

EDITION 1

DESIGN HANDBOOK

STRUCTURAL DESIGN AND MANUFACTURING IN HIGH-STRENGTH STEEL



SSAB

This handbook contains general suggestions and information without any expressed or implied warranty of any kind. SSAB hereby expressly disclaims all liability of any kind, including any damages, in connection with the use of the information and for their suitability for individual applications. It is the responsibility of the user of this brochure to adapt the recommendations contained therein to the requirements of individual applications.

Index

-
1. Designing and manufacturing products of high-strength steel
 2. Steel types and their properties
 3. Design principles
 4. Static design
 5. Fatigue design
 6. Manufacturing
-





1. Designing and manufacturing products of high-strength steel

1.1	Holistic approach – Crucial for the final result	1:1
1.2	Benefits for the end user and for the environment result in increased competitiveness	1:2
1.3	Choice of material	1:3
1.3.1	Material upgrade	1:3
1.3.2	Structural design	1:4
1.4	Development, accumulated knowledge and experience	1:4
1.5	Experiences within different fields of application	1:5
1.5.1	Lifting	1:5
1.5.2	Lorries	1:5
1.5.3	Trailers	1:6
1.5.4	Construction vehicles	1:6
1.5.5	Transport of people	1:8
1.5.6	Variety of applications	1:8
1.6	Possibilities	1:8



2. Steel types and their properties

2.1	Introduction	2:1
2.2	Steel types	2:2
	HSLA steels (High-Strength Low Alloy)	2:2
	Bainitic steel	2:2
	Rephosphorus (RP) and BH steel	2:2
	DP/DL/DPX steels (Dual Phase)	2:2
	Martensitic steel (M)	2:3
	Boron steel	2:3
	Corrosion-resistant steels	2:3
	Chemical composition	2:3
2.3	Material properties	2:4
2.3.1	Strength	2:4
	Directional dependence of strength	2:5
	Variation in strength	2:5
	Aging, bake hardening	2:5
	Strength at high strain rate	2:5
	Effect on strength due to short term heating	2:6
	High temperature strength	2:6
2.3.2	Toughness	2:6
2.3.3	Wear resistance	2:7
2.3.4	Physical properties	2:7
2.4	References	2:7



3. Design Principles

3.1 Basic concepts	3:1	Punch riveting	3:11
3.1.1 Resistance and loading	3:1	Blind rivets	3:11
3.1.2 Local buckling	3:2	3.3.4 Integral joints	3:11
3.1.3 Fatigue	3:2	3.3.5 Adhesive joints	3:11
3.2 Structural design	3:2	3.3.6 Combination joints	3:12
3.2.1 Material utilization	3:2	3.4 Forming	3:12
3.2.2 Load introductions	3:3	Shearing and punching	3:12
In- and out of plane bending for a structural members	3:3	Plastic forming	3:12
Load introduction	3:4	3.5 Corrosion and corrosion protection	3:13
Asymmetrical beams	3:4	3.5.1 Corrosion types	3:13
3.2.3 Stiffness	3:5	General corrosion	3:13
Open thin walled cross- sections	3:5	Local corrosion	3:13
3.2.4 Design with respect to fatigue	3:5	Crevice corrosion	3:13
3.2.5 Natural frequency	3:6	Galvanic corrosion	3:13
3.2.6 Stiffeners	3:6	Fretting corrosion	3:13
Out of plane bending	3:7	Stress corrosion cracking and corrosion fatigue	3:13
In-plane compression forces	3:7	3.5.2 Different types of corrosion protection	3:13
3.3 Joints	3:8	Weathering steel	3:14
3.3.1 Welded joints	3:8	3.5.3 Construction advices for corrosion prevention	3:14
Choice of filler metal	3:8	Avoid constructions that provide standing water or dirt accumulations	3:14
Under marching	3:8	Steel in contact with other materials	3:14
Marching or over marching	3:8	Corrosion in spot welds of metal coated steels	3:14
Practical design of welded joints	3:8	Corrosion of cut edges on metal coated steel	3:14
Spot welded joints	3:8	Environmental classification of corrosivity	3:15
3.3.2 Bolted connections	3:10	Water-filled crevices	3:15
Friction joints	3:10	Design for optimized surface treatment	3:15
Shear joints	3:10		
Axially loaded joints	3:10		
3.3.3 Riveting	3:10		
Clinching	3:11		



4. Static design

4.1	Basic concepts	4:1	Bending moment and axial force	4:31
4.1.1	Load capacity/resistance	4:1	Bending moment,	
	Serviceability limit state	4:1	axial force and shear force	4:32
	Ultimate limit state	4:1	Bending moment,	
	Instability	4:2	normal force and patch loading	4:32
4.1.2	Cross-sections	4:3	Torsional moment, bending moment,	
	Cold-formed sections	4:3	shear force and axial force	4:33
	Welded sections	4:3	4.3.10 Special effects	4:34
	Cross-section classes	4:4	Shear lag	4:34
4.2	Design methods	4:4	Flange curling	4:35
4.2.1	Relative design	4:4	Flattening of cross-section	4:35
4.2.2	Absolute design	4:4	Cross-section change of open	
	External load and load effect	4:4	cross-sections by shear stress	4:36
	Structural design and material selection	4:5	Natural frequency	4:37
4.2.3	Assessment of requisite safety	4:5	4.4 Design using FEM	4:39
	Resistance	4:6	4.4.1 Introduction	4:39
	Design load	4:6	4.4.2 Modeling	4:39
	Material yield point	4:6	Boundary conditions and loads	4:39
	Material's ultimate tensile strength	4:6	Discretization	4:39
4.2.4	Testing	4:7	Material modeling	4:40
4.2.5	Simulation	4:7	Through process effects	4:40
4.3	Design of plate fields and beams	4:7	Imperfections and instability	4:40
4.3.1	Limitations – Geometric proportions	4:7	Residual stresses from welding	4:42
4.3.2	Buckling	4:8	Cold forming effects	4:42
	Critical stress and slenderness	4:8	Lacquer hardening effects	4:42
	Design with respect to local buckling	4:8	Fluctuations in mechanical	
	Design of stiffeners	4:14	properties and nominal thickness	4:42
	Design with respect to		Modeling of joints	4:42
	local buckling of round pipes	4:16	4.4.3 Calculation	4:42
	Buckling between fastening points	4:17	4.4.4 Evaluation	4:43
4.3.3	Elastic behavior in slender parts	4:17	Convergence study, accuracy and check	4:43
4.3.4	Axial force	4:18	Design criteria	4:43
	Tension	4:18	Resistance	4:43
	Compressive	4:18	Limited plastic deformation	4:44
4.3.5	Bending moment	4:22	Stiffness/Natural frequency	4:44
4.3.6	Shear force	4:24	Energy absorption, pulses	4:44
	Large web openings/holes	4:26	Fracture	4:44
4.3.7	Load introductions and support	4:26	4.4.5 Design procedure	4:44
	Load introductions in		4.5 Energy absorption, dent and impact	4:45
	a cold-formed section	4:27	4.5.1 Dent resistance	4:46
	Load introduction in welded beams	4:28	4.5.2 Plastic energy absorption in components	4:46
4.3.8	Torsional moment	4:28	Axially loaded tubes	4:46
	Closed cross-sections	4:29	Beams subjected to a bending load	4:48
	Open cross-sections	4:29	4.6 Joints	4:48
	Varying cross-sections along beam	4:29	4.6.1 Welded joints	4:48
4.3.9	Interaction	4:31		

Residual stress	4:48
HAZ (Heat-Affected Zone)	4:49
Butt weld	4:49
Fillet weld	4:50
Spot weld	4:53
4.6.2 Bolted connections	4:54
Shear fracture in the bolt	4:54
Bearing failure	4:55
Material failure	4:55
Edge failure	4:55
Pre-stressing	4:56
Friction joints	4:56
Thin plate joints	4:56
4.6.3 Riveted joints	4:57
Self-piercing riveting	4:57
Clinching	4:58
4.6.4 Adhesive joints	4:58
Design	4:59
4.7 Low operating temperature	4:60
Correction of transition temperature for thin sheet	4:61
4.8 References	4:63



5. Fatigue Design

5.1	Introduction	5:1	5.6.2	Load analysis	5:27
5.1.1	The fatigue phenomenon	5:1		General information	5:27
5.1.2	Difference between parent metal and welded Joint	5:2		Rainflow count & range pair methods	5:28
5.1.3	Fatigue design standards	5:2	5.6.3	Stress history characterization	5:29
5.2	Effect of different factors on fatigue strength	5:3	5.6.4	Typified stress histories	5:30
5.2.1	Number of load cycles – S-N curve	5:3	5.6.5	Choice of design method	5:31
5.2.2	Load history	5:4		Nominal stress method	5:32
5.2.3	Notch effect – Stress concentrations	5:4		Hot Spot method	5:32
5.2.4	Mean stress and residual stress	5:5		Effective notch method	5:33
5.2.5	Temperature	5:5		Design based of fracture mechanics	5:33
5.2.6	Corrosion	5:5	5.6.6	Calculation procedure	5:34
5.3	Design with respect to fatigue	5:6		Calculation procedure, comments and instructions	5:35
5.3.1	Common design principles	5:6	5.6.7	Nominal stress method	5:38
5.3.2	Choice of joints – Structural details	5:6		Improvement techniques	5:40
5.3.3	High-strength steels in fatigue-loaded structures	5:6		Special cases	5:40
5.3.4	Placement and design of welded joints	5:7		Structural joints for parent material	5:41
5.3.5	Load introductions	5:9		Structural details for parent material with different surface and edge condition	5:42
5.4	Fatigue of non-welded material	5:10		Structural details for welded joints	5:44
5.4.1	General information	5:10	5.6.7	Hot Spot stress method	5:61
5.4.2	Material effect, effect of surface condition	5:10		Position of a Hot Spot	5:61
5.4.3	Galvanized surface	5:12		Type a and b Hot Spots	5:61
5.4.4	Quality of cut edges	5:12		Assessment using strain measurements	5:61
5.4.5	Mechanical notches	5:14		Assessment of Hot Spot stress using FE calculations	5:62
5.4.6	Strain hardening and bake hardening	5:14		Extrapolation for type a Hot Spot	5:63
5.4.7	Material factor	5:14		Extrapolation for type b Hot Spot	5:64
5.5	Fatigue in welded material and structures	5:16		Solution procedure	5:64
5.5.1	General information	5:16	5.6.9	Effective notch method	5:64
5.5.2	Different types of geometric notch effect in welded structures	5:16		Effective notch radius	5:65
5.5.3	Different types of joints, optimum throat thickness for fillet welds	5:17		FE modeling	5:65
5.5.4	Thickness effect	5:18		Element mesh	5:65
5.5.5	Residual stress in the weld – Stress relief treatment	5:19		FAT classes	5:66
5.5.6	Post-treatment of welds for increased fatigue strength	5:20		Solution procedure	5:66
5.5.7	Welding quality and assessment of weld defects	5:22	5.6.10	Linear damage calculation by the "Palmgren-Miner" rule	5:66
5.6	Design	5:26	5.6.11	Fatigue testing	5:67
5.6.1	Introduction	5:26		Component testing	5:67
				Determination of the S-N curve	5:69
			5.6.12	Fracture mechanics – Defect tolerance	5:69
				Fracture mechanisms	5:69
				Basic fracture mechanics	5:70

Critical crack size in connection with brittle fracture	5:70
Critical crack size in connection with ductile fracture	5:71
Crack growth under fatigue load	5:71
Data for fracture mechanical calculations	5:71
Threshold value for crack propagation, ΔK_{th}	5:71
Fracture toughness and impact toughness, Charpy	5:72
Crack propagation constants C and n	5:72
Geometry factor	5:72
Initial crack depth	5:73
Assessment if a defect is growing	5:74
Critical defect size with regard to brittle fracture	5:74
Defect tolerance diagram	5:74
Crack growth based on FE calculations and linear fracture mechanics	5:75
Service life calculations through direct determination of stress intensity	5:75
Service life calculations through approximate weight functions	5:75
5.6.13 General advice about FEM in connection with fatigue design	5:77
Beam elements	5:77
Solid elements	5:77
Shell elements	5:77
Polynomial degree for elements	5:78
Combinations of different types of elements	5:78
Assessment	5:78
5.6.14 Appendix A	5:79
5.6.15 Symbols	5:80
5.7 References	5:80

6. Manufacturing

6.1	General information	6:1	Length of the material [6.13]	6:16
6.2	Cutting	6:2	Some final viewpoints	6:16
6.2.1	Size shearing	6:2	6.4.2 Roll forming	6:16
	Power shearing	6:2	Additional operations	6:17
	Cutting force during power shearing	6:2	6.4.3 Presswork operations	6:17
	Recommendations for power shearing	6:3	Definitions and testing	6:17
	Punching	6:3	Deep drawing	6:18
	Cutting force during punching	6:4	Draw	6:18
	Recommendations for punching	6:4	Stretch forming	6:19
	Summary of advantages and disadvantages during size shearing of high-strength steels	6:5	Comments concerning drawing and stretch forming tests	6:19
6.2.2	Machining	6:5	6.4.4 Flanging	6:20
	Drilling	6:5	Forming limit curve (FLC)	6:21
	Milling	6:5	The effect of forming when choosing a high-strength steel	6:21
6.3	Thermal cutting	6:6	Springback	6:21
6.3.1	Plasma cutting	6:6	Measures for reducing springback during presswork operations	6:21
	Application	6:6	Formation of wrinkles	6:22
	How does plasma cutting work?	6:6	Formability	6:22
	Process gases	6:7	Stress on the tools	6:23
	High tolerance plasma arc cutting	6:7	6.5 Welding	6:24
	Cutting speed	6:8	6.5.1 Fusion welding	6:24
	Cut quality	6:8	Weldability	6:24
6.3.2	Laser cutting	6:8	Heat input	6:24
	Laser	6:9	Heat affected zone	6:25
	Laser cutting	6:9	Welding defects	6:25
	Cutting speed	6:10	Cold cracks	6:26
	Alloying elements	6:10	Hot cracks	6:26
	Plate surface	6:10	Defects influenced by the welding procedure	6:26
	Laser cutting of SSAB materials	6:11	Welding processes	6:26
	Production cost	6:11	MAG welding	6:28
6.4	Plastic forming	6:12	TIG welding	6:28
6.4.1	Bending	6:12	Manual metal arc welding	6:29
	Methods, nomenclature	6:12	Submerged arc welding	6:29
	Bendability	6:12	Laser welding	6:29
	Springback	6:12	Static strength of welded joint	6:30
	V-bending	6:13	Fatigue strength of the welded joint	6:30
	Air bending (free bending)	6:13	Impact toughness of the welded joint	6:31
	Springback during air bending	6:13	6.5.2 Fusion welding in Domex steel	6:31
	Bottom	6:14	Edge preparation and types of joints	6:31
	U-bending	6:14	Welded joints strength	6:31
	Methods for reducing springback during U-bending	6:14	Impact toughness of the welded joint	6:32
	Overbending	6:14	Filler metals for cold forming steels	6:32
	Intended bend	6:14		
	Bending force	6:14		

Filler metals for Domex W	6:33
Filler metals for Domex boron steel (014B, 024B)	6:33
6.5.3 Fusion welding in Docol steel	6:33
Filler metals	6:33
Strength of welded joints	6:33
6.5.4 Fusion welding of Dogal (metal-coated thin plates)	6:34
Filler metals	6:34
The effect of zinc on fusion welding	6:34
Recommendations	6:34
Corrosion of welded joints	6:34
6.5.5 Electrical resistance welding	6:35
Electrical resistance welding principle	6:35
Spot welding	6:35
Projection welding	6:36
Seam welding	6:37
Structural instructions	6:37
6.5.6 Spot welding	6:39
Testing of spot welded joints	6:39
Recommendations to avoid welding defects	6:40
Weldability	6:40
Width of the weldability lobe	6:40
Type of failure	6:41
Useful life of the electrode	6:41
Static strength of spot welds	6:41
6.5.7 Resistance welding in Docol steel	6:42
Soft Docol steel	6:42
Recommended welding variables for soft Docol steels	6:42
High-strength Docol steels	6:43
Spot welding in high-strength Docol steels	6:43
Static strength of high-strength Docol steels	6:44
6.5.8 Resistance welding in Domex steel	6:45
Soft Domex steels	6:45
High-strength Domex steels	6:45
6.5.9 Resistance welding in Dogal (zinc-coated thin plates)	6:45
Useful life of electrodes	6:45
Recommended welding variables for soft Dogal steels	6:45
Recommended welding variables for high-strength Dogal steels	6:46
6.6 Mechanical joining	6:46
6.6.1 Mechanical joining methods	6:46
Screwed joints	6:46
Clinching	6:47
Strength of butt riveted joints	6:48
Self piercing riveting	6:48
Strength of self pierced riveted joints	6:49
6.7 Bonding	6:49
The plate surface	6:49
Joint design	6:50
Long-term durability	6:50
Adhesive types and adhesive application	6:50
6.8 Soldering	6:51
Soldering methods	6:51
Thin plate soldering	6:51
6.9 Straightening	6:52
6.9.1 Roll flattening	6:52
6.10 Surface treatment	6:52
6.10.1 Cleaning and surface treatment	6:52
Mechanical cleaning	6:52
Degreasing	6:53
Pickling	6:53
6.10.2 Non-metallic, non-organic coatings	6:53
Chromating	6:53
Phosphatization	6:54
Enameling	6:54
6.10.3 Organic coatings	6:55
Passivations and TOC (Thin Organic Coatings)	6:55
Paint	6:56
Paint application	6:56
Corrosion protection by painting	6:56
Coil coating	6:57
Polyester	6:57
Prelaq 200	6:57
PVDF – Polyvinylidene Fluoride	6:57
6.10.4 Metallic coatings	6:58
Continuous metal coating	6:58
General galvanizing	6:58
Zinc plating	6:59
Nickel- and chrome-plating	6:59
PVD and CVD coatings	6:60
6.11 Tool steel for high-strength steels	6:60
6.11.1 Tool steel for punching operations	6:60
6.11.2 Tool steel for punching	6:60
6.11.3 Coating of tools	6:60
PVD (Physical Vapor Deposition)	6:61
CVD (Chemical Vapor Deposition)	6:61
6.12 References	6:62





1. Designing and manufacturing products of high strength steel

1.1 Holistic approach

– crucial for the final result

The use of high strength steel leads to better product performance in terms of higher payload, higher crashworthiness, longer service life and lower fuel consumption. The advantages, such as better transport economy, improved safety and greater environmental benefits, which the end user benefits from, increase. Work environment benefits and development opportunities strengthened through collaboration within stronger networks of many different competence areas also offer unique customer values. The competitive power in the form of stronger trademark and better profitability for both manufacturers and end-user companies increases. The best choice of material is therefore made based on a holistic approach and is a factor of decisive importance for greater profitability and competitiveness.

- To define the customer/end user requirements and product benefits; to further develop benefits in order to increase the competitive power.
- To systematically learn from end user experience and field measurement results. Increased product knowledge gives better prerequisites for developing even more competitive constructions.
- To get to know the material and all its properties. Strength, elasticity, strain hardening, density, hardness, fatigue strength, workability, weldability, corrosive properties.
- To identify the material properties which are of greatest importance for the end product performance.

- To select the design solutions that are best suited to the material and structure in question; to design for better recycling of the material.
- To describe the material requirements for an effective production adapted to the actual product volume.
- To consider even scrap, delivery forms, availability and logistics solutions.
- To select ecologically sustainable solutions, to reduce the impact on the environment during the entire life cycle of the product, to develop and select alternatives that offer environmental benefits.
- The collaboration between material suppliers, manufacturing companies and trade associations provides important knowledge and experience.

High economic growth results in a high demand for material and is in itself a driving force for efficient material use, i.e. increased use of advanced materials. More rigorous environmental requirements coupled with the diminishing availability of raw materials and energy further increase the value of a possible weight reduction. The more this development advances, the more the use of this high strength steel accelerates. The value of a weight reduction is one of the driving forces justifying the choice of high strength steel. Other materials, such as aluminium and composites, are often more of a complement rather than a competitive alternative. Choose the right material for the right place!

1.2 Benefits for the end user and for the environment result in increased competitiveness

High strength steel strongly contributes to increasing the benefits for end users within a large number of areas. Good transport economy, good driving characteristics, low maintenance costs and low fuel consumption of a concrete mixer on a semi-trailer chassis, *figure 1.1a*, are of vital importance for the end user. In this case the fatigue strength and wear resistance of the construction are considered important characteristics.

Another example is a road post, *figure 1.1b*, of high strength steel, where the high yield stress of the steel is used to ensure that the post straightens out after a collision. It is no longer necessary to send personnel to fix the

road posts after car collisions. As compared to previous designs, the construction work is also simplified. In other words, this leads to significant cost savings for the road administration.

An example where a design is available in several different materials is the LPG bottle, *figure 1.1c*. Current resistance calculation rules, design and manufacturing methods mean that high strength steel is an extremely advantageous alternative for this purpose. Lighter bottles result in fewer heavy lifts and better transport economy.

The sugar cane trailer, *figure 1.1d*, shows the benefits of high strength steel for the end user within the transport sector. In addition to more efficient transport, the increase in payload leads also to lower fuel consumption and lower road tolls.



Figure 1.1: a) Concrete mixer (Baryval Serviplem, S.A.). b) Road post with reflection (Dura Pty.Ltd)
c) LPG bottle (Liotard.) d) Sugar cane trailer (Industria Metallurgica Pastre).

1.3 Choice of material

SSAB's structural steels make it possible to build lighter and more innovative structures. Uniform mechanical properties give good manufacturing prerequisites to increase productivity and shorten production lead times. These properties are found in strength classes of up to $R_e = 1300$ MPa. Example applications are: trailers, bodywork, containers, goods wagons, cranes, lorries, buses, agricultural equipment and vehicles, vessels, bridges, buildings, contractor's machinery and tanks.

Hardox – SSAB's versatile wear plate increases payload and service life in tough environments. The combination of hardness and toughness makes the plate extremely resistant to wear, while user-friendliness in the workshop cuts production costs. Hardox combines durability and high resistance and in some cases it can be used as construction steel. Buckets, lorry and dumper truck platforms, railroad cars, bodywork, cutters and grates are a few example applications of Hardox.

Cold-rolled steel plate from SSAB covers the entire range from soft to high strength steel. Some of the advantages of using high strength steel include lightweight design (with the same strength), higher strength, lower material cost and simplified but retained production. It is widely used in different vehicle components (including safety components), radiators, refrigerators, containers and packaging straps. Strength classes of up to $R_m = 1400$ MPa.

SSAB's zinc-plated steel combines the workability and high strength that characterise modern steel plates with excellent corrosion resistance. It is used for products that need anticorrosion protection such as washing machines, fans and ventilation ducts. It is available in different versions with a wide spectrum of properties, from soft materials for manual processing or advanced pressing to high strength materials.

Greencoat – SSAB's prepainted steel sheet is a well established building material. It is usually used for roofing and wall cladding on buildings, for rainwater goods and fittings. It is available as a structural element in walls, roofs and beams. Prepainted sheets are available in numerous combinations of steel materials, metal coatings and paint coats. Roofing, rainwater goods and wall cladding are example areas of application.

Toolox is SSAB's tool and machine steel is used in press tools, moulds and machine components.

The different steel types, their properties and delivery forms are described in chapter 2 and in SSAB's product information.

1.3.1 Material upgrade

Design of high strength steel structures usually follow two main principles:

- absolute design; the whole structure is studied with respect to load capacity and expected load situations
- relative design; the material thickness of the existing structural parts are decreased in relation to the high strength material properties

Practical experience has shown that a first conservative approach in the case of relative design can be expressed by equation 1.1

$$t_{HS} = t_{MS} \sqrt{\frac{R_{e,MS}}{R_{e,HS}}} \quad (\text{Eq. 1.1})$$

where

- t_{HS} – plate/sheet thickness in high strength steel
 t_{MS} – plate/sheet thickness in mild steel
 $R_{e,HS}$ – yield stress high strength steel
 $R_{e,MS}$ – yield stress mild steel

The equation is based on local bending of the plate with retained resistance.

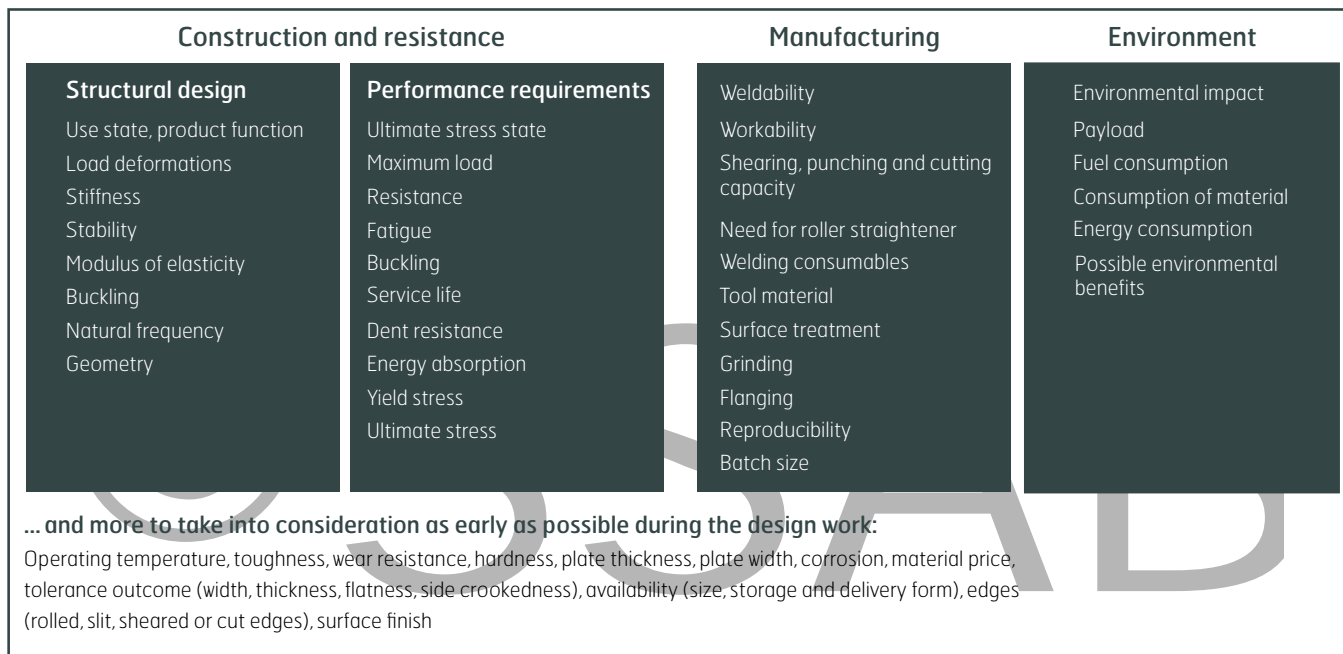


Figure 1.2: Questions concerning design, manufacturing, choice of material and environment are directly or indirectly associated with each other.

1.3.2 Structural design

For experienced designers with sound knowledge of materials, high strength steel is the natural choice for many different applications. Good structural design with regard to load transfer, instability and fatigue are of decisive importance for how well the strength of the material can be utilised. A good design philosophy requires easily applicable design methods often associated with experience of testing and use. Take into account quality results, tolerances and efficiency of selected production methods early in the product development project. When you want to establish the strength that is possible in practice in a certain structure, you should consider several different aspects, *figure 1.2*.

The material selection philosophy ought to choose as high strength a material as possible considering these factors, cf. *figure 1.2*, in combination with design solutions. The lightest possible weight and/or highest possible performance of the end product give best customer value and competitive edge.



Figure 1.3: Technical guidance in connection with product improvements.

1.4 Development, accumulated knowledge and experience

The individual ability to create and improve things is the most important prerequisite for growth. Dedicated people realise new ideas. Efficient collaboration between people competent in different fields is crucial for the further development of ideas to create innovations and new competitive products. Experts in research, process and product development projects learn from each other and work together with business developers, marketing specialists and sellers. Employees with growing expertise and competence work together to develop new technically and commercially products. The creativity and competence of our current employees and their network are already of decisive importance for the future competitiveness.

In addition to the physical plates, material delivery includes also a complete offer of quality, delivery reliability and service:

- Help desk – Assistance
- Manufacturing and technical support: troubleshooting, technical inspections
- FE (Finite Element) simulations
- Upgrades, collaboration and technical guidance in connection with product improvements
- Product development works, expert competence in product development
- Participation in research projects and implementation of results
- Test materials
- Component tests
- Training, courses
- Manuals

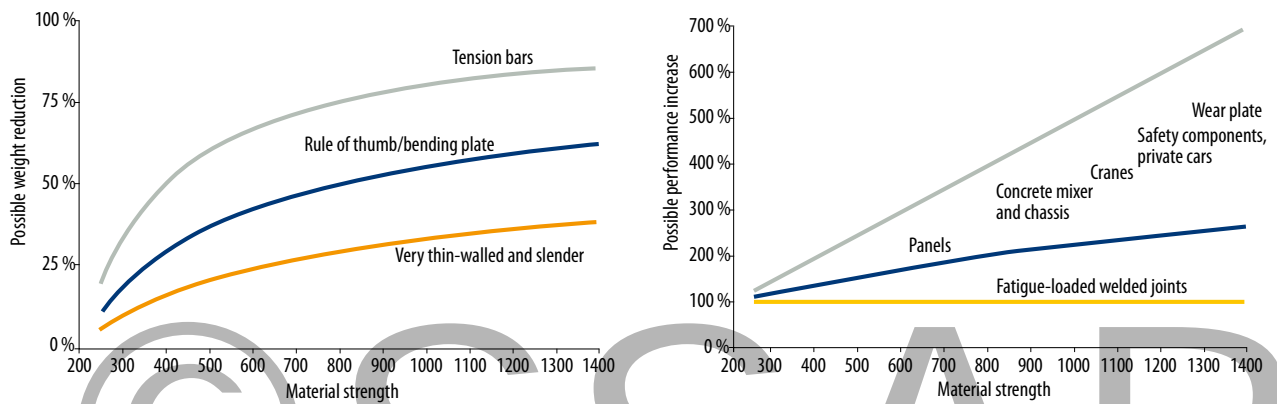


Figure 1.4: a) Possible weight cost savings in case of unchanged performance requirements and b) possible performance increase in case of unchanged weight (schematic).

1.5 Experiences within different fields of application

SSAB has been working with applications in high strength steel together with our customers for more than 25 years.

1.5.1 Lifting

The leading crane manufacturers have very long experience of using high strength hot rolled steel. High strength in combination with structural design is a key factor for the performance of modern cranes. Design and resistance calculation methods are well suited for high strength steel. A good hoisting crane is characterised by high lifting capacity within a wide range of work and low weight. The properties of high strength steel are utilised in full.

With a design that takes into account stiffness of the structure, fatigue strength of the basic material and welded joints, high strength steel can be utilized to a large extent. Special attention is paid to the execution and location of welds. A good description of the impact of the load on the structure, such as number of stress fluctuations and their distribution between the different ranges, is required.

Good design of all welded joints, load transfer and cross section shape are key factors, chapter 3.

Resistance calculations are subject to crane standard (EN 13001). Extreme fatigue testing of test rods, components and whole cranes is carried out. Load spectrum from operation can be gathered through measurements during the crane's service life, chapter 5.

Hot rolled high strength steel is usually used with yield points between 700–1200 MPa. With thinner plate thickness, and thereby higher working stress, the need for thorough structural design increases. Bending capacity and weldability are key properties for rational manufacturing. Low operating temperature requires good impact strength, particularly for thicker plates. Surface finish can be important if the plate is used as a sliding surface, cf. chapter 2.

Production takes place in small to average batches. The bending capacity in an edging press is cost effective. Shearing and punching are more and more often replaced by laser cutting. Welding, such as MAG, primarily takes place in automatic welders or is done by robots. The design should be such that edge preparation can be avoided. Laser cutting is expected to become more frequent, cf. chapter 6.

1.5.2 Lorries

The leading lorry manufacturers choose high strength steel in frame members, cross bars and other components. The use of high strength steel in modern chassis frames is exemplary. Good design of all joints, load transfers and transitions between the different cross sections and connections between bars as regards fatigue is crucial, cf. chapter 5. Design for energy absorption is made for lorry cab and other safety components, cf. section 4.5.

A good lorry is characterised by good manoeuvrability, high safety, high load capacity and low weight for reduced fuel consumption. Many different high strength steels are used, both hot rolled (in chassis) and cold rolled (in safety components).

Production takes place in average to large production series. Roll forming of frame members, bending and pressing of cross bars are standard manufacturing methods, just as punching and riveting of joints.

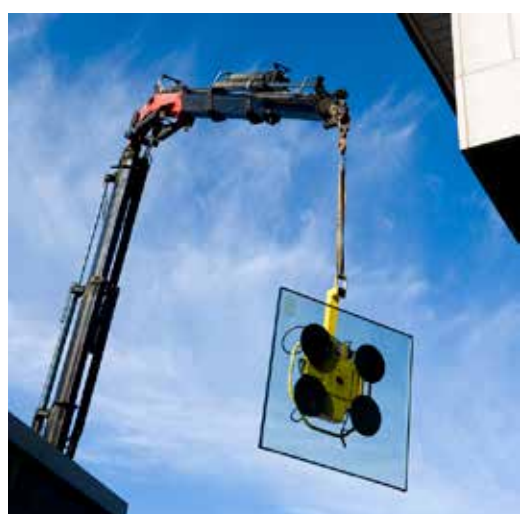


Figure 1.5: Truck cranes from Hiab.

1.5.3 Trailers

Trailers and trail cars are available in many versions with one and the same common denominator; they are connected to a tow car or a lorry. High strength steel is crucial for the total load capacity of the vehicle, both with regard to strength and permitted total weight. As compared to conventional steel, high strength steel offers more wear resistance which means fewer maintenance repairs.

With the use of thinner high strength plates, the payload increases and can be expressly associated with higher profit and smaller environmental impact thanks to lower fuel consumption or fewer trips for the same volume of goods. End users represented by vehicle owners and logistics companies also see the advantages of increased payload and steer the development towards lighter trailers. The benefits are very easy to notice.

Different types of recycling and waste management containers can be made of high strength steel. Important aspects to consider in the case of containers intended for both industrial use and household waste are minimum maintenance and durability. Increased payload and reduced environmental impact are arguments that drive the development towards using high strength steel in this sector. The design of recycling containers is governed by national laws and standards.

The structure of refuse trucks and recycling containers can often be improved by upgrading to high strength steel. The outcome is a design with thinner material thickness, fewer constituent components, decreased air resistance and

fewer maintenance interventions. A plainer design is less likely to cause corrosion-related problems because there are fewer nooks that are easier to keep clean.

Experience-based relative design criteria are often applied both with regard to stiffness and with regard to resistance. The elastic beam theory can be applied when calculating bending stress and deflection of chassis beams. The calculation of other load cases, such as torsional rigidity, and more complex structures are successfully assessed with the help of computer stimulations. Fatigue is very important to consider in design. Place and design welded joints, load transfers and beam connections properly!

The most common material is the hot rolled steel with a yield point of 700 MPa. However, the use of both hot and cold rolled steel with yield point up to 1300 MPa has increased.

Production takes place in series of any size from very small to average. Shearing is more and more often replaced by laser and plasma cutting ensuring higher edge quality and thus prolonging the fatigue life in many cases. Edge pressing and bending are frequently used but can be replaced by roll forming where the volume is large enough such as in different shapes of side floor beams for trailers and top lines for recycling containers. This way an advanced shape can be achieved with the help of narrow radii and integrated stiffeners. Welding, e.g. with MAG, both manual and using robots, offers better possibility for controlling welding parameters such as heat supply. This leads to improved productivity and better outcome with regard to shape requirements for straightness and flatness, for example.



Figure 1.6: MST timber trailer.



Figure 1.7: Many vehicle manufacturers use advanced high strength steel.

1.5.4 Construction vehicles

Construction vehicle manufacturers have long experience of high strength steel and provide good examples of excellent detailing, practical design and production in these fatigue stressed designs. The main structures such as frameworks, lifting frameworks, excavator booms, shafts and links are exposed to 1,000–5,000 significant fluctuating forces per hour of operation. The turbo aggregate and other speed-dependant components are exposed to 10–100 times more fluctuating forces. This means that main structures with less than 15,000 hours of operation are exposed to up to 15–50 million significant fluctuating forces.

Design with regard to fatigue is necessary in order to guarantee safety and service life for each detail or component!

Many structures in a construction machine are characterised by compact design, many load transfers, local reinforcement arrangements and many critical positions with respect to fatigue. The calculations are very extensive and often difficult to carry out from a technical perspective, even if FE-simulations are used, cf. figure 1.7.

Fatigue is a local phenomenon that limits the vehicle's service life. We strive to reduce the stress level and/or defect size locally in known areas through design. This increases service life. The plate thickness is thereby reduced since high strength steel can handle the increasing operating stress in the design.

To consider

To design and manufacture a lighter plate structure with a thickness greater than approx. 5 mm, you can use the following methods:

- Proper load evaluation and meticulous design calculations.
- Removal of critical welded joints by, for example, using bigger plate fields, cold-forming or moulding local welded details and geometrical shape optimisation of the design, at which welded joints etc. are placed in areas with lower stress levels.
- Use the thickness effects. (Thinner materials alone can mean longer service life).
- Better welding quality by, for example, improvement methods, edge preparation, better welding processes, etc.
- Efficient and process-controlled manufacturing methods.
- Cost effective production control methods.

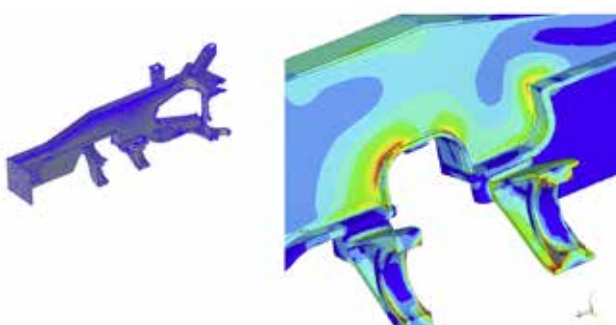


Figure 1.8: Computer simulation of a frame. The colours represent different stress levels.



Figure 1.9: Tipper body with modern design of high strength steel. The result is a vehicle with increased durability and load capacity.

Manufacturing takes place in average size series. Support structures in construction vehicles consist primarily of gas or laser-cut plates, joined together in different welding processes. In connection with load transfer and the position of the bearings, welding of simple geometries of high strength steel and of more complex geometries of cast steel. For further information, see chapter 6.

1.5.5 Transport of people

Traffic safety, reduced fuel consumption and CO₂ emissions are key factors for all transport of people. At the same time, the users' requirements concerning comfort and performance are growing. Cost-effective manufacturing must be achieved, often in large-volume series. Since more and more safety components and other equipment are put into the cars, it is difficult to reduce the weight of the vehicles. It is therefore vital to reduce the weight of each component. In passenger cars, high strength cold rolled steel is used in body reinforcements, bumpers, door beams, cap pieces and seats in order to increase collision safety while at the same time minimising the weight. Sub-contractors can manufacture complex components cost effectively even in the case of high strength steels. Pressing, roll forming, laser welding and spot welding are established methods when working with these materials.

The automotive industry is a forerunner as far as the use of high strength steel is concerned. Companies often have their own instructions which can differ from the instructions in this Handbook. The material selection philosophy, design principles, as well as the manufacturing aspects covered in this Handbook, however, apply and are of current importance in many cases, even within the automotive industry.

1.5.6 Variety of applications

Lorries, bridles, hoists, containers, safe boxes, chair legs, table frames, bed components, crash barriers, locks and building components are a few examples of other areas of application. Almost an unlimited number of examples exist today.

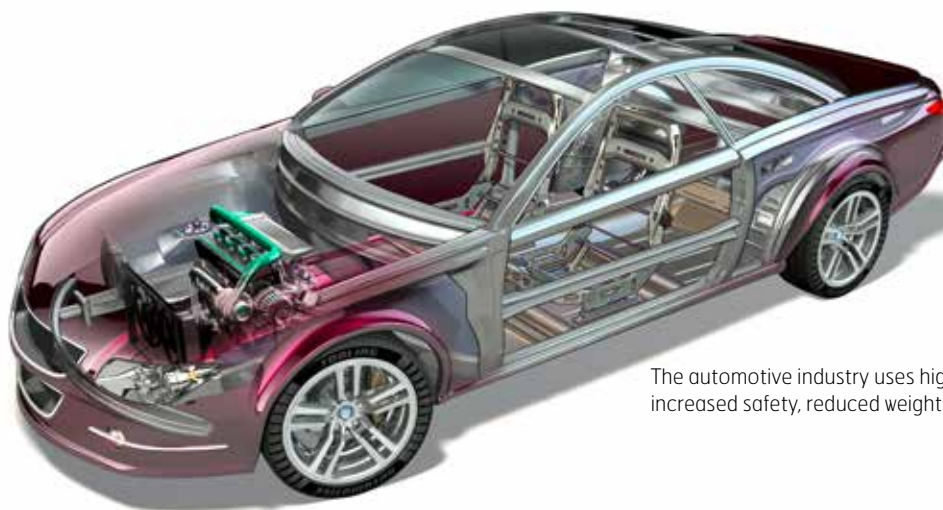
1.6 Possibilities

Properly used high strength steel has many advantages to offer. It is not only a matter of reducing thickness and weight, but also of increasing the benefits for the customer, of developing competence and innovation performance.

Innovative companies constantly stretch the limits of what is considered possible. Constant development and synergies between different industry sectors give new ideas for the use of high strength steel.



Figure 1.10: Front door mechanism in trains, Dellner Couplers.



AB

The automotive industry uses high strength steel to achieve increased safety, reduced weight and lower fuel consumption.

The working area and lifting capacity for cranes and sky-lifts is greatly improved by the use of high strength steel.



High strength steel supplies the robustness and lightness necessary for the manufacturing of vehicles within the heavy transport industry. Increased load capacity means environmental and economical benefits.





2. Steel types and their properties

At present, SSAB manufactures steel with a wide spectrum of strength levels. We focus primarily on high strength steel. Steel strength can be increased with the help of various hardening mechanisms. Below is a description of different steel types and what gives them their properties.

2.1 Introduction

Our steel plates are available in thicknesses from 0.4 to 160 mm. Our brands Hardox, Strenx, Docol, GreenCoat and SSAB Domex steels are well known for consistently high quality, as well as for SSAB's unique offering of support and cooperation for increasing competitiveness.

The product range is constantly evolving, new steel grades are launched regularly. Data sheets, brochures, materials data and delivery dimensions available on www.ssab.com.



Figure 2.1: Charger ring of pig iron for LD converter in Luleå.

2.2 Steel types

HSLA Steels (High Strength Low Alloy)

HSLA steels are alloyed with small amounts of niobium, titanium or vanadium. Despite the fact that the amounts are only a few hundredths of a weight percent, the elements can significantly increase the strength properties of the steel. Together with carbon and nitrogen, the elements form carbides and nitrides which are a prerequisite for fine grain size and precipitation hardening if the rolling process is carefully controlled. SSAB currently manufactures hot-rolled, cold-rolled and metal coated HSLA steels.

Modern strip-rolled HSLA steels have very good weldability thanks to their low carbon, phosphorus and sulfur content. The small amounts of carbon and sulfur also means that the steel can be bent at tight radii without breaking. Unlike older mild structural steels, these so called cold-formed steels also have guaranteed ductility. The ductility is very good even in the case of high strength steels. These steels have replaced the old, standardized mild structural steels to a great extent.

The HSLA steels have a very wide area of application. Examples of applications are crane arms, details of trucks and construction machinery. Thinner, cold-rolled and metal coated steels also are used in cars, furniture and various pressings in the manufacturing industry.

Bainitic steels

Microalloyed hot-rolled HSLA steels have yield point levels of up to 700 MPa. Increasing the strength requires harder phases like bainite and martensite. In general, the strength of these phases increases as a function of the carbon content.

By controlling the cooling process after hot rolling in a very meticulous manner, it is possible to build up bainite microstructures which in turn increase the strength of the steel. This is how yield

points from approx. 800 MPa can be obtained. The composition of the steel must be adapted to the cooling process so as to achieve the right strength while at the same time optimize the steel with regard to other requirements such as workability and weldability.

Bainitic steels are suitable for thin dimensions, generally under 10 mm. Areas of application where bainitic steels can be used in constructions are, in the first place, lifting and load handling. Other examples of application include heavy transport.

The ductility of bainite steels is also good. The high strength, however, places high requirements on tools and forming know-how.

Rephosphorus (RP) and BH steels

Rephosphorus steels (RP) are the so called solution-hardened steels, i.e. their strength is achieved through substances that form a solid solution with iron. The principle is that the atom size deviates from the size of the iron atom. This fact creates tensions in the structure thus resulting in increased strength. RP steels are alloyed with the elements manganese, silicon and phosphorus. The greatest effect is achieved via the use of phosphorus, which has given the name of this steel family.

Another version of these steels is the BH steel. BH stands for bake hardening, meaning that the increase in strength is achieved by painting a formed com-

ponent and then, when the varnish has hardened, subjecting it to thermal treatment.

These steels, despite their increased strength, have very good deep drawing properties. In this respect RP steels resemble mild steels. RP steels have guaranteed yield point of up to 300 MPa for cold-rolled and metal coated steels.

Because of the combination of high strength and good compressibility, these steels are used for complex pressings where low weight is essential. Passenger cars are one example of where these properties are useful.

DP/DL/DPX steels (Dual Phase)

Dual Phase or two-phase steels are transformation hardened steels. As the name suggests, the steel consists of two phases, one hard, which is martensite, and one mild – ferrite. Increasing the portion of martensite gives greater strength. Figure 2.2 shows an example of the microstructure of one of these steels. The steel shown contains approx. 30 % ferrite and 70 % martensite, which gives a minimum breaking point of 1000 MPa.

The strength is contingent upon the alloy content and the change of temperature during the entire thermal treatment. The most important alloy elements are carbon and manganese. The thermal treatment has two functions: to give the desired martensite and ferrite distribution, and to give the martensite the right hardness.

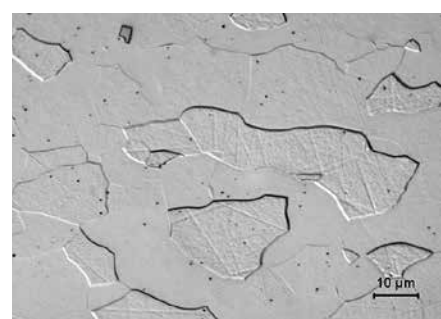
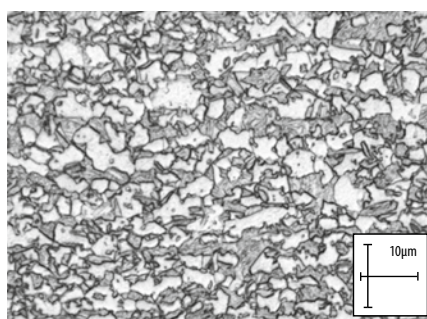


Figure 2.2: Microstructure of Docol 1000 DP to the left, HSLA material to the right.

Despite their high strength, DP steels have good workability. The above applies particularly for draw-pressing because these steels have a very low yield point/breaking point ratio. DL steels are a version of DP steels but with a lower yield point/breaking point ratio, which gives better workability. DPX steels have higher yield point than the equivalent DP steels, but improved properties when it comes to reverse bending. This is very useful in complex plate forming.

Weldability is also good. This is due to the fact that in our continuous annealing line for cold-rolled steel we can cool the steel in a water bath and thanks to the high cooling rate we can keep the alloy additive content low. Thanks to the great strain hardening of the steel, the finished component will have much higher yield point than the yield point at the time of delivery. The level is contingent upon the strain during the manufacturing process.

DP steels are available in both cold-rolled and hot-galvanized version. The difference between the manufacturing processes lies primarily in the cooling rate, which is much lower for hot-galvanized steel. This is compensated by additives, such as chromium, that increase the hardening capacity of the steel. When delivered DP, DL and DPX steels meet the minimum breaking point requirement. For example, the minimum breaking point of Docol 800 DP is 800 MPa.

The largest area of application for steels is energy absorbing components in vehicles, where the strain hardening can be used for absorbing energy in case of a collision.

Martensitic steels (M)

The cold-rolled product program also includes a series of completely martensitic steels. For these steels it is mainly the carbon content that determines the strength. Just as DP and DL steels, these steels are named accord-

ing to the minimum breaking point. Examples of steels in this series include Docol 1200 M and 1400 M. Despite their high strength, they have good forming and welding properties. Suitable applications of martensitic steels include primarily safety components in cars which require high yield point, as well as components exposed to collisions and wear such as container walls. The material is particularly suitable for roll forming at which complex profiles can be shaped. Another martensitic steel is our wear resistant steel, Hardox. The wear resistance is described in more detail in section 2.2.

Example areas of application include cement mixers, wagon bridges, dumpers, plow tools and pipeline systems where wear particles are found.

Boron steels

Boron steels are intended for hardening. They are carbon-manganese-chrome steels alloyed with a few thousandths of weight percent boron. Even though boron content is low, it significantly increases the hardening capacity. In other words, steels with carbon content below 0.20 % can be hardened too. There are boron steels with carbon content of up to approx. 0.5 %.

When delivered in hot- or cold-rolled and annealed condition, boron steels have a relatively low resistance, and mild annealing is normally not required before the production of components. After being produced, the components are hardened and achieve very high resistance. One of the advantages is that during the production process the components can be formed into complex forms thanks to the low resistance of the material. Furthermore, the resistance of the ready component after hardening is very high. In many cases the steels can replace more alloyed and thus more expensive steels.

The application of boron steels has augmented, such as wear components

for agricultural equipment, tools and collision protection components in cars.

Corrosion-resistant steels

Corrosion-resistant steels have 3–4 times better resistance to atmospheric corrosion than unalloyed or low alloy structural steels. This effect has been achieved through alloys of silicon, copper, chromium and, in some cases, phosphorus. When the standard structural steel starts to oxidize (corrode), porous, loose rust products are formed on the surface. This rust layer constitutes a very small obstacle for continued corrosion attacks because moisture can penetrate the steel. At the beginning, rust-resistant steels rust as unalloyed steels, but more and more dense oxide accumulates on the surface and the corrosion rate decreases over time. This is achieved through good adherence of the oxide layer, which prevents moisture from coming into contact with the plate surface.

Corrosion resistant steels are available in both hot- and cold-rolled version. Example steel types are Strenx 700W and Docol 700 W where W stands for "weather resistant".

Example areas of use of corrosion resistant steels are containers, garbage collection vehicles, rail wagons, chimneys and masts.

Chemical composition

In general, it is possible to say that the material has low carbon, sulfur and phosphorus content for the purpose of creating good prerequisites for welding and forming of the steel. The importance of silicon content for dip galvanizing is discussed in section 6.5.

The chemical composition of the steels is described in data sheets and product brochures which can be found at www.ssab.com.

2.3 Material properties

This section provides background information concerning the material properties one should be familiar with during structural work as well as some examples of test results for high strength steel.

2.3.1 Strength

A lot of information about the strength of the material can be found by carrying out tensile tests. With a tensile test it is possible to determine the material stress-strain response, cf. figure 2.3. At an early stage (low stress), the material is elastic, i.e. when stress is relieved, all deformation is reversible. The relation between stress and strain in this area is usually linear and is determined with the help of the modulus of elasticity, the E modulus. The E modulus is generally the same for all steel types and is approximately 210 GPa.

If the stress is high, the material starts to yield and the deformation is not completely reversible (plastic). This is reflected in the non-linear relation between stress and strain, cf. figure 2.3. The stress where yielding starts is called yield point and is given as R_{eH} for materials with a clear yield plateau and as R_{p02} for materials without a clear yield plateau, such as DP steels. R_{p02} is the stress that gives 0.2 % plastic strain after unloading. The stress can generally continue to increase after the yield point because the material strain-hardens. The stress then reaches a maximum level which coincides with necking during tensile tests.

This stress level is called ultimate strength or tensile strength, R_m , cf. figure 2.4. Despite its name, the material does not fail at this level. A neck forms and the strain is concentrated in the neck area. This leads to a decrease in

the tension force when continued loading is applied to the test specimen and eventually the material fractures. The plastic strain at this point is usually called elongation at failure. The measures are different depending on the gauge length, such as A80 for a gauge length of 80mm and A50 for 50mm. It should be noted that locally at the neck the strain is much higher than for standardized elongations at break A80 and A50, which is illustrated by the fact that A50 is usually 20–30 % greater than A80.

In the discussion above, stress is regarded as the stress at tensile tests divided by the original cross-section area, the so called engineering stress. In practice, the material is subjected to higher stress when the test specimen elongates and the cross-section area decreases during the test. By assuming that the plastic strain takes place under constant volume, it is possible to determine true stress with the help of equation 2.1. An associated relevant strain measure can also be defined according to equation 2.2.

The relation between the engineering and the true stress is only relevant as long as the stress condition is homogenous, i.e. up until necking, cf. figure 2.5.

The relation between true stress and strain is used, for example, during numeric simulations, but it can require extrapolation beyond the necking.

$$\sigma_{sann} = \sigma_{tekn} (1 + \varepsilon) \quad (\text{Eq. 2.1})$$

$$\varepsilon_{sann} = \ln(1 + \varepsilon) \quad (\text{Eq. 2.2})$$

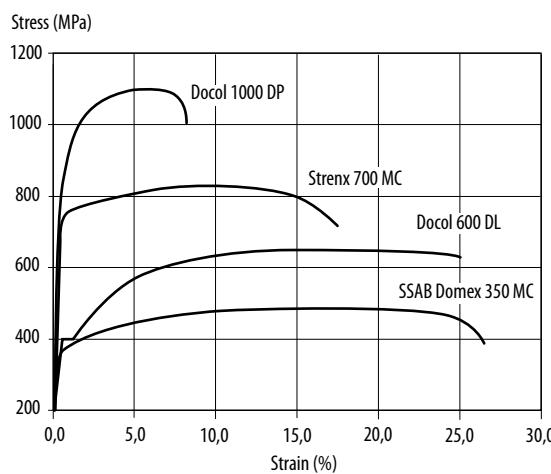


Figure 2.3: Example of stress-strain curves in different steels.

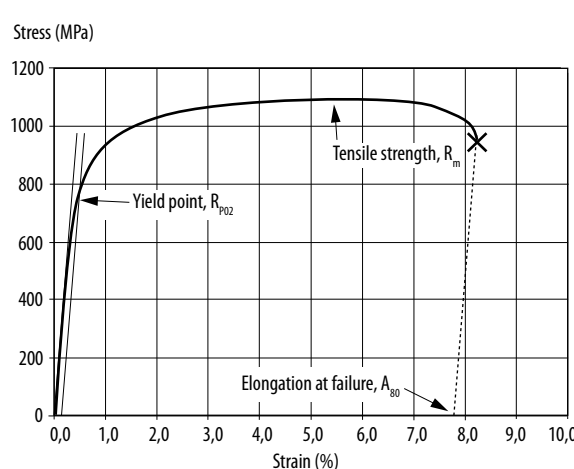
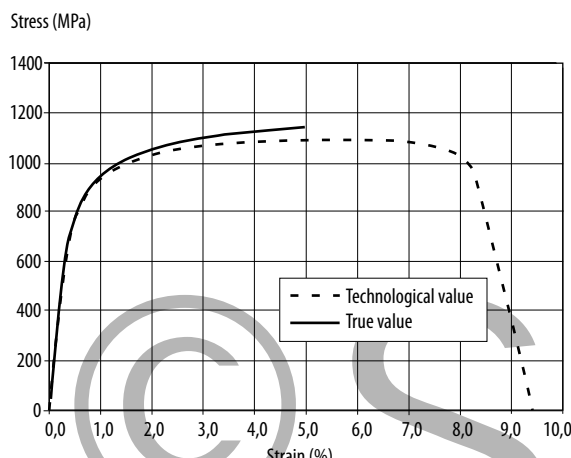


Figure 2.4: Example of yield point, ultimate strength and elongation at fracture for Docol 1000DP.



Figur 2.5: Example of engineering and true stress-strain response for Docol 1000DP.

Directional dependence of strength

The yield point and ultimate strength of the material can vary depending on the direction of the test specimen in relation to the rolling direction of the strip sheet. The properties of an isotropic material are the same regardless of the direction. DP steels are an example of isotropic steels. The properties of an anisotropic material on the other hand vary depending on the direction. Most SSAB steels are anisotropic and have higher yield point and ultimate strength perpendicular to the rolling direction. The yield point of hot-rolled HSLA steels perpendicular to the rolling direction can be, for example, 40–50 MPa higher than that along the rolling direction. The steels from the SSAB Domex MC- and Strenx-series are tested longitudinally to the rolling direction, which is the weakest direction.

Variation in strength

SSAB's steels undergo continuous casting, which ensures even chemical composition for all strips of the same charge. Rolling, annealing and metal coating are carried out on continuous computer-operated lines, which ensures uniform quality for all plates.

The steels will have a natural spreading of mechanical properties within the limits prescribed for chemical composition and process variables.

Ageing, bake hardening

Ageing is a physical metallurgy phenomenon. It means that skin passed steel hardens after a while and regains its yield range. The material loses some formability. The aging process is slow at room temperature but accelerates if temperature is increased. If the steel has been deformed, the effect is stronger.

For Rephosphorus (RP) and BH Steel, the aging effect can be utilized in a positive way by bake hardening. The yield point of a varnished pressing dried for 20 minutes at 170°C in an oven can increase with 30–80 MPa depending on the steel type.

Strength at high strain rate

All SSAB steels harden when the strain rate is increased. The degree of strain rate hardening is only remotely connected to

the strain condition. The hardening depends mainly on the rate of strain and temperature. High rate and low temperature make it more difficult to overcome the energy barriers that have to be passed for plastic strain of the material to be observed. Therefore, the stress required to achieve certain strain is higher at high rate than at low rate. This strain rate ratio shall not be confused with strain hardening.

Experiments and micromechanical analysis demonstrate that in principle the strain rate hardening can be described as a shifting of the stress-strain curve. Data about the tensile test curve shifting at high rates can be obtained by contacting SSAB, see www.ssab.com. An example of the effect of cold-rolled DP steel can be found in figure 2.5. The figure presents the true stress and the plastic strain. The stress is based on the actual cross section area of the test rod during the tensile test. Car collisions can involve tensile rates of 500 s⁻¹ and according to the figure, this corresponds to approx. 100 MPa.

Effect on strength due to short term heating

High strength is achieved through different hardening mechanisms such as precipitation hardening (HSLA steels) and transformation hardening (DP/DL steels and martensitic steels). There is, therefore, a risk of losing some of the durability during heating.

True stress (MPa)

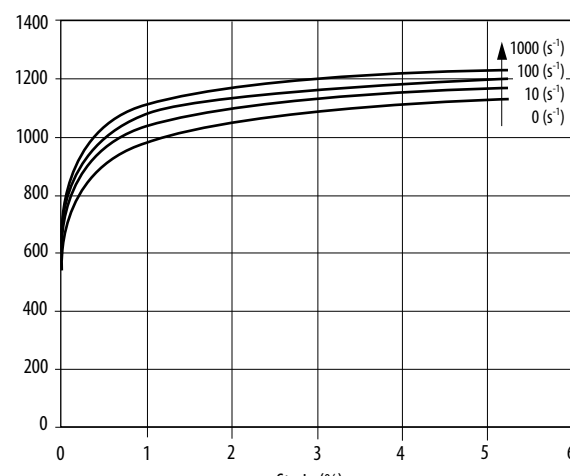


Figure 2.6: Strain rate dependencies for Docol 1000 DP.

Stålsort	20°C		100°C		200°C		300°C		400°C	
	R _{eff}	R _m	R _{p0,2}	R _m						
Domex 355 W	390	500	360	470	330	450	310	470	290	480
Domex 355MC	410	470	390	450	380	490	330	500	320	430
Domex 500MC	550	660	530	630	500	590	490	610	480	590
Domex 650MC	680	750	633	710	580	680	570	670	520	610
Domex 700MC	740	810	690	760	630	720	620	710	550	620

Figure 2.7: High temperature strength, MPa, standard values.

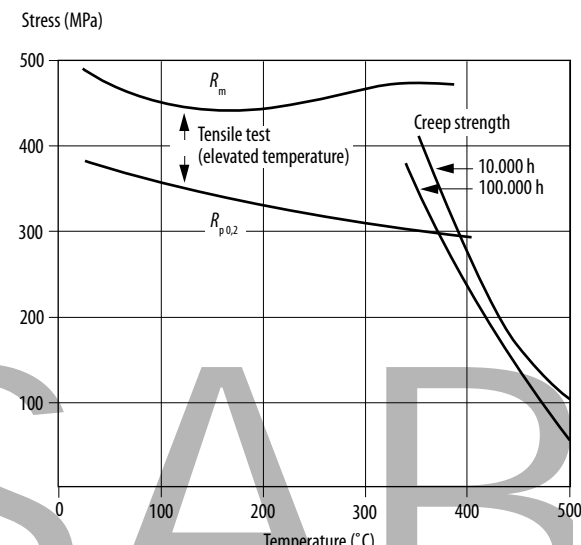


Figure 2.8: High temperature strength and creep strain strength for SSAB Weathering 350W.

DP/DL steels together with martensitic steels are the most sensitive types of steel. DP steels should not be heated to more than 300°C, while DL steels and martensitic steels should not be heated to more than 200°C. HSLA steels on the other hand can be heated to 650°C risk-free. It is also possible to use flame straightening if the temperature is limited to 650°C. Withstanding temperatures higher than that is possible only if small areas of the plate are heated. Local heating of DP/DL steels and martensitic steels results in reduced strength and thus better weldability which can be positively utilized.

Strength at elevated temperatures

Three properties determine the usability of steel at increased temperature:

- scaling temperature
- strength at elevated temperature
- creep strength

The scaling temperature, the temperature where the material loss exceeds 1 mm per year for both high strength and mild steels is approx. 520°C. The corrosion resistant SSAB Weathering 350 W steel has a scaling temperature of 560°C because it is alloyed with chromium and copper.

The high temperature strength is determined by means of tensile tests at different temperatures. The typical values for some high strength steels can be found in figure 2.7. The high strength steels lose less strength than conventional carbon-manganese steels at increased temperatures.

The creep strain strength is determined by measuring the load the material withstands at a constant temperature for a period of 10,000 or 100,000 hours.

The creep strain strength of SSAB Weathering 350 W can be found in figure 2.8. This figure presents the high temperature strength values as well. The figure shows that the high temperature strength is of relevance at temperatures below approx. 400°C, whereas the creep strength is relevant at temperatures of more than 400°C.

The highest recommended temperature of use for hot-galvanized plates is 230°C.

2.3.2 Toughness

High toughness is important for avoiding brittle fractures, i.e. instantaneous fracture without warning and limited plastic strain. The opposite of brittle fracture is ductile fracture at plastic strain and considerably lower distribution rate. A ductile break is characterized by the fact that separated surfaces do not match after the break.

To put it simple, the risk of brittle fracture is contingent upon the size of the load, the temperature of use and the thickness of the material. The risk of brittle fracture increases with the stress level in the construction, low temperatures and high degree of triaxial stress condition. The highest strength levels together with thicknesses of approx. 10 mm and upwards are checked with regard to the lowest service temperature.

A toughness gauge is obtained through impact toughness tests, Charpy-V test according to EN 10.045. In general, when it comes to steels, a test rod must be able to withstand 27J at test temperature in order not to be considered a brittle fracture. The impact toughness guarantee given for a steel is usually in force down to a certain temperature (the test temperature). This temperature can be found in the designation of the steel:

- B – no toughness guarantee
- C – impact toughness guarantee at 0°C
- D – impact toughness guarantee at -20°C
- E – impact toughness guarantee at -40°C
- F – impact toughness guarantee at -60°C

It is important to note that test temperature is not the same as the lowest service temperature of the steel, which is normally much lower than the test temperature. More detailed information about designs to avoid brittle fractures can be found in section 4.7.



2.3.3 Wear resistance

Wear is a very complex area. Abrasive wear is the most common mechanism for plate structures. Abrasion means that particles penetrate the plate surface which lead to plastic strain or removal of steel particles. The wear is contingent primarily upon the relation between the hardness of the abrasive material and hardness of the plate. Hardox wear plate is available with hardness from 350 Brinell to up to 700 Brinell.

A more detailed description of wear can be found in [2.1].

2.3.4 Physical properties

The physical properties of both mild and high strength steels are as follows:

Density: $\rho = 7.85 \times 10^3 \text{ kg/m}^3$

Coefficient of thermal expansion: $\alpha = 11 \times 10^{-6}$ (0°C)
 $\alpha = 14 \times 10^{-6}$ (200°C)
 $\alpha = 16 \times 10^{-6}$ (400°C)

Modulus of elasticity: $E = 210 \text{ GPa}$ (20°C)
 $E = 200 \text{ GPa}$ (200°C)
 $E = 180 \text{ GPa}$ (400°C)

Shear modulus: $G = 8.1 \times 10^4 \text{ MPa}$

Poisson's ratio: $\nu = 0.3$

To consider

- Mechanical properties for DP/DL and martensitic steels are isotropic.
- Other steels are unisotropic. Highest value of mechanical properties are transverse rolling direction. Different standards prescribe testing in different direction.
- SSAB Domex MC and Strenx are tested along rolling direction. I.e. weakest direction.
- HSLA can be heated up to 650° C without any loss in mechanical properties.
- DP steel should not be heated over 300° C and DL and martensitic steels not over 200° C.

2.4 References

[2.1] *Wear, a guide*, SSAB Oxelösund



SSAB

3. Design principles

The intention with this chapter is to provide suggestions and ideas for good design solutions in high strength steel.

The chapter describes basic concepts and common interesting areas from a structural design point of view. Both general but also referring to important phenomena for high strength steel structures.

3.1 Basic concepts

Using high strength steel generally puts higher demands on structural design to enable best possible use of the material. Extra care is required in material selection, structural design, and manufacture. Particular attention should be taken for slender plates in compression- and fatigue-loaded structural members. Plates in compression may need to be stiffened in order to allow the high stress permitted by the high strength steel. Fatigue loads may need special care in connection with the design and placement of joints, load introductions and notches for example.

There are several different ways to influence the function of a structure and the first step is to identify the requirements in order to subsequently find the right solutions.

3.1.1 Resistance and loading

Structures are exposed to different types of loading during their service life and it is important to find these in the design work and to associate them with a specific resistance.

Structural parts in high strength steel need to be studied, in particular, with regard to phenomena such as buckling and fatigue, this may affect the design with the purpose of achieving best results. Buckling is important with regard to high static loads and fatigue for dynamic loads, see figure 3.1.

For the load levels that arise in connection with ordinary use of a product, the resistance is often associated with deformations, elasticity or service life. Deformations are not expected to be permanent and cracks are not expected to form.

The maximum static load a structure can carry before collapsing is most often not subject to any requirements or restrictions to the extent or type of deformation; only the final resistance is important. The load level is determined, during design, usually by external loads often associated with safety. In many cases, the ability of the steel to plasticize can be used, which means that some of the deformation will be permanent.

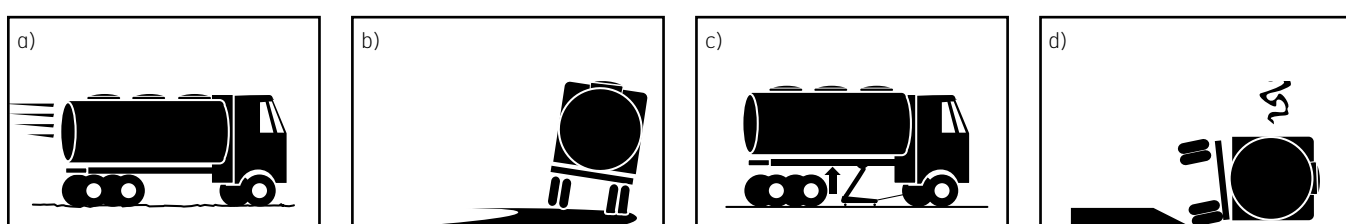


Figure 3.1: A structure is exposed to different loading during its service life; a) fatigue load – lower stress levels which are repeated many times; b) elastic behavior – restriction to the scope of the deformations; c) elastic behavior – no requirements to the scope of the deformation; d) maximum resistance – high stress levels in connection with an extreme load situation.

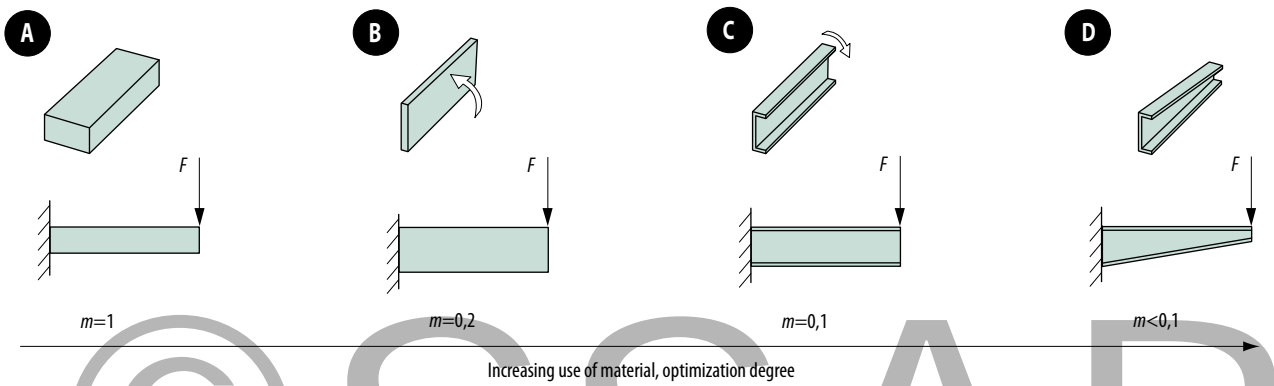


Figure 3.2: Example of weight reduction through gradual optimization of the beam section. m =relative weight.
The width of the sheet is the same in A, B, C and D.

3.1.2 Local buckling

Compressed slender parts in a cross-section can have limited load capacity due to local buckling. This local instability is important to pay attention to when using thinner material and higher working stresses but does not prevent the use of high strength steel. The full potential of the material can be utilized due to the fact that the effects are local and also that stiffeners, welded or formed, can be used to prevent local buckling.

The course of buckling is that at a certain stress level in the plate buckles start to form redistributing the stresses, see *figure 4.3*. The member can, however, continue to handle even higher loads utilizing the yield point in the rest of the cross-section. In other words, the actual carrying capacity/ resistance, is higher than what is allowed by the buckling stress permits.

It is sometimes stated that the gain in using high strength steel is limited as the local buckling stress is independent of the material yield point. This is wrong.

Local buckling is one of several instability phenomena which may need to be taken into account in connection with the design of structural members in high strength steel. Instability is further described in chapter 4.

3.1.3 Fatigue

Fatigue is the process of initiation and propagation of cracks in structures subjected to variating loads/ load cycles. The crack propagation happens without any visible plastic deformation and may therefore be difficult to discover. When the crack reaches a critical length, the final fracture may be instantaneous. The fatigue strength is generally significantly lower than the material yield point. Furthermore, welds have lower fatigue strength than parent material, which makes it important to place welds in areas with a lower stress levels. Cold formed sections and components provide opportunities for structural design with respect to fatigue. The advantages provided by laser cutting in combination with modern cold forming steels; with good-quality cutting edges giving and high fatigue strength in critical positions is one key factor to consider in the design work to be successful.

Fatigue is described exhaustively in chapter 5.

3.2 Structural design

This section discusses examples of detail- cross-section design for efficient material use. These are, in part, general tips but also practical solutions.

3.2.1 Material utilization

The material should always be placed where it is most useful. This fundamental idea can be illustrated with a beam subjected to a bending according to *figure 3.2*. The cantilever beam is loaded with an identical load in the free end and Beams A through D illustrate the relative weight (thickness) reduction of the member. *Figure 3.3* shows the equivalent for twisted bars. The material in the centre of the homogenous bar has low stress levels and contributes relatively little to the load capacity, which makes a thin-walled pipe a significantly more weight-optimized solution.

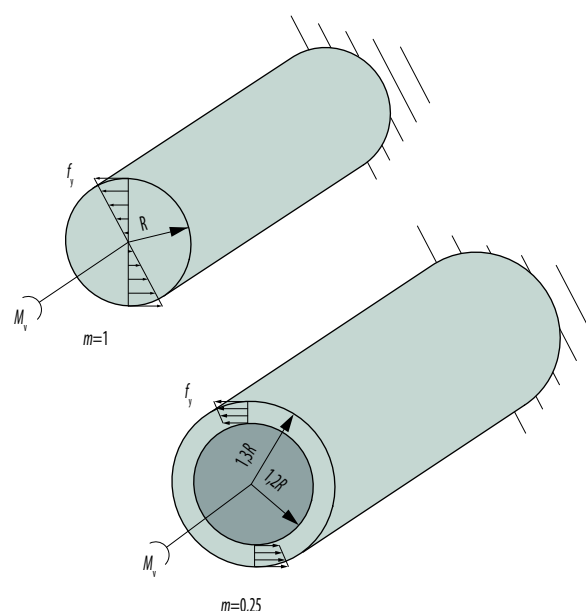


Figure 3.3: Material utilization illustrated with twisting of a homogenous bar contra a thin-walled pipe. m =relative weight.

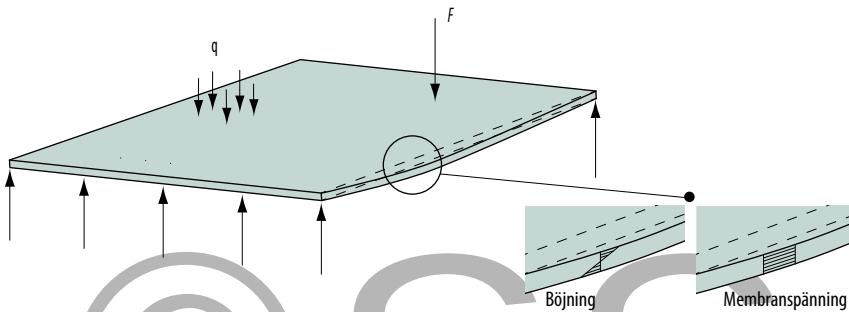


Figure 3.4: The sheet/plate subjected to out of plane bending.

3.2.2 Load introductions

It is important to design load introductions correctly when upgrading from mild to high strength steel and thinner plates.

In- and out of plane bending for a structural members
A structure responds to external loads by building up stress. In thin steel sheets/ plates, direction is absolutely decisive for the function. In the case of the loads applied perpendicular to the surface, the response will be out of plane bending or, in some cases, membrane stress, *figure 3.4*. With small deflections (of the order t), bending dominates and relatively small forces result in high compressive and tensile stress. The stress level from bending depends on the plate thickness and applied force according to *equation 3.1*.

If the loads are applied in the plane of the plate, the response will be according to *figure 3.5*. This leads to better material utilization and a stiffer structure. The relationship between load and stress becomes considerably more favorable, *equation 3.2*. This is particularly important to consider in detailing.

$$\sigma \sim \frac{F, q}{t^2} \quad (\text{Eqn. 3.1})$$

$$\sigma \sim \frac{F, q}{t} \quad (\text{Eqn. 3.2})$$

When a structural part is subjected to out of plane loading, there is a possibility to reduce sheet/plate thickness by 30 % by upgrading to a high strength steel with a yield point twice the original material. If the sheet/plate is subjected to in-plane bending the thickness reduction theoretically reach 50 % after the same upgrade.

Figure 3.6 displays practical examples of in- and out of plane bending.

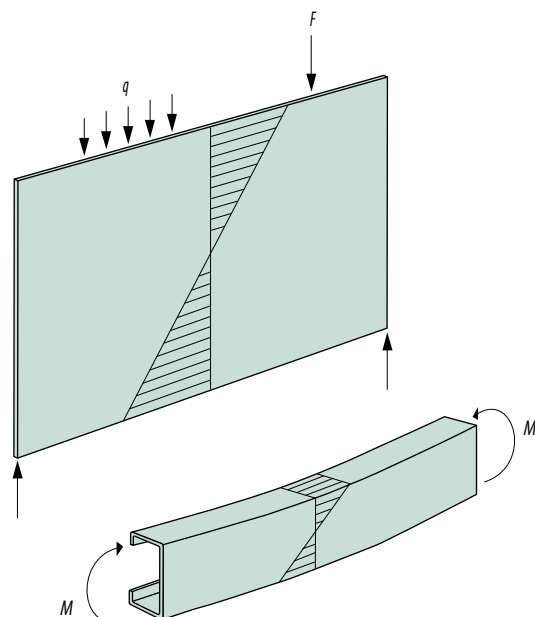


Figure 3.5: The sheet/plate subjected to in-plane bending.

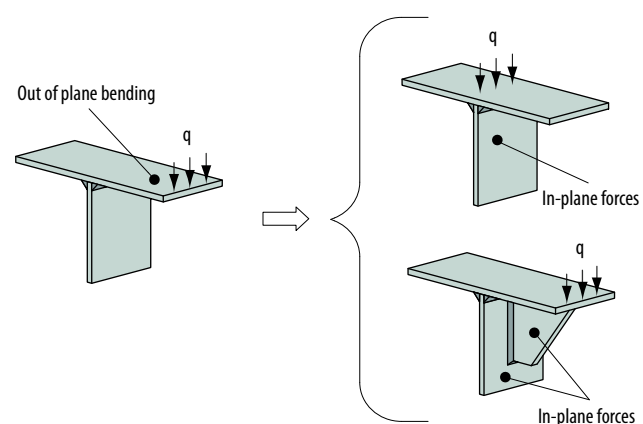
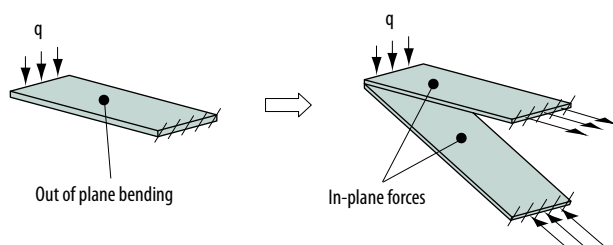
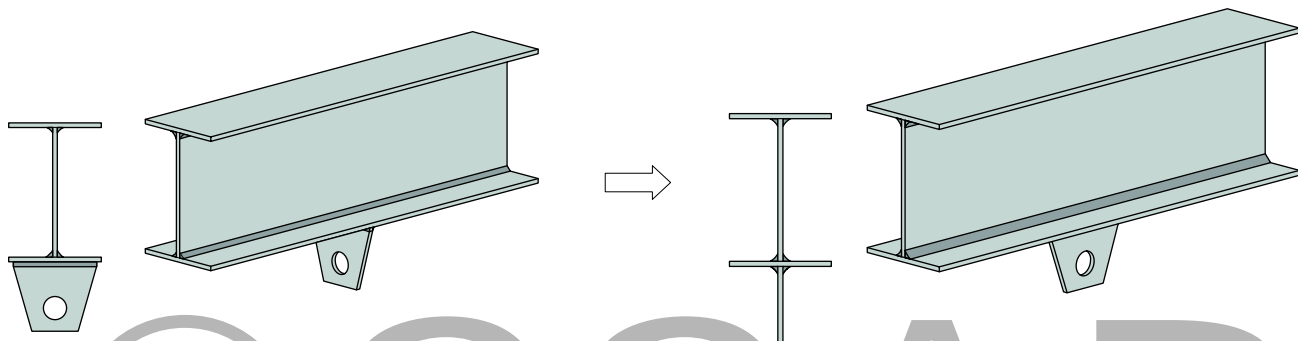


Figure 3.6: Example of designs where the sheet/plate is subjected to in- and out of plane forces.



a. The eye hook welded crosswise results in high local stress.

Figure 3.7: Beam with eye hook welded on the bottom flange.

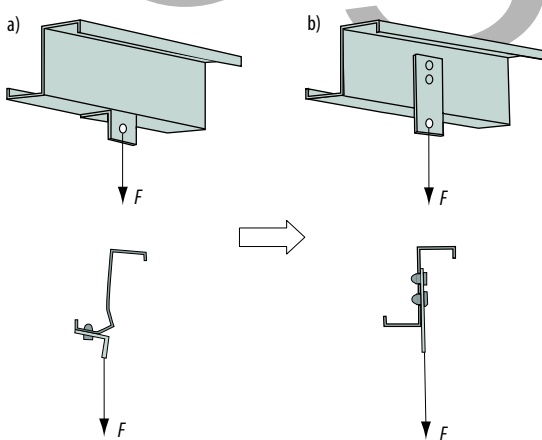


Figure 3.8: Load introduction into a Z-section.

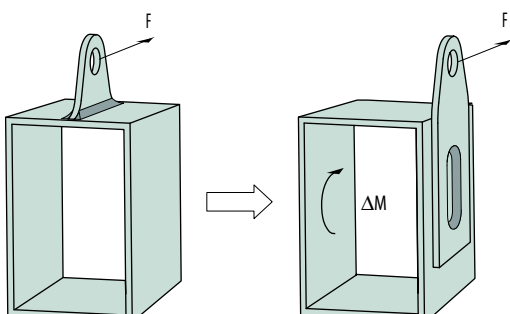


Figure 3.9: Examples of load transfers with diminishing local bending.

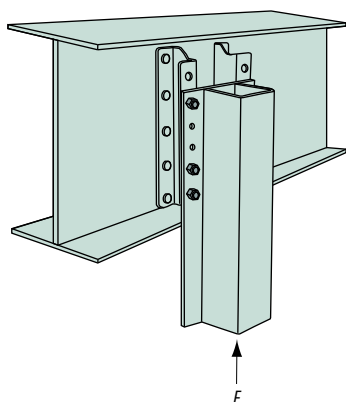


Figure 3.10: The load force goes directly to the beam web.

b: The load goes directly to the web of the beam.

Load introduction

Figure 3.7b shows how an eye hook should be placed under an I-beam. The load is introduced into the web resulting in in-plane bending for both the flange and the web.

If the eye hook is placed crosswise according to *figure 3.7a*, the flange of the beam will be subjected to out of plane bending, which means local high stress levels and thereby reduced load capacity.

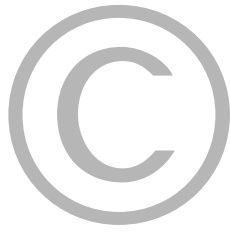
Figure 3.8 is another example of load introduction. An angle bracket attached to the flange results in high local stress whereas attachment directly into the web provides a significantly better response.

Figure 3.9 shows the load introduction in a box section improved by attaching the eye hook to the web avoiding out of plane bending of the flange. The same applies to the support in *figure 3.10*.

Asymmetrical beams

Asymmetrical beams such as C sections will twist because the load is not naturally applied at the shear centre of the cross-section, see *figure 3.11*. The load in illustration a) is applied through the web resulting in a rotation.

The joint in illustration b) prevents the rotation, i.e., stiffens the cross-section. The web, however, will be subjected to local bending. A solution with a web stiffener in illustration c) provides support under the shear center, and a load introduction without twisting and local bending.



SSAB

3.2.3 Stiffness

An upgrading from mild to high strength steel means that the material thickness can be reduced. Keeping the outer geometry of the upgraded structural member means that the deformation will increase for a given load. This is due to the fact that the stiffness depends only on geometry and the modulus of elasticity, E. If the load case is bending or twisting and if the same stiffness is required as for the original structure, cross-section geometry has to be redesigned, see for example *figure 3.12*. Increased cross-section height and reduced plate thickness can result in both reduced weight and higher stiffness.

Open thin walled cross-sections

Thin-walled cross-sections can, for different reasons, change their shape under a load, for example, according to *figure 3.13*. This may lead to an overestimation of both load capacity and stiffness, see also section 4.3.10.

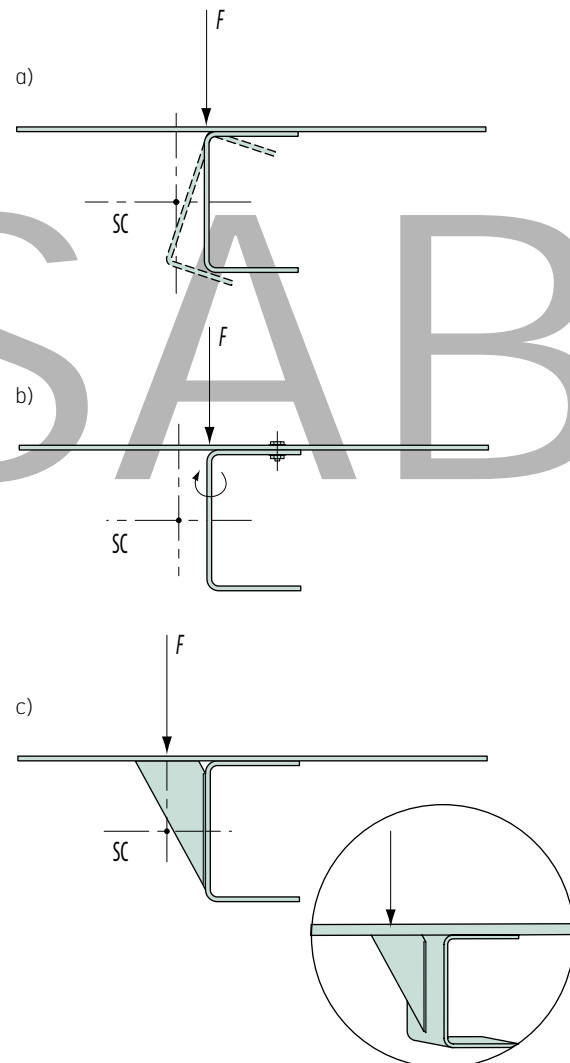
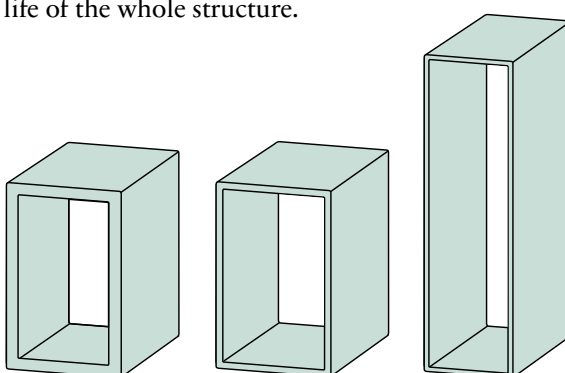


Figure 3.11: Load introduction in C-section.

3.2.4 Design with respect to fatigue

The fatigue strength of a joint is normally considerably lower than the fatigue strength of the material itself. This means that the design, placement and execution of welded joints is very important and often determines the fatigue life of the whole structure.



10 x 60 x 100

6 x 60 x 100

5 x 40 x 140

Weight: 1

Weight: 0,61

Weight: 0,61

Stiffness: 1

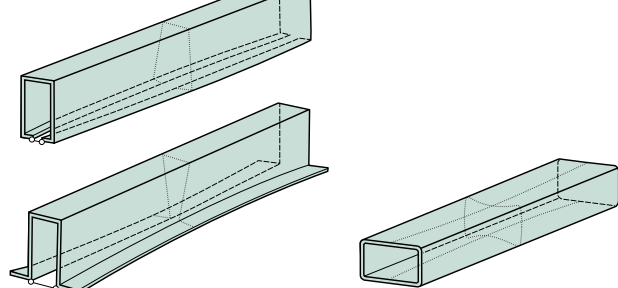
Stiffness: 0,67

Stiffness: 1,11

Deformation: 1

Deformation: 1,49

Deformation: 0,90



a) Cross-section change from shear flow.

b) Dishing of slender cross-section bending.

Figure 3.12: Lighter becomes stiffer.

Figure 3.13: Open thin cross-sections can change the shape of the cross-section under loading.

Avoid welded joints in areas subjected to high fatigue stress. If this is not possible, the joints should be designed for minimum stress concentration. Opt, for example, for butt welds rather than fillet welds.

Plug welds are good in fatigue-loaded joints as they can easily be placed in areas with lower stress, *figure 3.9*. A plug weld is also continuous.

The geometry of the loaded component itself should be designed to make the stress flow as smooth as possible. Cross-section changes and attachments can be introduced with a gradual stiffness change which results in lower stress concentrations, *figure 3.14* and *3.15*.

High local stress can be reduced by improving the micro geometry of the weld by using a post-treatment method such as grinding and TIG dressing of the transitional zone between the weld and the parent material.

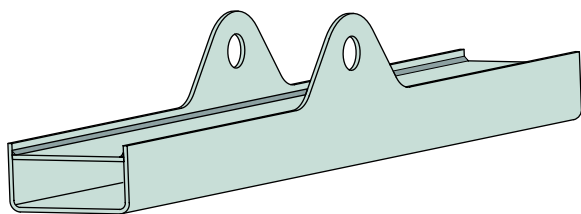


Figure 3.14: Eye hook fastened to the web for better static and fatigue strength.

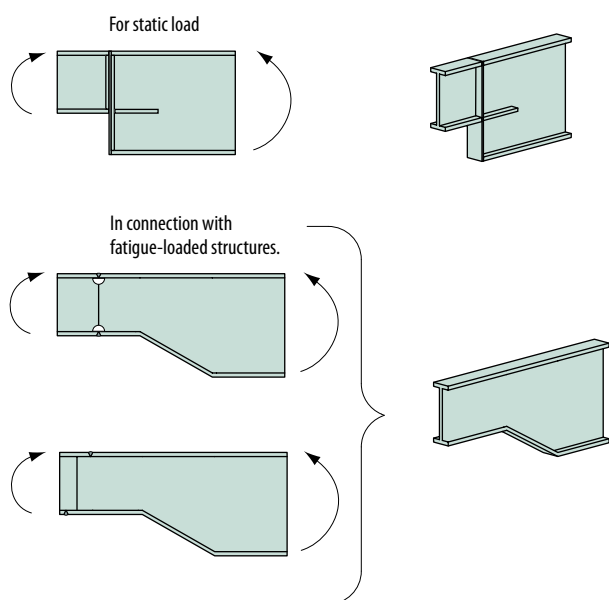


Figure 3.15: Joints intended only for static loads are displayed at the top, whereas the rest shows joints for fatigue loads.

3.2.5 Natural frequency

If the frequency of the load gets close to the natural frequencies of the structure this often causes problems with fatigue damage, noise and discomfort. The vibration properties of a structure change in connection with a transition to high strength steel. A thickness reduction with preserved cross-section geometry of a beam normally increases the natural frequency some, see also 4.3.10.

If the only occurring load has a constant frequency, it is relatively simple to adapt the structure. However, it is harder to avoid natural vibrations, e.g., for vehicles which are affected by varying loads and frequencies. Damping reduces vibration amplitudes but does not appreciably change the natural vibrations.

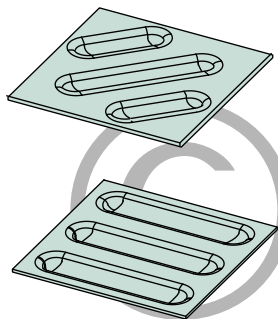
3.2.6 Stiffeners

Appropriately designed stiffeners increase the load capacity of slender plates with regard to buckling but are also used in connection with plates subjected to bending stress and load transfers. The need for stiffeners increases in connection with the design of optimized components in high strength steel. By keeping this in mind from the very beginning, you can often make the stiffeners an integrated part of the component or structure. Stiffeners can be manufactured by means of roll-forming, bending or pressing operations but can also be welded, *figure 3.16*.

To consider

- Avoid out of plane bending and introduce forces in the plane of the plate for efficient use of high strength steel in a structural member.
- A reduction of plate thickness affects the stiffness of a structural member.
- Appropriately designed stiffeners increase the load capacity of slender cross-sections with regard to local buckling.
- Avoid notches (welds, holes, etc.) in areas subjected to high fatigue stress. Use mechanical joints instead of welded joints, for example, screws and rivets.
- Edges and edge quality are important when it comes to fatigue life of a component. Laser and plasma cutting are preferable to cut and slit edges.
- If the structure is exposed to a corrosive environment, the fatigue strength is reduced drastically. In the worst cases, the reduction can be as much as 40 %.

A. Avstyrningar vid krafter vinkelrätt mot plåtens plan



B. Avstyrningar vid tryckkraft i plåtens plan.

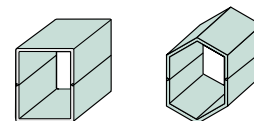
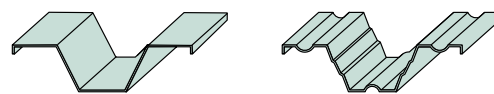
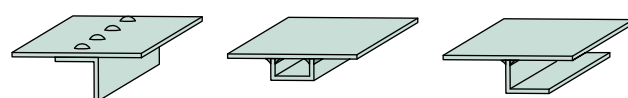


Figure 3.16: Examples of stiffeners. A: For stiffening with respect to out of plane bending. B: For compressive forces in the plane of the plate.

Plates with stiffeners can be divided into two main cases load-wise:

- Forces resulting in out of plane bending The stiffeners are designed for bending.
- Compressive forces in the plane of the plate The stiffeners increase the buckling stress of the plate.

Out of plane bending

Stiffeners are often closely spaced in order to achieve stiffness of a plate structure subjected out of plane loading. This does not apply if the aim is membrane stress in the plate.

One out of plane load case is impact, and depending on the type of application, there are two different approaches to consider. The first one is when no permanent deformation is permitted. The steel sheet in a car door, for example, should be able to handle flying stones without permanent dents. The yield point and thickness sheet are in this case very important.

The second case is when permanent deformations of a certain extent are permitted. An example of this is the basket for dumpers and trucks. In addition to the plate-thickness and the strength, cross-section geometry and distance between stiffeners are also of importance.

In most cases with high dent loading, it is preferable not to use any stiffeners whatsoever, for example, in dumper bodies where elastic deformation is used instead for energy absorption.

In-plane compression forces

Stiffeners are used in this case to increase the buckling stress. How the sheet/plate is stiffened depends on the load case. The effect of constraining slender plate fields with stiffeners increases the buckling stress. A weight-optimized cold formed structural member with stiffeners is often manufactured through roll-forming or bending. For welded structural members stiffeners are also welded.

Edge folds have a big influence on the load capacity with respect to buckling but may have more functions. For example, avoiding sharp trim edges and strengthens 'corrosion protection'.

3.3. Joints

An optimized structure requires correctly designed and produced joints as this is often the most critical part of a structure. This applies, in particular, if the structure is fatigue-loaded. First identify the loads on the structure and then try to place the joints in areas with low stress. Design the joints with as undisturbed stress flow as possible. Welding is also discussed more in chapter 6.5.

3.3.1 Welded joints

Welded joints are a common and often economical choice in a structure. An upgrade to a more high strength steel often reduces the plate thickness, which results in smaller throat thickness and lower costs in connection with welding.

High strength steels allow problem-free welding. Only minor adjustments of the welding parameters could be necessary, primarily during resistance welding.

A low heat input is better during fusion welding of high strength steels. This in order to preserve the mechanical properties of the material. A single run is often possible for structures in thin sheet material. More runs are required for thicker plates in order not to exceed the recommended heat input value.

Choice of filler metal

Welding in high strength steel, you can choose a filler metal which is under matching, matching or overmatching.

Undermatching

An under matching filler metal is chosen when the welded joint is in an area where the stress is not so high and/or when the load is not applied in the transverse-direction of the weld. An under matching filler metal can be chosen even for a fatigue-loaded joint and, under certain conditions, it will provide a more favorable geometry of the welded joint. The different weld defects and the geometry of the joint have a greater effect on the fatigue strength than the strength of the welded joint.

Matching or overmatching

A matching or over matching filler metal is required for welded joints which are in the most stressed areas, exposed to loads transverse the weld and where the joint is required to handle the properties of the parent metal. Meeting these requirements also requires the use of adapted welding energy inputs.

Practical design of welded joints

Examples of the different design of welded joints are displayed in figures 3.17 through 3.22. A design in accordance with the right sub-figures should be used for joints under a high level of stress and, in particular, for fatigue-loaded joints.

Spot welded joints

Spot welded joints are often used for sheet thickness of under 2 to 3 mm. These joints differ from the examples above as the sheets always overlap each other.

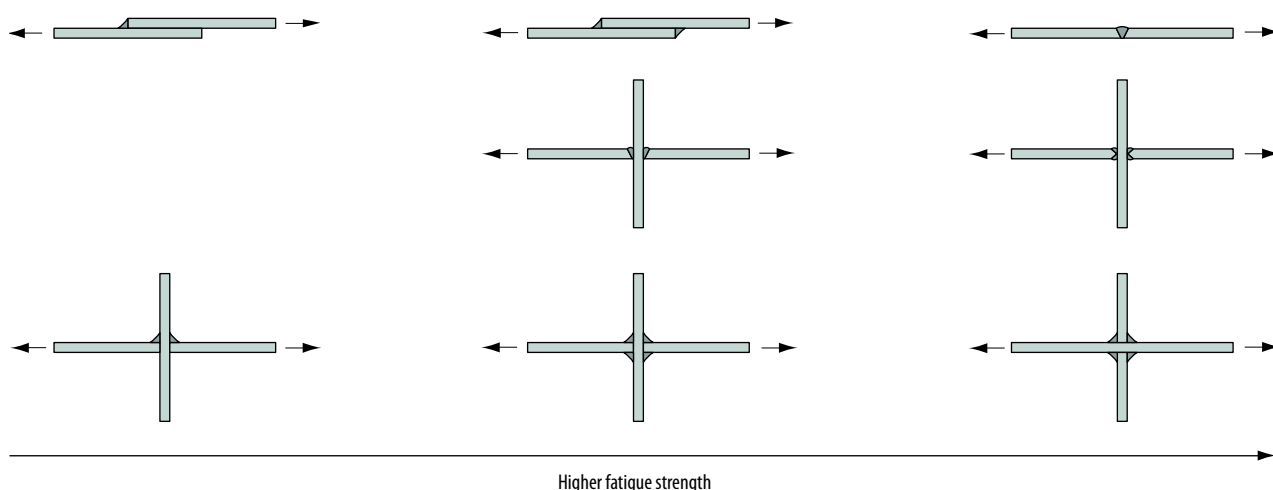


Figure 3.17: Butt welds are better than fillet welds in connection with fatigue load. If a butt weld is the necessary option, it is better to have a double-sided than a single-sided weld.

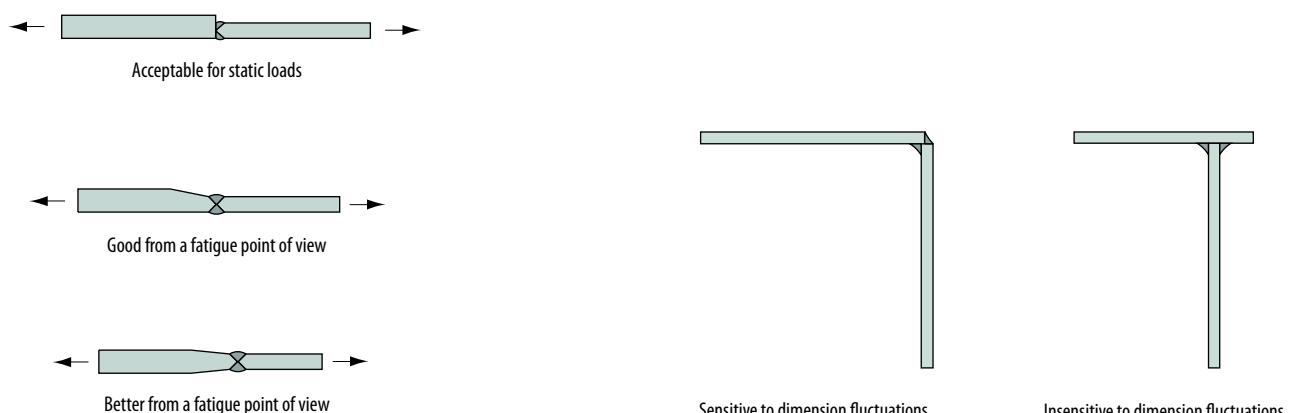
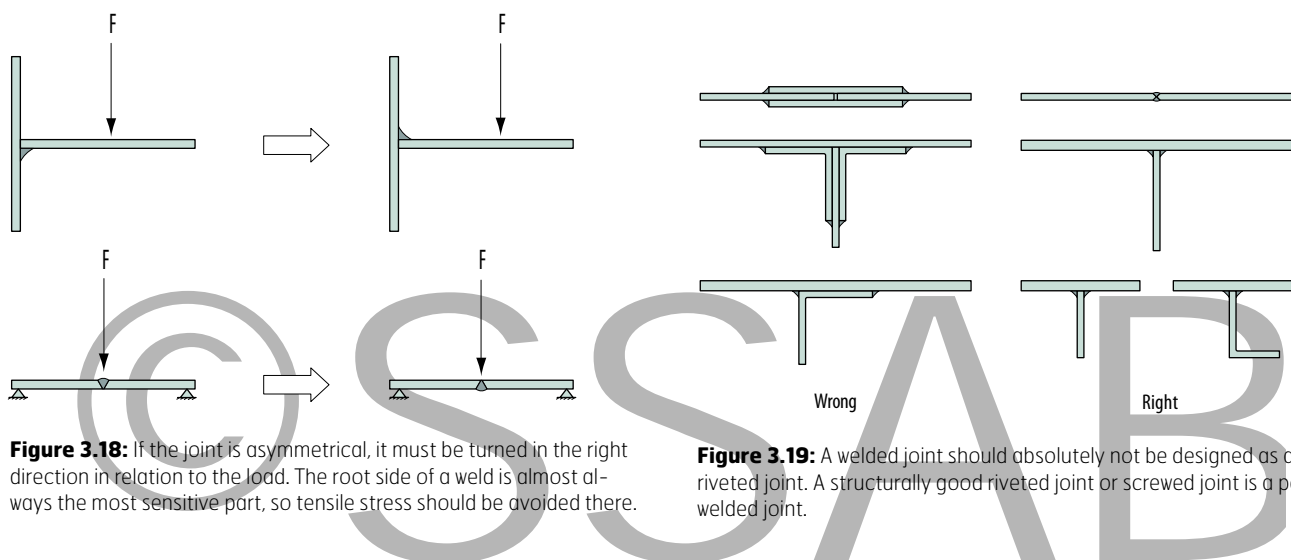
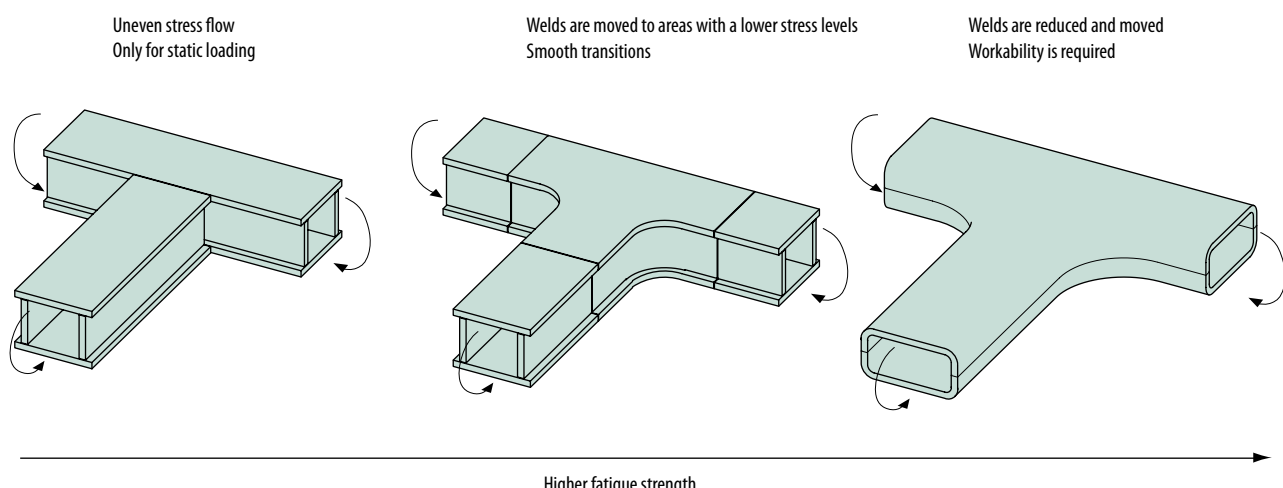


Figure 3.21: Design the welded joint so that its throat thickness not dependent on the dimensions of the constituent sheet/ plates. The tolerance requirements should not be raised unnecessarily.



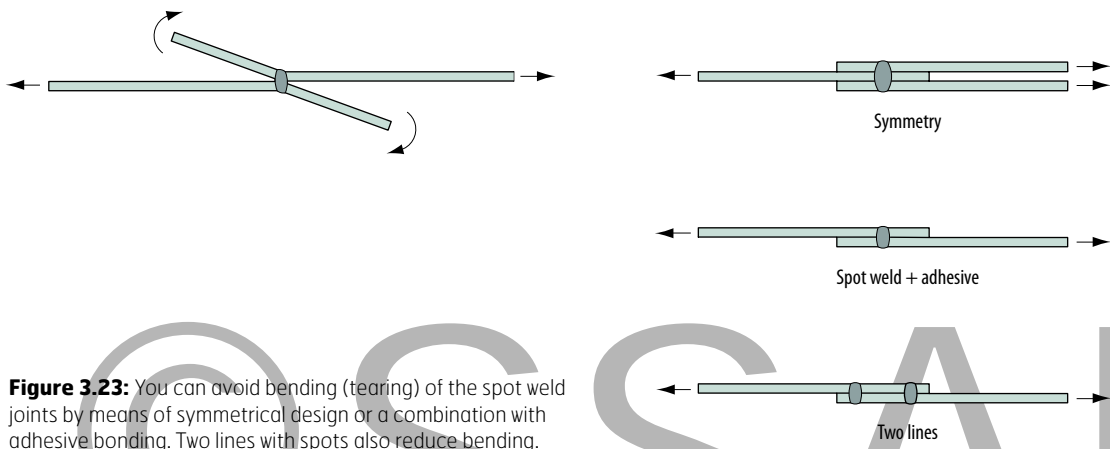


Figure 3.23: You can avoid bending (tearing) of the spot weld joints by means of symmetrical design or a combination with adhesive bonding. Two lines with spots also reduce bending.

Spot welded joints are sensitive to fatigue load. The fatigue strength can, however, be increased by reducing the distance between the weld spots and/or by increasing the electrode diameter. A clear improvement in the fatigue strength is achieved if the spot welding is combined with adhesive bonding, see *figure 3.23*.

More information about welded joints is available in chapter 6.

3.3.2 Bolted connections

The bolted connection has kept its relevance. Especially when using high strength steel with high stress levels from fatigue loads. Bolted connections can be designed with respect to fatigue. For example, bolted connections are generally used for attachments to truck frames. Preserved pre-stress is an absolute requirement in fatigue-loaded joints!

There are many versions of bolted connections, different types (shear or friction joints), with bolts of different designs and strength classes, as well as threads (cut, rolled or thread-forming).

Use as long bolts as possible in bolted connections and the clamp length at least three times the thread diameter. A given tightening torque will then deform the bolt more and the connection becomes less sensitive to settling and relaxation.

Paint coats pose a big risk of settling and relaxation. If the painting must be done prior to assembly, critical surfaces can be masked and any supplementary painting can be done with tightened bolts.

When the contact surface under the screw face or nut is too soft or has bad surface roughness, the use of tempered washers is required. Consider using washers when the strength in the connected parts is lower than that of the bolt or when the surface roughness is bad than what is achieved in connection with conventional machining ($R_a = 3$).

Only approximately 100 % of the tightening torque results in a pre-stressing force. The rest goes to overcoming friction in the threads and under the screw nut. Pre-stressing therefore becomes dependent on variations in the friction coefficients in threads and bases and on the design of the tightening.

Friction joints

Friction joints are preferable to shear joints as they are simpler to manufacture and assemble. Friction joints are designed structurally with pre-stressed screws in order to obtain sufficient friction force to resist the external load.

Shear joints

The external load in a shear joint is absorbed through shearing of the bolt stem. A good fit between the screw stem and hole is important and joint drilling of the holes in a screw group can therefore be required. Fatigue loads with a risk of sliding require close-tolerances. Keep in mind that it can be enough in a bolt group if several critical bolts are designed as shear connections in order to avoid sliding of the joint.

Axially loaded joints

By pre-stressing the connection, there is no backlash in connection with a change in the load direction and the force variation in the bolt becomes much smaller than the external force variation. This is particularly important for the service life of the fatigue-loaded connections.

3.3.3 Riveting

Clinching and punch riveting provide a low cost per joint spot and high productivity. This applies to an even higher extent if several joint spots are done at the same speed.

Since both clinching and punch riveting are cold joining methods, they do not result in any heat-affected zone in the material and most often do not ruin the properties of a possible surface layer. The fact that the methods are cold also means that flue gases and splash are avoided, even during jointing of coated plates. Self-piercing rivets and clinched joints have a high and even quality. One of the biggest advantages of clinching and punch riveting is the opportunity to join different types of materials. A disadvantage, however, could be the fact that the joint spot must be accessible from both sides and that the static strength is not as good as for other jointing methods.

Sheet thickness of 0.4 to 3 mm with an overall thickness of up to 6 mm can be used.

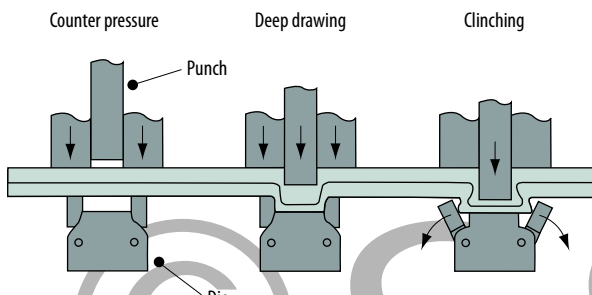


Figure 3.24: Examples of clinching.

Clinching

Clinching is a jointing method for thin sheets where structural continuity is ensured through mechanical locking. The locking is created by plastic forming of the materials in the joint spot; no joint element is added to the joint. The ready clinched joint has a dent on the one side of the sheet and a button-like bulge on the other; the riveting process is displayed in figure 3.24.

Punch riveting

A mechanical jointing method for thin plates that resembles clinching in certain respects. The main similarity is that you do not have to make a hole prior to the jointing. The difference is that punch riveting uses a loose joint element. In the first step of the punch riveting jointing process, the rivet cuts through the sheet. In the second part of the process, the rivet and/or the sheet are shaped in such a way as to form a mechanical lock.

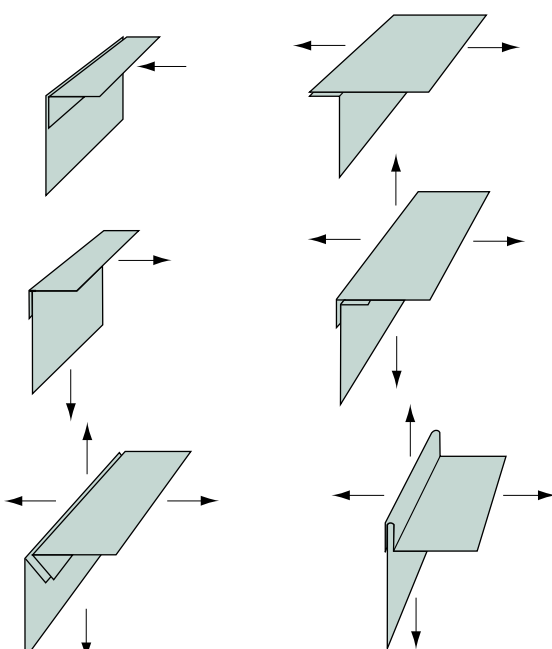


Figure 3.25: Examples of adhesive joints.

Blind rivets

Blind rivets, also known as pop rivets, are extensively used for jointing in both the sheet metal- and construction industries.

This type of rivet was originally developed for creating quick joints where one of the sides was inaccessible because of a block or counterforce. The simple and quick handling has led to a wide area of application – also when both sides are accessible.

3.3.4 Integral joints

The sheet in integral joints is bent and shaped so as to allow jointing without the addition of other materials. Integral joints can be made water- and steam-proof. The jointing can be done with a fillet or, if you do not wish to add an additional joint part, with folds.

3.3.5 Adhesive joints

An adhesive joint is designed in order to be able to absorb shear forces as the strength perpendicular to the adhesive surface is poor. Figure 3.25 shows examples of joint designs.

To consider

- Joints are often critical elements in a structure.
- High strength materials can be welded with under- or over matching filler metals.
- Friction joints are preferable when there is a fatigue load.
- Combination joints with adhesive bonding and mechanical joints provide good fatigue strength.



3.3.6 Combination joints

Combination joints are joints produced with a combination of two or more different types of jointing. Combination joints often include adhesive bonding in combination with mechanical jointing or spot welding.

Several advantages of combination joints:

- Adhesive bonding protects against corrosion and provides damping.
- The fatigue strength of adhesive spot welding is better than that of spot welding only.
- Adhesive bonding provides higher strength and stiffness compared to spot welding only.
- Adhesive bonding is often combined with a spot weld in order to fix the joint during the hardening process.

3.4. Forming

Forming can be divided into cutting and plastic forming. This is discussed in more detail in chapter 6.

Shearing and punching

The required cutting forces in connection with shearing of high strength materials do not need to be higher than for mildsteel. However, one should be aware that a so-called cutting angle is required and that the cutting clearance may need to be adjusted to achieve the best results. The material selection in the cutting steel should also be taken into consideration. It is possible to get a guideline for this from SSAB.

Plastic forming

When a high strength steel and a more conventional mild steel are compared, it is clear that the elongation values are lower for the high strength material. It is unfortunately common to draw the hasty conclusion that workability is reduced to the same extent as the elongation value in question. This is not correct. It is a fact that the workability of the high strength materials is significantly better than that. What limits their workability is, above all, their ductility. On the other hand, the material has excellent properties in connection with deep drawing, see figure 3.26. Everyone who has previously worked with forming knows that both

Figure 3.26: The deep drawing properties of the high strength materials are good despite the lower elongation values at break these materials have in comparison with milder materials.

stretching and drawing appear at the same time and to a different extent in the same forming process. It is possible to control this in different ways depending on the design of the geometry and process. By using the current forming simulation tools, it has become much simpler to do these optimizations, in particular, when it comes to high strength steel.

Stretched edges usually appear in, e.g., flanges or in connection with the performance of a flanging operation, see figure 3.27. The surface condition of the stretched edge is absolutely decisive for how high the flange can be formed, in particular, for high strength materials. In addition to the surface condition, the burr occurring in connection with both shearing and punching should also be taken into consideration. This blanking bar exercises a negative effect on the flanging capacity of the material. This is why it should be ensured that the blanking burr preferably ends up on the side where the stress is lowest. Flanging should be carried out, for example, in such a way that the burr ends up along the inner side of the flange. On the other hand, if there is a possibility to produce milled edges or laser-cut substances, this provides better conditions for forming stretched edges.

Spring-back in connection with forming is related to the material yield point. The effect therefore becomes larger during forming of high strength materials. In order to meet the set geometric tolerance requirements of the formed components, the spring-back must therefore be compensated. In connection to this, forming simulations are used more and more often for calculation of this compensation in parallel with practical experiences and methods for minimizing spring-back, figure 3.28.

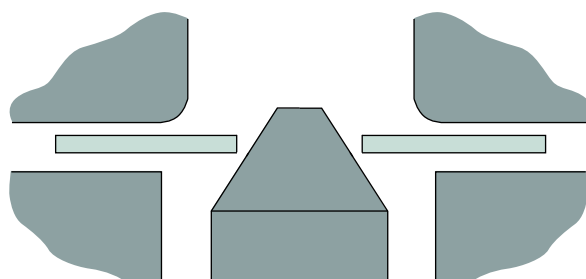
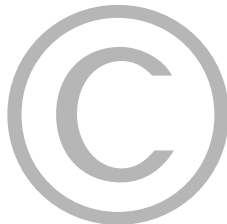


Figure 3.27: The surface condition of the edge is of great importance for achieving best results in connection with flanging of high strength materials.



3.5 Corrosion and corrosion protection

3.5.1 Corrosion types

There are different types of corrosion depending on, e.g., how the material corrodes and what causes the corrosion.

General corrosion

General corrosion proceeds by the same rate across all of the exposed surfaces. The average loss of material due to corrosion, i.e., the weight loss per surface unit during general corrosion is a good measure of the corrosion rate. General corrosion is common in on unalloyed and low-alloy steel, for example, during atmospheric corrosion.

Local corrosion

Local corrosion, also called pitting or pitting corrosion, means that the attack on the metal is localized in certain areas on the surface, whereas the remaining surface is more or less unaffected. In many cases, it takes a long time before the pit appears (initiation) but once the attack has started, it can grow very quickly (propagation). The attacks are most often very serious as they can quickly penetrate through the material or reduce the strength properties. The risk of pitting corrosion increases with the chloride content, the content of oxidizing agents, rising temperature and decreasing pH.

Crevice corrosion

Crevices, e.g., in a flange, under a gasket or a deposit, may initiate local corrosion in two different ways. If oxygen is prevented from reaching a surface, the surface can activate and a corrosion attack takes place.

The second reason why crevices initiate to corrosion attacks is that the crevice or deposit retains water. The presence of chlorides always speed up the corrosion attack and risk of crevice corrosion exists e. g. in flanges of stainless steel in sea water, under dirt deposits on car bodies or in gutters. Corrosion attacks between the laps in a steel coil during transportation and storage are also examples of crevice corrosion.

Figure 3.28: A method for reducing the effect of spring-back is to introduce grooves fixing the trestle.



Galvanic corrosion

If two different metallic materials are brought into contact with each other and are subsequently exposed to a humid environment, one of the materials will corrode faster than if they were exposed separated in the same environment. Which material corrodes faster is determined by how noble the materials are. The less noble material always corrodes faster. Basic knowledge of galvanic corrosion is always essential for SSAB's coated products in connection with cut edges and for the selection of fasteners.

Fretting corrosion

Fretting corrosion occurs at the interface of two metal parts in relative movement under a high load and in a corrosive environment. It may occur on metal-coated material, for example, during transport.

Stress corrosion cracking and corrosion fatigue

If a material is exposed to tensile stress and is simultaneously placed in a corrosive environment, usually containing chlorides or strong alkaline solutions, cracks and fractures may occur. The tensile stress in many cases can be residual stress in the structure after e. g. welding or forming.

A corrosion type similar to stress corrosion cracking is corrosion fatigue. The difference is that stress corrosion cracking arises under a static load, whereas corrosion fatigue occurs under varying load.

Cyclic mechanical stresses in conjunction with a corrosive environment may lead to corrosion fatigue. The fatigue strength of the material is lowered significantly by corrosion fatigue compared to only fatigue and no special fatigue limit occurs. Corrosion fatigue may quickly lead to formation of cracks or fractures in the material. The cracks are often transgranular and only slightly branched.

3.5.2 Different types of corrosion protection

Three different methods are used to prevent steel from corrosion.

- Alloying the steel with substances increasing the corrosion resistance. Typical examples are stainless steels and weathering steels.
- Coating the steel with a metal or an alloy which is more reactive to the environment than the steel and thereby protects it against corrosion.
- Apply an organic coating which delays the contact between the steel and the corrosive media.

Weathering steel

Weathering steels are low-alloy high strength steels which, when freely exposed in outdoor atmospheres, have significantly better corrosion resistance than ordinary carbon steels. Weathering steels initially rust in the same way as unalloyed steels, but a denser barrier layer of corrosion products is gradually formed and the corrosion rate decreases with time. The homogeneous and dense barrier layer (oxide layer) is formed by the presence of the alloying elements copper, chromium, phosphorus and silicon.

The rate and mechanism for the development of the barrier layer depends on several factors, mainly, the moisture content and air pollution. Wind direction and solar radiation can also play a minor role. The corrosion attack on weathering steels is already after 10 years significantly lower than on unalloyed steels and the difference is increasing with time.

The optimum corrosion protection for weathering steels is achieved in environments with alternating wet and dry periods where the protective barrier layer is formed in the best way. Under constant wet conditions, e.g., immersed in water or buried in soil, the protection by the barrier layer is less and the corrosion rate is similar to unalloyed steel. It is thus important to design constructions so accumulations of water and condensate pockets can be avoided.

3.5.3 Design advices for corrosion prevention

Corrosion can be prevented if the structures in the exposed environment are designed correctly. Following points should be experientially considered when designing a structure.

Avoid standing water or dirt accumulations

Standing water gives rise to corrosion on steel structures. Steel components in external structures should be designed in order to prevent the formation of pockets where dirt and moisture can collect, see figure 3.29.

Steel in contact with other materials

When selecting materials for a structure, you should take into consideration that the corrosion rate of steel is influenced by other materials in contact with the steel.

Various sealing and roofing felt materials are petrochemical products and contain bitumen and may cause bitumen corrosion. If the sealant or roofing material is exposed to UV radiation, some of the components may decompose and may be leached out by rain or water condensate, thus producing an acidic solution. If this solution comes into contact with steel or galvanized steel, it will cause increased corrosion. Make sure that no corrosive chemicals are leached out of the sealant or roofing material and that it contains a UV stabilizer or is covered with a radiation-proof surface layer.

Corrosion in spot welds in metal coated steels

Adjust the welding parameters so that a minimum amount of the layer is burnt off during welding.

Corrosion of cut edges on metal coated steel

Cut edges on metal-coated or coil-coated strips have sufficient corrosion protection in normal environments through the zinc content on the coated surface. This protection may become insufficient in very corrosive environments and additional measures may become necessary. Perforated materials are particularly exposed in this situation.

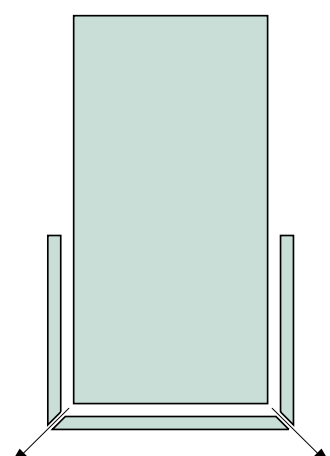


Figure 3.29: Example of vertical sheets placed in a U-shaped rail. If there is a risk of condensation in the construction there must be holes to ensure good drainage.

As a rule of thumb a zinc coating cannot protect a cut edge that is thicker than 1 to 2 mm. The lower limit, 1 mm, applies in environments with high humidity or condensed water. In more polluted or saline environments protection can be extended to a 2 mm thick edge.

On perforated materials, the perforations may not be placed too close if the perforation is done after surface treatment. The metallic coating is then not enough to protect the relatively big share of cut edges. A guideline value can be at least 10 to 15 mm between perforations.

Note that since the purpose of the perforated material is to ensure certain sound dampening properties through its perforation, this necessitates the use of a certain hole pattern. Consequently, painting or galvanizing after perforation stamping should be considered for the use in higher corrosivity categories.

In order to protect the cut edge of a coated strip, the end of the panel can be bended, see *figure 3.30*.

The cut edges of coated panels may also need to be painted in very corrosive environments.

Choose materials matching the environment

It is important to choose materials according to the environment in which they are going to be used. Different environments with varying amounts of substances affect the corrosion rate in different ways. The corrosivity of different environments have been classified in corrosivity categories, see SS-EN ISO 9223. The most corrosive environment nowadays is in the coastal areas but local industrial areas and big cities can also have a high corrosivity.

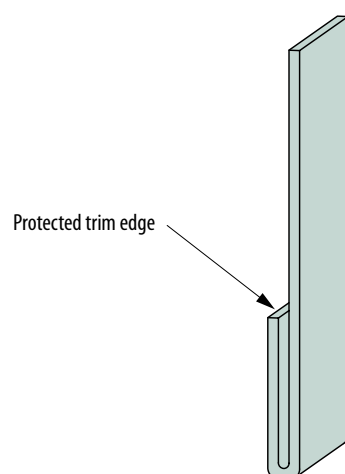


Figure 3.30: A bending preventing the exposure of the cut edge.

Water-filled crevices

The vertical strip on a wall should be finished so that the cut edge does not have any contact with the horizontal surfaces, such as the horizontal fittings or the floor, see *figure 3.31*. This prevents the formation of capillary water between the surfaces.

Crevice corrosion may occur in connection with discontinuous welded joints in a humid environment. All-welded joints are preferable.

Design for optimized surface treatment

In order to obtain the best surface treatment and corrosion protection it is important to avoid

- Undrained areas and narrow crevices where surface treatment residues can remain and subsequently cause corrosion.
- Sharp edges and corners, deep notches and a rough geometrical shape may cause irregular and inferior surface treatment quality in these areas.

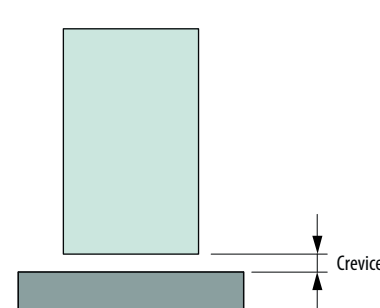


Figure 3.31: Avoid water-filled crevices.





4. Static design

This chapter discusses structures resistance to static loading where the requirements are connected to load capacity/resistance and deformations. Issues that needs to be addressed in order to use the full potential of high strength steel are highlighted. In structural design the resistance of a structure is to be compared to the load effects applied during service life.

Load analysis is an important part of the field work. Finding relevant critical loads differs a lot from one application to another and is therefore not within the scope of this book.

4.1 Basic concepts

Welded and cold-formed sections are described here. The calculation methods which are presented are based, for the most part, on the common European standard for steel structures, Eurocode 3 [4.1].

4.1.1 Load capacity/resistance

The criterion for resistance under a static load has previously often been that the relation between load and deformation ceases to be linear, for example, when the yield point or the elastic buckling stress is reached. This is closer to what can be designated as the service load, an often recurring load. The Design Handbook describes resistance primarily as an ultimate limit state, i.e., the largest load a structure can carry before collapsing. This means for example that plastic deformation and stress redistribution in a cross-section can be used in resistance calculations.

Serviceability limit state

Elastic behavior but also limitations of deformations under a certain load can be design requirement in the serviceability limit state. The limit for elastic response can be difficult to define in certain cases. Elastic buckling may occur for really thin high-strength steel plates, which means that the cross-section after unloading returns to its original form completely. Elastic behavior and deformation calculations are discussed briefly in section 4.3.3.

Ultimate limit state

The design load level in the ultimate limit state is most often significantly higher than in the serviceability limit state and permanent deformations after unloading are permissible. Several different types of failure modes may be relevant: material failure, instability or extensive plastic deformation. Instability is often a design parameter for slender structures in high-strength steel.

© SSAB

Instability

A high yield point permits slender structural parts, which means that buckling in different configurations may need to be analyzed. The most common failure modes due to instability are illustrated in *figure 4.1*. The calculation method for determining resistance with respect to instability is described in the next section. The resistance is determined with a theoretically calculated critical stress/load as a basis and a definition of slenderness, see *equation 4.4*.

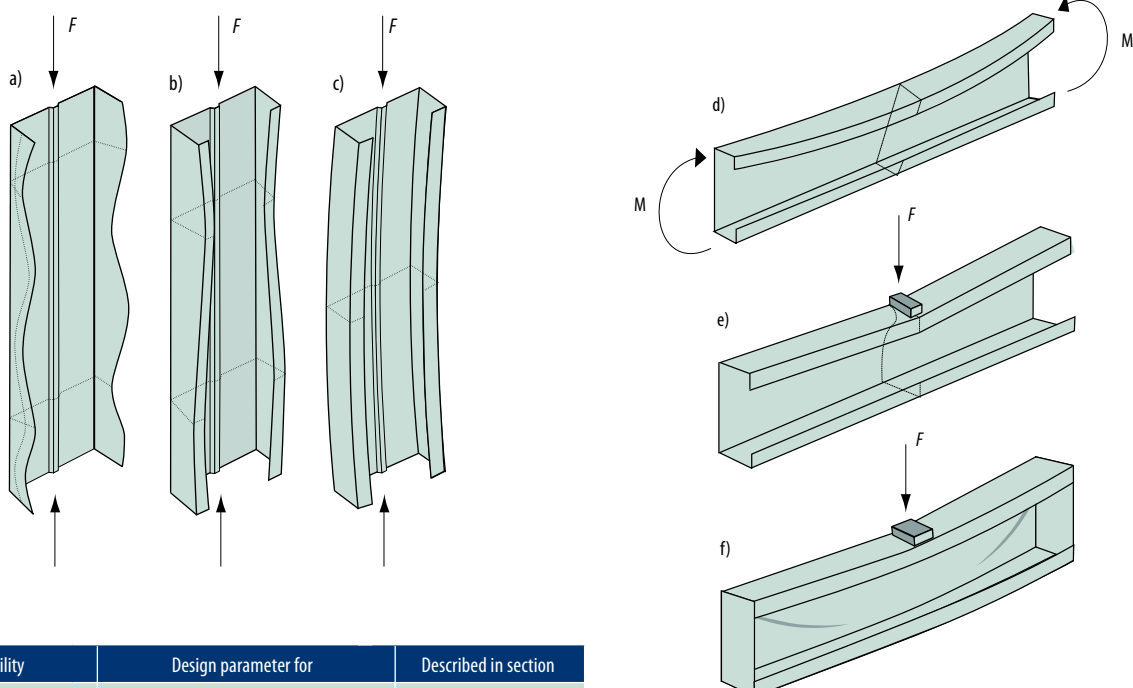
Local buckling and shear buckling are instability phenomena which can appear for slender plate surfaces exposed to compression- or shear stress respectively. The

buckling is local, which means that the actual resistance of the plate can be significantly higher than the critical buckling stress.

Stiffeners to support slender plates are used to increase the resistance. A design parameter for the design of stiffeners is distortional buckling.

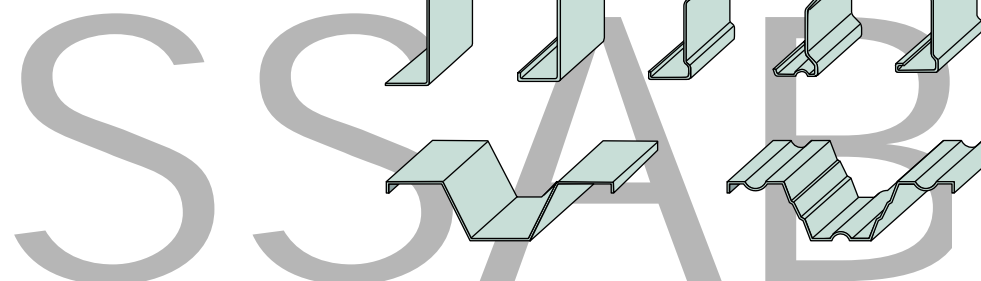
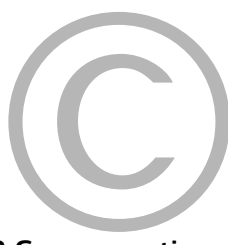
Patch loading may occur in connection with load introductions and at supports.

Flexural buckling and lateral-torsional buckling affect the whole length of a structure and are therefore global phenomenon. There is no so-called post-critical behavior, which means that failure occurs without warning.



Instability	Design parameter for	Described in section
a Local buckling	Slender plates in compression	4.3.2 Buckling
b Distortional buckling	Stiffened plates in compression	4.3.2 Buckling
c Flexural buckling	Long and narrow members in compression	4.3.4 Normal force
d Lateral-torsional buckling	High open cross-sections in bending	4.3.5 Bending moment
e Patch loading	Local load introduction in slender webs	4.3.7 Load Introductions and support
f Shear buckling	High slender webs in shear	4.3.6 Shear force

Figure 4.1: Instability phenomena which may govern the resistance for slender steel members.



4.1.2 Cross-sections

There are a number of different designations of standard cross-sections. However, when it comes to calculations for thin plate structures, cross-sections are divided into cold-formed and welded sections. Both types can be divided into open and closed sections with different types of stiffeners in the web and flange, see *figure 4.2*. Stiffener prevents or delays local buckling.

There are certain differences between cold-formed and welded sections; for example, welded cross-sections generally have higher residual stress, which reduces their resistance. The Design Handbook describes the calculation procedure for both of them in parallel.

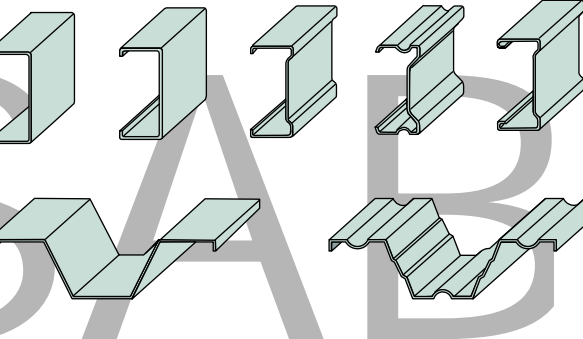
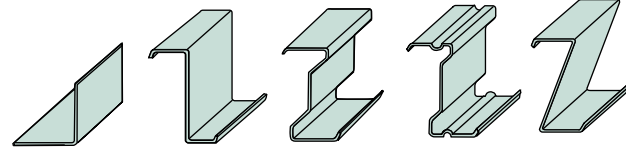
Cold-formed sections

Cold-formed sections can be manufactured of both cold- and hot-rolled sheets. The design is described, for the most part, in Eurocode 3 part 1-3 [4.2]. Common cross-sections include C- and Z-profiles but also built-up sections. Manufacture takes place through bending, roll-forming or pressing. Stiffeners are most often done in the form of folds and grooves, see *figure 4.2*.

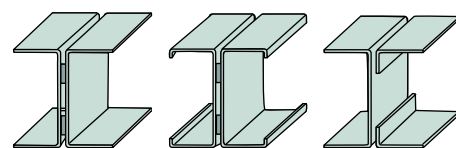
Welded sections

Welding together two or more plate surfaces provides great possibilities of tailoring optimum cross-sections for different purposes. Common cross-sections include box sections, I-beams with different plate thickness of the flange and web and larger plates with welded stiffeners. The design is described, for the most part, in Eurocode 3, part 1-1 [4.3] and Eurocode 3, part 1-5 [4.4].

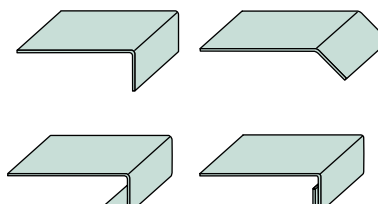
Cold-formed profiles



Built-up cold-formed sections



Single and double edge folds



Grooves



Welded cross-sections

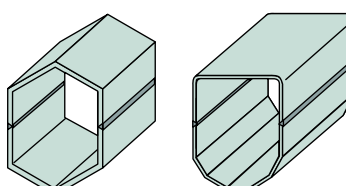
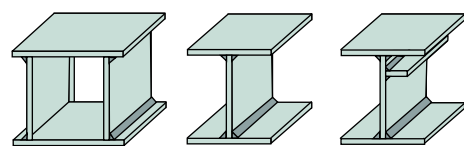


Figure 4.2: Standard cross-sections for thin-plate structures.

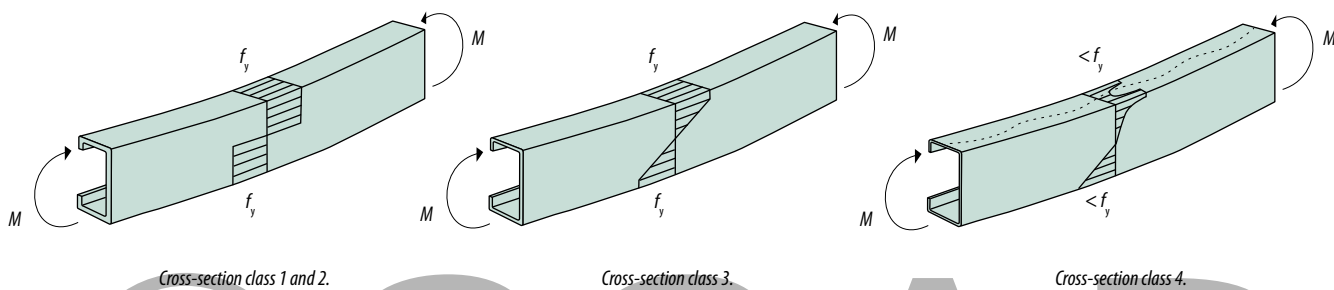


Figure 4.3: Stress distribution with maximum resistance for the different cross-section classes ($f_y = R_c$).

Cross-section classes

Four different cross-section classes are defined which makes it possible to determine if buckling limits the resistance of a certain cross-section or not. The cross-section class depends on plate geometry, stress distribution and material yield point, and determines which resistance can be utilized, *figure 4.3*. Design with respect to buckling and how the classification is done is described in section 4.3.2.

Cross-section class 1: The cross-section can form a plastic hinge with rotation capacity required for plastic analysis of moment distribution.

Cross-section class 2: The cross-section can develop full plastic moment resistance but have limited rotation capacity.

Cross-section class 3: The cross-section can reach elastic moment resistance with yield point of the material as highest stress level.

Cross-section class 4: The slender parts of the cross-section will limit the resistance due to local buckling.

Cross-section class 1 and 2 have the same resistance, whereas the system calculation can be done differently. Plastic hinge theory can be used for class 1 when the moment distribution is more favorable. The strain hardening of the material should not be too low. SS-EN 1993-1-1 [4.3] recommends $f_u/f_y > 1.1$ and [4.6] suggests the use of plastic hinge theory for steels up to S460. The issue has not been sufficiently analyzed above that limit.

Cross-section class 1 through 3 does not result in any difference in resistance for cross-sections exposed only to compressive forces.

4.2 Design methods

The structural design work when upgrading to a high-strength material can be done based on the resistance of the existing structure in mild steel. Alternatively, the structure can be analyzed based on the existing conditions, whether old or new ones. The alternatives are described here as relative and absolute design, respectively.

4.2.1 Relative design

The method is simple to apply and can be used in connection with an upgrade to a high-strength steel without any major structural changes. Thickness is proportioned with regard to the properties of the new material so as to achieve the same resistance. But, it can be an advantage to review the design of the cross-section for best results. For example, the stiffness of a structural member is reduced in with a thickness reduction, which can be compensated simply by changing the outer geometry. Slender parts of a cross-section may need stiffeners and the placement of welds is important in connection with fatigue loads.

The advantage of relative design is that it does not require any load analysis. On the other hand, the possibility to find an optimized solution is limited.

4.2.2 Absolute design

Absolute design provides greater possibilities for optimization and adjustment to new conditions. The structural requirements in the serviceability limit state and ultimate limit states are analyzed with regard to safety and function. This naturally requires more work but can turn out to be profitable. The work consists mainly of the following parts:

- Assessment of all relevant external loads and calculation of internal forces and moment (load effect).
- Structural design and material selection, as well as calculation of resistance using, e.g., the Design Handbook.
- Assessment of requisite safety.

External load and load effect

External loads could be constant (static) or vary in time (dynamic). As a rule of thumb; a load is a fatigue load if the number of load cycles, i.e., load fluctuations exceeds 1,000. A fatigue load requires a different design procedure than a static load and is thoroughly described in chapter 5 in the Design Handbook. A dynamic load can be a fatigue load but not necessarily, cf. an impact load.

Several load situations and load levels with different structural requirements can often be identified. An ultimate limit load should be viewed as the maximum load which

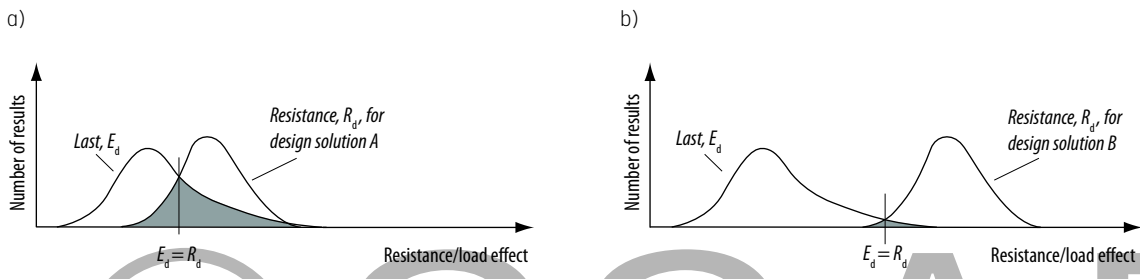


Figure 4.4: Load and resistance dispersion. The risk area for failure is shaded in both figures.

can affect the structure during its life where a collapse is not acceptable. For example, this can be a crash situation or another extreme load. A serviceability limit load refers to load levels during normal use where deformations often become a design requirement. Both of these should be analyzed in an absolute design. What is decisive for the design and material selection is different from one case to another.

Loads can be measured, estimated or calculated. During load measurement, it is possible to either measure the load itself with a load cell or its effect with a strain gauge. This can be an impossible or very difficult and expensive task and often requires statistical data for a successful safety assessment.

It is possible to find guideline values for different loads in standards and handbooks; crane standard [4.7], Eurocode 1 [4.8].

A system calculation is done in order to compute the internal forces and moments. The calculation methods for resistance described in the Design Handbook are based on an analysis of load effect according to the first-order theory. In other words, internal forces and moments are described on the basis of unchanged structural geometry.

Structural design and material selection

The creative part of the design work does not have any direct rules or standards to follow. It is rather practice, experience and often practical possibilities that are of great importance .

4.2.3 Assessment of requisite safety

The safety aspect is important both when it comes to relative and absolute design. It can be difficult to identify the safety margins and preserve them when upgrading an existing structure. Absolute design offers the opportunity to review different safety factors.

The design condition for a structure in an ultimate limit state is that the design resistance, R_d , should exceed the design load effect, E_d .

$$R_d \geq E_d$$

(Equ. 4.1)

The design values should be set with consideration for a statistical variation of the resistance and load effect, as well as the consequences of a failure.

Some form of statistical data or discussion is required. Figure 4.4 shows examples of probability density functions characteristics for load effect, E , and corresponding resistance, R . A frequency response characteristic is calculated by making a number of measurements or observations and registering results at different levels. This provides a good picture of how big the result spread is.

Figure 4.4 a and b illustrate how the risk of failure is affected by the choice of design values, E_d and R_d . The same load effect used in design according to equation 4.1 can result in a structural solution with resistance according to a) or b). The risk of failure, which is shaded in the figure, differs significantly for the two alternatives.

It is common to use the 5 % fractile (which means that 1 out of 20 fail) as a so-called characteristic value for both load effect and resistance which in turn gives the design values according to equation 4.2 and 4.3.

To consider

- For an impact load, it is usually a certain amount of energy which should be absorbed and not a certain force.
- Uneven temperature distribution may result in significant stress and strain in stiff structures.
- Accidental loads and loads which may arise in manufacture and transport must be considered.

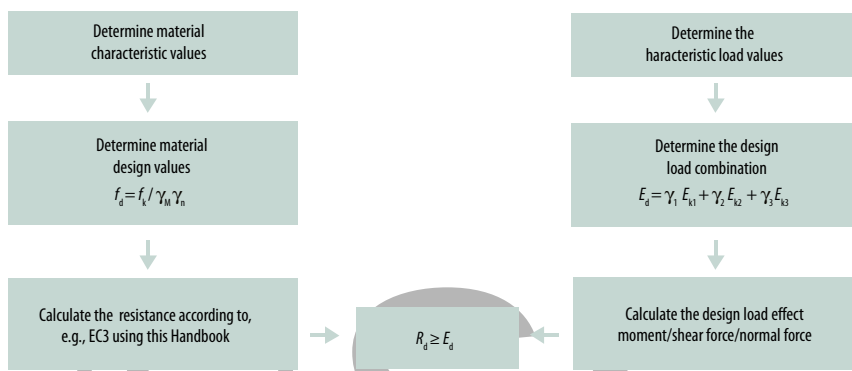


Figure 4.5: Calculation procedure during design.

Resistance

When it comes to resistance of a structural member, it is, above all, the fluctuations in material strength that produce a variation in result. Characteristic values are given as nominal values of yield strength and ultimate tensile strength in standards and data sheets, the design values are calculated according to *equation 4.2* and *table 4.1*. The so-called partial coefficients depend on type- and consequence of a failure.

$f_{yd} = \frac{f_{yk}}{\gamma_M \gamma_n}$	(Equ. 4.2)
$\gamma_M = 1.00$	For cross-sections where the resistance is limited by yield point
$\gamma_M = 1.00$	For cross-sections where the resistance is limited by instability
$\gamma_M = 1.25$	For cross-sections utilizing ultimate tensile strength
$\gamma_M = 1.25$	For joints/connections

The safety class can be translated into a risk of failure, see *table 5.11*.

Design load

Safety class	Consequence of failure	γ_n
1	Less serious	1.0
2	Serious	1.1
3	Very serious	1.2

Partial coefficient for materials based on safety class is a deviation from Eurocode 3.

Table 4.1: Partial coefficient for a number of defined safety classes [4.9].

Characteristic loads can be determined if statistic data is obtainable. Alternatively, a maximum load can be used, rated or the like. How this is handled depends wholly on the respective application.

The load most often consists of several different parts:

- a permanent load; consisting of the weight of the structural members and fixed equipment
- one or more variable loads; could be any type of load that the structure is expected to carry, of varying size and time frame.

More than one variable load can affect a structure at the same time, *equation 4.3*. But, the probability that the maximum values for these loads occur at the same time is often minimal. This is why one variable load can be selected as a so-called main load and the intensity of the remaining possible loads are reduced. This approach is described in EN 1990 [4.1]. Note that there can be several load cases with different combinations of loads. Finding possible scenarios is an important part of the structural work.

$$E_d = \gamma_{d1} E_{k1} + \gamma_{d2} E_{k2} + \gamma_{d3} E_{k3} + \gamma_{d4} E_{k4} \quad (\text{Equ. 4.3})$$

The design procedure is described schematically in *figure 4.5*.

Material yield point

The nominal value of material yield point for steel should be used by adopting $f_{yk} = R_{eh}$ directly from the product standard. See also chapter 2 for examples of material curves and definitions.

Material ultimate tensile strength

The nominal value of the ultimate tensile strength for steel should be used by adopting $f_{uk} = R_m$ directly from the product standard. See also chapter 2 for examples of material curves and definitions.

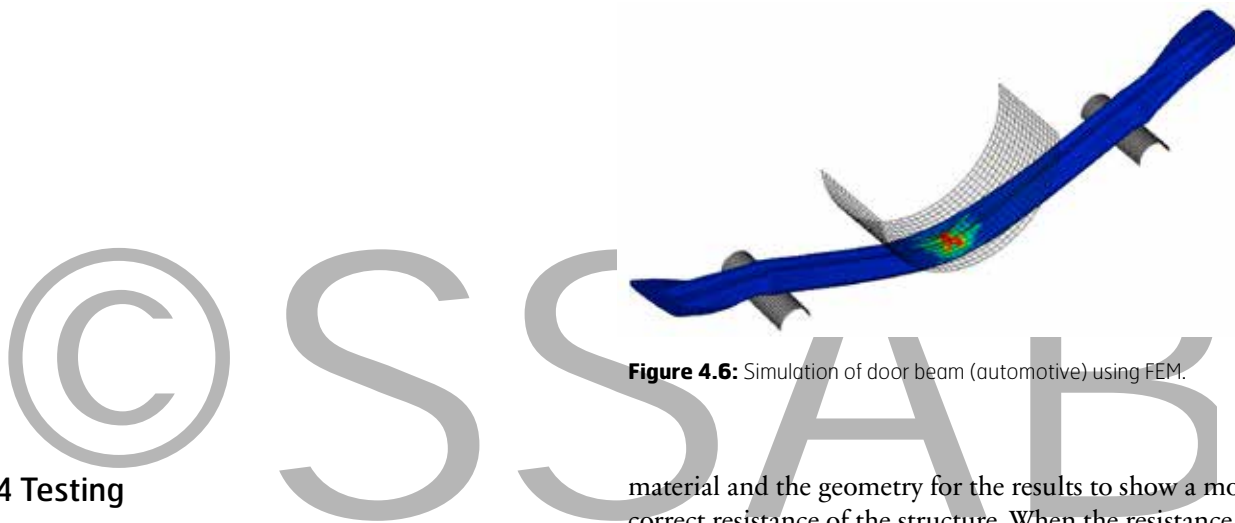


Figure 4.6: Simulation of door beam (automotive) using FEM.

4.2.4 Testing

Together with calculations, testing is often an important step in the development of a new product. Testing verifies that the defined functional requirements have been met. It is also a good way to define critical areas in a complicated structure as a supplement to simulations, see section 4.4.

The following should be taken into consideration in testing.

- Use a sufficient number of tests in order to be able to assess the dispersion and requisite safety.
- Material strength and geometry should be measured and the result evaluated to correspond to nominal values.
- Actual manufacturing methods should be used.
- Test specimens should be taken in the same direction as planned for the final production. This is particularly important for hot-rolled plates where the yield point and tensile strength across the plate can be greater than along the plate.
- Full-scale tests should be carried out in order to minimize the sources of errors.

Testing is particularly important if the geometry of a structural element is outside the area of application of the calculation procedure, see section 4.3.1.

Design through testing is also described in Eurocode [4.1].

4.2.5 Simulations

FEM (the Finite Element Method) is used successfully in design work. The advantages of FEM be used in cases where the structure is complex and the calculation of, for example, stress and deformations requires a greater effort. These programs can solve both linear and non-linear, static and dynamic problems. Linear calculations mean that the design is done in relation to a stress level which often becomes conservative and should not be used in normal cases. Most analyses require non-linear modeling of the

material and the geometry for the results to show a more correct resistance of the structure. When the resistance is governed by instability, this must be taken into account during modeling. This is discussed in section 4.4.

Design through simulation requires that you choose a safety level and take into consideration the insecurity in the constituent parameters.

4.3 Design of plates and beams

In order to take advantage of the actual resistance in an ultimate stress state, a certain degree of plasticization and stress re-distribution in cross-sections has to be allowed. A calculation of cross-section resistance, for example, bending or torsional moment, shear force and compressive force instead of stress enables this.

4.3.1 Limitations – geometric proportions

The calculation methods described here are verified for cross-sections where each part is within certain geometric limits. Outside these limits may give incorrect results and the resistance and response must instead be verified through testing and/or calculations.

In summary, it can be said that $b/t < 50$ applies to plated structural elements with one free edge and $b/t < 500$ applies to elements supported along two edges, see figure 4.11 and 4.12.

4.3.2 Local buckling

Local buckling is very important to address when using high strength steel. The thickness is decreased and the stress levels higher than in mild steel structures. The geometry of compressed parts in a cross-section has a significant effect on whether buckling will limit the stress level before reaching material yield point.

Local buckling is defined as a local instability of cross-section parts in compression or shear. The buckling is limited within a structural element which means there is a post critical resistance for the cross-section. When buckles starts to

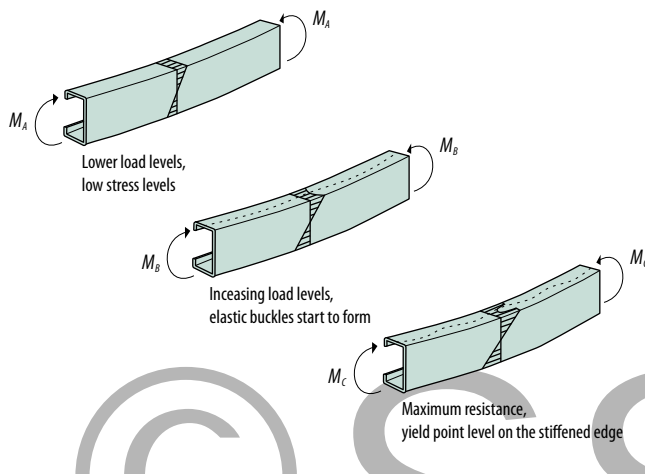


Figure 4.7: Stress distribution in a slender cross-section with increasing load levels. $M_A < M_B < M_C$

appear, the cross-section can still carry more load due to the fact that stress re-distribution is possible, see figure 4.7.

Figure 4.8 shows the stress distribution and how it varies in the compressed flange and the response in the load/deformation diagram. The flange begins to show buckles at A and the stress is no longer evenly distributed. As long as the yield point is not reached, the deformation remains elastic. The part of the flange connected to the web remains straight and the stress level can increase even more. Reaching yield point results in some plastic deformation, B. Material yield point therefore has an influence on the response. Maximum resistance is reached at C. For a mild steel with a corresponding geometry, the stress level at point A may exceed the yield point and buckling does not occur. The shape of the load/deformation curve depends wholly on the geometry and yield point.

The first step in calculating the resistance of a cross-section is to decide if buckling is a limiting factor for the different parts. This can be done by determining cross-section class according to figures 4.11 through 4.13. The material yield point, geometry and stress distribution and is used as input data. Design with regard to buckling needs to be done for each cross-section part in class 4.

Stiffeners can be used to stabilize slender compression plate surfaces. Stiffeners for a cold-formed section are often roll-formed grooves in the flanges and folds in the web, whereas welded stiffeners are used for plated cross-sections, see figure 4.2. Local buckling of a stiffened plate is limited to each individual plane part. Design of the stiffening itself is discussed on page 4.14.

In connection with buckling of round tubes, there is no post-critical behaviour and the structure is very sensitive to variations in initial imperfections. Tests show a large spread in the results [4.9]. Special rules for control of initial imperfection are available in Eurocode 3, part 1-6 [4.10]. Resistance calculations with regard to local buckling of round pipes is described on page 4.16.

Critical stress and slenderness

The design curves which describe the resistance with regard to stability are based on critical buckling stress according to the theory of elasticity. This governs for an ideal geometry without initial deformations and residual stress and can be both conservative and non-conservative for a real structural

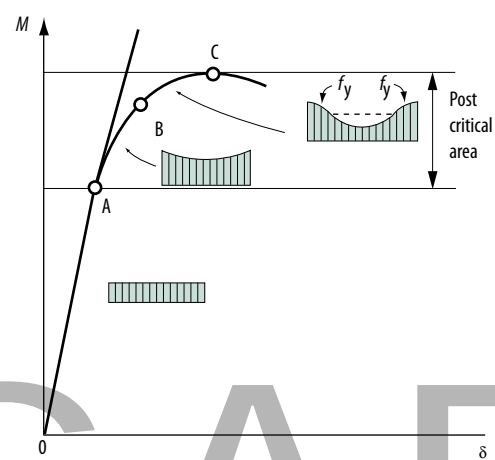


Figure 4.8: Applied moment vs. deflection during testing. Stress distribution for a slender flange in compression, see figure 4.7.

part. It is usually too low in the case of local buckling and too high for global buckling.

$$\lambda_p = \sqrt{\frac{f_y}{\sigma_{cr}}} \quad (\text{Eqn. 4.4})$$

This theoretical value is used to define a slenderness ratio, λ_p .

The definition of λ_p includes critical stress, σ_{cr} , together with material yield point, f_y , equation 4.4.

Using this equation with the theory for local buckling of a plate [4.10] leads to equation 4.5.

$$\lambda_p = \frac{b}{t} \sqrt{\frac{12(1-v^2) f_y}{\pi^2 E k_\sigma}} = 1,052 \frac{b}{t} \sqrt{\frac{f_y}{E k_\sigma}} = \frac{b/t}{28,4 \sqrt{k_\sigma}} \quad (\text{Eqn. 4.5})$$

k_σ and ε from figure 4.14 and figure 4.11, respectively.

Design with respect to local buckling

The resistance with regard to local buckling for cross-sections with one or more slender parts in class 4, figure 4.3, is calculated by using a fictitious effective area for each individual part. The basis is that the stress distribution is no longer even when buckling starts to occur. A simplified stress distribution with yield stress across an effective width provides a calculated resistance/force which corresponds to the actual one, figure 4.9.

Note that it is only the compression flange in the figure that is susceptible to local buckling and the width is reduced. This changes the position of the neutral axis.

Cross-section properties such as area (A_{eff}), moment of inertia (I_{eff}) and section modulus (W_{eff}) are calculated based on the effective cross-section surface and produces, together with the yield point, the resistance with regard to buckling.

The calculation procedure of the effective cross-section is described below.

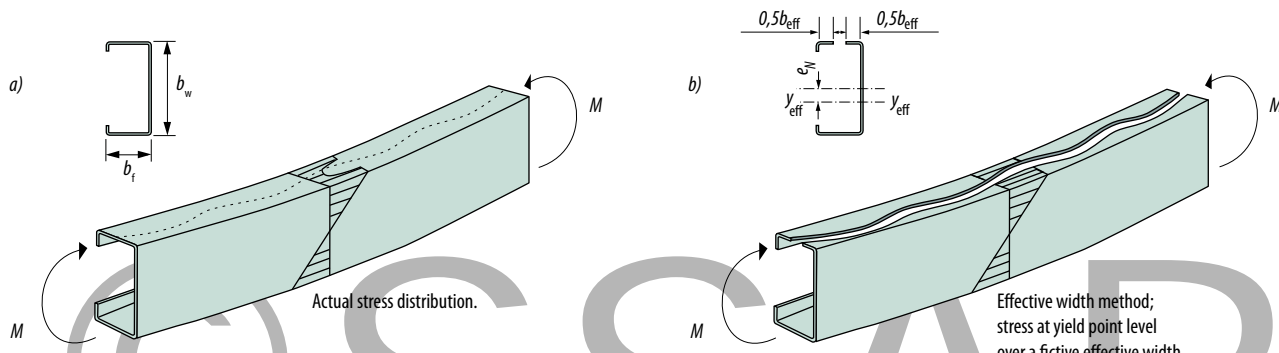


Figure 4.9: Method with effective cross-section.

Calculation procedure

Figures 4.10a and 4.10b can be used for the case of a compression flange. Figure 4.10a shows when buckling needs to be taken into consideration, with a maximum value of b/t for the flange as a function of the stress level introduced (i.e. yield point, f_y). Figure 4.10b provides the effective width of the flange as a portion of actual.

For other load cases, follow points 1 through 4 below.

1) Determine the cross-section class for each cross-section part pursuant to figure 4.11 or 4.12.

Class 4 cross-section parts are susceptible to local buckling and require the effective width to be calculated.

2) Determine the buckling coefficient, k_s , for the cross-section part from figure 4.14.

The division is the same as in connection with the classification; part supported along two edges or part with one free edge. The figure also represents different stress distributions.

3) Determine the slenderness of cross-section part as

$$\lambda_p = \frac{b/t}{28,4\epsilon\sqrt{k_s}} \quad (\text{Eq. 4.6})$$

4) A reduction factor, ρ , is calculated according to equation 4.7 or 4.8

Compressed part supported along two edges (web, flange in a box beam):

$$\rho = \frac{\lambda_p - 0,055(3+\psi)}{\lambda_p^2} \quad (\text{Eq. 4.7})$$

ψ from figure 4.14.

Compressed part with one free edge:

$$\rho = \frac{\lambda_p - 0,188}{\lambda_p^2} \quad (\text{Eq. 4.8})$$

ρ is never larger than 1.

5) The effective width is calculated and distributed according to figure 4.14.

6) When all slender cross-section parts have been reduced, the effective cross-section properties are calculated, $A_{\text{eff}}, I_{\text{eff}}, W_{\text{eff}}$.

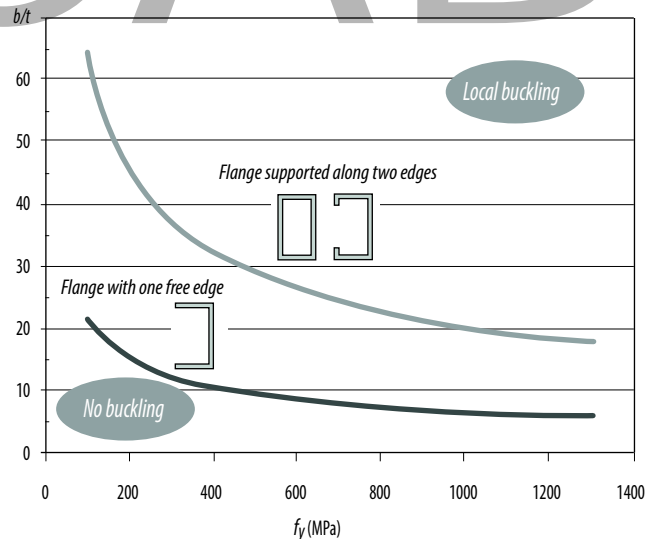


Figure 4.10 a: Maximum value for b/t for which local buckling will not occur. Flat sheet with even stress distribution in the compression flange with free edge (lower curve) and the compression flange supported along two edges (upper curve).

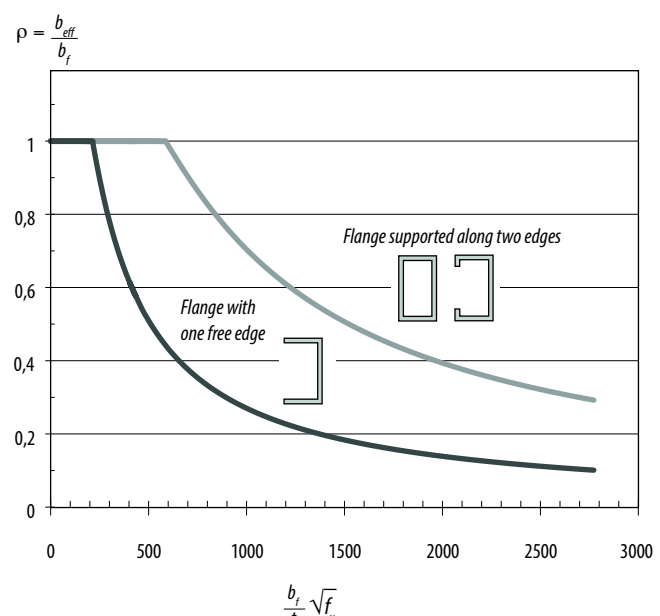
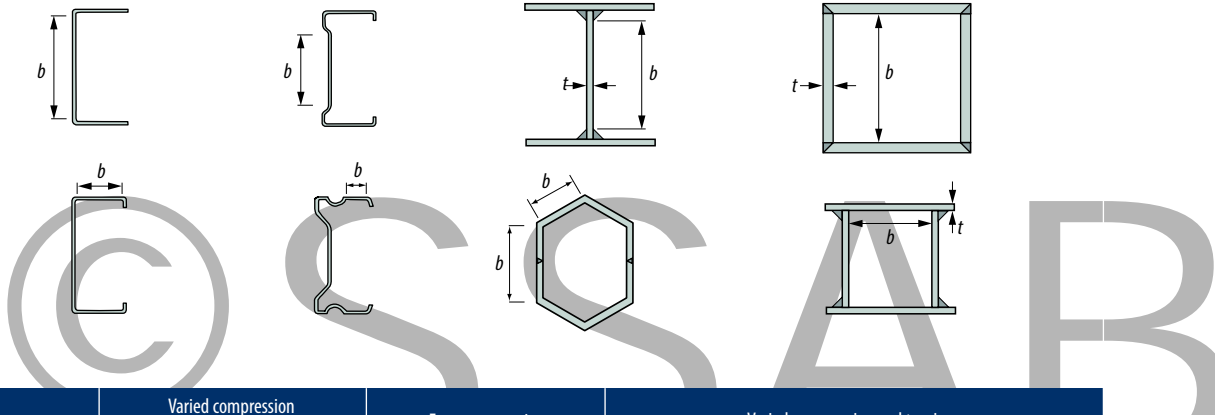
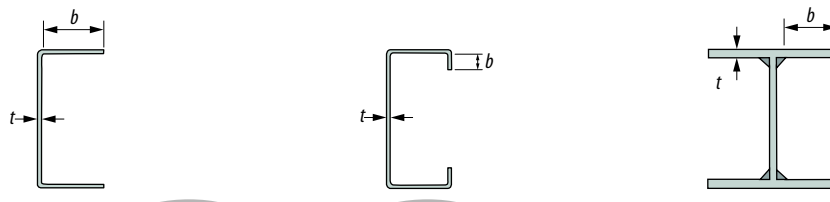


Figure 4.10 b: Reduction factor as a function of geometry and yield point in MPa for a compressed part, e.g. flange.



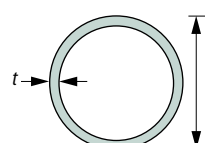
	Varied compression and tension, symmetrical	Even compression	Varied compression and tension				
Stress distribution Cross-section class 1 and 2							
Cross-section class 1	$b/t \leq 72\epsilon$	$b/t \leq 33\epsilon$	$b/t \leq \frac{396\epsilon}{13\alpha-1}$	$b/t \leq \frac{39\epsilon}{\alpha}$			
Cross-section class 2	$72\epsilon < b/t \leq 83\epsilon$	$33\epsilon < b/t \leq 38\epsilon$	$b/t \leq \frac{456\epsilon}{13\alpha-1}$	$b/t \leq \frac{41,5\epsilon}{\alpha}$			
Stress distribution Cross-section class 3							
Cross-section class 3	$83\epsilon < b/t \leq 124\epsilon$	$38\epsilon < b/t \leq 42\epsilon$	$b/t \leq \frac{42\epsilon}{0,67+0,33\psi}$	$b/t \leq 62\epsilon (1-\psi)\sqrt{(-\psi)}$ <i>*Fictitious stress level</i>			
Stress distribution Cross-section class 4							
Cross-section class 4	$b/t \geq 124\epsilon$	$b/t \geq 42\epsilon$	$b/t \geq \frac{42\epsilon}{0,67+0,33\psi}$	$b/t \geq 62\epsilon (1-\psi)\sqrt{(-\psi)}$ <i>*Fictitious stress level</i>			
$\epsilon = \sqrt{235/f_y} [\text{MPa}]$	f_y	235	355	420	500	700	960
	ϵ	1,00	0,81	0,75	0,69	0,58	0,49

Figure 4.11: Slenderness limits for cross-section parts in compression; parts supported along two longitudinal edges.



Stress distribution Cross-section class 1 and 2	Even compression		Varied compression and tension				
	Free edge under compression	Free edge under tension					
Cross-section class 1	$b/t \leq 9\epsilon$	$b/t \leq \frac{9\epsilon}{\alpha}$	$b/t \leq \frac{9\epsilon}{\alpha\sqrt{\alpha}}$				
Cross-section class 2	$9\epsilon \leq b/t \leq 10\epsilon$	$\frac{9\epsilon}{\alpha} \leq b/t \leq \frac{10\epsilon}{\alpha}$	$\frac{9\epsilon}{\alpha\sqrt{\alpha}} \leq b/t \leq \frac{10\epsilon}{\alpha\sqrt{\alpha}}$				
Stress distribution Cross-section class 3							
Cross-section class 3	$10\epsilon \leq b/t \leq 14\epsilon$		$b/t \leq 21\epsilon\sqrt{k_\sigma}$ k_σ see figure 4.14				
Stress distribution Cross-section class 4							
Cross-section class 4	$b/t \geq 14\epsilon$		$b/t \geq 21\epsilon\sqrt{k_\sigma}$ k_σ see figure 4.14				
$\epsilon = \sqrt{235/f_y} [\text{MPa}]$	f_y	235	355	420	500	700	960
	ϵ	1,00	0,81	0,75	0,69	0,58	0,49

Figure 4.12: Slenderness limits for cross-section parts in compression; parts with one free edge.



Even compression and bending							
Cross-section class 1	$d/t \leq 50\epsilon^2$						
Cross-section class 2	$50\epsilon^2 \leq d/t \leq 70\epsilon^2$						
Cross-section class 3	$70\epsilon^2 \leq d/t \leq 90\epsilon^2$						
Cross-section class 4	$d/t \geq 90\epsilon^2$						
$\epsilon = \sqrt{235/f_y} [\text{MPa}]$	f_y	235	355	420	500	700	960
	ϵ	1,00	0,81	0,75	0,69	0,58	0,49

Figure 4.13: Slenderness limits for circular tubes subjected to compression and bending.

Plate supported along two edges

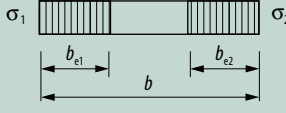
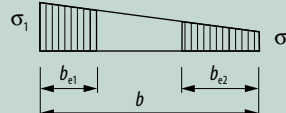
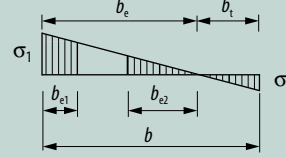
Stress distribution, positive compression			Effective width, exist		
			$\psi = 1:$ $b_{\text{eff}} = \rho b$ $b_{e1} = 0,5 b_{\text{eff}}$ $b_{e2} = 0,5 b_{\text{eff}}$		
			$1 > \psi > 0:$ $b_{\text{eff}} = \rho b$ $b_{e1} = \frac{2}{5-\psi} b_{\text{eff}}$ $b_{e2} = b_{\text{eff}} - b_{e1}$		
			$\psi < 0:$ $b_{\text{eff}} = \rho b_c = \rho b / (1-\psi)$ $b_{e1} = 0,4 b_{\text{eff}}$ $b_{e2} = 0,6 b_{\text{eff}}$		
$\psi = \sigma_2 / \sigma_1$	1	$1 > \psi > 0$	0	$0 > \psi > -1$	-1
Buckling coefficient, k_o	4,0	$8,2 / (1,05 + \psi)$	7,81	7,81 - 6,29 ψ + 9,78 ψ^2	23,9
					$-1 > \psi > -3$
					$5,98 (1 - \psi)^2$

Plate with one free edge

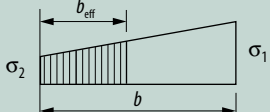
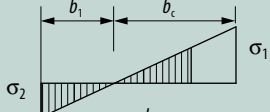
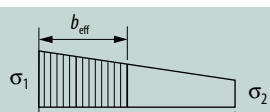
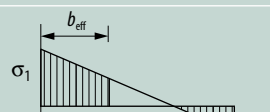
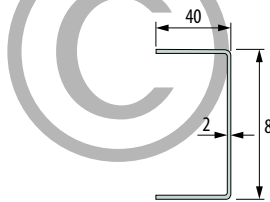
Stress distribution, positive compression			Effective width, exist				
			$1 > \psi > 0:$ $b_{\text{eff}} = \rho c$				
			$\psi < 0:$ $b_{\text{eff}} = \rho b_c = \rho c / (1-\psi)$				
$\psi = \sigma_2 / \sigma_1$	1	0	-1	$-1 > \psi > -3$			
Buckling coefficient, k_o	0,43	0,57	0,85	$0,57 - 0,21\psi + 0,07\psi^2$			
			$1 > \psi > 0:$ $b_{\text{eff}} = \rho c$				
			$\psi < 0:$ $b_{\text{eff}} = \rho b_c = \rho c / (1-\psi)$				
$\psi = \sigma_2 / \sigma_1$	1	$1 > \psi > 0$	0	$0 > \psi > -1$	-1		
Buckling coefficient, k_o	0,43	$0,578 / (\psi + 0,34)$	1,70	$1,7 - 5\psi + 17,1\psi^2$	23,8		

Figure 4.14: Effective width for parts supported along two longitudinal edges (on top) and for a free edge (on bottom).

Example 1

Determine the resistance with regard to bending of the C-profile, material yield point, $f_y = R_e = 700$ MPa.



From positive bending, the top flange is subjected to compressive stress and the web with a linearly varying stress. Each part of the cross-section is studied separately with regard to local buckling.

Upper flange:

1) Determine the cross-section class using *figure 4.12* (column 1). Part with one free edge and evenly distributed compression:

$$\frac{c}{t} = \frac{(40-2)}{2} = 19$$

Upper limit value for class 3

$$14 \sqrt{\frac{235}{700}} = 8,1$$

which means that the flange is in class 4. In *figure 4.10a* it is also clear that buckling needs to be considered.

2) The buckling coefficient is found in *figure 4.14*. Part supported by one free edge and evenly distributed compression:

$$\psi = 1 \rightarrow k_\sigma = 0,43$$

3) Now the slenderness of the flange can be calculated

$$\lambda_p = \frac{19}{28,4 \cdot \sqrt{\frac{235}{700}} \cdot \sqrt{0,43}} = 1,76$$

4) The reduction factor for plates with one free edge becomes

$$\rho = \frac{1,76 - 0,188}{1,76^2} = 0,5$$

See also *figure 4.10b*.

5) The effective width of the flange is calculated and distributed according to *figure 4.14*

$$b_{\text{eff}} = 0,5 \cdot b$$

Web:

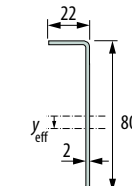
1) Determine the cross-section class using *figure 4.11* (column 3). Plates supported along two edges with varying stress; note that the neutral axis has moved 5 mm:

$$\frac{c}{t} = \frac{(80-2 \cdot 2)}{2} = 38$$

Upper limit value for class 3

$$\frac{42}{0,67 + 0,33 (-0,8)} \sqrt{\frac{235}{700}} = 60,0$$

which means that the web is in cross-section class 3 and no reduction for local buckling needs to be done. The effective cross-section, therefore, becomes in accordance with below. Note that the neutral layer has shifted.



An edge fold in accordance with figure below will prevent local buckling of the flange.

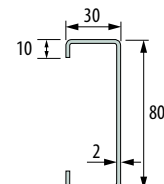


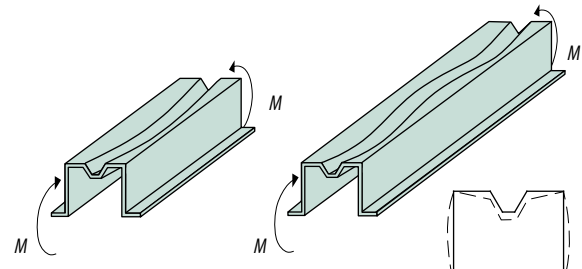
Figure 4.11 is now used in order to determine the cross-section class of the flange (column 2). Plate supported along two edges with evenly distributed pressure:

$$\frac{c}{t} = \frac{(30-2 \cdot 2)}{2} = 13$$

The upper limit value for cross-section class 2 is

$$38 \sqrt{\frac{235}{700}} = 22,0$$

which means that the flange is now in cross-section class 2 and does not need to be reduced. See also *figure 4.10a*. The stability of the edge fold, design of stiffener, is done in the next step.

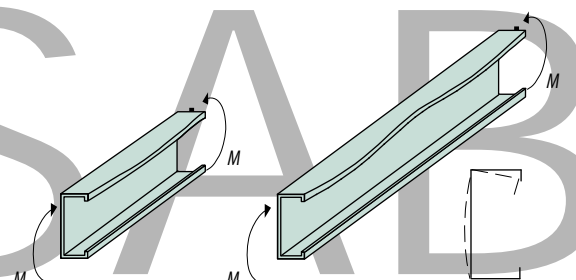


Design of stiffeners

Using edge folds and grooves is a way to stiffen slender parts. The geometry of the stiffener must be designed with regard to distortional buckling. Two common cases of distortion buckling are illustrated in *figure 4.15*; buckling of an edge fold in a C-profile and buckling of a groove in a hat-profile, both profiles subjected to bending.

The calculations are based on the theory of global buckling of a bar on an elastic support. The stiffener represents the bar and the resistance against distortion of the cross-section the elastic base. The calculation procedure described here results in an effective thickness for the stiffener if distortional buckling can occur. The aim should in most cases be to find a stiffener that is enough to support the cross-section from instability.

Figure 4.16 illustrates the cross-section data needed for the calculation and the procedure is, as follows.



Figur 4.15: Distortion buckling of beams subjected to bending.
a) buckling of a groove in a hat-profile
b) buckling of an edge fold in a C-profile

Calculation procedure

1) Determine the cross-section class for each part pursuant to *figure 4.11* or *4.12*.

Class 4 cross-section parts require calculation of effective widths.

2) Determine the critical buckling stress for global buckling of the stiffener, σ_{cr} , from *figure 4.16* depending on the type of stiffener and cross-section.

3) Determine the slenderness according to *equation 4.4*

$$\lambda_d = \sqrt{\frac{f_y}{\sigma_{cr,s}}}$$

where f_y is the material yield point.

4) The reduction factor for distortion buckling is calculated according to

$$\chi_d = 1,0 \quad \lambda_d \leq 0,65$$

$$\chi_d = 1,47 - 0,723 \lambda_d \quad 0,65 \leq \lambda_d \leq 1,38$$

$$\chi_d = \frac{0,66}{\lambda_d} \quad \lambda_d \geq 1,38$$

5) The effective thickness of the stiffener and adjacent parts, A_s , is calculated as

$$t_d = \chi_d \cdot t \quad (\text{Eq. 4.9})$$

6) When all slender cross-section parts have been reduced, the effective cross-section properties are calculated, A_{eff} , I_{eff} , W_{eff}

Example 2

Is an edge fold of 10 mm sufficient to offer full support to the flange from example 1?

1) The whole flange contributes (cross-section class 2) from before.

2) Determine the critical buckling stress using *figure 4.16*. C-profile with an edge fold subjected to bending:

$$b_{el} = 13 \text{ mm}$$

$$b_i = 24 \text{ mm}$$

$$I_s = 356 \text{ mm}^4$$

$$A_s = 46 \text{ mm}^2$$

$$\sigma_{cr} = \frac{1,05 \cdot 210 \cdot 10^9}{46 \cdot 10^6} \sqrt{\frac{356 \cdot 10^{-12} \cdot 0,002^3}{(0,024^2 \cdot 0,08 + 0,024^3)}} = 1045 \text{ MPa}$$

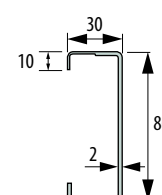
3) Calculate the slenderness

$$\lambda_d = \sqrt{\frac{700}{1045}} = 0,8$$

4) Reduction factor

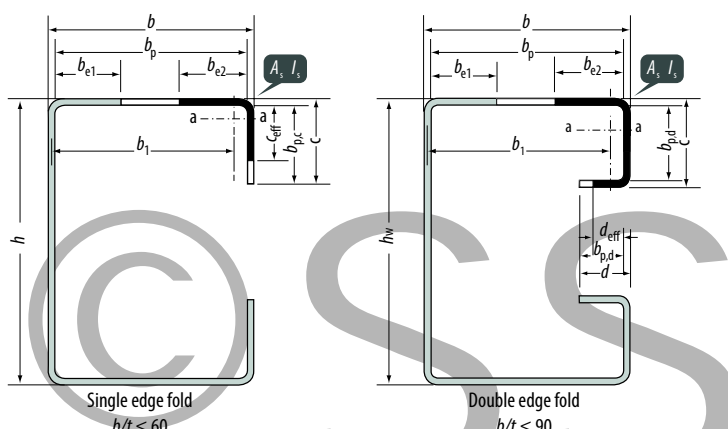
$$\chi_d = 1,47 - 0,723 \cdot 0,8 = 0,88$$

This means that the edge fold is not sufficient to offer full support and that the resistance is calculated with a reduced area according to figure.



By increasing the edge fold to 15 mm, the whole cross-section contributes during bending and the full potential of the material can be used.

Edge fold, symmetrical C- or Z-section



Normal force

$$\sigma_{ct} = \frac{1,05E}{A_s} \sqrt{\frac{I_s t^3}{(b_1^2 h_w + b_1^3 + 0,5 b_1^2 h_w)}}$$

Bending

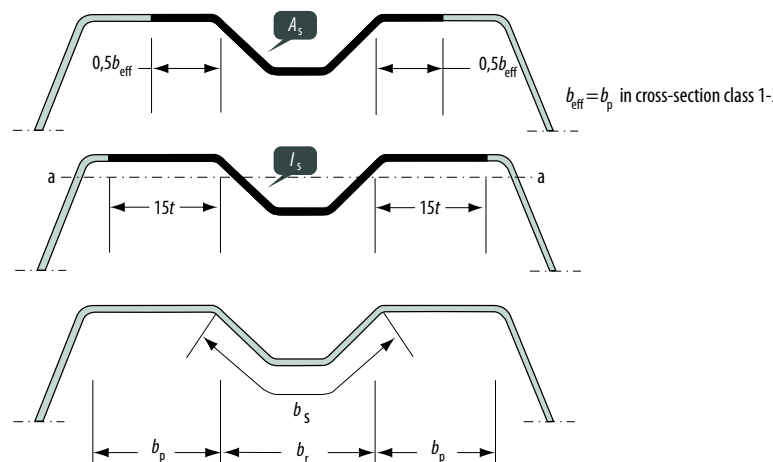
$$\sigma_{ct} = \frac{1,05E}{A_s} \sqrt{\frac{I_s t^3}{(b_1^2 h_w + b_1^3)}}$$

I_s – Moment of inertia for effective area with regard to a-a

$$b_{e1} = \frac{b_p}{2} \quad b_{e2} = \frac{b_p}{2} \quad (\text{Cross-section class 1-3})$$

$$b_{e1} = \frac{b_{\text{eff}}}{2} \quad b_{e2} = \frac{b_{\text{eff}}}{2} \quad (\text{Cross-section class 4})$$

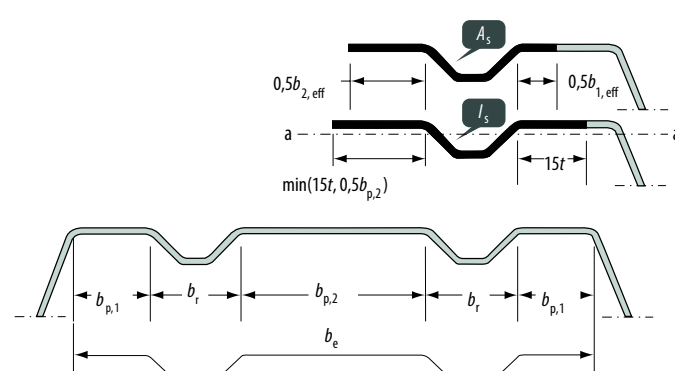
Intermediate groove(s)



One groove

$$\sigma_{ct,s} = \frac{4,2 E}{A_s} \sqrt{\frac{I_s t^3}{4 b_p^2 (2 b_p + 3 b_s)}}$$

I_s – Moment of inertia for effective area with regard to a-a



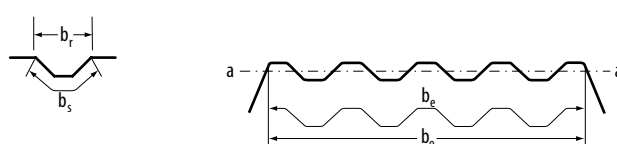
Two grooves

$$\sigma_{ct,s} = \frac{4,2 E}{A_s} \sqrt{\frac{I_s t^3}{8 b_e^2 (3 b_e - 4 b)}}$$

$$b_e = 2 b_{p,1} + b_{p,2} + 2 b_s$$

$$b = b_{p,1} + 0.5 b_r$$

I_s – Moment of inertia for effective area with regard to a-a



More grooves

$$\sigma_{ct,s} = 1,8 E \sqrt{\frac{I_s t}{b_0^2 z_e^3}} + 3,6 \frac{E t^2}{b_0^2}$$

I_s – Moment of inertia for gross area with regard to a-a

Figure 4.16: Cross-section properties for calculation of resistance with regard to distortion buckling.

Design with respect to local buckling of round tubes

Round tubes should be regarded as shell structures and are described in Eurocode 3, part 1-6 [4.11]. There are special requirements of initial imperfections and caution is recommended when dents strongly reduces the resistance and there is no post-critical area.

The resistance with respect to buckling in cross-section class 4 is calculated according to figure 4.13. The geometry of a round tube preserves its form until collapse and the resistance of slender tubes is calculated with a limited stress level. The calculation procedure for bended and axially loaded tubes, according to figure 4.17, is described here.

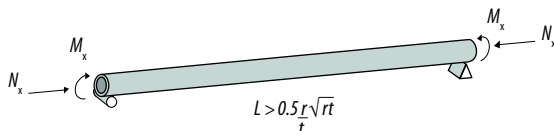


Figure 4.17: Circular tube loaded with a normal force and bending moment.

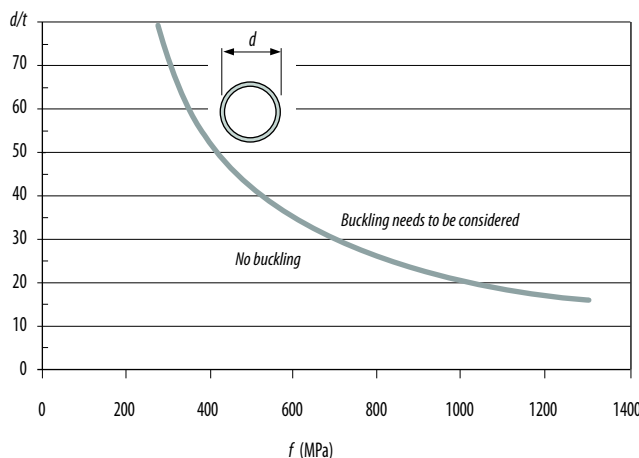


Figure 4.18 a: Maximum value of d/t for round pipe where design with regard to local buckling is not required.

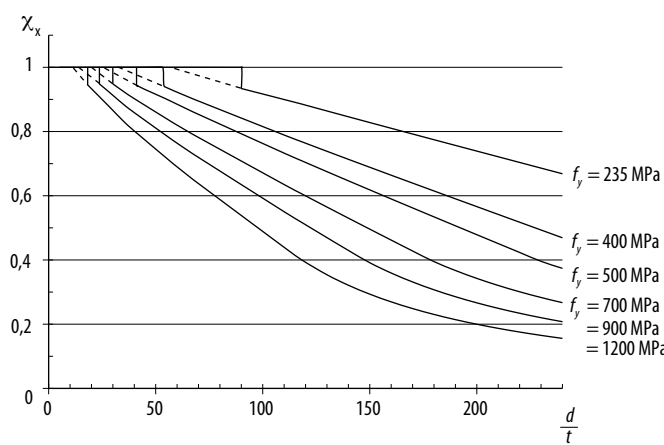


Figure 4.18 b: Reduction factor with regard to local buckling as a function of diameter and thickness.

Calculation procedure

Use figure 4.18a and 4.18b. When buckling needs to be taken into consideration can be determined in figure 4.18a; the reduction factor for design with respect to buckling is found in figure 4.18b. Full calculation of the design value is done according to point 5 below.

Alternatively, follow points 1 through 5.

1) Determine the cross-section class according to figure 4.13.

The permissible stress, $\sigma_{x,Rd}$, for cross-sections in class 4 is calculated according to point 5 below.

2) Determine the critical buckling stress, σ_{cr} , according to

$$\sigma_{cr} = 0.726 \cdot E \cdot \frac{t}{d} \quad (\text{Eqn. 4.10})$$

where

E – modulus of elasticity (210 GPa)

t – thickness (mm)

d – outer diameter (mm)

3) Determine the slenderness.

$$\lambda = \sqrt{\frac{f_y}{\sigma_{cr}}}$$

where

f_y – material yield point

4) The reduction factor, χ_x , for local buckling of a round pipe is calculated according to

$$\begin{aligned} \chi_x &= 1,0 & \lambda &\leq 0,2 \\ \chi_x &= 1-0,6 \left(\frac{\lambda-0,2}{\lambda_p-0,2} \right) & 0,2 < \lambda < \lambda_p \\ \chi_x &= \frac{\alpha}{\lambda^2} & \lambda_p \leq \lambda \end{aligned}$$

where

$$\alpha = \frac{0,62}{1 + \left(\frac{d}{208t} \right)^{0,72}}$$

$$\lambda_p = \frac{\alpha}{0,4}$$

5) Design value of the acting stress is

$$\sigma_{x,Rd} = \chi_x \cdot f_{yd} \quad (\text{Eqn. 4.11})$$

6) Resistance with regard to buckling is now calculated based on the cross-section magnitudes for gross cross-section and reduced design value of the acting stress.

Buckling between fastening points

The resistance of a spot welded or bolted section according to *figure 4.19* can be limited by buckling between the fastening points. The minimum distance, p_1 , according to *equation 4.12* prevents buckling of the plates separately and the double plate thickness can be used in slenderness calculation and resistance [4.12]. By placing the joint so that it is in tension, instability is avoided.

$$p_1 = t \sqrt{\frac{E}{\sigma_c}} \quad (\text{Eqn. 4.12})$$

where

E – modulus of elasticity (MPa)

σ_c – compressive stress in the current plate (MPa)

$$p_1 \leq 3 \cdot b$$

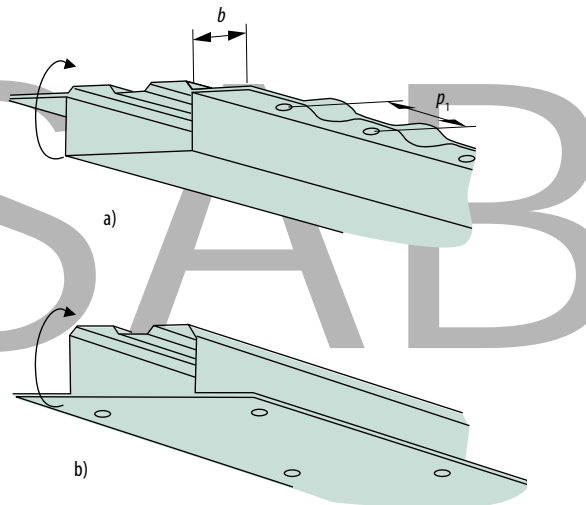


Figure 4.19: a) Buckling between fastening points in a compressed flange with one free edge, b) Place the joint on the tension side, if possible.

4.3.3 Elastic behavior in slender parts

Local buckling starts at a certain stress level in slender parts of a cross-section. After this the response from the structure is no longer linear, see point A in *figure 4.8*. A conservative approach for determining at what stress level this can be expected is presented in *table 4.2*. There is a post critical resistance in the structure after buckling starts, in particular for slender parts in high-strength steel. Practical testing and FEM calculations can give an answer to how much.

If the stress level does not exceed the values in *table 4.2*, the gross cross-section is used to calculate deformations, *figure 4.20*.

The effective, reduced, cross-section and the effective bending stiffness, EI_{eff} , is used for calculation of deformations in the ultimate limit state, i.e at point C in *figure 4.8*.

Calculation of the effective cross-section based on working stress instead of yield point gives the bending stiffness for load levels between A and C, *figure 4.8*.

Box flange web in compression (σ is indicated in MPa)	Web with varied stress (σ is indicated in MPa)	Free edge subjected to compression (σ is indicated in MPa)
$\sigma \leq 0.41 \cdot 10^6 \cdot \frac{t^2}{b^2}$	$\sigma \leq 3.6 \cdot 10^6 \cdot \frac{t^2}{b^2}$	$\sigma \leq 0.046 \cdot 10^6 \cdot \frac{t^2}{b^2}$

Table 4.2: Stress level in cross-section parts for linear behavior, σ in MPa.

This handbook contains general suggestions and information without any expressed or implied warranty of any kind. SSAB hereby expressly disclaims all liability of any kind, including any damages, in connection with the use of the information and for their suitability for individual applications. It is the responsibility of the user of this brochure to adapt the recommendations contained therein to the requirements of individual applications.

Load case	Deformation, d_{\max}
	$d_{\max} = \frac{FL^3}{48EI}$
	$d_{\max} = \frac{5qL^4}{384EI}$
	$d_{\max} = \frac{FL^3}{3EI}$
	$d_{\max} = \frac{qL^4}{8EI}$
	$d_{\max} = \frac{FL^3}{192EI}$
	$d_{\max} = \frac{qL^4}{384EI}$

Figure 4.20: Deformation calculations for elastic behavior.

4.3.4 Axial force

An axial force can be tensile or compressive. For tensile forces it is material- and cross-section properties that governs, whereas for compressive forces the resistance can be limited by instability. In design of compression members in a high-strength material several geometrical parameters are important for the possibility to utilize the yield stress, see *figure 4.22*. Local buckling of individual cross-section parts also needs to be checked.

Tension

The resistance with respect to tensile force, $N_{t,Rd}$, is calculated as

$$N_{t,Rd} = \frac{f_y A_g}{\gamma_M \gamma_n} \quad (\text{Eq. 4.13})$$

$$N_{t,Rd} = \frac{0,9 f_u A_{net}}{\gamma_M \gamma_n} \quad (\text{Eq. 4.14})$$

where

f_y – material yield point (MPa)

A_g – gross cross-section area (mm^2)

A_{net} – net cross-section area (with holes) (mm^2)

$\gamma_M \gamma_n$ – partial coefficients, see section 4.2.3

Compression

The resistance can be limited by global buckling (torsional, flexural and torsional-flexural) and/or local buckling depending on the cross-section geometry and the length of the member. The resistance is calculated according to

$$N_{b,Rd} = \frac{\chi A f_y}{\gamma_M \gamma_n} \quad \text{Cross-section class 1-3} \quad (\text{Eq. 4.15})$$

$$N_{b,Rd} = \frac{\chi A_{eff} f_y}{\gamma_M \gamma_n} \quad \text{Cross-section class 4} \quad (\text{Eq. 4.16})$$

where

A – cross-section area (mm^2)

A_{eff} – cross-section effective area, see section 4.3.2

f_y – material yield point (MPa)

$\gamma_M \gamma_n$ – partial coefficients, see section 4.2.2

χ – the reduction factor for global buckling, *figure 4.21*

$\chi < 1.0$ means that buckling must be considered.

Buckling curve	a	b	c
a	0,21	0,34	0,49
e ₀	300	250	200

Table 4.3: Imperfection factor and initial curvature.

The cross-section class is defined in section 4.1.2.

The reduction factor, χ , is based on the theoretically calculated critical load (torsional, flexural and torsional-flexural buckling), *figure 4.22*. Depending on type of cross-section this load has to be adjusted to fit real behavior, see *figure 4.22* and *4.23*. It is, above all, initial curvature and residual stresses that makes the theoretical value overestimate the final resistance. For tolerances regarding initial curvature and inclination, including the effect of residual stress, see *figure 4.23* or, alternatively, Eurocode 3, part 1-1 [4.3]. The tolerance for geometric curvature only is $L/750$.

Calculation procedure

1) Determine the cross-section class according to *figures 4.11* through *4.13*.

2) Determine the critical load, see *figure 4.22*.

3) Determine the slenderness, λ , which

$$\lambda = \sqrt{A f_y / N_{cr}} \quad \text{Cross-section class 1-3}$$

$$\lambda = \sqrt{A_{eff} f_y / N_{cr}} \quad \text{Cross-section class 4}$$

where

f_y – material yield point (MPa)

A – cross-section area (mm^2)

A_{eff} – cross-section effective area, see section 4.3.2

4) The reduction factor for global buckling is calculated according to

$$\chi = \frac{1}{\phi + \sqrt{\phi^2 - \lambda^2}} \quad \chi < 1 \quad (\text{Eq. 4.17})$$

where

$$\phi = 0,5(1+\alpha(\lambda-0,2)+\lambda^2)$$

α the imperfection factor, see *table 4.3*; the buckling curve is determined according to *figure 4.24*. See also *figure 4.21*.

5) The resistance is calculated according to *equation 4.15* or *4.16*.

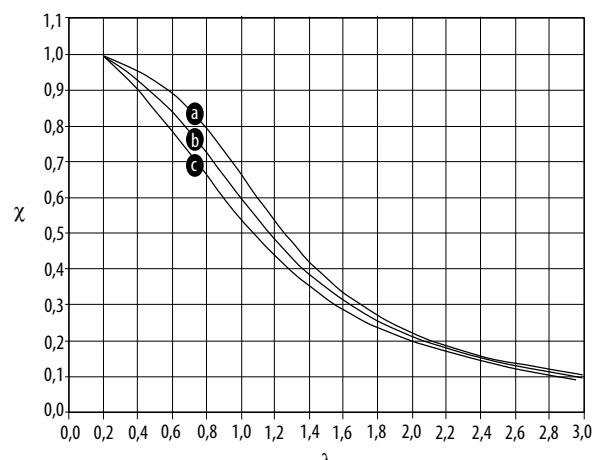
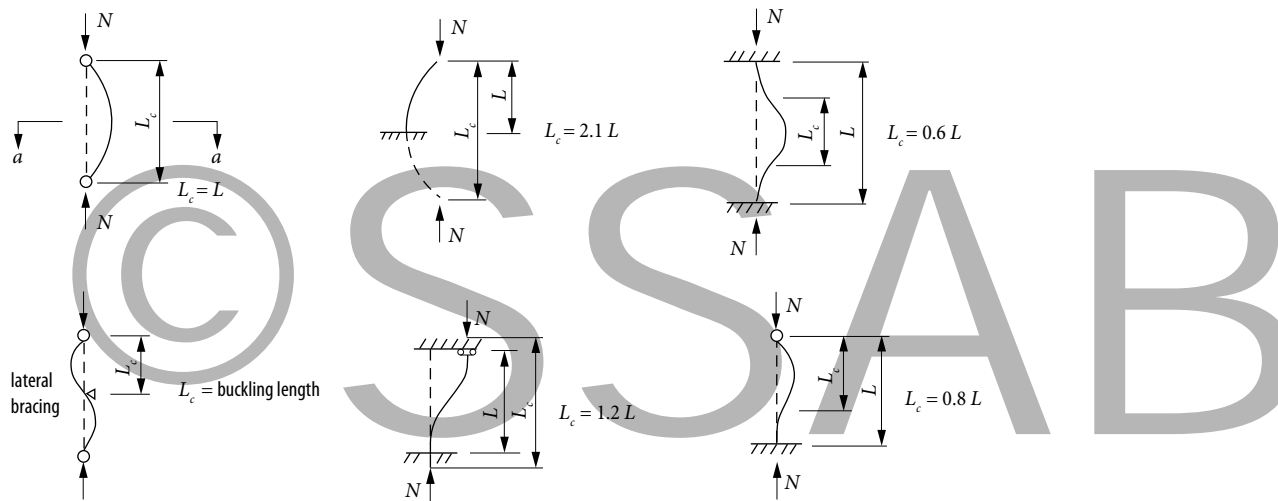


Figure 4.21: Reduction curves for different buckling curves. See also *figure 4.24*.

Global buckling

Under a compressive force, the whole length takes part in the instability. Boundary conditions and lateral bracing affect the buckling length (L_c) used in the resistance calculation. N_c is based on the gross cross-section, i.e., without any reduction, also in cross-section class 4. The governing buckling mode (flexural-, torsional- or torsional-flexural buckling) will be the lowest calculated value.

Buckling length



Flexural buckling

Buckling in one of the cross-section symmetry plane.

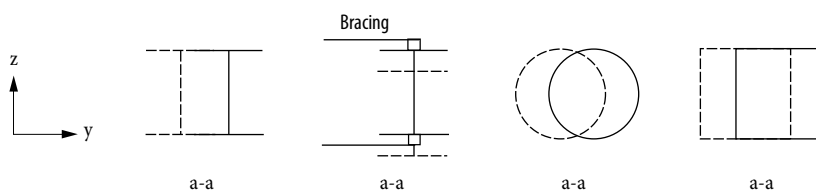
- For example, double-, polar symmetrical- and closed cross-sections.

$$N_{cr,z} = \frac{\pi^2 EI_z}{L_c^2}$$

I_z – moment of inertia in current buckling direction;

I_z – weak direction;

I_y – strong direction can govern in connection with bracing



Torsional buckling

The deformation during buckling takes place in the form of rotation/twisting.

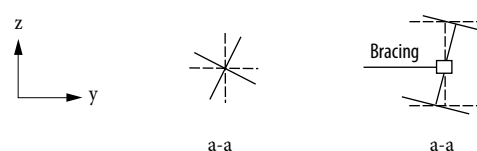
- For example, cross-sections with little torsional stiffness; certain open cross-sections and cross-sections according to the figure.

$$N_{cr} = \frac{A}{I_p} (C + \frac{\pi^2 C_w}{L_c^2})$$

$$I_p = I_y + I_z$$

C – GI_v torsional stiffness, see section 4.3.8

C_w – EI_w warping stiffness, see section 4.3.8



Torsional-flexural buckling

The deformation during buckling takes place in the form of bending and twisting.

- For example, single- and asymmetrical open cross-sections or braced cross-sections according to the figure.

For critical loads, refer to [4.5]

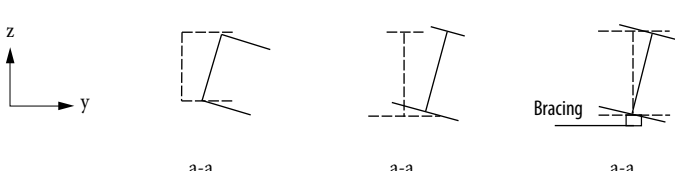
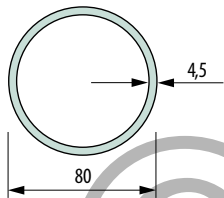


Figure 4.22: Calculation of critical load under axial compression.

This handbook contains general suggestions and information without any expressed or implied warranty of any kind. SSAB hereby expressly disclaims all liability of any kind, including any damages, in connection with the use of the information and for their suitability for individual applications. It is the responsibility of the user of this brochure to adapt the recommendations contained therein to the requirements of individual applications.

Example 3

Calculate the resistance of the circular tube with regard to an axial compression force, $L_c = 1,5$ m, and material yield point, $f_y = R_e = 275$ MPa.



1) Determine the cross-section class using figure 4.11.

$$\frac{d}{t} = \frac{80}{4,5} = 20$$

Upper limit value for cross-section class 1

$$50 \cdot \frac{235}{275} = 42,7$$

which means that the tube is in cross-section class 1 and yield stress can be used in the cross-section, i.e. local buckling is not a limitation. Check global buckling.

2) Determine the critical load according to figure 4.24.

$$I = \frac{\pi}{64} (80^4 - (80-2 \cdot 4,5)^4) = 0,76 \cdot 10^6 \text{ mm}^4$$

$$N_{cr} = \frac{\pi^2 \cdot 210 \cdot 10^9 \cdot 0,76 \cdot 10^6}{1,5^2} = 700,8 \text{ kN}$$

3) Determine the slenderness.

$$A = \frac{\pi}{4} (80^2 - (80-2 \cdot 4,5)^2) = 1067 \text{ mm}^2$$

$$\lambda = \sqrt{\frac{1067 \cdot 275}{700,8 \cdot 10^3}} = 0,65$$

4) Determine the reduction factor using figure 4.22 and table 4.4. Alternatively, directly from figure 4.23.

$$\alpha = 0,49$$

$$\phi = 0,5(1 + 0,49(1,86-0,2) + 1,86^2) = 0,82$$

$$\chi = \frac{1}{0,82 + \sqrt{0,82^2 - 0,65^2}} = 0,76$$

5) The resistance becomes

$$N_{b,Rd} = \frac{0,76 \cdot 1067 \cdot 275}{\gamma_m \gamma_n} = \frac{222,2}{1,2} = 185,1 \text{ kN}$$

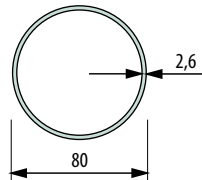
in safety class 3 (see table 4.1)

Upgrade the tube to a material with a yield point $f_y = 800$ MPa. The resistance should be the same.

Dent resistance is important to take into account for slender round tubes as such deformations will initiate local buckling. It is possible to calculate the material thickness necessary for preserving dent resistance, see section 4.5.1.

$$t_{HS} = 4,5 \sqrt{\frac{275}{800}} = 2,6 \text{ mm}$$

In this case calculate the resistance with $t_{HS}=2,6$ mm.



1) Determine the cross-section class using figure 4.11.

$$\frac{d}{t} = \frac{80}{2,6} = 30,7$$

Upper limit value for cross-section class 3

$$90 \cdot \frac{235}{700} = 26,4$$

which means that the tube belongs to cross-section class 4 and has to be calculated with regard to local buckling, see figure 4.18.

$$\frac{d}{t} = 30,7 \rightarrow \chi_x = 0,95$$

The permissible stress becomes

$$\sigma_{x,Rd} = \chi_x \cdot f_y = 0,95 \cdot 800 = 760 \text{ MPa}$$

2) Determine the critical load according to figure 4.24.

$$N_{cr} = 432,9 \text{ kN}$$

3) Determine the slenderness.

$$\lambda = 1,0$$

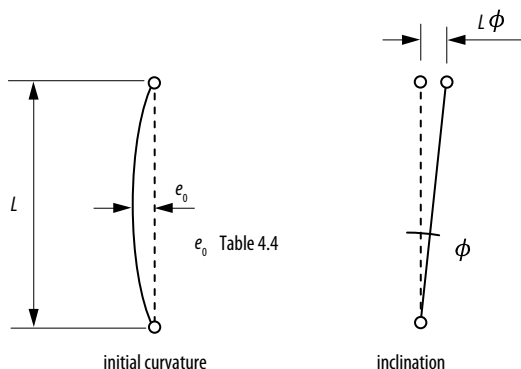
4) Determine the reduction factor using figure 4.22 and table 4.4 or, alternatively, directly from figure 4.23.

5) The resistance becomes

$$N_{b,Rd} = \frac{0,50 \cdot 632 \cdot 760}{\gamma_m \gamma_n} = \frac{237,6}{1,2} = 198,0 \text{ kN}$$

in safety class 3 (see table 4.1)

198,0 kN > 185,1 kN, which results in a matching resistance for the tube with $t = 2,6$ mm in a high-strength material, weight reduction is 42%.



$$\phi = \frac{1}{200}$$

For $4 \text{ m} < L < 9 \text{ m}$ the inclination tolerance decreases linearly to 1/300.

Figure 4.23: Tolerance value for inclination and curvature.

Global buckling

Residual stress in the cross-section affects the resistance. Different production methods and buckling directions thereby result in different design curves in figure 4.21.

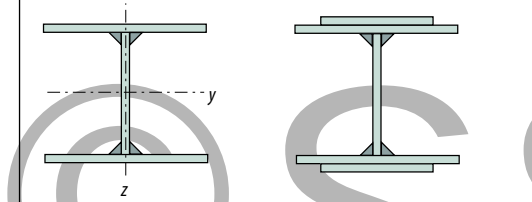
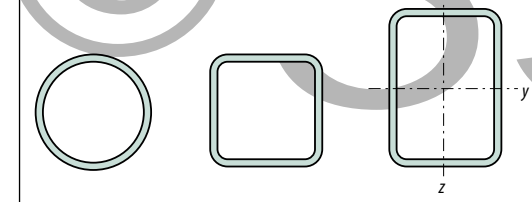
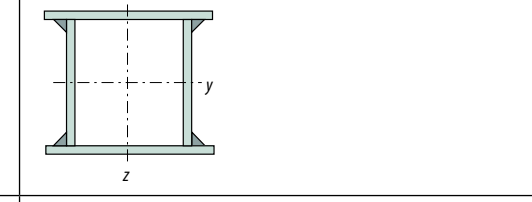
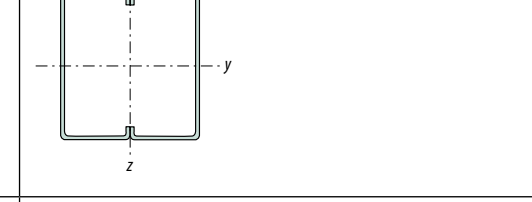
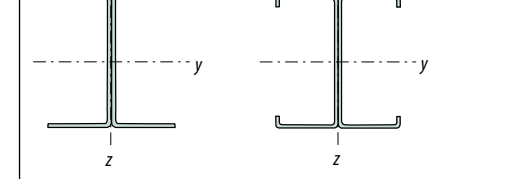
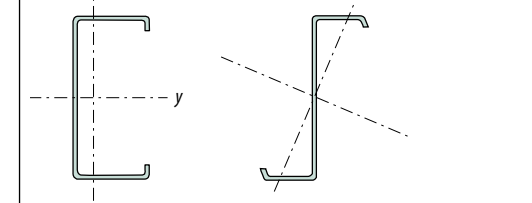
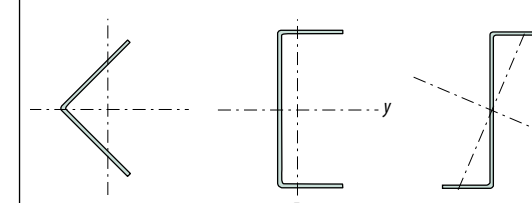
	Cross-section	Global buckling around axis	Buckling curve
Welded open cross-section		y - y z - z	b c
Cold-formed tubes		y - y z - z	c c
Welded closed cross-section		y - y z - z	b c
Cold-formed closed cross-section built-up		y - y z - z	b b
Cold-formed open cross-section built-up		y - y z - z	a b
Cold-formed open cross-section		y - y z - z	b b
Cold-formed open cross-section		y - y z - z	c c

Figure 4.24: Buckling curve for different types of cross-sections.

This handbook contains general suggestions and information without any expressed or implied warranty of any kind. SSAB hereby expressly disclaims all liability of any kind, including any damages, in connection with the use of the information and for their suitability for individual applications. It is the responsibility of the user of this brochure to adapt the recommendations contained therein to the requirements of individual applications.

4.3.5 Bending moment

Resistance with regard to bending can be limited by material yielding, global buckling (lateral-torsional buckling) and/or local buckling depending on the cross-section geometry and length of the beam.

In lateral-torsional buckling the compression flange becomes unstable twisting the whole cross-section. There are often different types of bracing which prevent lateral-torsional buckling, e.g., connection structural elements, see *figure 4.25*.

The resistance is calculated as

$$M_{c,Rd} = \chi_{LT} W_{pl} \cdot f_y / \gamma_M \gamma_n \quad \text{Cross-section class 1 and 2} \quad (\text{Eq. 4.18})$$

$$M_{c,Rd} = \chi_{LT} W_{el} \cdot f_y / \gamma_M \gamma_n \quad \text{Cross-section class 3} \quad (\text{Eq. 4.19})$$

$$M_{c,Rd} = \chi_{LT} W_{eff} \cdot f_y / \gamma_M \gamma_n \quad \text{Cross-section class 4} \quad (\text{Eq. 4.20})$$

where

$\gamma_M \gamma_n$ – are partial coefficients, see section 4.2.3

f_y – material yield point (Pa)

W_{pl} – section modulus corresponding to full plastic stress distribution (m^3)

W_{el} – section modulus corresponding to elastic stress distribution (m^3)

W_{eff} – section modulus calculated across the effective cross-section (m^3) according to section 4.3.2

χ_{LT} – reduction factor for lateral-torsional buckling

$\chi_{LT} = 1.0$ means that lateral-torsional buckling does not limit the resistance.

Lateral-torsional buckling can limit the design for high open cross-sections exposed to bending in a strong direction. It does not need to be taken into consideration for beams where the compression flange is braced laterally, for bending only around the weak axis or for closed cross-sections with $h/b \leq 1.5$.

Cross-section	Height/width ratio	Buckling curve
Rolled sections	$h/b \leq 2$ $h/b > 2$	b c
Welded sections	$h/b \leq 2$ $h/b > 2$	c d
Other	–	d

Table 4.4: Selection of lateral-torsional buckling curve for cross-section.

The reduction factor, χ_{LT} , is based on a theoretically calculated critical lateral-torsional buckling moment which is adjusted depending on cross-section type, the same procedure as for global buckling. Initial curvature and residual stresses causes the critical lateral-torsional buckling moment to overrate the resistance.

Calculation procedure

- Determine the cross-section class according to section 4.3.2. The effective cross-section for class 4 cross-sections is calculated according to *figures 4.11 through 4.13*.
- Determine the critical lateral-torsional buckling moment M_{cr} according to *figure 4.25*.

If lateral-torsional buckling is not relevant, proceed to point 5, $\chi_{LT} = 1.0$.

- Determine the slenderness λ as

$$\lambda = \sqrt{W_{el} f_y / M_{cr}} \quad \text{Cross-section class 1-3}$$

$$\lambda = \sqrt{W_{eff} f_y / M_{cr}} \quad \text{Cross-section class 4}$$

where

f_y – material yield point (Pa)

W_{el} – elastic section modulus (m^3)

W_{eff} – effective section modulus (m^3), see section 4.3.2

- The reduction factor for lateral-torsional buckling is calculated according to

$$\chi_{LT} = \frac{1}{\Phi_{LT} + \sqrt{\Phi_{LT}^2 - \beta \lambda_{LT}^2}} \quad (\text{Eq. 4.21})$$

where

$$\Phi_{LT} = 0.5(1 + \alpha_{LT}(\lambda - 0.2) + \lambda^2)$$

$$\Phi_{LT} = 0.5[1 + \alpha_{LT}(\lambda_{LT} - \lambda_{LT,0}) + \beta \lambda_{LT}^2]$$

The imperfection factor is the same as for global buckling, *table 4.3*; the curve is determined according to *table 4.4*.

$$\lambda_{LT,0} = 0.4$$

$$\beta = 0.75$$

χ_{LT} can never be more than 1

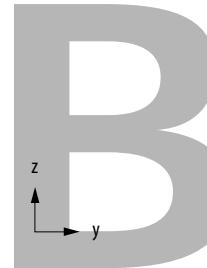
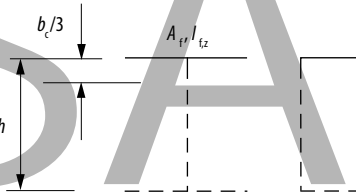
- The resistance is calculated according to *equations 4.18 through 4.20*.

Lateral-torsional buckling

If a beam with an open cross-section is subjected to transverse loads and/or bending moment in a strong direction, it can experience lateral-torsional buckling. The calculation of the critical lateral-torsional buckling moment, M_{cr} , is not trivial. There are solutions, for example in [4.10]. M_{cr} is based on the gross cross-section, i.e., no reduction in cross section class 4.

The critical buckling moment, M_{cr} , can be calculated conservatively from a critical stress level referring to lateral buckling of the compression flange. Buckling between lateral bracing according to the figure below, gives the critical stress

$$\sigma_{cr} = m \cdot \frac{\pi^2 EI_{f,z}}{L_c^2 A_f}$$



where

I_{fz} – the moment of inertia for global buckling around the z-axis for a flange, including part of the web, $b_c/3$

b_c – compression zone

h – beam height

L_c – buckling length in accordance with below

m – factor depending on moment distribution in accordance with the table

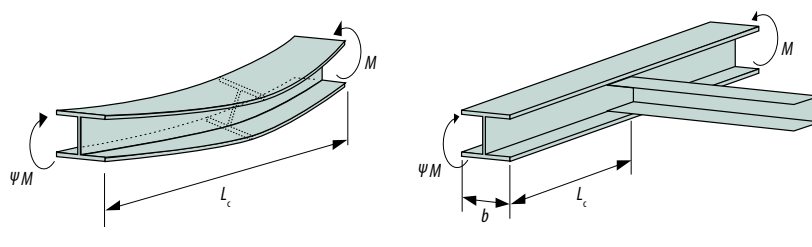
The critical moment for symmetrical cross-sections can then be calculated as

$$M_{cr} = m \cdot \frac{\pi^2 EI_{f,z}}{L_c^2} \cdot h \quad (\text{Ekv 4.22})$$

where

m – factor which takes moment distribution into consideration, see the table below

Moment distribution	m
	1.0
	$\frac{1.8}{(1+0.89\psi)}$
	1.3



Symmetrical I-beams do not experience lateral-torsional buckling if

$$\frac{L_c}{b} \leq 1.2(0.6-0.2\Psi-0.1\Psi^2)\sqrt{\frac{E}{f_y}}$$

C-sections do not experience lateral-torsional buckling if

$$\frac{L_c}{i_f} \leq 4.2(0.6-0.2\Psi-0.1\Psi^2)\sqrt{\frac{E}{f_y}}$$

Figure 4.25: Lateral-torsional buckling, calculation of critical lateral-torsional moment.

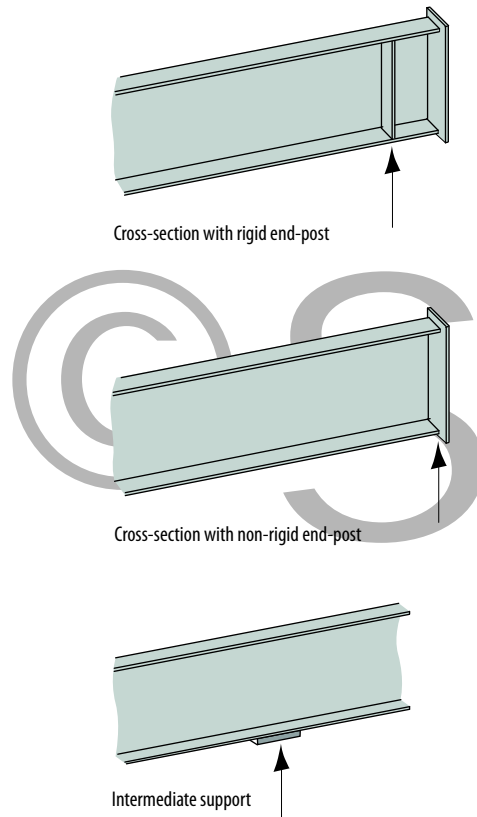


Figure 4.26: Different design of beam end and intermediate support.

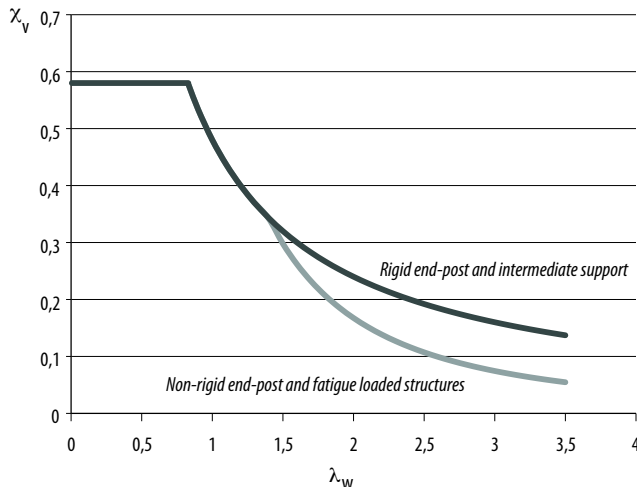


Figure 4.27: Reduction factor for cold formed sections and welded profiles with regard to shear buckling, table 4.5.

4.3.6 Shear force

Resistance with regard to shear force can be limited by material yielding or shear buckling, which depends on cross-section geometry. At load introduction or support shear forces are often high and detailing is of important for the final resistance, see *figure 4.26*. Patch loading can be the failure mode when there are no stiffeners, see section 4.3.7. The resistance is calculated differently depending on if the web is inclined or not, see *figure 4.28*.

$$V_{b,Rd} = \chi_v \frac{S_w t f_y}{\gamma_M \gamma_n} \quad (\text{Eqn. 4.23})$$

or

$$V_{b,Rd} = \chi_v \frac{h_w t_w f_y}{\gamma_M \gamma_n} \quad (\text{Eqn. 4.24})$$

where

f_y – material yield point (MPa)

h_w – web height (mm), see *figure 4.28*

s_w – web inclined height (mm), see *figure 4.28*

t – web thickness (mm)

$\gamma_M \gamma_n$ – partial coefficients, see section 4.2.3

χ_v – reduction factor for shear buckling, see *figure 4.27* or *table 4.6*.

$\chi_v = 0.58$ means that shear buckling does not limit the resistance.

χ_v is based on the slenderness of the web and a cross-section design which includes stiffeners in the form of grooves or welded plates.

Calculation procedure

- 1) Determine the slenderness of the web, λ_w , according to *figure 4.28*.
- 2) Determine the reduction factor based on *figure 4.27* or, alternatively, *table 4.5* for cold-formed and built-up welded sections.
- 3) The resistance is calculated according to *equation 4.23* or *4.24*.

Slenderness of the web according to <i>figure 4.28</i>	Non-rigid end post and fatigue load	Rigid end-post and intermediate support
$\lambda_w \leq 0,83$	0,58	0,58
$0,83 < \lambda_w < 1,40$	$0,48/\lambda_w$	$0,48/\lambda_w$
$\lambda_w \geq 1,40$	$0,67/\lambda_w^2$	$0,48/\lambda_w$

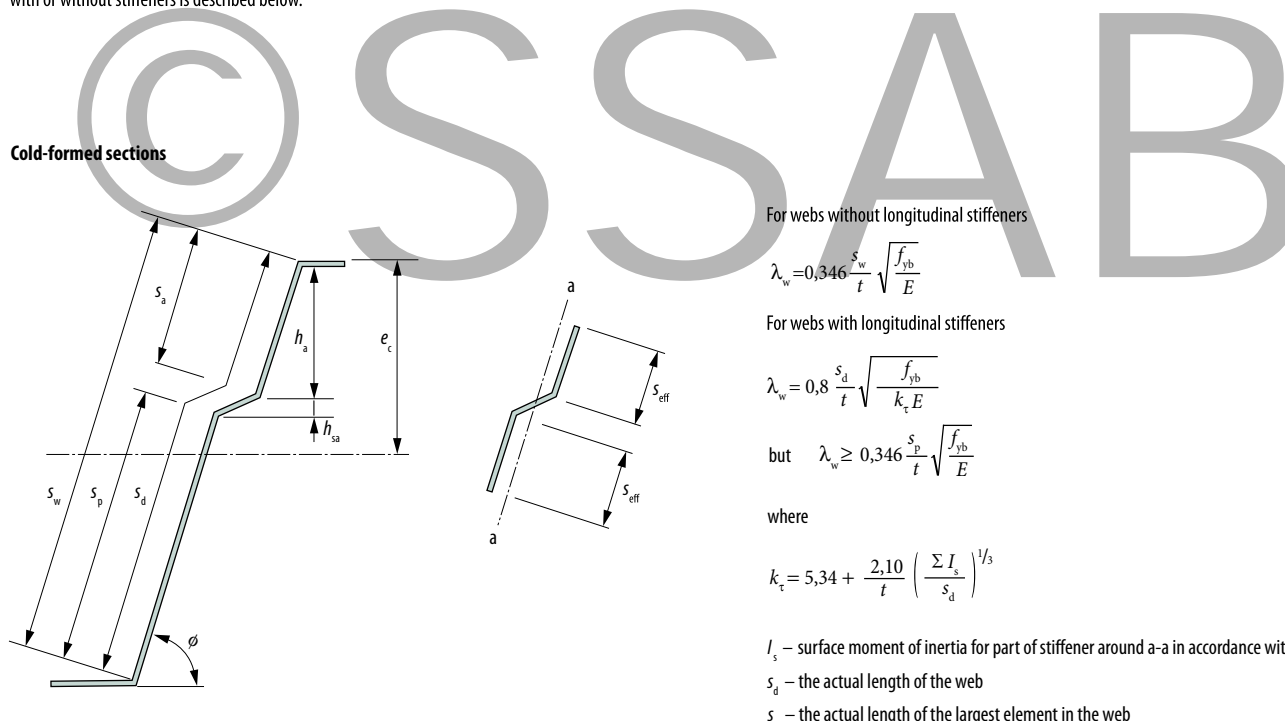
Table 4.5: Reduction factor for cold-formed sections with regard to shear buckling.



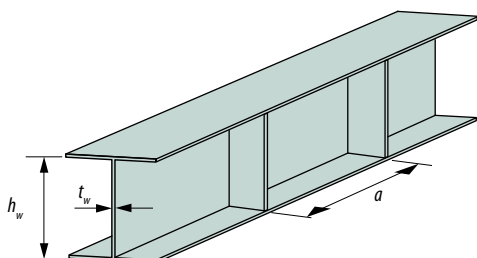
Shear buckling of container side.

Shear buckling

The resistance with regard to shear force is affected by grooves and welded stiffeners. A calculation of slenderness with or without stiffeners is described below.



Welded sections



For webs without stiffeners

$$\lambda_w = 0,346 \frac{h_w}{t_w} \sqrt{\frac{f_{yb}}{E}}$$

For webs with transverse longitudinal stiffeners according to figure

$$\lambda_w = 0,8 \frac{h_w}{t_w} \sqrt{\frac{f_{yb}}{k_t E}}$$

where

$$k_t = 5,34 + 4 \left(\frac{h_w}{a} \right)^2 \text{ for } \frac{a}{h_w} \geq 1$$

$$k_t = 4 + 5,34 \left(\frac{h_w}{a} \right)^2 \text{ for } \frac{a}{h_w} < 1$$

For contributions of horizontal web stiffeners, see Eurocode 3, part 1-5 [4.2]

Figure 4.28: Slenderness calculations with regard to shear buckling of shear force.

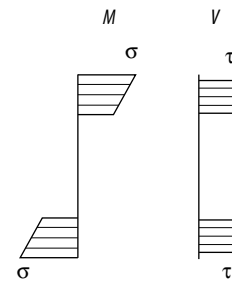
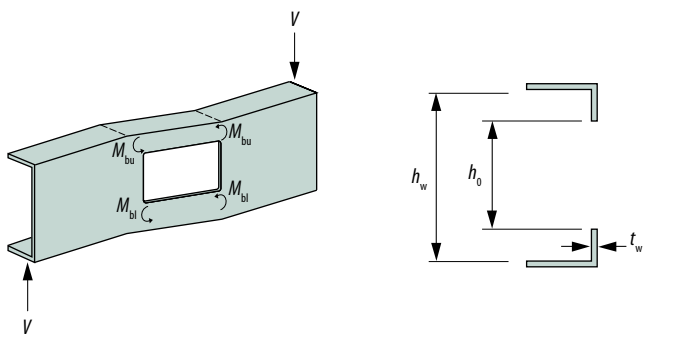


Figure 4.29: Beam with a hole in the web.

Large web openings/holes

For webs with openings/holes has a minor effect on the moment resistance but can significantly reduce shear force. Instability can be a design requirement for thin high-strength structures.

Moment and shear force resistance are calculated for the net cross-section where the shear force is absorbed by the remaining part of the web. The cross-section class is checked for compressed parts where the web is treated like a part with one free edge according to section 4.3.2.

With a slender web where

$$\frac{h_w}{t_w} > 72 \sqrt{\frac{235}{f_y}} \quad (\text{Eq. 4.25})$$

the shear force resistance is limited by shear buckling and the resistance is calculated as;

$$V_{R,d} = \chi_v \left(1 - \frac{\sqrt{h_0 l_0}}{h_w}\right) \cdot h_w t_w f_y \quad (\text{Eq. 4.26})$$

where

- f_y – material yield point (MPa)
- χ_v – reduction factor for shear buckling according to 4.27
- h_0 – height of the hole (mm), see figure 4.29
- l_0 – length of the hole (mm), see figure 4.29
- h_w – web height (mm)
- t_w – web thickness (mm)

For long web openings subjected to shear, local bending (so-called Vierendeel bending) has to be added to the net cross-section due to significant shear deformations, see figure 4.29. The shear force resistance must then also be checked with regard to equation 4.27.

$$V_b = \frac{2M_{bl} + 2M_{bu}}{l_0} \quad (\text{Eq. 4.27})$$

where

- M_{bl} – moment resistance (kNm), see figure 4.29
- M_{bu} – moment resistance (kNm), see figure 4.29
- l_0 – length of the hole (mm)

In long web openings, the compression part of the cross-section may need to be checked for global buckling (torsional buckling or y, z alignment). In circular holes, the latter can take place only in extreme cases.

There can also be instability vertically in the web between the holes when the holes are close to each other.

4.3.7 Load introductions and support

Load introductions should be designed to prevent local bending of the plate. For example, a vertical load on a beam should be placed in direct connection to the web or via a load distribution plate, see figure 3.10.

Local resistance at load introductions and supports, referred to as patch loading, can be limited by instability, see figure 4.30. The load distribution is of significant importance for slender webs in high strength material. Resistance with regard to patch loading is treated differently for cold-formed thin plate sections and welded beams.

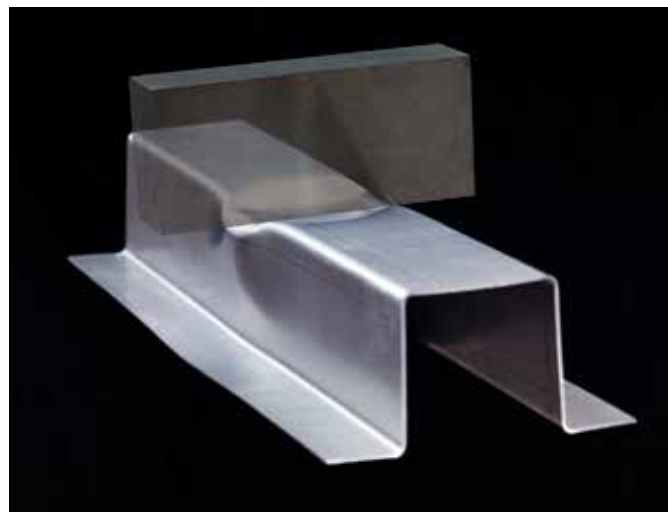


Figure 4.30: Patch loading during load introduction in slender webs.

Load introductions in cold-formed sections

Figure 4.31 displays different forms of cross-sections and designations. Resistance with regard to patching loading is calculated per web according to equation 4.28.

$$R_{wd} = \alpha \cdot t^2 \cdot \sqrt{f_y E} \cdot (2,4 + (\frac{\phi}{90})^2) \cdot (1 - 0,1 \sqrt{\frac{r}{t}}) \cdot (0,5 + \sqrt{0,02 \frac{l_s}{t}}) \quad (\text{Eqn. 4.28})$$

where

- f_y – material yield point (MPa)
- r – inner bending radius for bending against support (mm)
- ϕ – angle of inclination (deg) for web with regard to flange, see figure 4.31
- l_s – effective support width (mm), see below
- α – coefficient depending on the type of support and cross-section

α for external support, $c < 1.5 h_w$ in figure 4.32

- $l_s = 10$ mm (independent of the actual length)
- $\alpha = 0.075$ (sections where the flanges are braced laterally plus troughed sheet)
- $\alpha = 0.057$ (other sections)

α for internal support, $c < 1.5 h_w$ in figure 4.32

- l_s , see figure 4.32, however, $l_s < 200$ mm
- $\alpha = 0.15$ (sections where the flanges are braced laterally plus troughed sheet)
- $\alpha = 0.115$ (other sections, including cross-sections with one web such as C- or Z-sections)

This is a deviation from Eurocode 3 [4.13]).

Equation 4.28 is multiplied by a factor κ for webs with folds

$$\kappa_{a,s} = 1,45 - 0,05 \frac{e_{\max}}{t}$$

$$\kappa_{a,s} < 0,95 + 35000 \frac{t^2 e_{\min}}{b^2 s_p}$$

where

- b_d – width of loaded flange (mm), see figure 4.31
- s_p – distance to the nearest web groove (mm), see figure 4.31
- e_{\max} – maximum distance (mm) according to figure 4.31
- e_{\min} – minimum distance (mm) according to figure 4.31

The expressions for patch loading of cold-formed webs are based on testing.

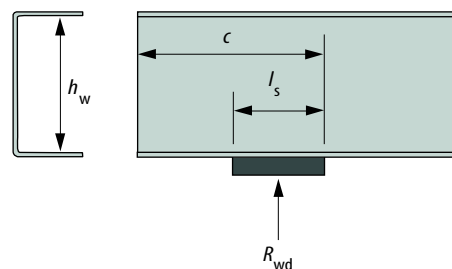


Figure 4.32: Distance to the free end and width of load introduction or support force.

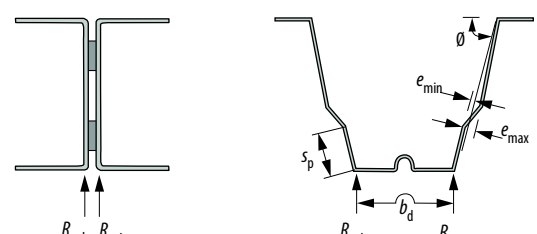
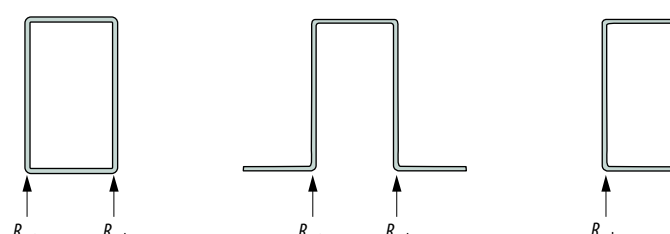


Figure 4.31: Load introductions and support force for sections with one or more webs.

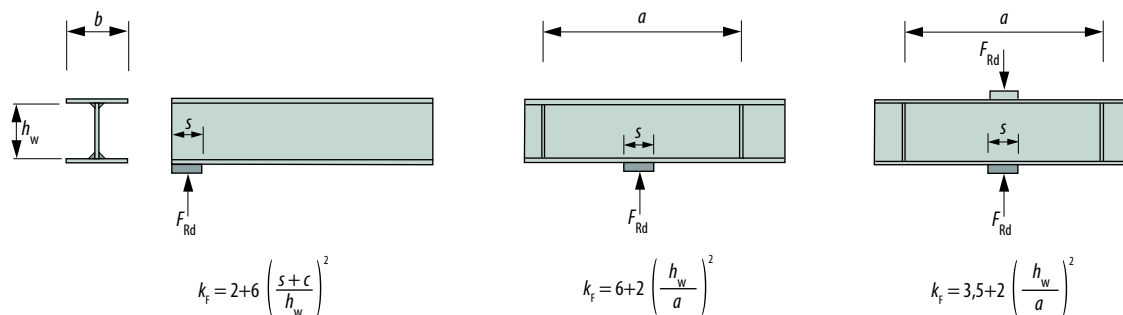


Figure 4.33: Patch loading of web in connection with load introductions and support for welded sections.

Load introduction in welded beams

The resistance can be limited by material yielding or instability. Figure 4.33 displays different load situations and designations. Resistance is calculated per web according to equation 4.29. See also [4.40]

$$F_{Rd} = \chi_F f_y l_y t_w \quad (\text{Eq. 4.29})$$

where

- f_y – material yield point (MPa)
 - l_y – effective support length (mm), see figure 4.33
 - t_w – web thickness (mm)
 - χ_F – reduction factor for patch loading
- $\chi_F = 1.0$ means that material yield point can be reached

Calculation procedure

- 1) Determine the critical load, F_{cr} , with regard to patch loading, k_f , according to figure 4.33.

$$F_{cr} = 0,9 k_f E \frac{t_w^3}{h_w} \quad (\text{Eq. 4.30})$$

- 2) Determine the slenderness, λ_F , as

$$\lambda_F = \sqrt{\frac{f_y \cdot l_y \cdot t_w}{F_{cr}}}$$

where

$$l_y = s + 2t_f \left(1 + \sqrt{\frac{f_y b_f}{f_{yw} t_w}} \right)$$

- 3) The reduction factor for patch loading is calculated according to

$$\chi_F = \frac{1}{\phi_F + \sqrt{\phi_F^2 - \lambda_F^2}} \leq 1.0 \quad (\text{Eq. 4.31})$$

where

$$\phi_F = 0,5(1+0,5(\lambda_F - 0,6) + \lambda_F)$$

- 4) The resistance is calculated according to equation 4.29

4.3.8 Torsion moment

A torsional moment can be applied direct load on a structure or as an effect of eccentricity or such.

Torsion results in shear stresses; and for open cross-sections also normal stress. The so-called Saint-Venant torsion results only in shear stress according to figure 4.34 a, whereas Vlasov torsion results in both shear and normal stress according to figure 4.34 b-c. Normal stress is often overlooked but can be very substantial and affect the resistance, in particular, in connection with fatigue loads.

Pure torsion of a massive or closed section results mainly in Saint-Venant shear stress, see figure 4.35 a. When a beam with an open section is twisted so-called warping will take place, see figure 4.35 b. If the warping is prevented, shear and normal stress arise in the flanges, so-called Vlasov stress pursuant to figure 4.35 c. Warping is normally prevented by the connecting parts of a structure. The degree of Vlasov stress generally increases with reduction in plate thickness and this phenomenon is particularly important to consider for open cross-section in upgrading from a mild to a high-strength.

The types sometimes occur simultaneously, so-called mixed torsion. This can be decided with a parameter, α .

For $0.05 \leq \alpha \leq 20$, the design is for mixed torsion.

$$\alpha = 0.04 \frac{I_v}{I_w} L^2 \quad (\text{Eq. 4.32})$$

where

- I_v – the cross-section factor of torsional stiffness (mm^4), see figure 4.36
- I_w – the cross-section factor of warping stiffness (mm^4), see figure 4.36
- L – beam length

In most cases, closed cross-sections can be designed for Saint-Venant stress and open cross-sections for Vlasov stresses.

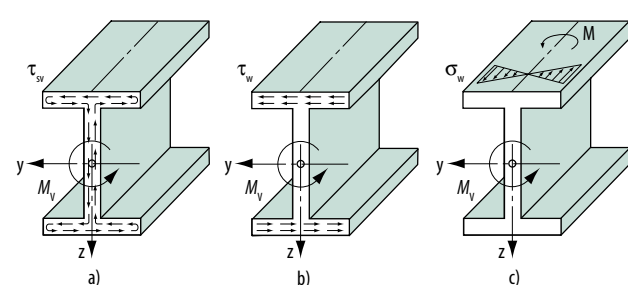


Figure 4.34: Stress distribution from torsion: a) shear stress in cross-section, b) shear stress in flange, c) normal stress in flange.

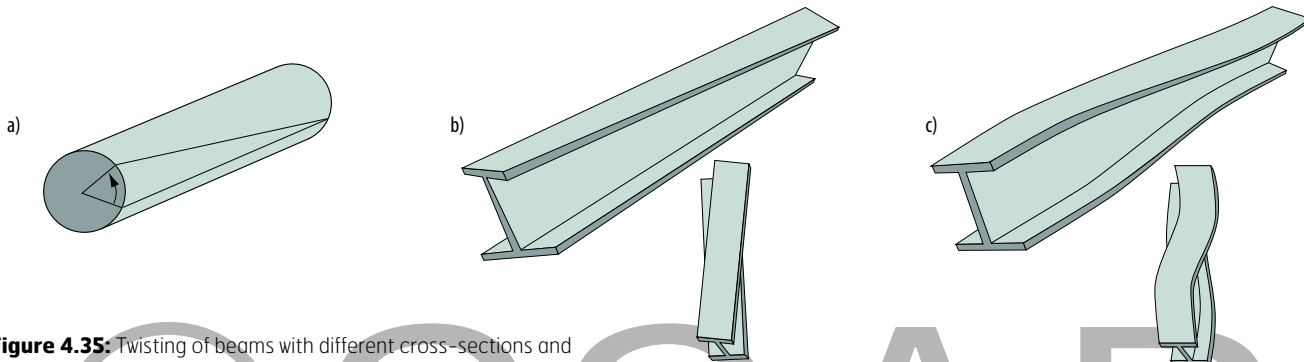


Figure 4.35: Twisting of beams with different cross-sections and boundary conditions

- a) Massive cross-sections – no warping (Saint-Venant)
- a) Open thin-walled cross-sections – free warping (Saint-Venant)
- a) Open thin-walled cross-sections – prevented warping (Vlasov)

Closed cross-sections

Resistance with regard to torsional moment is calculated with regard to shear stress, *figure 4.34 a*), and is limited by material yielding or shear buckling. For stress calculations, see section 4.3.9.

The resistance is calculated according to *equation 4.33*.

$$M_{v,Rd} = \chi_v \cdot W_v \cdot f_y / \gamma_M \gamma_n \quad (\text{Eq. 4.33})$$

where

f_y – material yield point (Pa)

W_v – cross-section elastic torsional resistance (m^3), see *figure 4.38*

$\gamma_M \gamma_n$ – partial coefficients, see section 4.2.3

χ_v – reduction factor according to section 4.3.6.

$\chi_v = 0.58$ means that shear buckling does not limit the resistance

Determine the reduction factor, χ_v , from *figure 4.27* for the part of the cross-section with the highest slenderness, λ_w , according to *figure 4.28*.

Open cross-sections

In most cases, resistance with regard to torsional moment is determined by normal stress from restrained warping, *figure 4.35 c*). Shear stress can govern for very short beams. The stress calculations are described in section 4.3.9.

Resistance with regard to normal stress is calculated according to *equation 4.34*

$$M_{v,Rd} = \frac{\eta_w}{L} \cdot W_w \cdot f_y / \gamma_M \gamma_n \quad (\text{Eq. 4.34})$$

where

f_y – material yield point (Pa)

η_w – coefficient according to *figure 4.36*

W_w – cross section elastic warping resistance (m^3), see *figure 4.38*

L – beam length (m)

$\gamma_M \gamma_n$ – partial coefficients, see section 4.3.2

Varying cross-sections along beam

In cases with variations in stiffness along the beam, *figure 4.38*, the different parts can be regarded separately. Weaker parts can be described as fixed to the stiffer parts whereas the weaker parts only offer vertical support. Changes in torsional stiffness should be avoided from a structural point of view, see *figure 4.38*, since it can cause high local stress.

Boundary conditions and load	η_w
	8
	2
	1
	4

Figure 4.36: Relation between the external twisting moment and the internal moment in the flanges from prevented warping.

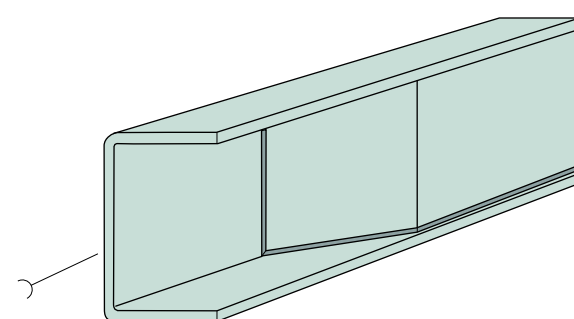


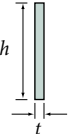
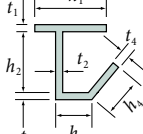
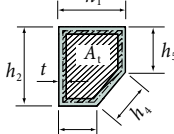
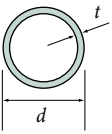
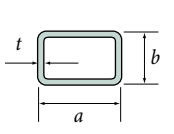
Figure 4.37: Suitable transition between a soft and a stiff structural component.

Torsional stiffness and torsional resistance in cross-sections

I_v – torsional stiffness (mm^4)

W_v – elastic torsional resistance (mm^3)

Z_v – plastic torsional resistance (mm^3)

				
$I_v = c_1 h t^3$	$I_v = \sum h_n t^3 / 3$	$I_v = 4A_t^2 t / \sum h_n$	$I_v = \pi(d-t)^3 t / 4$	$I_v = 2a^2 b^2 t / (a+b)$
$W_v = c_2 h t^2$	$W_v = I_v / t_{\max}$	$W_v = 2A_t t$	$W_v = \pi(d-t)^2 t / 2$	$W_v = 2abt$
$Z_v = \sum h_n t_n^2 / 2$	$Z_v = W_v$	$Z_v = W_v$	$Z_v = W_v$	$Z_v = W_v$

b/t	1	1,5	2	4	8	20	∞
c1	0.141	0.196	0.229	0.281	0.307	0.323	0.333
c2	0.208	0.231	0.246	0.282	0.307	0.323	0.333

Warping stiffness and warping resistance in cross-sections

I_w – warping stiffness (mm^4)

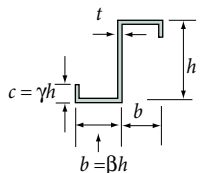
W_w – elastic warping resistance (mm^4)

Z_w – plastic warping resistance (mm^4)

The warping stiffness for a random open cross-section is calculated using sector coordinates [4.14].

The results for certain common cross-sections are presented here.

The warping stiffness is negligible compared to the torsional stiffness for a closed cross-section.



$$I_w = (ht/3) [(3 + 2\zeta) \omega_1^2 + 2(\beta + \gamma - \zeta) \omega_2^2 + 2\gamma \omega_3 (\omega_2 + \omega_3)]$$

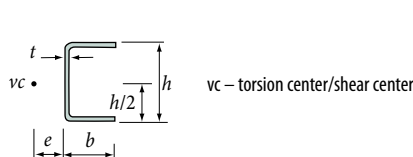
$$\zeta = \beta[\beta + 2\gamma(1 + \gamma)]/[1 + 2(\beta + \gamma)]$$

$$\omega_1 = \zeta h^2/2$$

$$\omega_2 = (\beta - \zeta) h^2/2$$

$$\omega_3 = \omega_2 + \gamma \zeta h^2$$

$$W_w = I_w / \omega_3$$



$$I_w = b^2 h^2 t_f (2b - 3e) / 12$$

$$e = 3b^2 / (6b + h)$$

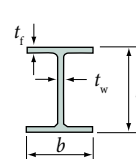
$$\epsilon = 3\beta^2 / (1 + 6\beta)$$

$$\beta = b/h$$

$$\omega_1 = \epsilon h^2/2$$

$$\omega_2 = (\beta - \epsilon) h^2/2$$

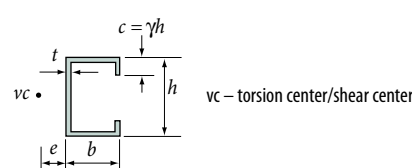
$$W_w = I_w / \omega_2$$



$$I_w = b^3 h^2 t_f / 24 = I_z (h/2)_2$$

$$W_w = b^2 h t_f / 6 = W_z h/2$$

$$Z_w = b^2 h t_f / 4 = Z_z h/2$$



$$I_w = (ht/3) [(1 + 2\epsilon) \omega_1^2 + 2(\beta + \gamma - \epsilon) \omega_2^2 + 2\gamma \omega_3 (\omega_2 + \omega_3)]$$

$$\epsilon = \epsilon h$$

$$\epsilon = \beta [2\gamma (3 - 4\gamma^2) + 3\beta] / [1 + 2\gamma (4\gamma^2 - 6\gamma + 3) + 6\beta]$$

$$\beta = b/h$$

$$\omega_1 = \epsilon h^2/2$$

$$\omega_2 = (\beta - \epsilon) h^2/2$$

$$\omega_3 = \omega_2 + \gamma (\beta + \epsilon) h^2$$

$$W_w = I_w / \omega_3$$

Figure 4.38: Cross-section properties in connection with twisting of open and closed cross-sections.

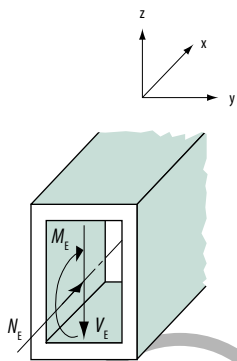


Figure 4.39: Cross-section forces; moment, shear force and axial force.

4.3.9 Interaction

Different section forces; moment, shear, axial force, etc. often interact in cross-sections along a structural member. The stress levels and, in certain cases, also the stability needs to be checked for combinations.

Bending moment and axial force

For cross-sections subjected to axial force and bending moment the combined elastic stress levels are calculated and compared to material yield point. Additionally, for compressive force in combination with bending moment stability needs to be considered.

Material yielding in cross-sections is calculated according to *equation 4.35* for all class 1-3 cross sections and *equation 4.36* for all class 4 cross-sections

$$\left(\frac{N_E}{A \cdot f_y}\right) + \left(\frac{M_E}{W \cdot f_y}\right) \leq 1 \quad (\text{Eq. 4.35})$$

$$\left(\frac{N_E}{A_{\text{eff}} \cdot f_y}\right) + \left(\frac{M_E + N_E \cdot e_N}{W_{\text{eff}} \cdot f_y}\right) \leq 1 \quad (\text{Eq. 4.36})$$

where

- f_y – material yield point (Pa)
- N_E – load effect (N), axial force in cross-section
- M_E – load effect (Nm), bending moment in current cross-section
- W – section modulus for bending (m^3)
- W_{eff} – effective section modulus for bending (m^3), section 4.3.2.
- A – cross-section area (m^2)
- A_{eff} – effective cross-section area (m^2)
- $N_E e_N$ – additional moment from center of gravity changing with an effective cross-section (Nm), see *figure 4.9*

With additional bending moment in other direction this is added to *equation 4.35* and *4.36*.

For welded class 1 and 2 cross-sections, where full plastic resistance can be used, calculation is done according to *equation 4.37*. This governs for bending in strong direction of a bisymmetrical I-section.

$$\left(\frac{N_E}{N_{\text{pl}}}\right) + \left(\frac{M_E}{M_{\text{pl}}}\right) \left(1 - 0,5 \frac{A_w}{A}\right) \leq 1 \quad (\text{Eq. 4.37})$$

where

- M_E – load effect (Nm), bending moment in cross-section
- N_E – load effect (N), axial force in cross-section
- M_{pl} – plastic moment resistance (Nm) for cross-sections subjected to a bending moment
- N_{pl} – resistance to axial force (N) for cross-section
- A – cross-section area (m^2)
- A_w – flange area (m^2)

Cold-formed and welded sections are treated differently with respect to stability. *Equation 4.38* applies to cold-formed sections and *equation 4.39* applies to welded sections

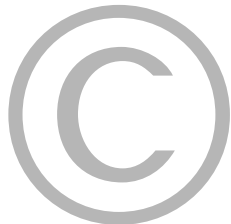
$$\left(\frac{N_E}{N_{\text{b,d}}}\right)^{0,8} + \left(\frac{M_E}{M_{\text{b,R}}}\right)^{0,8} \leq 1 \quad (\text{Eq. 4.38})$$

$$\left(\frac{N_E}{N_{\text{b,R}}}\right) + \left(\frac{M_E + N_E \cdot e_N}{M_{\text{b,R}}}\right) \leq 1 \quad (\text{Eq. 4.39})$$

where

- M_E – load effect (Nm), bending moment in cross-section
- N_E – load effect (N), axial force in cross-section
- $N_{\text{b,R}}$ – resistance to axial force (N) with respect to global and local buckling (effective cross-section), section 4.3.4
- $M_{\text{b,R}}$ – moment resistance (Nm) with respect to lateral-torsional and local buckling (effective cross-section), section 4.3.2
- $N_E e_N$ – additional moment from center of gravity changing with an effective cross-section (Nm), see *figure 4.9*

With additional bending moment in other direction this is added to *equation 4.38* and *4.39*.



SSAB

Bending moment, axial force and shear force

Shear forces affects the overall resistance if $V_E > 0,5 V_{b,Rd}$. A reduction due to material yielding is done in this case and the design stress level from bending moment and axial force is limited according to *equation 4.40*. For cross-sections where shear buckling can occur, see section 4.3.6, *equation 4.41* applies.

$$\left(1 - \left(\frac{2V_E}{V_{b,R}} - 1\right)^2\right) \cdot f_y \quad (\text{Eq. 4.40})$$

where

- f_y – material yield point (MPa)
 V_E – load effect, shear force in current cross-section
 $V_{b,R}$ – shear force resistance, section 4.3.6.

$$\left(\frac{N_E}{N_{b,R}}\right) + \left(\frac{M_E + N_E \cdot e_N}{M_{b,R}}\right) + \left(\frac{M_f}{M_{pl}}\right) \left(\frac{2V_E}{V_{b,R}} - 1\right) \leq 1 \quad (\text{Eq. 4.41})$$

- M_E – load effect (Nm), bending moment in cross-section
 N_E – load effect (N), axial force in cross-section
 V_E – load effect (N), shear force in cross-section
 $N_{b,R}$ – resistance to axial force (N) with respect to local buckling (effective cross-section), section 4.3.4
 $M_{b,R}$ – moment resistance (Nm) with respect to local buckling (effective cross-section), section 4.3.2.
 $V_{b,R}$ – shear force resistance (N) with respect to shear buckling, section 4.3.6.
 M_f – moment resistance (Nm) for the cross-section if only the flanges are contributing
 M_{pl} – plastic moment resistance (Nm) for the gross cross-section

Bending moment, normal force and patch loading

The interaction is calculated empirically and there is a significant spread in test results [4.15]. The combination of bending moment and patch load is often a design parameter for profiled sheets. Welded and cold-formed sections are treated differently.

The interaction for cold-formed thin plate sections is according to *equation 4.43* and for welded sections *equation 4.42*.

$$0,8 \cdot \left(\left(\frac{N_E}{N_{b,R}} \right) + \left(\frac{M_E + N_E \cdot e_N}{M_{b,R}} \right) \right) + \frac{F_E}{F_R} \leq 1 \quad (\text{Eq. 4.42})$$

$$\frac{M_E}{M_{b,R}} + \frac{F_E}{F_R} \leq 1,25 \quad (\text{Eq. 4.43})$$

- M_E – load effect (Nm), bending moment in cross-section
 N_E – load effect (N), axial force in cross-section
 F_E – load effect (N), transverse force in cross-section
 $N_{b,R}$ – axial force resistance (N) with respect to local buckling (effective cross-section), section 4.3.4
 $M_{b,R}$ – moment resistance (Nm) with respect to local buckling (effective cross-section), section 4.3.2.
 F_R – resistance to patch loading (N)

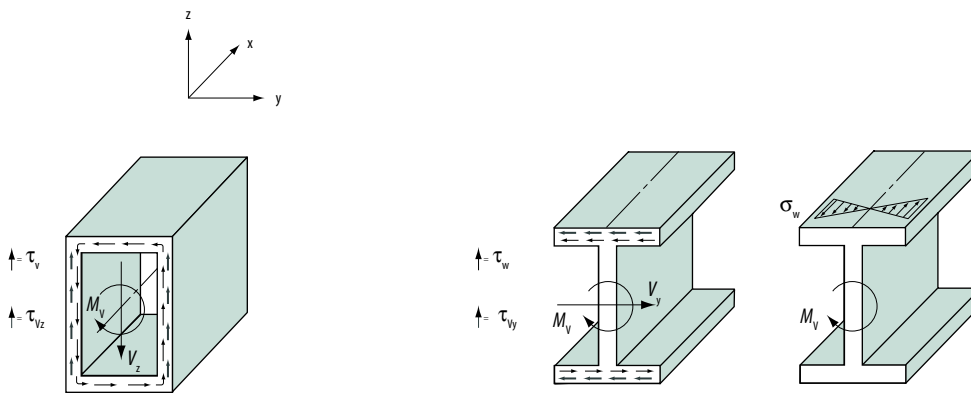


Figure 4.40: Load effects from torsional moment and shear force.

Torsional moment, bending moment, shear force and axial force

Twisting of closed cross-sections causes shear stress and for open sections also normal stress. Stress levels and stability are checked in interaction.

The shear force from twisting of closed sections is calculated according to *equation 4.44*.

$$\tau_v = \frac{M_{vE}}{I_v} t \quad (\text{Eq. 4.44})$$

where

M_{vE} – load effect (Nm), torsional moment in cross-section

τ_v – Saint-Venant shear stress (Pa) in the gross cross-section

I_v – the cross-section torsional stiffness (m^4), see *figure 4.36*

t – thickness (m)

Shear stress from other external loads are added, see *figure 4.40*, and compared with the design shear stress according to section 4.3.6.

$$\tau_{vz} + \tau_v \leq \chi_v \frac{f_y}{\gamma_M \gamma_n}$$

where

τ_{vz} – shear stress of shear force V_z (gross cross-section)

The design load effect in connection with torsion of open cross-sections is calculated as

$$\tau_w = \frac{M_v}{I_w t} S_\omega \quad (\text{Eq. 4.45})$$

$$\sigma_w = \frac{M_v}{W_w \eta_w} \quad (\text{Eq. 4.46})$$

where

τ_w – Vlasov shear stress calculated in the gross cross-section

σ_w – Vlasov normal stress calculated in the gross cross-section

I_w – the cross-section warping stiffness, see *figure 4.36*

S_ω – sectorial static moment, see [4.14]

η_w – according to *figure 4.37*

t – thickness

Shear and normal stress from other external loads are added, see *figure 4.40*, and compared with the design normal and shear stress. χ_v , according to section 4.3.6.

$$\sigma_N + \sigma_{My} + \sigma_{Mz} + \sigma_w \leq f_y / \gamma_M \gamma_n$$

where

σ_{My} – direct stress of bending moment M_y (effective cross-section)

σ_{Mz} – direct stress of bending moment M_z (effective cross-section)

σ_N – direct stress of axial force N (effective cross-section)

$$\tau_{vy} + \tau_w \leq \chi_v \frac{f_y}{\gamma_M \gamma_n}$$

where

τ_{vy} – shear stress from shear force V_y (gross cross-section)

Yielding of material is checked according to

$$\sqrt{\sigma_{tot, Ed}^2 + 3\tau_{tot, Ed}^2} \leq 1,1 \frac{f_y}{\gamma_{M0}}$$

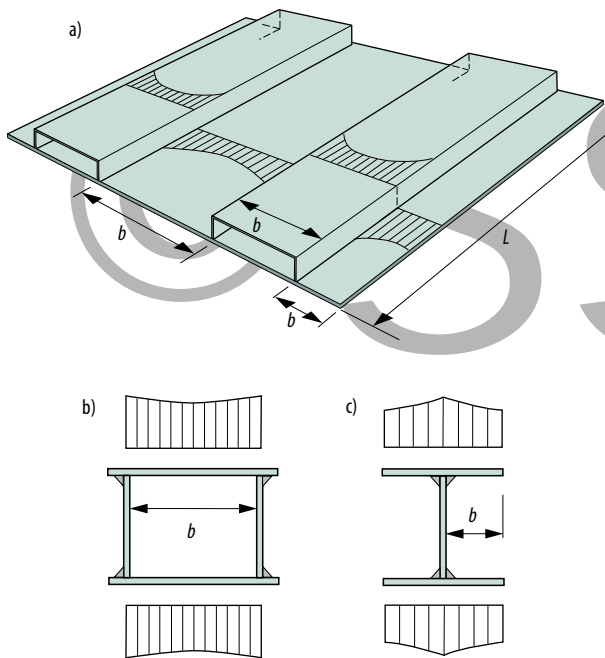


Figure 4.41: Designations in connection with resistance calculation regarding shear lag.

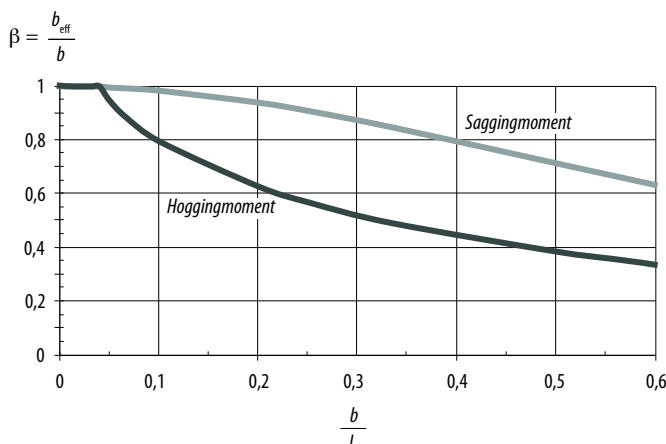


Figure 4.42: Reduction factor with regard to shear lag for flange supported along two edges.

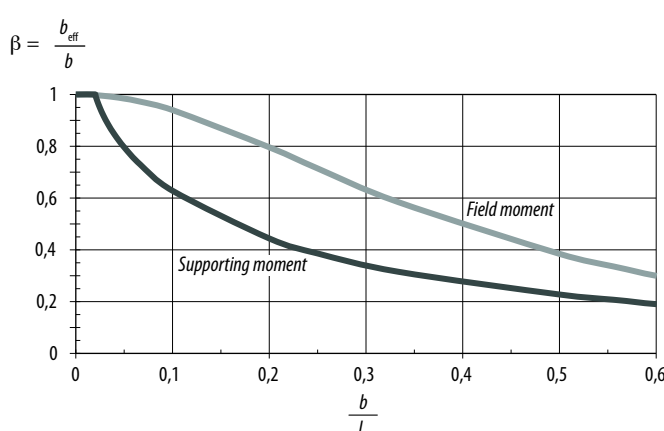


Figure 4.43: Reduction factor with regard to shear lag for flange with one free edge.

4.3.10 Special effects

Beam theory which is the basis of most resistance calculations does not always apply to very thin-gauged cross-sections. This can lead to overestimation of both resistance and stiffness of a member.

The stress distribution for very high beams with a short span, e.g., $b/L >$ approx. 1/3 for a simply supported beam, is not linear and such beams should therefore be treated differently [4.14]. For cross-sections with wide flanges and short spans the stress distribution can resemble that for local buckling, *figure 4.41*. This phenomenon is called shear lag.

The available calculation methods also usually assume that the cross-section shape does not change during loading. This may not be the case for thin-gauged cross-sections. Flange curling is a phenomenon where the flanges bend towards the neutral axis and thereby change the cross-section height, see *figures 3.13* and *4.44*. Open cross-sections are particularly sensitive to high shear stress see *figures 3.13* and *4.47*.

Shear lag

The stress distribution from bending of a structure with wide flanges can vary according to *figure 4.41*. The reason for this is large shear deformations in the flange. The phenomenon is called shear lag and applies to both compression and tension flanges. The width of the flange (b) in relation to the span (L) in *figure 4.41* determines if the effect of shear lag should be taken into consideration in design.

The following applies in serviceability limit state and fatigue load (elastic behavior of a cross-section)

$$b > \frac{L}{50} \quad \text{Part with one free edge}$$

$$b > \frac{L}{25} \quad \text{Part with two supported edges}$$

and in ultimate stress state (yielding of material in cross-section allowed)

$$b > \frac{L}{20} \quad \text{Part with one free edge}$$

$$b > \frac{L}{10} \quad \text{Part with two supported edges}$$

The effective width with regard to local buckling is used as a basis for cross-section class 4 flanges.

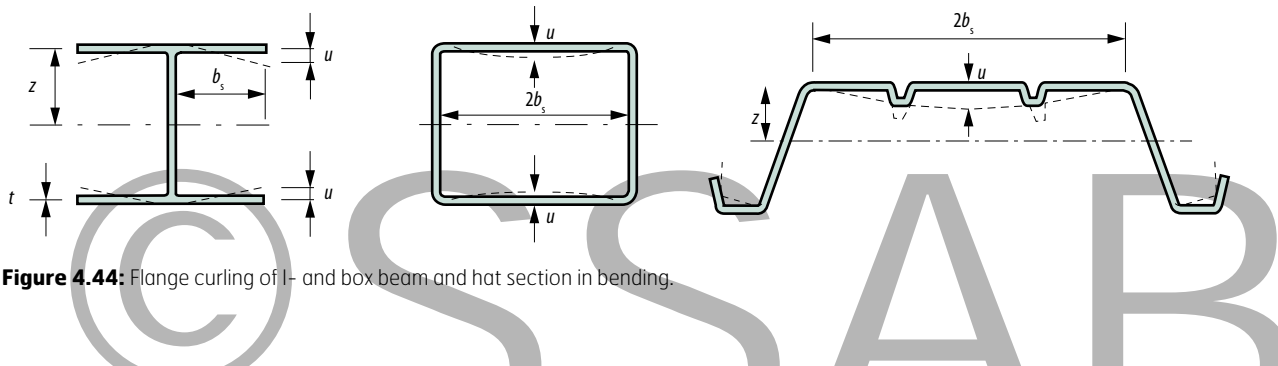


Figure 4.44: Flange curling of I- and box beam and hat section in bending.

Resistance with respect to shear lag is considered in a similar way as local buckling, see section 4.3.2. An effective flange width is calculated for which yield stress can be reached. *Figure 4.42* and *4.43* gives the reduction factor β in relation to b/L and the effective flange width is calculated according to *equation 4.47*

$$b_{\text{eff}} = \beta b \quad (\text{Eqn. 4.47})$$

The difference between sagging and hogging moment in *figure 4.42* and *4.43* is the moment distribution gradient (inclination) which governs the magnitude of the shear stress. Shear stress is larger at support (hogging moment) and the effect of shear lag is therefore greater.

Flange curling

In bending the flanges of a cross-section are subjected to a force component directed towards the neutral axis. This can result in flange curling, *figure 4.44*, and this geometric change can reduce the resistance. The effect is negligible for welded beams but may become noticeable for slender flanges in high-strength steel.

The magnitude of the flange curling, see *figure 4.44*, is for initially straight beams according to *equation 4.48*.

$$u = 2 \frac{\sigma_a^2}{E^2} \frac{b_s^4}{t^2 z} \quad (\text{Eqn. 4.48})$$

where

- σ_a – the stress in the flange calculated from gross area
- z – distance from the cross-section center of gravity to the flange
- b_s – distances available from *figure 4.33*
- t_f – flange thickness

If flange curling is less than 5% of the beam height, it can, as a rule, be neglected. Flange curling is taken into consideration by calculating the resistance of the deformed cross-section.

Flattening of cross-section

For a low cross-section with a strongly inclined web and where the relationship between the height and width of the cross-section is small, bending can cause flattening. Rough estimates show that the compression can be regarded as negligible if the thickness exceeds the calculated value in *equation 4.49* [4.12]:

$$t > \frac{1,5 b_t^2 f_y}{z E} \quad (\text{Eqn. 4.49})$$

See *figure 4.45* for an explanation of designations; the yield point is f_y .

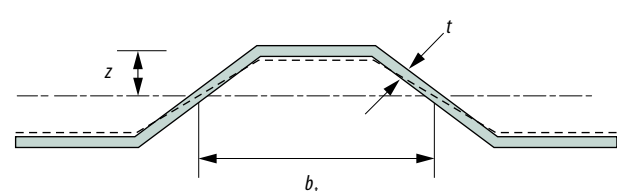


Figure 4.45: Flattening of cross-section, low section with an inclined web.

Cross-section change of open cross-sections by shear stress

The shear flows that arise from bending of a beam can result in substantial forces acting on the flange and significant deformations of thin-walled open cross-sections, *figure 4.46*.

The forces are according to *figure 4.46* and for an evenly distributed load have a magnitude of

$$k_h q$$

alternatively, for a point load

$$k_h F$$

where

$$k_h = \frac{3b_u^2(h+b)}{h^2(h+2b+4b_u+6bb_u/h)}$$

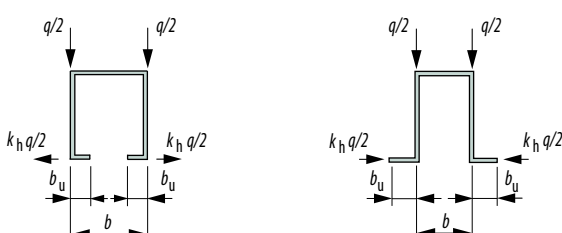
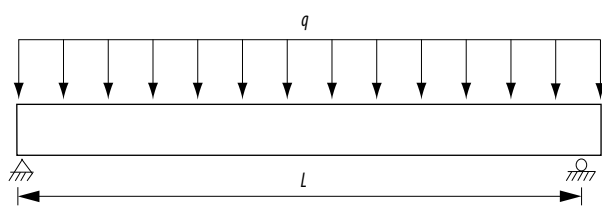


Figure 4.46: Lateral forces on flange [4.8].

Examples of lateral bending stress and deformations are given in *figure 4.47*.

In order to avoid unfavorable changes of the cross-section shape, the flanges should be locked or designed in such a way that the deformation stiffens the cross-section rather than weakens it, *figure 4.47*.

The flange forces may produce resulting side forces and torsional moment in asymmetrical cross-sections, *figure 4.49* [4.12].

$q = 20 \text{ N/mm}$				
t (mm)	b_u (mm)	σ (MPa)	d (mm)	
5	10	2	0	
2	10	14	1	
1	10	57	7	
0,5	10	230	58	
5	20	8	0	
2	20	50	3	
1	20	200	25	
0,5	20	(800)	(203)	

() values corresponding to such big deformation that calculation model does not apply.

Figure 4.47: Examples of lateral bending stress and cross-section deformations.

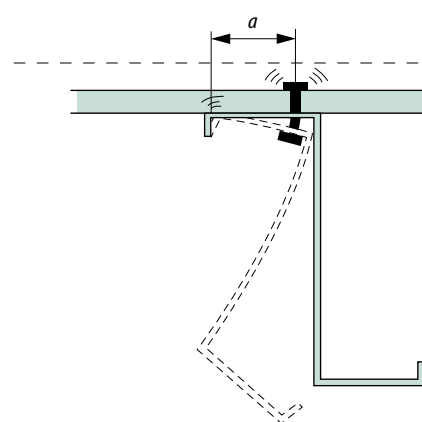


Figure 4.48: Asymmetrical cross-sections may give rise to a twisting moment and lateral forces.

Natural frequency

Geometric changes in a structure or structural element leads to changes in oscillatory properties; lower weight increases the natural frequency and lower stiffness decreases the natural frequency. Problems often arise if the frequency of the load and the natural frequency of the structure are similar to each other.

Most structures have several degrees of freedom and thereby several natural frequencies. The lowest is most often the one to create problems. The calculation procedure here assesses the five lowest natural frequencies for beams and the lowest natural frequency for rectangular plates. Note that this applies without an external load, i.e., only with a dead weight.

Natural frequencies of beams are calculated according to equation 4.50.

$$f_0 = \frac{\xi}{L^2} \cdot \sqrt{\frac{I}{A}} \quad (\text{Eq. 4.50})$$

where

- f_0 – natural frequency of the beam (Hz)
 ξ – frequency parameter according to figure 4.50
 I – moment of inertia of the beam (mm^4)
 L – balklängd (mm)
 A – cross section area of beam (mm^2)

Which means that the natural frequency can be calculated according to equation 4.51.

$$f_{\text{HS}} = f_{\text{MS}} \cdot \sqrt{\frac{I_{\text{HS}} \cdot m_{\text{HS}}}{I_{\text{MS}} \cdot m_{\text{MS}}}} \quad (\text{Eq. 4.51})$$

where

- f_{MS} – natural frequency of beam in mild steel (Hz)
 f_{HS} – natural frequency of beam in high-strength steel (Hz)
 I_{MS} – moment of inertia of beam in mild steel (mm^4)
 I_{HS} – moment of inertia of beam in high-strength steel (mm^4)
 m_{MS} – weight of beam in mild steel (kg)
 m_{HS} – weight of beam in high-strength steel (kg)

Natural frequencies of a plates are calculated according to equation 4.52.

$$f_0 = \frac{\xi \cdot t}{a^2} \quad (\text{Eq. 4.52})$$

where

- f_0 – natural frequency of the beam (Hz)
 ξ – frequency parameter according to figure 4.51
 a – short side of plate (mm)
 t – plate thickness (mm)

The effect for a plate becomes significantly higher in connection with an upgrade according to equation 4.53.

$$f_{\text{HS}} = f_{\text{MS}} \cdot \frac{t_{\text{HS}}}{t_{\text{MS}}} \quad (\text{Eq. 4.53})$$

where

- t_{MS} – material thickness (mm) in mild steel
 t_{HS} – material thickness (mm) in high-strength steel

Keep in mind that both different parts and the whole structure may begin to vibrate.



Figure 4.49: Example of an application where the natural vibrations should be checked.



Boundary conditions	Natural frequency				
	1:a	2:a	3:e	4:e	5:e
	$1.85 \cdot 10^7$	$5.09 \cdot 10^7$	$9.98 \cdot 10^7$	$1.65 \cdot 10^8$	$2.47 \cdot 10^8$
	$2.90 \cdot 10^6$	$1.82 \cdot 10^7$	$5.09 \cdot 10^7$	$9.98 \cdot 10^7$	$1.65 \cdot 10^8$
	$1.27 \cdot 10^7$	$4.13 \cdot 10^7$	$8.61 \cdot 10^7$	$1.47 \cdot 10^8$	$2.25 \cdot 10^8$
	$4.62 \cdot 10^6$	$2.50 \cdot 10^7$	$6.16 \cdot 10^7$	$1.15 \cdot 10^8$	$1.84 \cdot 10^8$
	$8.15 \cdot 10^6$	$3.26 \cdot 10^7$	$7.34 \cdot 10^7$	$1.30 \cdot 10^8$	$2.04 \cdot 10^8$
	$2.04 \cdot 10^6$	$1.83 \cdot 10^7$	$5.09 \cdot 10^7$	$9.98 \cdot 10^7$	$1.65 \cdot 10^8$

Figure 4.50: Frequency parameter for a beam with different boundary conditions.

Length/width ratio, b/a Boundary conditions: F=fixed H=articulated	1.0	1.5	2.0	2.5	3.0	∞
	$4.96 \cdot 10^6$	$3.58 \cdot 10^6$	$3.10 \cdot 10^6$	$2.88 \cdot 10^6$	$2.76 \cdot 10^6$	$2.48 \cdot 10^6$
	$9.04 \cdot 10^6$	$6.79 \cdot 10^6$	$6.18 \cdot 10^6$	$5.97 \cdot 10^6$	$5.83 \cdot 10^6$	$5.62 \cdot 10^6$
	$7.28 \cdot 10^6$	$4.37 \cdot 10^6$	$3.44 \cdot 10^6$	$3.05 \cdot 10^6$	$2.86 \cdot 10^6$	$2.48 \cdot 10^6$
	$7.28 \cdot 10^6$	$6.30 \cdot 10^6$	$5.99 \cdot 10^6$	$5.85 \cdot 10^6$	$5.78 \cdot 10^6$	$5.62 \cdot 10^6$

Figure 4.51: Frequency parameter for plates with different geometry and boundary conditions.



4.4 Design using FEM

4.4.1 Introduction

The Finite Element Method (FEM) is a numerical method which is well-suited for structural calculations. The result shows, e.g., stress distribution, deformations and resistance of a complete structure or member. It is important to note that the method generates an approximate solution and that the accuracy completely depends on the input. The user needs to have good knowledge about the method and the problem itself. The approach in modeling, calculation and evaluation is described in general herein and presupposes certain previous experience in FE simulation and engineering models.

FE simulations can be used in cases where an analytical solution does not exist, for example, non-linear problems (significant deformations, instability, non-linear material properties, etc.). FE simulation can also be relevant in cases where the structure is of a magnitude and complexity that signifies a superior work effort. Numerical simulations are a natural preliminary stage of practical testing of actual components in a product development stage and in the interpretation of results from practical testing. In many cases it is a cheaper alternative to practical testing and well-suited in geometry and material upgrade studies, i.e., a parameter studies. Thin sheet structures are preferably optimized using FEM.

Fatigue design using FEM is discussed separately in chapter 5.6.

4.4.2 Modeling

The Finite Element Method is not only approximate by nature but it also requires certain assumptions to be made. These can consist of simplified boundary conditions, material models and modeling of joints and are described briefly in the following.

Boundary conditions and loads

In many cases the behavior of a part of a structure can be calculated separately. This can be done with sub-modeling where boundary conditions are transferred from the global

model. Alternatively, the sub-model can be analyzed using simplified boundary conditions. There are a large number of possibilities to apply boundary conditions, they are important for the result and it can be a good idea to perform a sensitivity analysis. Symmetrical boundary conditions are diligently applied but note that it is not only the geometry that should be symmetrical but also loads and possible imperfections.

In applying loads it is common to prescribe forces or deformation to certain nodes or element surfaces. This approach can be used when local effects at load introductions are not being studied. If the load is applied through contact with other parts, for example, a lifting bracket or a load distribution plate, local stress patterns and failure at the load introduction can be studied. There is a lot to gain if the load-introducing part can be considered as stiff in relation to the analyzed component.

Discretization

FEM is based on the discretization of the problem. Components are modeled using a large number of geometrically simple elements where the response is determined locally in integration points. The response in remaining parts of the elements are determined using interpolation methods. Shell elements are recommended for thin sheet structures. These elements are geometrically two-dimensional but there are a number of integration points in the thickness direction to describe variations. The advantage of shell elements is that they can handle all types of instability, including local buckling, unlike beam elements which can handle only global instability. Most beam elements cannot handle twisting with prevented warping and this is why, for example, torsional-flexural buckling and lateral-torsional buckling must be included in another way. The advantage of beam elements is that the number of degrees of freedom becomes smaller, which reduces calculation time.

There is an abundance of different element types which can be characterized, among other things, by the number of nodes, number of degrees of freedom, element formulation and integration method. There are, e.g., shell elements which allow shear deformation (Mindlin's theory) and thin shell elements where the shear deformation is considered to be negligible (Kirchoff's theory). As a rule, general shell elements which can handle both cases are to be used.

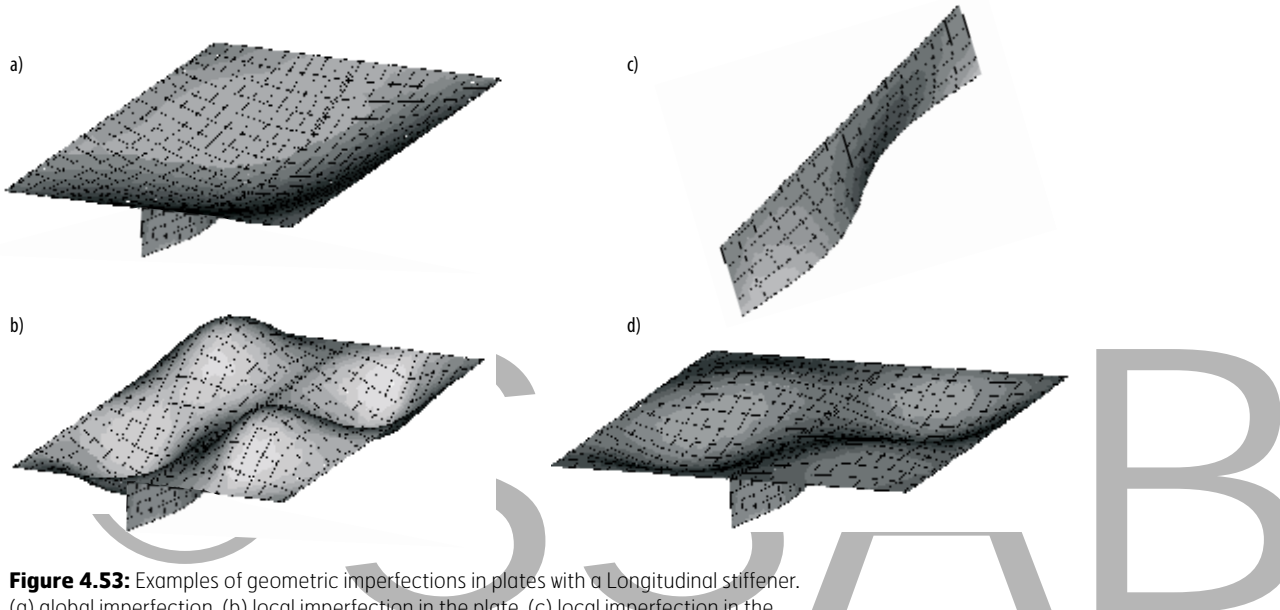


Figure 4.53: Examples of geometric imperfections in plates with a Longitudinal stiffener.
(a) global imperfection, (b) local imperfection in the plate, (c) local imperfection in the stiffener and (d) all imperfections added together.

Material modeling

Modeling of the non-linearity in material properties is required for most analyses. As a rule, the behavior during uniaxial tensile testing is enough as input data where true stress and strain values should be used, see *figure 2.5*. As a suggestion; use data from actual uniaxial tensile tests. Most steel types show only small differences in mechanical properties in different directions and can be modeled as isotropic.

Since the stress state is not purely uniaxial after necking of the specimen in a tensile test, the true curve needs to be extrapolated. This is not discussed in detail here but, as a suggestion, can be done with a Bergström model [4.16] or a “power-law” function adapted for strain in an interval right before necking. It can be worth noting that strain during fracture, e.g., the A80 value, is not the same thing as the actual ductility of the material. The stresses are localized after necking and can locally reach values many times higher than the average value across the extensometer measuring length, e.g., 80 mm.

If a dynamic problem is studied, the steel dependence on the strain rate should be included. If there is uncertainty about the magnitude of the strain rate that occurs locally in the problem, the strain rate effect can be excluded in the first simulation, assess it and then include relevant material data in the sharp simulation. Local strain rates of up to 500 s^{-1} are typical for a car collision, which corresponds to a yield stress increase of approx. 100 MPa. This effect can affect the total energy absorption by as much as 20%, [4.17].

Different material data is available for download from www.ssab.com. Data for the rate dependence in certain materials can be ordered from SSAB.

Through process effects

In order to obtain a realistic measure of the actual resistance using FEM, it is generally required to pay attention to the through process effects. These can be, for example, geometric imperfections, cold forming and lacquer hardening effects, as well as residual stresses.

Imperfections and instability

Geometric deviations (imperfections) play an important role in slender structures where local- and global buckling can be the failure mode. Due to these production-caused imperfections a slender structural member can have less load capacity than a geometrically perfect and, in certain cases, the FE simulation does not find the relevant instability mode. This means that if imperfections are neglected in a FE simulation, the resistance may come to be significantly overrated.

The imperfections are usually modeled using selected eigen-modes which are obtained from an eigen-value analysis in FEM. The relevant eigen-modes are then scaled to reasonable size with amplitude of the imperfections related to production tolerances. As a suggestion, the respective amplitude is set at 80% of the production tolerance. In the event of a combination of several imperfections, one should be taken at its full value and the others should be reduced to 70%. *Figure 4.52* gives recommendations for the magnitude and shape of such imperfections, both including and excluding the effects of residual stress. The latter means that residual stress from welding can either be included in the model as an imperfection or explicitly as a stress pattern, see next section.

If there are many parts in the structure where local instability can occur, the above method means that the relevant eigen-modes can be of a very high order and difficult to find. It may be simpler to assign the most relevant imperfections based on experience. The failure mode is often similar to the geometry of the most critical imperfection. *Figure 4.53* can function as an illustration of the latter way of introducing imperfections.

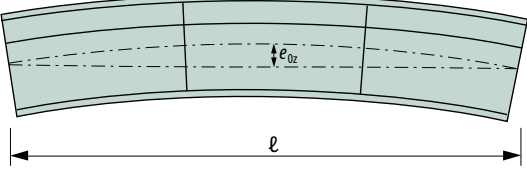
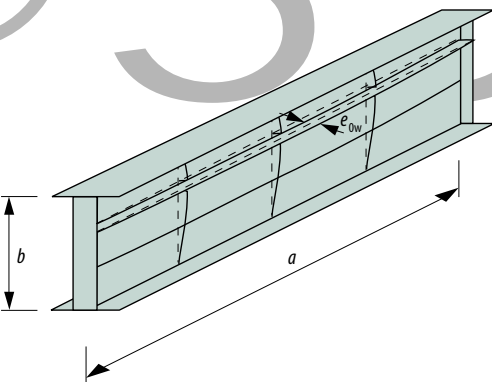
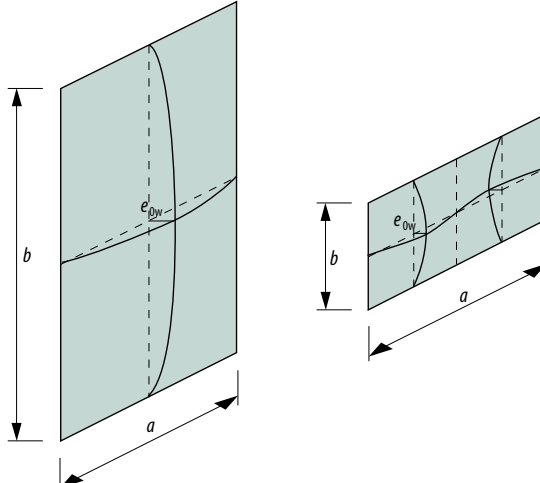
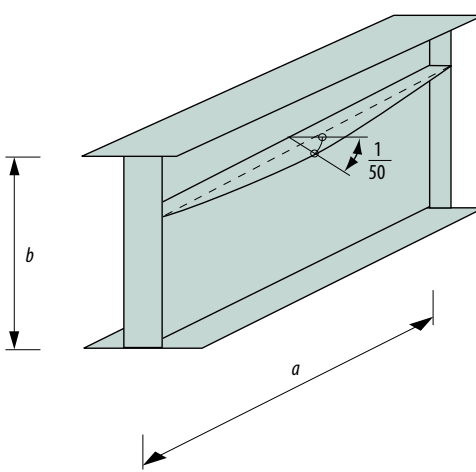
Type of imperfection	Structural member	Shape	Magnitude with the effect of residual stress	Magnitude without the effect of residual stress
Global Bar with length l		Arc	See table 4.3	80% of the value in table 4.3
Global Longitudinal stiffener with length a		Arc	min (a/400, b/400)	min 00, b/500
Local Plate field or part of plate field		Buckling mode	min (a/200, b/200)	min 50, b/250
Local Twisting of flange or stiffener		Twisting	1/50	1/60

Figure 4.52: Equivalent geometric imperfections for structural members.

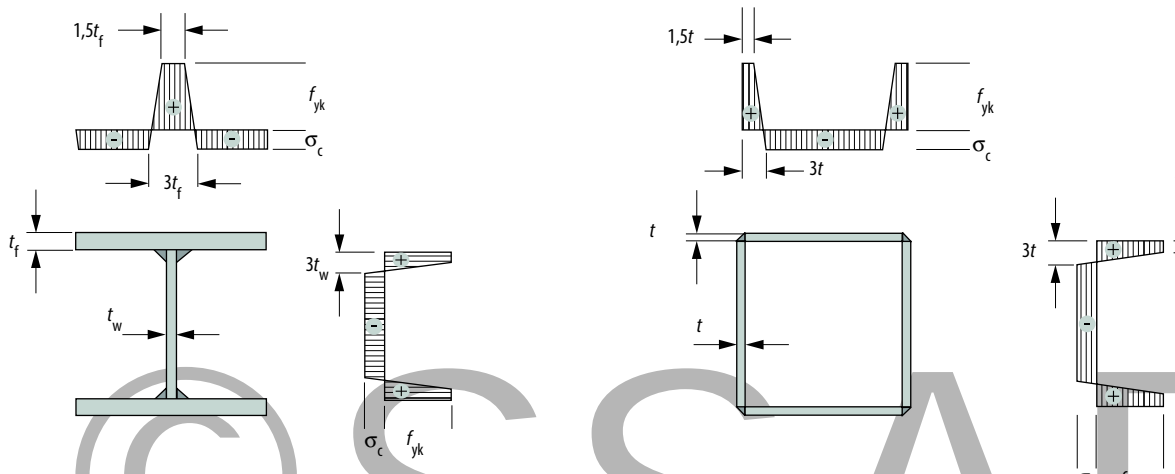


Figure 4.54: Schematic residual stress distributions. Longitudinal direction according to BSK 99 [4]. The compressive stress σ_c is calculated based on equilibrium; the resultant force across the cross-section is zero. f_{yk} is replaced with 500 MPa for high-strength steels with the yield point above 500 MPa of a parent or base material.

Residual stresses from welding

There are two simplified ways to handle residual stress from welding in static design. The simpler of the two is to replace the effect of the residual stress with fictitious geometric imperfections which, together with the actual geometric imperfections, form the so-called equivalent imperfections. This approach can, however, give conservative results for local buckling of plates. An alternative and often more specific way is to assign a simplified distribution of residual stress in the model.

If the residual stress distribution is unknown, stresses from welding can be taken as tensile stress at yield point level in an area 1.5 to 3 times the thickness of the plate, see *figure 4.46*. However, the yield point for high-strength steel is high and the residual stress can instead be set at 500 MPa, even if the actual yield point is higher. This tensile stress must naturally be supplemented with a compressive stress in the remaining parts of the cross-section in order to achieve equilibrium. Compressive residual stress influences the global buckling resistance of a member in compression. As a suggestion, the element mesh should be adapted to include the residual stress distribution.

Cold forming effects

Cold forming in thin sheet leads to local strain hardening and thickness changes. In many cases, the sheet is thinner where the forming and consequently the strain hardening is largest. These subversive mechanisms with regard to strength may produce an overall negligible contribution for conventional steels. The forming effect may need to be included with pressing of strong strain hardening materials such as dual-phase (DP) steel. An approach that considers the most important aspects is to transfer plastic strain in the sheet and actual thicknesses from a forming simulation to the structural calculation. The mesh is not required to be identical during forming simulation and structural calculation. If this is not the case, data can be transferred using mapping procedures.

Lacquer hardening effects

Certain steels (RP, BH, DP, etc.) have a strong bake hardening effect. This is a consequence of lacquering of formed

components and can result in an increase in the yield point by 50 to 100 MPa. This can be included in FE simulations but should in that case be connected to the strain level from the forming stage.

Fluctuations in mechanical properties and nominal thickness

An aspect which is as important to pay attention to as the above through process effects is the fluctuations in mechanical properties and nominal thickness between different sheets/ plates. FEM typically uses characteristic values of mechanical properties and thickness supplemented with a sensitivity analysis. The more holistic concept of “robust structure” implies optimization with consideration for input fluctuations in order to find a structure which performs well in reality. The effect of fluctuations is treated using the Monte-Carlo method or more advanced, yet less time-consuming methods based on response functions.

Modeling of joints

Fatigue design puts high demands on joint modeling, see chapter 5.6. Joints are not as critical in static design. There is a wealth of methods of modeling joints in FEM. As a rule, joints can be modeled with shell elements, beam elements or spring elements in thin plate structures. A warning can be issued for shell modeling of single-sided fillet welds. The bending state can be strongly over exaggerated since the forces have a larger lever than in reality.

4.4.3 Calculation

There are two classes of numerical methods with different time integration procedures in FEM; implicit and explicit method. If the model is linear, an implicit method is used. If, on the other hand, the model is material- or geometrically non-linear, a stepwise integration is required and in this case the explicit method can also be applied. The implicit method iterates until equilibrium is achieved in each step, whereas an explicit method uses a large number of short time steps. An explicit method is typically used in dynamic problems and an implicit method in static problems. In order to analyze problems with long duration or

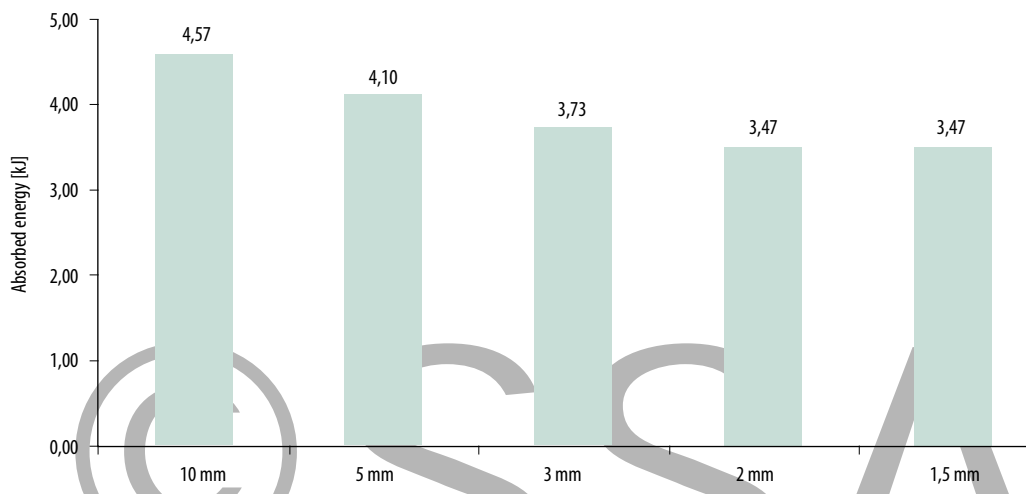


Figure 4.55: Energy absorption as a function of element size for axial crushing of rectangular tube (60x60x1,5) in Docol 800DP. Four-node shell elements with reduced integration and uniform element size with non-linear geometry.

purely static problems using an explicit method, time- or mass scaling may need to be employed in order to prevent the calculation time from becoming insurmountable.

Other choices that need to be done before a calculation can start are the iteration procedure, whether a formulation of large deformations should be assigned, etc. As a rule, these settings are handled easily but the theory behind them is complicated. A description can be found in each respective FE program manual.

4.4.4 Evaluation

The first part of the assessment procedure should consist of a convergence study, appraisal of accuracy and other checks. Once satisfactory results have been obtained, stress, plastic strain, reaction forces, deformations, etc., are assessed.

Convergence study, accuracy and control

In order to verify that the results from the FE simulations are credible, a convergence study can be made. This is done by repeating the analysis with more and more degrees of freedom in the problem to check the convergence of the solution, as well as an estimate of the error. The study typically covers global or local parameters such as stress, force or deformation of the geometry with a different number of elements. Folding puts high demands on the element mesh and can work as an example. The effect of the element size on the energy absorption in an axially crushed square tube is showed in figure 4.55. The FE simulation shows overrated energy absorption of significant amount for element sizes larger than two millimeters. A general rule is also that when too few degrees of freedom are used, the finite element method gives too high resistance and stiffness.

It should also be noted that even if the FE simulation generates a solution with significant local errors, global measures such as resistance can show good accuracy. Singularities are a result of, for example, corners or radii modeled sharp or loads applied in nodes. This gives local extreme values but the effect quickly abates and satisfactory results for global magnitudes or in areas of interest can be found. It should also be noted that there are often

big differences in the thickness direction in the apparently two-dimensional elements in the post-processor during the assessment of local stress and strain in shell element models.

Many modeling and logical errors can be discovered by appraising during the assessment if the results are reasonable. Check that the reaction forces correspond to the applied forces and that deformations are reasonable both with regard to shape and size. There are possibilities to visually enlarge deformations in the post-processor for this purpose. In order to additionally confirm the credibility of a solution, set an upper and lower boundary using calculations according to standards or analytical solutions for a simplified problem. This handbook also works well for this purpose.

This type of preliminary work is particularly important when instability can be expected to govern the resistance. Instability phenomena can be difficult to find in FE simulations unless there are initial imperfections which to some extent correspond to the expected failure mode.

Design criteria

Static design criteria can consist of requirements on the structure ultimate limit state (resistance) or serviceability limit state (limited deformation). A couple of comments regarding possible design criteria are discussed here.

Resistance

Resistance is the maximum load a structure can carry, see section 4.1.1. It can be determined by studying load vs. deformation in the FEM model where an increasing load is applied. The maximum load is the theoretical resistance. Even though resistance is a global measure, it requires correct modeling of local phenomena such as local buckling of thin sheet structures.



Limited plastic deformation

Permanent deformations after unloading can be a design criterion. These can be limited in size or not acceptable at all. Permanent deformations are obtained through a single linear unloading step in the FE simulation or plastic strain can be observed during loading.

Stiffness/Natural frequency

The stiffness or natural frequency of a structure can be a design criterion. More focus is put on this issue through the general trend of increased use of high-strength steel and reduced thicknesses. The elastic stiffness and natural frequencies are calculated in FEM in linear analyses. Joints in the structure affect stiffness to a large extent.

Energy absorption, pulses

FEM is well-suited analysing energy absorption of components or determining pulses in structures. Energy absorption through folding or plastic hinges puts high demand on the element mesh and the assumption of large deformations. Something to consider in studying the energy absorption of individual thin sheet components in larger structures is that they can only absorb limited amount of deformation before the load is redistributed to another part of the structure.

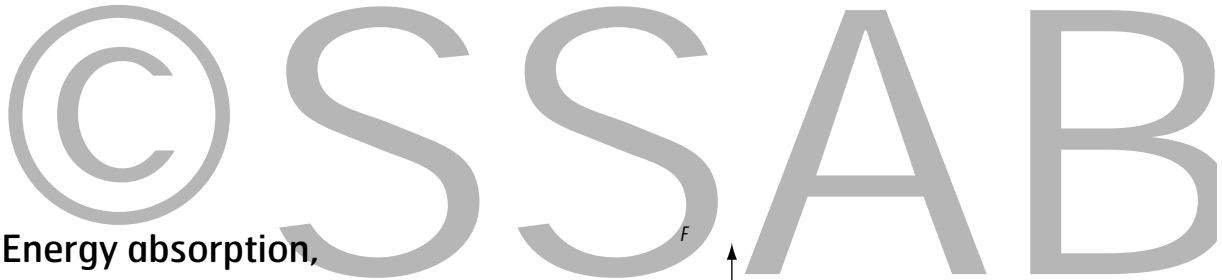
Fracture

Modeling of fracture in thin sheet structures is complicated. In general, the fracture is initiated by local plastic instabilities (often in the thickness direction), growth of cavities or from an edge due to local defects or microstructural factors. The latter, e.g., high stress concentration in the boundary layer between a soft and a hard phase. This leads to difficulties in finding satisfactory continuum-based fracture criteria. It is common to use fracture criteria based on maximum shear stress. It should be noted that thin sheet structures most often experience plastic collapse and load redistribution or lost function before material fracture.

4.4.5 Design procedure

During design with FEM, it is of course important to use an as correct model as possible when it comes to boundary conditions, load introductions and material data. It is important to differentiate between design and another simulation such as, e.g., different parametric studies for development of optimized components. Design with FEM should contain both a certain amount of safety due to the fact that FEM is an approximation method but also other uncertainties such as material strength, thickness- and other geometric tolerances. In order to match the previously described design procedure, nominal values should be used for material properties and thicknesses. In order to obtain conservative FE results, a stress-strain response should be used where the material is deformed elastically up to the nominal yield point followed by weak linear deformation hardening, e.g., with a modulus of elasticity/100 inclination. Both local and global imperfections should be included in the model, see section 4.4.3. Residual stress from welding should also be included, either explicitly as stress or through equivalent geometric imperfections.

If the model is subjected to a combination of design loads, these should be assumed to be proportional and increased to the same extent with a load multiplier. This means that the calculation must be load-controlled in order to preserve the proportions. The loads are increased from a low value until either it becomes impossible to reach an equilibrium state or unloading starts. The highest value of the load or loads corresponds to the characteristic resistance. This value is subsequently to be divided by safety factors and the design resistance is determined. There can be systematic differences between such a calculation and test results and this is the reason for recommending calibration with regard to tests. There are normally no test results for the current component or structure but the calibration can be made for something resembling it. This procedure is practice in research and there are a number of publications containing test results and calibrations that can be used. It is important to conduct any such calibrations under the same prerequisites as are intended for the current problem.



4.5 Energy absorption, dent and impact

Some structures are designed to absorb a certain amount of energy without any permanent deformation, whereas others are intended to absorb a maximum amount of energy during the collapse of the structure. These two types are called elastic and plastic energy absorption. An example of elastic energy absorption is a minor dent on the door of a refrigerator or a car. Plastic energy absorption is used, e.g., as safety components in cars.

During elastic energy absorption, it is material yield point and the stiffness of the structure that determine how well the energy is absorbed. Note that the material yield point in a completed component can be significantly higher than for the base material. This applies, in particular, to DP steels which have strong deformation hardening. Plastic energy absorption produces substantial local strain, which means that the energy absorption capacity rather depends on the tensile strength of the material.

Absorbed energy, both elastic and plastic, is calculated according to equation 4.54.

$$E = F_{\text{medel}} \cdot s \quad (\text{Eqn. 4.54})$$

where

E – energy (J)

F_{medel} – mean force, see figure 4.56 (N)

s – deformation of force F (m)

The deformation, s , is dependent on the stiffness of the structure. A non-rigid behavior means larger deformations but also more energy absorption for the same force.

Choice of material is decisive for the energy absorption capacity. In general, higher strength results in more energy absorption. If the process takes place at high speed, the energy absorption is given an additional boost as steel has positive dynamic properties, see figure 4.57.

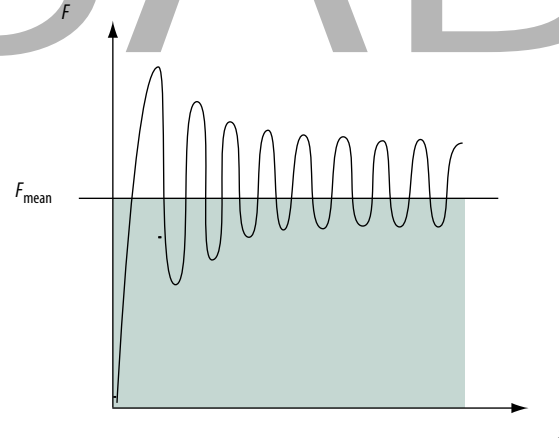


Figure 4.56: Absorbed energy,

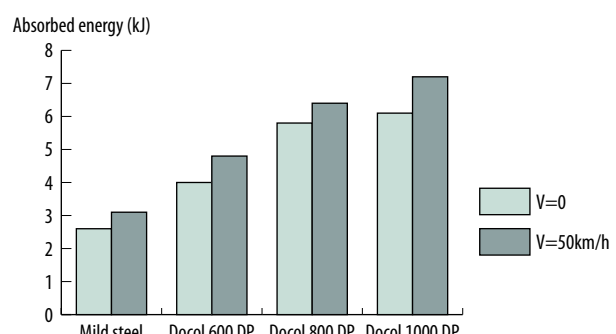


Figure 4.57: Material selection has a big effect on the energy absorption capacity.

4.5.1 Dent resistance

Surfaces, e.g., in the white goods and motor vehicle industries are expected to handle moderate dents and impacts without any permanent deformations. In other applications, e.g., dumper bodies, certain plastic deformation must be allowed in order to limit the total weight.

Dent resistance with a permanent deformation of 0.1 mm can be described by *equation 4.55*.

$$F = K \cdot R_e \cdot t^n \quad (\text{Eq. 4.55})$$

where

F – point load, the force which hits the surface (N)

K, n – geometry-dependent constants the common values for level plate are $K = 1.4$ and $n = 2.0$

If you want to keep the dent resistance when upgrading to a high-strength material, the thickness can be calculated by re-writing *equation 4.55*.

$$t_{\text{HS}} = t_{\text{MS}} \cdot \sqrt{\frac{R_{\text{eMS}}}{R_{\text{eHS}}}} \quad (\text{Eq. 4.56})$$

where

t_{HS} – thickness in high-strength steel (mm)

t_{MS} – thickness in mild steel (mm)

R_{eMS} – yield point, mild steel (MPa)

R_{eHS} – yield point, high-strength steel (MPa)

In applications where plastic deformations are allowed, the formula below can be used, [4.26]. The required plate thickness is calculated based on mass, material, fall height and permissible plastic deformation.

$$t = \sqrt{\frac{E_{\text{tilf}}}{\pi R_e \Delta p_m}} - \frac{5}{36} \Delta p_m^2 \quad (\text{Eq. 4.57})$$

where

t – requisite plate thickness (mm)

E_{tilf} – energy input (Nmm)

R_e – material yield point (MPa)

Δp_m – maximum plastic deformation (mm)

Note that the formula applies at impact velocities of under 10 m/s and only if:

$$\Delta p_m < 1,3 \left(\frac{E_{\text{tilf}}}{R_e} \right)^{1/3}$$

and is correct if

$$\Delta p_m < \left(\frac{E_{\text{tilf}}}{R_e} \right)^{1/3}$$

4.5.2 Plastic energy absorption in components

There are analytical solutions for certain special case of energy absorption. Regression formulas for common geometries can also be found. Other cases must resort to numerical simulation using FEM.

Some formulations applicable to energy absorption in tubes are presented below. These equations are derived and empirically tested primarily under quasi-static circumstances. In reality, the collapse process is often dynamic. As a rule, the quasi-static solution is reliable if the impact velocity is below 15 m/s. If the speed is higher refer to the literature where solutions for certain cases can be found. Otherwise, refer to FEM simulations, see chapter 4.4. The design of energy-absorbing components should always be concluded with practical tests.

Axially loaded tubes

In order to be able to rank a component from energy absorption point of view of, a definition of different merit figures can be done. Weight efficiency or energy efficiency are common.

Weigh efficiency = E / m (J/kg)

Energy efficiency = $F_{\text{medel}} s / F_{\text{max}} L$

where

m – mass (kg)

L – original length (m)

E, F, s – according to *figure 4.57*

In order to isolate the importance of geometry, the structural efficiency, η , can be defined for different geometries, *equation 4.58* [4.20, 4.27].

$$\eta = \frac{\sigma_{\text{medel}}}{R_m} \quad (\text{Eq. 4.58})$$

where

σ_{medel} – mean stress during the collapse process (MPa)

R_m – material yield point (MPa)

The structural efficiency, η , for a tube is described as

$$\eta = m \phi^n \quad (\text{Eq. 4.59})$$

where

ϕ – relative area (the area of the cross-section/ enclosed area)

m, n – factors depending on geometry and collapse mode, from *table 4.6*

The material stiffness is not included in the equation and is therefore not suitable for a comparison between different materials, e.g., steel and aluminum.

The values in the table come from a large number of tests found in literature which also correspond well to SSAB hot- and cold-rolled steels, see *figure 4.58*. Note that the results presuppose that energy absorption takes place through progressive folding and without any significant forming of cracks.

In the design of energy-absorbing components is important for the collapse mode to be stable for. When the thickness is small compared to the external geometry the collapse can become unstable in axial compression of tubes. According to Thornton [4.20] the critical relation between material thickness and compressed section part width can be described with *equation 4.60*.

$$\frac{t}{w} \geq 0,48 \sqrt{\frac{1-v^2}{E}} R_e \quad (\text{Eq. 4.60})$$

where

- t, w – geometry according to *figure 4.59* (mm)
- v – Poisson's ratio (0.3 for steel)
- E – modulus of elasticity (210 GPa)
- R_e – material yield point (MPa)

Otherwise, there is a risk of irregular folding. By creating initiation points, so-called triggers, regular folding can be achieved even when *equation 4.60* is not been met.

If the structure is long, instability can occurs in the form of global bending. Keep in mind that the bending stiffness of the cross-section during folding can become significantly lower than originally.

The following rule of thumb applies to thin-walled circular tubes according to Jones [4.21]:

- | | |
|--|----------------------|
| $(L/2)_{\text{crit}} > 2,54e^{0,124R/t}$ | Global bending |
| $(L/2)_{\text{crit}} < 3,35e^{0,06R/t}$ | Progressive buckling |

The corresponding rules for square Tubes are:

- | | |
|---|----------------------|
| $(L/W)_{\text{crit}} > 2,54e^{0,08W/t}$ | Global bending |
| $(L/W)_{\text{crit}} < 3,42e^{0,04W/t}$ | Progressive buckling |

where

- L – tube length (mm)
- W – length of side (mm)
- R – radius (mm)
- t – thickness (mm)

Section	Collapse mode	m	n
Circular	Buckling	2	0,7
Circular	Formation of cracks	1,16	0,56
Rectangular	Buckling	1,4	0,8
Rectangular, spot-welded	Buckling	$2,82-4,35\rho_i$	1
Hexagonal	Buckling	1,4	0,6

Table 4.6: The values of m and n for different geometry and collapse mode. ρ_i is the flange part of the cross-section total area. Formation of cracks refers to the fact that the collapse takes place through buckling but the tube cracks in the folds.

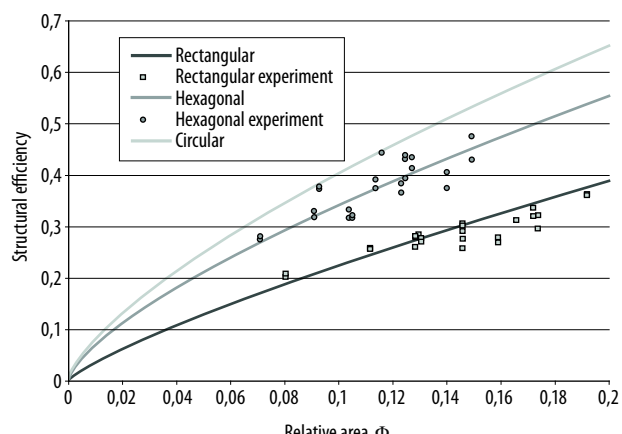


Figure 4.58: Structural efficiency as a function of relative area for rectangular, hexagonal and circular cross-sections according to table 4.6. Empirical results for rectangular and hexagonal tubes with a big variation of material properties and geometries are also included in the form of hot- and cold-rolled steels with yield points of between 330 and 860 MPa and thicknesses of between 1.2 and 4.0 mm.

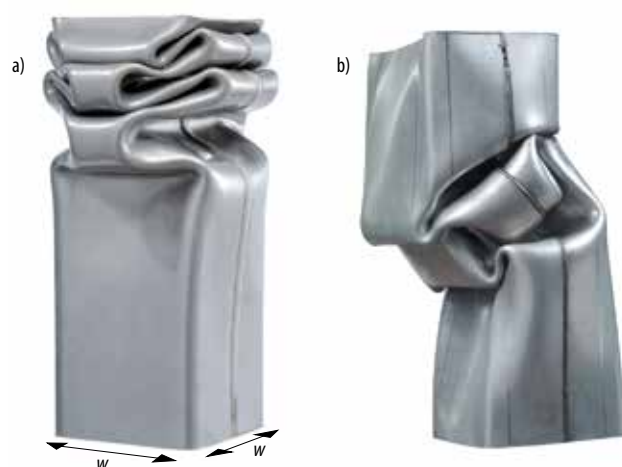


Figure 4.59: Collapse modes. a) Regular formation of folds. b) Irregular formation of folds.

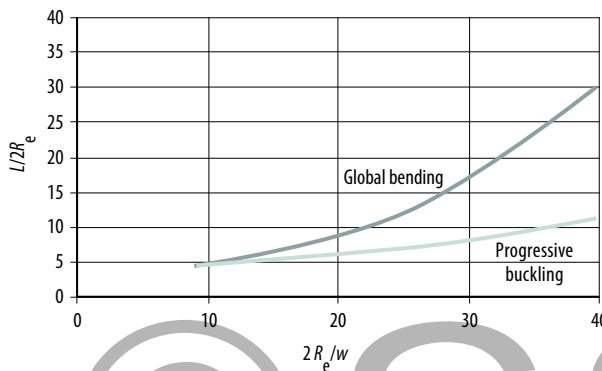


Figure 4.60: Collapse mode for circular and square tubes.

How the geometry parameters affect the global bending and folding collapse modes is graphically illustrated in figure 4.60. The modes can alternate in the area between these limit values during the collapse process.

These limits are derived for quasi-static cases. In dynamic situations, as a rule, the risk of irregular folding increases and the risk of global bending decreases with increasing speed.

It can be mentioned that tubes with flanges (for spot welding) behaves in a different way than the above-described butt-welded tubes. Additional parameters such as flange width and spot weld distance will affect the energy absorption. Generally, flanges contribute less than the tube itself, which provides a less weight-efficient solution. Therefore, the width of necessary flanges should be as small as possible.

Beams subjected to bending load

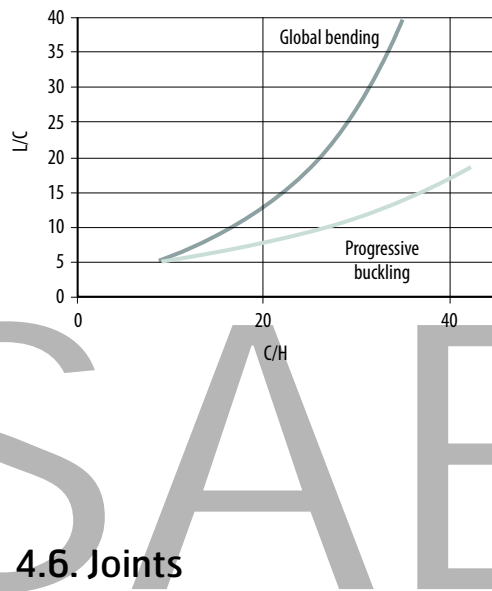
The energy absorption capacity from three-point bending tests of any cross-section can be calculated according to equation 4.61 [4.25]:

$$E = 0,73 \sqrt{\delta_{\text{linj}}} K \delta^{1,5} - 0,16 \frac{\delta_{\text{linj}} K^2}{F_{\text{max}}} \delta^2 \quad (\text{Eq. 4.61})$$

where

- δ_{linj} – the deflection at which the most strained beam fiber reaches the yield point
- K – equivalent spring stiffness, F/δ ($48EI/L^3$ for a freely supported beam)
- δ – maximum deflection
- F_{max} – maximum force

The equation has proven to be in relatively good agreement with extensive practical testing carried out at SSAB in Borlänge. The tests comprised circular tubes, rectangular pipes, open and closed hat sections (single and double).



4.6. Joints

A selection of design criteria for welded-, bolted-, riveted- and adhesive joints subjected to static loading are presented. Design with respect to fatigue loaded joints is described in chapter 5.

4.6.1 Welded joints

The most common joining method is welding. Different welding methods and joining types are described in chapter 6 and even more detailed in the Joining Handbook [4.32]. This section focus on design of fusion welded joints (MAG, MMA, plasma) and spot welds.

A large number of parameters can be varied in designing welded joints. There are different types of joints, welding methods, welding geometries, filler material, welding classes, heat input, weld run sequences, post-treatment methods, etc., see, for example, Karlebo Svetshandbok, [4.33].

Residual stress

During cooling after welding, residual stresses are formed. As a rule, there will tensile residual stress in the vicinity of the weld (primarily along the joint) and compressive residual stress in part with less heat input from welding. The residual stresses are normally not taken into consideration during design of the welded joint itself. However, the tensile stress can be of interest in fatigue analyses and the compressive stress affect resistance of a member susceptible to instability.



HAZ (Heat-Affected Zone)

Regarding material strength in the heat-affected zone, HAZ, it can be stated that soft zones are formed in HAZ from welding in hot rolled cold-formed steel with a yield point over 550 MPa. However, with normal heat input and temperatures, these soft zones do not have any major effect on the strength of the joint due to high triaxiality in the limited area. The fact that soft zones are formed during welding of steels with a very high yield point applies even to cold-rolled steels. As a result for these thin cold-rolled sheets, the strength of the joint is less than that of the parent material, even if a matching filler material is used, see figure 4.61. The strength of a welded joints in material with a lower tensile strength is, however, at least equal to that of the parent material.

Butt weld

A joint with matching or overmatching butt- or T-welds is probably as strong as the parent material in hot-rolled plates subjected to static load. This holds provided that the weld is done with a sufficiently low heat input, see chapter 6. For fatigue loads it is the weld defects rather than the strength of the filler material that governs failure and the weld must be analyzed in detail, see chapter 5.

In principle, the same reasoning also applies to cold-rolled steels. However, it can be more difficult to adjust the heat input in this case and there are no matching filler materials for the highest strength levels in SSAB product range.

Undermatching welds can be given a significantly higher strength if the excess weld metal (reinforcement) is not removed. Undermatching filler material is common in fillet welds, but can also be used in butt welds placed in less stressed areas of the cross-section or when the main load does not act perpendicular to the weld.

Single-side welded lap joints are also common for cold rolled steels, figure 4.62. The static resistance of these is lower compared to that of butt welds due to the additional bending introduced.

Partial penetration butt welds should be treated as fillet welds in design calculation.

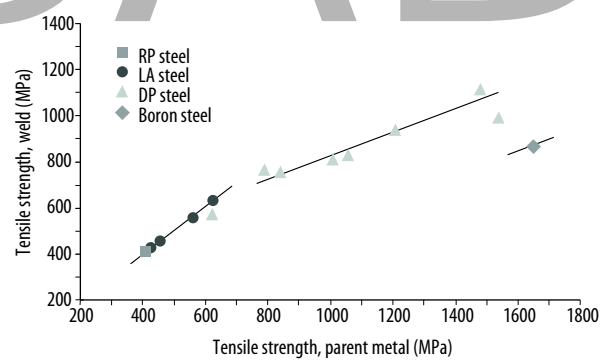
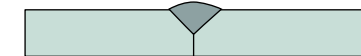


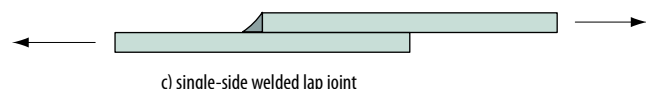
Figure 4.61: Strength of welded joint compared to parent metal for cold rolled steels. MAG welding, transversal weld load, reinforcement removed by grinding, matching filler metals [4.32].



a) welded butt weld



b) non-welded butt weld



c) single-side welded lap joint

Figure 4.62: Butt weld: a) welded; b) non-welded; c) single-side welded lap joint.

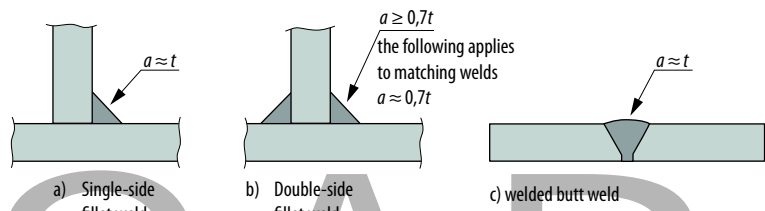


Figure 4.63: Rules of thumb for load-carrying welds effective throat thickness.

Fillet weld

In Eurocode 3 matching and overmatching welds are described. But, the effective throat thickness in fillet welds can be designed with undermatching filler materials to make the welded joint as strong as the parent material. In addition, there are many cases where the weld in a cross-section can be placed in a low stressed area, close to the neutral axis.

Some recommendations for effective throat thickness of static loaded welds are presented in *figure 4.63*. Cases b and c with matching filler materials result in joints which are just as strong as the parent material. Do not opt for unnecessarily big fillet welds.

SSAB experience indicates that it is reasonable to utilize the mean value of the strength of the parent and filler material in calculations through the effective throat thickness – at least in those cases where the welded joint can be made in one bead.

The tensile strength (f_u) of the parent material in *equation 4.63* and *4.64* is then replaced by the tensile strength (f_{uw}) of the weld material, which can be calculated according to *equation 4.62*.

$$f_{uw} = \frac{f_u + f_{euk}}{2} \quad (\text{Eq. 4.62})$$

where

f_{euk} – tensile strength of filler material.

It should be noted that if EN 1993-1-12 governs, the tensile strength (f_{euk}) of the filler material should be used in calculations through the effective throat thickness of the weld as the welding is carried out with undermatching electrodes.

A simplified design method for a fillet weld is to check the resultant from all acting forces, F_s , (on a unit long weld) with the condition in *equation 4.63*

$$F_s \leq \frac{af_u}{\sqrt{3}\gamma_M}, \quad (\text{Eq. 4.63})$$

where a is the effective throat thickness regardless of how the load is oriented to the plane where the effective throat thickness is determined.

In design of fillet welds, the stress state is analyzed in the cross-section of the effective throat thickness, see *figure 4.64*.

In calculations, the effective throat thickness is usually defined as the height in the largest triangle that can be drawn between the joint surfaces and the weld surface. Penetration, if any, can, however, be taken into account during calculations – if sufficiently verified. For more information, see [4.42].

The load, F_s , which acts on a fillet weld is divided into stress components according to *figure 4.65*. The stresses are assumed to be evenly distributed over the section. The weld length, i.e., the actual weld length minus end craters ($2a$), should not be shorter than $10a$. The normal stress parallel to the weld, $\sigma_{//}$, can be neglected. Stresses can also be obtained from a FE analysis.

The resistance of a matching fillet weld is sufficient if the conditions below are met; *equation 4.64* and *4.65*.

$$[\sigma_\perp^2 + 3(\tau_\perp^2 + \tau_{//}^2)]^{1/2} \leq \frac{f_u}{\gamma_M} \quad (\text{Eq. 4.64})$$

and

$$\sigma_\perp \leq \frac{0,9f_u}{\gamma_M} \quad (\text{Eq. 4.65})$$

where

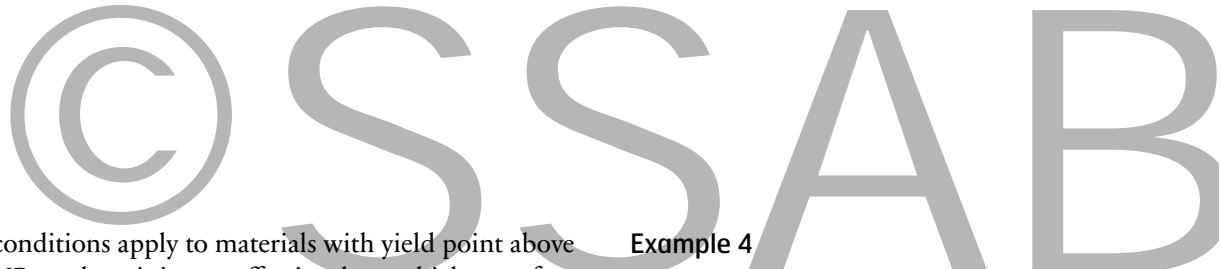
σ_\perp – normal stress perpendicular to the section

τ_\perp – shear stress (in the calculation section) perpendicular to the weld

$\tau_{//}$ – shear stress (in the calculation section) in parallel with the weld

f_u – characteristic yield point of the weaker material in the joint

γ_M – safety factor according to 4.2.3, $\gamma_M = 1.25$



The conditions apply to materials with yield point above 355 MPa and a minimum effective throat thickness of 3 mm. The condition can be too conservative for material with lower yield point. Eurocode 3, part 1-8 [4.34] describes to what extent a higher effective stress can be permitted for these materials.

For materials with strong strain hardening it is advisable to add a safety factor of 1.2 in order to compensate for the difference between yield point and ultimate tensile strength.

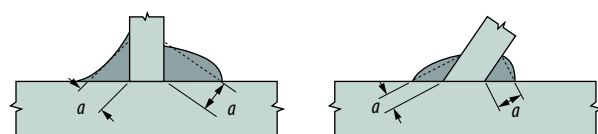


Figure 4.64: The definition of effective throat thickness for fillet welds.

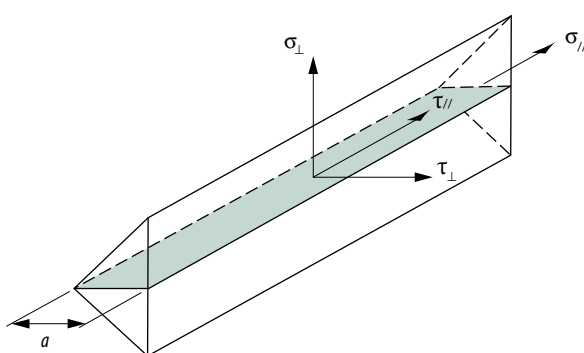
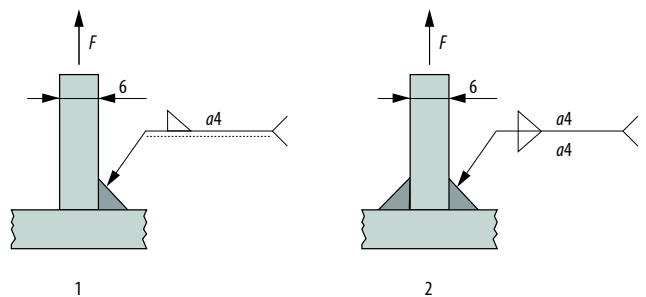


Figure 4.65: Stress components in a fillet weld.

Example 4

Statically loaded fillet weld

What load capacity (F) does a single-sided, 1, and double-sided, 2, fillet weld according to the figure below have? The yield point and ultimate tensile strength of the material: $R_{eH} = 700$ MPa and $R_m = 750$ MPa, respectively, and the filler material $R_m = 560$ MPa.



Since the weld material is undermatching, the weld electrode strength value should be used during analysis of the section through the weld effective throat thickness.

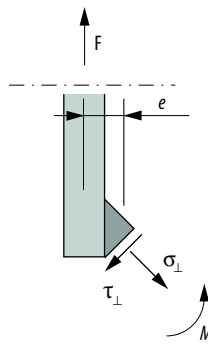
$$f_{uw} = 560 \text{ MPa}$$

Safety factors according to section 4.2.3

$$\gamma_M = 1.25$$

1. Single-sided fillet weld:

Find equilibrium between external and internal forces in the effective throat thickness of the weld.



Horizontal equilibrium gives

$$\sigma_{\perp} = \tau_{\perp}$$

Vertical equilibrium gives

$$\sigma_{\perp} = \tau_{\perp} = \frac{F}{\sqrt{2}al}$$

where l is the weld length.

Bending moment from external load in the weld.

$$M = F \cdot e$$

where

$$e = \frac{6}{6} + \frac{4}{2\sqrt{2}} = 4,41$$

If plastic stress distribution is accepted in the weld, the internal moment can be described as

$$M = 2 \cdot \Delta\sigma_{\perp} \frac{a}{2} \cdot \frac{a}{4} \cdot l = \frac{\Delta\sigma_{\perp} a^2 l}{4}$$

The contribution to the normal stress in the weld therefore becomes

$$\Delta\sigma_{\perp} = \frac{4F \cdot e}{a^2 l}$$

and the total stress in the effective throat thickness of the weld:

$$\sigma_{\perp} = \frac{F}{\sqrt{2}al} + \frac{4F \cdot e}{a^2 l} = \frac{F}{l} \left(\frac{1}{\sqrt{2} \cdot 4} + \frac{4 \cdot 4,41}{16} \right) = 1,28 \frac{F}{l}$$

$$\tau_{\perp} = \frac{F}{\sqrt{2}al} = \frac{F}{\sqrt{2} \cdot 4l} = 0,177 \frac{F}{l}$$

Equation 4.64 gives conditions for the resistance of the weld

$$\frac{F}{l} \sqrt{1,28^2 + 3 \cdot 0,177^2} \leq \frac{560}{1,25}$$

which gives

$$F \leq 347 \text{ N/mm}$$

Finally, the stress should also be checked using *equation 4.65*

$$1,28 \frac{F}{l} \leq \frac{0,9 \cdot 560}{1,25}$$

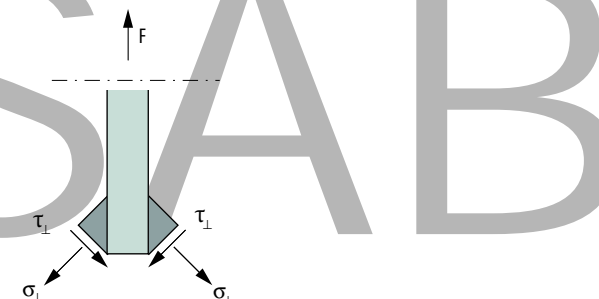
which gives

$$F \leq 315 \text{ N/mm}$$

By ensuring fusion penetration, the load capacity can be significantly higher in a single-sided fillet welded joint. 2 mm of fusion penetration give an effective throat thickness of 6 mm, which results in double load capacity.

2. Double-sided fillet weld:

Find equilibrium between external and internal forces in the effective throat thickness of the weld.



Assume that $\sigma_{\perp} = \tau_{\perp}$

Vertical equilibrium gives

$$\sigma_{\perp} = \tau_{\perp} = \frac{\sqrt{2}F}{4al}$$

where l is the weld length.

Equation 4.64 gives

$$\frac{\sqrt{2}F}{8l} \leq \frac{560}{1,25}$$

and

$$F \leq 2534 \text{ N/mm}$$

Equation 4.65 gives

$$\frac{\sqrt{2}F}{4al} \leq \frac{0,9 \cdot 560}{1,25}$$

and the force

$$F \leq \frac{0,9 \cdot 560 \cdot 4 \cdot 4}{1,25 \sqrt{2}} = 4562 \text{ N/mm}$$

Compared with the single-sided weld, the double-sided is 8 times stronger!

In order for the load capacity in the fillet weld to be the same as for the plate (see *equation 4.14*)

$$N_{t,Rd} = \frac{0,9 \cdot 6 \cdot 750}{1,25} = 3240 \text{ N/mm}$$

the effective throat thickness needs to be $4 \cdot 3240 / 2534 = 5.1 \text{ mm}$.

Spot weld

A practical and economical weld method for thin (< 3 mm) sheets is through spot welding. Spot welding is common in the car industry and the strength of an individual spot weld is often tested through practical tests, e.g., shear, peel, tensile, torsional and fatigue tests. The resistance of joints is then generally determined through a FE analysis of the actual structure with simplified models of the spot welds. The mechanical properties of the spot weld are typically defined through the shear and tensile strength, possibly supplemented with ductility.

How forces are distributed in a joint with several spot welds is complicated. This depends, among other things, on the geometric distribution of spot welds, the load and the ductility of the joint. Experiments carried out under controlled conditions (well-centered load, etc.), e.g., shear testing of single-line joints, have showed that the forces in certain cases are distributed evenly between the welds. In practice numerical methods has to be used (FEM) or, alternatively, practical testing in order to determine the resistance of a specific spot welded joint.

The resistance of a spot welded joint under a shear load is determined by weld nugget edge failure (in the surrounding plate material), net area fracture and finally shear fracture in the weld nugget.

A common requirement with spot welding is that the weld nugget diameter (d) should meet

$$d \geq 4\sqrt{t} \quad (\text{Eqn. 4.66})$$

where

t – plate thickness (mm)

The weld nugget diameter should not be confused with the electrode tip diameter. For more information, see section 6.5.5 and the SSAB Joining Handbook [4.32].

For an overall well designed structure, with the condition for minimum weld nugget diameter fulfilled, it is edge failure of weld nugget under a shear load that governs.

Following conditions apply to the resistance of a joint with a shear-loaded individual spot weld

Steel type	k mean (min–max)	k_{fu}
FeP01–FeP05	3,5 (3,0–4,0)	1050
Docol 220RP–300RP	3,4 (3,1–3,6)	1220–1560
Docol 220LA–500LA	3,4 (3,2–3,6)	1220–2160
Docol 600DP–600DL	3,2 (3,0–3,5)	2080
Docol 800DP	2,9 (2,4–3,7)	2490
Docol 1000DP	2,7 (1,9–3,3)	2970
Docol 1400DP	2,3 (2,1–2,5)	3330
Docol Borstäl	2,1	3360

$$F_{td} = \frac{ktdf_u}{\gamma_M} \quad (\text{Eqn. 4.67})$$

where

- t – thickness of the thinner plate
- d – weld nugget diameter
- f_u – tensile strength
- k – values are obtained in *table 4.7* for some of SSAB steels.
- γ_M – safety factor according to 4.2.3, $\gamma_M = 1.25$

The factor k as a rule, decreases with increasing strength in the steel. However, it can be stated $k \cdot f_u$, which is proportional to shear load resistance, generally increases with the increasing strength for cold rolled steels. *Table 4.7* gives typical values of the factor for *equation 4.67*, and also the maximum and minimum values. These give indication of a relatively big spread. For additional information, see to the Joining Handbook [4.32].

The plate width can also affect the resistance of the joint subjected to shear. Unlike thickness and weld nugget diameter, the relationship between width and resistance is non-linear. The effect decreases with the increasing width and can be neglected for wide joints, typically 50 mm.

Worth mentioning is that spot welds should not be subjected to large tensile loads, in particular, for high-strength steels. The load capacity in tension has only a small influence from material strength. Tensile cross testing carried out at SSAB indicates that load capacity is $1200 \cdot t \cdot d$ for cold rolled steels (with the exception of 1400M and hardened boron steel). This should however not be viewed as a design value, see Joining Handbook [4.32]. It is not uncommon for the resistance of an individual spot weld in DP steel to be only 50% for a tensile load compared to shear load.

It should finally be mentioned that fatigue is the most common cause of failure for a spot weld in many applications, not the static resistance, see chapter 5. A way to improve the resistance of a spot weld, both with respect to static and fatigue loads, is to combine spot welds and adhesive bonding.

Table 4.7: Experimental results from one weld point, 2-plate joint with the same thickness and steel type (cold rolled steel) in both plates. The Joining Handbook [4.32]. For information about additional steels, refer to www.ssab.com.

4.6.2 Bolted connections

There are many types of bolted joints and many different joint classes (shear-, fitted-, friction-, injection joints, etc.), with different bolts (strength classes, drilling, tapping, etc.), with or without pre-stressing, washers, etc. Some of the most important design criteria for bolted connections using bolt and nut are listed below.

Four failure modes can be identified from shear loading.

Shear failure in the bolt

The bolt is sheared off in the section/sections between the plates in the joint. Similar with an undermatching weld, cf. figure 4.66. The shear area should be the nominal area at the position of critical cross-section.

Hole bearing failure in steel plate

If the distance between bolt and plate edge is not critical a hole bearing failure can occur. This means that the bearing pressure reach yielding for the plate material see figure 4.67.

Material failure

Failure in the reduced net cross-section of the plate, see figure 4.68.

Edge failure

If the distance between bolt and plate edge is limited, the joint can fail through shearing along "parallel" lines, see figure 4.69.

The four failure mechanisms are analyzed individually in order to find the governing design load. A combination of the different mechanisms is also a possible failure mode.

Joints in thin sheet structures should not be subjected to a big peel- or tensile load. Different types of bolted connections behave differently under a tensile load, and to determine the final resistance practical testing is often the best approach.

Practical testing is important in the design of bolted connections to supplemented calculations. Recommendations regarding testing are available in ECCS, Publ. No. 21 och No. 42 [4.37, 4.38]. Some key design criteria for calculation according to Eurocode 3 are presented in the following. These are valid for plate thicknesses > 4 mm. Note that there are also other exceptions and limitations to this.

Shear failure in the bolt

Tests results have shown that the relation between shear and tensile strength of a bolt is independent of the diameter. The shear resistance can be described by equations 4.68 and 4.69.

$$F_{td} = \frac{0.6f_{buk}A_s}{\gamma_M} \quad (\text{Eq. 4.68})$$

for bolt strength classes 4.6, 5.6 and 8.8

$$F_{td} = \frac{0.5f_{buk}A_s}{\gamma_M} \quad (\text{Eq. 4.69})$$

for strength classes 4.8, 5.8, 6.8 and 10.9

where

f_{buk} – tensile strength of the bolt (MPa)

A_s – nominal bolt area (mm^2)

γ_M – safety factor according to 4.2.3, $\gamma_M = 1.25$

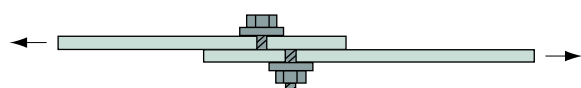


Figure 4.66: Schematic description of shear failure in the screw.

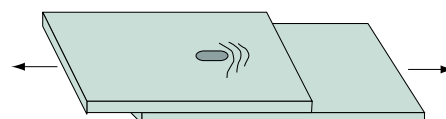


Figure 4.67: Schematic description of failure in steel plate

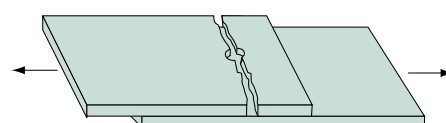


Figure 4.68: Schematic description of net failure.

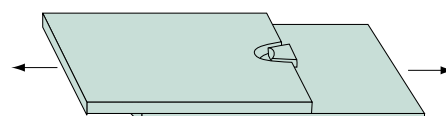


Figure 4.69: Schematic description of edge failure.

Bearing failure

A number of parameters govern the bearing pressure resistance. The most important are covered by *equation 4.70*.

$$F_{\text{td}} = \frac{2.5 f_{\text{uk}} dt}{\gamma_M} \quad (\text{Eq. 4.70})$$

where

- d – bolt diameter (mm)
- t – plate thickness (mm)
- f_{uk} – tensile strength of material (MPa)
- γ_M – safety factor according to 4.2.3, $\gamma_M = 1.25$

This presupposes disposition of the bolts in accordance with recommendations eliminating edge failure, *equation 4.71*.

Material failure

The net area of a bolted section is reduced which increases the stress level locally. *Equation 4.71* governs for thick plates, > 4 mm. The effect of stress concentrations may need to be taken into consideration for thinner plates.

$$F_{\text{td}} = \frac{A_{\text{net}} f_{\text{uk}}}{\gamma_M} \quad (\text{Eq. 4.71})$$

where

- A_{net} – section net area (mm^2)
- f_{uk} – tensile strength of material (MPa)
- γ_M – safety factor according to 4.2.3, $\gamma_M = 1.25$

Edge failure

Longitudinal shear failure caused by insufficient edge distance can be avoided by the disposition of the bolts. The following is recommended;

$$\begin{aligned} e_1 &\geq 3d; & e_2 &\geq 1.5d \\ p_1 &\geq 3d; & p_2 &\geq 4d. \end{aligned} \quad (\text{Eq. 4.72})$$

where

e_1 , e_2 , p_1 and p_2 according to *figure 4.70*

If distance, e_1 , to the free edge in the direction of the force is smaller than recommended, the resistance can be estimated with respect to edge failure using *equation 4.73*.

$$F_{\text{td}} = \frac{e_1 t f_{\text{uk}}}{1.2 \gamma_M} \quad (\text{Eq. 4.73})$$

where

- e_1 – according to *figure 4.70* (mm)
- t – plate thickness (mm)
- f_{uk} – tensile strength of material (MPa)
- γ_M – safety factor according to section 4.2.3

If edge distances are below recommended, the reduced resistance can be calculated using Eurocode 3-1-8 [4.34].

The ultimate shear resistance of a joint is given by the governing failure mechanism, i.e., the lowest resistance from *equations 4.70–4.73*.

As mentioned, practical testing is the first resort in design of axially loaded bolted joints. The axial resistance of the bolt under a tensile load can, however, be determined according to *equation 4.74*

$$F_{\text{dd}} = \frac{0.9 A_s f_{\text{buk}}}{\gamma_{Mn}} \quad (\text{Eq. 4.74})$$

where

- A_s – bolt area (mm^2)
- f_{buk} – tensile strength of material (MPa)
- γ_{Mn} – safety factor according to section 4.2.3

Note that pull-through affects the resistance of the whole joint under an axial load.

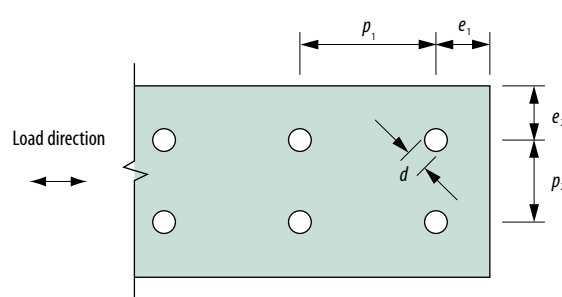


Figure 4.70: Relevant dimensions in connection with recommendations for the placement of screw in a screwed joint.

If the load applied is a combination of a tensile and shear force, the combined effect can conservatively be computed according to *equation 4.75*.

$$\frac{F_{\perp}}{1,4F_{dd}} + \frac{F_{//}}{F_{td}} \leq 1 \quad (\text{Eq. 4.75})$$

where

- F_{\perp} – tensile load (N)
 $F_{//}$ – shear load (N)
 F_{dd} – resistance under a tensile load, *equation 4.74* (N)
 F_{td} – resistance under a shear load, *equation 4.73* (N)

$$F_{td} = \frac{0.7f_{buk}A_s\mu n}{\gamma_M} \quad (\text{Eq. 4.76})$$

where

- A_s – stress area of bolt (mm²)
 f_{buk} – tensile strength of bolt (MPa)
 γ_M – safety factor according to section 4.2.3
 μ – friction coefficient
 n – number of cuts

Pre-stressing

By tightening the bolts of a joint with a certain torque, a clamping force is applied. This clamping force can be utilized in friction joints, fatigue-loaded joints and to avoid a loose fit. In friction joints the clamping force is required to transfer shear. Pre-stressing can reduce the load variation in axially loaded bolts, which is of importance from a fatigue point of view. Eliminating a loose fit also prevents leakage and sliding, the latter resulting in wear.

Friction joints

The difference between shear- and friction joints is that a significant part of the shear force in the latter is absorbed by friction between the plates in the joint. The possibility to design an efficient friction joint, however, decreases with the decreasing plate thickness. Considering only friction, the resistance of a friction joint, is according to *equation 4.76*.

Guidelines for friction coefficients:

Pure mill scale	$\mu = 0.3$
Blast or flame-cleaned surface	$\mu = 0.5$
Hot-dip galvanized surface	$\mu = 0.15$
Hot-dip galvanized and blast surface	$\mu = 0.35$
Spray-galvanized surface (layer thickness > 50µm)	$\mu = 0.3$
Surface alumetized by spraying (layer thickness > 50µm)	$\mu = 0.5$
Zinc silicate paint (layer thickness <100µm)	$\mu = 0.4$

A typical clamping force is assumed in *equation 4.75*. If settling and external axial loads are taken into consideration, a more sophisticated expression for the clamping force can be found. The stiffness of the foundation must also be determined in that case. The gap between hole and bolt can also affect the relation in *equation 4.75*.

If shear failure in the bolts is not governing, the load can be assumed distributed evenly among the individual bolts in the joint. As a rule, this applies to joints with identical bolts and plates with similar materials and thicknesses.

Thin plate joints

Other types of bolted connections are often used for lower load levels and applications with joining and fastening of thin sheet structures such as corrugated sheet, panels and fittings. These can be penetrating, drilling or tapping bolts. There are additional mechanisms which must be included in the design of such joints, e.g., angular misalignment of the bolt, etc. A summary of these type of joints and design recommendations are available in [4.39].

4.6.3 Riveted joints

Riveting is used for joining of thin sheets and design calculations resembles that of bolted joints. Recommendations and test results of self-piercing riveted joints and clinched joints are presented in this section.

Riveted joints can generally be divided into:

- Self-piercing riveted joints

An external rivet punches a hole and then joins the plates.

- Clinched joints

Mechanical locking through plastic deformation of existing plates.

- Blind riveted (POP riveted) joints

An external hollow rivet is fitted into a hole. Requires access only from one direction.

Design of blind riveted joints is not discussed further.

Self-piercing riveting

Self-piercing riveted and clinched joints are found mainly in applications where different materials, or surface-treated sheets, need to be joined together. It is also a solution where higher high-cycle fatigue strength is required than for spot welds. Comparing self-piercing riveting and clinching to spot welding, the riveted joints often show better energy absorption due to more elongation at failure.

The static resistance of self-piercing riveted joints is affected by the strength of the sheet and the rivet, sheet thickness, rivet type and rivet geometry.

The effect of the rivet diameter is illustrated in *figure 4.71*. The fact that spot welds, as a rule, handle higher loads compared to self-piercing rivets but have lower elongation at break can also be observed in *figure 4.71*.

The effect of the sheet thickness is presented in *table 4.8* where shear resistance and peeling, respectively, is presented for joints in mild steel of varying thickness.

Experiments carried out with DC test specimens also gives a measure of the resistance for combined load directions, see *table 4.9*.

The results are based on experiments carried out in mild steel. The resistance of a self-piercing riveted joint increases with the strength of the sheet material. There are examples of this from tests carried out in Docol steels, see *figure 4.72*. This figure also shows the difference in shear resistance between clinching, self-piercing riveting and spot welding. The difference between riveting and spot welding increases with the increase in plate thickness.

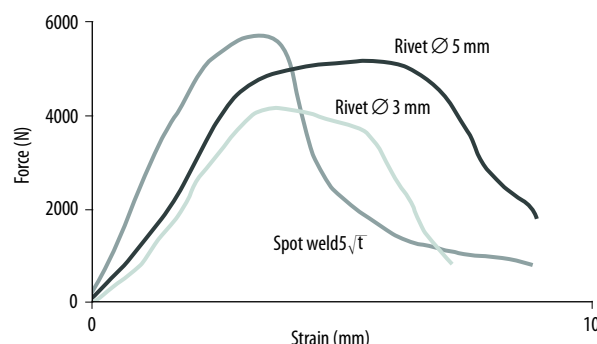


Figure 4.71: Typical results from diagonal tension test of spot welded and self-piercing joints. Low carbon mild steels with a plate thickness of $1.0 + 1.0$ mm, [4.32].

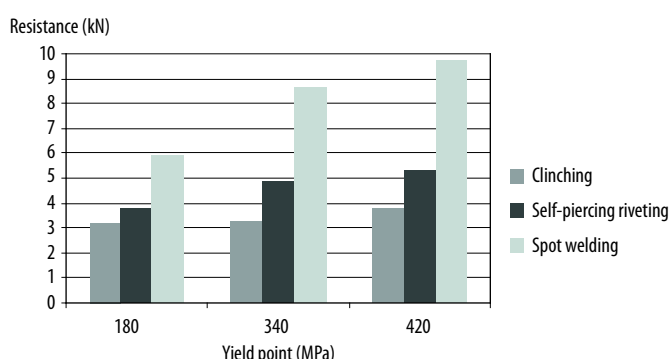


Figure 4.72: Static resistance under a shear load for clinching, self-piercing riveting and spot welding as a function of the yield point. Cold-rolled material with a thickness of $1.0 + 1.0$ mm, [4.32].

Plate thickness (mm)	Resistance, shearing (kN)	Resistance, peeling (kN)
1+1	3,5	1,5
2+2	7,0	2,8
3+3	12	4,5

Table 4.8: Static resistance in self-piercing joints for different plate thicknesses. Ø 5-mm rivets in mild thin sheet, [4.32].

Load direction	Resistance (kN)
0° (shearing)	3,5
30°	2,8
60°	1,9
90° (peeling)	1,7

Table 4.9: Static resistance in self-piercing joints as a function of load direction. Ø 6.4-mm rivets in mild thin sheet with a thickness of $1.0 + 1.0$ mm, [4.32].



Clinching

The factors that primarily affect the resistance of a clinched joint are the material strength, thickness, type of clinched joint and its size. The resistance increases with increasing material strength, thickness and the rivet diameter.

The static resistance of clinched joints, as a rule, is lower than for both self-piercing riveting and spot welding, as indicated in figure 4.72. However, there is a large spread in properties of the different types of clinched joints. This has been studied in tests using different materials (with similar strength levels) and clinched joint types and for the same sheet thickness. Figure 4.73 presents shear resistance for different materials and rivet types (diverse round and rectangular). The diagram should be regarded as a general example of how the failure load is affected by the strength of the parent material. Additional information is available from SSAB or in the reference [4.32]. It can be stated that round clinched joints show higher resistance than rectangular (except for torsional loads). As a rule, the best way to increase the resistance of a self-piercing joint or a clinched joint is to increase the number of rivets.

Even high strength material can be clinched. A higher yield point of the sheet, however, requires a higher pressing force. This leads to more tool wear, which can limit the method use for high-strength steels. For example, clinched joints in cold rolled dual phase Docol 1000DP steel (yield point of max 950 MPa) are not formed under the same pressing force that forms satisfactory clinched

joints for steels with a yield point of up to 400 MPa. If the force is increased by 50%, clinched joints can be produced with cold rolled Docol 1000DP. These have a significantly higher shear resistance compared to materials with a yield point of, e.g., 400 MPa. This is due to the high yield point and the strain hardening of the dual phase steel.

As evident from above, a large part of the design procedure for clinched and self-piercing joints is based on testing. But, progress have recently been achieved also when it comes to the FE analysis of these joints. Note that the data presented above for self-piercing riveting and clinching is the result of experimental testing for a specific setup of material and geometry parameters. This should not be regarded as absolute design values. Additional test results are available in the Joining Handbook [4.32] or can be obtained by contacting SSAB.

4.6.4 Adhesive joints

The adhesive joint is relatively new compared to bolted and welded joints for thin sheet structures. The development of adhesives is going quickly. In general, the design procedure is not as established as for bolted and welded joints. Eurocode 3 does not cover the combination of thin sheet and adhesive. A large number of parameters control the joint properties, e.g., adhesive type, hardening procedure, wetting, fixing, temperature and residual stresses, see the Joining Handbook [4.32].

In general there is a lot to gain by considering adhesives already in the design stage. A large contact surface is required and the joint should be subjected mainly to a shear. Minimizing Peel and Cleavage Load

Limiting factors for the strength in an adhesive joint can be both the strength of the adhesive and the adhesion in the interface. The design sections below discuss primarily the strength of the adhesive, whereas adhesion is affected by wetting, roughness and purity, etc. The chapter is primarily descriptive by nature.

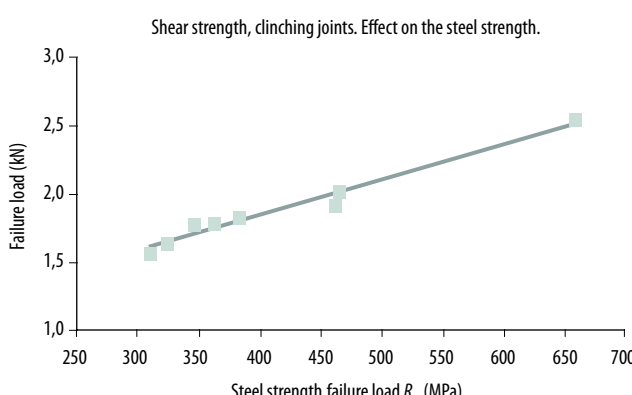


Figure 4.73: Examples of shear strength in clinching joints. Round rivet with a diameter of 7 mm, sheet thickness of 0.7 mm, [4.32].



Design

Design of adhesive joints is to a higher extent than for other joints done with numerical analysis and/or practical testing. There are few standards and established methods on the subject. The resistance of lap joints under a shear load is often calculated according to *equation 4.77*.

$$F_s = \tau_{lim} b L \quad (\text{Eqn. 4.77})$$

where

b – contact surface width (mm)

L – joint length (mm)

τ_{lim} – shear strength of the adhesive,
see *figure 4.74* (MPa)

Test results for single-sided lap joints with thin sheet subjected to a shear show that the yield point of the material in the sheet also affects the static resistance of the joint [2]. The reason is the joint tendency to rotate due to an applied bending moment. The highest local stress due to bending of sheets with the same thickness is three times the nominal tensile stress. Material yielding due to this will result in rotation and peeling of the adhesive joint which can lead to a failure. For calculation of the resistance, Adams [3] suggests the load level at yielding, i.e.

$$F_s = \frac{f_y b t}{4} \quad (\text{Eqn. 4.78})$$

where

f_y – yield point of sheet material (MPa)

t – thickness (mm)

b – width (mm)

The shear strength of the adhesive is not an absolute material parameter as the stress distribution is not even over the joint. The shear stress is typically distributed lengthwise, *figure 4.74*, with high stress at the joint edges. τ_{lim} is defined as the mean shear stress depending on the design of the joint. What determines the stress concentrations is the joint length, sheet thickness and type of joint (beveling, double sheets, etc.) If *equation 4.77* is used (with bulk shear strength equal to that of the adhesive) in design, a large safety margin is advised, a factor of 10 to 20 is not uncommon.

Equation 4.78 can be regarded as a lower limit value. The upper limit is given by the force which corresponds to maximum shear stress in the adhesive in the joint. This upper limit is given by *equation 4.77* when τ_{lim} is the actual shear stress (bulk shear strength) of the adhesive.

In order to obtain a more correct assessment of the resistance and a detailed description of how different parameters affect the joint resistance, a numerical analysis (FE analysis) can be done. This is an efficient tool for parametric studies but to verify the numerical results practical testing is strongly recommended. The challenge using FE analysis is in describing the adhesive, material model and material properties. The stress and strain curve is typically non-linear and the true shear strength of the adhesive cannot be obtained from a typical shear test of a lap joint. The adhesive bulk properties have to be examined on adhesive test specimens or by using especially designed joints (rough double plates subjected to shear or tubes/shafts subjected to twisting).

A way to find design parameters from different testing is to compile a joint factor diagram. The specific resistance (force/joint area) of each tested joint is plotted for a unique setup of joint parameters, see [4.19].

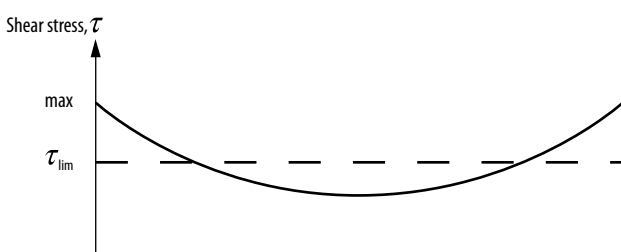


Figure 4.74: Schematic distribution of shear stress in an adhesive joint.

Despite high stress concentrations along the edges of an adhesive joint, the resistance increases with increasing joint length. The reasons for this is that; increasing the length reduces the bending moment; that adhesives, as a rule, have good ductility and that stress is distributed more even in the adhesive joint than in many other types of joints. A good designed adhesive joint often has higher stiffness than a corresponding spot welded joint.

If materials with different Young's modulus (E) is joined together, the joint achieves maximum strength when the strain is compatible. Strain compatibility is obtained by adjusting the thicknesses (t), so that $E \cdot t$ is constant.

By combining different types of joints, the best of what each respective joint has to offer can be utilized. Adhesives are typically combined with spot welding or riveting.

The advantages of adhesives are:

- Excellent fatigue properties
- High stiffness
- Load distribution
- Sealing
- Sound- and vibration dampening

Advantages that can be achieved through a combination with spot welding:

- Peeling strength
- Long-term properties
- No fixation is required

Through bending, folding, etc, it is possible to design thin sheet joints to be subjected to pure shear, see chapter 3. In addition to the possibilities offered by combination joints, rubber-modified epoxy-adhesive can give the joint a certain resistance to peeling. Numerical analysis and peel test and/or cleavage test can provide information about a joint strength with respect to peeling.

The strength properties of an adhesive joint degenerate with time. This is caused mainly by moisture, which diffuses into the adhesive from the free surface or the contact surface. It is important for the adhesive to cover the sheet surface roughness well. The long-term durability can also be determined by how strong and durable oxides are formed by the steel.

4.7 Low operating temperature

High toughness is important to avoid brittle failure, i.e. instantaneous failure without any warning and at negligible plastic strain. The opposite of brittle- is ductile failure with high degree of plastic deformation and lower propagation rate. A ductile failure is characterized by the fracture surfaces not matching. Toughness is normally determined with an impact toughness test, Charpy V, according to EN 10.045. According to this standard, a test specimen must be able to withstand 27 J at the test temperature in order for the steel not to be considered brittle. The impact toughness guarantee given for a certain type of steel normally applies to a certain temperature (the "test temperature").

It is important to note that the test temperature is not the same as the lowest operating temperature. The lowest operating temperature is usually significantly lower. Higher requirements have to be put on toughness for high strength steels. The reason for this is that the risk of brittle failure primarily depends on the thickness and secondly on the operating temperature and the magnitude of the load. Cold forming is accompanied by strain hardening which increases the transition temperature from ductile to brittle failure by 2–3° C per % deformation. If a cold formed area is welded, ageing can lead to an additional increase in the transition temperature of 5–10° C. This is called strain ageing. The risk of brittle failure increases with the stress level in a structure and the degree of triaxial stress condition. Triaxial stress conditions exists, to a larger extent, in structures with thick plate. For high-strength steels delivered as thin sheet with good impact toughness, the increased transition temperature seldom has any practical meaning. The test specimen which is normally used in impact toughness testing has a cross-section area of 10x10 mm² and a 2 mm deep notch. A test specimen with a smaller cross-section area must be used for thicknesses less than 10 mm, see *table 4.11*.

Guaranteed impact value from Charpy V testing can vary between different steel producers, between different steels and different standards. The most common is that the guarantees are min. 27 J or min. 40 J from testing 10x10 mm² specimens. The corresponding values from testing thinner material using a reduced test specimen size is 34 J/cm² or 50 J/cm², respectively. The toughness guarantees that are usually given for SSAB high-strength hot rolled MC have additional denotation according to *table 4.10*.

This table should not be used for all Domex steels. For more information see product data sheet for the respective steel.

Figure 4.75 can be used to determining the lowest permissible operating temperature with regard to the risk of brittle failure.

The figure concerns a welded structure subjected to a static load. It indicates that decreasing thickness strongly influences the lowest operating temperature. This also corresponds well to practical experience showing that brittle failures seldom occur for thin sheet.

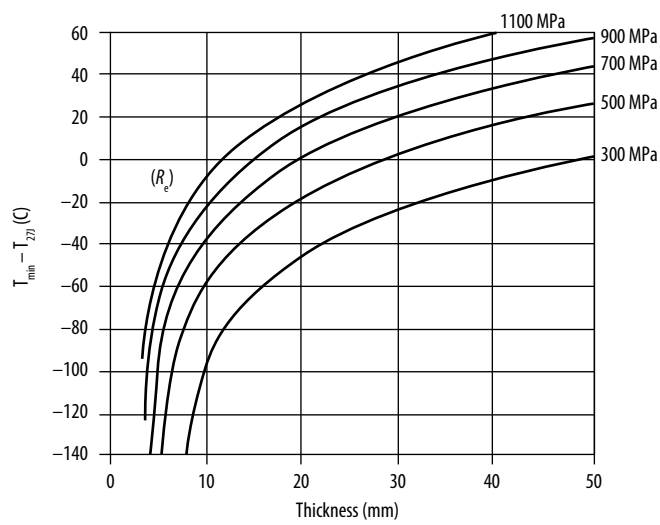
$T_{\min} - T_{27J}$ is indicated on the y axis of the diagram, i.e., the difference in temperature between the lowest operating temperature and the transition temperature. If there the actual transition temperature for the welded joint is unknown, the test temperature (Charpy V) at which the impact toughness guarantees for the steel apply, see *table 4.10* or the current product data sheet can be used. The basis for the diagram is made from practical testing on different types of beams and with a wide material strength range (up to a yield point of approx. 1300 MPa).

If the transition temperature at 40 J (T_{40J}) is known instead of at T_{27J} , the difference between T_{27J} and T_{40J} can be used. For common high-strength steels, this difference is approx. 10° C (i.e., $T_{27J} = T_{40J} - 10^\circ \text{C}$). If both transition temperatures are unknown, T_{27J} and T_{40J} , for the respective steel, the test temperature at which the impact toughness guarantees apply can be used instead (see section 2.3.2). T_{27J} must in this case be at least as low as the testing temperature.

The recommendation is that if the actual T_{27J} value is not known, the test temperature can be used as input value for T_{27J} instead.

Correction of transition temperature for thin sheet

Using *figure 4.75* for thin sheet $\leq 10 \text{ mm}$ an adjustment of the transition temperature must be done. The reason is testing of reduced test specimen, *table 4.11*. *Figure 4.76* can be used for the corrected T_{27J} -value.



T_{\min} = Lowest operating temperature

T_{27J} = The transition temperature at 27 J, i.e., the temperature at which impact toughness measured with Charpy V (big enough test rod 10x10 mm) is 27 J.

Figure 4.75: Diagram for assessment of the lowest operating temperature, T_{\min} . Welded structure and static load. T_{27J} is the transition temperature.

Additional designation	Test temperature	Energy level
B	No impact testing	
D	-20°C	40J
E	-40°C	27J

Table 4.10: Temperatures for which impact toughness guarantees based on 10x10 mm² impact test rods are usually given, as well as associated additional designations for hot rolled HS and EHS.

Sheet thickness (mm)	Test rod (mm ²)
>10mm	10 x 10
7,5–10,0	10 x 7,5
5,0–7,5	10 x 5

Table 4.11: Test rod dimension during toughness test according to Charpy V for different plate thicknesses.

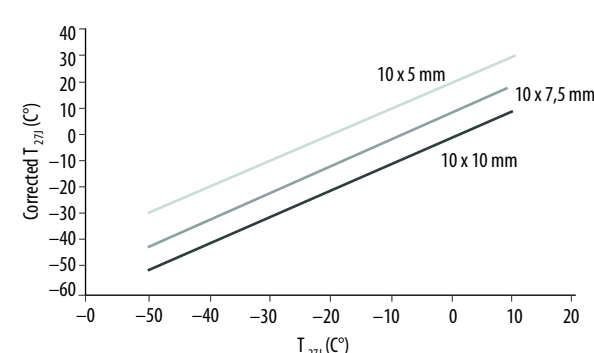


Figure 4.76 Corrected T_{27J} value as a function of size on the reduced impact test rod.

Calculation procedure

1. Start from t , R_e and T_{27J} .

t – sheet thickness (mm)
 R_e – yield point (MPa)
 T_{27J} – transition temperature ($^{\circ}$ C)

2. Determine T_{min} from figure 4.75

If data for the actual transition temperature of the steel is not available, use the test temperature as a value for T_{27J} .

Correct T_{27J} for $t < 10$ mm using figure 4.76.

Example 5

SSAB Domex 500 MCE is used in a welded structure. The plate thickness is 12 mm. Specify an approximate value for the lowest operating temperature for the structure.

Solution:

Since the case involves a MC steel with additional designation E, the impact toughness guarantee is 27 Joule at -40° C.

$T_{min} - T_{27J} = -50^{\circ}$ C according to figure 4.75.

$T_{27J} = -50^{\circ}$ C (E steel with a guarantee of 27 J at -40° C) results in $T_{min} = -50^{\circ}$ C + $T_{27J} = -50^{\circ}$ C -40° C = -90° C.

Example 6

A steel with a yield point of 1100 MPa and a thickness of 6 mm is used in a welded structure. The toughness guarantee is 27 J (34 J/cm^2) at -40° C. What is the lowest operating temperature?

Solution:

Since the plate thickness is <10 mm, a reduced test specimen has been used during the impact toughness test. See the flow chart in the calculation procedure. A specimen with dimensions 10x5 mm (see table 4.11) is used for a plate thickness of 6 mm.

The corrected T_{27J} value according to figure 4.76 becomes:

T_{27J} (corrected) = -20° C

According to figure 4.75, this results in

$T_{min} - T_{27J} = -40^{\circ}$ C.

When a corrected test specimen has been used:

$T_{27J} = T_{27J}$ (corrected)

The condition according to the equation above gives:

$T_{min} = -40^{\circ}$ C + T_{27J} (corrected) = -40° C -20° C = -60° C

Answer:

Lowest operating temperature, $T_{min} = -60^{\circ}$ C.

To consider

- Structures in high strength steel may need to be checked with regard to their lowest operating temperature. This becomes more important for thick plates.
- Pay attention to additional denotations and impact toughness guarantees.
- The risk of brittle failure is reduced with reduced thickness, increased impact toughness, reduced degree of triaxial stress condition.
- Always follow the recommendations for maximum allowed heat input during welding. One weld bead is often possible for thin sheets. More weld beads are required for thicker plates in order not to exceed the recommended heat input value.
- The heat input recommendations regarding welding should be followed in connection with TIG re-melting.
- In critical cases, it is advisable to avoid welding in bent areas.

4.8 References

- [4.1] SS-EN 1990
Eurocode – Grundläggande dimensioneringsregler för bärverk.
SIS Förlag AB.
- [4.2] SS-EN 1993-1-3:2005
Eurocode 3 – Dimensionering av stålkonstruktioner, Del 1-3: Kallformade profiler och profilerad plåt.
SIS Förlag AB, 2005.
- [4.3] SS-EN 1993-1-1:2005
Eurocode 3 – Dimensionering av stålkonstruktioner, Del 1-1: Allmänna regler och regler för byggnader.
SIS Förlag AB, Stockholm 2005.
- [4.4] SS-EN 1993-1-5:2005
Eurocode 3 – Dimensionering av stålkonstruktioner, Del 1-5: Plåtbalkar.
SIS Förlag AB, 2005.
- [4.5] Höglund, T.
Modul 6: Stabilitet för balkar och stänger.
Stålbyggnadsinstitutet, Stockholm 2006.
- [4.6] Johansson, B.
Modul 4: Bärverksanalys.
Stålbyggnadsinstitutet, Stockholm 2006.
- [4.7] SS-EN 13001-1:2004+A1:2009
Lyftkranar – Dimensionering – Del 1: Allmäna principer och krav
SIS Förlag AB, 2009.
- [4.8] SS-EN 1991
Eurocode 1 – Laster och bärverk
SIS Förlag AB, 1991.
- [4.9] BSK 99.
Boverkets handbok om stålkonstruktioner.
Boverket, 1999
- [4.10] Timoshenko, S. P., Gere, J. M.
Theory of elastic stability.
McGraw-Hill Book Company, 2nd Ed. 1961
- [4.11] SS-EN 1993-1-6: 2005
Eurocode 3 – Dimensionering av stålkonstruktioner, Del 1-6: Skal.
SIS Förlag AB, 2005.
- [4.12] StBK-N5
Tunnplåtsnorm
Statens Stålbyggnadskommitté, AB Svensk Byggtjänst, Stockholm 1980.
- [4.13] Gozzi, J., Pétursson, E.
Lokal intryckning av slank C-profil.
Intern rapport nr. 10045, SSAB EMEA, Borlänge 2010.
- [4.14] *Handboken Bygg, band A,*
Liber Förlag, Stockholm 1983
- [4.15] Höglund, T, Strömberg, J.
Modul 7: Kallformade profiler.
Stålbyggnadsinstitutet, Stockholm 2006.
- [4.16] Bergström, Y.
A Dislocation Model for the Stress-Strain Behaviour of Polycrystalline a – FE with Special Emphasis on the Variation of the Densities of Mobile and Immobile Dislocations
Materials Science and Engineering 5, s193-200, 1969/70
- [4.17] Carlsson, B.
Effects on Strain Rate on Absorbed Energy in Crushing of Box Columns,
Esaform Conference, Krakow, Poland, 2002.
- [4.18] *Strain rate dependent steel material properties in CAE analysis for crashworthiness.*
ULSAB – AVC Technical Transfer Dispatch #3A, January 2000.
- [4.19] Jones N. and Wierzbicki T.
Static and dynamic finite element analysis of structural crashworthiness in the automotive and aerospace industries, in Structural crashworthiness.
Butterwoths, London, 1983, pp. 175–217.
- [4.20] Thornton, P. H., Mahmood, H. F., Magee, C. L.
Energy absorption by structural collapse.
Structural Crashworthiness, edited by Jones N. and Wierzbicki T., Butterwoths, London, 1983, pp. 96–117.
- [4.21] Jones, N.
Some Phenomena in the structural crashworthiness field.
IJCrash 1999, Vol 4, No 4, pp 335–350.
- [4.22] Wierzbicki, T.
Crushing behaviour of plate intersections,
Structural Crashworthiness edited by Jones N. and Wierzbicki T., Butterwoths, London, 1983, pp. 66–95.
- [4.23] Sperle, J-O. Olsson.
High Strength and ultra high strength steels for weight reduction in structural and safety related applications.
29th International Symposium on Automotive Technology & Automation (ISATA). Florence, Italy, 3rd–6th June 1996. Internal SSAB Report No. 970095.

- [4.24] Borlecht, Subbaraman.
Design of Ultra-High strength sheet steel beams,
SAE Technical Papers 900428. International congress
and exposition Detroit, Michigan
February 26 – March 2, 1990.
- [4.25] Eckerlid, J.
Sammanställning av provresultat från trepunkts böjprov.
Intern rapport nr 980144, SSAB Tunnplåt AB, Borlänge.
- [4.26] Bergqvist.
Något om Fallförsök på plåtfält.
Teknisk rapport TR 12/80, SSAB Oxelösund.
- [4.27] Eckerlid, J., Söderberg, A.
Krossningsförsök för att verifiera Plåthandboken.
Intern rapport nr 040123, SSAB, Borlänge 2004.
- [4.28] Abaqus Standard.
*Hibbitt Karlsson & Sorensen Inc, 1080 Main Street,
Pawtucket, RI 02860-4847, USA.*
<http://www.abaqus.com>
- [4.29] Engberg, G., Carlsson, B.
*The strain-rate sensitivity and deformation hardening of
ferritic steels,*
Intern rapport nr 980144, SSAB Tunnplåt AB.
- [4.30] Söderberg, A.
Materialmodellering vid numerisk krocksimulering.
Intern Rapport N1.95AS.04.0049-22,
SSAB Tunnplåt, Borlänge 2004.
- [4.31] Thornton, P. H.
*Energy absorption by structural collapse of
spot-welded sheet metal sections.*
Transactions SAE, 89(2), 1473, 1980.
- [4.32] Fogningshandboken – Sammanfogning av höghållfast stål.
SSAB Tunnplåt AB, 2004.
- [4.33] Svetshandbok (Karlebo)
Liber AB, 1999.
- [4.34] SS-EN 1993-1-8:2005
*Eurocode 3 – Dimensionering av stålkonstruktioner,
Del 1-8: Dimensionering av knutpunkter och förband.*
SIS Förlag AB, Stockholm 2005.
- [4.35] BSK 07
Boverkets handbok om stålkonstruktioner.
Boverket, november 2007.
- [4.36] Olsson, C.,
Konstruktionshandbok för svetsade produkter
Liber AB, 2008.
- [4.37] ECCS publ. No21
*European Recommendations for the Design and Testing of
Connections in Steel Sheetings and Sections.*
ECCS, English, 1990, 176pp.
- [4.38] ECCS publ. No42
Mechanical Fasteners for Steel Sheetings.
ECCS, English, 1983.
- [4.39] Höglund, T., Johansson, B.
Fästdom och förband i stålkonstruktioner
Stålbyggnadsinstitutet, publ. 172, 2001.
- [4.40] Clarin, M..
*Plate Buckling Resistance - Patch Loading of
Longitudinally Stiffened Webs and Local Buckling*
Luleå University of Technology,
Doctoral Thesis 2007:31
Luleå, 2007
2007:31 /ISSN:I402-I544/ISRN: LTU-DI—07/31--SE
- [4.41] Gozzi, J.
*Patch Loading Resistance of Plated Girders -Ultimate
and serviceability limit state*
Luleå University of Technology, Doctoral Thesis
2007:30
Luleå 2007
2007:30 /ISSN:I402-I544/ISRN:LTU-DT—07/30—SE



Most failures in load-carrying structures are caused by fatigue. The major reason is that the material strength under cyclic loading, fatigue strength, is much lower than the static strength in particular at sharp notches (e.g. welds). This fact is not always taken into consideration during the design process.

5.1 Introduction

Lighter and more optimized structures achieved through the use of high-strength steel entail better material efficiency and higher working stresses. This turns fatigue, into a design parameter of a higher extent and it pays off to devote time and effort to perform accurate fatigue design.

Sections 5.1 through 5.5 shed light on the fatigue phenomenon and the most important factors affecting fatigue strength. The fatigue design section, 5.6, provides guidance on fatigue design itself. It is largely based on the IIW's (International Institute of Welding) Recommendations [5.1], the new Crane Standard [5.2] and earlier editions of this handbook [5.26]. Deviations and supplements have been made based on our own research and experience in the area.

5.1.1 The fatigue phenomenon

Fatigue is the behavior of cracks, how they form and grow through the material under cyclic loading. Fatigue is therefore a local phenomenon and fatigue fractures are characterized by little plastic deformation. Hence fatigue cracks can be difficult to discover.

The fatigue life is usually divided into initiation and growth of the crack. These two phases are completely different from a physical point of view. The initiation phase generally dominates in connection with mild notches and the crack growth phase in connection with sharp notches such as welds.

The surface of a fatigue crack is formed when it gradually grows through the material. The visible lines in the fractured surface are called beach marks which forms

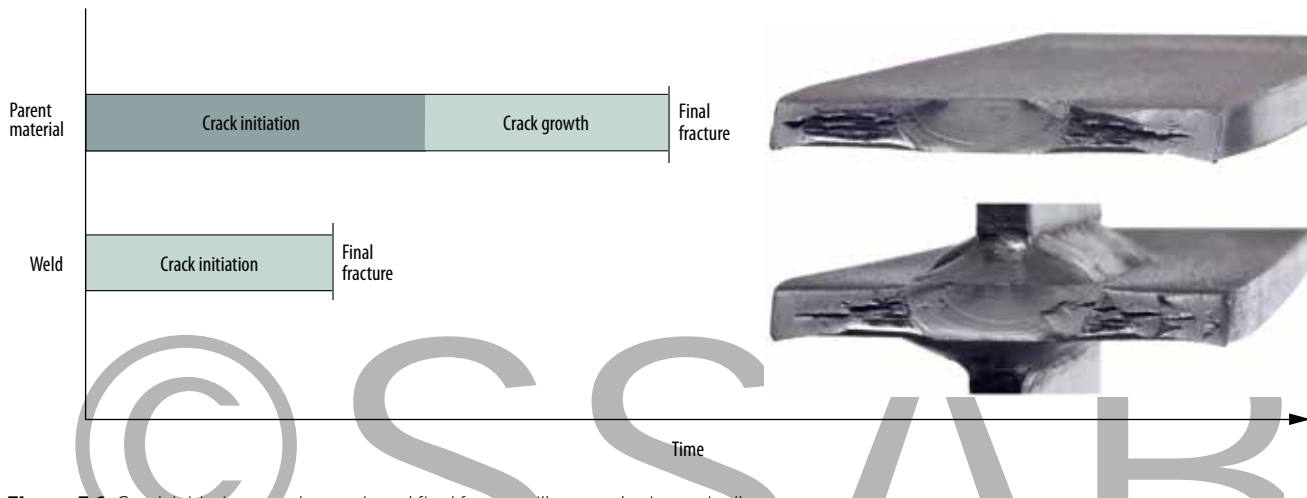


Figure 5.1: Crack initiation, crack growth and final fracture illustrated schematically.

under periods of a low loads. The distance between these lines increases the greater the distance from the initiation point, which therefore often makes it possible to trace back where the fatigue crack has originated. The final fracture occurs when the remaining material cannot resist the applied load. The final fracture can be ductile or brittle depending on the steel type and temperature, see figure 5.1.

Fatigue strength is affected by a number of factors, many hard to trace physically. Fatigue should therefore be viewed as empirical science and knowledge in the area has been amassed through extensive testing.

The number of load cycles, distribution and intensity of loads (stress history) and the notch effect are the factors which exercise the greatest influence on fatigue strength. Other factors include the steel's static strength, surface conditions, welding defects, mean stress, residual stress, plate thickness, temperature and corrosion.

5.1.2 Difference between parent material and welded joints

One of the most important areas of knowledge in the area of fatigue is to be familiar with the principal difference in the fatigue resistance of materials with none or mild mechanical notches and materials with crack-like imperfections such as welded joints. Welded joints often have sharp notches at the weld toe (the zone between the weld and the parent material) and in the weld root. This result in rapid initiation of fatigue cracks and the fatigue life is thereby dominated by crack growth, see figure 5.1. The crack propagation rate is independent of the steel grade.

The stress needed to initiate fatigue cracks in parent material, on the other hand, is related to the static strength. The fatigue resistance therefore increases with increased strength of the non-welded steel and the fatigue life is dominated by the initiation phase.

This is illustrated in figure 5.2 in a Kittagawa diagram, where the fatigue strength is displayed as a function of the defect size a . The significant parameter in the area dominated by crack growth is the fracture mechanical unit called stress intensity range, ΔK . Also see section 5.6. Thus proper structural design and good weld quality is very important factors for good material efficiency in fatigue loaded structures made of high strength steel.

5.1.3 Fatigue design standards

Standards for fatigue design are available only for certain types of structures, e.g. civil engineering structures, cranes, ships and pressure vessels.

There are normally no standards for other types of steel structures, just well-prepared recommendations which have become the de facto standard in many industries. The recommendations for fatigue design of welded structures published by the IIW (International Institute of Welding) and the AWS (American Welding Society) are particularly noteworthy. A disadvantage of these recommendations is however, that there is often no guidance available to assess the effect of the steel's strength and how the quality of welds affects fatigue resistance.

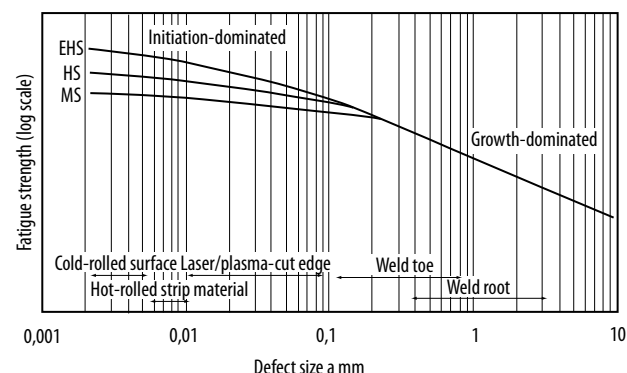
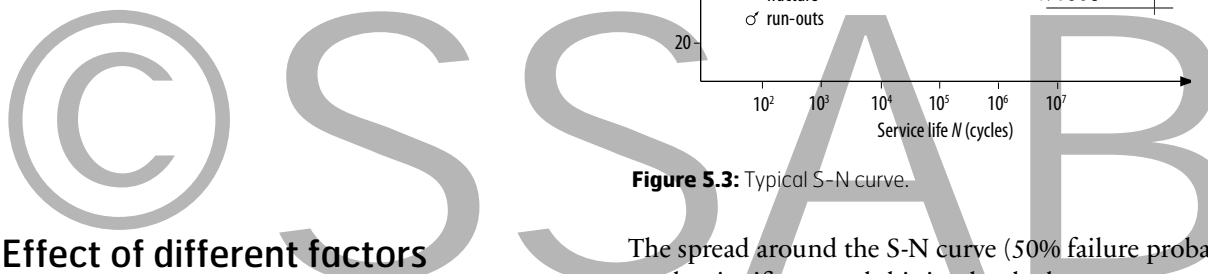


Figure 5.2: Fatigue strength as a function of defect size illustrated schematically.



5.2 Effect of different factors on fatigue strength

5.2.1 Number of load cycles – the S-N curve

Fatigue strength decreases with increase of service life. The decrease is small for non-notched parent material but can be significant when the notch effect is high. For example, the fatigue strength for a fillet weld at $2 \cdot 10^6$ load cycles is only 20% of the value at 10^4 . The connection between fatigue strength and life (number of load cycles) is called S-N curve, see figure 5.3. If fatigue data is presented in a log-log diagram, the connection with limited life becomes linear.

This part of the S-N curve is usually described with the equation

$$N = \frac{C}{\Delta\sigma^m} \quad (\text{Eq. 5.1})$$

where

- N – number of load cycles until failure
- $\Delta\sigma$ – stress range
- C, m – material constants

Under certain conditions the fatigue life can be infinite, the so-called fatigue limit, and the S/N curve becomes horizontal. The transition from the linear part to the horizontal part is in the region of 10^6 to 10^7 load cycles.

For non-notched parent material the slope the S/N curve is rather flat and the fatigue limit could be reached before 10^6 load cycles and at high stress ranges. For welds the slope the S/N is steep and the fatigue limit could be reached as late as 10^7 load cycles and at low stress ranges. Physically, the fatigue limit is the stress range required for initiation and/or propagation of a fatigue crack at all. The fatigue limit does not exist in cases of variable amplitude, unless all load cycles in the load history is below the fatigue limit. Variable amplitude is the most common type of loads in real life.

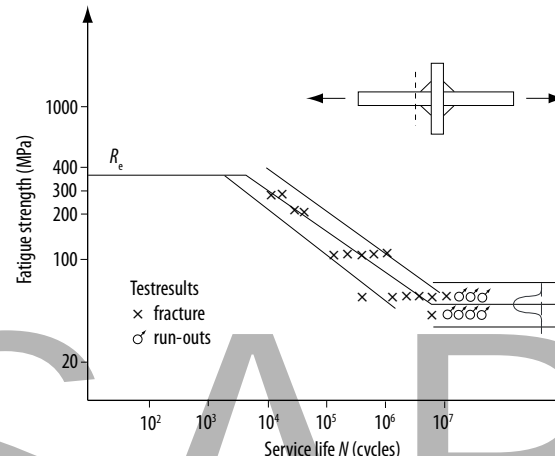


Figure 5.3: Typical S-N curve.

The spread around the S-N curve (50% failure probability) can be significant and this is why the lower 2.3% quartile is usually selected as characteristic fatigue strength for design purpose. In practice a structure is considered as exposed to a fatigue load first when the number of load cycles exceeds 1 000.

Figure 5.4 defines the most common concepts used to describe a fatigue load.

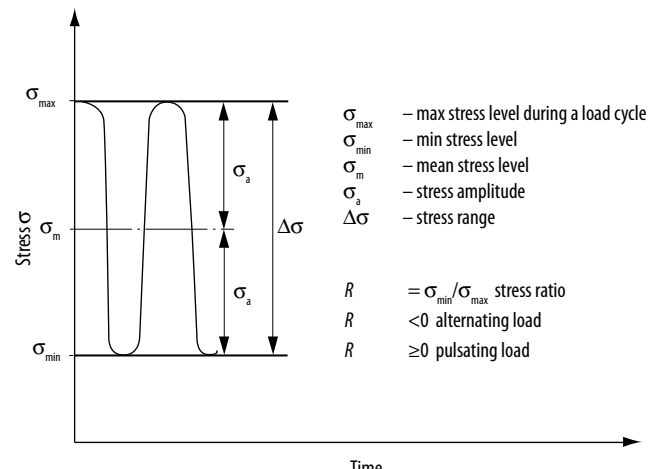


Figure 5.4: Definitions of stress and ratios during a load cycle.



Figure 5.5: Recorded signals of constant amplitude load (A) and from a wheel-loader in operation (B).

5.2.2 Load history

Most structures are exposed to loads which vary irregularly over time. As examples, a loading machine works under varying ground conditions or a crane which makes different lifts over time, see *figure 5.5*. In other words, the structure is exposed to a load history, which in turn leads to a stress history.

Designing a structure based on an assumption that each load cycle is equal to the highest load, i.e. constant amplitude loading (A), it often leads to extreme conservative design. If a structure is exposed to a common load history (B), such assumption would lead to overestimation by 50 to 70% of the required strength, *figure 5.6*. This emphasizes the importance of a careful load analysis in order to utilize good material efficiency.

The relevant stress history is determined by assessing or measuring of actual loads or strains. The stress history parameter then sets the basis for the analysis. An alternative is to perform a cumulative damage sum calculation according to the Palmgren-Miner rule. For these calculations, see sections 5.6.3 or 5.6.10.

5.2.3 Notch effect – Stress concentrations

Notch effect is without a doubt the most important factor affecting fatigue strength. It is also the factor which can be influenced the most by the designer, production engineer and individual welder. The disruption in the stress field caused by a geometric notch is usually described with the stress concentration factor, K_t . It indicates how many times higher the maximum stress in the notch is compared to the nominal stress. Stress concentrations can be caused by, e.g. surface roughness, mechanical notches such as holes and indentations, abrupt cross-section changes or welds.

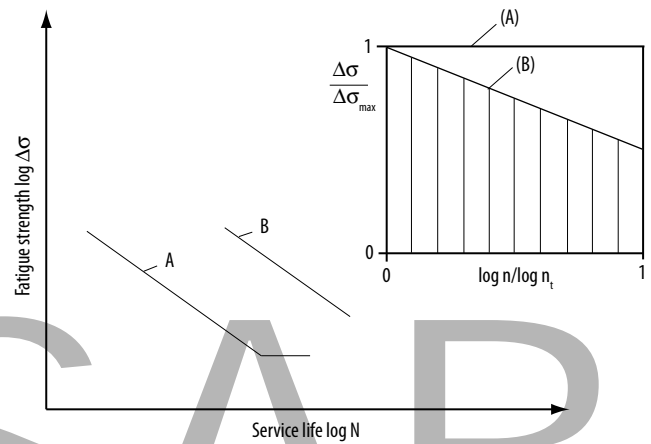


Figure 5.6: Influence of different load spectrums.

If the notch is small in relation to other dimensions, the stress concentration factor can in many cases be approximated with the solution for an elliptical notch and then K_t can be written

$$K_t = 1 + 2\sqrt{\frac{a}{r}} \quad (\text{Eq. 5.2})$$

where

- a – the notch's depth, see *figure 5.7*
- r – tip radius, *figure 5.7*

The formula above allows us to draw the general conclusion that stress concentration can be reduced and that fatigue strength can be increased by reducing the depth of the notch and/or by increasing its radius. It is also easy to deduce that the stress concentration for a hole (radius $a=r$) is $K_t = 3$.

Stress concentrations for different mechanical notches are available in handbooks such as Peterson's "Stress Concentration Factors" [5.3].

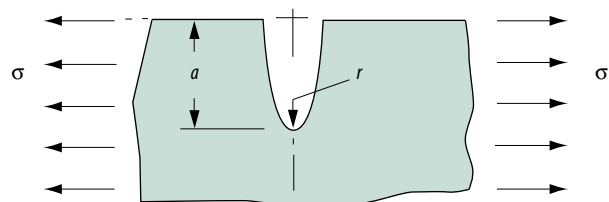


Figure 5.7: Tip radius and depth of a notch.

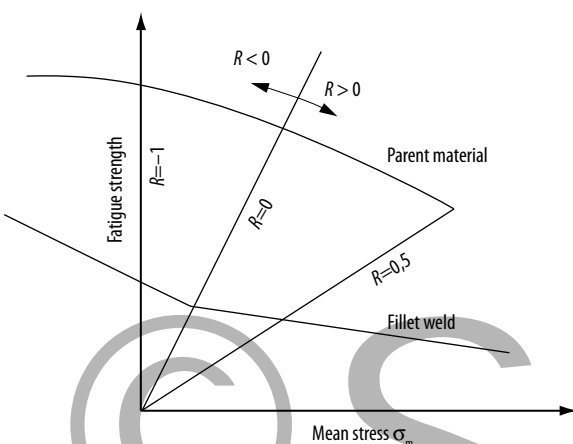


Figure 5.8: Effect of mean stress on fatigue strength.

Stress concentration factors are difficult to determine in welds since notch depths and radii vary. In addition, crack-like imperfections also produce singularities and the stress concentration is made up of global and local notch effect. To meet these demands methods such as "Notch Stress" and "Hot Spot Stress" which, to a higher extent, take the actual stress in the welded area into consideration have been developed. But still fatigue design of welds is usually made with the nominal stress method which uses different fatigue resistance values (FAT) and corresponding S-N curve, dependent on the type of welded joint. See also section 5.6.7.

5.2.4 Mean stress and residual stress

The effect of the mean stress on fatigue strength is usually described with a Goodman, Haigh or $\Delta\sigma$ - σ_m diagram, see figure 5.8.

The effect of mean stress in practice is positive for alternating load, i.e. when the stress ratio $R = \sigma_{\min}/\sigma_{\max} < 0$ (see figure 5.4). For $R = \sigma_{\min}/\sigma_{\max} > 0$ the effect is negative and the fatigue strength is reduced for parent material. The significant parameter for welded joints is the stress range $\Delta\sigma$ due to the high local residual tensile stresses at the weld. For this reason the local stress range varies from the yield strength and downwards independently of the nominal R value, also see section 5.5.5.

Residual stress exerts a great influence on fatigue resistance and the difference in fatigue strength between areas with tensile or compressive residual stresses is substantial. The positive effect on fatigue strength exercised by compressive residual stress such as "peening" is well-documented in [5.4]. Residual stresses are usually unknown for welded joints. The tensile residual stresses are commonly assumed to be as high as the yield strength for the parent material for a welded joint in design contexts. This applies for the as-welded condition. As fatigue in welded joints primarily deals with crack growth, residual stresses have a significant effect on the degree of crack closure and thereby on fatigue strength, in particular in the vicinity of the fatigue limit.

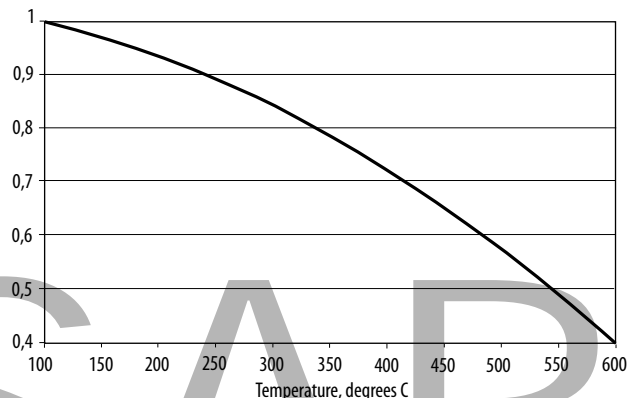


Figure 5.9: Fatigue strength reduction factor for steel at elevated temperatures, IIW [5.1].

5.2.5 Temperature

Temperature affects fatigue strength to a different extent for both parent and welded material. The temperature dependence for welded material, where the fatigue process is dominated by crack growth, follows the temperature dependence of the Young's modulus. The temperature dependence for parent material, where the initiation of fatigue cracks is dominant, is approximately the same as for the yield strength, see figure 2.8. Creep phenomena become critical above 400° and creep and fatigue must be treated at the same time.

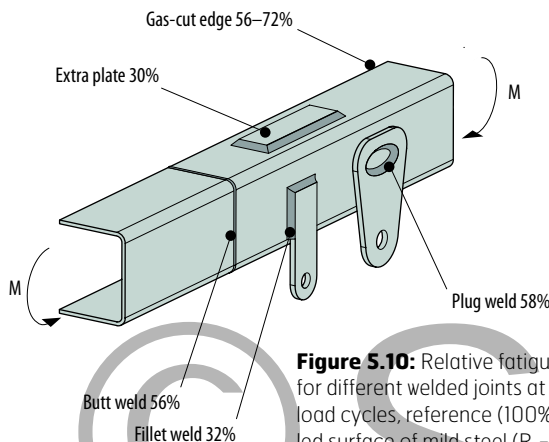
The IIW recommendation [5.1] indicates a reduction factor for fatigue strength at an increased temperature according to figure 5.9. It applies to weld material and is conservative compared to the temperature dependence which is normally calculated for the modulus of elasticity.

Note that variations of temperature in structures which are sensitive to temperature gradients can lead to substantial reversible plastic strain and a short fatigue service life. High plastic strains can develop if materials with different coefficients of thermal expansion are part of structures exposed to temperature variations, for example, if carbon steel interacts with stainless steel.

5.2.6 Corrosion

Corrosion affects fatigue strength negatively and the term "corrosion fatigue" is normally used when a corrosive environment reduces the time for initiation of cracks or accelerates crack growth in connection. The effect of corrosion fatigue, i.e. when the corrosive medium acts at the same time as the fatigue load is greater and results in lower fatigue strength compared to the effect of increased surface roughness on weather resistance steels. This should be kept in mind during design.

Painted structures used in normal environment are not considered to be exposed to corrosion fatigue since the phenomenon is observed only in harsh corrosive environments such as offshore.



Factors which must specifically be taken into consideration when considering corrosion fatigue are that the load frequency and time exert a greater influence when compared to conditions in an air environment. The effect of the steel's strength can also disappear for parent material and the fatigue limit can decrease or disappear completely.

Reductions in fatigue strength of up to 40% compared to the conditions in an air environment have been reported. The use of sacrificial anodes of zinc as cathode protection is a common way of protecting offshore structures in salt water environments. Such protection ensures fatigue resistance which corresponds to the fatigue resistance achieved under "normal" conditions.

Metallic coating normally provides good protection against corrosion fatigue but the coating can, as in the batch hot-dip galvanization process, result in a reduction in fatigue strength, also see section 5.4.3.

5.3 Design with respect to fatigue

5.3.1 Common design principles

The magnitude of stress concentration in combination with different notches is decisive for a structure's fatigue resistance. The structural design should be done to ensure as little disturbance of the stress flow as possible. This applies to both the local and global stress flow. Structural elements should be subjected to tension or compression instead of bending which will result in better prerequisites for reducing the thickness without subsequent high increases in local bending stress. The fundamental principles for, e.g. skins, plates and load introductions as described in sections 3.2.2 through 3.2.4 and 3.3 are also highly applicable here.

Start and stop positions of welds should generally be avoided in areas exposed to high stress since they have low fatigue resistance.

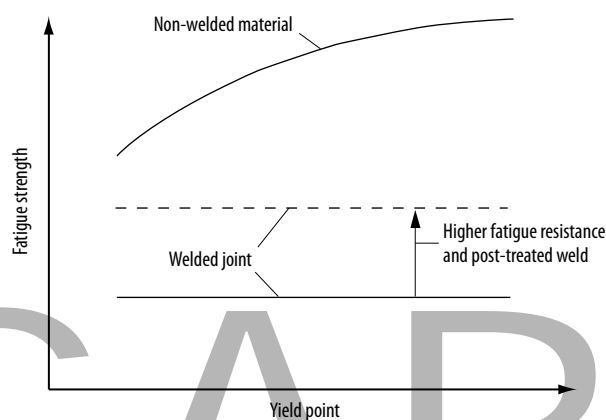


Figure 5.11: Fatigue strength as a function of yield strength illustrated schematically; effect of higher fatigue resistance and post-treatment of weld.

Since fatigue is a local phenomenon, it is always the weakest link in the structure that determines the total fatigue resistance. It is important to analyze where these weak points are located and then improve the fatigue resistance at these points in order to improve the whole structure.

5.3.2 Choice of joints – Structural details

Structural details with corresponding fatigue resistance value, FAT, is available for a selection of joints. FAT is, by definition, the characteristic fatigue strength for the joint in question at $2 \cdot 10^6$ load cycles and a failure probability of 2.3%.

Fatigue strength varies a lot among different types of welded joints. It is important to choose a joint with a low notch effect in areas exposed to high stress levels. *Figure 5.10* displays the relative difference in fatigue strength between different joints. The reference (100%) is parent material with as rolled surface in mild steel ($R_e = 240 \text{ MPa}$). Welding an additional plate with the intention of strengthening the structure can apparently have the complete opposite effect when it is subjected to a fatigue load. Likewise, an apparently harmless fillet-welded connection may, even if it is not load-carrying, have devastating consequences for the fatigue resistance.

5.3.3 High-strength steels in fatigue-loaded structures

High strength steels gives an opportunity for higher working stress. In order to match it, the fatigue strength in welded components must be improved in order to utilize the full potential of these steels in fatigue loaded structures, *figure 5.11*. Select welded joints with a high fatigue resistance and/or give critical welds with high notch effect a post-treatment.

As a designer, it is very practical to work with comparisons of different possible joints in the selection process of

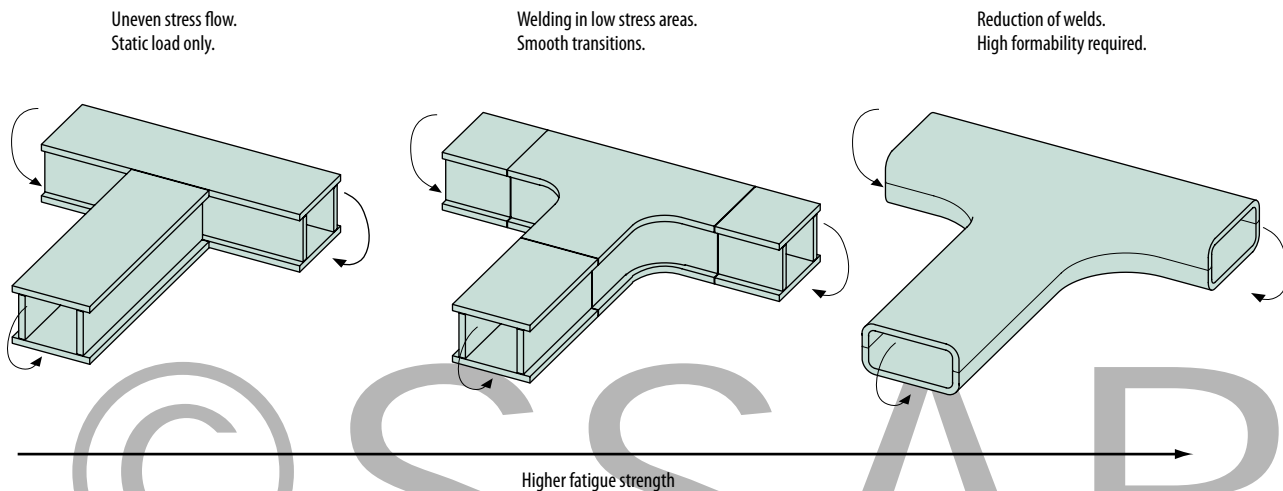


Figure 5.12: Smart design and placing of welds results in longer fatigue life and higher material efficiency.

design solutions. The fatigue resistance is proportional to the FAT of the structural detail, and the life to FAT^m where $m=3$ for welded joints and $m=5$ for parent material. This means that a moderate increase in the fatigue resistance value can result in a significant increase in life.

5.3.4 Placement and design of welded joints

Avoiding stress concentrations in areas with high nominal stress is the guiding principle for structural design of joints in fatigue-loaded structures. When it comes to welded joints, the reasons for stress concentrations in weld-affected zones must be reduced and the welds should be placed in parts of the structure which have low nominal stress e.g. close to the neutral layer in a beam subjected to bending moment. Imagine a square section which is made out of two U-sections which have been welded longitudinally. When it is subjected to a bending moment, the weld is in the neutral layer, see *figure 5.13*. In such case, the high fatigue strength of the parent material can be fully utilized. This is an example of good structural design and weld placement.

In general, welding should be avoided in and in the vicinity of flanges in beams subjected to bending moment.

There are often possibilities to reduce the number of welds by using a different structural design and to improve the weld placement by using the good cold forming properties of modern steels and by pressing, bending or roll-forming parts of the structure. Instead of working with welded stiffeners, these can be replaced with bends and grooves. The elimination or transfer of welds ensures greater fatigue resistance or lower weight, see *figure 5.12*.

A better alternative to welded joints for fatigue loaded structures, which also takes advantage of the fatigue resistance of high strength steel, is the use of screws and riveted joints.

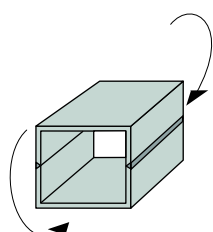


Figure 5.13: Welding in the neutral layer means utilizing the fatigue strength of the parent material.

It is important to avoid abrupt stiffness changes and to strive to achieve an as even stress flow as possible during the design of joints between structural elements with different thicknesses, see *figure 5.14 a*.

If it is possible to avoid placing the weld in the transition, the stress concentration is reduced and the fatigue resistance will be increased. *Figure 5.14 b* shows how a butt weld joint can be placed next to the transition between different plate thicknesses and how the fatigue resistance is increased from $FAT=71$ in case a) to $FAT=90$ in case b). This corresponds to a doubling of life, $(90/71)^3 = 2$.

It is particularly important to avoid abrupt stiffness changes during the transition from closed to open cross-sections loaded in torsion. Design the transition with a successive change of torsional stiffness. The torsional stiffness of the closed cross-section is proportional to the enclosed area and a design according to *figure 5.15* will lead to a successive reduction in torsional stiffness.

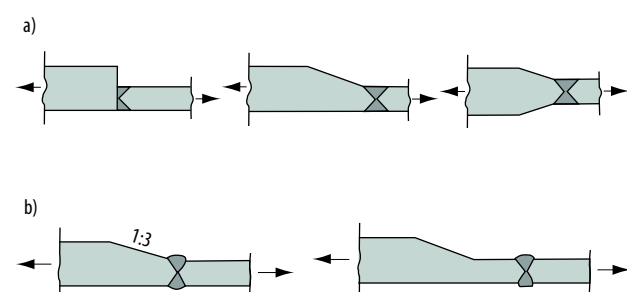


Figure 5.14: Avoid abrupt stiffness changes and to superpose notch effects.

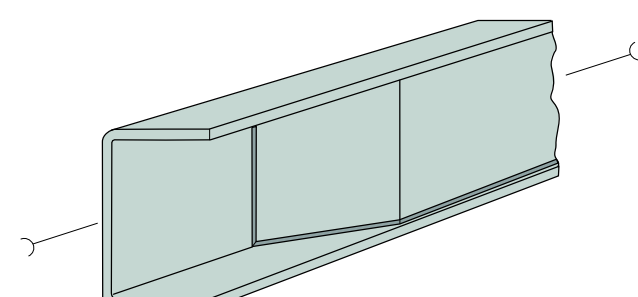


Figure 5.15: Use smooth transition from closed to open cross-section under torsional loading.

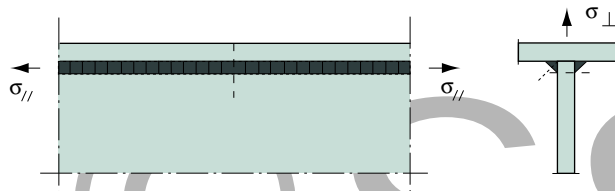


Figure 5.16: Fillet weld in beam; loaded parallel (left illustration) or perpendicular (right illustration) to the longitudinal direction.

Welds have a higher fatigue resistance when they are loaded parallel than when they are loaded perpendicularly to the weld's longitudinal direction. This is exemplified in *figure 5.16* with a fillet weld between a flange and a web in a beam where a load parallel to the weld gives the weld a fatigue resistance value $FAT=90$ MPa, whereas a perpendicular loaded only have $FAT=56$ MPa.

The higher fatigue resistance for the longitudinal welds is a result of the much smaller disruptions of the stress flow caused by the weld geometry in this case. This also means that the potential of increasing the welded joint's fatigue strength with different improvement methods is limited when the load is in the weld's longitudinal direction.

A fillet weld which is loaded in parallel to the weld's longitudinal direction ($\sigma_{//}$) in accordance with the above does not transfer a lot of force and the stress is low. Relatively small throat thicknesses are used and there is seldom any requirement on strength of the filler material. When there are high loads perpendicular to the weld (σ_{\perp}), it is recommended as large throat thickness as necessary to prevent any fatigue cracks in the weld root. A crack which starts from the weld toe is easier to discover than a crack which starts from the weld root. If the static part of the load is high and perpendicular to the weld matching filler material is recommended.

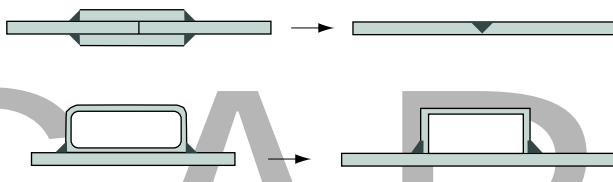


Figure 5.18: Do not design welded joints as bolted or adhesive joints.

Butt welds are preferable in connection with fatigue as the stress flow through the weld is relatively undisturbed and the local bending moments are small. Welds with V- and K-grooves are preferable to fillet welds. If fillet welds cannot be avoided, they should be double and/or with deep penetration. For an assessment of the optimum throat thickness in connection with penetration, refer to section 5.5.3.

Welding with deep penetration gives advantages according to, *figure 5.17*. Since deep penetration reduces the stress in the weld due to smaller local bending moment, as in a single-sided fillet weld, and the fatigue strength increases. The throat thickness can be reduced if a significant penetration is achieved.

Do not design a welded joint as a screwed or adhesive joint, see *figure 5.18*. Avoid crevices which may lead to corrosion and which impair the fatigue strength. If crevices cannot be avoided, seal them with some form of a sealant and/or use some corrosion protection.

The effort in welded structures should be to place the root side of the weld in areas exposed to compressive stress. This applies, in particular, if the root is not sealed, see *figure 5.19*. The root side of the weld often contains defects which are possible initiating points of fatigue cracks. Fatigue cracks can start in welds with nominal compressive stress, due to tensile residual stress. But these fatigue cracks are stopped once it comes out of the residual stress field.

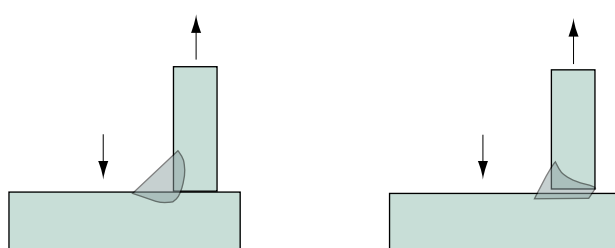


Figure 5.17: Take advantage of the penetration connected to machine welding for high fatigue strength and lower production cost.

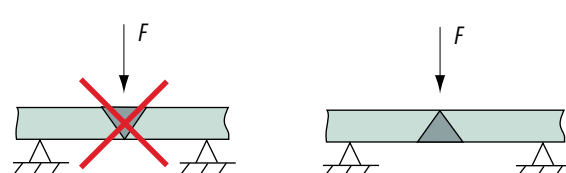
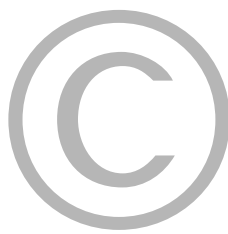


Figure 5.19: Place the weld's root side in areas with compressive stress.



5.3.5 Load introductions

Two main principles for structural design in connection with load introductions are described in 5.2.2 and 5.2.4. The first principle is to avoid local bending. This is achieved by introducing loads into the plane of a plate (see figure 5.20.b) and not perpendicular (see figure 5.20.a).

Aiming for reduction in plate thickness the principle above is important or the result is significant increases in local stress and deformations, see figure 5.20.

An analogous example is closed beams where local bending occurs if the load is introduced too far from the stiffening web. The principle during load transfers between telescopic arms as in figure 5.21, where the load is transferred via lugs, is to reduce the lever to a minimum by choosing narrow bending radiiuses in the corners.

The second principle which serves as guidance during the design of load introductions is to place the welded joints as close to the neutral layer as possible, e.g., according to the examples in figure 5.22. The use of plug welds which are almost continuous, without start position and thereby have a high fatigue resistance is recommended. Seal the gap between the plates if required. Start and stop positions of welds should generally be avoided in areas exposed to high stress.

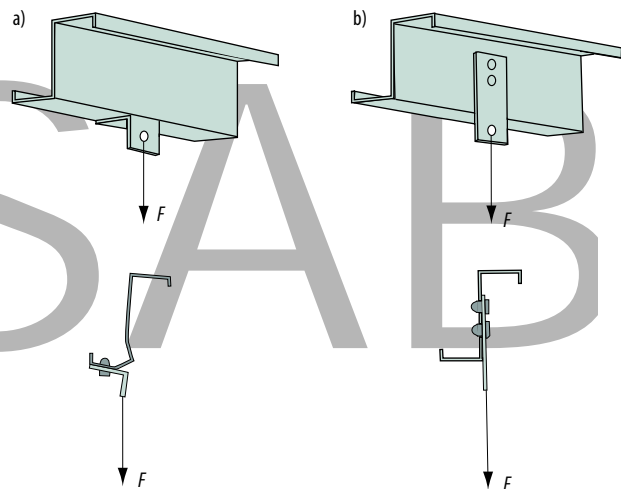


Figure 5.20: Load introduction into a Z-beam. (a) the flange is subjected to local bending (b) the whole cross-section is subjected to in-plane bending.

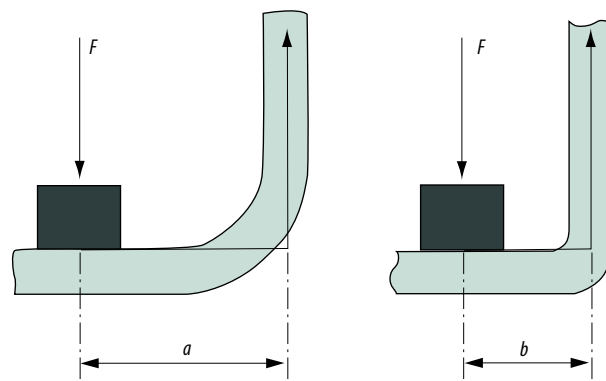


Figure 5.21: Load introduction into closed sections.

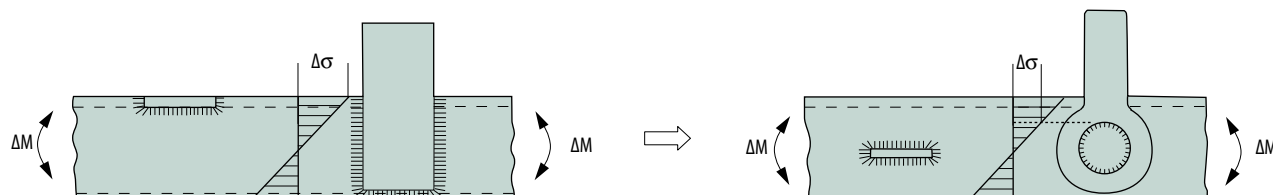


Figure 5.22: Put welded attachments close to the neutral layer.

5.4 Fatigue of non-welded material

5.4.1 General information

Parent material which has not been welded can be fully utilized if the structural design has been successful. The fatigue resistance is determined by the stress range required for initiation of a crack, a range which increases with higher steel strength. Hence the fatigue strength of high strength steels is higher than mild steels. How much higher is dependent on the steel's strength, the roughness

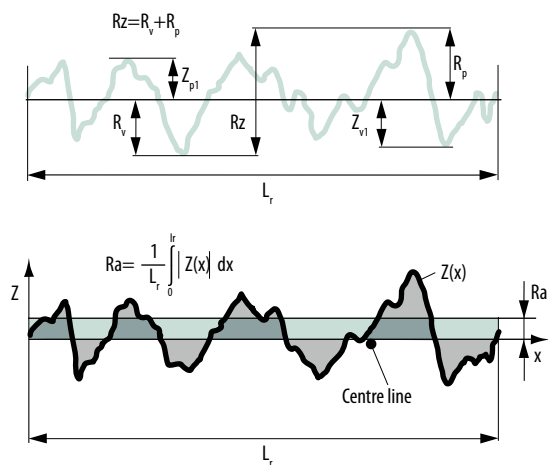


Figure 5.23: Definition of surface roughness and mean surface deviation.

of the plate surface, the quality of the edges and notches such as holes, indentations or screwed or riveted joints.

5.4.2 Material effect, effect of surface condition

The fatigue strength of non-welded steel increases with increased steel strength. The rate of this increase depends, among other things, on the surface condition of the material. The fatigue strength is better in cold-rolled than in hot-rolled surfaces due to the surface quality.

Research [5.5 and 5.6] shows that a surface's notch effect from a fatigue point of view can be described by the surface roughness (R_z or R_a value). These are assessed during surface topography measurements and defined according to *figure 5.23*. R_z is usually assessed as the mean value of five measurements and is designated R_{z_s} . Herein R_z here refers to this value.

The value $\Delta\sigma^*$ of fatigue strength for materials with a smooth surface ($R_z \approx 0$) can be described with a correlation between the fatigue strength and yield strength in accordance to *figure 5.24* from [5.6]. Fatigue strength refers to the value at 50% failure probability, 10^6 load cycles and a stress ratio $R=0$.

Based on the correlation in *figure 5.24*, the fatigue strength can be calculated using the respective steel's strength values and the surface condition (R_z value) as input.

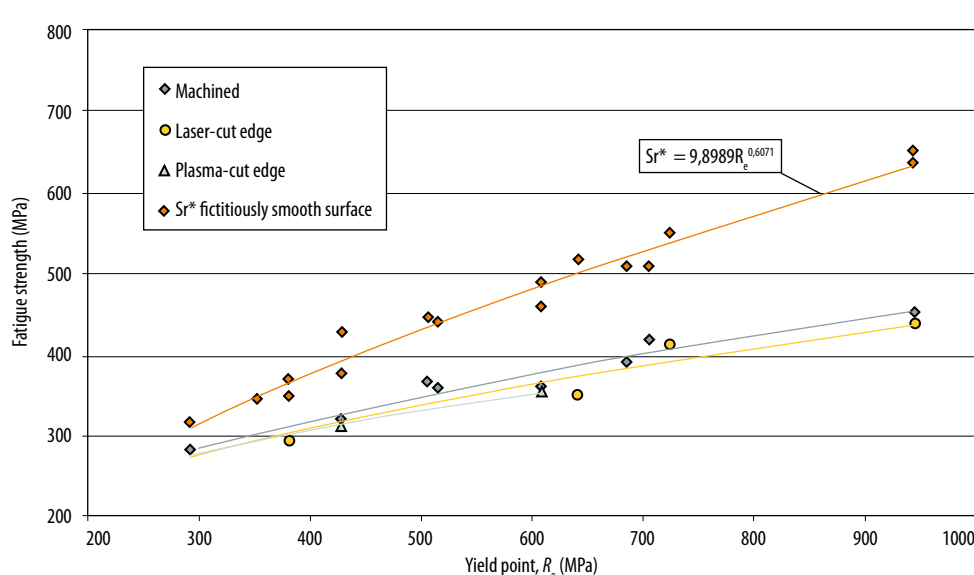


Figure 5.24: Correlation between the calculated fatigue strength for a fictitious smooth test specimen and the yield strength; test results corrected for different surface and edge conditions, constant amplitude, $R=0$ [5.6], failure probability 50%.

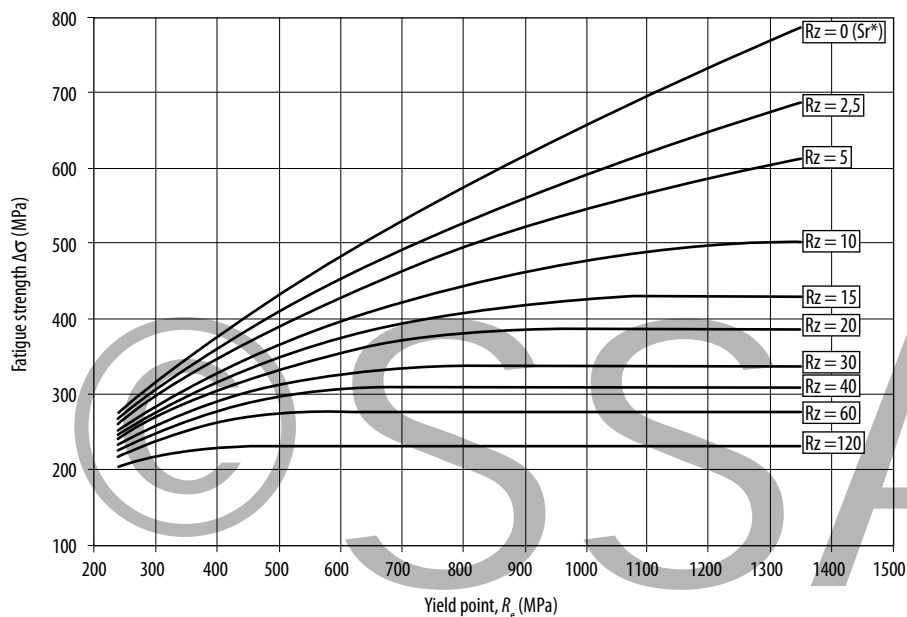


Figure 5.25: Fatigue strength at $N=10^6$ load cycles and $R=0$, failure probability 50%, for non-welded parent material with different surface condition (Rz value).

The fatigue strength $\Delta\sigma$ is then calculated in accordance with the following

$$\Delta\sigma = \frac{\Delta\sigma^*}{K_r} \quad (\text{Eq. 5.3})$$

where

$\Delta\sigma^*$ – the fatigue strength of a fictitious smooth test specimen, *equation 5.4*

K_r – surface factor

$$\Delta\sigma^* = 9.8989 \cdot R_e^{0.6071} \quad (\text{Eq. 5.4})$$

$$K_r = \frac{1}{1 - 0.000254 \cdot R_m \cdot \ln(\frac{Rz}{6} + 1)} \quad (\text{Eq. 5.5})$$

where

R_e – yield strength (MPa)

R_m – tensile strength (MPa)

The correlation for K_r applies when the fatigue life is dominated by crack initiation. When the formula $\Delta\sigma = \Delta\sigma^*/K_r$ above gives a falling curve in *figure 5.25*, $\Delta\sigma$ is cho-

sen equal to the maximum value and the curve continues horizontally, which represents a fatigue life dominated by crack growth.

The correlation above is illustrated in *figure 5.25* where the fatigue strength as function of the yield strength has been calculated for a number of Rz values. In order to calculate the fatigue strength for other than $N=10^6$, *equation 5.1* is used, [5.2]. The exponent is $m=5$.

Figure 5.25 indicates that the increase in fatigue strength with the increase in the yield strength diminishes if the surface condition is impaired. The increase stops completely at a certain yield strength which, in turn, gets lower with increased Rz value. At this yield strength the fatigue life switches from initiation domination to crack growth type.

Measurements of surface condition in the form of mean surface deviation R_a and the Rz values, have been performed on hot-rolled, cold-rolled, machined and blast surface, *figure 5.26* [5.6]. The measured steel grades had $R_e \leq 700$ MPa.

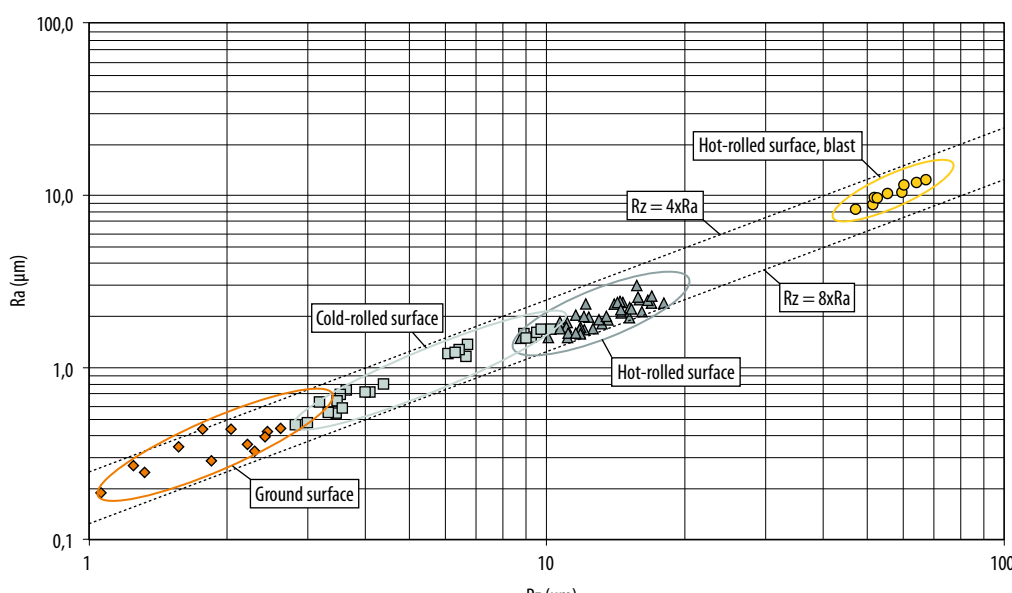


Figure 5.26: Results from surface roughness measurement of rolled, ground and blast surfaces [5.6].



To sum up, the results of the measurements are presented below in *table 5.1*.

Surface roughness measurements show that there is a connection between the Rz and Ra values and that $Rz \approx 6 Ra$.

Measurements of shot-blast surfaces gives Rz values of 35 to 50 without corresponding decreases in fatigue strength due to the “better” surface topography and the presence of a compressive stress state due to the cold working during blasting.

5.4.3 Galvanized surface

Galvanization provides good corrosion protection and is thereby also positive for fatigue resistance in corrosive environments. A plate which has electrolytically galvanized or continuously hot-dip galvanized surface has the same fatigue strength in a non-corrosive environment as a non-galvanized surface in a corresponding steel type. Batch hot-dip galvanizing results in a thicker zinc layer and a thicker brittle so-called ζ phase can develop in the boundary layer between the steel and the zinc. This phase can crack under load and result in micro cracks which can

reach critical size from fatigue point of view. The practical consequence is that the fatigue strength does not improve with increased yield strength if it exceeds 500 MPa. Fatigue strength material dependence for hot-dip galvanized surface can then be described by the curve for Rz = 60 in *figure 5.25*. This has been verified with fracture mechanical calculations and test results [5.5 and 5.8].

5.4.4 Quality of cut edges

The quality of the plate edge is of great importance for fatigue resistance. Different cutting methods result in different edge quality. *Figure 5.27* shows results of fatigue testing of Strenx 700MC where the plate edge has been milled, laser-cut and sheared. Laser-cut edges are considerably better than sheared edges.

The quality of a sheared edge depends on the settings of the scissors and the quality of the steel cutter. A sheared edge with a poor quality may provide very low fatigue resistance. In order to achieve better fatigue resistance, the edge must be given a post-treatment in order to eliminate crack-like imperfections. Machining removes such defects

Surface	Rz (μm)	Ra (μm)
Ground	1,1–2,6	0,2–0,4
Cold-rolled	3–10	0,5–1,7
Hot-rolled	8–18	1,5–3,0

Table 5.1: Measured surface roughness in the form of mean surface deviation Ra and the Rz value.

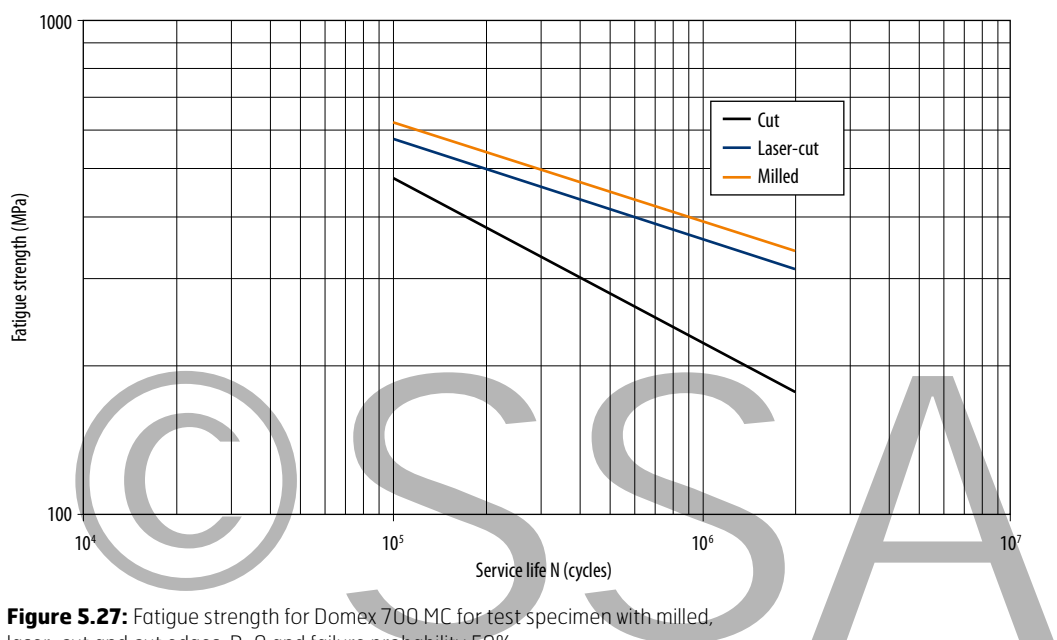


Figure 5.27: Fatigue strength for Domex 700 MC for test specimen with milled, laser-cut and cut edges, R=0 and failure probability 50%.

and provides good fatigue resistance see the curve for milled edges in *figure 5.27*. Another method is to introduce compressive residual stress by shot blasting. A slotted edge usually gives higher quality than a sheared one but the dependence on tool settings is substantial. Edge cornering rolling of slotted material has substantial effect on the fatigue strength.

Fatigue resistance of thermally cut edges varies depending on the method and quality of cutting, *figure 5.28*. Laser cutting can give fatigue resistance almost on a par with a machined edge. However, it is hard to achieve a good cutting quality with manually operated tools.

To improve the fatigue resistance of thermally cut edges one can chamfer the edge corners and avoid start/stop positions in critical sections with high stresses. Blasting of a structure with cut edges usually has a positive effect on the fatigue resistance.

In order to reduce the effect of cut edges on the fatigue resistance of C-profiles subjected to bending moment, edge folds can be introduced so that the stress range in the cut edge is lowered, see *figure 5.29*.

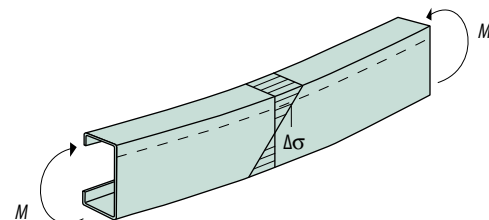


Figure 5.29: C-profiles with edge folds subjected to a bending moment provide an opportunity to reduce the stresses in the cut edges.

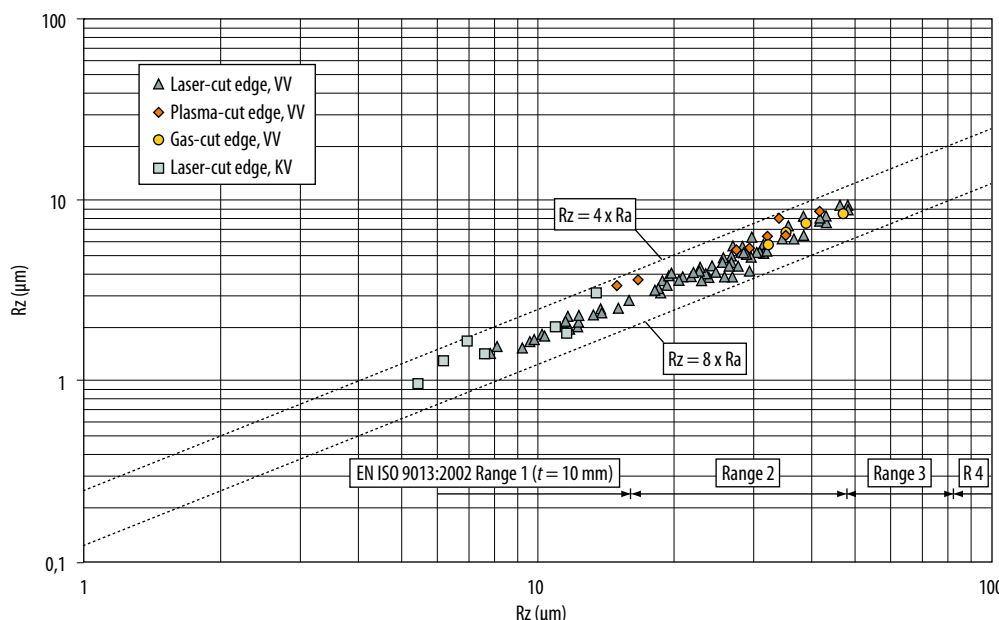


Figure 5.28: Results from surface roughness measurements of thermally cut edges [5.6].



As a rule, untreated sheared or gas-cut edges often result in relatively poor edge quality, with a risk of crack-like imperfections. The practical consequence is in such case that the fatigue strength does not improve at all with increased yield strength. Fatigue strength material dependence can then be described by the curve L in *figure 5.25*.

Material dependence is during calculations handled with the material factor ϕ_m , see also sections 5.4.7 and 5.6.6.

The correlations described above apply primarily to the description of the effect of the static strength with different surface qualities. When the surface becomes so rough that the material dependence is lost (Rz values greater than 120) the notch effect is included in the respective fatigue class, FAT.

5.4.5 Mechanical notches

For mechanical machined notches such as holes, indentations and mechanical joints, so-called mild notches, the notch effect is described by the stress concentration factor K_t .

The reduction in fatigue strength is determined by the notch factor K_f and the correlation between K_f and K_t is described by the correlation:

$$K_f = 1 + \frac{K_t - 1}{1 + \frac{0,6}{\sqrt{r}}} \quad (\text{Eqn. 5.6})$$

where

K_t – stress concentration factor
 r – notch radius

*Neuber constant = 0.6 ($R_e=220$ MPa for mild steels)

Note that the material effect is handled separately with the material factor ϕ_m according to *figure 5.30* and not through different values of the Neuber constant.

The stress concentration factor K_t for different mechanical notches is available in handbooks such as Peterson's "Stress Concentration Factors" [5.3].

To simplify the assessment of the fatigue strength in a structure which consists of both mechanical and weld notches, section 5.6 describes a method of converting the

notch effect for mechanical notches (K_t) into a fatigue class FAT. The notch effect for certain mechanical joints is directly specified with a fatigue class, see section 5.6.7. The material effect for mechanical notches is taken into consideration by using the material factor ϕ_m .

In connection with high fatigue loads reversible plastic strain may occur in mechanical notches which may lead to cyclical softening or hardening.

5.4.6 Strain hardening and bake hardening

Dual phase steels have high strain hardening which increase the yield strength considerably during plastic forming, such as bending and pressing. Furthermore, the yield strength increases additionally if the part is heated to 170° C after pressing, the effect is called bake hardening. As the yield strength of these steels increases during strain and bake hardening the fatigue strength also increases. Strain and bake hardening is thoroughly described in chapter 2.

Using the origin yield strength as basis for fatigue strength makes the design in these cases conservative. Usually the yield strength after 2% strain and bake hardening is used.

The calculations which form the basis for the correlations in *figure 5.25*, which present the influence on fatigue strength by the yield strength, have taken the factors above into account.

5.4.7 Material factor

Based on the correlations presented in section 5.4.2, the material factor has been calculated as a function of yield strength and surface conditions. The curves with designation A-K in *figure 5.30* correspond to Rz values from 3 to 120 ($R_a=0.5-20$). The L curve corresponds to $\phi_m=1$, i.e., no material dependence and applies to parent material with crack-like imperfections or welded joints. The fatigue strength of parent material is calculated by multiplying FAT for actual the structural detail with the material factor, ϕ_m . In order to be able to associate the different curves in *figure 5.30* with different surface and edge conditions in practice, the data presented in sections 5.4.2 through 5.4.4 above has been analyzed [5.6]. The result of this analysis is summarized in *table 5.2*. For the structural details of parent material, see to *table 5.17*.

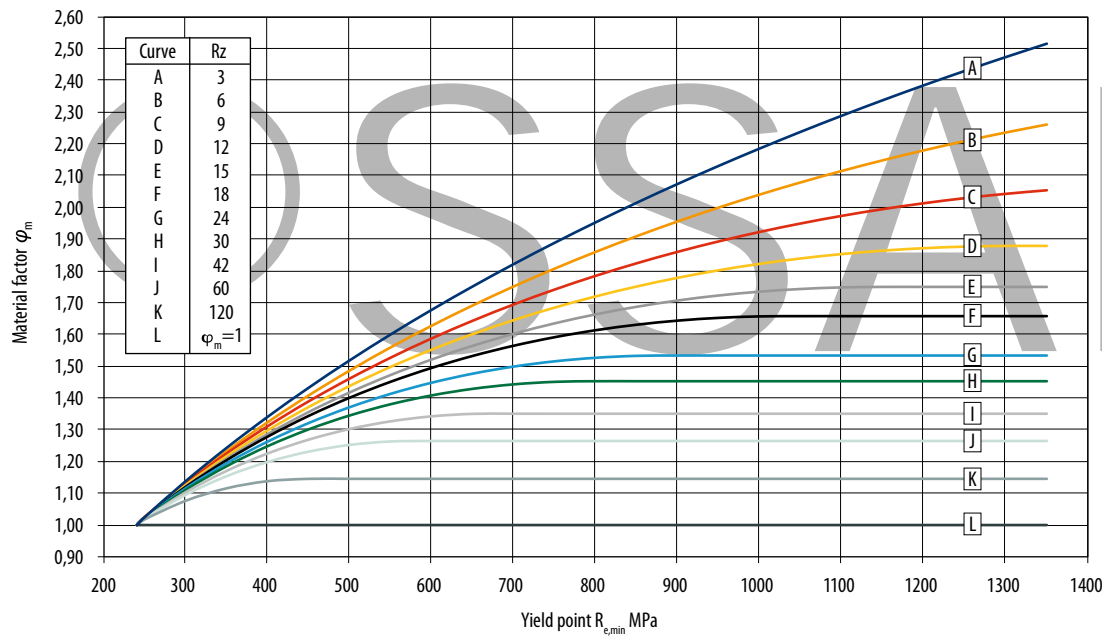


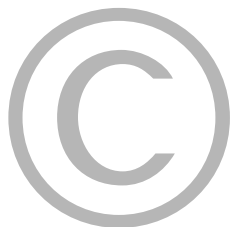
Figure 5.30: The material factor as a function of yield strength and surface condition.

Type of surface or edge	Comment/quality specification	Surface condition Rz	ISO Range ¹⁾	φ_m -curve
Ground	Corners deburred	3		A
Machined	Corners deburred	6		B
Surface of cold-rolled or continuously hot-dip galvanized strip material		6	(1)	B
Surface of hot-rolled strip material	High quality	12	(1)	D
	Good quality	15	(1)	E
	Moderate quality	18	(1–2)	F
Blasted surface of quenched and tempered plate material		42	–	I
Punched edge in cold-rolled strip material ²⁾	Good	15	–	D
Slitted edge in hot-rolled strip material ²⁾	Good quality, all visible imperfections are remedied	30	–	H
Laser-cut edge ²⁾	Very high quality, only cold-rolled strip material	9	1	C
Laser-cut edge in hot-rolled strip material ²⁾	High quality	15	1	E
	Good quality	18	2	F
	Moderate quality	24	2	G
		30	2	H
Plasma-cut edge in hot-rolled strip material ²⁾	High quality	15	2	E
	Good quality	18	2	F
	Moderate quality	24	2	G
		30	2	H
Gas-cut edge	Good quality	40	2–3	L
	Moderate quality	50	3	L

¹⁾SS-EN-ISO 9013 ($t = 10$ mm) [5.10]

²⁾Free from crack-like imperfections

Table 5.2: Correlation between surface/edge condition and the material factor in figure 5.30.



5.5 Fatigue in welded material and structures

5.5.1 General information

Welding makes the material undergo a transformation due to the heat input during the process. The heat input leads to metallurgical transitions, increased hardness and soft zones in HAZ, see section 6.4. It also leads to residual stresses in and nearby the weld. The weld reinforcement changes the geometry in the welded area and the critical part is the weld toes which have a very small radius. During automatic high efficiency welding it is difficult to avoid surface welding defects in the form of "cold-laps". Methodology errors in the form of undercuts, root defects, lack of fusion, inclusions, porosity, etc., may also appear. In general are embedded flaws less sensitive than surface flaws for fatigue.

In contradiction to common expectations, metallurgical changes in the structure and hardness of the weld, including the soft zones, exert only a marginal effect on the fatigue strength. It is instead the weld's local geometry at the welds toes and root that are decisive for a weld's fatigue resistance. It is the toe radius and flank angle, the geometry at the root and the residual stresses that most important factors. It is the weld's quality and the individual welder ability to perform a good weld in these aspects that have a decisive effect on fatigue resistance, see also section 5.5.7.

Methods which improve the local geometry of a weld are very effective to increase the fatigue strength since the local geometry has such impact on the fatigue strength, also see section 5.5.6.

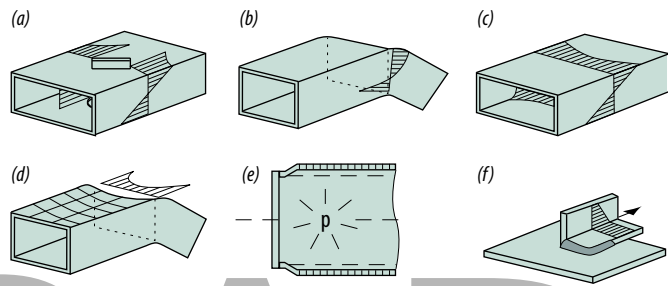


Figure 5.31: Stress distribution due to geometric disruptions in the stress flow.

5.5.2 Different types of geometric notch effect in welded structures

Disruptions in the stress flow at welded joints have different origins. They can be caused by global geometric transitions or macro or micro geometric notch effects from welds.

The global disruption in the stress flow can be caused by big indentations and bent sections, membrane effects in connection with thin-walled sections, see figure 5.31, or bending due to secondary bending moment as illustrated in figures 5.20 and 5.21. There can also be additional stress due to axial or angular misalignment, figure 5.32. The increase in stress from global disruption in the stress flow

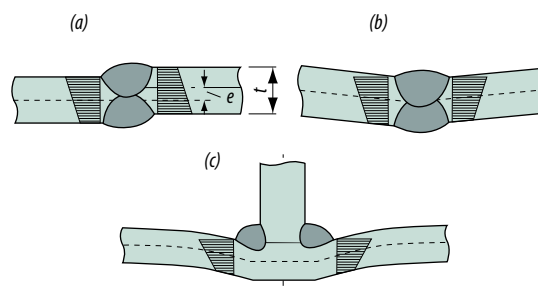


Figure 5.32: Addition of secondary bending stress due to axial or angular misalignment.

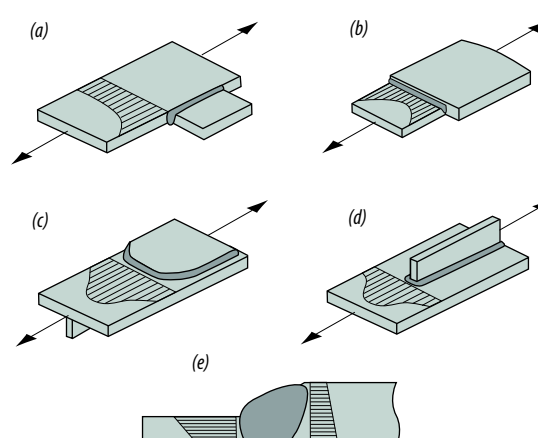


Figure 5.33: Welded structural details and geometrical stress.

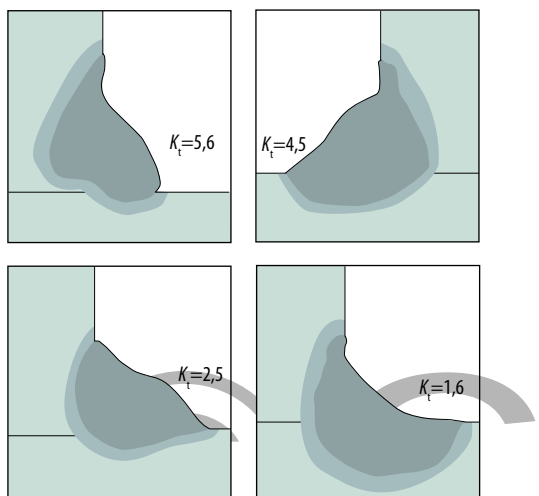


Figure 5.34: Stress concentration factors at weld toes of real fillet welds, made by FE analysis. Refers to the weld toe at the horizontal plate.

should be taken into consideration for fatigue life analysis. The increase of stress generated due to axial or angular misalignment is to a certain extent taken into account in the structural details for fatigue life analysis, see point 8 of section 5.6.6.

The local stress which is a result of the welded joint's geometric design is usually called geometrical stress or structural "Hot Spot" stress, see figure 5.33.

There is also a non-linear additional stress peak due to the weld's local geometry. This stress peak is governed by the weld's flank angle and weld toe radius and can vary significantly depending on the value of these parameters, see the different values of K_t in figure 5.34.

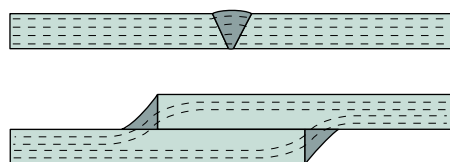


Figure 5.35: Stress flow disruptions in a load-carrying butt weld and fillet weld.

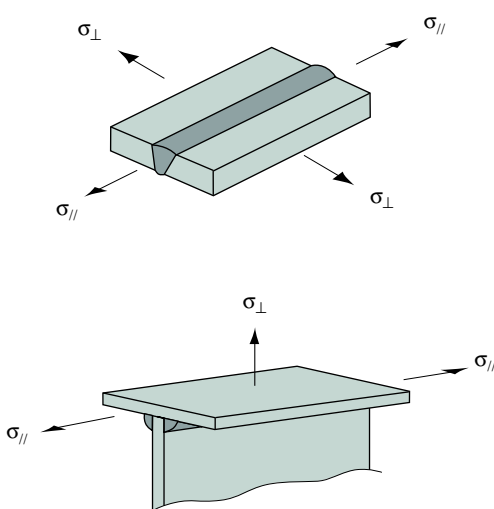


Figure 5.36: Effect of load direction on fatigue resistance value, FAT.

This handbook contains general suggestions and information without any expressed or implied warranty of any kind. SSAB hereby expressly disclaims all liability of any kind, including any damages, in connection with the use of the information and for their suitability for individual applications. It is the responsibility of the user of this brochure to adapt the recommendations contained therein to the requirements of individual applications.

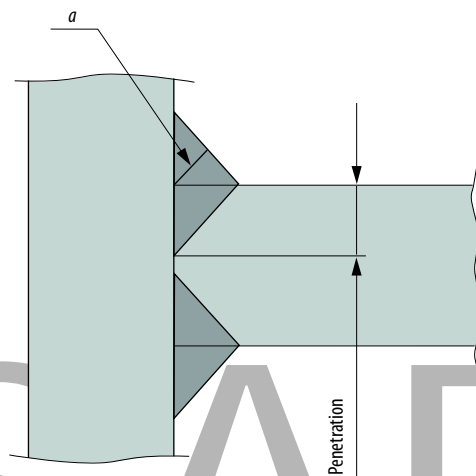


Figure 5.37: Definition of throat thickness, a and penetration.

5.5.3 Different types of joints, optimum throat thickness for fillet welds

Transverse load-carrying fillet welds generally produce a greater disturbance in the stress flow than corresponding butt welds, figure 5.35.

The load direction is also of great importance and welds which are loaded perpendicular exert a greater notch effect than welds which are primarily loaded parallel to the weld, figure 5.36. This effect of the load direction is also greater for a fillet weld than for a butt weld.

There is a risk combined with fillet welds of initiation of fatigue cracks from the root, in particular if the penetration is low and/or the throat thickness is small. The risk increases if the weld toe has been given post-treatment in order to increase the fatigue strength. This is why it is important to choose a sufficient throat thickness and penetra-

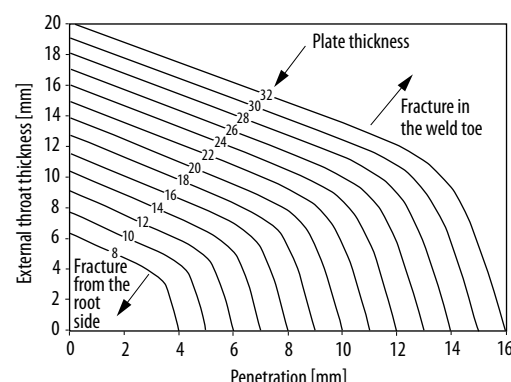


Figure 5.38: Optimum throat thickness for a tensile load [5.11].

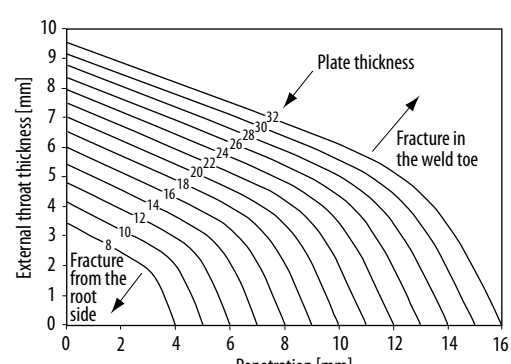


Figure 5.39: Optimum throat thickness for a bending load [5.11].

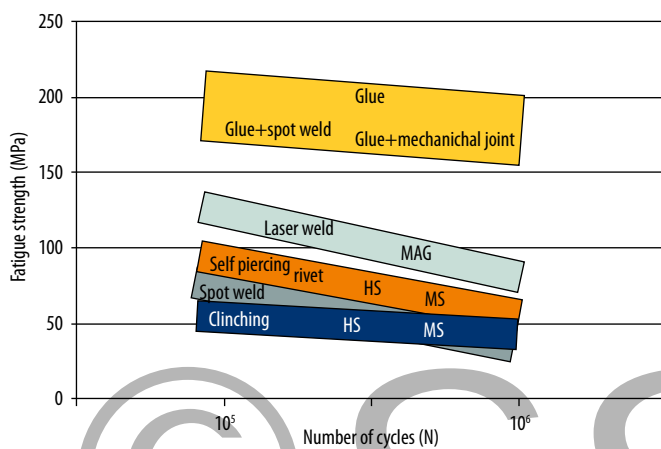


Figure 5.40: Fatigue strength for different jointing methods, shear-loaded lap joints, spot distance 40 mm, continuous laser and MAG weld, adhesive joints with epoxy glue. ($R = 0$)

tion in fillet welds in order to avoid crack initiation from the root. Figures 5.37 through 5.39 provide the basis for such an evaluation for welds which have not been given a post-treatment.

Post-treatment of welds gives an increase of the fatigue strength at the weld toe. To accomplish uniform strength in fillet welds the design of the root side is important. This is done by calculating the needed increase of throat thickness to compensate for the higher stress at the weld toe which the post-treatment allows. Calculations can also be performed by using the Notch stress method or a fracture mechanical analysis. Guidance for this is given in [5.1 and 5.11] and section 5.6.

The structural details according to IIW are based on experiments with hot-rolled material and the IIW Recommendation [5.1] therefore covers only a few joints that are typical for cold-rolled material. The fatigue strength of different types of welded joints used for thin material can, however, differ a lot and it is important to know these differences. Combining spot welding or mechanical jointing with adhesive bonding provides significant advantages for fatigue strength, just like choosing joints with continuous welds. Figure 5.40 clearly shows these differences for shear-loaded lap joints in plate with a thickness of 1 mm. The fatigue strength is expressed as the nominal stress for 40-mm wide test specimens. The yield strength has influence for mechanical jointing and joints in high-strength steel (HS) has higher fatigue strength than mild steel (MS).

Chapter 7 of the Joining Handbook [5.12] and [5.13 and 5.14] contains more information and also comparisons of the fatigue strength of different joints.

Joint category	Condition	n
Cruciform joints, transverse T-joints, plates with transverse attachments, ends of longitudinal stiffeners	As-welded	0,15
Cruciform joints, transverse T-joints, plates with transverse attachments, ends of longitudinal stiffeners	Post-treated weld	0,1
Transverse butt weld	As-welded	0,1
Machined butt weld reinforcements, longitudinal welds or attachments to plate edges	All	0
Non-welded parent material	All	0

Table 5.3: Recommended values for n according to research at SSAB.

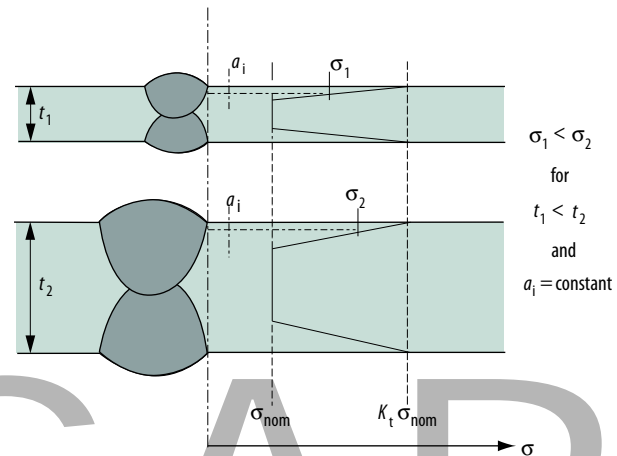


Figure 5.41: Schematic illustration of the higher stress generated in a weld in thick compared to thin material. When subjected to equal nominal stress at a given defect depth, a_i .

5.5.4 Thickness effect

A reduction in the sheet thickness increases the fatigue strength in terms of stress. In non-welded structures, this is mainly caused by statistic volume dependence. This means that the less volume exposed to stress the smaller probability for fracture and therefore higher fatigue strength. This effect is small in structures with no or mild notches but become substantial for welded joints as there is an additional geometric thickness effect present. A propagating crack will remain longer in a high stress field with increased thickness of the weld joint and the fatigue strength will thereby decrease, figure 5.41. Since the defect depth a_i of a weld is not dependent of thickness.

This effect increases when the global stress gradient increases and this is why the thickness effect is larger under bending load than under tensile load. The impact of the thickness effect is also influenced by of the notch effect, e.g., whether it is a butt or a fillet weld, the weld is loaded perpendicular or parallel and the weld is as welded or post-treated. The correlation between fatigue strength and thickness is described by equation 5.7.

$$\Delta\sigma = \Delta\sigma_0 \left(\frac{t_o}{t} \right)^n \quad (\text{Eq. 5.7})$$

where

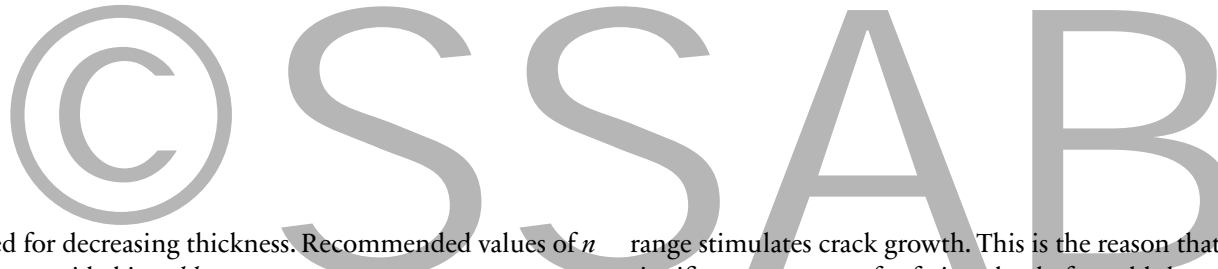
n – exponent which varies between 0 and 0.15

t_o – reference thickness

t – thickness

If the reference thickness t_o is set to 15 mm, the relation above states that a weld in 5 mm material has up to 25% higher fatigue strength than a weld in 15 mm material. The IIW Recommendations [5.1] have a reference thickness of 25 mm. A thickness effect which increases in the FAT values should be verified with testing according to IIW. Such testing have been performed and shows that the fatigue strength increases for sheet thickness down to 4 mm [5.15 and 5.16]. For thicknesses thinner than 4 mm the correction for 4mm is used.

It was also found that the value for n had to be reduced by 50% compared to the IIW Recommendations, when it



is used for decreasing thickness. Recommended values of n for are provided in *table 5.3*.

The thickness effect is considered in the nominal stress method by multiplying the FAT value with the thickness improvement factor ϕ_t . The thickness correction is not used in the Hot Spot, notch stress and the fracture mechanics methods see also point 3 of section 5.6.6.

5.5.5 Residual stress in the weld – Stress relief treatment

Residual tensile stress is formed in the area close to the weld due to shrinkage during cooling. Residual stresses in the weld exert a great effect on fatigue resistance and the difference in fatigue strength between areas with tensile and compressive residual stress is substantial. However, tensile residual stress equal to the parent material yield strength is commonly assumed during fatigue design of welded joints. The residual stress is added to the stress caused by an external load. The stress range close to the weld will then pulsate from a maximum at yield strength and downwards independently of the R-ratio of the external load range. Due to this phenomena the effective stress range does not decrease even if $R<0$ and crack closure occurs at compressive load. So the complete nominal stress

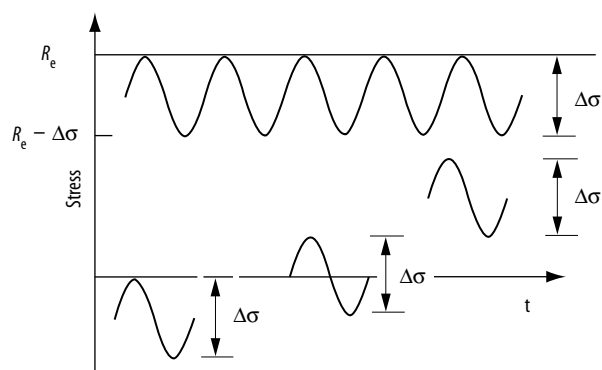


Figure 5.42: Combination of residual stress and applied stress.

range stimulates crack growth. This is the reason that the significant parameter for fatigue load of a weld the stress range $\Delta\sigma$, *figure 5.42*.

Figure 5.43 shows results from fatigue tests of specimens with longitudinal stiffeners which have been tested at different mean stress. It appears that the mean stress only marginally affects the fatigue strength, $\Delta\sigma$, for specimens in as welded condition. Stress relief treatment, however, provides a significant increase in fatigue strength when a part of the load cycle is compressive, i.e. for $R<0$. The reason is that crack closure strongly reduces the effective stress range when the residual stresses are removed.

The consequence is that it does not pay off to give a stress relief treatment to a welded structure in order to improve the fatigue strength unless some part of the stress cycle is compressive.

The IIW has chosen in its recommendations to allow enhancement of welds with low residual stresses. Herein this is We considered with a stress alternation factor, φ_e , whose effect is somewhat different, see also section 5.6.6.5

If the residual stresses in a weld is known, e.g., by measurements, the local R ratio based on nominal stress and residual stress can be used to determine the stress alternation factor φ_e .

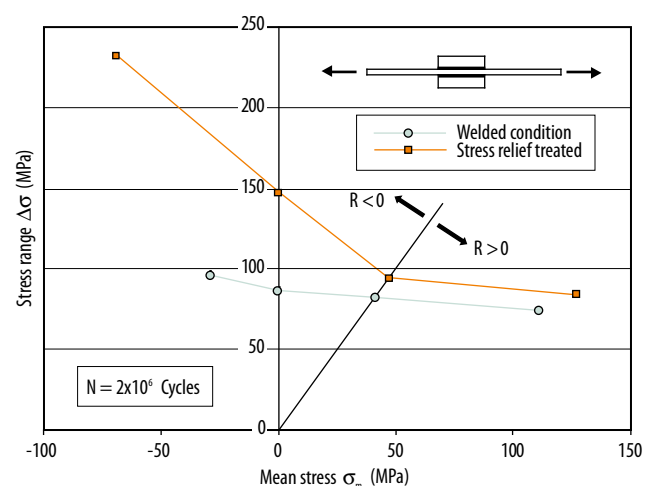
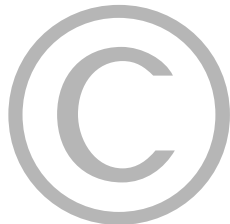


Figure 5.43: Fatigue strength as a function of nominal mean stress for test specimen with welded longitudinal stiffeners [5.17].



SSAB

5.5.6. Post-treatment of welds for increased fatigue strength

The occurrence of local stress concentrations, different types of defects and residual stresses in the vicinity of the weld is decisive for the weld's fatigue resistance. The need for methods to improve the fatigue life is evident.

If it is not possible to avoid welds in high stress regions, it could pay off to introduce some post-treatment method. Post-treatment of welds in a limited area normally results in a significantly increased fatigue life of the whole structure. In general it could be stated that, the lower the fatigue resistance of a welded joint, the greater potential to increase the fatigue life by post-treatment.

The methods available for post-treatment of welds are aimed at treating the area next to the weld toe and hence improving the local geometry or introducing compressive residual stresses. Based on that, examples of different methods could be divided into two groups:

Methods for improving the local geometry (a):

- machining or surface grinding of the weld reinforcement
- machining or grinding of the weld toe
- local remelting with TIG, plasma or laser

Methods for introducing compressive residual stresses b):

- Cold hammering – Peening (Hammering, Needle Hammering, Shot Peening, "Ultrasonic Peening" (UP) and "Ultrasonic Impact Treatment" (UIT))
- local compression
- overloading
- HFMI, (High Frequency Metal Impact)

The primary purpose of the methods according to (a) is to remove or reduce crack-like imperfections in the weld toe and thereby prolong the initiation stage of the fatigue process. They also produce a smoother transition between the plate and the weld, hence increasing the radius and decreasing the stress concentration.

Methods according to (b) introduce advantageous compressive stresses in the area next to the weld toe. The weld toe is thereby going to be "pre-stressed" with compressive stresses which must first be overcome by a possible tensile stress in order to propagate a fatigue crack. The effective stress range decreases due to crack closure and hence the fatigue strength increases.

An improvement method according to (a) is preferable since geometric improvements stand a better chance of being preserved than introduction of compressive stresses which have a risk of relaxation due to extreme loads. Some methods, like UIT, affect both the geometry and the residual stresses in a positive way.

A short review of different post-treatment methods follows below.

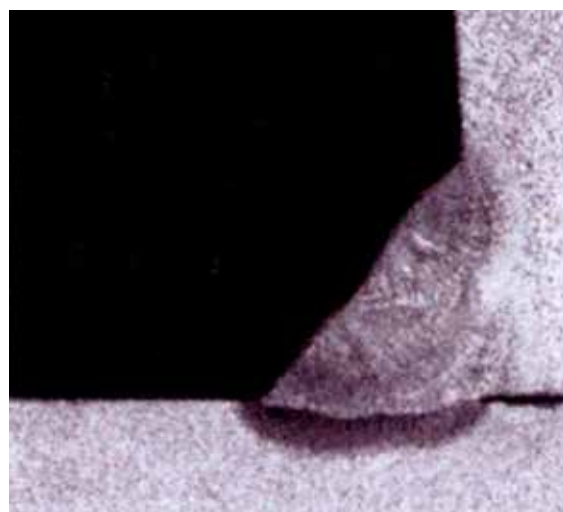
Machining and grinding are historically the most common methods of post-treating welds. They are performed with a disc grinder or rotary burr grinder in order to improve the local geometry in the transition zone between the weld and the parent material (the weld toe). It is important to grind off completely any undercuts and other defects and the recommended grinding depth is the *defect depth + 0.5 mm*. The depth is simultaneously maximized so that the area reduction does not exceed 10%. Otherwise, the area reduction due to grinding must be taken into consideration.



During *TIG dressing*, the transition zone between the weld and the parent material is melted using a TIG welding machine. The geometry of the transition zone is improved and porosity and inclusions float up. A special procedure is applied at the start and stop positions. The method, which is relatively quick and environmentally-friendly, is nowadays implemented in industrial serial production. Figure 5.44 shows a cross-section of an undressed and a TIG-dressed fillet weld.

The extra heating of the steel during TIG dressing can produce a soft zone in steels with very high strength. This normally does not affect fatigue resistance but in static situations this should take into consideration if the weld is exposed to a high load. Further information the Joining Handbook [5.12].

Cold hammering (peening) is a process where the material is cold worked with a vibrating tool or through shot peening. It builds compressive stresses and also provides a certain improvement of local geometry. Blasting of welded structures could also provide them with an “overall protection” when it comes to premature fatigue failures. Ultrasonic Peening (UP) and Ultrasonic Impact Treatment (UIT) are new methods which are relatively easy to use and which are also better from an environmental point of view (lower sound level and less vibrations) than traditional cold hammering.



Local compression (coining) is realized by pressing structural elements between two tools in order to plastically deform the material and build in compressive stresses. The technology is used for well-defined local areas with a high notch effect, e.g. next to spot welds or at the end of stiffeners.

Overloading can be used for certain structures where the load direction does not change, e.g. pressure vessels and cranes. The structure is loaded up to the nominal yield strength, which causes plastic deformations in areas with a high notch effect. Compressive stresses are then introduced in these areas during unloading. The advantage of this method is that it can generate compressive residual stresses even in internal notches and the root side of welds.

Stress relief annealing is used seldom only for the purpose of boosting the fatigue strength. There are usually other simultaneous reasons for its use. It can, however, result in positive effects for the fatigue strength if some part of the nominal stress cycle is compressive stress (see section 5.5.5).

HFMI, (High Frequency Metal Impact) is a new manual method where a metallic cylinder plastically deforms the transition zone between the weld and the base material. Used locally in critical areas, [5:53]

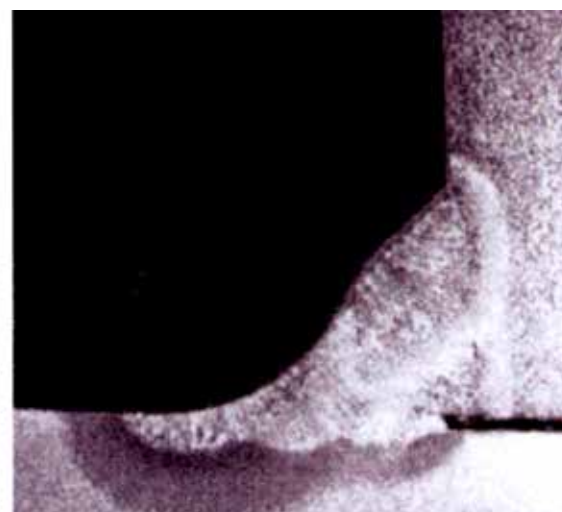


Figure 5.44: Cross-section of an welded and a TIG-dressed fillet weld.

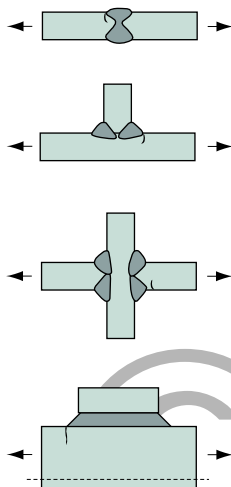


Figure 5.45: Welded joints suitable for post-treatment (IIW).

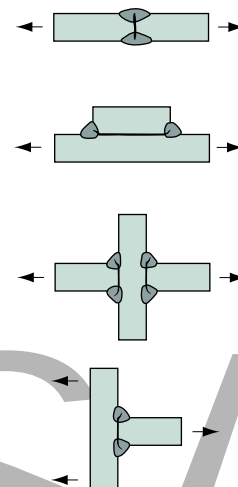


Figure 5.46: Welded joints which crack from the root side are unsuitable for post-treatment (IIW).

Since most herein mentioned methods can be used to improve the weld toe only, other parts of the welded joint, e.g. the root side in fillet welds, can instead become critical. The full effect of the post-treatment can then be diminished. This is why it is important to also analyze secondary initiation positions with respect to fatigue failure. For this reason *figure 5.45* and *5.46* give examples of joints which are suitable and unsuitable for post-treatment aimed at increasing the fatigue strength. There is a big risk of crack initiation from the root in the joints in *figure 5.46*.

Certain guidance for choosing the throat thickness for fillet welds with partial penetration is given in section 5.5.3 and for post-treated ones in [5.11].

The effect of post-treatment depends on the welded joint load direction and the number of load cycles.

The effect of post-treatment on welds which are loaded along their longitudinal direction is marginal.

Such situations often show a very high fatigue resistance and it is only the weld reinforcement's wave pattern and possible start/stop positions that produce a notch effect.

The welding end of a longitudinal stiffener, however, should be viewed as a transverse weld with a high notch effect.

The effect of post-treatment is greatest at a high number of load cycles and decreases with a decrease in the number of cycles to failure – the more, the higher the R-value, since the maximum allowable stress could be limited by the yield strength. Nevertheless, IIW has chosen to adopt, until further notice, the same slope of the S-N curve ($m=3$) for both post-treated and as-welded joints.

In its recommendations for post-treatment of welds (grinding, TIG dressing and peening), IIW [5.1] has specified the improvement effect as a factor which increases the load carrying capacity by approximately 30%. The design

stress range for the post-treated welded joint is calculated by multiplying this factor by the characteristic stress range based on the current FAT class for the as-welded joint. Approximately it corresponds to an increase by two steps in the series of FAT classes. However, the maximum stress level it can be raised to is the stress level corresponding to fatigue class FAT 112, see also section 5.6.7 under the "Improvement Methods" heading. The increase in fatigue strength is normally greater than the conservative 30% put down by the IIW. Higher improvement factors can be allowed, in particular in connection with longer service lives, if they are verified by practical testing.

5.5.7 Welding quality and assessment of weld defects

Good welding quality in a fatigue context normally means smooth transitions between the weld and the parent material, flat flank angle, a large weld toe radius, the smallest possible undercut and absence of cold laps. It is also these parameters that are a decisive for quality when it comes to fatigue-loaded structures. For a welded joint without full penetration it is important that the penetration depth does not decrease due to lack of fusion or other root defects. Low penetration increases the risk of initiation of cracks from the weld root.

Imperfections such as inclusions, porosity, minor undercuts and lack of fusion can be allowed to a certain extent without affecting the welded joint's fatigue resistance. The permissible extent of these imperfections is related to the structural detail correlated with the joint.

There are different types of welding defects. It can be a matter of axial and angular misalignment which increases the geometrical stress (*figure 5.32*), welding imperfections

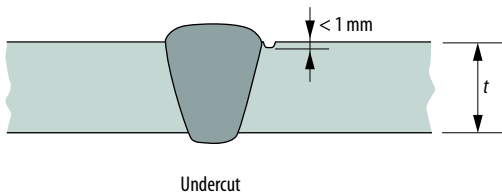
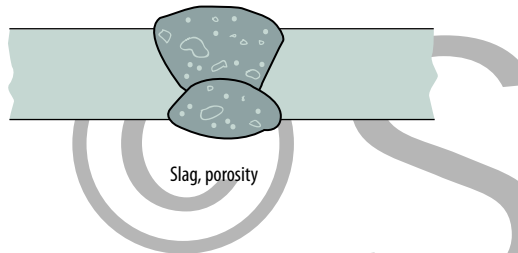


Figure 5.47: Example of non-crack-like weld imperfections; slags and undercut shallower than 1 mm.



which interact with the natural stress concentration in the weld toe or internal defects.

A certain effect of misalignment, defects in joints without full penetration and undercuts is covered by the fatigue resistance values. The stress increase in connection with misalignment is expressed with a factor, ω . It is included in the fatigue resistance values only to a certain extent and in section 5.6.6.8 this is further described.

Other types of defects are usually divided into crack-like and non-crack-like imperfections. The latter group includes undercuts which are shallower than 1 mm, as well as slag and porosity, see 5.47.

The acceptance level of undercuts for different FAT values is specified in *table 5.4* and regarding slag and porosity in *table 5.5*.

When it comes to undercuts and other plane welding defects oriented in the weld's longitudinal direction, these do not affect the fatigue resistance with respect to longitudinal loads.

Undercuts deeper than 1 mm should be viewed as crack-like imperfections and their effect on fatigue strength is assessed using fracture mechanics, see *figure 5.47* and section 5.6.12.

Examples of defects which do not interact with the weld toe are embedded crack-like imperfections, e.g. partial penetration and lack of fusion, see *figure 5.48*. These are also analyzed with fracture mechanics.

Fatigue resistance value FAT	Permitted relative defect depth of an undercut a/t	
	Butt weld	Fillet weld
100	0,025	–
90	0,05	–
80	0,075	0,05
71	0,10	0,075
63	0,10	0,10
< 56	0,10	0,10

Table 5.4: Acceptance levels for weld toe undercut.

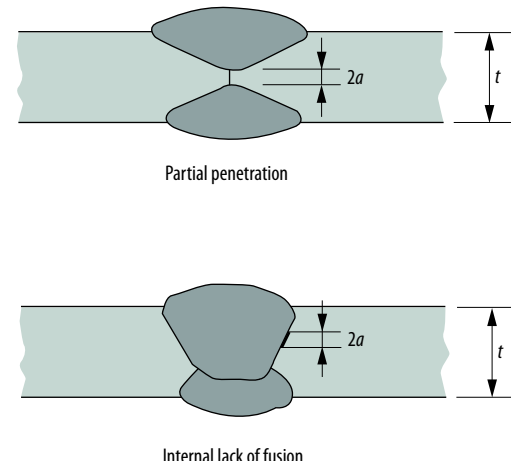


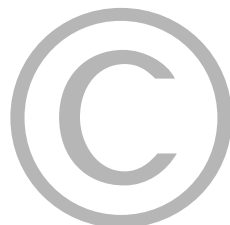
Figure 5.48: Example of crack-like imperfections which are assessed with fracture mechanics

Fatigue resistance value FAT	Max. length of inclusions in mm		Porosity % area ^{*)}
	Welded	Stress-treated	
100	1,5	7,5	3
90	2,5	19	3
80	4	58	3
71	10	—	5
63	35	—	5
< 56	—	—	5

***) Length of weld with porosity according to non-destructive testing divided by the weld length.
Max. pore diameter t/4 or 6 mm.**

Table 5.5: Acceptance levels for inclusions and porosity in welds

This handbook contains general suggestions and information without any expressed or implied warranty of any kind. SSAB hereby expressly disclaims all liability of any kind, including any damages, in connection with the use of the information and for their suitability for individual applications. It is the responsibility of the user of this brochure to adapt the recommendations contained therein to the requirements of individual applications.



SSAB

The IIW specifies a simplified procedure for assessing the highest FAT class in connection with different defect depths in crack-like imperfections [5.1]. Guidance on the assessment of defect sizes based on NDT (non-destructive testing) indications is provided in *figure 5.49*.

The defects are regarded as elliptical (embedded flaws) or semi-elliptical (surface flaws) according to *figures 5.50* through *5.52*. If a flaw inside the material lies less than 0.75 a below the surface, it is regarded as a surface flaw with a depth of 2 a .

The highest FAT class at different defect depths for crack-like imperfections is specified in *figure 5.53*. It is based on the simplified procedure by IIW. L is the distance between the weld toes. In addition to the cases included in *figure 5.53*, the simplified procedure by IIW also covers cases with edge defects.

For more detailed information about the background of what is treated within this section, refer to section 3.8 and 6.2 in [5.1]

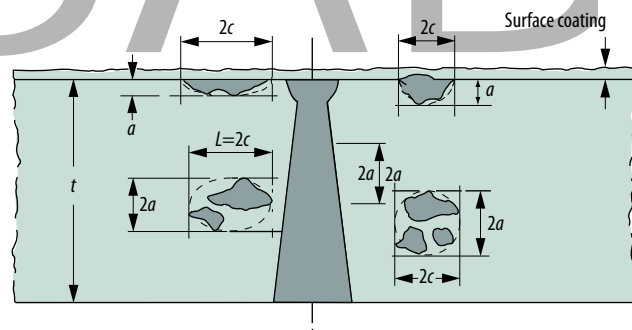


Figure 5.49: Assessment of defect sizes based on NDT indications.

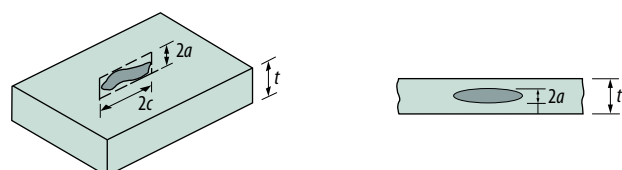


Figure 5.50: Dimension definitions in crack-like embedded flaws.

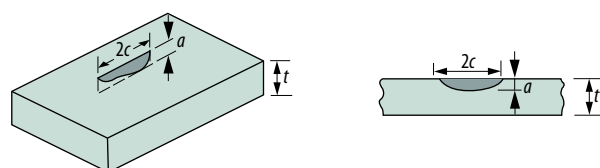


Figure 5.51: Dimension definitions in crack-like surface flaws.

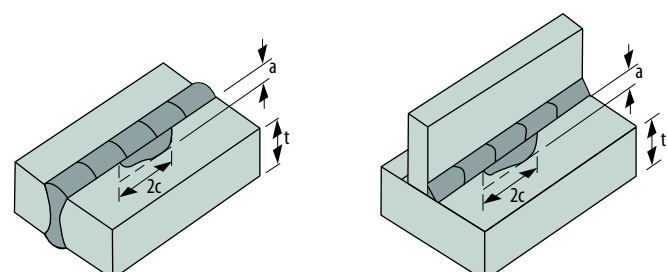


Figure 5.52: Dimension definitions in crack-like surface flaws in welds.

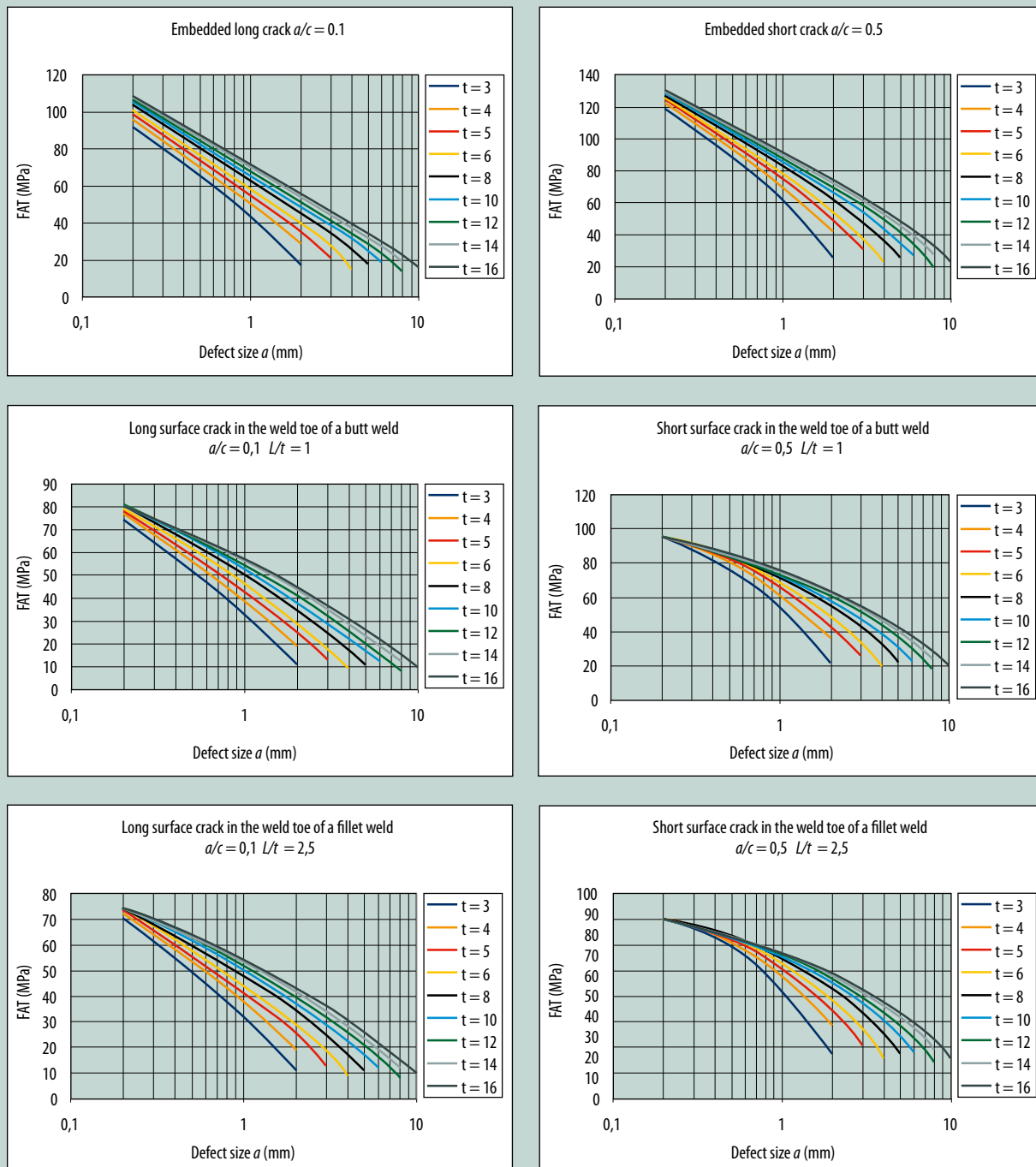
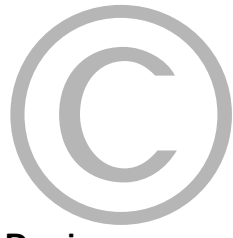


Figure 5.53: Highest FAT class at different defect depths in crack-like imperfections.



SSAB

5.6 Design

5.6.1 Introduction

Design refers to validate that the resistance of a structure expressed as fatigue strength, which has taken into account notch effect, stress history and service life, is larger or equal to the stresses exerted by external loading. By taking into account the uncertainties in assumed loads and distribution in fatigue strength. *Figure 5.54* shows this schematically, where the failure risk is dashed.

Fatigue-loaded structures are often exposed to stresses which vary in magnitude and intensity over time. The service life of a structure is strongly dependent on the stress history parameter. This is why it is of the utmost importance to perform a careful load analysis in order to obtain the best possible material efficiency. This is why this section describes the load analysis in a relatively great detail.

The nominal stress, structural Hot Spot stress and effective notch stress methods and fracture mechanics are discussed here. Fatigue resistance values, FAT, for welds originates mainly from the IIW Recommendation for fatigue design [5.1]. Load history calculations are based on the Crane Standard [5.2]. It uses S-N curves with a constant

slope as in the figure on the right below, *figure 5.55*. This simplifies the calculations but gives a more conservative result for a load history with many small loads compared to the traditional approach with a flatter slope after a knee point, the figure on the left. Section 5.6.7 is based on S-N curves without a knee point. Section 5.6.10 provides an opportunity to apply both alternatives. Using S-N curves with a knee point is recommended for better material efficiency in structures with a load history with many small loads.

Partial coefficients are equal as in previous editions of this handbook [5.26] and are comparable with the ones specified in the IIW Recommendations and the Crane Standard. The material factor which takes into consideration the effect of static strength and surface roughness on the fatigue strength of parent materials has been updated for higher strength steels. The thickness improvement factor, which takes into account the higher fatigue strength in thin welded joints, has also been updated. Section 5.6.12 fracture mechanics and defect tolerance is updated with actual crack growth data.

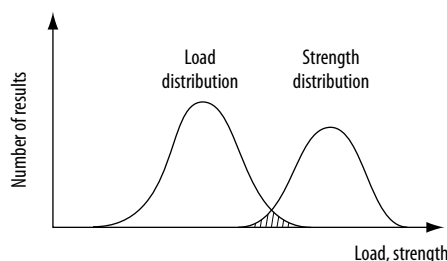


Figure 5.54: Load and strength distribution schematically.

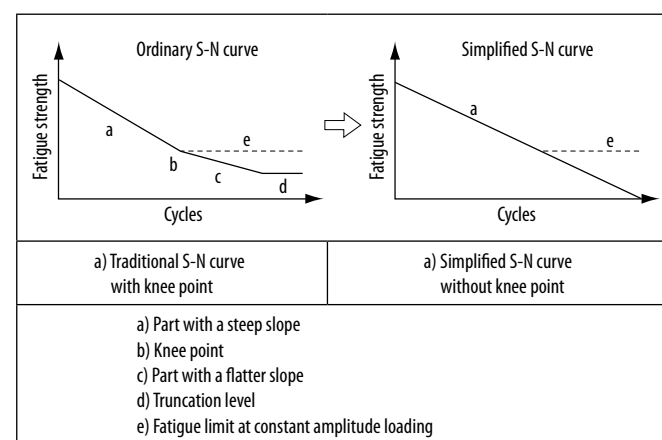
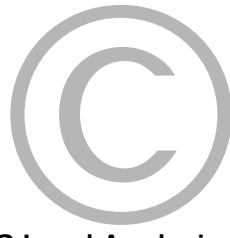


Figure 5.55: Traditional and simplified S-N curve, respectively. The knee point is left out of the simplified S-N curve.



5.6.2 Load Analysis

SSAB

General information

An accurate load analysis is the most important and also the most difficult thing during fatigue design. An underestimation of the loads by 20% corresponds to a twice as short service life of a welded joint. On the other way around an overestimation of the stress spectrum easily leads to substantial over sizing. These are strong arguments for collecting information about the loads that affects the structure.

The load analysis is aimed at systematizing the occurring loads into a load history e.g. stress history. The intensity is described with a stress history parameter. This is an important parameter in fatigue design. The stress history can be different in different parts of a structure. One example is a wheel suspension part which is exposed to a stress history that is different to the one found in the vehicle frame.

Assumptions must often be made about the loads during the development of a new product. Many times it is necessary to develop a prototype and perform measurements under realistic conditions in order to find appropriate load data. Component testing in a test rig is often conducted in order to verify the product based on the recorded load data. Strain measurements can be performed in order to verify stress calculations during rig tests, see *figure 5.56*.

In order to determine the stress history for a structure one can make strain measurements in service or perform dynamic simulations. It is also possible to use a standardized load history from a standard, norm or recommendation if available. See also section 5.6.4. A measurement should be conducted under as realistic conditions as possible. The required time to collect a representative load history during a measurement is at the very least a 0.1 % of the service life [5.19].

Strain measurements are often preceded by FE analyses to identify critical areas in the structure. After the measurements it is possible to calibrate the FE model with the measured strains and perhaps identify overlooked critical points without the need for new measurements. The choice of strain gauge placement is determined by the purpose of the measurement and evaluation method. When measurements are based on the Hot Spot method, strain gauges are put in direct connection with the welded joints, see also section 5.6.8.

The measuring system which collects the signals from the strain gauges is called a logger. The chosen sampling frequency in the logger should not be less than 10 times the highest frequency in the measured signal. The strain signals recorded by the logger must be converted to a stress and arranged in a stress history by the methods described in next chapter to be useful in fatigue evaluation. To simplify the following sections, it is presumed that the signals have been converted into stress.

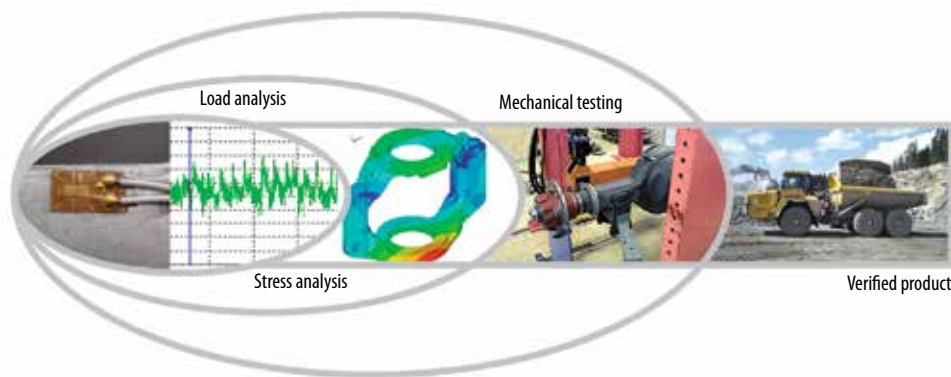
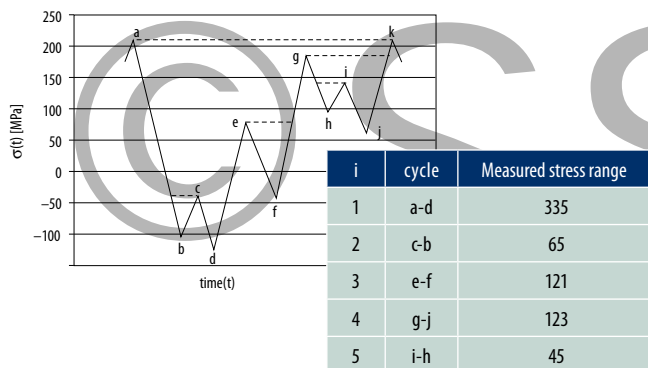


Figure 5.56: The figure describes a methodology when a new product is developed and designed.

1. Measured data



2. Division into intervals

i	Intervall $\Delta\sigma$ (MPa)		
1	320	-	340
	300	-	320
	..	-	..
3,4	120	-	140
	100	-	120
	80	-	100
2	60	-	80
5	40	-	60
	20	-	40
	0	-	20

3. Range pair

$\Delta\sigma_i$ (MPa)	n_i	Σn_i
330	1	1
310		1
..		1
130	2	3
110		3
90		3
70	1	4
50	1	5
30		5
10		5

Figure 5.57: The range pair method illustrated with the reservoir analogy, i.e., the graph is filled with “liquid”. All “containers” are drained, beginning with the lowest point of the sequence. The drained heights in the respective container correspond to the stress range in the sequence.

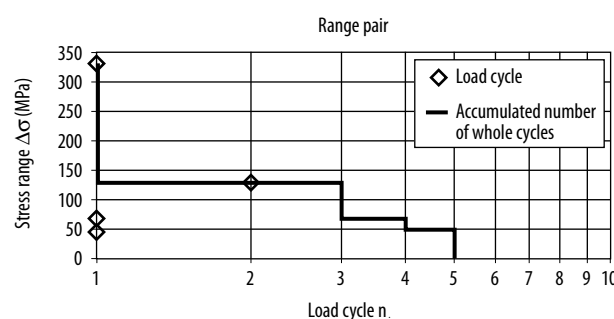
CSAB

Rainflow count & range pair methods

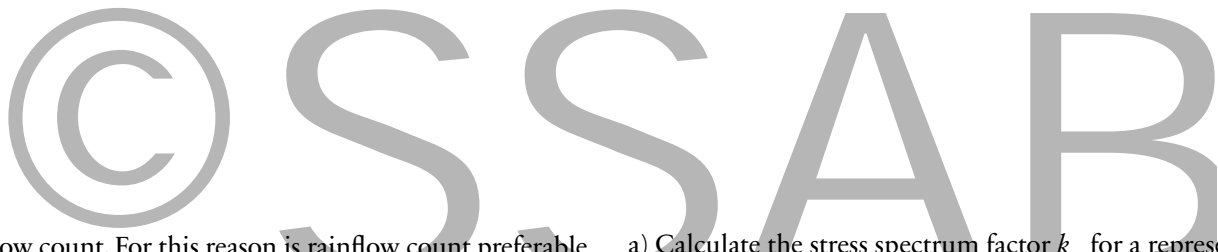
A way of handling the big amounts of data from a measurement is to form whole or half cycles based on local max and min stress. The rainflow count and range pair methods are most common algorithms for signal processing and are more reliable than the level crossing method [5.19]. These algorithms are usually included in the logger’s software. The algorithms are standardized according to ASTM E 1049-85, Cycle Counting in Fatigue Analysis [5.21]. As suggested by the name, the application of the range pair method registers stress ranges and number of load cycles. This method is sometimes called the reservoir counting method, cf. figure 5.57.

When the range pair method is used, the measured stress ranges are sorted into intervals with the corresponding number of load cycles. Each level is represented by the mean value of the adjacent interval boundaries. The number of levels is determined by the scope of the signals and the precision that is required. 64 levels can be chosen as a guideline value. The steps between the levels are uniform in linear scale.

The rainflow count and range pair methods give equivalent results. The significant differences are that half load cycles and corresponding mean stress are recorded with the



Graphical representation.



rainflow count. For this reason is rainflow count preferable for short measuring sequences.

Fatigue evaluation is most common based on stress ranges and particularly for welded structures where the mean stress has negligible influence, see section 5.5.5. The range pair method is sufficient in such cases.

5.6.3 Stress history characterization

For fatigue evaluation it is necessary to determine the stress history parameter for critical parts. This is done by determining the stress spectrum factor, k_m . The methodology of the stress spectrum factor k_m is based on the Crane Standard [5.2] with an assumption of constant slope of the S-N curve in accordance with section 5.6.1. It is common that the stress spectrum factor is the equal all over a part.

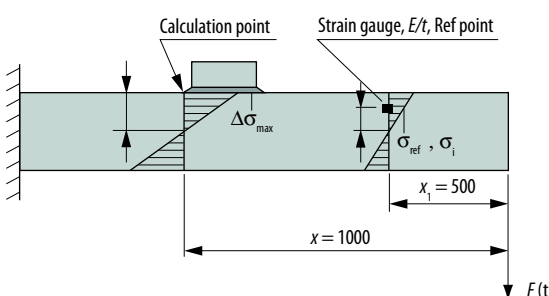


Figure 5.58: Calculation point and reference point.

a) Calculate the stress spectrum factor k_m for a representative part of the total stress history. The stress spectrum factor is determined from measured stress ranges on the field or an assessment based on the usage.

$$k_m = \sum_i \left(\frac{\Delta\sigma_i}{\Delta\sigma_{ref}} \right)^m \cdot \frac{n_i}{n_t} \quad (\text{Eq. 5.8})$$

$$n_t = \sum_i n_i \quad (\text{Eq. 5.9})$$

Equation 5.8 is then formed

$$k_m = \left(\frac{\Delta\sigma_1}{\Delta\sigma_{ref}} \right)^m \cdot \frac{n_1}{n_t} + \left(\frac{\Delta\sigma_2}{\Delta\sigma_{ref}} \right)^m \cdot \frac{n_2}{n_t} + \left(\frac{\Delta\sigma_3}{\Delta\sigma_{ref}} \right)^m \cdot \frac{n_3}{n_t} + \dots$$

where

- n_i – load cycles at level i
- n_t – total number of load cycles
- $\Delta\sigma_i$ – stress range at level i
- $\Delta\sigma_{ref}$ – selected reference value for calculation of k_m
- m – the slope of the S-N curve.

$m=3$ is selected for the slope of the S-N curve for welded joints. $m=5$ is selected for parent material, screwed or riveted joints and welded joints loaded under shear stress. The greatest stress range measured in the stress history can be selected as reference value $\Delta\sigma_{ref}$. It is important that the maximum stress range $\Delta\sigma_{max}$ at the calculation point is determined with the same external load as $\Delta\sigma_{ref}$, see the example according to figure 5.58.

b) The stress history parameter is s_m , subsequently calculated according to

$$s_m = \frac{N_t}{2 \cdot 10^6} \cdot k_m \quad (\text{Eq. 5.10})$$

where

- N_t – Design life in load cycles, i.e., the total number of load cycles the structural element is exposed to during its usage.

5.6.4 Typified stress histories

A simplified way of representing stress histories graphically is to use linear functions and specify stress ranges as a function of the accumulated number of load cycles. The accumulated number of load cycles for a given stress range is then made up of the sum total of all load cycles on this and higher level.

The stress histories which are standardized with regard to the design number of stress cycles and maximum stress range are linear in a lin-log scale and are seven, *figure 5.59*. A value of the stress spectrum parameter κ belongs to each stress history. The value of κ is the same as the quotient between the smallest and the largest stress range in the spectrum. When $\kappa=1$, it therefore corresponds to a load with a constant stress range, i.e., constant amplitude loading. A spectrum with a low value of κ is called a loading history with many small loads and a spectrum with a high value of κ is called a loading history with constant amplitude loading. It can be assigned to one of the typified stress histories for a given structure or component. This is possible as both the stress range and the design stress cycle figures are standardized for the typified stress histories. If you want to make a graphic comparison between a measured and a typified stress history, the hundred largest stress cycles should be truncated. When a graphic comparison is made, you should first ensure that the measured stress history agrees well with the typified stress history at high numbers of load cycles.

Loading histories with many small loads allow higher permitted working stress than loading histories with constant loads at any given service life. In those cases where a structure is exposed to a stress spectrum which can be assigned to one of the typified stress histories and

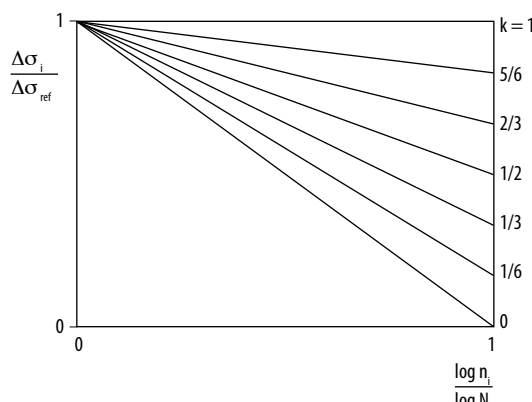


Figure 5.59: Typified stress histories. The ratio between the number of stress cycles n_i at the respective stress range and the total number of stress cycles N_t is represented along the X-axis. The stress ranges in relation to the maximum stress range in the spectrum on the Y-axis.

if the maximum stress range and design stress cycle figures are known, the design can be based on the approximate connection between κ and k_m . The conversion figures between the values of κ and the stress spectrum factor k_m at a different number of stress cycles are indicated in *figure 5.60* and *figure 5.61*. The current κ value for a certain number of stress cycles gives a value of k_3 or k_5 ($k_3=k_m$ for $m=3$, $k_5=k_m$ for $m=5$) which is used in the design condition in section 5.6.6.

The values are produced under the prerequisite that the S-N curves have a constant slope without a knee point according to section 5.6.1.

Empirical values for a design number of stress cycles and stress history exists for certain types of structures, see *table 5.6*. The table is not intended as design data in any specific case but should be viewed more as an example of the stress spectra different structures are exposed to. A corresponding value for k_3 is computed from *figure 5.60*.

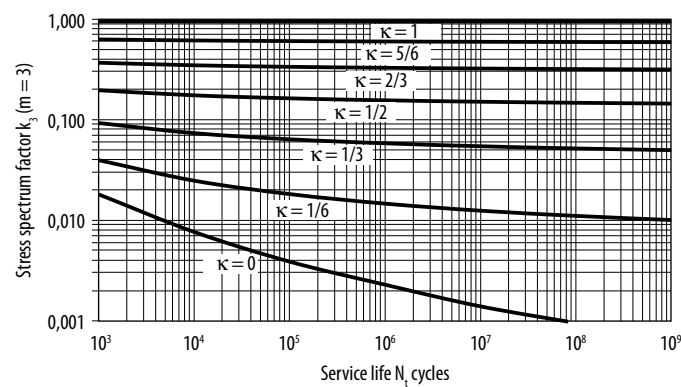


Figure 5.60: Stress spectrum factor k_3 for $m=3$.

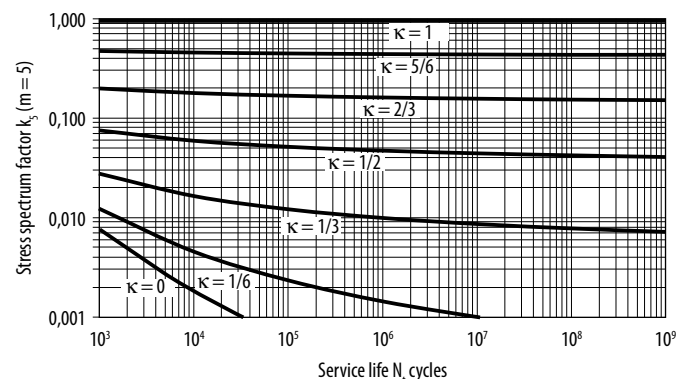


Figure 5.61: Stress spectrum factor k_5 for $m=5$.

Type of structure	κ	N_t
Bridges	1/3	$2 \cdot 10^6$
Steel buildings	1/2	*)
Mobile cranes	1/2	$2 \cdot 10^5$
Steel cross members	2/3–1	$2 \cdot 10^6$
Container cranes	2/3	*)
Ship's bottoms	0	10^8
Excavators (boom, stick)	1/2–2/3	*)
Vehicle frames:		
Dumpers, tipper lorries	2/3	$2 \cdot 10^6$
Forestry machinery	1/2–2/3	*)
Trailers, road lorries	0	10^8
Mobile cranes chassis	0–1/2	*)
Forks on forklift trucks: Sawmill transports	1/3	$2 \cdot 10^6$
Lifting arms on wheel-loaders:		
Hard operation, regular cycle	1/4	*)
Normal, varied driving	0–1/6	*)

*) Different, depending on application

Table 5.6: Example of approximate values of the stress history parameter κ , and typical number of stress cycles for certain structures.

5.6.5 Choice of design method

The purpose of the calculations, the design's complexity and desired accuracy are decisive for the choice of design method. Fatigue design according to the Design Handbook covers the nominal stress method, the Hot Spot method, the effective notch method and defect tolerance based on fracture mechanics. The Hot Spot method and the effective notch method are FE based methods.. Nowadays, also fracture mechanical analysis and the nominal stress method are often based on FE calculations although the methods are originally based on analytical calculations. It should be kept in mind that each method has its strengths and weaknesses and that the results of the different methods are not always in exact agreement with each other. A schematic description which illustrates the work effort for the methods, the complexity of the respective structure and the accuracy of the fatigue life estimation can be viewed in figure 5.62.

For simple geometries with well-defined stress, the nominal stress method is a simple method which provides a satisfactory result with relatively little work effort. A method providing better accuracy is used for more complex geometries where nominal stress cannot be defined. More or less extensive testing of components or whole structures is often necessary when mass production is relevant for the purpose of verifying the calculations. A brief comparison between the different methods is provided below. For a more detailed comparison, see [5.23].

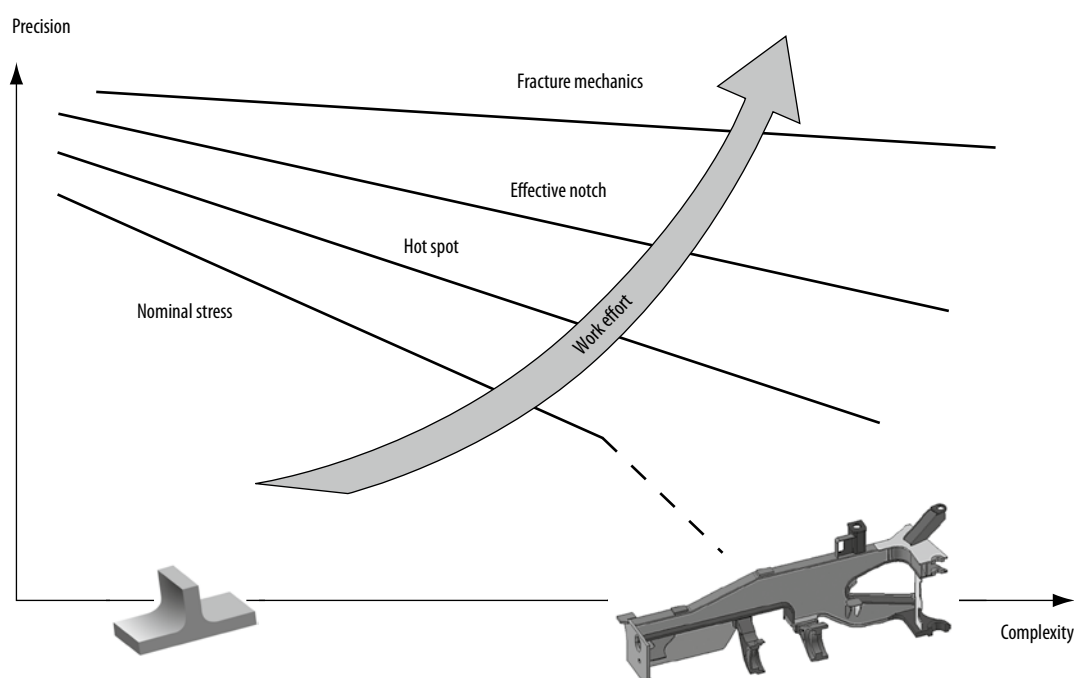
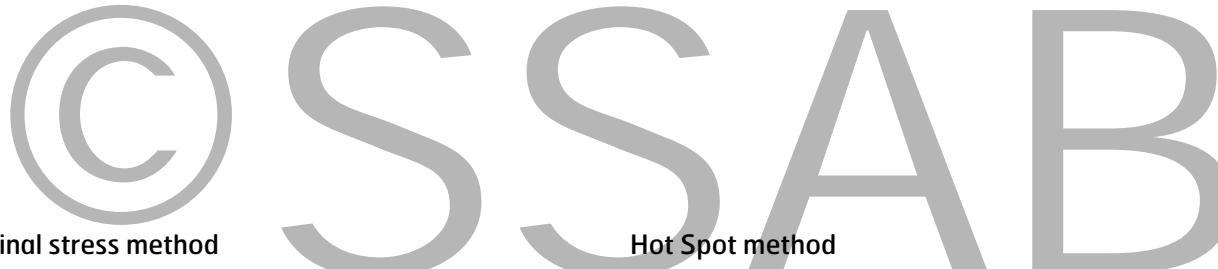


Figure 5.62: The different methods for fatigue life evaluation [5.22].



Nominal stress method

Fatigue design is based on nominal stresses and the fatigue class for different types of joints was the first method developed among methods mentioned above and is still the most common one used today.

Prerequisites:

- Nominal stress must be possible to determine.
- The geometry and load direction of the respective joint have an equivalent in a known fatigue class.
- The current calculation point meets the requirements for tolerances, e.g., angular and axial misalignment compared to what is specified for the joint in the fatigue class table. Otherwise, the additional bending stress needs to be accounted for.

Advantages:

- Simple method, calculations without advanced calculation programs often possible.
- Works for certain joints where notch stress and Hot Spot cannot be applied, e.g., in connection with a load in the weld's longitudinal direction in fillet welds or butt welds.
- Covered by many standards and recommendations.

Disadvantages:

- Does not work in complex welded structures where nominal stress cannot be defined.
- Fatigue class tables often become extensive (50 to 100 joints) in order to cover commonly occurring geometries.

Hot Spot method

The Hot Spot method is intended for fatigue design of welded joints. The method is based on geometrical stress, primarily perpendicular to the weld toe and can be used when nominal stress is difficult to define in the vicinity of the relevant weld and the nominal stress method is therefore not applicable. Measurements in accordance with this method can be performed locally, in the vicinity of the weld toe.

Prerequisites:

- The method is applicable only to welded joints only when the weld toe is critical.
- Smaller, so-called sub-models with refined element division are often required during FE calculations of larger structures.
- The respective FE model must be modeled with the actual angular and axial misalignment during FE calculations aimed at capturing secondary bending stress.

Advantages:

- The method is applicable to complex structures where nominal stress is difficult to define.
- Joints which are not listed in fatigue class tables associated with the nominal stress method can be analyzed using the Hot Spot method.
- Direct connection between results from strain gauge measurements and the FE analysis.
- Angular and axial misalignment can be modeled.
- Secondary bending stress is captured during strain measurements locally at the weld.
- The fatigue resistance table for this method comprises only approx. 9 structural joints and 2 FAT values.

Disadvantages/limitations:

- Greater work effort required compared with the nominal stress method.
- Does not work for fatigue design of weld roots.
- The method covers stress mainly perpendicular to the weld toe but not parallel to the weld toe.



Effective notch method

During the application of the effective notch method, which is a local method, a fictitious radius of 1 mm is modeled using FEM, either in the weld toe or in the weld root.

Prerequisites:

- The method is applicable only to welded joints.
- So-called sub-models with refined element division during FEM calculations of larger structures.

Advantages:

- The method is applicable to complex structures where nominal stress is difficult to define.
- In addition to the weld toe, this method also allows design of the weld root.
- The method can be used when a comparison of different weld geometries or penetration depths is necessary.
- Joints which are not listed in fatigue class tables associated with the nominal stress method can be analyzed using this method.
- The method can be applied in connection with substantial angular and axial misalignment. However, it is required that the respective FE model be modeled with the actual angular and axial misalignment during FE calculations.
- Only one fatigue class is used for this method, depending on the thickness and stress type evaluated.

Disadvantages/limitations:

- Greater work effort required than when the nominal stress method is applied.
- The method covers stress mainly perpendicular to the weld toe but not when the stress is parallel to the weld.
- The effective strain in the notch radius itself of the weld toe cannot be measured, due to its fictive nature. This is why there is no direct connection between the measurement results from the strain gauge and the FE analysis.

Design based of fracture mechanics

Fracture mechanical design is based on the assumption that a structure contains cracks, which is reasonable during fatigue design of welded joints. Fracture mechanics can be used in the following cases:

- In connection with an assessment if a defect will grow under a fatigue load.
- Determine the critical crack/flaw size for fracture for stable – and unstable crack growth and final failure
- In connection with assessments of how many stress cycles are necessary for a defect to reach critical size.
- When the effect of local geometry, such as, e.g., weld toe radius and angle in welded joints is studied, i.e., the effect of weld quality.
- In connection with failure analyses.
- When the fatigue strength in a weld root needs to be inspected.
- When the effect of different penetration depths, e.g., in a load-carrying fillet weld has to be studied.
- When a growing crack in a structure causes unloading of part of the structure and the load transfer causes a greater load on other parts, i.e. redundancy effects.
- When the interaction of several cracks in a joint is studied, e.g., simultaneous crack growth from the bottom and top side of a double-sided fillet welded joint.

5.6.6 Calculation procedure

First identify the structure's critical areas from a fatigue point of view.

These areas are often welds that subjected to a transverse stress flow and start/stop positions of welds, in particular in combination with stiffness discontinuities or load introductions. The calculation procedure below is followed for each critical point in a structure which is subjected to any stress history. This procedure can be applied with the nominal stress method, the Hot Spot method and the effective notch method. Note that if the total number of load cycles is smaller than 10^3 load cycles, fatigue design is not necessary but a static analysis should always be conducted regardless of the total number of load cycles; see chapter 4.

- Determine the effect of the stress history through the stress history parameter s_m

$$s_m = \frac{N_t}{2 \cdot 10^6} \cdot k_m \quad (\text{Eq. 5.10})$$

where

$$k_m = \sum_i \left(\frac{\Delta\sigma_i}{\Delta\sigma_{ref}} \right)^m \cdot \frac{n_i}{n_t} \quad (\text{Eq. 5.8})$$

$k_m < 1$ for variable amplitude loading.

$k_m = 1$ for constant amplitude loading.

- Determine relevant structural detail and corresponding *FAT* using *tables 5.17, 5.18 and 5.19*
- Determine the thickness enhancement factor φ_t ; see *equation 5.11* and *table 5.9*
- Determine the material factor φ_m ; see *figure 5.63*
- Determine the stress alternation factor φ_e ; see *equations 5.12 through 5.14*
- Determine the partial coefficients for load and resistance, γ_f and γ_m ; see *table 5.11*
- Determine the permitted stress range $\Delta\sigma_{Rd}$

$$\Delta\sigma_{Rd} = \frac{\text{FAT} \cdot \varphi_t \cdot \varphi_m \cdot \varphi_e}{\gamma_m \cdot \sqrt[m]{s_m}} \quad (\text{Eq. 5.15})$$

- Check the angular and axial misalignment, ω ; see *equations 5.16 through 5.18*
- Determine the maximum stress range $\Delta\sigma_{max}$

$$\Delta\sigma_{max} = \sigma_{max} - \sigma_{min} \quad (\text{Eq. 5.19})$$

- At the point of evaluation this criterion must be fulfilled $\Delta\sigma_{max} \gamma_f < \Delta\sigma_{Rd}$

Symbol	Explanation
k_m	stress spectrum factor
$\Delta\sigma_i$	stress range at level i
n_i	number of cycles at level i for a representative part of the stress history
n_t	total number of cycles for a representative part of the stress history
s_m	stress history parameter
$\Delta\sigma_{ref}$	stress range reference value
$\Delta\sigma_{max}$	maximum stress range
σ_{max}	maximum stress at current calculation point
σ_{min}	minimum stress at current calculation point
$\Delta\sigma_{Rd}$	permitted stress range
γ_f	partial safety factor with regard to load
γ_m	partial safety factor with regard to fracture risk
<i>FAT</i>	fatigue resistance value
φ_t	thickness improvement factor
φ_m	material factor
φ_e	fatigue enhancement factor
N_t	design total service life

Table 5.7: Symbols.

Calculation procedure, comments and instructions

1. Stress history parameter s_m

The stress history parameter is calculated as a function of the stress history factor, k_m , and the design number of load cycles, N_t , according to section 5.6.3.

2. Structural detail

Determine the structural detail and corresponding FAT for the current calculation point from the table of fatigue resistance values for actual method.

- For the nominal stress method, see *tables 5.17 through 5.19*.
- For the Hot Spot stress method, see *table 5.22*.
- FAT=225 is used for the effective notch method for thickness $t > 5$ mm.

The fatigue resistance values specified for welds in *table 5.19* corresponds to normal production quality. For welded joints with better welding quality, we recommend the requirements according to Volvo's quality standard, which form the basis for the work in the IIW and whose background is described in [5.24]. The quality requirements for the different weld classes and the possible increase in fatigue strength (FAT) are presented briefly in *table 5.8*. Otherwise, refer to [5.24].

Type of discontinuity	Welding class VD normal quality	Welding class VC high quality	Welding class VB post-treated
"Cold lap"	$a < 0,5$ mm	$a < 0,1$ mm	Not permitted
Lack of fusion	Not permitted	Not permitted	Not permitted
Weld toe radius	$r > 0,3$ mm	$r > 1$ mm	$r > 4$ mm
Axial misalignment	$a < 0,1t$ mm (max 2 mm)	Not permitted	Not permitted
Undercut	$a < 0,05t$ mm (max 1 mm)	$a < 0,025t$ mm (max 0,5 mm)	Not permitted
FAT correction	FAT	FAT + 2 steps ¹⁾	FAT + 4 steps ¹⁾

¹⁾ In the series of FAT classes according to *table 5.13*. FAT may be increased, as a maximum, to 125.

Table 5.8: Maximum size of discontinuities for different weld classes [5.24].

3. Thickness enhancement factor, φ_t

When using the nominal stress method, the thickness enhancement factor is calculated according to

$$\varphi_t = \left(\frac{t_0}{t} \right)^n \quad (\text{Eq. 5.11})$$

where

- t_0 – reference thickness, set here to 15 mm
- t – thickness in the actual joint
- n – exponent for the thickness improvement factor according to *table 5.9*

The thickness enhancement factor is used when a welded joint is loaded perpendicular to the weld's direction and when the weld toe is critical i.e. a fatigue crack is assumed to start from the weld toe and not from the weld root.

Joint category	Condition	n
Cruciform joints, transverse T-joints, plates with transverse attachments, ends of longitudinal stiffeners	As-welded	0,15
Cruciform joints, transverse T-joints, plates with transverse attachments, ends of longitudinal stiffeners	Post-treated weld	0,1
Transverse butt weld	As-welded	0,1
Machined butt weld reinforcements, longitudinal welds or attachments to plate edges	All	0
Non-welded parent material	All	0

Table 5.9: Recommended values of the exponent n for the thickness improvement factor.

It is conservative to set to $\varphi_t=1.0$ for thicknesses less than 15 mm. For joints with a thickness less than 4 mm φ_t is equal to φ_t at $t=4$ mm. $\varphi_t=1.0$ for spot welds and non-welded parent material.

During analysis with the Hot Spot stress and the effective notch stress method, the thickness improvement factor is set to $\varphi_t=1.0$.

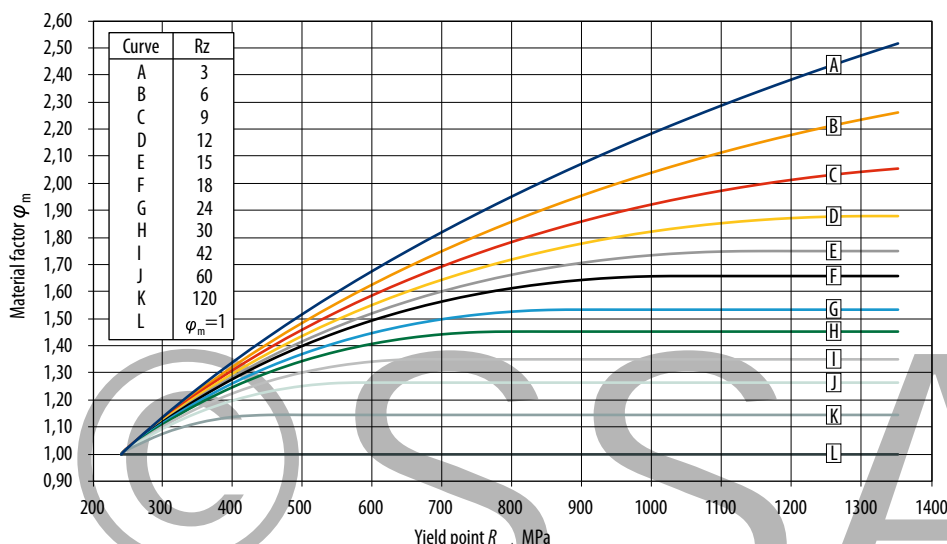


Figure 5.63: Material factor φ_m as a function of yield strength, edge condition and surface roughness. If only Ra is known, the correlation $Rz=6$ Ra can be used.

4. Material factor, φ_m

The fatigue strength increases with increased static strength (R_e) if no crack-like imperfections are present in the material at the point for analysis. The material factor is selected according to figure 5.63, curve A-K based on what is specified in table 5.17 and table 5.18. The fatigue strength for welded joints is independent of the static strength in both the parent material and filler material and $\varphi_m = 1$ in such case (curve L in figure 5.63). Since the Hot Spot and effective notch methods only are applicable for welded joints the material factor is always one ($\varphi_m = 1$) when they are used.

5. Stress alternation factor, φ_e

Higher fatigue loads can be allowed for structures with low residual stress if the nominal stress range contains compressive part, i.e. if $R > 0$, see section 5.5.5. The increased fatigue strength is calculated by multiplying the fatigue strength, FAT, by the stress alternation factor, φ_e . The residual stress is often low for small and thin-walled welded structures and structures which have been given a stress relief treatment. For welded joints which have been post-treated with methods introducing compressive residual stress the stress $\varphi_e = 1$ should be applied.

Residual stress of less than 50 MPa is normally considered to be low and, depending on the stress ratio, R , the stress alternation factor, φ_e , is then selected according to

$$\begin{aligned}\varphi_e &= 1 && \text{Welded material} \\ \varphi_e &= 1 - 0,3 \cdot R && (0 \leq R \leq 0,5, \sigma_{\max} > 0) \\ \varphi_e &= 1 - 0,3 \cdot R && \text{Parent material}\end{aligned}\quad (\text{Equ. 5.12})$$

$$\begin{aligned}\varphi_e &= 1 - 0,2 \cdot R && \text{Welded material} \\ \varphi_e &= 1 - 0,3 \cdot R && \text{Parent material}\end{aligned}\quad (\text{Equ. 5.13})$$

$$\begin{aligned}\varphi_e &= 1 - 0,2 \cdot R && \text{Welded material} \\ \varphi_e &= 1,05 - 0,2 \cdot R && \text{Parent material}\end{aligned}\quad (\text{Equ. 5.14})$$

$$\begin{aligned}\varphi_e &= 1,3 && \text{Welded material} \\ \varphi_e &= 1,35 && \text{Parent material}\end{aligned}$$

Figure 5.64 illustrate the stress alternation factors, φ_e , for different stress ratios, R .

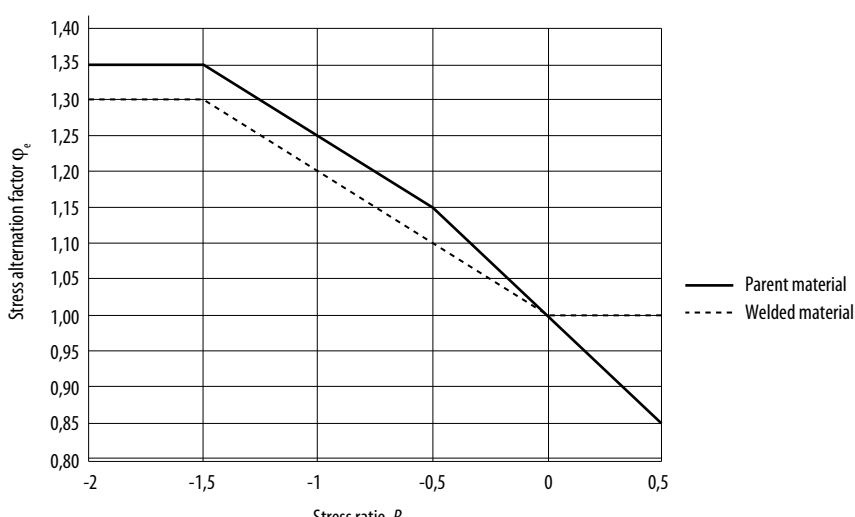


Figure 5.64: Stress alternation factor as a function of stress ratio. Equations 5.12–5.14.

Type of analysis	Nominal stress method	Hot spot stress method and effective notch stress method	
Type of welded joint	ω_1 Already covered in FAT class	ω_1 Already covered in S-N curve	ω Effective default value to be considered in stress
Butt joint made in shop in flat position	1,15	1,05	1,10
Other butt joints	1,30	1,05	1,25
Cruciform joints	1,45	1,05	1,40
Fillet weld welded on one of the sides of a plate	1,25	1,05	1,20

Table 5.12: Consideration of stress magnification due to misalignment.



6. Partial coefficients γ_f and γ_m

Determine the partial coefficient γ_f with regard to the uncertainty in the load assumptions. γ_f is usually set to 1.0 for a load history based on field measurement.

The consequence of failure and the consideration of an acceptable fracture risk determine the choice of γ_m according to *table 5.11*.

Consequence of failure	Partial safety factor γ_m	Approximate failure risk
Negligible	1.0	10^{-2}
Less serious	1.1	10^{-3}
Serious	1.21	10^{-4}
Very serious	1.32	10^{-5}

Table 5.11: Partial safety factor γ_m for permitted stress and acceptable failure risk.

7. Permitted stress range $\Delta\sigma_{Rd}$

The permitted stress range $\Delta\sigma_{Rd}$ is calculated according to

$$\Delta\sigma_{Rd} = \frac{\text{FAT} \cdot \varphi_t \cdot \varphi_m \cdot \varphi_e}{\gamma_m \cdot \sqrt[m]{s_m}} \quad (\text{Equ. 5.15})$$

8. Angular and axial misalignment, ω

Angular or axial misalignment causes secondary bending stresses see sections 5.5.2 and 5.5.7. A certain degree of misalignment expressed as ω_1 is included in the structural joints, see *table 5.12*. This type of defects does not need to be taken into consideration when the nominal stress method is used, if normal work shop practice is followed. If the angular and axial misalignment in the current structures is not known, the ω values according to *table 5.12* can be used [5.1].

The correlation factor ω for larger misalignment is calculated according to Appendix A. The simultaneous effect of angular and axial misalignment is summed up according to

$$\omega = \omega_{ax} + \omega_{ang} - 1 \quad (\text{Equ. 5.16})$$

In those cases where ω exceed the limit values ω_1 , the applied stress range $\Delta\sigma_{max}$ is multiplied by the effective correlation factor ω_{eff} i.e. when

$$\omega > \omega_1 \quad (\text{Equ. 5.17})$$

The effective correlation factor ω_{eff} compensates for the extra bending stress that occur when the limit values according to *table 5.13* is exceeded and is calculated according to

$$\omega_{eff} = \frac{\omega}{\omega_1} \quad (\text{Equ. 5.18})$$

In a FE model of a complex structure it is unrealistic to take into consideration all existing misalignment. Usually a FE model is perfect in this respect (angular and axial misalignment is not modeled) and the evaluated stress is in such case non conservative. So it is beneficial to determine the misalignments in a structure through measurements.

9. Maximum stress range

The maximum stress range in the point of evaluation is determined from the stress history and is defined according to *figure 5.65*.

$$\Delta\sigma_{max} = \sigma_{max} - \sigma_{min} \quad (\text{Equ. 5.19})$$

Note that signs must be included in the calculation of stress range according to *equation 5.19* when $\sigma_{min} < 0$.

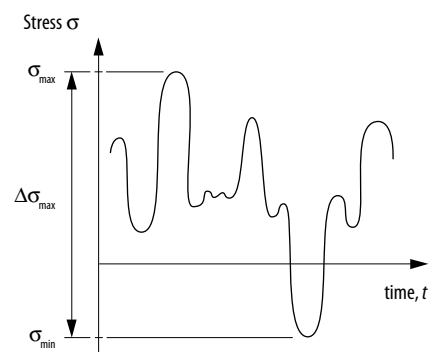


Figure 5.65: Definitions of stress range.

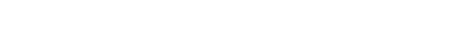
Geometry of structural element and load	Corresponding joints from the fatigue resistance value table
	 FAT = 71 MPa

Figure 5.66: Application of the nominal stress method.

10. At the point of evaluation this criterion must be fulfilled
The design value of stress range $\Delta\sigma_{sd}$ should be smaller
than or equal to the permitted stress range according to

$$\Delta\sigma_{\text{Sd}} \leq \Delta\sigma_{\text{Rd}} \quad (\text{Equ. 5.20})$$

i.e.

$$\Delta\sigma_{\max} \cdot \gamma_f \leq \frac{FAT \cdot \varphi_t \cdot \varphi_m \cdot \varphi_e}{\gamma_m \cdot \sqrt[m]{s_m}}$$

where

$$\Delta\sigma_{\text{sd}} = \Delta\sigma_{\text{max}} \cdot \gamma_e$$

γ_f is often presumed to be equal to 1; see item 6, partial coefficients.

In those cases where misalignment (see step 8 above) must be taken into consideration, the criterion is formulated

$$\omega_{\text{eff}} \cdot \Delta\sigma_{\max} \cdot \gamma_f \leq \frac{FAT \cdot \varphi_i \cdot \varphi_m \cdot \varphi_e}{\gamma_m \cdot \sqrt[m]{s_m}} \quad (\text{Eqn. 5.21})$$

5.6.7 Nominal stress method

The nominal stress method is based on testing of many different types of structural joints. The result of these is summed up in a number of S-N curves (Stress range – Number of load cycles). A fatigue resistance value, FAT, is associated to each S-N curve and corresponds to the fatigue strength at $2 \cdot 10^6$ load cycles with a failure probability of 2.3%. The nominal stress is the stress which can be calculated by using conventional solid mechanics. Stress concentrations which are caused by welds, holes or notches are not part of the nominal stress but where of course present during the tests and are by such manners included in the fatigue resistance value, FAT, see figure 5.66.

When a part is analyzed with the nominal stress method the first step is to find a structural joint which is relevant in respect of geometry and load; see *table 5.16* to *table 5.19*. In the situation of constant amplitude loading, it is possible to determine the service life through the S-N curves in *figure 5.67* and *figure 5.68* and *equation 5.22*.

If the figures are compared, it turns out that the curves have different slope. The slope is $m=3$ for welded joints and $m=5$ for non-welded parent material without crack-like imperfections, *table 5.13*.

For shear loading the slope of the S/N curve is 5 for both welded and parent material

The structural joints for parent material also refer to screwed and riveted joints, holes, and free edges according to tables 5.16 to 5.18. The increase in fatigue strength related to increased yield strength of the parent material is computed with the material factor φ_{m} .

The (nominal) stress range should be within the limits of the elastic properties of the material. The stress range shall not be exceed $1.5 \cdot R_e$, for nominal normal stresses or $1.5 \cdot R \sqrt{3}$ for nominal shear stresses.

Table 5.13: Series of FAT classes (2.3% failure probability) and associated slope of the S-N curve, m

This handbook contains general suggestions and information without any expressed or implied warranty of any kind. SSAB hereby expressly disclaims all liability of any kind, including any damages, in connection with the use of the information and for their suitability for individual applications. It is the responsibility of the user of this brochure to adapt the recommendations contained therein to the requirements of individual applications.

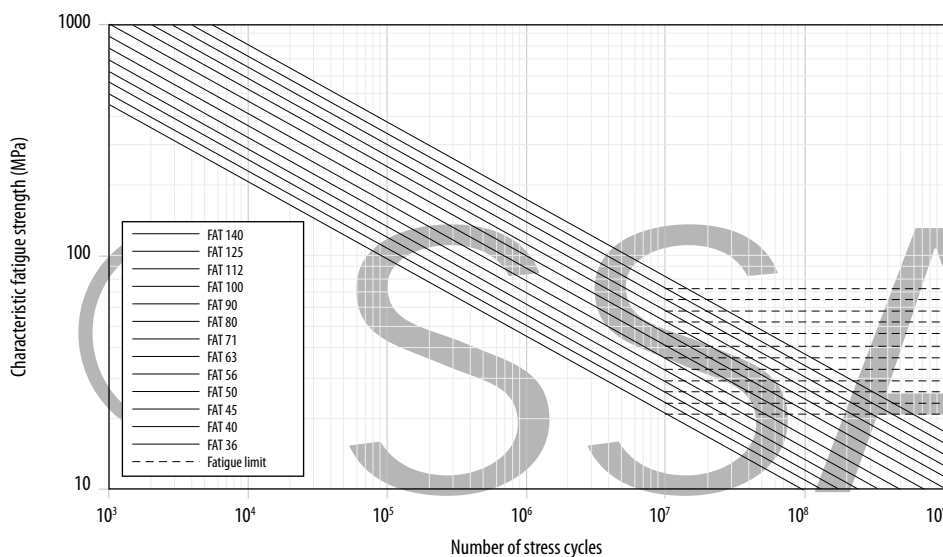


Figure 5.67: S-N curves with a slope $m=3$ for welded joints. Knee points are left out in accordance with section 5.6.1. The broken line indicates the fatigue limit at a constant amplitude loading.

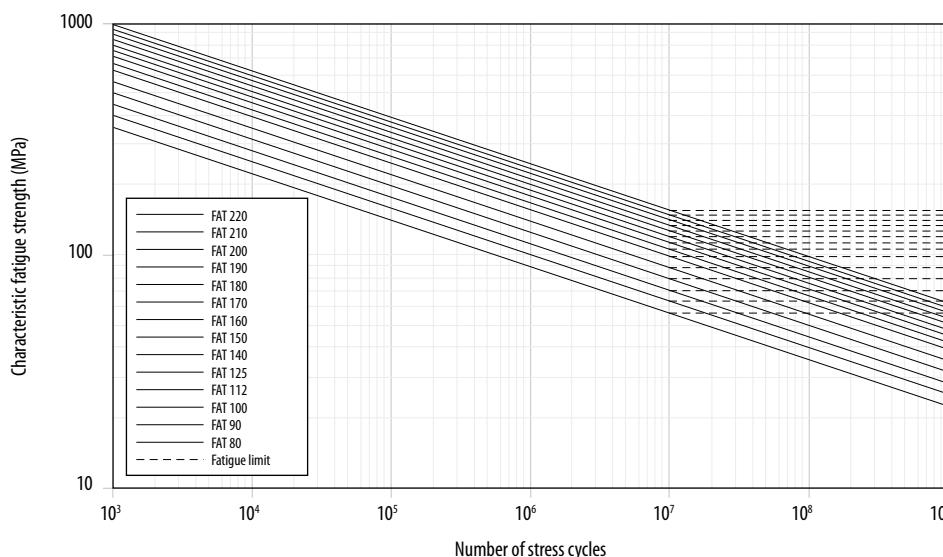


Figure 5.68: S-N curves with a slope $m=5$ for parent material and cut edges. Knee points are left out in accordance with section 5.6.1. The broken line indicates the fatigue limit at a constant amplitude loading.

The number of load cycles at a specific stress range and fatigue resistance value is provided by

$$N = 2 \cdot 10^6 \cdot \left(\frac{FAT}{\Delta\sigma} \right)^m \quad (\text{Eq. 5.22})$$

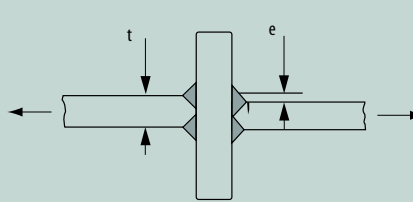
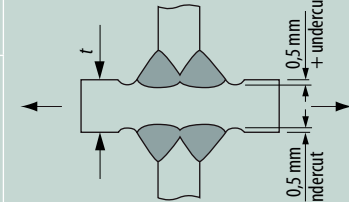
The stress range at a specific number of load cycles and fatigue resistance value is provided by

$$\Delta\sigma = FAT \cdot \left(\frac{2 \cdot 10^6}{N} \right)^{1/m} \quad (\text{Eq. 5.23})$$

where

- N – number of load cycles
- FAT – fatigue resistance value (MPa)
- m – slope of the S-N curve, $m=3$ or 5
- $\Delta\sigma$ – stress range

Evaluation with respect to the fatigue limit (the broken lines) is performed when the stress range from a constant amplitude loading is lower than the fatigue limit or a load history which have the largest stress range ($\Delta\sigma_{\max}$) lower than the fatigue limit. The continuous lines are used for damage sum calculations of load histories.

Joints	Post-treatment	FAT	Comment under cut
	Undressed weld	80	
	Post-treated weld • TIG - remelting • Grinding • Cold hammering (HAP, UP, UIT) ¹⁾	100–112 ²⁾	 <p>0.5 mm + under cut</p>

¹⁾ HAP Hammer peening, UP ultrasonic peening, UIT ultra sonic peening

²⁾ Depending on method and parent material yield strength.

Figure 5.69: Post-treatment of fillet weld.

Improvement techniques

The fatigue strength of a weld can be improved through post-treatment if the weld toe is critical; see figure 5.69. If a weld toe is improved it is necessary to check if the corresponding weld root becomes a critical for fatigue. When welds are given a post-treatment using TIG or grinding, the fatigue resistance value FAT increase 2 steps in the series of fatigue classes, but FAT=112 MPa is the highest value which can be achieved. The increase for penning methods is 3 steps but limited to FAT=125 MPa if the parent material has a yield strength over 350 MPa, see table 5.14.

Note that the skill of the individual operator is very important for the result of a post treatment process in the same manner as for welding; see also [5.22-5.25].

All post treatment methods that introduce compressive residual stresses are sensitive for high tensile loads. As compressive residual stress can be released during loading, the nominal R-ratio must be taken into consideration during the assessment of the improved fatigue strength [5.25], figure 5.70. This effect is illustrated in table 5.15.

The post-treatment of welds through grinding should take into consideration the reduction in the cross-section, see figure 5.69. The nominal stress shall be recalculated if the cross-section area is reduced by more than 10%. Grinding is carried out to a depth of 0.5 mm below the occurring undercuts.

See also the abstract of Volvo's standard in table 5.8, which allows larger increases in the fatigue resistance for post-treated welds.

Nominal method	Improvement expressed as steps in the series of FAT classes		
	Grinding	TIG-dressing	"Peening"
	Number of steps ¹⁾	Number of steps ¹⁾	Number of steps ¹⁾
$R_e < 350 \text{ MPa}$	2 (Max FAT 112)	2 (Max FAT 112)	2 (Max FAT 112)
$R_e \geq 350 \text{ MPa}$	2 (Max FAT 125)	2 (Max FAT 112)	3 (Max FAT 125)

¹⁾ Refers to the number of steps the original FAT is increased by post-treatment.

Table 5.14: FAT values in connection with post-treatment of welds, design with nominal stress.

Special cases

If two welds are interacting the lowest fatigue resistance value is reduced one step in the series of fatigue classes. If more than two welds are interacting the lowest fatigue resistance value is reduced two steps in the series of fatigue classes.

Holes close to a weld are considered to exert an effect if the distance between the edge of the hole and the weld is smaller than the diameter of the hole. In such case the effect of the hole is taken into consideration by increasing the nominal stress by 50% [5.53]. Depending on load direction, the notch stress method can be applied.

Structural details in accordance with table 5.16 are used for pure shear loading and the slope of the S/N curve is 5 for both welded and parent material. The fatigue limit is found at 10^8 load cycles for constant amplitude loading.

Stress ratio R	Improvement ¹⁾
$R \leq 0.15$	Up to 3 FAT classes
$0.15 < R \leq 0.28$	Up to 2 FAT classes; the same as for grinding and TIG dressing
$0.28 < R \leq 0.4$	One class for FAT 90 and lower
$R > 0.4$	No increase if it cannot be verified through testing

¹⁾ Refers to the number of steps the original FAT value is increased by post-treatment.

Table 5.15: Effect of the R ratio for improvement methods which introduces compressive residual stress.

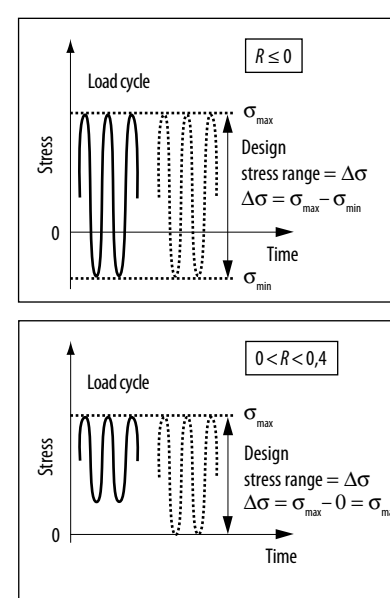


Figure 5.70: Nominal R-ratio considering compressive residual stress.

Joint under shear load	Slope m	FAT (MPa)	Load cycles at fatigue limit
Parent material or butt weld with full penetration	5	100	10^8
Butt weld or fillet weld with partial penetration	5	80	10^8

Table 5.16: Fatigue resistance values for structural details on the basis of shear stress.

Structural joints for parent material

Structural joints for parent material with holes or different edge and surface conditions are listed in *table 5.17*. The data for this table is based on a compilation of a large number of fatigue tests of our steels which have taken into consideration the surface roughness of the critical edge or surface. The influence of holes has also been tested. [5.5, 5.6, 5.7, 5.27]. The increase in fatigue strength related to increased yield strength of the parent material is computed with the material factor φ_m , *figure 5.63*.

Handbooks, e.g., Peterson [5.3] are used to determine the stress concentration factor, K_t , for notches, which are not covered by the tables of structural details. K_t can also be approximated by the simplified expression in *equation 5.2*. The fatigue resistance value, FAT, can then be determined approximately from *figure 5.71*.

The figures are based on the correlation

$$FAT = 215/K_f \quad (\text{Eq. 5.24})$$

$$K_f = 1 + \frac{K_t - 1}{1 + \frac{0,6^*}{\sqrt{r}}} \quad (\text{Eq. 5.25})$$

where

K_f – notch factor

K_t – stress concentration factor

r – notch radius

*Neuber constant = 0.6 ($R_e = 220$ MPa for mild steels)

Note that the material effect is handled separately with the material factor φ_m according to *figure 5.63* and not through different values of the Neuber constant.

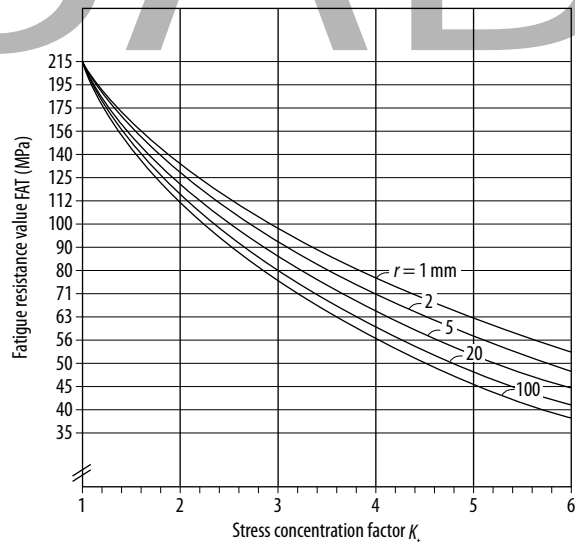
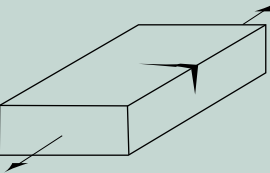
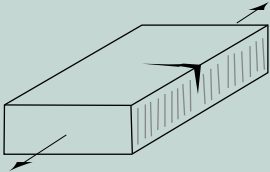
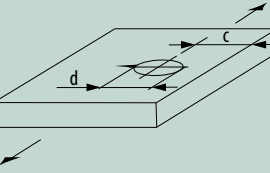
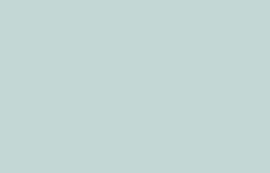


Figure 5.71: Correlation between the stress concentration factor K_t and the fatigue class FAT. r = radius of the notch.

Structural details for parent material with different surface and edge condition

Table 5.17 lists fatigue resistance values (2.3% failure probability at $2 \cdot 10^6$ load cycles) for parent material. The increase in fatigue strength related to increased yield strength of the parent material is computed with the mate-

rial factor ϕ_m , figure 5.63. The data for this table is based on a compilation of a large number of fatigue tests which have taken into consideration the yield strength of the parent material and the surface roughness of the critical edge, surface or, where appropriate, hole, [5.26 and 5.27].

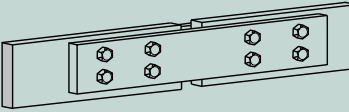
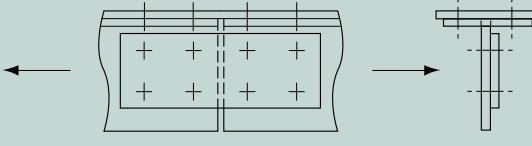
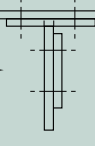
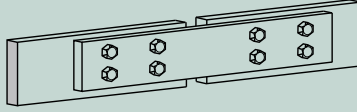
No	Structural detail	Description of design surface or edge	Comment/quality specification	Surface finish Rz	FAT (MPa)	Slope S-N, m	ϕ_m -curve
01		Ground	Corners deburred.	3	220	5	A
02		Machined	Corners deburred.	6	210	5	B
03		Surface of cold-rolled or continuously hot-dip galvanized strip material.		6	200	5	B
04		Surface of hot-rolled strip material.	High quality.	12	180	5	D
05			Good quality.	15	170	5	E
06			Moderate quality.	18	160	5	F
07			Exposed surface of weathering steel.	-	150	5	I
08			Blasted surface. ¹⁾	70	170	5	E
09		Blasted surface of quenched and tempered plate material.		42	180	5	I
10		Batch hot-dip galvanized surface.	Good quality.	-	170	5	J
11		Punched edge, cold-rolled strip material.	Good quality.	15	170	5	D
12		Slotted edge, hot-rolled strip material ²⁾	Good quality. All visible signs of defects to be removed. Edge corner rolling or blasting can increase FAT by 30%.	30	180	5	H
13		Punched edge, hot-rolled material.		-	140	3	L
14		Cut edge (power-shearing).		-	140	3	L
15		Laser-cut edge	Very high quality. Only cold-rolled strip material.	9	190	5	C
16		Laser-cut edge hot-rolled strip material.	High quality.	15	170	5	E
17			Good quality.	18	160	5	F
18		Plasma-cut edge hot-rolled strip material.	Moderate quality.	24	150	5	G
19			High quality.	30	150	5	H
20			Good quality.	15	170	5	E
21			Moderate quality.	18	160	5	F
22			24	150	5	G	
23			30	150	5	H	
24		Machine gas-cut edges with subsequent machining, no cracks or visible defects.	All visible signs of defects to be removed. Cut surfaces to be milled or grinded, all burrs to be removed. No repairs by welding permitted! Rz not determined.	-	140	3	L
25		Machine thermally cut, corners removed, no cracks or notches by inspection.	Rz not determined.	-	125	3	L
26		Machine thermally cut, without cracks and sharp notches.	Rz not determined.	-	100	3	L
27		Machine thermally cut, uninspected, no notches deeper than 0.5 mm.	Rz not determined.	-	80	3	L
28		Circular open holes If $1.5d < c < 3d$, FAT is reduced by one step. The stress range can be calculated on the gross area if $A_{hole}/A_{gross} < 0.1$. Reamed holes with deburred edges, allows the FAT class to be raised one step. FAT class can be raised two steps for holes with tightened screws. ³⁾	Drilled and punched hole, cold-rolled plate	15	112	5	E
29			Drilled hole, hot-rolled plate.	15	100	5	E
30			Punched hole, hot-rolled plate.	-	80	3	L

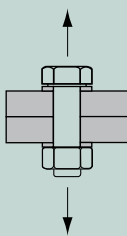
¹⁾ The positive effect of compressive stress as due to blasting, is not included in FAT class [5.4.2].

²⁾ Note that the fatigue strength is strongly reduced if the cut edge surface has lower quality.

³⁾ See also FE E21 hole close to weld

Table 5.17: Structural details for parental material.

Bolted and riveted joints					
		Double-shear joints.	See joint no. 17, 19.		
		Single-shear joint with support (example).	See joint no. 17, 19.	The bolts in a friction joint do not need to be checked for fatigue. Gas-cut or untreated punched holes are not permitted.	Nominal stress is calculated per net area for parent metal and per stress area for bolts.
		Single-shear joint.	See joint no. 18, 20.		

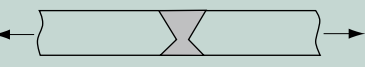
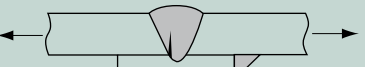
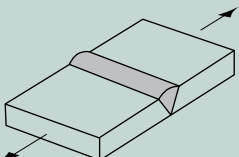
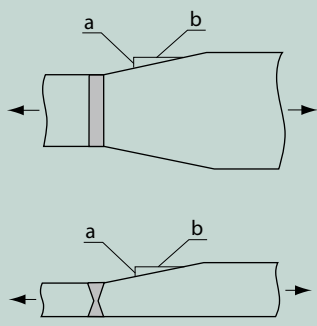
No	Structural details	Comment	FAT (MPa)	m	φ_m -curve ²⁾	
16	Holed parts in a friction joint loaded with normal stress.		125	5	D	
17	Holed parts in a friction joint loaded with normal stress. Double- and single-shear joint with support.		125	5	E	
18	Holed parts in a friction joint loaded with normal stress. Single-shear joint without support.		80	5	E	
19	Bolts or rivets in a shear joint. Double- or single-shear joint with support.	Evenly distributed stress assumed. Shear stress ($\Delta\tau_c$) Hole bearing stress ($\Delta\sigma_c$)	112 310	5 5	E E	
20	Bolts or rivets in a shear joint. Single-shear joint without support.	Evenly distributed stress assumed. Shear stress ($\Delta\tau_c$) Hole bearing stress ($\Delta\sigma_c$)	90 220	5 5	E E	
21		Threaded bolt exposed to normal stress (Strength class 8.8 or higher). Cut thread Rolled thread > M30 Rolled thread ≤ M30	The stress range is calculated using the additional force, i.e., the difference between the pre-stressing force and the applied force. The stress area, A_s , and the force range in the bolt shank should be used.	50 63 71	3 3 3	L L L

²⁾ φ_m should be assessed with the respective min yield point for parent metal or bolt metal depending on the design section

Table 5.18: Structural details for bolted and riveted joints.

Structural details for welded joints

Table 5.19 lists fatigue resistance values (2.3% failure probability at $2 \cdot 10^6$ load cycles) for welded joints. The data for this table is primarily based on the IIW [5.1] and is supplemented, to a certain extent, with joints from [5.26].

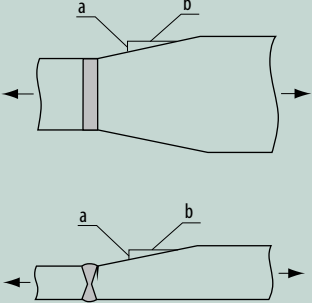
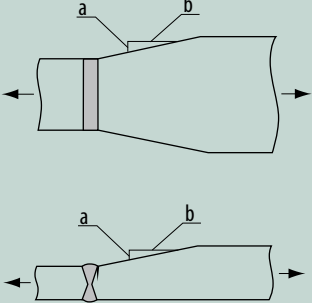
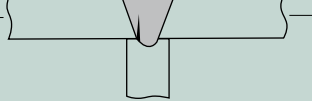
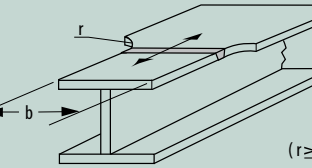
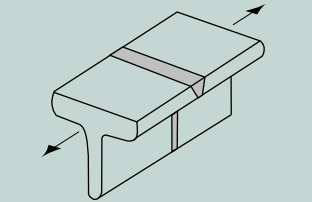
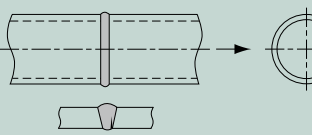
Welded joints				
No	Structural details	FAT (MPa) $m=3$	Description	Comment
Transverse butt welds				
22		112	Transverse butt weld (X-groove or V-groove), ground flush to plate, 100% NDT.	All welds ground flush to surface, grinding parallel to direction of stress. Weld run-on and run-off pieces to be used and subsequently removed. Plate edges ground flush in direction of stress. Welded from both sides. Misalignment < 5% of plate thickness. Proved free from significant defects by appropriate NDT.
23		90	Transverse butt weld made in shop in flat position, NDT, weld reinforcement < 0.1 times thickness.	Weld run-on and run-off pieces to be used and subsequently removed. Plate edges ground flush in direction of stress. Welded from both sides. Misalignment < 5% of plate thickness.
24		80	Transverse butt weld which does not meet the requirements in 23, NDT.	Weld run-on and run-off pieces to be used and subsequently removed. Plate edges ground flush in direction of stress. Welded from both sides. Misalignment < 10% of plate thickness.
25		80	Transverse butt weld welded on non-fusible temporary backing, root crack.	Backing removed, root visually inspected. Misalignment < 10% of plate thickness.
26		71	Transverse butt weld on permanent backing bar.	Misalignment < 10% of plate thickness.
27		71 36	Transverse butt weld, welded from one side without backing bar, full penetration root controlled by appropriate NDT no NDT	Misalignment < 10% of plate thickness.
28		36	Transverse butt weld, partial penetration, analysis based on stress in weld throat sectional area, weld overfill not to be taken into account.	The detail is not recommended for fatigue-loaded members. Assessment using notch stress or fracture mechanics preferred.
29		112 100 90	Transverse butt weld ground flush, NDT, with smooth transition in thickness and width slope 1:5 slope 1:3 slope 1:2	All welds ground flush to surface, grinding parallel to direction of loading. Weld run-on and run-off pieces to be used and subsequently removed. Plate edges ground flush in direction of stress. Welded from both sides. Misalignment < 5% of plate thickness.

Non Destructive Testing, NDT

¹⁾ FAT from Plåthandboken utgåva VII [5.26]

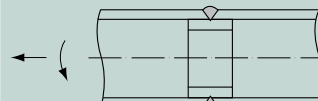
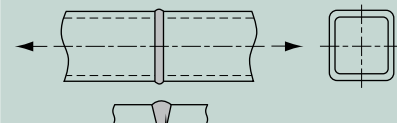
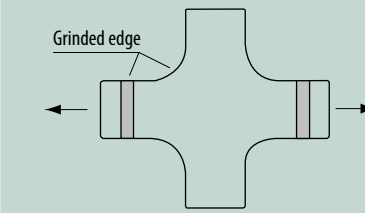
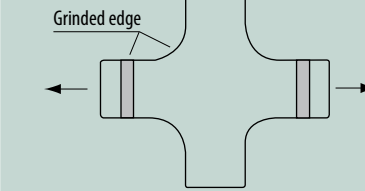
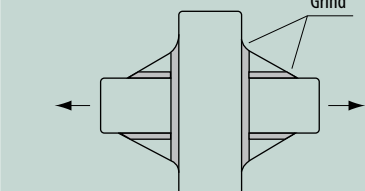
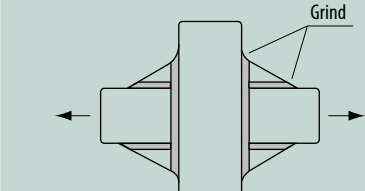
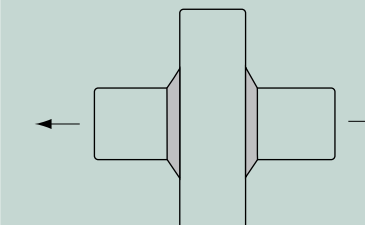
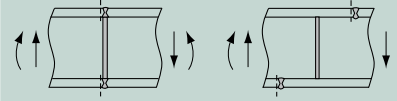
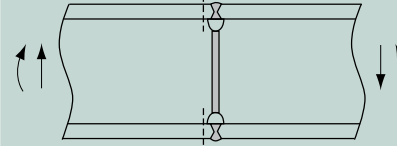
²⁾ FAT is increased by two steps in the series of fatigue classes (table 5.13) compared to Plåthandboken utgåva VII [5.26]

Tabell 5.19: Structural details for welded material.

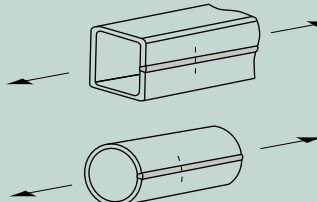
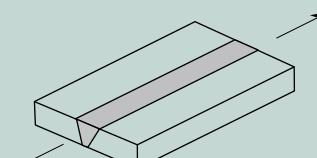
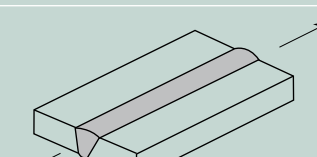
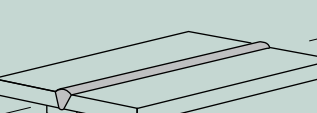
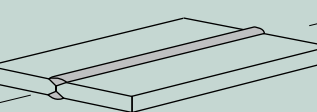
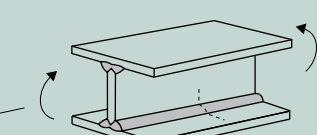
Welded joints				
No	Structural details	FAT (MPa) $m=3$	Description	Comment
Transverse butt welds				
30		90 80 71	Transverse butt weld made in shop, welded in flat position, NDT, smooth transition in thickness and width slope 1:5 slope 1:3 slope 1:2	Weld run-on and run-off pieces to be used and subsequently removed. Plate edges ground flush in direction of stress. Welded from both sides. Misalignment < 5% of plate thickness.
31		80 71 63	Transverse butt weld, NDT, with smooth transition in thickness and width slope 1:5 slope 1:3 slope 1:2	Weld run-on and run-off pieces to be used and subsequently removed. Plate edges ground flush in direction of stress. Welded from both sides. Misalignment < 10% of plate thickness.
32		71	Transverse butt weld, different thicknesses without smooth transition in thickness, centers aligned. In cases where the weld profile is equivalent to a moderate slope, 31 can be used.	Misalignment < 10% of plate thickness. If centers are deliberately misaligned, this misalignment has to be considered.
33		71	Three plate connection, potential crack from root.	Misalignment < 10% of plate thickness.
34		100	Transverse butt weld flange splice in welded cross-section. Welded prior to the assembly, ground flush, with radius transition, NDT.	All welds ground flush to surface, grinding parallel to direction of stress. Weld run-on and run-off pieces to be used and subsequently removed. Plate edges ground flush in direction of stress.
35		80	Transverse butt weld splice in rolled section or bar besides flats, ground flush, NDT.	All welds ground flush to surface, grinding parallel to direction of stress. Weld run-on and run-off pieces to be used and subsequently removed. Plate edges ground flush in direction of stress.
36		71 36	Transverse butt weld joint in circular hollow section, welded from one side, full penetration, potential crack from root. root controlled by NDT no NDT	Welded in flat position.

Tabell 5.19 cont.

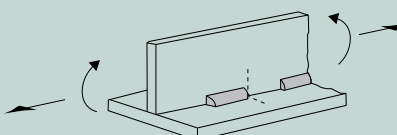
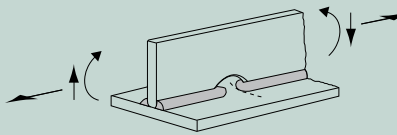
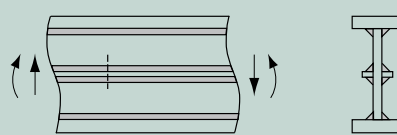
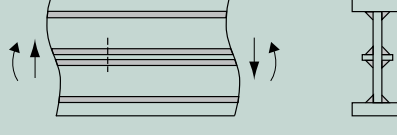
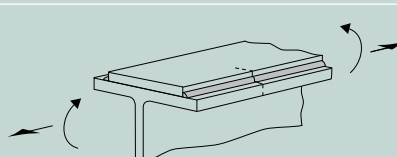
This handbook contains general suggestions and information without any expressed or implied warranty of any kind. SSAB hereby expressly disclaims all liability of any kind, including any damages, in connection with the use of the information and for their suitability for individual applications. It is the responsibility of the user of this brochure to adapt the recommendations contained therein to the requirements of individual applications.

Welded joints				
No	Structural details	FAT (MPa) $m=3$	Description	Comment
Transverse butt welds				
37		71	Tubular joint with permanent backing.	Welded in flat position. Full penetration weld.
38		56 36	Transverse butt weld splice in rectangular hollow section, welded from one side, full penetration, root crack root controlled by NDT no NDT	Welded in flat position.
39		100	Transverse butt weld ground flush, weld ends and radius ground, 100% NDT at crossing flanges, radius transition.	All welds ground flush to surface, grinding parallel to direction of stress. Weld run-on and run-off pieces to be used and subsequently removed. Plate edges ground flush in direction of stress. Welded from both sides. No misalignment. Requisite weld quality cannot be controlled with NDT.
40		90	Transverse butt weld made in shop in flat position, weld profile controlled, NDT at crossing flanges, radius transition.	Weld run-on and run-off pieces to be used and subsequently removed. Plate edges ground flush in direction of stress. Welded from both sides. Misalignment < 5% of plate thickness.
41		80	Transverse butt weld at intersecting flange, weld ground flush, NDT at crossing flanges, with welded triangular transition plates, weld ends ground. Crack starting at butt weld. For crack of continuous flange, see joint no 80 and 81!	All welds ground flush to surface, grinding parallel to direction of stress. Plate edges ground flush in direction of stress. Welded from both sides. Misalignment < 10% of plate thickness.
42		71	Transverse butt weld at intersecting flange, NDT at crossing flanges, with welded triangular transition plates, weld ends ground. Crack starting at butt weld. For crack of continuous flange, see joint no 80 and 81!	Plate edges ground flush in direction of stress. Welded from both sides. Misalignment < 10% of plate thickness.
43		50	Transverse butt weld at intersecting flange. Crack starting at butt weld. For crack of continuous flange, see joint no 80 and 81!	Welded from both sides. Misalignment < 10% of plate thickness.
44		80	Butt weld at beam splice. ¹⁾	Butt weld with welded root. Rolled or welded cross-section. For execution without welded root, the FAT value is reduced by two steps.
45		80	Butt weld at beam splice, rolled section. ¹⁾	Welded root, drilled or ground hole. For execution without welded root, the FAT value is reduced by two steps.

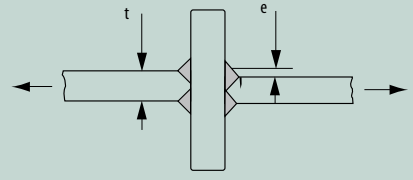
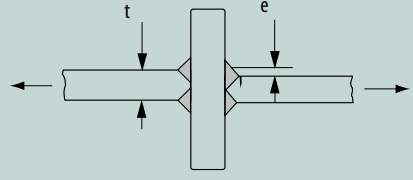
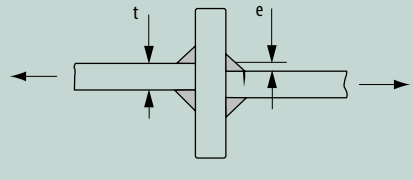
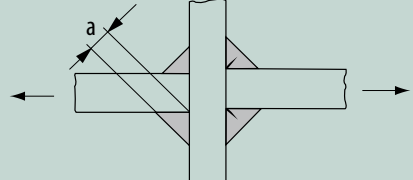
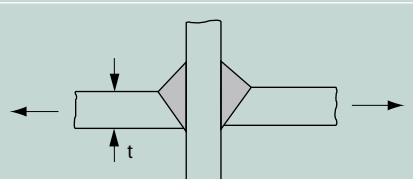
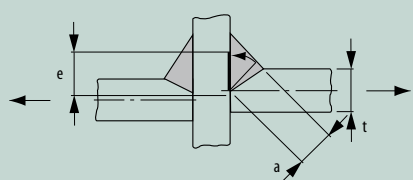
Tabell 5.19 cont.

Welded joints				
No	Structural details	FAT (MPa) $m=3$	Description	Comment
Longitudinal welds				
46		125 90	Automatic longitudinal seam welds without start/stop positions in hollow sections. with start/stop positions.	
47		125	Longitudinal butt weld, both sides ground flush parallel to load direction, NDT.	
48		100 90	Longitudinal butt weld, without start/stop positions, NDT. with start/stop positions.	
49		90	Longitudinal butt weld in V-groove with permanent backing strip. ¹⁾	
50		90	Longitudinal butt weld, partial penetration. ¹⁾	
51		125	Continuous automatic longitudinal fully penetrated K-butt weld without start/stop positions (based on stress range in flange), NDT.	No start/stop positions permitted except when the repair is performed by a specialist and inspection is carried out to verify the proper execution of the weld.
52		100	Continuous automatic longitudinal double-sided fillet weld without start/stop positions (based on stress range in flange).	
53		90	Continuous manual longitudinal fillet or butt weld.	Calculation based on stress range in flange.

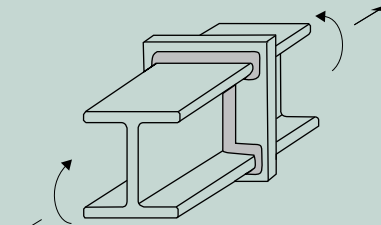
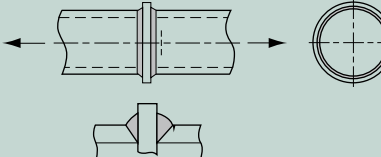
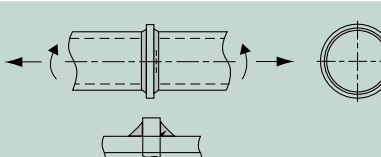
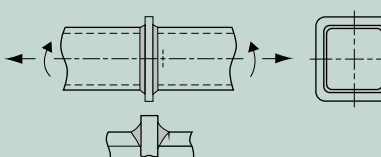
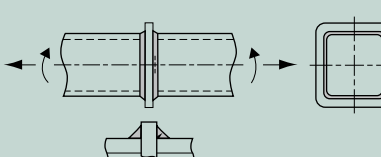
Tabell 5.19 cont.

Welded joints				
No	Structural details	FAT (MPa) m=3	Description	Comment
Longitudinal welds				
54		80 71 63 56 50 45 40 36	Intermittent longitudinal fillet weld. $\tau/\sigma =$ 0 0,0–0,2 0,2–0,3 0,3–0,4 0,4–0,5 0,5–0,6 0,6–0,7 >0,7	Calculation based on normal stress in flange and shear stress in web at weld ends.
55		71 63 56 50 45 40 36	Longitudinal butt weld, fillet weld or intermittent weld with cope holes. Holes not higher than 40% of web height. $\tau/\sigma =$ 0 0,0–0,2 0,2–0,3 0,3–0,4 0,4–0,5 0,5–0,6 >0,6	Calculation based on normal stress in flange and shear stress in web at weld ends.
56		100 ¹⁾	Automatically welded longitudinal web stiffeners. ¹⁾	Without start/stop positions.
57		90 ²⁾	Manually welded longitudinal web stiffeners. ¹⁾	
58		90	Beam with additional plate. ¹⁾	Refers to sections at least one flange width from the end of the additional plate. Cruciform joints and T-joints.

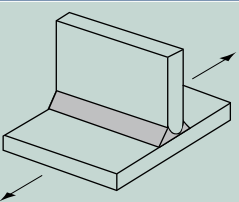
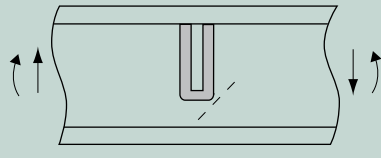
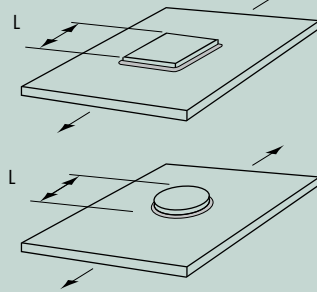
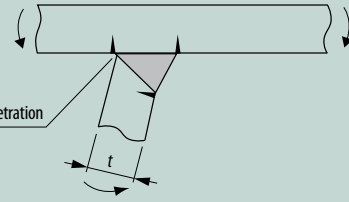
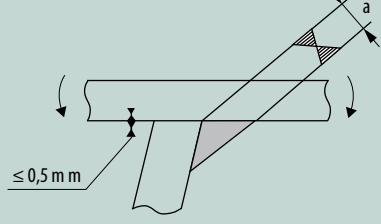
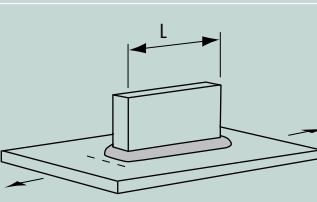
Tabell 5.19 cont.

Welded joints				
No	Structural details	FAT (MPa) $m=3$	Description	Comment
Cruciform joints and T-joints				
59		80 90	Cruciform joint or T-joint, K-butt weld, full penetration, no lamellar tearing, $e < 0.15 \cdot t$, weld toes ground, potential failure from weld toe. Single-sided T-joints and cruciform joints without axial misalignment.	Advisable to ensure inspection of the intermediate plate with regard to susceptibility to lamellar tearing. Misalignment < 15% of loaded plate thickness.
60		71 80	Cruciform joint or T-joint, K-butt weld, full penetration, no lamellar tearing, $e < 0.15 \cdot t$, potential failure from weld toe. Single-sided T-joints and cruciform joints without misalignment.	Advisable to ensure inspection of the intermediate plate with regard to susceptibility to lamellar tearing. Misalignment < 15% of loaded plate thickness.
61		63 71	Cruciform joint or T-joint, fillet welds or partial penetration K-butt welds, no lamellar tearing, $e < 0.15 \cdot t$, potential failure from weld toe. Single-sided T-joints and cruciform joints without misalignment	Advisable to ensure inspection of the intermediate plate with regard to susceptibility to lamellar tearing. Misalignment < 15% of loaded plate thickness. Also to be inspected as 62.
62		36 40	Cruciform joint or T-joint, fillet welds or partial penetration K-butt welds including toe ground joints, potential failure from weld root. For $a/t \leq 1/3$	Stress included in weld's throat thickness. Also to be inspected as 61. $\sigma_w = \frac{F}{\sum(a \cdot l)}$ The a/t ratio is calculated with the weld throat through plate thickness.
63		71 36	Cruciform joint or T-joint, single-sided arc or laser beam welded V-butt weld, full penetration, no lamellar tearing, misalignment $e < 0.15 \cdot t$, potential failure from weld toe. Full penetration checked by inspected of root. If root is not inspected, then root crack.	
64		71	Cruciform joint or T-joint, single-sided arc welded fillet or partial penetration Y-butt weld, no lamellar tearing, misalignment of plates $e < 0.15 \cdot t$, stress at weld root. Penetration verified.	Analysis based on axial and bending stress in weld throat. Misalignment e to be considered in the analysis. Stress at weld root: e = misalignment between the center of the plate and weld throat, including penetration, rotated into vertical leg plate using root tip as pivot. An analysis using the effective notch stress method is recommended.

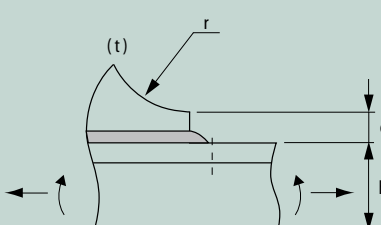
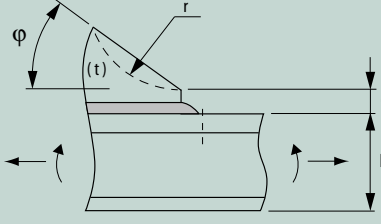
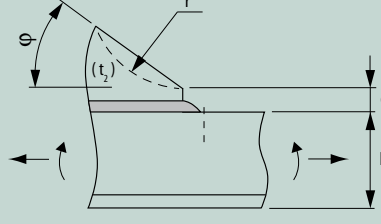
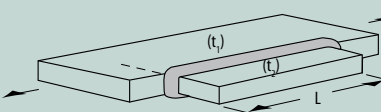
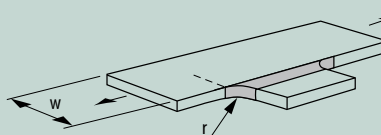
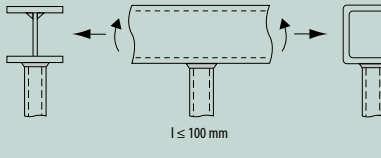
Tabell 5.19 cont.

Welded joints				
No	Structural details	FAT (MPa) $m=3$	Description	Comment
Cruciform joints and T-joints				
65		36	Splice of rolled section with intermediate plate, fillet welds, potential failure from weld root. Analysis based on stress in weld throat.	
66		56 60	Splice of circular hollow section with intermediate plate, single-sided butt weld, potential failure from weld toe. wall thickness > 8 mm wall thickness < 8 mm	NDT of welds in order to ensure full root penetration.
67		45 40	Splice of circular hollow section with intermediate plate, fillet weld, potential failure from root. Analysis based on stress in weld throat. wall thickness > 8 mm wall thickness < 8 mm	
68		50 45	Splice of rectangular hollow section with intermediate plate, single-sided butt weld, potential failure from weld toe. wall thickness > 8 mm wall thickness < 8 mm	NDT of welds in order to ensure full root penetration.
69		40 36	Splice of rectangular hollow section with intermediate plate, fillet welds, potential failure from weld root. Analysis based on stress in weld throat. wall thickness > 8 mm wall thickness < 8 mm	

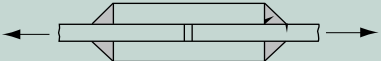
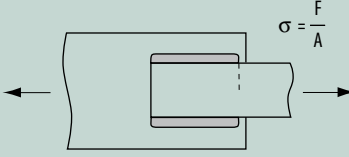
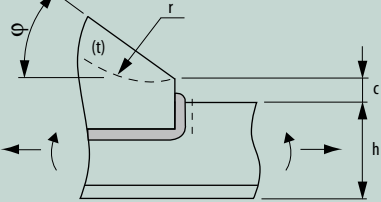
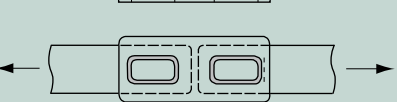
Tabell 5.19 cont.

Welded joints				
No	Structural details	FAT (MPa) $m=3$	Description	Comment
Non-load-carrying attachments				
70		100 100 80 71	Transverse non-load-carrying attachment, not thicker than the main plate, K-butt weld, toe ground Double-sided fillet weld, toe ground Fillet weld(s), as welded Thicker than the main plate	Grinding in the direction of stress. An angular misalignment corresponding to $k_m = 1.2$ is included in the FAT value.
71		100 100 80 71	Transverse stiffener welded on girder web or flange, not thicker than the main plate, K-butt weld, toe ground Double-sided fillet weld, toe ground Fillet weld(s), as welded Thicker than the main plate	Assessed with regard to the maximum main stress.
72		80 71 63 50	Non-load-carrying rectangular or circular flat studs, pads or plates. $L \leq 50 \text{ mm}$ $50 < L \leq 150 \text{ mm}$ $150 < L \leq 300 \text{ mm}$ $L > 300 \text{ mm}$	
73		63	Weld stud	Automated flash-butt welding with quality requirements according to the Swedish National Road Administration.
74		71	Trapezoidal stiffener to deck plate, full penetration butt weld.	Calculation based on stiffener plate thickness.
75		50	Trapezoidal stiffener to deck plate, fillet weld or partial penetration weld, out-of-plane bending.	Calculation based on stiffener plate thickness or weld throat; maximum stress value used.
76		80 71 63 50	Longitudinal fillet welded gusset with length L $L \leq 50 \text{ mm}$ $50 < L \leq 150 \text{ mm}$ $150 < L \leq 300 \text{ mm}$ $L > 300 \text{ mm}$	For gusset on edge, see 80. Suitable for structural hot spot analysis.

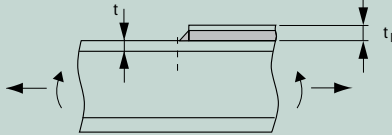
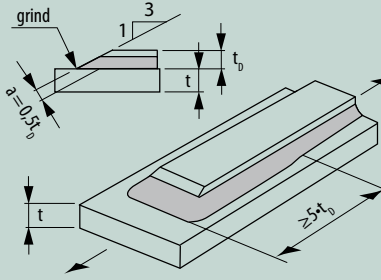
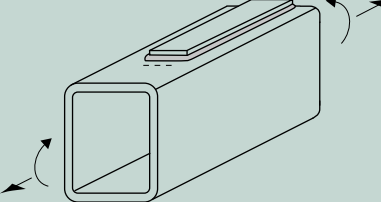
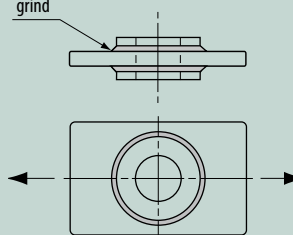
Tabell 5.19 cont.

Welded joints				
No	Structural details	FAT (MPa) $m=3$	Description	Comment
Non-load-carrying attachments				
77	 A diagram showing a longitudinal fillet-welded gusset. The gusset has a thickness t , a radius r at the transition, and a height c . The base plate has a thickness h . Arrows indicate stress directions.	90	Longitudinal fillet-welded gusset with radius transition, fillet weld around and toe ground, $c < 2t$, max 25 mm $r > 150$ mm	t = thickness of attachment Suitable for structural hot spot analysis.
78	 A diagram showing a longitudinal fillet-welded gusset with a smooth transition (sniped end or radius). The gusset has a thickness t , a radius r , and a height c . The base plate has a thickness h . Arrows indicate stress directions. Parameters: $c < 2t$, max 25 mm, $r > 0.5h$, $r \leq 0.5h$ or $\varphi < 20^\circ$.	71 63	Longitudinal fillet-welded gusset with smooth transition (sniped end or radius), welded or beam flange or plate, fillet weld around end. $c < 2t$, max 25 mm $r > 0.5h$ $r \leq 0.5h$ or $\varphi < 20^\circ$	t = thickness of attachment If attachment thickness < 1/2 of base plate thickness, the FAT value is increased by one step (not applicable to welding on profiles!) Suitable for structural hot spot analysis.
79	 A diagram showing a longitudinal flat side gusset with a smooth transition (sniped end or radius) welded on a plate edge or beam flange edge. The gusset has a thickness t_2 , a radius r , and a height c . The base plate has a thickness h . Arrows indicate stress directions. Parameters: $c < 2t_2$, max 25 mm, $r > 0.5h$, $r = 0.5h$ or $\varphi < 20^\circ$.	50 45	Longitudinal flat side gusset with smooth transition (sniped end or radius) welded on plate edge or beam flange edge, fillet weld around end. $c < 2t_2$, max 25 mm $r > 0.5h$ $r = 0.5h$ or $\varphi < 20^\circ$	t_2 = thickness of attachment FAT is increased by one step for $t_2 < 0.7t_1$ Suitable for structural hot spot analysis.
80	 A diagram showing an in-plane or out-of-plane longitudinal gusset welded to a plate or beam flange edge. The gusset has a length L and a thickness t_2 . The base plate has a thickness t_1 . Arrows indicate stress directions. Parameters: $L \leq 150$ mm, $150 < L \leq 300$ mm, $L > 300$ mm.	50 45 40	In-plane or out-of-plane longitudinal gusset welded plate or beam flange edge, gusset length L : $L \leq 150$ mm $150 < L \leq 300$ mm $L > 300$ mm	t_1 = continuous plate thickness t_2 = thickness of attachment FAT is increased by one step for $t_2 < 0.7t_1$
81	 A diagram showing a longitudinal flat side gusset welded on the edge of a plate or beam flange. The gusset has a width w and a radius r . Arrows indicate stress directions. Parameters: $r > 150$ mm or $r/w > 1/3$, $1/6 < r/w \leq 1/3$, $r/w \leq 1/6$.	90 71 50	Longitudinal flat side gusset welded on edge of plate or beam flange, radius transition ground. $r > 150$ mm or $r/w > 1/3$ $1/6 < r/w \leq 1/3$ $r/w \leq 1/6$	Smooth transition radius formed by grinding the weld area in transition in order to remove the weld toe completely. Grinding in the direction of stress.
82	 A diagram showing a circular or rectangular hollow section fillet-welded to another cross-section. The gusset has a width l and a height h . Arrows indicate stress directions. Parameter: $l \leq 100$ mm.	71	Circular or rectangular hollow section, fillet-welded to another cross-section. Cross-section width parallel to the direction of stress < 100 mm, otherwise as a longitudinal attachment.	Non-load-carrying welds.

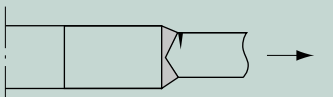
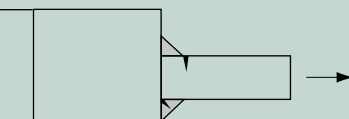
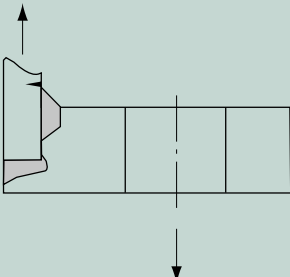
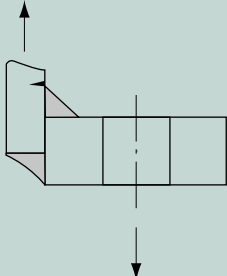
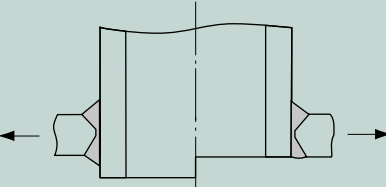
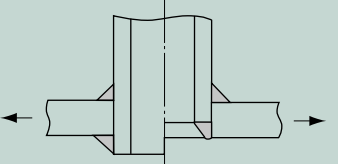
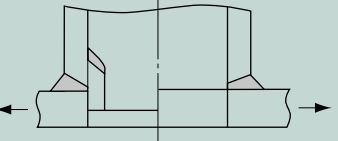
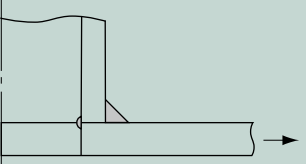
Tabell 5.19 cont.

Welded joints				
No	Structural details	FAT (MPa) $m=3$	Description	Comment
Lap joints				
83		63 45	Transverse loaded lap joint with fillet welds Crack at weld toe Fatigue of weld throat	Stress to be calculated in the main plate using a plate width corresponding to the weld length. Avoid global buckling for this type of joint!
84		50 50	Longitudinally loaded lap joint with side fillet welds Fatigue of parent metal Fatigue of weld (calculated with a max. length of 40 times the throat of the weld)	Weld ends more than 10 mm from main plate edge. Avoid global buckling for this type of joint! The higher of the stress values of the two members should be used for parent metal verification.
85		63 50	Lap joint gusset, fillet welded, non-load-carrying, with smooth transition (sniped end with <math>\varphi < 20^\circ</math> or radius), welded to loaded element <math>c < 2r</math>, but $c \leq 25$ mm to flat bar to angle bar	t = thickness of gusset plate
86		63 36	Transverse loaded overlap joint with fillet welds. Stress in plate at weld toe (toe crack) Stress in weld throat (root crack)	Stress to be calculated using a plate width corresponding to the weld length. Misalignment to be considered for stress in plate. Both failure modes to be inspected separately.
87		90	Plug-welded lap joint ¹⁾	

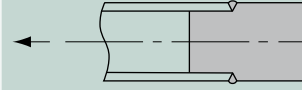
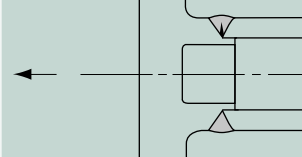
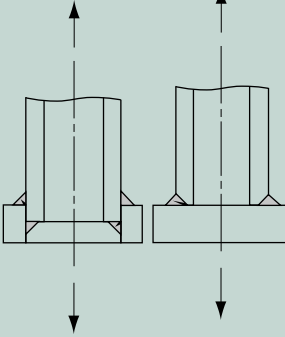
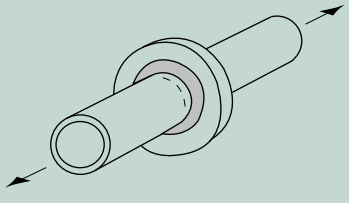
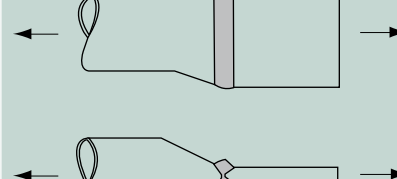
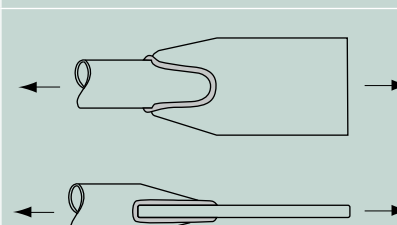
Tabell 5.19 cont.

Welded joints				
No	Structural details	FAT (MPa) $m=3$	Description	Comment
Reinforcements				
88		56 50 45	End of long doubling plate on I-beam (based on nominal stress range in flange at weld toe). $t_d \leq 0.8t$ $0.8t < t_d \leq 1.5t$ $t_d > 1.5t$	End zones of single or multiple welded cover plates, with or without transverse welds. If the cover plate is wider than the flange, a transverse weld is needed. No undercut at transverse welds!
89		71 63 56	End of long doubling plate on beam, reinforced welded ends ground (based on stress range in flange at weld toe). $t_d \leq 0.8t$ $0.8t < t_d \leq 1.5t$ $t_d > 1.5t$	Grinding in the direction of stress. One or more beads for improvement of the weld section with preserved throat thickness. Start and stop positions at least $5t_d$ on the long side.
90		50	End of reinforcement plate on rectangular hollow section. wall thickness: $t < 25$ mm	No undercut at transverse welds!
91		80 71	Fillet-welded reinforcement weld toe ground as welded	Grinding in the direction of stress. The hot spot method recommended as an alternative.

Tabell 5.19 cont.

Welded joints				
No	Structural details	FAT (MPa) m=3	Description	Comment
Flanges, branches and nozzles				
92		71	Stiff block flange, full penetration weld.	
93		63 36	Stiff block flange, partial penetration weld or fillet weld crack at weld toe root crack in weld throat	
94		71	Flat flange with at least 80% full penetration butt welds, modified nominal stress (according to Section 5.5.2) in pipe, toe crack.	The hot spot method recommended as an alternative.
95		63	Fillet welded pipe to flat flange, modified nominal stress (according to Section 5.5.2) in pipe, toe crack.	The hot spot method recommended as an alternative.
96		80	Tubular branch or pipe penetrating a plate, K-butt welds	If diameter > 50 mm, stress concentration of cutout has to be considered. The hot spot method recommended as an alternative.
97		71 36	Tubular branch or pipe penetrating a plate, fillet welds, toe cracks. Root cracks (based on stress in weld throat)	If diameter > 50 mm, stress concentration of cutout has to be considered. The hot spot method recommended as an alternative.
98		71	Nozzle welded on plate, root pass removed by drilling.	If diameter > 50 mm, stress concentration of cutout has to be considered. The hot spot method recommended as an alternative.
99		63	Nozzle welded on pipe, root pass as welded.	If diameter > 50 mm, stress concentration of cutout has to be considered. The hot spot method recommended as an alternative.

Tabell 5.19 cont.

Welded joints				
No	Structural details	FAT (MPa) m=3	Description	Comment
Tubular joints				
100		63	Butt welded circular tube or pipe to solid bar joint. Potential failure.	Based on stress in tube or pipe. The weld root must penetrate to the solid bar to avoid spaces perpendicular to the direction of stress.
101		63	Circular tube or pipe welded to component with single-sided butt weld with integral backing. Potential crack from weld root.	The weld root must penetrate to the component to avoid spaces perpendicular to the direction of stress.
102		50	Circular tube or pipe welded to component with single-sided butt weld or double fillet welds. Potential crack from weld root.	The impaired possibility to inspect root cracks by NDT should be compensated by adequate safety considerations or by downgrading two FAT classes.
103		90 90 71	Circular hollow section with welded-on disc, potential failure from toe in hollow section. K-butt weld, toe ground Fillet weld, weld toe ground Fillet weld(s), as welded	Unloaded weld.
104		63	Tube plate joint, tube flattened, butt weld (X-groove). Tube diameter < 200 mm and Plate thickness < 20 mm	
105		63 45	Tube plate joint, tube slotted and welded to plate Tube diameter < 200 mm and plate thickness < 20 mm Tube diameter > 200 mm and plate thickness > 20 mm	

Tabell 5.19 cont.

Welded joints				
No	Structural details	FAT (MPa) $m=3$	Description	Comment
Spot-welded				
106		50	Spot weld ¹⁾	
107		112	Spot-welded hat beam ¹⁾	
108		125	Box beam with non-load-carrying spot welds ¹⁾	
109		60	Box beam with load-carrying spot welds ¹⁾	

Tabell 5.19 cont.

Example 1

The fatigue life of a welded joint has to be estimated. A measurement has revealed that the stress range is 25% larger than what was expected in the beginning. How does this affect the fatigue life of the joint?

Solution:

Equation 5.22 gives the fatigue life of a given weld:

$$N = 2 \cdot 10^6 \cdot \left(\frac{FAT}{\Delta\sigma} \right)^m$$

The relationship between measured ($\Delta\sigma_{mät}$) and calculated ($\Delta\sigma_{ber}$) stress range is: $\Delta\sigma_{mät} = 1.25 \Delta\sigma_{ber}$

The stress range is the only parameter that has changed. The reduction service life can then be calculated according to:

Answer:

The fatigue life is reduced to 50% of what was expected in the beginning.

$$\frac{N_{mät}}{N_{ber}} = \frac{\frac{2 \cdot 10^6 \cdot \left(\frac{FAT}{\Delta\sigma_{mät}} \right)^3}{2 \cdot 10^6 \cdot \left(\frac{FAT}{\Delta\sigma_{ber}} \right)^3}} = \frac{\left(\frac{FAT}{1,25 \cdot \Delta\sigma_{ber}} \right)^3}{\left(\frac{FAT}{\Delta\sigma_{ber}} \right)^3} = \left(\frac{1}{1,25} \right)^3 \approx 0,5$$

Answer:

The fatigue life is reduced to 50% of what was expected in the beginning.

Example 2

The weld between the main member and a cross member in a trailer shall be analyzed in terms of fatigue life since the cross member is a new development. In order to get accurate load data a field measurement of a prototype was conducted for 24 hours a day during one week. The measurement was performed under such conditions as that there is a little risk that trailers will be subjected to a tougher load history in the future. For this reason γ_f is set

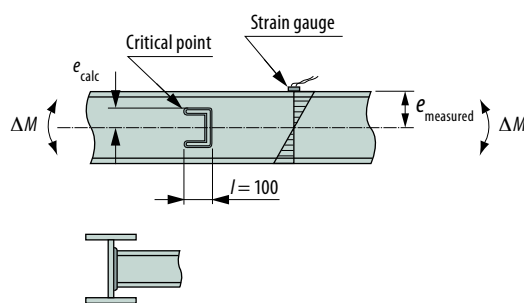


Figure 5.72: Frame member with cross beam connection.

to 1.0 during the calculations. The requirement for service life is 9 years and the trailer will spend two-thirds of this time in traffic, i.e. 16 hours a day. A critical point has been identified in the connection between the frame member and cross member according to the sketch below.

The web of the main member has a thickness of 5 mm. The consequence of failure is assessed to be serious and γ_m is set to 1.21. The misalignments are acceptable for structural joint in question. Figure 5.73 and table 5.20 shows the

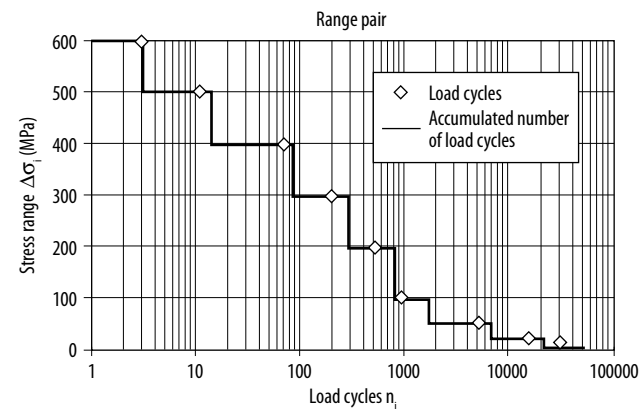


Figure 5.73: Graphic representation of stress history from field measurement.

Range pair values from field measurement			Calculated values	
i	(MPa)	$n_i^{(1)}$ (load cycles)	k_{3i} ($\Delta\sigma_{ref} = \Delta\sigma_i = 600$ MPa)	Accumulated number of load cycles ⁽²⁾
1	600	3	$5,80 \cdot 10^{-5}$	3
2	500	11	$1,23 \cdot 10^{-4}$	14
3	400	70	$4,01 \cdot 10^{-4}$	84
4	300	201	$4,85 \cdot 10^{-4}$	285
5	200	511	$3,66 \cdot 10^{-4}$	796
6	100	913	$8,17 \cdot 10^{-5}$	1709
7	50	5015	$5,61 \cdot 10^{-5}$	6724
8	20	15025	$1,08 \cdot 10^{-5}$	21749
9	10	30012	$2,68 \cdot 10^{-6}$	51761
Sum:		51761	$0,00158 = k_3$	

Table 5.20: Results from field measurement and calculation of the stress spectrum factor k_m .

measured data in form of range pair values for stress ranges and load cycles. Does the critical point meet the requirement for service life under the conditions stated above?

Solution:

Apply the nominal stress method, calculation procedure according to section 5.6.6 and 5.6.7.

1. Stress history parameter, s_m

According to the calculations in *table 5.20*, $k_3 = 0.00158$.

The service life is (when the trailer is used 16 hours a day):

$9 \cdot 2/3 \cdot 52$ weeks = 312 weeks. The total number of load cycles n_t from the field measurement shall be multiplied 312 to get the total number of load cycles for a service life N_t .

$$N_t = 312 \cdot n_t = 312 \cdot 51761 = 1.61 \cdot 10^7 \text{ load cycles}$$

The stress history parameter is calculated according to *equation 5.10*.

$$s_m = \frac{N_t}{2 \cdot 10^6} \cdot k_m = \frac{1,61 \cdot 10^7}{2 \cdot 10^6} \cdot 0,00158 = 0,0127$$

2. The structural joint is identified using *table 5.20*.

Joint no. 76 with $l=100$ gives $FAT = 71$, $m=3$ for welds.

3. The thickness improvement factor is calculated according to *equation 5.11*

$$\varphi_t = \left(\frac{15}{t} \right)^n = \left(\frac{15}{5} \right)^{0,15} = 1,18$$

($n=0,15$ for fillet welds)

4. The material factor $\varphi_m = 1$ for welds

5. The stress alternation factor is set to $\varphi_e = 1$ since the residual stress is not known for weld

6. Partial coefficients $\gamma_f = 1.0$ and $\gamma_m = 1.21$ see above

7. The permitted stress range in the critical point is calculated according to

$$\Delta\sigma_{Rd} = \frac{FAT \cdot \varphi_t \cdot \varphi_m \cdot \varphi_e}{\gamma_m \cdot \sqrt[m]{s_m}} = \frac{71 \cdot 1,18 \cdot 1 \cdot 1}{1,21 \cdot \sqrt[3]{0,0127}} = 296 \text{ MPa}$$

8. No effect of angular and axial misalignment ($\omega_{eff} = 1.0$)

9. Maximum stress range, $\Delta\sigma_{max}$, in the critical point. The main member is exposed to pure bending and the nominal stress distribution is equal at the strain gauge and the critical point. The distance to the neutral layer governs the relationship between the maximum stress range at the strain gauge and the maximum stress range in the critical point according to

$$\Delta\sigma_{max} = \Delta\sigma_{ref} \cdot \frac{e_{calcd}}{e_{measured}}$$

The reference stress range is 600 MPa and $e_{ber} = 150$ mm and $e_{mat} = 70$ mm

$$\Delta\sigma_{max} = \Delta\sigma_{ref} \cdot \frac{e_{calcd}}{e_{measured}} = 600 \cdot \frac{70}{150} = 280 \text{ MPa}$$

10. The criterion is given by

$$\Delta\sigma_{sd} \leq \Delta\sigma_{rd}$$

$$\Delta\sigma_{sd} = \Delta\sigma_{max} \cdot \gamma_f = 280 \cdot 1,0 = 280 \text{ MPa}$$

$$\Delta\sigma_{rd} = 296 \cdot 1,0 = 296 \text{ MPa}$$

280 MPa < 296 MPa OK!

Answer:

The welded joint meets the requirement for an operating life of 9 years.

Comment: The number of stress range intervals i is reduced compared to a real case.

Example 3

Calculate the ratio between the permitted stress ranges for a welded joint when it is subjected to different stress histories. Assume $\kappa = 1/2$ in one case and $\kappa = 5/6$ in the other. The number of load cycles is 10^6 in both cases.

Solution:

$\kappa = 1/2$ at 10^6 load cycles gives $k_3 = 0.16$ according to *figure 5.60*.

$\kappa = 5/6$ at 10^6 load cycles gives $k_3 = 0.60$ according to *figure 5.60*.

Use the expressions according to *equation 5.10* and *equation 5.15* for the stress history parameter s_m and permitted stress range.

$$\Delta\sigma_{Rd} = \frac{FAT \cdot \varphi_t \cdot \varphi_m \cdot \varphi_e}{\gamma_m \cdot \sqrt[m]{s_m}}$$

$$s_m = \frac{N_t}{2 \cdot 10^6} \cdot k_m$$



Figure 5.74: Critical cross-section in mobile crane.

The only parameter that varies is k_3 . The ratio between the permitted stress ranges in the different cases is calculated by

$$\frac{\Delta\sigma_{Rd}(\kappa=1/2)}{\Delta\sigma_{Rd}(\kappa=5/6)} = \sqrt[3]{\frac{1/k_{3(1/2)}}{1/k_{3(5/6)}}} = \sqrt[3]{\frac{k_{3(5/6)}}{k_{3(1/2)}}} = \sqrt[3]{0,60} = 1,5$$

Answer:

The ratio is 1.5, i.e., a 50% higher stress range is possible for a welded joint which is exposed to a stress history with $\kappa=1/2$ instead of $\kappa=5/6$ provided that the number of load cycles is $1 \cdot 10^6$ in both cases.

Comment: This example shows the importance of the stress history for the permitted stress range. A loading history with many small loads permits 50% higher maximum stress range, $\Delta\sigma_{max}$.

Example 4

A new mobile crane needs to be evaluated for fatigue and a first attempt at cross section dimensions gives a maximum stress range of $\Delta\sigma_{max} = 430$ MPa in a longitudinally loaded butt weld which is assumed to be critical, see figure 5.74. The service life N_t is $1 \cdot 10^5$ load cycles and the stress history parameter is estimated at $\kappa=1/3$.

It is assumed that $\gamma_f=1$ and $\gamma_m=1.21$ and that the misalignment are within the permitted tolerances for the applicable structural joint and does not need to be taken into further consideration. Does the weld fulfill the intended service life?

Solution:

The calculation procedure according to section 5.6.6 is applied with the use of typified stress histories according to section 5.6.3 and the nominal stress method, section 5.6.7.

1. The stress history parameter, s_m , equation 5.10

$$s_m = \frac{N_t}{2 \cdot 10^6} \cdot k_m$$

$k_m \approx 0.07$ for $\kappa=1/3$
and

SSAB

$N_t = 1 \cdot 10^5$ load cycles according to figure 5.60 gives

$$s_m = \frac{1 \cdot 10^5}{2 \cdot 10^6} \cdot 0,07 = 0,0035$$

2. Fatigue resistance value $FAT=100$ MPa for longitudinally loaded butt weld according to table 5.20, joint no. 23, and slope of S/N curve $m=3$
3. The thickness improvement factor $\varphi_t=1.0$ for longitudinally loaded butt weld
4. The material factor $\varphi_m=1$ for welds
5. The stress alternation factor $\varphi_e=1$ for welds if residual stresses are unknown
6. Partial coefficients $\gamma_f=1.0$ and $\gamma_m=1.21$
7. The permitted stress range is calculated according to equation 5.15
- $$\Delta\sigma_{Rd} = \frac{FAT \cdot \varphi_t \cdot \varphi_m \cdot \varphi_e}{\gamma_m \cdot \sqrt[3]{s_m}} = \frac{100 \cdot 1,0 \cdot 1,0 \cdot 1,0}{1,21 \cdot \sqrt[3]{0,0035}} = 544$$
 MPa
8. Angular and axial misalignment $\omega_{eff}=1.0$
9. The maximum stress range is 430 MPa
10. Criterion, equation 5.20

$$\Delta\sigma_{Sd} \leq \Delta\sigma_{Rd}$$

$$\Delta\sigma_{Sd} = \Delta\sigma_{max} \cdot \gamma_f = 430 \cdot 1,0 = 430$$
 MPa

$$\Delta\sigma_{Rd} = 544$$
 MPa

430 MPa < 544 MPa OK!

Answer:

The critical cross-section meets the requirements.

Comment: The calculation should be regarded as a rough estimate since the value of the stress history parameter κ is estimated.

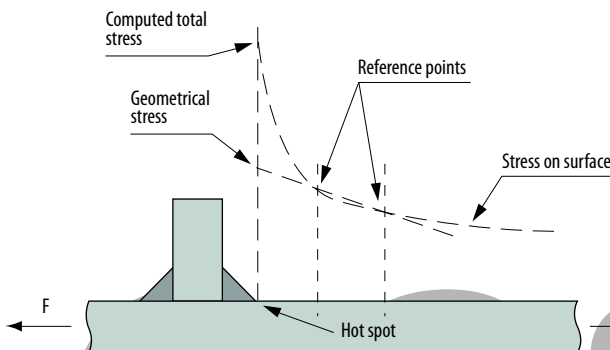


Figure 5.75: Definition of structural hot spot stress [5.1].

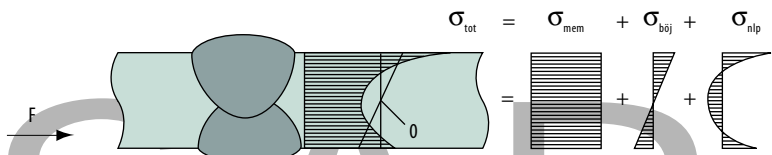


Figure 5.76: Non-linear stress distribution at weld toe separated to components [5.1].

5.6.8 Hot Spot stress method

The Hot Spot method was originally developed for strain measurements within the offshore industry. During the years it has been developed to also apply for assessments of stresses obtained with FE analysis. The Hot Spot method is based on geometrical stress at the weld toe, see figure 5.75. This means that two or more reference points at certain distances from the weld toe are evaluated. The stresses in the reference points are extrapolated to the weld toe for determination of the Hot Spot stress. The Hot Spot stress is subsequently used together with structural joints that are specifically prepared for the method.

The Hot Spot method is suitable, for example, in the following cases.

- when it is not possible to define a nominal stress
- when there is no structural joint in the nominal method which is applicable

Some of the limitations for the Hot Spot method are

- it is limited to studies of the weld toe
- it is intended for stresses which are mainly perpendicular to the weld

Our experience of the Hot Spot method is that it requires some kind of normal throat thickness even if it is not specified in the recommendations [5.1 and 5.23]. In thin material with a large throat thickness (for example $t=3.5\text{ mm}$, $a=5\text{ mm}$) a very conservative result is found. In thick material with a small throat thickness (for example $t=45\text{ mm}$, $a=6-7\text{ mm}$) a non conservative result is found. It all ends up at the distance between the reference points and the weld toe and thereby the ability to find the relevant stress distribution.

The structural Hot Spot stress includes all stress components except the non-linear stress distribution due to the local weld geometry, see figure 5.76.

σ_{tot} is the total stress, σ_{mem} the membrane stress, $\sigma_{bøj}$ the bending stress and σ_{nlp} the non-linear stress peak.

Position of a Hot Spot

A Hot Spot for assessment can be found in different ways. The Hot Spot is a critical point where a fatigue crack can be assumed to initiate. Critical points can be identified by means of [5.1 and 5.23]

- FE calculations using a global model
- identifying initiation points in failed structures
- strain measurements in areas which are assessed to be critical

Type a and b Hot Spots

There are two types of structural Hot Spot type a and b, see figure 5.77. Type a refers to welded joints where a crack is expected to grow from the surface of a plate. Type b refers to joints where a crack is expected to grow from the edge of a plate. Different extrapolation methods are used for the respective type, which is described below and according to table 5.21.

Assessment using strain measurements

The recommended placement and number of strain gauges depends on the extent of shell bending stresses, the plate thickness and the type structural stress (type a or b). The methodology is to measure strains at the reference points and convert the extrapolated Hot Spot strain to stress. The requirements on placement of the strain gauges with regard to the plate thickness make it impossible to measure on thin plates according to these recommendations. Precise positioning is not necessary if multi-grid strip gauges are used, since the results can be used to plot the stress distribution approaching the weld toe. The stresses at the required positions can then be read from the fitted curve. [5.1].

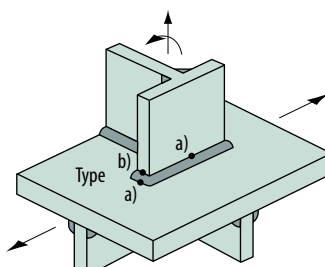


Figure 5.77: Type a and b Hot Spots [5.1].

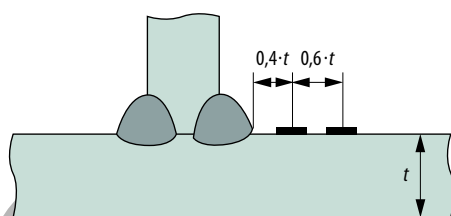


Figure 5.78: Placement of strain gauges for linear extrapolation [5.1].

The centre point of the first gauge, whose gauge length should not exceed $0.2 \cdot t$, is located at a distance of $0.4 \cdot t$ from the weld toe. The centre point of the second gauge is located at a distance of $1.0 \cdot t$ from the weld toe, see *figure 5.78*.

In this case, the Hot Spot strain is extrapolated according to *equation 5.26*.

$$\varepsilon_{hs} = 1,67 \cdot \varepsilon_{0,4t} - 0,67 \cdot \varepsilon_{1,0t} \quad (\text{Eq. 5.26})$$

Three gauges at reference points $0.4 \cdot t$, $0.9 \cdot t$ and $1.4 \cdot t$, and quadratic extrapolation. This method is particularly suitable for cases of pronounced non-linear structural stress increase towards the Hot Spot. *Equation 5.27*.

$$\varepsilon_{hs} = 2,52 \cdot \varepsilon_{0,4t} - 2,24 \cdot \varepsilon_{0,9t} + 0,72 \cdot \varepsilon_{1,4t} \quad (\text{Eq. 5.27})$$

The stress distribution for a Hot Spot type b does not depend the plate thickness so fixed distances from the weld toe are used. Three strain gauges are attached to the plate edge at reference points 4, 8 and 12 mm distant from the weld toe. The Hot Spot strain is determined by quadratic extrapolation to the weld toe. *Equation 5.28*.

$$\varepsilon_{hs} = 3 \cdot \varepsilon_{4\text{ mm}} - 3 \cdot \varepsilon_{8\text{ mm}} + \varepsilon_{12\text{ mm}} \quad (\text{Eq. 5.28})$$

Special recommendations exist for determining the structural Hot Spot stress in tubular joints [5.29]. In general these allow linear extrapolation from the measured or calculated stresses at two reference points. Parametric formulae have been established for the stress concentration factor in many joints between circular and rectangular section tubes, see [5.29].

If the stress state is close to uniaxial, the approximation to the structural Hot Spot stress is obtained approximately from *equation 5.29*.

$$\sigma_{hs} = E \cdot \varepsilon_{hs} \quad (\text{Eq. 5.29})$$

For biaxial stress state, the use of rosette strain gauges is recommended. If the ratio of longitudinal and transversal strains $\varepsilon_y / \varepsilon_x$ is available, for example from FE analysis, the structural Hot Spot stress can then be resolved from *equation 5.28*, assuming that this principal stress is approximately perpendicular to the weld toe. [5.1]

$$\sigma_{hs} = E \cdot \varepsilon_x \frac{1 + \nu \frac{\varepsilon_y}{\varepsilon_x}}{1 - \nu^2} \quad (\text{Eq. 5.30})$$

Assessment of Hot Spot stress using FE calculations

The principal stress is used if its direction is perpendicular within $\pm 60^\circ$ to the weld toe. If the angle is greater than 60° , use the larger of the following two – the stress component that is perpendicular to the weld toe or the lower principal stress [5.1].

In addition to the basic requirements to the FE model according to section 4.4, there are a number of aspects which should be taken into consideration during the use of the Hot Spot method, e.g. size and orientation of the elements closest to the weld. A sub-model of the joint, where the stress is determined by means of FE calculations of the complete structure, is often required due to precision requirements. There is a decisive difference in the joint is modeled with solid or shell elements. Solid elements give a better model but the disadvantage is that it becomes more complex and the degrees of freedom increases markedly. In general, 8-noded shell elements or 20-noded solid elements are recommended [5.30].

The representation of the weld in the FE-model is of different importance for the different types of joints and loads. The weld is not modeled at all in simpler models. When solid elements are used, the geometry of the weld can be modeled and the stiffness of the joint is such case correct.

If shell elements are used, there are a number of methods to model the weld. One way is to let the joined plates share nodes and give adjacent elements larger thickness. In such manner, the stiffness of the joint can be represented better, see *figure 5.79* [5.23]. For additional methods to represent the weld, refer to [5.28 and 5.30].

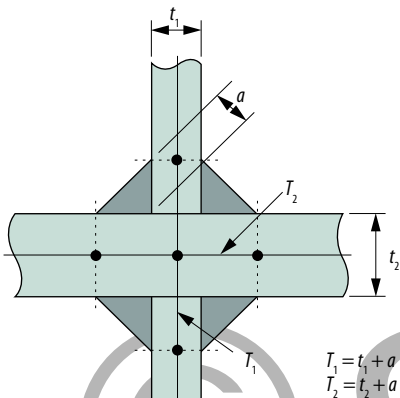


Figure 5.79: One way to model welded joints is to let the plates share nodes and increase the thickness of the adjacent elements. Throat thickness together with plate thicknesses governs the range of the increase in thickness [5.23].

The type and size of elements determine the position of the reference points. Two alternative applicable element sizes are presented in [5.1]: a relatively coarse and a relatively fine model. The size of the elements is determined by the thickness for Hot Spot type a. Fixed element sizes are used for Hot Spot type b. See *table 5.21* and *figure 5.80*.

Extrapolation for type a Hot Spot

The structural Hot Spot stress is determined using the reference points and extrapolation equations as given below, see *figure 5.80*. The reference point closest to the weld toe must be chosen to avoid any influence of the notch due to the weld itself (which leads to a non-linear stress peak). This is practically the case at a distance of $0.4 \cdot t$ from the weld toe, where t is plate thickness.

Fine mesh with element length not more than $0.4 \cdot t$ at the Hot Spot: Evaluation of nodal stresses at two reference points $0.4 \cdot t$ and $1.0 \cdot t$, and linear extrapolation according to *equation 5.31*.

$$\sigma_{hs} = 1,67 \cdot \sigma_{0,4t} - 0,67 \cdot \sigma_{1,0t} \quad (\text{Eq. 5.31})$$

Type of model and hot spot	Relatively coarse model		Relatively coarse model	
	Type a	Type b	Type a	Type b
Element size	Shells	$t \cdot t$	$10 \cdot 10 \text{ mm}$	$\leq 0,4 \cdot t \cdot t$
	Solids	$t \cdot t$	$10 \cdot 10 \text{ mm}$	$\leq 4 \cdot 4 \text{ mm}$
Extrapolation-points	Shells	$0,5 \cdot t$ and $1,5 \cdot t$ mid-side points	5 and 15 mm mid-side points	$0,4 \cdot t$ and $1,0 \cdot t$ nodal points
	Solids	$0,5 \cdot t$ and $1,5 \cdot t$ surface center	5 and 15 mm surface center	$4,8$ and 12 mm nodal points

Table 5.21: Element sizes and extrapolation points.

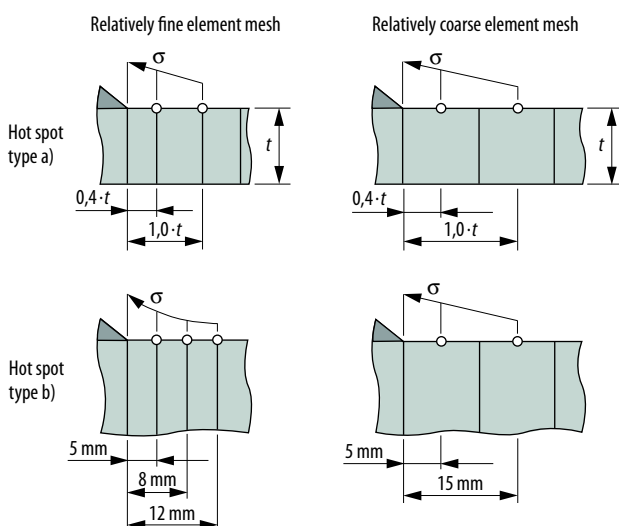


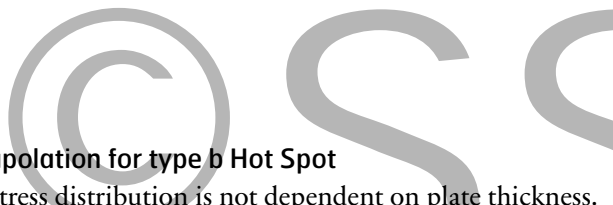
Figure 5.80: Element sizes and extrapolation points [5.1].

Fine mesh as defined in above: Evaluation of nodal stresses at three reference points $0.4 \cdot t$, $0.9 \cdot t$ and $1.4 \cdot t$, and quadratic extrapolation (*equation 5.32*). This method is recommended for cases of pronounced non-linear structural stress increase towards the Hot Spot, at sharp changes of direction of the applied force or for thick walled structures.

$$\sigma_{hs} = 2,52 \cdot \sigma_{0,4t} - 2,24 \cdot \sigma_{0,9t} + 0,72 \cdot \sigma_{1,4t} \quad (\text{Eq. 5.32})$$

Coarse mesh with higher-order elements having lengths equal to plate thickness at the Hot Spot: Evaluation of stresses at mid-side points or surface centres respectively, i.e. at two reference points $0,5 \cdot t$ and $1,5 \cdot t$, and linear extrapolation according to *equation 5.33*.

$$\sigma_{hs} = 1,5 \cdot \sigma_{0,5t} - 0,5 \cdot \sigma_{1,5t} \quad (\text{Eq. 5.33})$$



Extrapolation for type b Hot Spot

The stress distribution is not dependent on plate thickness. Therefore, the reference points are given at absolute distances from the weld toe, or from the weld end if the weld does not continue around the end of the attached plate.

Fine mesh with element length of not more than 4 mm at the Hot Spot: Evaluation of nodal stresses at three reference points 4 mm, 8 mm and 12 mm and quadratic extrapolation according to *equation 5.34*.

$$\sigma_{hs} = 3 \cdot \sigma_{4\text{ mm}} - 3 \cdot \sigma_{8\text{ mm}} + \sigma_{12\text{ mm}} \quad (\text{Eq. 5.34})$$

Coarse mesh with higher-order elements having length of 10 mm at the Hot Spot: Evaluation of stresses at the mid-side points of the first two elements and linear extrapolation according to *equation 5.35*.

$$\sigma_{hs} = 1,5 \cdot \sigma_{5\text{ mm}} - 0,5 \cdot \sigma_{15\text{ mm}} \quad (\text{Eq. 5.35})$$

Solution procedure

The Hot Spot stresses are determined as described above and the fatigue life evaluation is done in accordance to section 5.6.6, but $\Delta\sigma_{\max}$ is replaced by $\Delta\sigma_{hs}$. Alternatively the fatigue life can be evaluated using the cumulative damage sum according to section 5.6.10. The structural joints are obtained from *table 5.22*. The material factor φ_m is set to 1 as the calculation refers to welds. The stress alternation factor φ_e is usually set to 1 since the residual stresses often are unknown. The thickness enhancement factor φ_t can conservatively be set to 1. The design value of the structural Hot Spot stress range $\Delta\sigma_{hs}$ shall not exceed $2 \cdot R_e$.

When the stress ranges have been determined through strain measurements the effects of misalignment, if any, are included in the measured results. If FE analysis is used the misalignments can be modeled or the stress-increasing effects can be handled separately by approximations from *table 5.12*, which is less time consuming.

Structural details for post treated welds are given in *table 5.22*. General information is given in 5.5.6. Post treatment of welds for increased fatigue strength. Recommendations for assessment is given in 5.6.7 section Improvement techniques.

No	Structural detail	Description	Requirements	FAT
1		Butt joint.	As-welded, NDT (non-destructive testing).	100
2		Cruciform or T-joints with full penetration K-butt welds.	K-butt welds, no lamellar tearing.	100
3		Non-load-carrying fillet welds.	Transverse non-load carrying attachment, not thicker than the main plate, as-welded.	100
4		Bracket ends, ends of longitudinal stiffeners.	Fillet weld around the bracket ends/stiffener or not, as-welded.	100
5		Cover plate ends and similar joints.	As-welded.	100
6		Cruciform joints with load-carrying fillet welds.	Fillet welds, as-welded.	90
7		Lap joint with load-carrying fillet welds.	Fillet weld, as-welded.	90
8		Type "b" joint with short attachment.	Fillet or full penetration weld, as-welded.	100
9		Type "b" joint with long attachment.	Fillet or full penetration weld, as-welded.	90

Fatigue resistance values for post treated welds				
Yield strength	Grinding or TIG-treatment		"Peening"	
	Load carrying	Nonload carrying	Load carrying	Nonload carrying
$R_e < 350 \text{ MPa}$	112	125	112	125
$R_e \geq 350 \text{ MPa}$	112	125	125	140

Table 5.22: Structural details for hot spot method [5.1].

5.6.9 Effective notch method

The effective notch stress method, allows an analysis of fatigue from both the weld toe and the weld root. The effective notch stress is the total stress at a welded joint's toe or root if linear elastic material behavior is assumed. It is determined with FE calculations where the structure's geometry, including the weld, is modeled. The weld toe and weld root are modeled with a fictitious radius r , see *figure 5.81*. The greatest principal stress is first calculated and used together with the FAT class which is applicable to the respective fictitious radius.

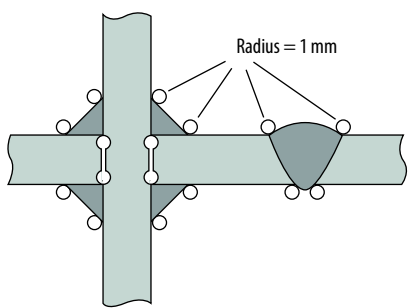


Figure 5.81: Fictitious rounding of weld toes and roots [5.1], [5.31].

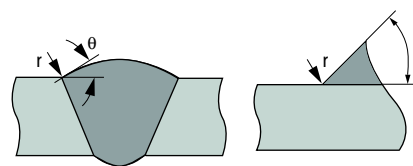


Figure 5.82: Flank angle for butt weld and for fillet weld [5.1], [5.31].

The effective notch method is applicable, among other things, in the following cases

- when neither the nominal stress method, nor the Hot Spot method is applicable.
- in connection with comparative studies of different types of geometries and welded joints

Assessing all welded joints in a structure is often unrealistic design joints can instead be identified using

- FE calculations using a global model
- identification of initiation points in failed applications
- strain measurements in areas which are assessed to be critical
- the nominal stress method

Effective notch radius

The local geometry of the welds often differs a lot and this is why the exact modeling of each weld is complicated. A fictitious radius of a given magnitude is used instead. The method originates in the offshore and shipping industry and this is why it has originally been used for plate thicknesses of more than 5 mm where a radius of 1 mm is used. The use of a radius of 1 mm for thicknesses of less than 5 mm means that the cross-section changes so much that the stress distribution and size are no longer relevant. This is why a radius of 0.05 mm, which has been studied primarily with regard to spot and lap joints [5.28 and 5.31], is used for plate thicknesses of less than 5 mm. Even a measured, greater radius can be used, [5.31].

FE modeling

The effective notch can be applied using either 2-dimensional elements with plane deformation condition or solid elements, depending on the relevant structure and application. If a 2-dimensional model is used, plane deformation is assumed, in which case it is important to keep the load on the weld primarily perpendicular to the weld's longitudinal direction and not to change the weld's geometry and thereby allow the identification of a representative section [5.31]. Idealized weld geometry with a constant flank angle θ and the respective radius is modeled for the alternatives

with a radius of 1 and 0.05 mm, respectively. Flank angles of $\theta=30^\circ$ and $\theta=45^\circ$ are generally recommended for butt welds and fillet welds, respectively, see figure 5.82.

The weld toe is modeled using the current radius and the flank angle. The weld root can be omitted in certain cases with full penetration but a conservative modeling includes a radius even for the weld root. If the fusion penetration depth is known, the radius is modeled at the end of the fusion penetration. If the fusion penetration is not known, the fictitious radius is modeled conservatively without fusion penetration.

As a rule, two different techniques are used for the weld root: a so-called key hole or a U-shape, see figure 5.83.

The U-shape gives lower stress concentrations than the key hole in non-load-carrying joints, which can lead to an underestimation of the stress in the root. The U-shape can lead to a higher stress concentration in the weld toe in load-carrying welds due to the reduced stiffness. Both methods produce basically the same stress level in the weld root in load-carrying joints [5.31].

A relatively coarse element mesh is usually used in the global structure and a fine element mesh in the vicinity of the notch. In larger structures, where several welds need to be analyzed, this is realized in practice through sub-modeling. This means that calculations are first carried out of the whole structure, whereupon the result from them is used to define loads and boundary conditions on a sub-model of the studied joint with a finer mesh, see section 5.6.13.

Element mesh

The element mesh needs to grow gradually finer towards the notch so as to prevent large size or shape differences in the adjacent elements. The recommended element size and number of elements around the radius are different for elements with a linear or quadratic displacement func-

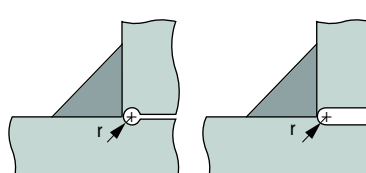


Figure 5.83: The weld root can be modeled in the form of a key hole or in the form of a U. In this case without penetration [5.1].

tion, respectively. At least one element per 15° of curvature is recommended for elements with quadratic displacement function, which means an element size of not more than 0.25 mm for a radius of 1 mm. See figure 5.84 and figure 5.85, as well as table 5.23 [5.31].

FAT Classes

A FAT value of 225 MPa is used for a radius of 1 mm and a FAT value of 630 MPa for a radius of 0.05 mm [5.32 and 5.33]. New articles regarding these FAT values are continuously presented and this is why we recommend that the readers keep up to date, primarily via the IIW.

Solution procedure

To produce a design, you may need to calculate several stresses for a relevant notch in order to compute the stress ranges. The design is then carried out in a corresponding way as in section 5.6.6, with the difference that is replaced with the stress range which has been calculated for the current notch. Alternatively, a cumulative damage calculation can be conducted according to section 5.6.10. The relevant FAT class is then obtained in accordance with the above. The material factor ϕ_m is set to 1 as the calculations refer to a weld. The stress alternation factor ϕ_e is usually set to 1 as it refers to undressed welds and the thickness improvement factor ϕ_t is then conservatively set to 1, as well. Angular and/or axial misalignment can be taken into consideration through modeling. A less time-consuming way of managing these stress-increasing effects is to use table 5.6.6.

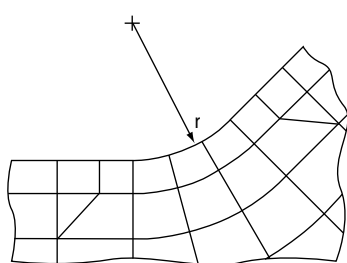


Figure 5.84: Typical element mesh for a weld toe when elements with quadratic displacement function are used [5.31].

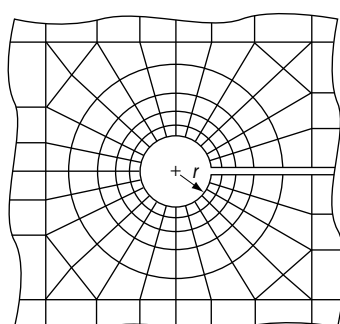
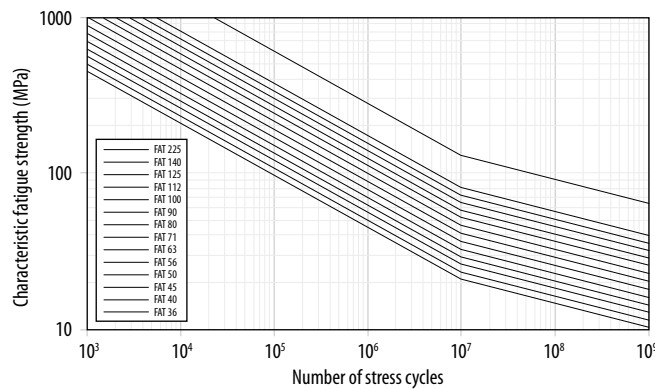


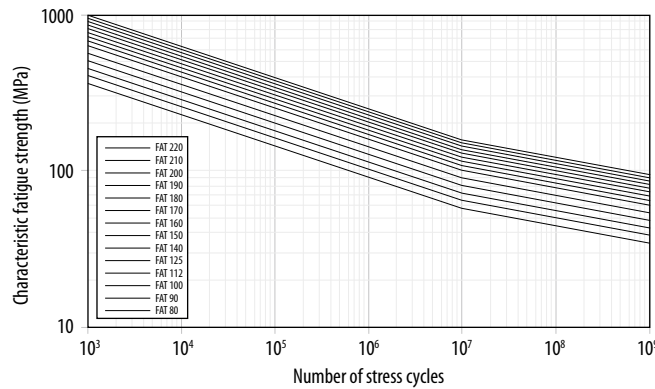
Figure 5.85: Typical element mesh for a weld root with a shape of a key hole when elements with quadratic displacement function are used [5.31].

5.6.10 Linear damage calculation by the “Palmgren-Miner” rule

The Palmgren-Miner cumulative damage sum can be used in with the nominal stress, the Hot Spot and the effective notch method. A damage sum calculation with a simplified S-N curve (without a knee point, section 5.6.1) will give the same result as a calculation according to section 5.6.6. The advantage with the damage sum calculation is that it can be used for S-N curves with a knee point. In the case of a load history with many small load cycles an S/N curve with knee point is beneficial since it avoids a too conservative design approach. S-N curves with knee point applicable for the nominal stress, the Hot Spot and the effective notch method are shown in figure 5.86.



a) Welds (FAT 225 refers to the effective notch method).



b) Parent material (only for the nominal stress method).

Figure 5.86: S-N curves with a knee point at 10^7 load cycles.

Element formulation (displacement function)	Size for $r = 1 \text{ mm}$	Size for $r = 0,05 \text{ mm}$	Number of elements for 45° vinkel
Quadratic	$\leq 0,25 \text{ mm}$	$\leq 0,012 \text{ mm}$	≥ 3
Linear	$\leq 0,15 \text{ mm}$	$\leq 0,008 \text{ mm}$	≥ 5

Table 5.23: Recommended element sizes at the weld [5.31].

Calculation procedure

1. Calculate the permitted stress range at $2 \cdot 10^6$ load cycles, equation 5.15:

$$\Delta\sigma_{Rd} = \frac{FAT \cdot \varphi_t \cdot \varphi_m \cdot \varphi_e}{\gamma_f \cdot \gamma_m}$$

2. Truncate the stress ranges which are lower than the stress range which corresponds to 10^9 load cycles for the actual S-N curve.

3. Determine the maximum permitted number of load cycles, N_i , for each stress level, $\Delta\sigma_i$ for the actual S-N curve.

$$N_i = \left(\frac{\Delta\sigma_{Rd}}{\Delta\sigma_i} \right)^{m_i} \cdot 2 \cdot 10^6$$

$m_i=3$ for welds, $m_i=5$ for parent material.

N_i is calculated according to for stress ranges which are below the knee point,

$$N_i = \left(\frac{\Delta\sigma_{Rd}}{\Delta\sigma_i \cdot 5^{(1/m_i)}} \right)^{m_2} \cdot 1 \cdot 10^7$$

Where $m_2=2 \cdot m_i - 1$ ($m_i=5$ for welds, $m_i=9$ for parent material)

4. At the point of evaluation this criterion must be fulfilled:

$$\sum_i \frac{n_i}{N_i} \leq d$$

$d=1$ (Failure criterion)

We have chosen to apply $d=1$ as failure criterion in accordance with the Crane Standard [5.2]. This is also practice within Swedish engineering industry. Values between 0.5 and 1 can be used according to the IIW [5.1]. According to our experience is values lower than 1 a conservative approach. The criterion at the point of evaluation is then with $d=1$

$$\sum_i \frac{n_i}{N_i} = \frac{n_1}{N_1} + \frac{n_2}{N_2} + \dots + \frac{n_i}{N_i} \leq 1,0$$

where

- i – index for level i from the stress history.
- n_i – number of load cycles at stress range σ_i from the stress history.
- N_i – maximum permitted number of load cycles at stress range σ_i from the S-N curve.

5.6.11 Fatigue testing

Fatigue testing is an important part of the product development process. Testing can be used to verify that a part, structure or product has the required fatigue strength. Fatigue testing is always a simplification of reality but is of course much faster in terms of time to failure compared to products in real service. The usable information from a single fatigue test is limited but in combination with previous testing or experience from real service it can contribute with very valuable information.

Variation in welding quality is often the explanation for differences in service life; see section 5.5.2 and 5.5.7. For this reason it is important to strive for a quality of the tested specimens which correspond to the outcome of normal production.

It is common to make strain measurements of a test specimen during a test for correlation with strength calculations. The result from constant amplitude testing in the region of the fatigue limit is very scattered in terms of life so it is important to keep testing within the sloping part of the S/N curve. Too high loads should be avoided since plastic strains also have large impact on life.

Component testing

The absolute majority of fatigue tests performed is made with constant amplitude loading. The scatter of the S/N curve associated to the test has smaller scatter at high loads especially for welded components. The most common failure criterion of a fatigue tests is rapture but decreased stiffness of the test specimen or a certain crack length is also used but is harder to control for the test machine.

Constant amplitude testing is usually performed even if the actual loading history different i.e., $k_3 < 1$. This is an accelerated testing, which is acceptable if the stress history parameter s_3 (i.e., fatigue damage) is the same during testing as in the calculation assumptions or, alternatively, during actual operation. The corresponding number of load cycles at testing N_{prov} can be calculated based on N_t and k_3 as $k_3 = 1$ during constant amplitude load testing according to equation 5.36.

$$N_{prov} = N_t \cdot k_3 \quad (\text{Eq. 5.36})$$

Failure probability P	$n = 1$	$n = 2$	$n = 3$	$n = 4$	$n = 5$
20%	1.19	1.03	0.97	0.94	0.92
10%	1.81	1.57	1.48	1.43	1.40
5%	2.33	2.01	1.90	1.84	1.80
1%	3.29	2.85	2.69	2.60	2.55

Equation 5.36 applies if the stress range $\Delta\sigma_{\max}$ in the calculation or the largest stress range $\Delta\sigma_{\max}$ during operation is the same as the stress range at testing. An acceleration of the testing can be achieved by using a stress range $\Delta\sigma_{\text{prov}}$, which is higher than $\Delta\sigma_{\max}$.

$$N_{\text{prov}} = N_t \cdot k_3 \cdot \left(\frac{\Delta\sigma_{\max}}{\Delta\sigma_{\text{prov}}} \right)^3 \quad (\text{Eqn. 5.37})$$

There are also risks associated with accelerated testing. Real components have many possible initiation points for fatigue cracks. Each and every one of these has "its own" S-N curve. The critical point changes at different load levels. If the S-N curve for a weld (typically $FAT=80, m=3$) and the S-N curve for a hole (typically $FAT \cdot \varphi_m = 150, m=5$) are compared, you can see that they cross each other. See figure 5.86. In practice this means a switch of critical point. If fatigue testing is performed with too high loads the critical point in real service may not be found.

Fatigue testing involves a certain probability that a randomly chosen component would not meet its nominal fatigue life. The failure probability P depends on the scatter in fatigue life. To lower the failure probability P the testing has to be extended with more load cycles. If several components are tested, the number of load cycles can be reduced for the same failure probability P .

Assuming a static normal distribution, the lowest acceptable the number of load cycles can be calculated for a certain failure probability and a certain number of tested components. The scatter in fatigue tests is expressed as the standard deviation σ of $\log(N)$ and usually is within the range of 0.05 to 0.2. Table 5.24 indicates how many standard deviations, x , the required number of load cycles is adjusted at different failure probabilities, P , and number of tested components [5.52].

The required number of load cycles the tested components should fulfill for approval is given by:

$$N_{\text{prov}, P} = 10^{\log(N_{\text{prov}}) + x \cdot \sigma} \quad (\text{Eqn. 5.38})$$

Example 5

A welded component for a mobile crane needs to be verified through constant amplitude testing with three test specimens which are identical to the welded component. The crane is designed for a loading history with many small loads, $\kappa=1/6$ and total number of load cycles is $N_t=10^6$ load cycles. The maximum stress range the component is exposed to during operation is $\Delta\sigma_{\max}=700$ MPa.

Table 5.24: The S-N curve displacement, x , expressed in standard deviations for the number, n , of tested components.

The standard deviation σ in $\log(N)$ is assumed to be 0.17 [5.19]. How many load cycles do the three test specimens need to last in order to fulfill the failure probability of $P=1\%$. The fatigue testing will be performed at a stress range equal to the maximum stress range.

Solution:

$\kappa=1/6$ and $N_t=10^6$ load cycles according to figure 5.60 give $k_3 = 1 \cdot 5 \cdot 10^{-2}$

The number of load cycles for 50% failure probability is provided by equation 5.36

$$N_{\text{prov}} = N_t \cdot k_3 = 1 \cdot 10^6 \cdot 1,5 \cdot 10^{-2} = 15\,000 \text{ cycles}$$

1 % failure probability for $n=3$ gives $x=2.69$ according to table 5.24

The number of load cycles that all test specimens must pass for acceptance is then computed from equation 5.38.

$$N_{n=3, P=1} = 10^{\log(N_{\text{prov}}) + x \cdot \sigma} = 10^{\log(1,5 \cdot 10^4) + 2,69 \cdot 0,17} = 10^{4,63}$$

$$N_{n=3, P=1} = 42\,990 \text{ cycles}$$

Answer:

Mean value from the three test specimens must pass 43 000 load cycles at a constant amplitude load with a stress range of $\Delta\sigma_{\max}=700$ MPa.

Comments:

1) There is no formal requirement in this example to continue testing after 43 000 load cycles and aim for failure in order to meet the requirement for 1% failure probability. On other hand, it can be useful to continue testing until failure as this can provide information if the component is oversized. The additional cost for testing until failure is often small compared to the overall testing cost.

2) A possible outcome of the testing is that the first specimen lasts significantly longer than the 43 000 load cycles, for example, 60 000 load cycles until failure. An assessment can then be made if more testing should be performed. It is possible to calculate the required number of load cycles for one component to fulfill the failure probability of 1%. Table 5.24 gives a value of $x=3.29$ for $n=1$.

The required number of load cycles for one specimen is calculated according to

$$N_{n=1, P=1\%} = 10^{\log(N_{\text{prov}}) + x \cdot \sigma} = 10^{\log(1,5 \cdot 10^4) + 3,29 \cdot 0,17} \approx 10^{4,70}$$

$$N_{n=1, P=1\%} \approx 54\,400 \text{ cycles}$$

The requirement for failure probability is met even if the two remaining specimens are not tested. Continued testing of the two remaining specimens can tell if the com-

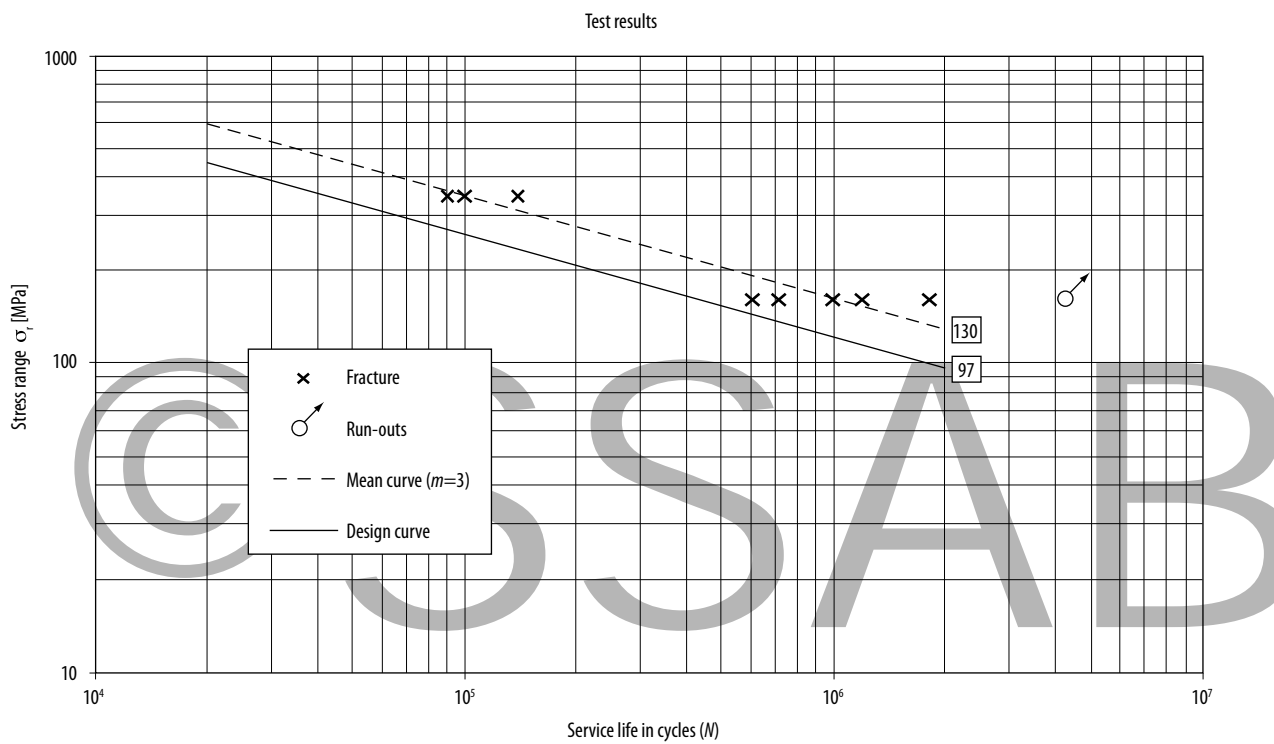


Figure 5.87: Examples of fatigue test results for a welded joint. The FAT class is estimated to $0.75 \cdot 130 = 97$ MPa.

ponent is oversized. This is the case if the two remaining specimens last 60 000 load cycles. An increased number of specimens which are tested allows for smaller margins on number of load cycles that are required for approval. Such approach gives better opportunities for optimized structures which utilizes the properties of high strength steel.

Determination of the S-N curve

Fatigue testing which is performed to establish an S-N curve is usually focused on the sloping part of the curve and the fatigue limit is of secondary interest. A minimum recommendation is that at least 10 test results are within the sloping part of the curve, i.e. in the range of 10^4 to 10^6 load cycles. So a larger number of test specimens have to be prepared for the test since fractures in the gripping heads can occur and some specimen are used before suitable load levels have been found. The S/N curve is fitted to the test results with a slope $m=3$ for welds and $m=5$ for parent material during the assessment, see figure 5.87.

The FAT class (stress range at $2 \cdot 10^6$ load cycles and 2.3% failure probability) is estimated by multiplying the stress range at $2 \cdot 10^6$ load cycles of the mean curve by a factor of 0.75. A methodology to establish a FAT class in a statistically correct manner which takes into consideration the number of test specimens and scatter in test result is described in [5.1].

If the testing is conducted in bending of flat specimens the fatigue strength will be higher compared to results from tensile testing. The explanation is the varying stress distribution through the cross-section in bending. A propagating crack will be affected by lower stress the deeper it gets into the material. The phenomenon is to some extent similar to the thickness effect in welds, section 5.5.4. The fatigue strength found in a tensile test is approximately 80%.

5.6.12 Fracture mechanics – Defect tolerance

Regardless of how much work is done to produce “perfect” structures it is impossible, especially in welded structures, to avoid defects completely. This section describes how to analyze the effect of different defects on carrying capacity or service life using fracture mechanics. Examples of questions which can be described using fracture mechanics are:

- Will a defect grow under the applied fatigue load?
- Which defect size is critical with regard to the risk of brittle failure?
- How many load cycles are required for the defect to reach critical size?

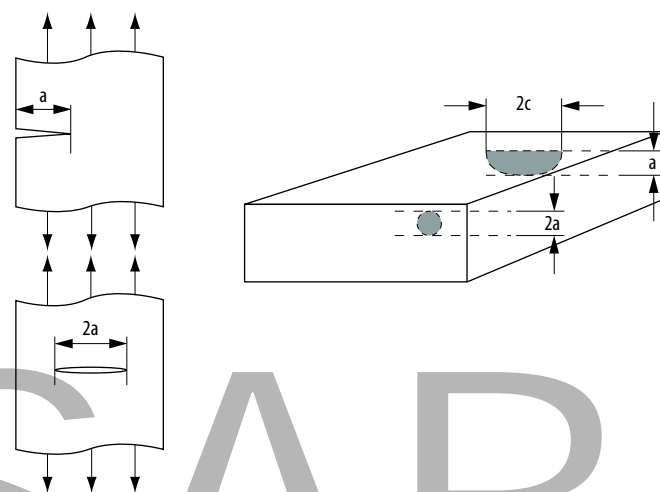
Fracture mechanisms

Different types of fractures occur at different geometrical and loading conditions and as a result of material characteristics. The different types of fractures can roughly be divided as:

- brittle fracture
- ductile fracture
- fatigue fracture

Brittle fractures are characterized by the fact that the fracture happens under a negligible plastic deformation, on a macroscopic scale, and the fracture advances rapidly through the material.

Ductile fractures are accompanied by considerable plastic deformation. The fracture surfaces cannot be fitted together after failure and the propagation rate is significantly lower than for brittle fractures. Ductile fracture can



also be stable and unstable fracture. The latter case is very similar to brittle fracture and is sometimes taken as brittle fracture.

Fatigue fractures happen when a crack or a defect grows to a critical size under a fatigue load. The crack growth itself takes place in very small increments (10^{-2} – 10^{-6} mm/load cycle) and in most cases without any visible plastic strain. *Figure 5.1* shows so called beach mark, which are very typical for fatigue fracture. These lines, observed in *figure 5.1*, should not be confused with so called striation, which can only be observed with a scanning electron microscope, SEM. The final fracture after the fatigue crack propagation can be brittle or ductile.

Basic fracture mechanics

Fracture mechanics is discussed in detail in for example [5.34]. Fracture mechanics can be divided from the user point of view into determination of critical crack size with respect to static failure and analysis of crack propagation under fatigue loading.

Critical crack size in connection with brittle fracture

A risk of brittle fracture exists if the following three conditions are met:

A brittle fracture can occur if the following three conditions are met:

- sufficiently high stress in the structure
- sufficiently low temperature
- sufficiently high degree of triaxial stress state

Triaxial stress state often requires large plate thicknesses and this is why brittle fractures rarely occur for plate thicknesses $t \leq 16$ mm, this thickness depends however the strength of the material. SSAB high strength steels allow for higher working stress in structural members and should be checked with regard to operating temperature, see also section 4.7. Critical crack size for brittle fractures is determined by using linear fracture mechanics.

The stress level in the vicinity of the crack tip is scaled be the so called stress intensity factor, K . The practically most interesting load is a load perpendicular crack, see *figures 5.88* and *5.96*, and this loading is called modus I , and the corresponding stress intensity is designated K_I according to

Figure 5.88: Definition of crack depth.

$$K_I = \sigma \sqrt{\pi a} \cdot f \quad (\text{Eq. 5.39})$$

where

- σ – nominal stress (disregarding the crack) plus residual stress, if any
- a – crack depth, *figure 5.88*
- f – geometry function which includes the effect of the crack and the component concerned and the load type (tension or bending). See next section, Data for Fracture Mechanical Calculations, below.

Fracture occurs when:

$$K_I = K_{IC} \quad (\text{Eq. 5.40})$$

where

K_{IC} = plain strain fracture toughness.

It should be noted in connection with the introduction of a safety factor, e.g., in *equation 5.39* that a factor 2 for stress corresponds to a factor 4 for the crack depth. Plain strain fracture toughness is a material property but in order to obtain valid values during testing, the conditions for linear fracture mechanics need to be met:

$$\left\{ \frac{t}{a} \geq 2,5 \cdot \left(\frac{K_{IC}}{R_c} \right) \right\} \quad (\text{Eq. 5.41})$$

Fracture toughness, which decreases with as temperature drops, is determined by standardized testing.

Fracture toughness should not be confused with impact toughness according to Charpy. Impact toughness is used as a qualitative measure of material toughness but cannot be used for direct calculation of critical defect sizes. There is, however, a very rough approximate connection between impact toughness and fracture toughness, see next section, Data for Fracture Mechanical Calculations. If only the requirement for crack length in *equation 5.41* is met, the fracture condition in *equation 5.40* is replaced by

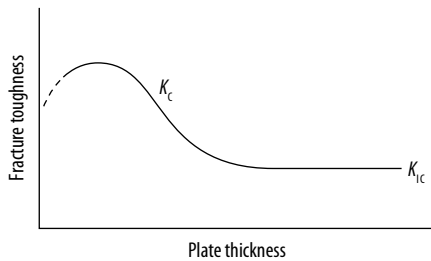


Figure 5.89: Principal correlation between fracture toughness and plate thickness.

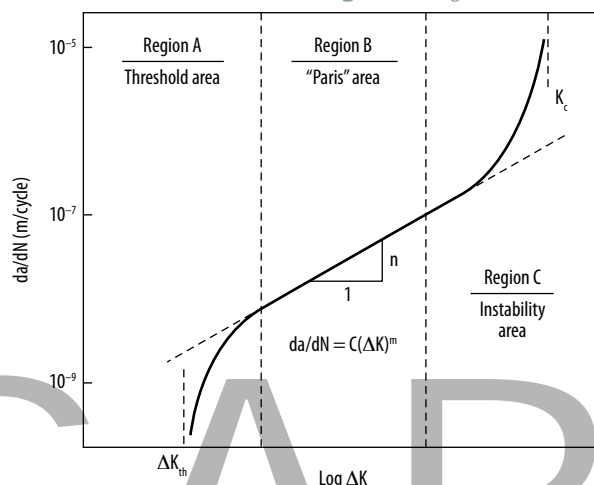


Figure 5.90: Correlation between crack growth rate and variation in stress intensity [5.36].

$$K_i = K_c \quad (\text{Eq. 5.42})$$

where

K_c – the material fracture toughness at the current thickness.

In this case, the material is tested with the same thickness it has in the structure as fracture toughness varies with thickness, see *figure 5.89*.

Critical crack size in connection with ductile fracture

When the conditions for linear fracture mechanics are not satisfied, non-linear fracture mechanics can be used. An engineering method, which is particularly useful in welded joints, is the CTOD method (Crack Tip Opening Displacement). The method is based on the assumption that the material toughness can be defined by the opening of the tip of the crack, which can happen before the initiation of the fracture. Toughness is specified in critical CTOD which is usually designated as δ_c and has the dimension of length. Typical values of δ_c in welded joints range from 0.1 to 0.3 mm. The method is very suited for toughness in welded joints, see also [5.35].

Crack growth under fatigue load

The crack-driving parameter under a fatigue load is the variation in stress intensity range, ΔK . Modus I is usually dominant, i.e., crack growth is primarily driven by a stress component perpendicular to the crack. The stress range variation is then formulated

$$\Delta K_i = \Delta \sigma \sqrt{\pi a} \cdot f \quad (\text{Eq. 5.43})$$

where

$\Delta \sigma$ – $\sigma_{\max} - \sigma_{\min}$ for welded joints where the residual stress has not been eliminated or if $\sigma_{\min} > 0$
 $\Delta \sigma$ – σ_{\max} for all other cases

The correlation between the crack-driving parameter ΔK (the "I" index is often left out in fatigue contexts) and the crack growth rate da/dN is displayed in *figure 5.90*. The figure has three different regions. The curve tips downwards on the far left, next to the lowest ΔK values (the threshold region or region 1) and there is no crack growth under $\Delta K = \Delta K_{th}$ (the threshold value). In the linear intermediate region, region 2, the correlation between da/dN and ΔK can be described by the Paris law:

$$\frac{da}{dN} = C \cdot \Delta K^n \quad (\text{Eq. 5.44})$$

where

C and n – material-specific crack propagation constants

$$\Delta K = \Delta \sigma \sqrt{\pi a} \cdot f \quad (\text{Eq. 5.45})$$

K_{\max} approaches the material toughness (K_{IC}, K_c) at ΔK values above region 2 and crack growth increases very quickly with a rising ΔK (the instability area)

Data for fracture mechanical calculations

Fracture mechanical calculations require knowledge about material data ($K_{IC}, K_c, \Delta K_{th}, C, n$), the geometric factor, f , in the expression for stress intensity and about existing defects or crack depths.

Threshold value for crack propagation, ΔK_{th}

The threshold value depends mainly on the microstructure of the steel and local R ratio, including residual stress. It is reasonable to assume that there is high residual stress in welded joints and therefore it can be conservatively assumed an R ratio above 0.5, when using *table 5.25* to estimate the threshold value.

Fracture toughness and impact toughness, Charpy

As mentioned above, fracture toughness and impact toughness should not be mixed up. Fracture toughness for structural steels is generally in the interval of $50 < K_{IC} < 250 \text{ MP}\sqrt{\text{m}}$. Impact toughness for hot-rolled plates in delivery condition can generally be specified; see also section 4.7. If fracture toughness data is not available, the following correlations can give a very rough approximation based on impact toughness data [5.37]. See also figure 5.91. For fatigue calculation based on fracture mechanics the fracture toughness is rarely necessary, because of a very high fatigue crack growth rate in region 3, see figure 5.90.

$$\begin{cases} K_c = 11,76 \cdot KV^{0,66} & KV \leq 45 \text{ J} \\ K_c = 54,40 \cdot KV^{0,26} & KV > 45 \text{ J} \end{cases} \quad (\text{Eqn. 5.46})$$

Crack propagation constants C and n

Crack growth is less dependent on microstructure and the R relationship in the linear Paris region than in the threshold and instability region. This means that the same crack propagation data can be used for parent material and weld material. Crack growth is, furthermore, independent of yield strength and tensile strength in both parent and

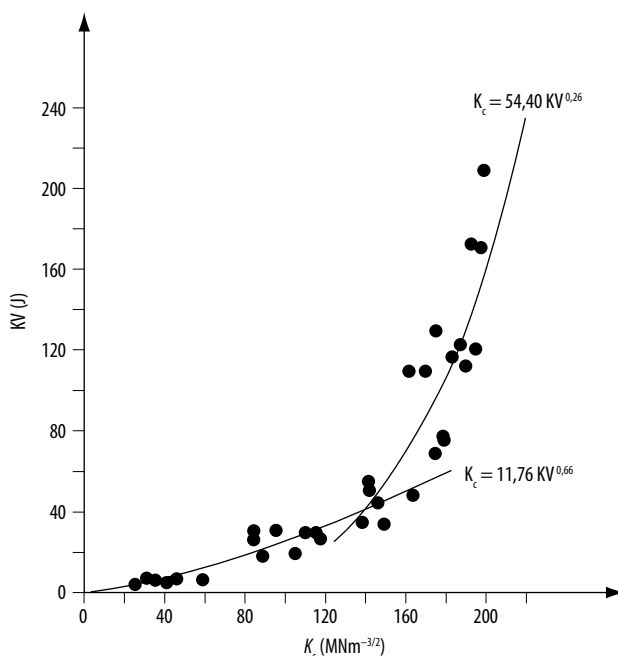


Figure 5.91: Correlation between notch toughness and fracture toughness [5.36].

weld material. Since time (or number of load cycles) for initiating a fatigue crack in welded joints is negligible and the fatigue process is dominated by crack growth in the Paris area, fatigue strength in welded joints is independent of the parent and filler material yield strength.

The crack propagation constants C and n and the threshold value DK_{th} according to the IIW are listed in table 5.25. These values apply for a 2.3% failure probability and agree well with testing and calculations for welded joints in SSAB steel [5.38].

Stress intensity unit and crack propagation rate	C	n	Threshold value ΔK_{th}			
			R ≥ 0,5	0 ≤ R ≤ 0,5	R < 0	Surface crack $a < 1\text{mm}$
$K(\text{Nmm}^{-3/2}) da/dN (\text{mm/cycle})$	$5,21 \cdot 10^{-13}$	3,0	63	170-214-R	170	≤ 63
$K(\text{MPa}\sqrt{\text{m}}) da/dN (\text{m/cycle})$	$1,65 \cdot 10^{-11}$	3,0	2,0	5,4-6,8-R	5,4	$\leq 2,0$

Table 5.25: Crack growth constants according to the IIW.

Geometry factor

The geometry factor, f, is often divided into a number of sub-factors, each of which takes into account a special geometry effect [5.39]. If the distance between the crack front and the external surface of the body in front of the crack is significantly larger than a , f can be approximated with

$$f = 1,12 f_{10} \quad \text{surface crack} \quad (\text{Eqn. 5.47})$$

$$f = f_{10} \quad \text{inner crack} \quad (\text{Eqn. 5.48})$$

where f_{10} is taken from figure 5.92.

Sufficient accuracy for the most common fatigue cracks in welded joints (shallow surface cracks, $a/t < 0,2$, and long crack, $a/c < 0,1$) is usually obtain by approximating f with

$$f = 1,12 M_k \quad (\text{Eqn. 5.49})$$

where M_k is a factor that corrects the for the crack being situated in a region with external stress concentration. M_k depends on the degree of stress concentration, K_t , and the crack depth, a . For $a \rightarrow 0$ means that $M_k \rightarrow K_t$.

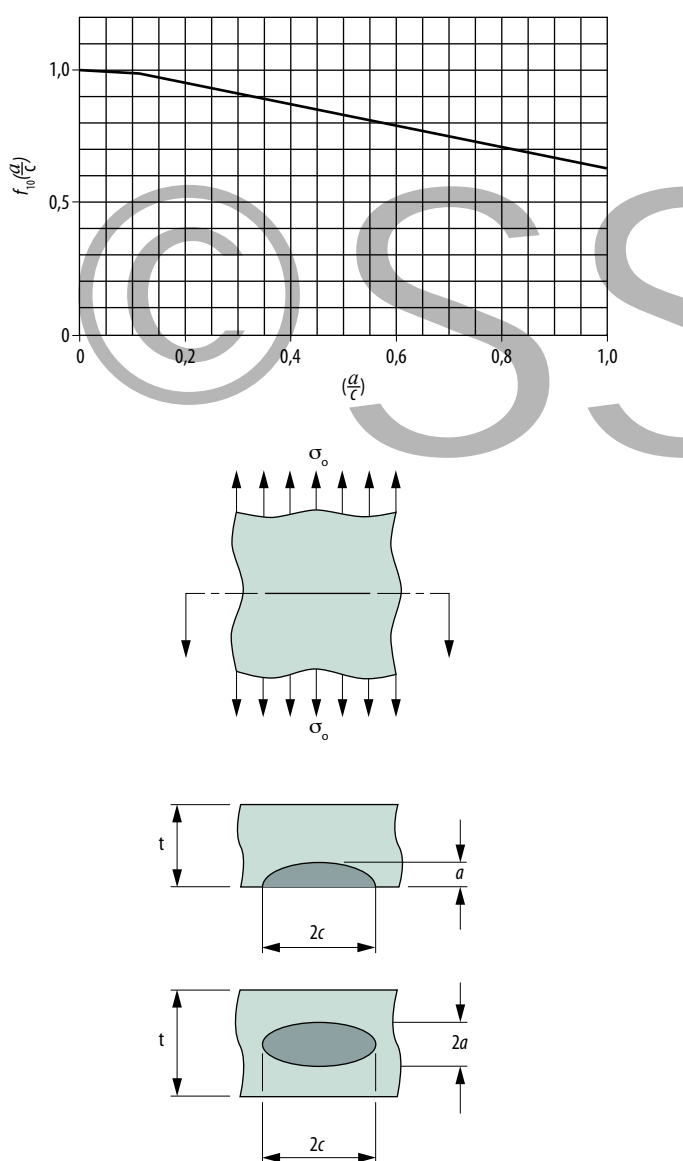


Figure 5.92: Geometry factor f_{10}' [5.40].

a/t	M_k in connection with pure tension								
	0,500	1,000	1,000	1,000	1,000	1,000	1,000	1,000	1,000
0,200	1,000	1,000	1,000	1,019	1,057	1,111	1,157	1,146	1,146
0,100	1,000	1,013	1,067	1,113	1,173	1,259	1,335	1,316	1,316
0,050	1,029	1,075	1,151	1,216	1,301	1,441	1,557	1,557	1,557
0,020	1,111	1,240	1,423	1,558	1,715	1,914	2,068	2,069	2,069
0,010	1,377	1,537	1,764	1,931	2,127	2,373	2,564	2,564	2,564
0,005	1,707	1,905	2,186	2,394	2,636	2,941	3,179	3,179	3,179
0,002	2,268	2,530	2,904	3,181	3,502	3,907	4,223	4,223	4,223
0,001	2,811	3,137	3,600	3,943	4,341	4,844	5,235	5,235	5,235
L/t	0,2	0,3	0,5	0,7	1,0	1,5	2,0	3,0	5,0

a/t	M_k in connection with pure bending								
	0,500	1,000	1,000	1,000	1,000	1,000	1,000	1,000	1,000
0,200	1,000	1,000	1,000	1,000	1,000	1,000	1,000	1,000	1,000
0,100	1,000	1,000	1,000	1,021	1,054	1,054	1,054	1,054	1,054
0,050	1,021	1,058	1,113	1,154	1,202	1,202	1,202	1,202	1,202
0,020	1,156	1,212	1,309	1,404	1,514	1,514	1,514	1,514	1,514
0,010	1,338	1,457	1,622	1,741	1,876	1,876	1,876	1,876	1,876
0,005	1,659	1,807	2,011	2,158	2,326	2,326	2,326	2,326	2,326
0,002	2,204	2,400	2,672	2,367	3,090	3,090	3,090	3,090	3,090
0,001	2,732	2,975	3,312	3,554	3,831	3,831	3,831	3,831	3,831
L/t	0,2	0,3	0,5	0,7	1,0	1,5	2,0	3,0	5,0

Table 5.26: M_k for butt and fillet welds. Note that when a/t is relatively big, say, $a/t > 0,2$, the approximation $f = 1,12 M_k$ does not apply.

M_k in tension and bending for butt welds and non-load-carrying fillet welds is indicated in table 5.26 [5.41]. If the weld geometry is known in detail (flank angle, cathetus length and thickness of connecting part), more exact correlations can be used, [5.36, 5.39, 5.42 and 5.43].

The designations for crack length a , plate thickness t and length L between the weld edges of the joint are clear from figure 5.93.

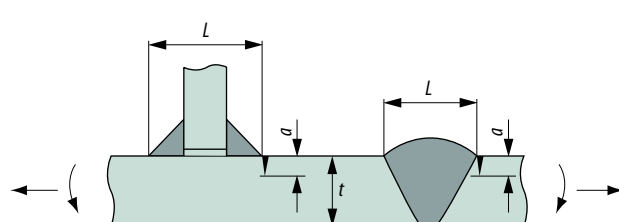


Figure 5.93: Geometries pertaining to table 5.26 in connection with determining M_k for butt and fillet welds, ref [5.41].

Initial crack depth

Fracture mechanical analyses are usually not performed for defects that normally appear in materials or welded joints but when unexpected major defects are found. Different studies show that defects of 0.3 to 0.4 mm can exist in normal untreated (not ground or TIG dressed) butt and fillet welds, see section 5.5.7.

Assessment if a defect is growing

Based on the threshold value, we can calculate the maximum stress range, $\Delta\sigma_{th}$, which will not propagate a known crack, or the size of crack, a_{th} , which will not propagate under a certain stress range. *Equation 5.45* gives

$$\Delta\sigma_{th} = \Delta K_{th}/(\sqrt{\pi}af) \quad (\text{Eq. 5.50})$$

$$a_{th} = \frac{(\Delta K_{th}/(\Delta\sigma f))^2}{\pi} \quad (\text{Eq. 5.51})$$

Critical defect size with regard to brittle fracture

The critical size of the defect is obtained directly from *equation 5.39* and *equation 5.40*

$$a_c = \frac{(K_{IC}/(\sigma_{max}f))^2}{\pi} \quad (\text{Eq. 5.52})$$

Assessment of the number of load cycles until critical crack size.

Paris law can be used directly to compare how quickly different cracks will grow.

In order to calculate how many load cycles are required for growth of a crack from a certain size, a_i , to another, a_f , *equation 5.44* must be integrated according to

$$\frac{da}{dN} = C \cdot \Delta K^n = C[\Delta\sigma \sqrt{\pi}af(a)]^n$$

which gives

$$\frac{da}{[\sqrt{a}f(a)]^n} = C[\Delta\sigma \sqrt{\pi}]^n dN$$

and

$$\int_{a_i}^{a_f} \frac{da}{[\sqrt{a}f(a)]^n} = \int_{N_i=0}^{N_f} C[\Delta\sigma \sqrt{\pi}]^n dN$$

finally

$$N_f = \frac{1}{C[\Delta\sigma \sqrt{\pi}]^n} \cdot \int_{a_i}^{a_f} \frac{da}{[\sqrt{a}f(a)]^n}$$

The calculations can be simplified by assuming a constant geometry factor, f . Start with small increments and vary the increment size in order to see what is best with regard to the desired accuracy.

Select a number of different relevant crack depths and adapt a polynomial to them that can be integrated; see *figure 5.94*.

The variation in stress intensity governs the progress of fatigue under a fatigue load. In general, the risk of unstable fracture should be investigated. Stress intensity must be calculated using maximum nominal stress plus any residual stress.

Defect tolerance diagram

A defect tolerance diagram, which provides the approximate correlations between defect depth, a , and stress, is shown in *figure 5.95*. The curves for limited service life are calculated with $n = 3$ and $C = 5,21 \cdot 10^{13}$. The diagram applies for $a/t < 0.2$ and $R = 0$. The geometry factor $f = 1.0$. If the geometry factor $f \neq 1$, $\Delta\sigma$ in the diagram can instead be set to $\Delta\sigma \cdot f$.

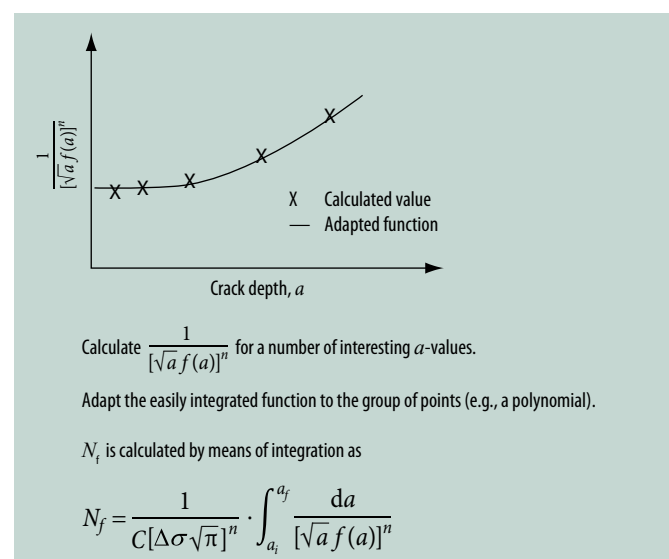


Figure 5.94: Integration of Paris' law.

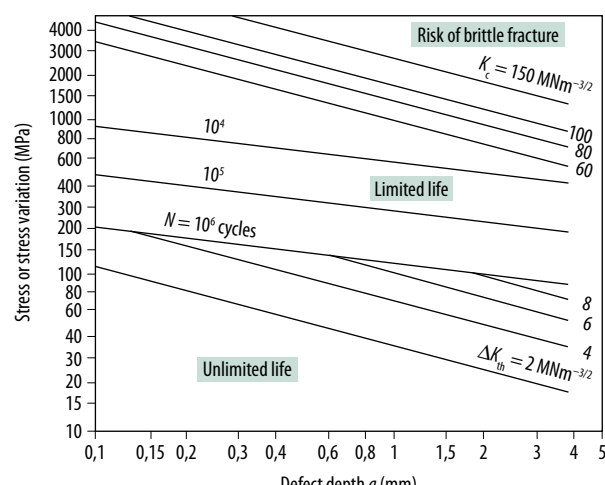


Figure 5.95: Defect tolerance diagram [5.34].

Crack growth based on FE calculations and linear fracture mechanics

As FE calculations are used for the purpose of making service life assessments using linear elastic fracture mechanics, this can be done by direct determination of the stress intensity, K , at different crack depths or by using approximate weight functions.

Service life calculations through direct determination of stress intensity

The crack tip is made up of a singular point in 2D and of a line in 3D. Despite the singularity, there are a number of commercial FE-software that offer the possibility to calculate the stress intensity K via special routines. If the variation in load is known, the variation in stress intensity ΔK can be calculated. If the load is applied perpendicular to the crack (most often the load that dominates crack growth), ΔK , is obtained; see figure 5.96.

The most basic calculation is by using two-dimensional geometry, e.g., with plane strain elements. The crack is then represented one-dimensionally and corresponds to a line crack. The service life length can then be integrated when the stress intensity has been determined for several different crack depths. This is time-consuming if automatic re-meshing cannot be used. Using this as guidance, you can model a correct crack path for geometries where the path of the crack is known, e.g., due to testing or breakdowns. Special programs (FE or based on a standard) focusing only on crack growth through fracture mechanical calculations can be an efficient aid many times; see, e.g., [5.44 and 5.45]. Quite many programs have built-in functions for automatic re-meshing after each increment in the

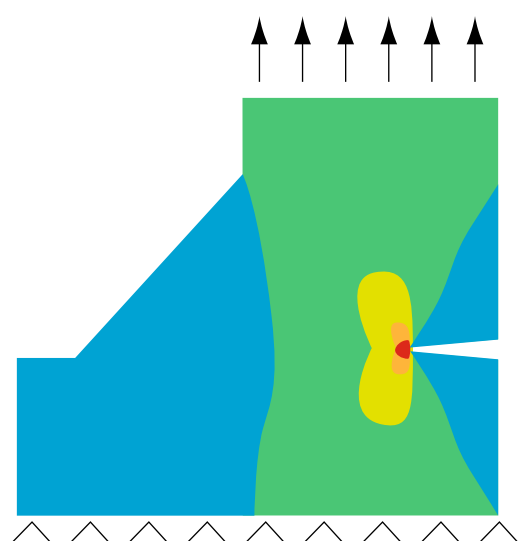


Figure 5.96: Root crack in fillet welded joint.

crack propagation, see also ref. Programming these functions into ordinary FE programs requires a lot of work, in particular, if the direction of the crack growth needs to be handled automatically; see also [5.46, 5.47 and 5.48].

Service life calculation through approximate weight functions

An engineering method for crack growth calculations is to use FE programs in combination with software based on weight functions [5.34]. The methodology is based on assumptions about the crack path and a stress gradient is calculated for a given load on the intact component using the FE program, see figure 5.97. Guidance for crack paths for common geometries can be obtained from table 5.19, which indicates the beginning of the crack in certain cases or, alternatively, from experience with the respective component. The stress gradient in the y -direction, see figure 5.97 is the input for the fracture mechanical calculation. The weight function approach enables calculations with a great number of crack geometries, e.g., line or half-elliptical cracks. The crack propagation constants n and C and the initial crack depth constitute the main input data. It is also possible to simulate the R value dependence provided that the respective residual stress state is known; see also [5.49].

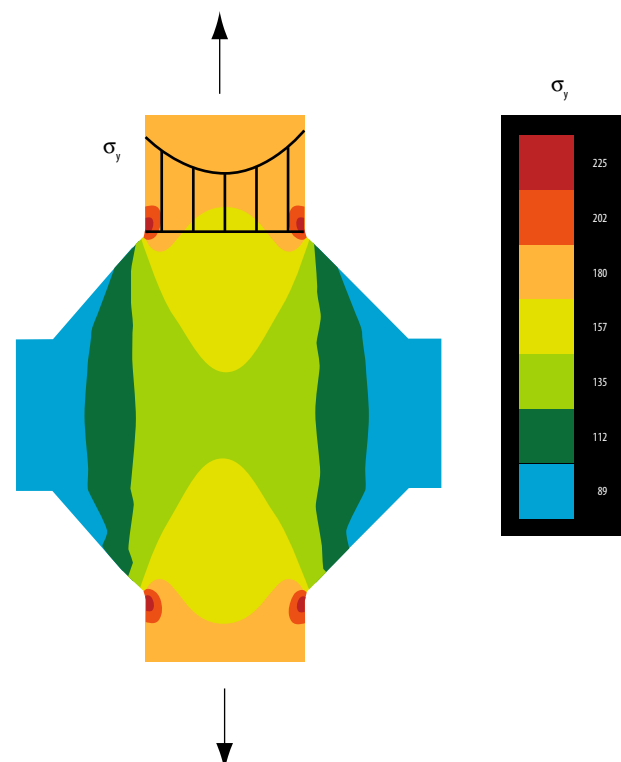


Figure 5.97: Stress gradient along the assumed crack path for toe crack in fillet welded joint.

Example 6

An approx. 1-mm-deep crack-like surface defect has been found in a 12-mm plate. The defect has a length of 10 mm and lies perpendicular to the highest stress level. The plate will be exposed to a fatigue load of $\Delta\sigma = 60 \text{ MPa}$ and a static max load of $\sigma_{\max} = 590 \text{ MPa}$. Is the defect acceptable if infinite service life is desired?

$$K_C = 60 \text{ MPa}\sqrt{\text{m}}, \Delta K_{\text{th}} = 6 \text{ MPa}\sqrt{\text{m}}.$$

Solution:

Surface crack gives equation 5.39, 5.47

$$K_I = \sigma\sqrt{\pi a} \cdot f$$

$$f = 1,12 f_{10}$$

$$K_I = 1,12 \cdot \Delta\sigma\sqrt{\pi a} \cdot f_{10}$$

Fatigue

$$\Delta\sigma \cdot f = 1.12 \cdot 60 \cdot 1 = 67 \text{ MPa}$$

Figure 5.99 gives the critical defect depth. Read a_{th} as the intersecting point between $\Delta\sigma \cdot f = 67 \text{ MPa}$ and $\Delta K_{\text{th}} = 6 \text{ MPa}\sqrt{\text{m}}$.

$$a_{\text{th}} \approx 2.4 \text{ mm}$$

“Brittle fracture”

$$\sigma_f = 1.12$$

$$\sigma_{\max} = 1.12 \cdot 590 = 661 \text{ MPa}$$

$$\text{Critical defect depth } a_C \approx 2,5 \text{ mm.}$$

Answer:

Fatigue is decisive and the critical defect size $a_{\text{th}} \approx 2.4 \text{ mm}$, i.e., a safety factor of 2.4. A defect of 1 mm is therefore acceptable.

5.6.13 General advice about FEM in connection with fatigue design

As FE calculations are used for fatigue design, in addition to the guidance given in section 4.4 and the prerequisites applicable to the respective method (nominal stress, Hot Spot and effective notch), it is also important to have knowledge about the prerequisites and element definitions applicable to the current FE program. Some common element types and their use are described briefly and based on [5.23 and 5.29].

Beam elements

Beam elements can transfer tension, compression, bending, shear and torsion. Beam elements have the advantage of being easy to use, which makes modeling work go relatively fast. Beam elements can be used to calculate nominal stress. If the fatigue class for this joint is known, fatigue design can be carried out according to the nominal stress method. The limitation faced by beam elements is that they cannot be used to analyze local stress in a weld and are therefore not directly usable in connection with the application of the Hot Spot and the effective notch methods. In principle, all FE programs support Saint-Venant torsion for beam elements. On the other hand, there are extremely few programs that support Vlasov torsion for beam elements. Vlasov torsion gives rise to normal stress, above all, in thin-walled open cross-sections where warping is prevented. Such stress can be significant and, in such cases, is important to quantify during fatigue design. The program must therefore be able to handle the warping stiffness cross-section factor, K_w ; see also section 4.3.8. The reason why few FE programs support Vlasov torsion is that beam elements usually get their properties (area, surface moment of inertia, torsional stiffness) in the cross-section's gravity center. Beams with cross-sections which are bisymmetric and are exposed to torsion can be affected by these problems as the torsion center and gravity center do not coincide for them. If a force affects, e.g., a C-section in its center of gravity, a torsional moment is going to give rise to Vlasov normal stress if warping of the cross-section is prevented. If beam elements are then used to calculate the effect of this, the relevant element type must support the axial misalignment between the torsion center and the center of gravity. If this is not possible, the use of shell elements is recommended instead.

Solid elements

Solid elements can be said to be the most versatile elements but also the elements that require the most in the form of calculation and work effort. Solid elements usually exist in the form of prismatic, pyramid or tetrahedral elements. The latter are often associated with automatic mesh generation based on a CAD model. Brick elements often require manual generation but, on the other hand, provide better calculation precision than tetrahedrons. Solid elements are often required for analyzing stress in welded nodes. As solid models require more in the form of modeling and even more calculation effort than shell models, sub-models made of solid elements in combination with a global model built only of shell elements are often used. Displacements along section surfaces in the global model are transferred to the sub-model as boundary conditions. Alternatively, no sub-model is made. Smaller parts of the global model can instead be made of solid elements and the rest of, e.g., shell elements. As solid elements are used in combination with the Hot Spot method and the geometrical stress has to be extrapolated from the current FE model, it should be made sure that the non-linear stress component that exists in direct connection with the weld toe is actually excluded. This is done by dividing the stress distribution into membrane stress, bending stress and the non-linear stress peak, whereupon only membrane and bending stress are added to the respective extrapolation points and the extrapolation is subsequently carried out.

Shell elements

Shell elements are often used for welded structures containing thin plates. Beam structures are often modeled using shell elements. A global model built up with relatively coarse element distribution and of shell elements can be used to identify points which are critical with regard to fatigue. Refined studies can subsequently be performed of these points. Shell elements can be used to calculate geometric stress when the Hot Spot method is applied. The Hot Spot method presupposes that the non-linear stress component that exists in direct connection with the weld toe is excluded. This function can be said to be built into the shell elements as they automatically exclude the non-linear stress component. See also section 5.6.8. It should be known that sometimes there is local bending arising in the connection between different plates modeled as shell elements, e.g., in connection with reinforcements. If the nominal stress method is used in combination with shell elements during fatigue design, it should be checked if the local bending is covered by the relevant fatigue class. If this is the case, the additional local bending should not be included in the nominal stress according to the FE model.



Polynomial degree for elements

As models are built up with shell elements or solid elements, these should, as a rule, be parabolic. Parabolic elements analyze stress gradients better than linear elements and give a better approximation of curved edges. Linear elements provided a faceted stress picture of a notch made up of a curved edge. An example of a curved edge is when the effective notch method is applied. A radius of 1 mm is then modeled at the weld toe and the stress is read locally. As solid elements are used for assessing Hot Spot stresses, a limitation of the polynomial degree can, in certain cases, be used to exclude the non-linear stress peak.

Combinations of different types of elements

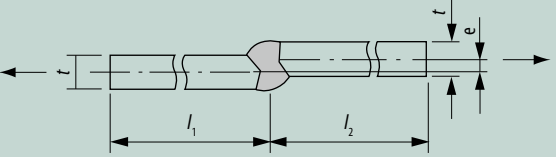
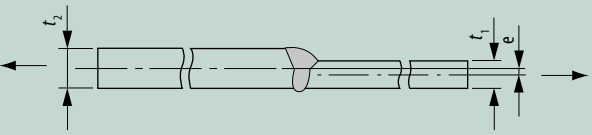
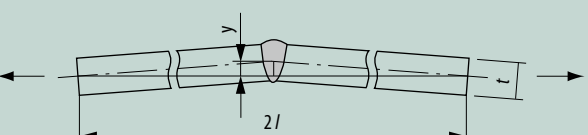
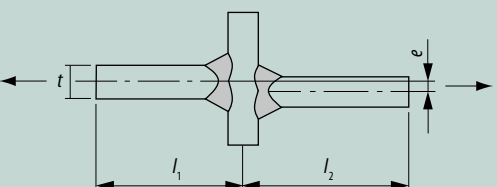
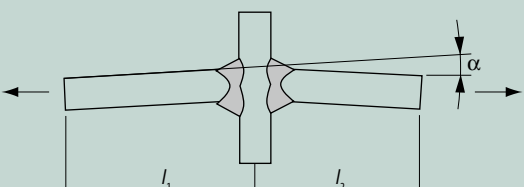
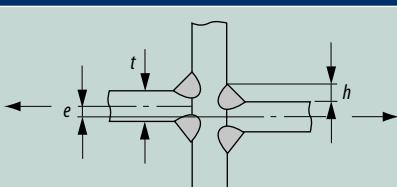
Different element types are often combined to save calculation efforts but also for modeling reasons. This is done automatically for most FEM software available. When different element types are combined, the displacement and rotations that affect the results are able to transfer among the different types of elements. An example of this is a transition between solid elements and shell elements where the shell element has five degrees of freedom (three displacements and two rotations per node) and the solid element has three degrees of freedom (three displacements per node). This means that a shell element in this case cannot transfer moment in all directions to the solid elements. This can be remedied sometimes by using MPC (Multi Point Constraint) where, for example, a shell element can

be forced to transfer a bending moment. Another way is to cover the surface section of the solid element with shell elements or to pull the shell elements a bit into the solid elements. Both these methods, however, increase the stiffness in the model.

Assessment

The Hot Spot method and the effective notch method are based on a calculation of stress components perpendicular to the weld. Assessing comparative stress according to, e.g., von Mises should be avoided. You should instead use principal stress or divide the stress into components parallel or perpendicular to the weld's longitudinal direction. Comparative stress should be used only in order to identify critical areas in a structure. Stress should then not be assessed in singular points as stress in a singular point depends on the element distribution and convergence cannot be achieved. Attention during shell modeling should be paid to which side the results are read on. The assessment will be facilitated if all shell elements are oriented unambiguously, e.g., with their normal direction from a structure in a global model. Not only nodal stresses should be assessed as these are made up of the mean values from the adjacent elements' corner nodes. Stress builds up in critical points, e.g., in a splice between two plates of different thicknesses assessed with FEM, which leads to stress underestimation. Then it is important to continuously check during the calculations that the calculated reaction forces correspond to the applied loads. It is also important during sub-modeling to cut out the sub-model at a sufficiently large distance from the current notch so that the original stress field around it is not affected. Finally, it is good to check the reasonability in results with estimated calculations. Studies comprising assessments using the nominal stress method, the Hot Spot method, the effective notch method, fracture mechanics and full-scale tests of complex welded structures are available in [5.46, 5.50 and 5.51].

5.6.14 Appendix A – Calculation of correlation factor for angular and axial misalignment

Axial misalignment between flat plates	
	$\omega_{ax} = 1 + \lambda \cdot \frac{e \cdot l_1}{t \cdot (l_1 + l_2)}$
λ is dependent on restraint, $\lambda=6$ for unrestrained joints. For remotely loaded joints assume $l_1=l_2$.	
Axial misalignment between flat plates of differing thickness	
	$\omega_{ax} = 1 + \frac{6 \cdot e}{t_1} \cdot \frac{t_1^n}{t_1^n + t_2^n}$
Relates to remotely loaded unrestraint joints. The use of $n=1.5$ is supported by tests.	
Angular misalignment between flat plates	
	$\beta = \frac{2 \cdot l}{t} \cdot \sqrt{\frac{3 \cdot \sigma_m}{E}}$
Fixed ends	
	$\omega_{ang} = 1 + \frac{3 \cdot \gamma}{t} \cdot \frac{\tanh(\beta/2)}{(\beta/2)}$
Pinned ends	
	$\omega_{ang} = 1 + \frac{6 \cdot \gamma}{t} \cdot \frac{\tanh(\beta)}{\beta}$
The tanh correction allows for reduction of angular misalignment due to the straightening of the joint under tensile loading. It is always ≤ 1 and it is conservative to ignore it, σ_m is membrane stress range. When a reduction due to angular misalignment is calculated, shall every stress range $\Delta\sigma_i$ and $\Delta\sigma_{max}$ according to equation 8 be multiplied by the effective correlation factor according to equation 17.	
Axial misalignment of cruciform joints (toe cracks)	
	$\omega_{ax} = 1 + \lambda \cdot \frac{e \cdot l_1}{t \cdot (l_1 + l_2)}$
λ varies from $\lambda=3$ (fully restrained) to $\lambda=6$ (unrestraint). For unrestrained remotely loaded joints assume; $l_1=l_2$, and $\lambda=6$.	
Angular misalignment of cruciform joints (toe cracks)	
	$\omega_{ang} = 1 + \lambda \cdot \alpha \cdot \frac{l_1 \cdot l_2}{t \cdot (l_1 + l_2)}$
If the in-plane displacement of the transverse plate is restricted, λ varies from $\lambda=0.02$ to $\lambda=0.04$. If not, λ varies from $\lambda=3$ to $\lambda=6$.	
Axial misalignment in fillet welded cruciform joints (root crack)	
	$\omega_{ax} = 1 + \frac{e}{t + h}$
ω_{ax} refers to the stress range in weld throat.	

There are more examples according to IIW [5.1] which deal with angular and axial misalignment for cylindrical structures.

5.6.15 Symbols

$\Delta\sigma_{\max}$	Maximum stress range
$\Delta\sigma_{\text{ref}}$	Stress range reference value
$\Delta\sigma_{\text{Sd}}$	Design value of stress range
$\Delta\sigma_{\text{Rd}}$	Permitted stress range
γ_f	Partial safety factor with regard to load
γ_m	Partial safety factor with regard to fracture risk
FAT	Fatigue resistance value, FAT stands for fatigue
φ_t	Thickness improvement factor
φ_m	Material factor
φ_e	Fatigue enhancement factor
s_m	Stress history parameter
σ_{\max}	Maximum stress at current calculation point
σ_{\min}	Minimum stress at current calculation point
k_m	Stress spectrum factor
N_t	Design total service life
$\Delta\sigma_i$	Stress range at level i
n_i	Number of load cycles at level i for a representative part of the stress history
m	Exponent or index for the inclination of S-N curve (not for γ_m and φ_m)

5.7 References

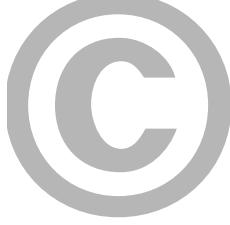
- [5.1] Hobbacher, A.
Recommendations for fatigue design of welded joints and components.
International Institute of Welding,
document XIII-1965-03/XV-1127-03.
- [5.2] CEN/ TC 147, prEN 13001-3-1:2009
Cranes – General Design – Part 3-1: Limit States and proof of competence of steel structures, 2009–10.
- [5.3] Pilkey, W. D.
Peterson's Stress Concentration Factors.
John Wiley & Sons Inc., 1997, ISBN 0-471-53849-3.
- [5.4] Haagensen, P.J., Maddox, S.J.
Recommendations on post weld improvement of steel and aluminium structures.
International Institute of Welding, document XIII-1815-00, rev. 2006.
- [5.5] Sperle, J-O., Nilsson, T.
The application of high strength steel for fatigue loaded structures.
Proceedings from HSLA Steels Conference, Beijing 1992.
- [5.6] Sperle, J-O.
Influence of parent metal strength on the fatigue strength of parent material with machined and thermally cut edges.
Welding in the World, Vol. 52 No 7/8, 2008, pp.79–92.
- [5.7] Larsson, J.
On the fatigue strength of Domex 1200.
SSAB Strip Products, Technical Report 090435, 2009.
- [5.8] Nilsson, T., Engberg, G., Trogen, H.
Fatigue properties of hot-dip galvanized steels.
Scandinavian Journal of Metallurgy 18 (1989), pp. 166.
- [5.9] Sperle, J-O.
Fatigue strength of high strength dual-phase steel sheet.
International Journal of Fatigue, No 2 (1985) pp 79–86.
- [5.10] SS-EN-ISO 9013
Thermal cutting – Classification of thermal cuts – Geometrical product specification and quality tolerances.
(ISO 9013:2002), revision 2.
- [5.11] Eriksson, Å., Lignell, A-M., Olsson, C., Spennare, H.
Svetsutvärdering med FEM
Handbok för utmattningsbelastade konstruktioner
(in Swedish).
VI, Industrilitteratur 2002, ISBN 91-75-636-9.
- [5.12] Fogningshandboken
Sammanfogning av höghållfast stål.
SSAB Tunnplåt AB, 2004.
- [5.13] Nilsson, T.
Manufacturing Guidelines when Using Ultra High Strength Steels in Automotive Applications.
ECSC Final report from SSAB - Part 2: Fatigue, 2004.
- [5.14] Sperle, J-O.
Strength of spot welds in high strength steel sheet.
Metal Construction (1983), Vol. 15, No. 4.
- [5.15] Gurney, T. R.
Fatigue of thin walled joints under complex loading.
Abington Publishing special report, Cambridge, England, 1997.

- [5.16] Gustafsson, M.
A Study of Thickness Effect on fatigue in thin welded high strength steel joints.
Steel Research International, No 77, (2006), pp. 873–881, 2006.
- [5.17] Maddox, S. J.
Fatigue strength of welded structures.
TWI, Abington Publishing Ltd, 2nd edition, 1991.
- [5.18] Dahle, T.
Spectrum Fatigue of Welded Components, Licentiate Thesis, Report 2001–11.
Royal Institute of Technology, Stockholm, 2001.
ISSN 0280-4646.
- [5.19] Olsson, Claes.
Konstruktionshandbok för svetsade produkter.
Stockholm: Industrilitteratur AB, 2005. Utgåva 3.
ISBN 91-7548-677-6.
- [5.20] Olsson, Claes.
Cumulative Damage Analysis, computer program for cummulative damage analysis of welded structures.
TechStrat of Sweden AB, 2008.
- [5.21] ASTM. ASTM E1049 - 85(2005)
Standard Practices for Cycle Counting in Fatigue Analysis.
American Society for Testing and Materials, ASTM, 2005.
- [5.22] Samuelsson, J. [ed.].
Design and Analysis of Welded High Strength Steel Structures.
Stockholm: Emas Publishing Ltd., 2002. Conference proceeding.
ISBN 1 901 537 34.
- [5.23] Eriksson, Å., Lignell, A-M., Olsson, C., Spennare, H.
Svetsutvärdering med FEM. Handbok för utmattningsbelastade konstruktioner.
Stockholm: VI Sveriges Verkstadsindustrier AB, 2002.
På svenska. Translated in English, *Weld evaluation using FEM, A guide to fatigue-loaded structures,*
ISBN 91-7548-665-2. ISBN 91-7548-636-9.
- [5.24] Jonsson, B., Samuelsson, J. och Marquis, G.
Development of weld quality criteria based on fatigue performance.
IIW-dokument XIII-2317-10, 2010.
- [5.25] Haagensen, P. J. IIW
Recommendations on Post Weld Improvement of Steel and Aluminium Structures. Revised July 2010. XIII-2200r7.
- [5.26] Plåthandboken, utgåva VII. SSAB Borlänge: s.n., 1997.
- [5.27] Sperle, J-O.
Proposal for characteristic fatigue strength for holes in a plate under normal stress.
prEN 13001-3-1:2008(E), Annex D, Table D.1, Detail No. 1.3. s.l.: SSAB Tunplåt AB, 2009. Remiss till Europeiska kranstandarden för nya FAT klasser avseende hål där hän syn tas till kanttillstånd, ytjämhet och statisk hållfasthet.
- [5.28] Radaj, D., Sonsino, M., Fricke, W.
Fatigue assessment of welded joints by local approaches.
2:nd edition. Cambridge: Woodhead Publishing, 2006.
ISBN-13: 978-1-85573-948-2.
- [5.29] Zhao, X.-L., Packer, J. A.
Recommended fatigue design procedure for welded hollow section joints.
Cambridge: Abington publishing, 2000.
IIW doc XIII-1772-99.
- [5.30] Niemi, E., Fricke, W., Maddox, S. J.
Fatigue Analysis of Welded Components/Designer's guide to the structural Hot Spot stress approach.
Cambridge: Woodhead Publishing Ltd, 2006. IIW-1430-00.
ISBN-13:978-1-84569-124-0.
- [5.31] Fricke, W.
Guideline for fatigue assesment by notch stress analysis for welded structures.
2008. IIW-Doc XIII-2240r1-08/XV-1289r1-08.
- [5.32] Sonsino, C. M.
Suggested allowable equivalent stresses for fatigue design of welded joints according to the hotch stress-concept with reference radii ref=1.00 and 0.05 mm. s.l.:
2008. IIW-XIII-2216-08/XV-1285-08.
- [5.33] Krantz B., Sonsino, C. M.
Verification of the notch stress concept for the reference radii of ref=1.00 an 0.05 mm.
IIW XIII-2274-09/XV-1312-09.
- [5.34] Andersson, T. L.
Fracture mechanics, Fundamentals and Applications. s.l.: CRC Press, Inc., 2005. ISBN: 9780849316562.
- [5.35] Dawes, M. G.
The CTOD design curve approach: limitations, finite size and application. s.l.:
Welding Institute. Rapport 278/1985.
- [5.36] Almar-Naess, A.
Fatigue Handbook, offshore steel structures.
Trondheim: Tapir, Norges Tekniske Høgskole, 1985.
- [5.37] Sperle, J-O.
Framtagning av grafiskt samband mellan brottseghet och slagseghet.
Borlänge: Svenskt stål AB, 1983. Teknisk rapport SF 154/83.

- [5.38] Gustafsson, M.
Study of thickness effect on fatigue in thin welded high strength steel joints. 77, s.l.:
Steel Research International, No 77, (2006),
pp 873–881, 2006.
- [5.39] Samuelsson, J., Dahlberg, L.
Tillämpning av brottmekanik i utmattningsbelastade konstruktioner.
Stockholm: Jernkontoret, 1978. TO 41-01.
- [5.40] Hedner, G.
Formelsamling i hållfasthetsslära.
Stockholm: KTH, 1986.
- [5.41] Hobbacher, A.
Reccomendations for assesment of weld imperfections in respect to fatigue. s.l.:
International institute of welding, 1987.
Second Draft 12.87, IIW JWG XIII-XV-86-87.
- [5.42] Gurney, T. R.
Stress intensity facors for cracks at the toes of transverse butt welds.
TWI, 2979. Rapport 88/1979.
- [5.43] Gurney, T. R.
Theoretical analysis of the influence of attachment size on the fatigue strength of transverse non-load carrying fillet welds.
TWI, 1979. Rapport 91/1979.
- [5.44] Cornell Fracture Group. [Online] 06 2009.
Fri programvara, *Franc 2D*, program för FE-baserade spricktillväxtberäkningar.
<http://www.cfg.cornell.edu/>.
- [5.45] Automation of fracture and fatigue assessment procedures (BS 7910) for engineering critical assessment.
Cambridge: s.n.
<http://www.twisoftware.com/crackwise>.
- [5.46] Martinsson, J.
Fatigue Assesment of Comlex Welded Structures.
Stockholm: KTH, department of Aeronatutical and Vehicle Engineering, 2005. Doctoral Thesis. ISBN 91-2783-968-6.
- [5.47] Barsoum, Z.
Residual Stress Analysis and Fatigue Assesment of Welded Steel Structures.
Stockholm: KTH, Department of Aeronautical and Vehicle Engineering, 2008. Doctoral Thesis. ISSN 1651-7660.
- [5.48] Björkblad, A.
Fatigue Assessment of Cast Components – Influence of Cast Defects,
Ph.D thesis. Dep. of Lightweight Structures.
Stockholm: KTH, ,KTH, Sweden, 2008.,
ISBN 978-91-7415-101-5.
- [5.49] Afgrow
Fracture Mechanics and Fatigue Crack Growth Analysis software tool, 2009, <http://www.afgrow.net/>.
- [5.50] Byggnevi, M.
LEFM Analysis and Fatigue Testing of Welded Structures.
Stockholm: KTH, 2005. Licentiate Thesis.
ISBN 91-7178-094-7.
- [5.51] Petterson, G.
Fatigue assesment of welded structures with non-linear boundary conditions.
Stockholm: KTH,department of Aeronautical and Vehicle Engineering, 2004. Licentiate Thesis.
- [5.52] Rydahl, L.
Beräkning av S-N kurvans förskjutning med hänsyn till antalet provade komponenter.
Teknisk rapport nr 100444, SSAB 2010.
- [5.53] Inverkan av ett hål nära svets.
Teknisk rapport N1.95LB.12.0305
SSAB, 2012.
- [5.54] Stemne, D.
HFMI-behandling -metod för förbättrade utmattningsegenskaper i svetsförband
Artikel. <http://sbi.se/uploads/source/files/Artiklar/HFMI.pdf>







SSAB

6. Manufacturing

Forming and joining of high strength sheets is nothing new or revolutionary and the processes are not considerably different as compared to mild steel sheet processing. On the other hand, when it comes to forming, for example, certain parameters have to be taken into account such as springback and cutting clearance, as well as the fact that certain joining methods are more suitable for high strength steels than for other steels. Welding processes that induce too much energy are less suitable than other processes where energy input is easy to control.

The development of methods for joining high strength steels is progressing all the time, which means that the properties of high strength steels are increasingly utilized.

6.1 General information

There are no major differences between high strength and mild steels as far as manufacturing is concerned. This statement is especially true for HSLA, Rephosphorus (RP) and DP (Dual Phase) steels, which have excellent formability and low content of alloying elements. A comparison between high strength and mild steels shows that:

- Better trim edges are obtained by size shearing of high strength steel if the cutting clearances are adjusted to the strength and thickness of the steel. However, the requirements on the tool steel are stricter than in the case of mild steel shearing.
- The bending and forming properties are very good even for high strength steel. When choosing high strength steel two major aspects is the larger springback and lower formability as compared to mild steels. More details about processing and forming can be found in SSAB's Forming Handbook.

High strength steels allow problem-free welding. Minor adjustments of the welding parameters may be necessary, mainly during resistance welding.

Surface treatment of high strength steels does not differ so much from the surface treatment of mild steels.

There are many different methods for joining steels, of which welding is the most common. Methods other than welding are also used, such as mechanical joining, adhesive bonding and soldering, cf. *figure 6.48*. Joining of SSAB's high strength steels can be done by all these methods and from a technical perspective it is not so different from the joining of mild steels.

This chapter will primarily describe the standard and most frequently used joining methods with an emphasis on welding. Welding, however, is not always the best option. Other methods can be more appropriate in certain applications. The thickness of the sheet metal and the surface coating also influence the choice of joining method.



Figure 6.1: Trim Edge Definition.

6.2 Cutting

Machine processing can be divided into two main groups of processing methods:

- size shearing; shearing, punching.
- chip removal; drilling and milling. (Turning and sawing are used to a lesser extent.)

Thermal cutting is a high-temperature method, whose closest equivalent is size shearing. Thermal cutting is carried out using an open gas jet, plasma or laser beam.

6.2.1 Size shearing

This group includes shearing, punching, fine blanking and slitting. Fine blanking is an advanced punching method for direct shearing into the final form. The method gives excellent accuracy. An alternative to fine blanking is punching with subsequent adjustment shearing that offers excellent precision as well. Fine blanking and slitting are not discussed in more detail in this chapter. More information about fine blanking and slitting can be found in SSAB's Forming Handbook.

Power shearing [6.1]

There are a few things to take into account during shearing. What should the trim edge look like? How much force do you need to apply? The trim edge quality is of upmost importance. The definition of "trim edge" can be seen in figure 6.1. Other definitions can be found in figure 6.2.

Cutting force during power shearing

The force (F) required to cut a material can be estimated if the tensile strength, thickness and cutting angle are known, see equation 6.1.

$$F = K_{sk} \cdot A = \frac{0.8R_m \cdot t^2}{2 \tan \alpha} \quad (\text{Eqn. 6.1})$$

The cutting shear strength K_{sk} is proportional to the tensile strength of the material and can be expressed as a factor e times the tensile strength. When making rough estimates for mild steels, the factor e can be set to 0.8.

It is evident from equation 6.1 that reducing the sheet thickness by half would reduce the cutting force by 75 %.

Shearing experiments conducted at SSAB show that the e -factor decreases from 0.8 for mild steel to 0.6 for steels with tensile strength of more than 800 MPa. The e factor is clearly shown in figure 6.3.

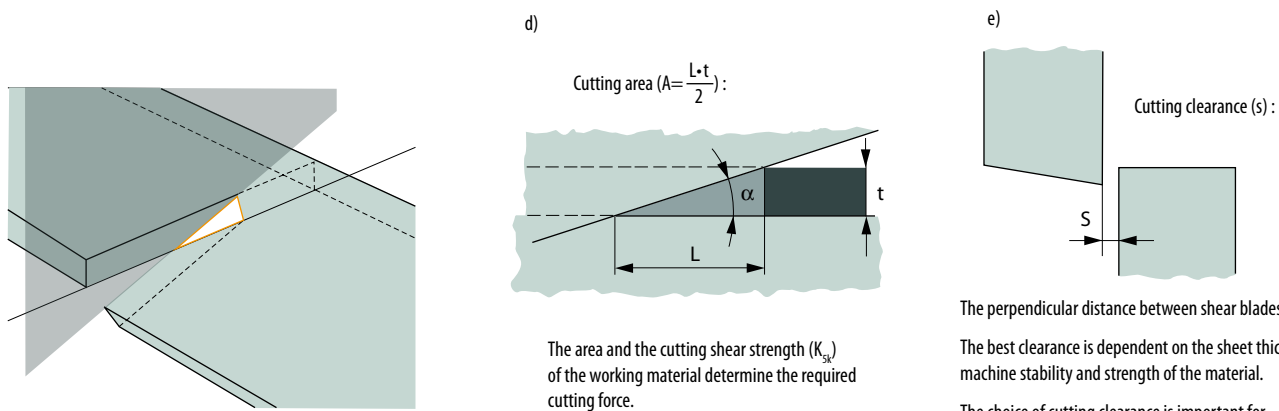
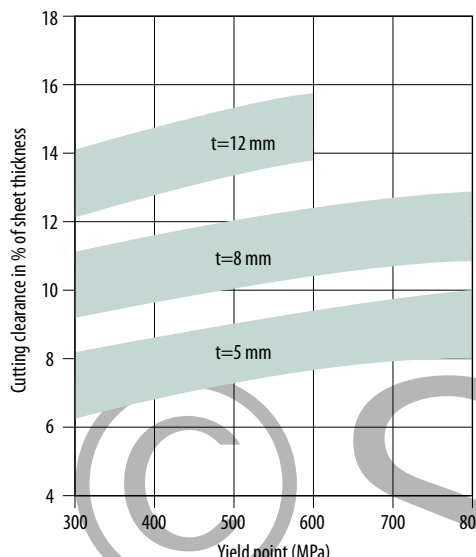


Figure 6.2: Definition of cutting area and cutting clearance.

This handbook contains general suggestions and information without any expressed or implied warranty of any kind. SSAB hereby expressly disclaims all liability of any kind, including any damages, in connection with the use of the information and for their suitability for individual applications.



Recommendations for power shearing

The cutting clearance is the most important parameter for achieving satisfactory results. A good trim edge is also essential for subsequent plastic forming of high strength steel. A bad trim edge can be the starting point for defects during the forming process.

Since machine stability and tool steel condition vary significantly from case to case, it is impossible to give recommendations that apply in all circumstances. The following guideline values obtained at SSAB can be used in order to achieve an optimal trim edge:

If the edge of the sheet metal is to be subject to large plastic deformation, thermal cutting is recommended for high strengths and thicknesses.

A too small cut-off can cause defects in the cutting surface of the remaining sheet metal. For high strengths it is therefore recommended not to make the cuts smaller than four times the sheet thickness.

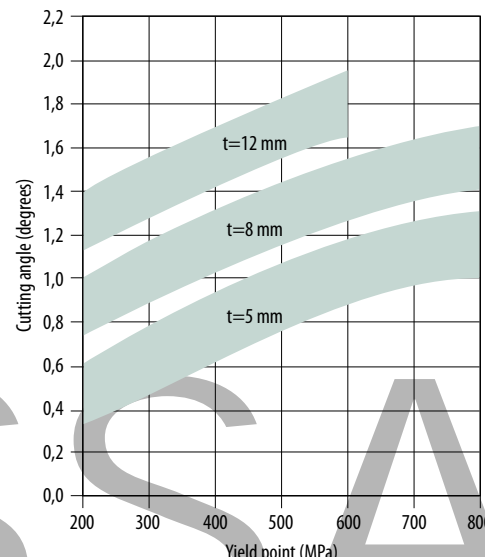


Figure 6.4: Cutting clearance and cutting angle during power shearing as a yield point function.

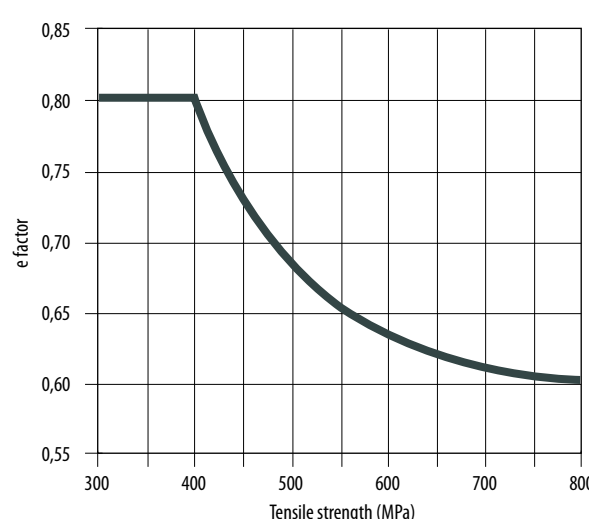


Figure 6.3: The e factor as a function of the tensile strength of the steel.

This handbook contains general suggestions and information without any expressed or implied warranty of any kind. SSAB hereby expressly disclaims all liability of any kind, including any damages, in connection with the use of the information and for their suitability for individual applications. It is the responsibility of the user of this brochure to adapt the recommendations contained therein to the requirements of individual applications.

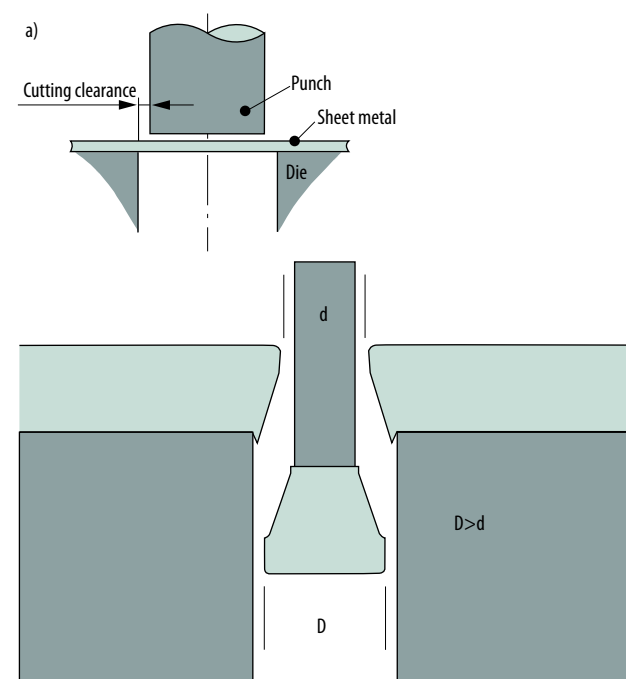


Figure 6.5: Definitions in hole punching.

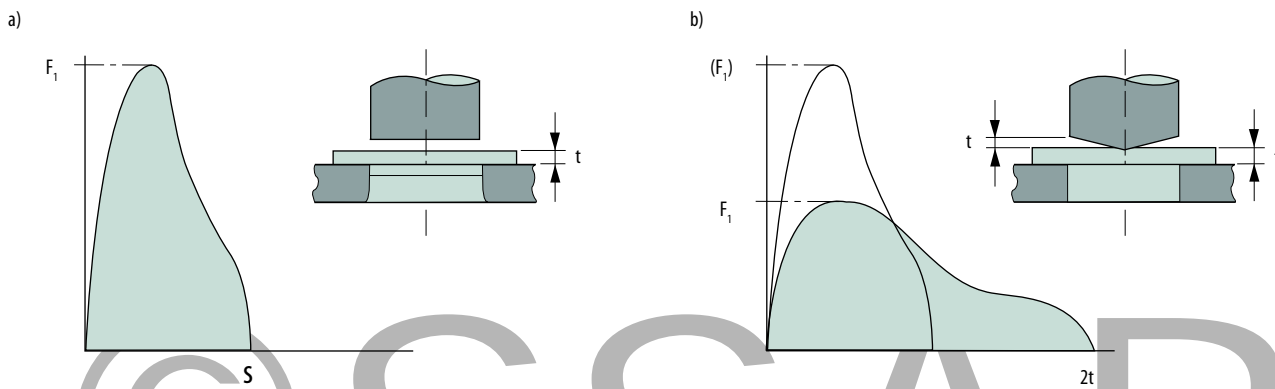


Figure 6.6: A rough estimate of the cutting force for face-and edge-ground punch. L = circumference of the cut hole [6.1].

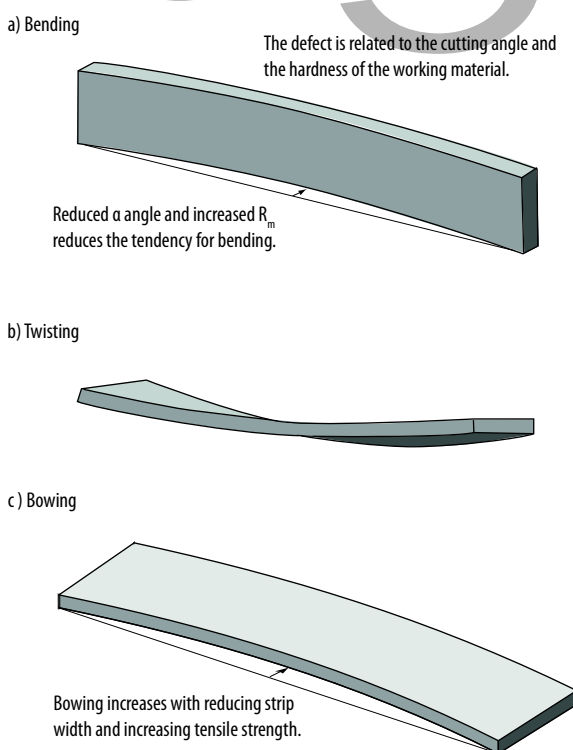


Figure 6.8: Different shape deviations during narrow strips shearing.
Top: twisting, Middle: bending, Bottom: bowing.

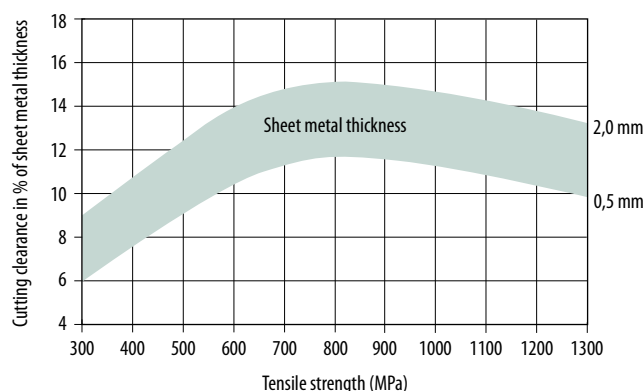


Figure 6.7: Recommended cutting clearance for punching.

Cutting force during punching

In general, it can be stated that wear reduces with increasing clearance and the right-angleness of the cut deteriorates.

The cutting force, F , as a function of the punch path through the sheet metal, is displayed in figure 6.6. If the punch is oblique the necessary force can be reduced by up to 50% as compared to the force applied on a plane-parallel cut surface, cf. figure 6.6. The noise level during punching with an oblique punch is lowered compared to a square punch. Equation 6.2 is used for a rough estimation of the punch force. F_1 is for square punch whereas F_2 is for oblique punch. However, tool wear is greater when oblique punches are used.

$$F_1 = 0.8 \cdot R_m \cdot L \cdot t$$

$$F_2 = 0.67 (0.8 \cdot R_m \cdot L \cdot t) \quad (\text{Eqn. 6.2})$$

Recommendations for punching

During closed geometry cutting (punching), only two parameters can be changed, namely the oblique punches/dies and the cutting clearance.

Oblique punches/dies are used primarily for the purpose of reducing the punching force.

Cutting clearance is decisive for the lifetime of the tool when punching high strength materials. The recommended cutting clearance is customized for a trim edge

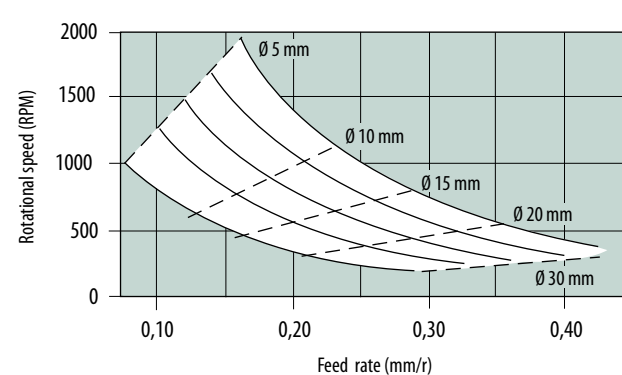


Figure 6.9: Rotation speed and feed rate for drill diameters between 5 and 30 mm during steel sheet metal drilling, Rm approx. 400–850 MPa [6.2].

	Working material Rm (MPa)	End face mills	Slitting cutter	Side-milling cutter	Long edge milling cutter	Cutter heads
Max feed rate (mm/tooth)	< 500	0,13	0,08	0,15	0,2	0,25
	500–700	0,1	0,05	0,13	0,18	0,2
	> 700	0,08	0,05	0,1	0,13	0,15
Max cutting speed (m/min)	< 500	18–28	40–55	16–24	16–24	20–30
	500–700	18–28	40–55	16–24	16–24	18–28
	> 700	17–23	30–45	16–20	15–20	16–24

Table 6.1: Machining data for Domex at high speed steel milling[6.3].

and minimum tool wear, cf. *figure 6.7*. For tensile strengths above 800 MPa, the chipping tendency increases. Chipping can be reduced by reducing the cutting clearance.

Summary of advantages and disadvantages during size shearing of high strength steels

A brief comparison between the cutting properties of high strength and mild steels can be found below:

Trim edges: Burr height, conicity and roll over, cf. *figure 6.1*, are smaller when shearing high strength steels as compared to mild steels. This is so provided that the cutting clearance is customized to the high strength level and thickness of the sheet metal.

Geometrical stability: When shearing narrow strips using power shears, bending and twisting reduces in the case of high strength steels. The bowing, on the other hand, is somewhat higher in sheet metal thicknesses above three mm, cf. *figure 6.8*.

Required force: The cutting force increases with increasing strength. Mild steel sheet are often replaced by thinner high strength sheets and, given the optimization of shearing parameters, the cutting force does not need to increase significantly.

Tool wear: Tool wear increases when shearing high strength steels. It can be reduced through the use of better tool materials, surface treatment and lubrication.

6.2.2 Machining

Machining for thin sheets mainly concern drilling and milling. Turning, planing and sawing are generally used only when working with thick plate($t > 15$ mm). These methods are therefore not discussed here.

Drilling

Holes in hot rolled and zinccoated sheet steel are usually made by punching. An exception is the assembly works where manual drilling is usually used. In these cases, the operator must try to find the best machining data for the object, amongst other things, depending on fixing possibilities and stability.

When drilling in hot-rolled steels please use the guide values in *figure 6.9*. The diagram requires that drilling is done in well-controlled and stable machines and fixing of the work piece takes place close to the drilling area. Holes $\phi > 10$ mm should be pre-drilled. Drilling in high strength steels can be carried out by a high-speed steel or cemented carbide drill. Individual holes can be made using a standard HSS drill. For a rational production, please use a coated, micro-alloyed (HSS-E) drill or a cobalt-alloyed (HSS-Co) drill.

The requirement for effective cooling and lubrication increases with an increase in sheet metal thickness and tensile strength of the working material.

Milling

The recommendations apply for hot-rolled steels and the most common milling types.

Machining data in the following tables, *table 6.1* and *table 6.2*, refer to mills with high-speed steel bits or respectively mills with soldered cemented carbide bits.

The specified cutting speeds correspond to 90 minutes of wear time during conventional milling. In the case of down-cut milling the cutting speeds can be increased by 20%.

	Working material Rm (MPa)	End face mills	Slitting cutter	Side-milling cutter	Long edge milling cutter	Cutter heads
Max feed rate (mm/tooth)	< 500	0,18	0,1	0,2	0,28	0,36
	500–700	0,18	0,1	0,2	0,28	0,36
	> 700	0,15	0,08	0,18	0,25	0,3
Max cutting speed (m/min)	< 500			120–200		
	500–700			100–160		
	> 700			80–120		

Table 6.2: Machining data, hot-rolled steels high speed steel mill [6.4].



6.3 Thermal cutting

Thermal cutting is a generic term for cutting processes that use a heat source to heat the material to melting or ignition temperature, respectively. The heat source can be an open gas jet, an electric arc or a laser beam. Gas comes from the same nozzle. It blows away the molten material so as to form a cut section. The gas can either be inert or active. The active gas (oxygen) oxidizes the molten material and contributes with energy through the exothermal reaction between oxygen and iron. Common for these cutting processes is that a cut section is obtained in a very controlled manner.

To continue, as far as thermal cutting is concerned, the processes have the advantage of not being affected by the hardness of the material, i.e. it is just as easy to cut high strength steel as it is to cut soft steel. Certain alloying elements can affect the cutting result. To find out how and in what way, please contact SSAB.

Two of these methods are discussed below, namely, plasma and laser cutting.

6.3.1 Plasma cutting

Plasma cutting as a machining process saw the light of day at the beginning of the 1960s. Back then it was a relatively expensive process, so only very few workshops were able afford investing in plasma cutting. However, with the advancement of the development, the equipment became less expensive.

Plasma cutting is an alternative to gas cutting, just as high tolerance plasma arc cutting (HTPAC) is an alternative to laser cutting. The subject will be discussed later in this chapter.

Application

As mentioned above, plasma cutting is considered an alternative to gas cutting. Plasma cutting is usually used for materials with a thickness between 6 and 75 mm.

Some of the characteristics of plasma cutting include: No contact between the nozzle and the material; can be used for cutting different types of electrically conductive

materials; plasma cutting produces less heat (linear energy input) than gas cutting, which contributes to achieving narrow cuts and lower thermal deformation. Furthermore, plasma cutting results in a narrower and harder heat-affected zone during the cutting of heat-treated materials as compared to gas cutting. However, the sound level is high (90–120 dBA) and the process generates a lot of fumes (unless it takes place under water).

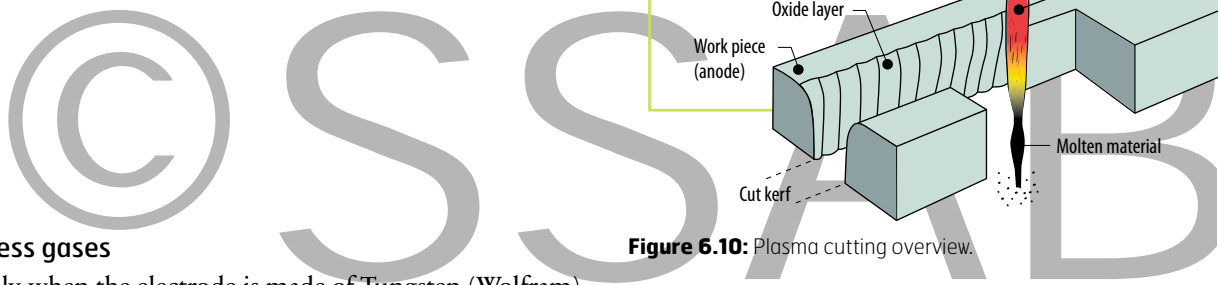
How does plasma cutting work?

Plasma cutting is a fusion cutting process where a beam of ionized gas (plasma) melts the material (the work piece) and blows away the molten material from the cut kerf. To be more exact, during the plasma cutting process, a plasma arc is formed between the electrode and the work piece. The plasma arc becomes concentrated because it is surrounded by a water-cooled nozzle. The temperature of the plasma arc can be very high, up to 30 000° C depending on the gas and the other parameters that are used. When the nozzle approaches the work piece, the arc is transferred between the nozzle and the material, the effect increases and the plasma arc cuts the material. The molten material is blown away from the cut kerf by the strong plasma gas flow, cf. figure 6.10.

Plasma cutting differs from gas cutting by the fact that during plasma cutting the plasma arc melts the material whereas during gas cutting the gas arc ignites the material and the oxygen gas reacts exothermally with the material, which then melts and is blown away from the cut kerf.

The distance between the material and the nozzle varies, but is usually 3–10 mm. Common plasma gases are argon, argon/hydrogen or nitrogen gas. Inert gases are preferable when high cut quality is desired.

In addition, plasma cutting is usually automatic, but manual plasma cutting exists too. Many nozzles can be used during automatic cutting, which naturally increases the productivity, cf. figure 6.11.



Process gases

Usually, when the electrode is made of Tungsten (Wolfram), an inert plasma gas such as argon is used. Oxidizing plasma gases can be used, but in that case the electrode must be made of copper/hafnium. The plasma gas flow is also important. If the gas flow is too low in relation to the set power level or the power level is too low in relation to the nozzle diameter, we will get two plasma arcs in a row. One from the electrode to the nozzle and one from the nozzle to the work piece. Double plasma arcs are usually catastrophic and can cause the nozzle to melt.

Many different gas combinations can be used during plasma cutting, both with regard to the plasma gas and with regard to the shielding gas. Usually, an air/air or an oxygen/air (plasma gas/shielding gas) combination is used during plasma cutting of steels. The important thing is to obtain good cut quality. Good cut quality is often defined as vertical cuts, even surface (low Ra and Rz), as well as a cut that is free from dross (burr). A good advice is to contact the machine supplier in order to get information about appropriate gas combinations for the current application.

High tolerance plasma arc cutting

High tolerance plasma arc cutting (HTPAC) is a further development of the traditional plasma nozzle. In the case of HTPAC, the plasma arc is more concentrated thanks to the fact that it rotates in the nozzle and also that a secondary gas is added outside the plasma arc. HTPAC is most often used during cutting of materials with a thickness below 23–35 mm. The immediate advantage of HTPAC as compared to traditional plasma is that the cut is narrower and that the heat affected zone is smaller. *Figure 6.12* shows a HTPAC nozzle.

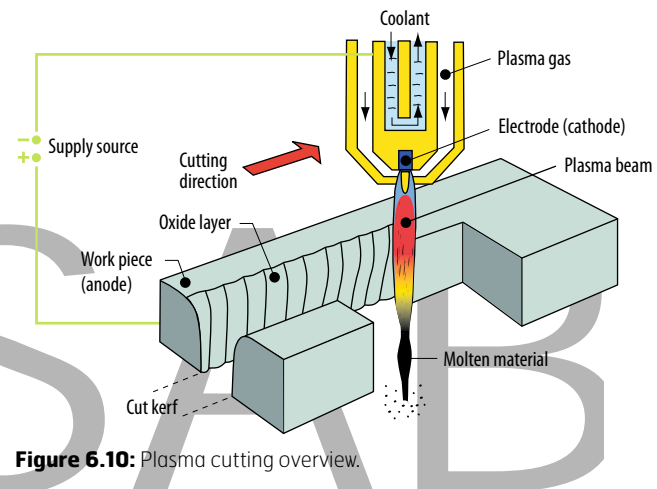


Figure 6.10: Plasma cutting overview.



Figure 6.11: Automatic plasma cutting.

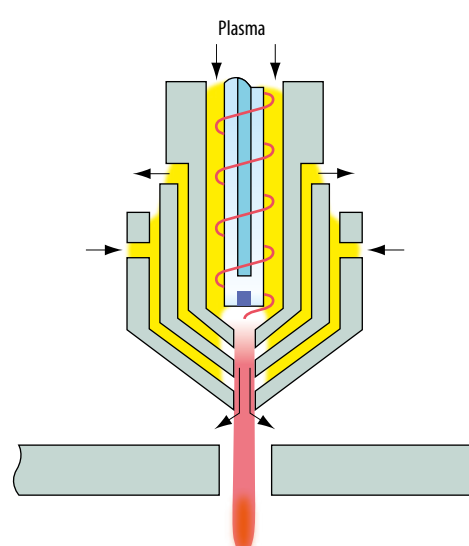


Figure 6.12: Fine plasma nozzle.

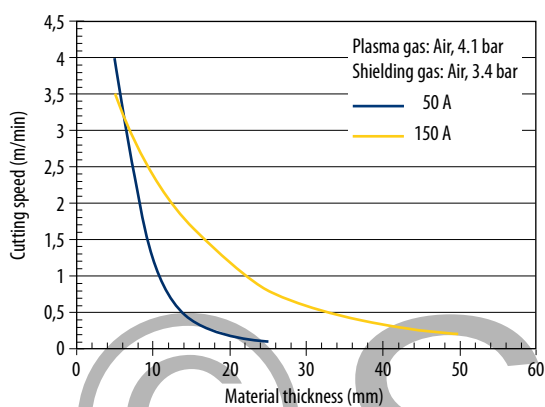


Figure 6.13: Cutting speed as a function of the material thickness (plasma).

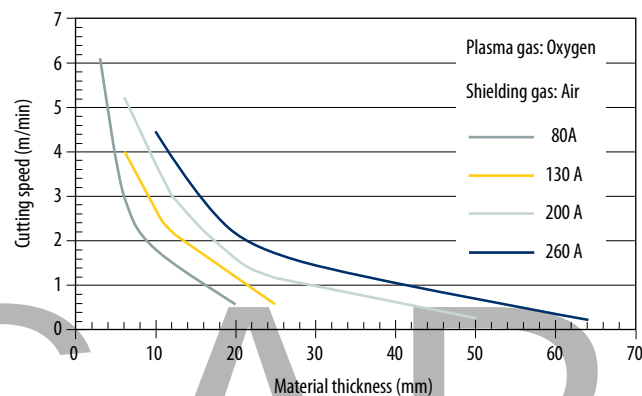


Figure 6.14: Cutting speed as a function of the material thickness (HTPAC).

Cutting speed

The cutting speed can vary depending on the setting of different parameters. The process parameters that affect the cutting speed immediately are voltage (V), current (A), plasma gas type and the choice of shielding gas. The choice of parameters must be relatively correct for a specific cutting speed in relation to the thickness of the work piece. Too high or too low a cutting speed can lead to a rough surface of the cut section as well as to the formation of dross (burr) on the lower part of the cut edge. In extreme cases, far too high a cutting speed can prevent the plasma beam from cutting through the entire material.

As already mentioned, the mechanical properties of the material do not play any role in plasma cutting/ HTPAC. The cutting parameters are the same for soft and high strength steels.

In general, what applies is that a high current makes it possible to cut a material with a certain thickness faster. At an unchanged power, the cutting speed is reduced if the thickness of the material is increased, cf. figure 6.13. Figure 6.13 shows plasma cutting of steels. Figure 6.14 shows the cutting speed for HTPAC as a function of the material thickness.

Cut quality

There are several different criteria that determine the quality of the cut surface. Some of them, such as dross, burr, pitting and striations can be observed with a naked eye. Others, such as perpendicular alignment, surface roughness (R_a and R_z) and kerf width have to be measured using different appliances. The first step in determining the quality of a cut surface is to set it in a relation with the intended purpose of the component. Is it going to be welded or painted? Is the cut surface going to be visible?

Plasma cutting or HTPAC generates cut surfaces with relatively low surface roughness, i.e. R_z values of 50 μm or lower. As with most thermal processing methods, the surface roughness increases with the increase in material thickness. Typical surface roughness values can be obtained from the EN ISO 9013:2002 [6.5] standard.

6.3.2 Laser cutting

Many processing methods use large machines and enormous power to cut or punch a component. Laser cutting on the other hand can handle the most complex of components without touching the work piece. As mentioned earlier, the hardness of the material is of no relevance, i.e. laser cutting works equally well for high strength steels and for soft steels.

During the past 30 years laser cutting has evolved from a processing method used in laboratories to an important processing method at numerous workshops. The industry has noticed the many advantages of laser cutting as compared to traditional profiling methods.

Below you can find some of the advantages of laser cutting:

Extremely fine/detailed components can be cut thanks to the small kerf widths (0.1–0.5 mm), as well as to the small turning radius (~ 0.1 mm)

In principle, laser cutting can be used on all materials, i.e. steel, plastics, other metals and ceramics

Completely computerized manufacturing (CNC)

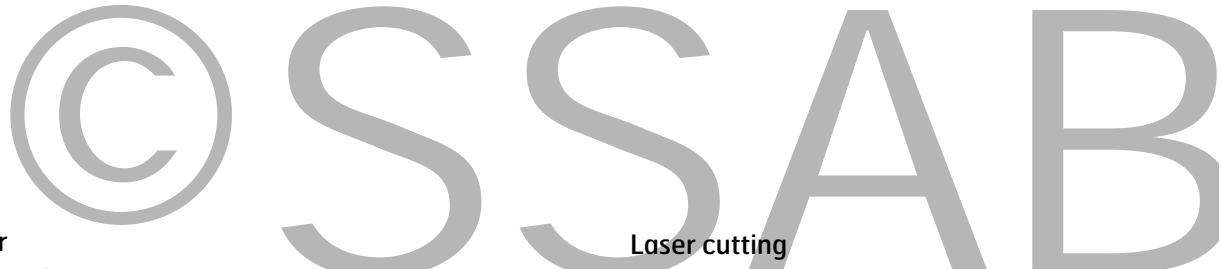
Minimum tool costs

Small thermal effect on the material as compared to other thermal cutting processes

Little or no jiggling or clamping

Fine cut edges, free from dross (burr) and usable immediately after the laser cutting operation

High cutting speeds (e.g.: a 4 kW laser: 2 mm steel is cut at a speed of 7 m/min, 6 mm – at a speed of 3 m/min)



Laser

Why prefer laser light to the light of a traditional source? The question is pertinent! The answer is that the laser light can be focused much more effectively than standard light. White light from a lamp consists of many different colors (wave lengths) and it is not parallel. If white light is focused by a lens, the focal point will be spread. The light of a laser is monochrome (it consists of only one wave length) and is parallel. As a result, laser light can be focused in one point [6.6].

There are many different laser sources. These, however, will not be described in this document. They will be only mentioned. CO₂ laser: The most common laser used in the engineering industry. The laser beam has a wave length of 10.6 µm (infra red). The laser light is angled from the laser to the work piece with the help of mirrors and it is focused with the help of a lens or a mirror. Nd:YAG laser: This laser is an excellent choice because it is possible to guide the light through a fiber. Thanks to this, the laser is easy to use in combination with a robot. The Nd:YAG laser is the second best selling laser after the CO₂ laser.

Laser cutting

As mentioned before, there are alternatives to laser cutting, but there are also many reasons why laser cutting has succeeded in establishing itself so well on the market. Amongst these:

Laser cutting does not affect the mechanical properties of the material. No tool costs.

This is a high-precision process. Extremely fine components can be cut with the help of a laser.

Only local and very limited heating result in a small heat affected zone and minimum thermal stress in the material.

A very flexible process.

Henceforth, economy and quality will be the prioritized factors when studying laser cutting. The advantages of laser cutting must be weighed against the investment cost. How does the laser cutting process work then? The laser beam heats the material to ignition or alternatively to melting temperature. The molten material is blown out of the cut kerf with the help of process gas, cf. figure 6.15.

Laser cutting itself can be divided into two types depending on what process gas is used, e.g. either oxygen or nitrogen. Oxygen is an active gas that reacts exothermally with the molten iron. An exothermal reaction means that heat (energy) is generated and this energy adds up to the total amount of energy applied on the material (the rest of the energy comes from the laser beam). The result is higher cutting speed than when cutting the material with the help of nitrogen as a process gas. The most common gas in laser cutting of steels (carbon steels) is the oxygen. When nitrogen is used as a process gas, the cut edge obtained is free from oxides, which means that components can be welded without any problems as far as stainless steel is concerned.

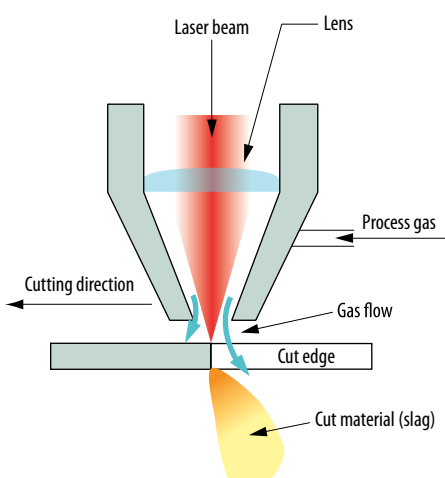


Figure 6.15: Diagram of laser cutting.

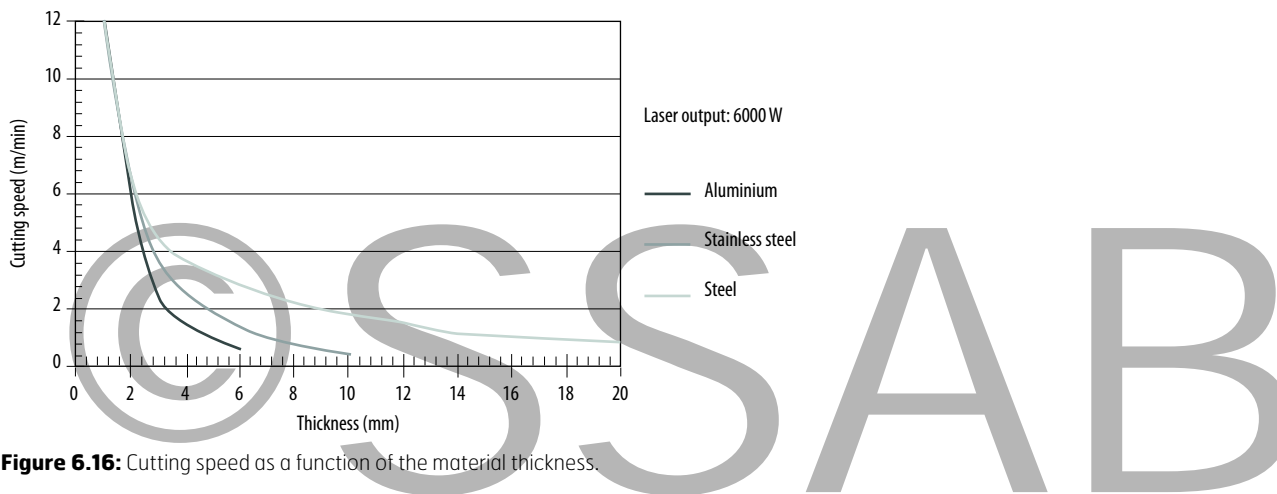


Figure 6.16: Cutting speed as a function of the material thickness.

Cutting speed

The laser output power and the cutting speed have to match. Too high or too low a cutting speed in relation to laser output may reduce the quality of the cut (higher Ra and Rz values) and can result in dross (burr) at the bottom of the cut edge. In extreme cases, too high a cutting speed can mean that it is no longer possible to cut through the material.

In general, the cutting speed increases with the increase in laser output power. At a constant laser output power, the cutting speed decreases when the material thickness is increased, cf. figure 6.16.

The cutting speed must, of course, be customized to the shape of the respective component. Corners, for example, are often cut at lower speeds. If the cutting speed is reduced, the laser output power will be automatically reduced as well. An approximate rule to remember: laser output of 1.5 kW can cut 1 mm steel at a speed of approximately 10 m/min and 10 mm steel at approx. 1 m/min.

Naturally, the cutting speed is an important parameter when choosing laser equipment, but you should not forget that it is not only the cutting speed that you should consider. Most CO₂ laser users cut with a speed between 80 and 90% of the maximum cutting speed because the reliability of the laser is extremely high in this range. For this reason it is unusual to cut at maximum laser output. When cutting corners and small circles, for example, the cutting speed is reduced. Table 6.3 shows standard cut data for different thicknesses as well as an outline of both corners and holes.

Alloying elements

As we all know, steel does not consist solely of iron, but also of many different alloying elements that help achieve the desired mechanical properties. It is important to know that alloying elements affect the laser cutting process. Molten or chemically reactive alloying elements affect the laser cutting process. For example, contaminating the oxygen and by that reducing the energy input to the cutting process or alternatively by impairing the viscosity and reducing the surface tension of the molten material. Some of the alloying elements that affect the cutting characteristics are silicon, sulfur, carbon and chrome [6.6]. For more information please contact SSAB.

For the above reason it is interesting to laser cut materials with as low alloying content as possible, such as all SSAB materials (all brands and strength levels).

Plate surface

For thicknesses of less than approx. 3 mm, the material is cold rolled, which gives a clean and bright surface. For thicknesses of more than 3 mm, the material is hot rolled and its surface is either dark grey or black. This surface is oxidized, which has taken place during the hot rolling process. The oxide may affect the possibility to cut the material with a laser, which will be discussed below.

Plates (both cold- and hot-rolled) can be zinc-coated or painted to prevent corrosion. Both zinc-coated and painted surfaces can be cut with a laser. Depending on the layer (zinc/paint), it can be necessary to adjust the process parameters during laser cutting. Below is a short summary of the different types of surfaces and how they affect the laser cutting process.

Material thickness (mm)	1	2	3	4	5	6	8	10	12	15	20	25
Focal length (inches)	5	5	5	7,5	7,5	7,5	7,5	7,5	7,5	7,5	7,5	7,5
Nozzle diameter (mm)	0,8	0,8	0,8	0,8	1,0	1,0	1,2	1,2	1,4	1,7	2,0	2,3
Laser output power (W)	1200	1100	2000	4000	4800	4800	4800	4800	4800	4800	4800	4700
Cutting speed (m/min)	8,3	5,4	4,9	4,3	4,0	3,3	2,8	2,4	1,9	1,55	1,1	0,8
Oxygen pressure (bar)	4	3,5	0,8	0,8	0,8	0,8	0,7	0,8	0,7	0,6	0,6	0,6

Table 6.3: Cut parameters for carbon steels.

This handbook contains general suggestions and information without any expressed or implied warranty of any kind. SSAB hereby expressly disclaims all liability of any kind, including any damages, in connection with the use of the information and for their suitability for individual applications. It is the responsibility of the user of this brochure to adapt the recommendations contained therein to the requirements of individual applications.

Yield strength/hardness	Thickness	Laser output power (W)	Oxygen pressure (bar)	Nozzle diameter (mm)	Nozzle-material standoff (mm)	Cutting speed (m/min)
Re 355, 420 and 700 MPa	4	4000	0,8	0,8	1,5	4,3
Re 355, 420 and 700 MPa	8	4800	0,7	1,2	1,5	2,8
Re 700 MPa	10	4800	0,7	1,4	1,5	2,4
Re 355, 420 MPa	12	4800	0,7	1,4	1,5	1,9
Re 960 MPa	4	4000	0,8	0,8	0,7	4,3
Re 960 MPa	5	4800	0,8	1,0	1,0	4,0
Re 960 MPa	6	4800	0,8	1,0	1,2	3,3
Re 960 MPa	8	4800	0,5	1,4	1,5	1,9
Re 1200 MPa	4	3500	0,8	1,0	0,7	4,3
Re 1200 MPa	6	4600	0,8	1,2	1,1	2,8
Re 1200 MPa	8	4800	0,7	1,2	1,5	2,6
Wear 400 HB	3	3000	0,7	0,8	0,7	4,9
Wear 400 HB	4	4000	0,8	0,8	0,7	4,3
Wear 400 HB	5	4800	0,8	1,0	1,0	4,0
Wear 400 HB	6	4800	0,8	1,0	1,2	3,3

Table 6.4: Cutting speeds for hot rolled steels.

Cold-rolled plates: The plates are perfect for laser cutting.

Pickled and oil-coated plates: Similarly too cold-rolled plates, perfect for laser cutting.

Black plate: A hot-rolled plate with a thin oxide layer on the surface. This oxide layer is often no problem during laser cutting. Problems can occur if the layer is too thick (in rare cases).

Zinc-covered plate: A thin zinc layer is often no problem for laser cutting. Some dross or burr can be observed but they are both easy to remove. Hot-dip galvanized plates have a thicker zinc layer that has a negative effect on the laser cutting process.

Paint: Some paint and the thickness of the paint can affect the laser cutting process negatively.

Blast surface: Sand or ceramic beads used for shot blasting affects the laser cutting process. This is so because of the presence of silicon.

Rust: Rust on the surface of the material can affect the laser cutting process (especially if the rust is thick and loose).

Laser cutting

All of the hot rolled material can be laser cut with similar process parameters as for the material S235JR. *Table 6.4* show typical cutting speeds for hot-rolled steel strips. Only Strenx 960 (8 mm) and Strenx 1200 (the 6 and 8 mm) is to be cut with reduced speed. The reason for this is that both have a primer on the surface. Cut edges have a good surface finish with low Ra and Rz values. Ra ranges between 0.5 and 14 microns and the Rz between 3 and 60 microns (the lower values apply the thickness of 4 mm and the higher values of thickness 12 mm). Cut surfaces roughness are below the values specified in the standard EN ISO 9013: 2002 [6.5]. Typical appearance see *Figure 6.17*.

SSAB Laser Plus Steels are specially developed for laser cutting and ensure a maximum flatness tolerance of 3 mm / m after laser cutting and a bending radius of 0 – 1.5 times the material thickness. These characteristics make it possible to meet the highest requirements for automated processes.

Some of the benefits with SSAB Laser Plus are high cutting speed, premium quality cut edges. Cutting of complex components with high precision and tight contours can be made without finishing work. The cold forming properties of SSAB Laser Plus are excellent with an inner bending radius of 0 – 1.5 times the material thickness, depending on the combination of strength and thickness. SSAB Laser Plus is available both as QT (quarto plate) and hot rolled coil products for the mechanical engineering industry, automotive and electronics.

Production cost

Like any other industry steel users constantly strive to reduce production costs. Upgrading the construction with a stronger material is a means of achieving this.

Below is an example of the benefits from an upgrading to a higher strength level. In the example costs are reduced by upgrading from Re = 355 (6mm thick) to Re = 420 (5 mm thick).

Example: 1000 details are to be cut out. Every detail has a cutting length of 1.7 meters. The cutting speed for Re = 420 (5 mm) is 3.4m/min and 3.0m/min for Re = 355 (6 mm). This means that we reduce the total cutting time by 60 minutes. The material cost difference should be added, Re = 420 (5 mm) instead of Re = 355 (6 mm). Further, easier handling is achieved due to the lighter 5 mm sheet compared to the older 6 mm sheet (assuming equal width and length). The total cost for each part is reduced both with respect to the laser cutting cost and material cost.

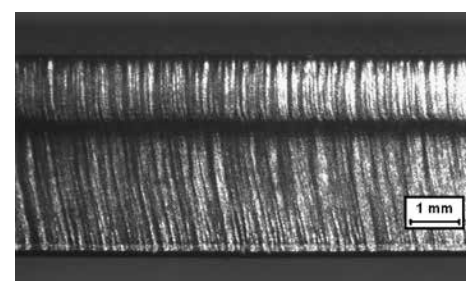


Figure 6.17: Cut edge of hot-rolled steel with a yield strength of 420 MPa (4 mm).

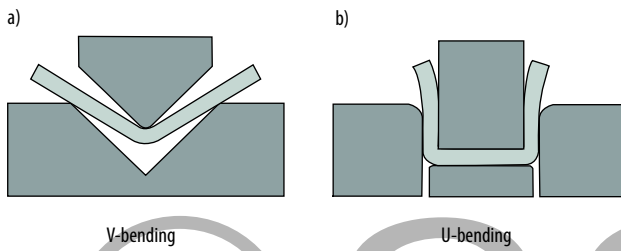


Figure 6.18: Bending methods [6.7] a) V-bending b) U-bending.

6.4 Plastic forming

This chapter discusses bending, roll forming, presswork operations and flanging.

When replacing mild steels with high strength steels, the greater springback and the lower formability must be taken into account. The necessary design changes (as compared to conventional steel grades) do not have to be very extensive. Lower formability, for example, can be compensated by greater radii and lower friction.

6.4.1 Bending

SSAB's high strength steels are produced with high precision in all process steps. The variations in strength are therefore small, resulting in small springback variations during bending. The steels have low carbon and sulfur content, high slag purity and a beneficial slag shape. The result is a significant increase in bendability as compared to traditional structural steels.

In general, the same rules apply both for bending high strength and mild steels. Remember, however, that the springback and the smallest bending radius increase with the strength.

Methods, nomenclature

Spring back angle β

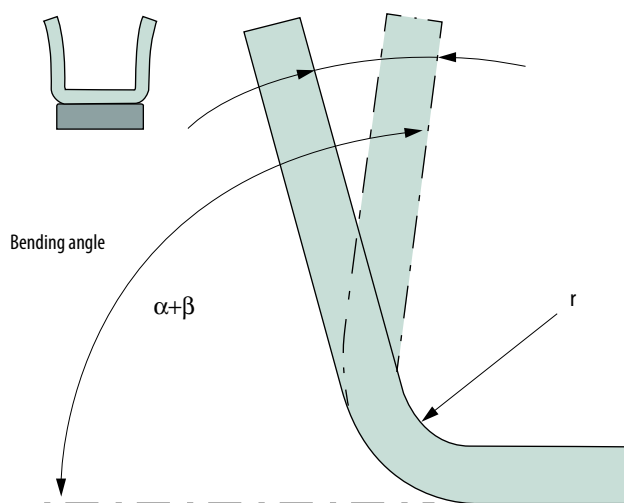


Figure 6.19: Angle definitions.

Bending is a plastic manufacturing process where sheet metals are formed by the application of a bending moment. The method is used to give the sheet metals a single bent shape, *figure 6.18*. Air bending (free bending) in V-shaped dies is the most frequently used method, *figure 6.18 a).* U-bending is shown in *figure 6.18 b).*

Most bending operations are carried out in mechanical or hydraulic press breaks. Folding machines are primarily used for small production runs. Read more about bending in the Forming Handbook.

Bendability

When bending, the outside of the sheet metal is stretched and the inside is compressed. The strain increases as the bending radius is reduced. The bendability of the material is therefore normally given as the minimum bending radius without failure. The recommended minimum bending radii for SSAB's materials can be found in leaflets as well as at www.ssab.com.

Springback

Springback is caused by elastic strain. The springback increases with the yield point, the strain hardening and the die width. The influence of the yield point is greatest. Springback reduces with a reduction of the bending radius.

The safest way to determine springback (and the inner radius of the bend) is by making a bending test. Over-bending is the most common springback compensation method. Another method is bending by bottoming, which also reduces springback.

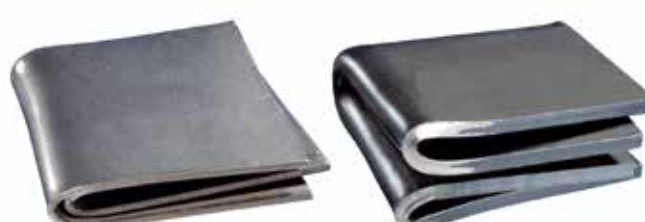
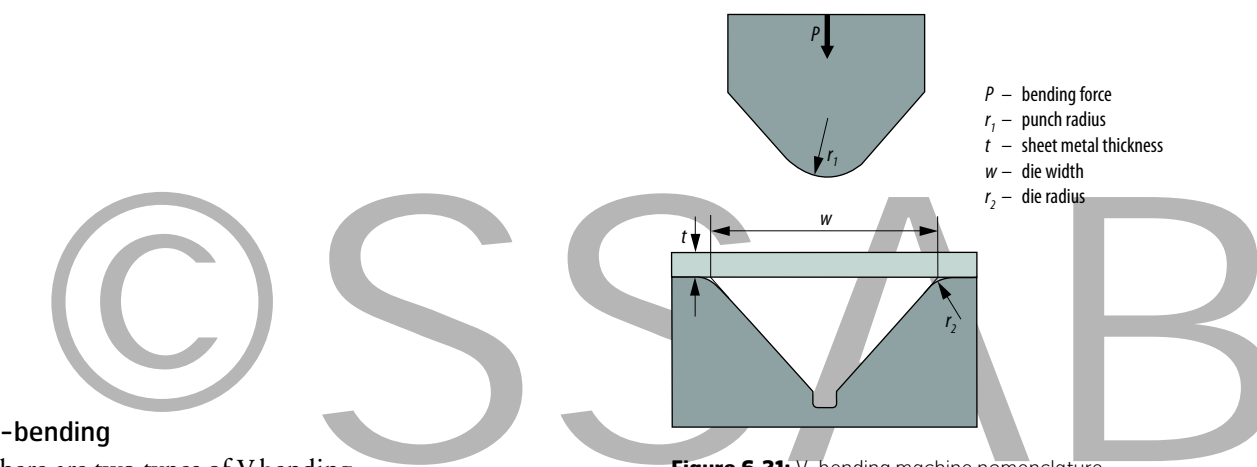


Figure 6.20: "Handkerchief folding" of Docol 1000 DP t=1.5 mm and Strenx 700 MC, t=4.0 mm.



V-bending

There are two types of V-bending:

- air bending (free bending) and
- bending by bottoming (bottom stroke)

Air bending (free bending)

During air bending of thin mild steel, the punch radius does not have any effect on the shape of the bend, figure 6.22. The shape is determined by the relation between the die width and the thickness of the sheet metal.

When bending thicker materials and UHS materials, it has been discovered that the inner radius of the bend is raised from the punch. This means that the inner radius of the bend is smaller than the radius of the punch.

This change is observed at a yield point of approximately 500 MPa.

Die width $>10 \cdot t$ might be necessary when bending thicker materials ($t > 10$ mm) and materials whose yield strength exceeds 700 MPa.

Springback during air bending

It is difficult to calculate springback accurately. In practice, however, a simple rule of thumb is applied: overbend 1° per 100 MPa yield point. For example, Strenx 700MC (yield point 700 MPa) needs to be overbent approximately 7°.

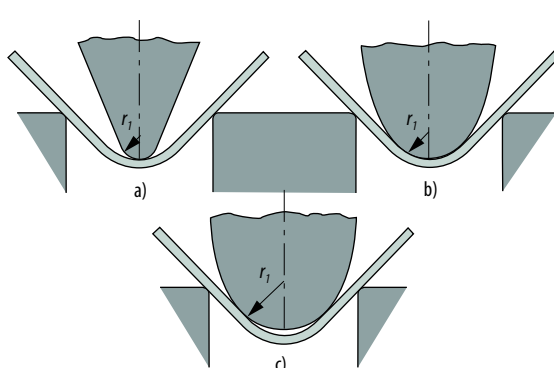


Figure 6.22: The bending radius is dependent on the material, die width and punch radius. The figure to the right shows the bending of mild steels. The figure to the left shows the behavior during bending of high strength steels.

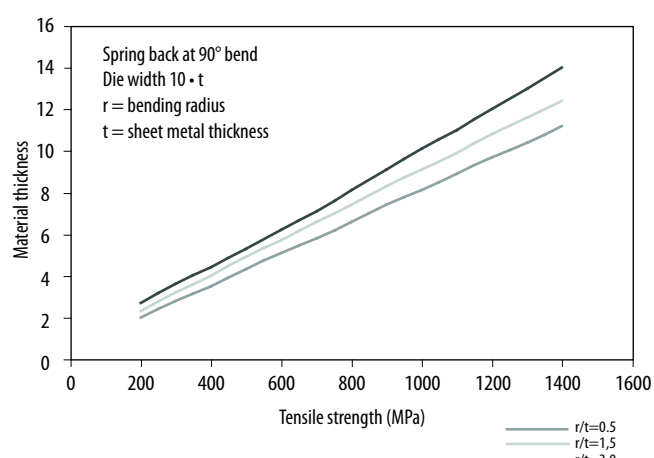
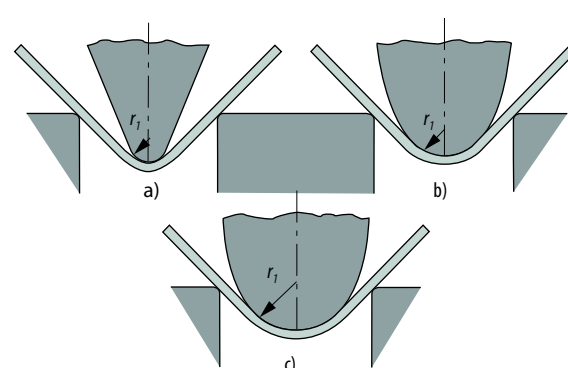


Figure 6.23: Overbending angle during air bending to 90°, θ , as a function of tensile strength for different R/t . Die width $10 \cdot t$.



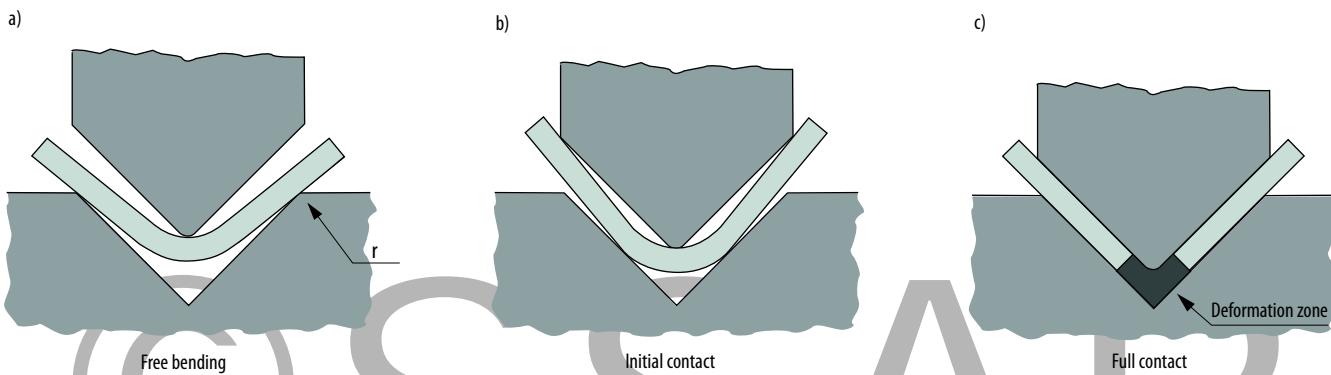


Figure 6.24: V-bending by bottoming [6.8].

Bottoming

During bottoming of thin sheet metals, *figure 6.24*, it is possible to achieve good shape accuracy.

If the bend is bottomed, the material will go into a fully plastic state, which practically eliminates springback. *Figure 6.25* shows different forms of bending by bottoming. The bottoming effect is difficult to estimate. The best way to evaluate is to make a practical test.

U-bending

U-shaped bends can be made in a special U-bending die, *figure 6.26*. It is important to have a pressure pad in the U-bending machine in order to have a product with an accurate shape.

The strains in the sheet metal are greater during V-bending than during U-bending to same angle.

Methods for reducing springback during U-bending

Combined air bending and bottoming with a punch angle $< 90^\circ$ is a frequently used method for bending accurate acute angles. The punch radius must be well-rounded off and polished. The risk of crack initiation/fracture increases both on the outside and on the inside of the bend.

Overbending

Overbending suitable for the current springback can be achieved by using a customized die, cf. *figure 6.27*.

Indented bend

By indenting the bend with stiffening grooves, springback is reduced to a minimum. An example of an indented bend are displayed in *figure 6.28*.

When bending metal-coated steels it is important to design the component and machine keeping in mind that scaling can occur at high friction and shearing forces. The right choice of tool and/or steel grade can reduce the risk of scaling.

Bending force

The force during air bending in V-dies is proportionate to the yield point of the material. For rough estimations, the bending force can be calculated using *equation 6.3*. For a more thorough calculation of the bending force, please use simulations.

$$P = \frac{C \cdot L \cdot t^2}{I} \cdot \frac{R_e + R_m}{2} \quad (\text{Eqn. 6.3})$$

P	- bending force (N)
L	- bend length (mm)
t	- sheet metal thickness (mm)
I	- effective moment arm length (mm)
R_e	- yield point (MPa)
R_m	- tensile strength (MPa)
C	- a constant, obtained from the diagram in <i>figure 6.29</i>

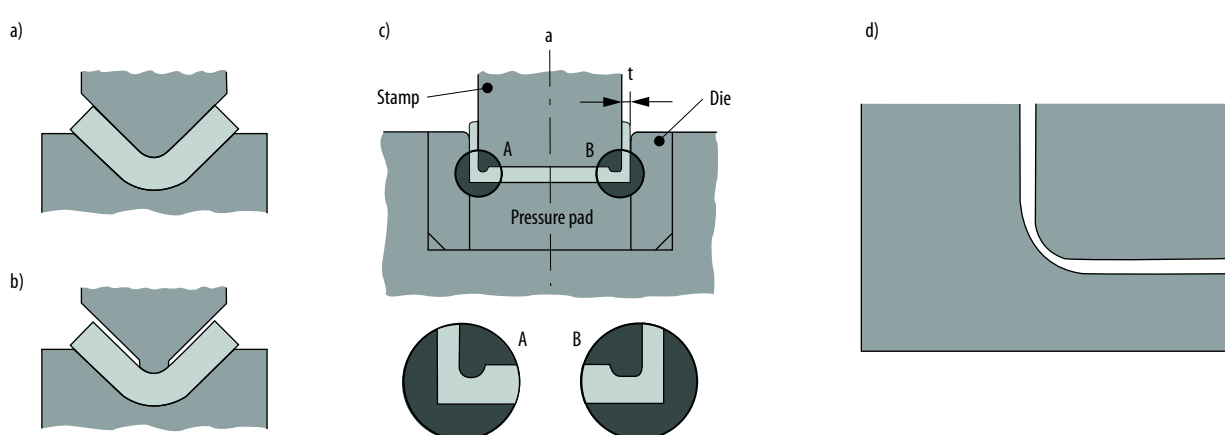


Figure 6.25: Bottoming punch a) standard punch b) punch with clearance [6.9] c) stamp with embossing edge d) Punch and die with different radii.

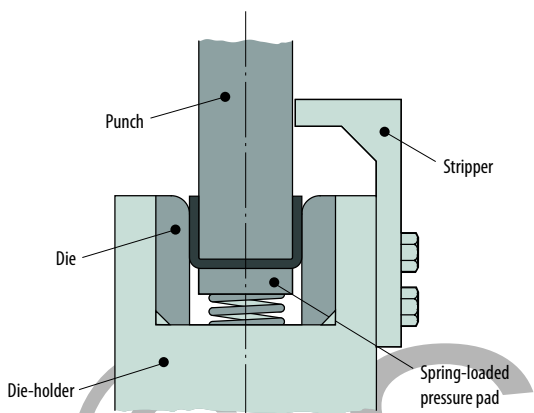


Figure 6.26: U-bending tool [6.10].



Figure 6.28: Broken edge to minimize springback.

Provided that the same machines are used, Strenx 650 MC, for example, requires double as much bending force as hot rolled steel with $Re=315$ MPa. The required force is inversely proportional to the width of the die, which means that if the die width is doubled, the bending force will be reduced by half. A reduction of the thickness by 30% reduces the bending force by half. This means that replacing mild steels with high strength ones in a bent component can result in lower bending force despite the fact that the sheet metal is harder. Thin sheet metals and greater die widths are two key factors that reduce the bending force.

When calculating the bending force with bending methods other than V-bending, the working beam must be taken into account, *figure 6.30*.

There are no reliable formulas for calculating the required force during bending by embossing of thin sheet metals, but experiments show that two to five times greater a force is required than during air bending.

The force during U-bending is the total of the bending force and the pressure pad force. In practice, the required force is greatly dependent on the tool radius and the friction.

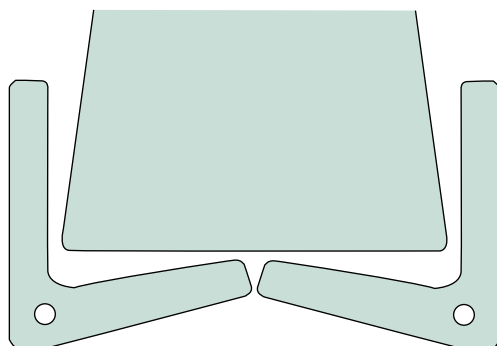


Figure 6.27: Spring die for overbending.

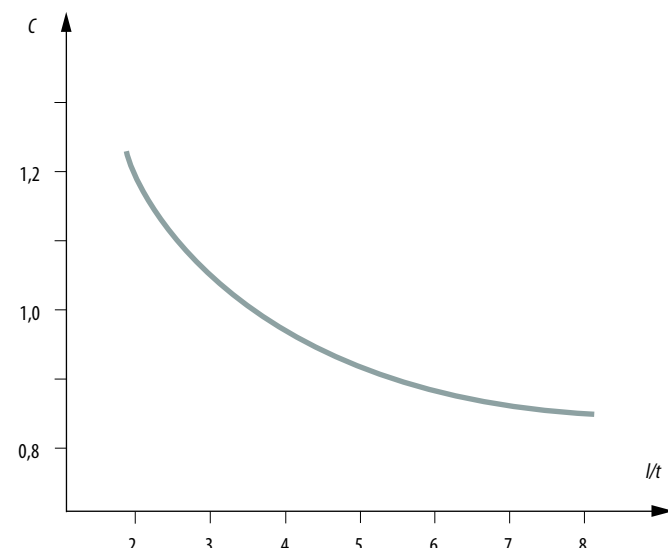


Figure 6.29: C constant for bending force calculation [6.11]

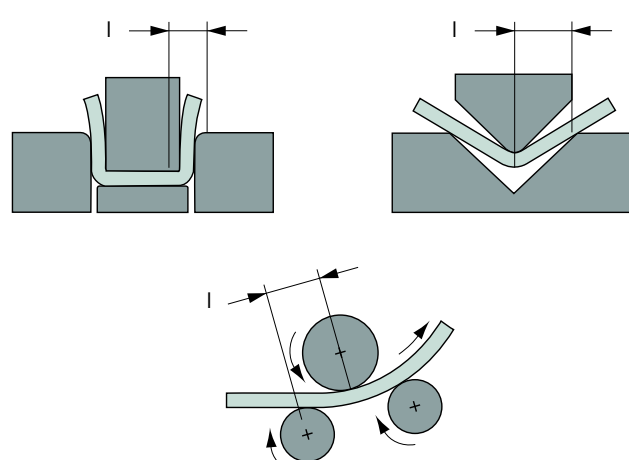


Figure 6.30: Effective moment arm length, l , in different bending methods [6.12].

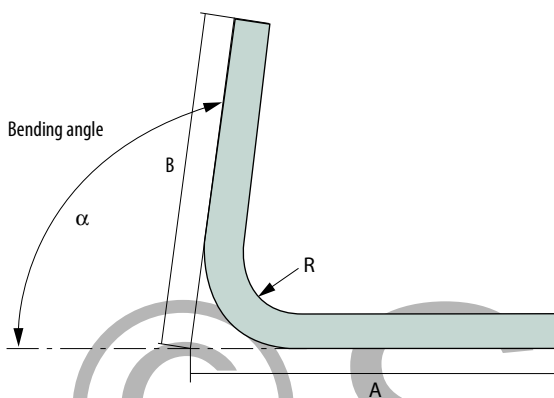


Figure 6.31: Formulas for calculating the V factor for determination of the length of material.

Length of the material [6.13]

The length of the material is calculated with the help of *equation 6.4*.

$$\Delta = 0.7 \cdot R + 0.06 \cdot t \cdot \alpha - 3.7 \cdot t \quad (\text{Eq. 6.4})$$

R – bending radius

t – sheet metal thickness

α – bending angle according to *figure 6.25*

Δ – the difference between the original length and the total of A and B according to: $L = \Delta + A + B$

In connection with long production series or when greater accuracy is required, bending samples that show the actual material length outcome must be taken.

Some final viewpoints

The trimmed edge has a great effect on the formation of cracks in edges during bending. The greatest and most serious cause for this is the burr. Therefore, the burr shall be turned to the inside of the bend where possible, or the trimmed edge shall be polished/ground before bending. Gas-cut components shall have a well-beveled edge.

The die should have large edge radii and fine surface quality to reduce the risk of dents and scratching of the sheet metal. The so called roll die with roller inserts in the die edges reduces the friction additionally and is recommended for bending of high strength steels. For sheet metal thicknesses of up to 2 mm, the radius of the die should be greater than the sheet metal thickness. In case of larger thicknesses, the radius of the die shall be at least $t/2$ (min 2 mm). The friction between the die and the sheet metal also increases the strain in the outer layer which makes failures occur more easily.

The smaller the inner radius, the greater the plasticity of the material has to be. Therefore, do not choose unnecessarily small bending radius. If possible, always use a radius greater than half the sheet metal thickness even if the material is guaranteed to bend to a sharp corner. Small radii also require more frequent resharpening of the tool.

When the sheet metal shanks are folded up during 180° bending, the bend must also be left a bit open.



Figure 6.32: Forming of a sheet metal profile in a forming pass.

6.4.2 Roll forming

Roll forming means that a flat sheet is transformed into a profile by incremental bending. You can see an example in *figure 6.32*. The sheet metal has passed several live shaft pairs equipped with profile-shaped rolls, *figure 6.33*. Many engineers regard roll forming as a two-dimensional technique, but it is in fact an exceedingly three-dimensional technique, see *figure 6.34*.

Several examples are shown in *figure 6.35* in order to illustrate the possibilities of roll forming.

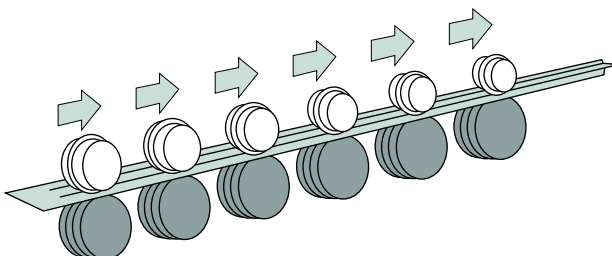


Figure 6.33: The sheet metal passes several live shaft pairs with profile-formed rolls.

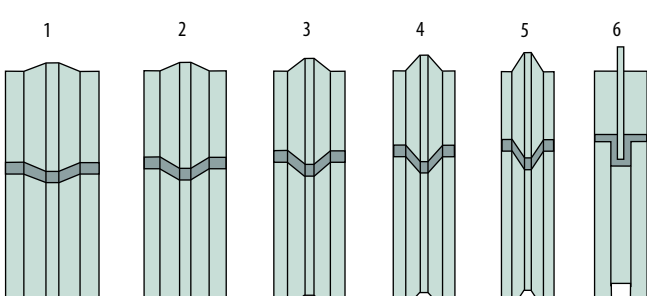


Figure 6.34: The successive profile folding during rolling means that the forming operation must be calculated three-dimensionally.



Figure 6.35: Examples of roll formed profiles.

Additional operations

Most linear profiles can be created by roll forming. In addition, a subsequent curving can give a curved profile. Examples of other supplementary operations associated with roll forming can be seen in figure 6.36.

SSAB works closely with Jensen A/S in Denmark, a manufacturer of roll forming machines. Tests conducted in collaboration with Jensen have shown that sharper radii can be achieved through roll forming of high strength steels than during bending. In a test by Jensen it was possible to manufacture a simple hat profile of Docol 1400 M with an inner radius of $1 \cdot t$. In comparison, the minimum recommended bending radius for this material is $3 \cdot t$, see figure 6.37.

6.4.3 Presswork operations

This chapter discusses fundamental definitions and test procedures. It also provides information about the differences between mild and high strength steels during presswork operations. Furthermore, it contains many examples of the use of SSAB's high strength steels. The result of a presswork operations is determined by the press, the tool, the sheet metal and the shape of the component. How these factors affect presswork operations and how a change in circumstances affects the quality of the result is generally known. The problem is that most of the knowledge and experience has not been quantified.

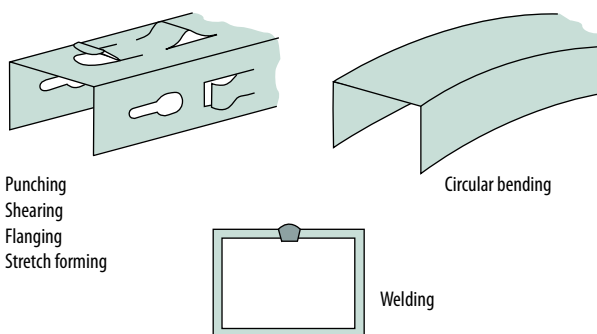


Figure 6.36: Additional roll forming operations.

SSAB

The main differences between high strength and mild steels during presswork operations are, as follows:

The elastic springback increases with the increase in strength. The springback can be counteracted by over crowning the punch or by increasing the plastic strain over the radius, by increasing the blank holder force. Springback is generally proportional to the yield point.

Formation of wrinkles and creases increases with increased strength and reduced thickness. It can be counteracted by increasing the blank holder force or by inserting draw beads to restrain and guide the surplus material.

As a rule, the formability decreases with the increase of strength. Reduced formability can be compensated by larger radii, reduced friction or multi-stage forming. The shape of the blank also affects the forming and the importance of the shape grows the greater the strength of the steel is.

The stress on the tool increases with increased sheet metal strength. Increased wear can be counteracted by a greater radius, better lubrication and/or better tool materials. Surface-coating of exposed areas can be necessary.

Definitions and testing

This part is of general nature and is not specific to high strength steels. Type examples of SSAB high strength steel values are mentioned.



Figure 6.37: The minimum guaranteed bending radius for Docol 1400M is $3 \cdot t$ for standard air bending. During roll forming, the same material is bent to a radius of $1 \cdot t$.

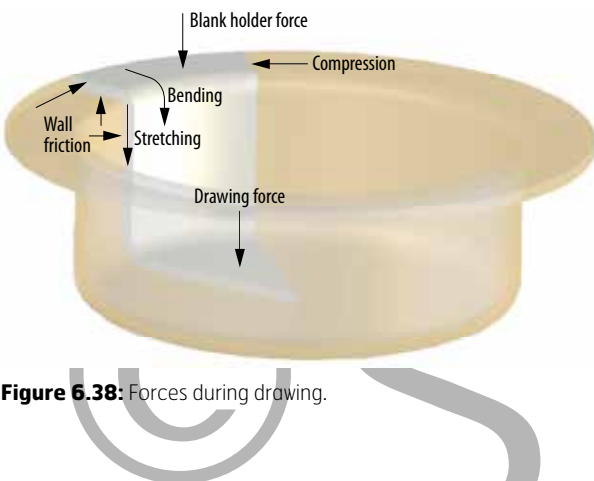


Figure 6.38: Forces during drawing.

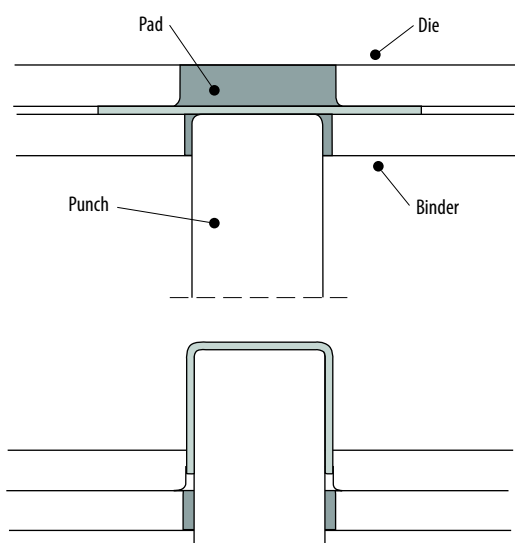


Figure 6.39: Drawing nomenclature.



Figure 6.40: High strength steels have remarkable deep drawing properties. Docol 1400M has five times higher tensile strength than SSAB Form 04, but the maximum drawing ratio is reduced by just 20%.

SSAB

Deep drawing

Deep drawing of sheet metals can be divided into two main types: drawing and stretch forming. In practice, most presswork operations are a combination of draw and stress forming. The material properties required for good draw or stretch forming ability, respectively, are not identical.

Drawing

Drawing is characterized by the fact that all of the material, or most of it, go through the die and that the blank holder pressure is balanced so as to prevent the formation of creases. The forces that act on the material during deep drawing are displayed in *figure 6.38*.

The ability of a material to withstand drawing is primarily dependent on two factors:

The tendency for plastic deformation in the plane of the sheet metal, i.e. how easily “the flange material” flows and turns into “side wall material” during drawing. A low yield point in the plane of the sheet metal as compared to the thickness of the sheet metal is therefore desired.

“The side wall material” must be possible to resist plastic deformation in the thickness direction so as to minimize the risk of fracture. The yield point should be higher in the thickness direction of the sheet metal than in the plane.

A measure for these two factors is the so called “strain ratio” or the coefficient of anisotropy, r . The drawability increases with the increase of the r value. The r value is defined as the relation between the plastic strain in width, ϵ_{22} , and the plastic strain in thickness, ϵ_{33} , during uniaxial drawing in longitudinal direction of a narrow strip specimen, $r = \epsilon_{22}/\epsilon_{33}$. The R value is around one for all steels



but cold rolled deep drawing steels which have much higher r values.

Drawing tests are carried out by cup and can drawing. Several circular blanks of different diameters are drawn to a cup, see *figure 6.40*. The critical, or limiting drawing ratio, LDR, is defined as the ratio between the greatest blank diameter, D, that can be drawn without fracture and the punch diameter d.

The limiting drawing ratio LDR values can be found in SSAB's leaflets at www.ssab.com.

Stretch forming

Stretch forming means that the material is locked by the blank holder force and that all plastic deformation takes place above the punch. The material is exposed to equibiaxial strain with a thickness reduction as a consequence. Fracture occurs when the local deformation is too large. The stretchability depends primarily on the deformation hardening ability of the material and its ability to distribute strains. The deformation hardening of the material is described by the n value. The stretchability increases with increasing n value. The n value can be obtained from the stress-strain curve of the material. A stretchability test (over semispherical stamp) resembles the Erichsen test used by SSAB. In this test, a blank is fixed into position and stretched to fracture by a punch with a diameter of 100 mm. The height at fracture is determined. The ratio between this height, H, and the punch diameter, d, is the measure for the stretchability of the material.

The H/d value can be found in leaflets and at www.ssab.com.

Comments concerning drawing and stretch forming tests

The LDR and H/d that have been prepared give an indication of the drawability/stretchability of the material. The test results from different test machines can be different due to the different test conditions and should therefore not be compared. Stretchability and drawability tests, however, can be used for internal comparisons or to compare the formability with other materials.

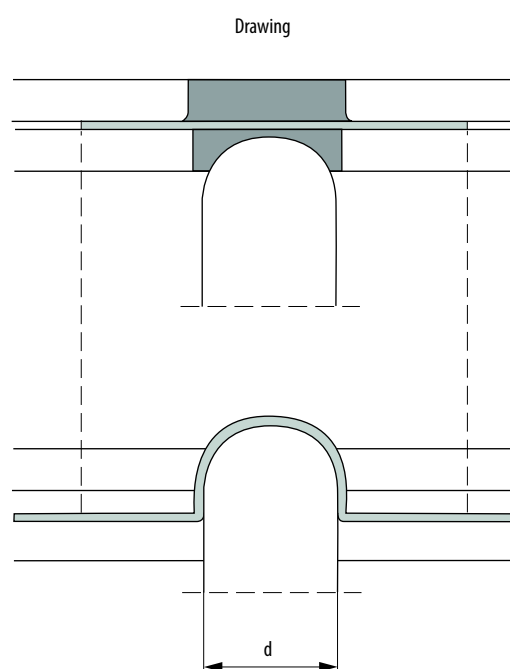
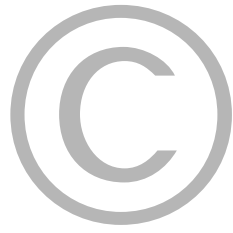


Figure 6.41: Drawability testing, limiting drawing ratio, LDR.



Figure 6.42: Stretchability testing, maximum relative draw depth, H/d.



6.4.4 Flanging

The formability during flanging is usually reduced with an increase of the strength of the material. Higher strength can be compensated by pre pressing, which increases the amount of material available for flanging. During flanging, the outside of the flange is exposed to greater strain than its inside. It is therefore important to cut the hole in one direction, if possible, and do the flanging in the opposite direction in order to have the blanking burr on the inside. Flanging requires good edge quality for best results.

The maximum strain in the cut edge during flanging is proportionate to the maximum flanging ratio, i.e. the relation between the diameter of the hole before and after flanging. The maximum flanging ratio is dependent on the mechanical properties of the sheet metal, its microstructure, the design of the tool and, last but not least, the edge quality of the hole that is to be flanged.

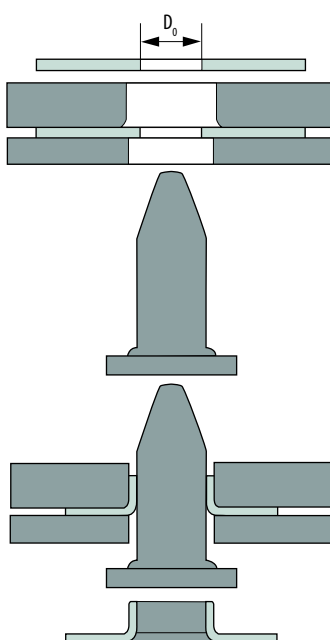


Figure 6.43: Outline diagram of how SSAB tests and measures the flangability.

The lower flanging ratio of high strength steels can be compensated in many different ways.

- Shearing and flanging shall be done in opposite directions, i.e. the blanking burr shall end up on the inside of the flange.
- Fine processing of the punch hole edges to minimize the punch impact. This is not always possible in practice.
- The height of the flange is increased while the flanging ratio is maintained via pre-pressing, *figure 6.44*. This results in more material that can be used in the flange.

The maximum flanging ratio is reduced with increasing thickness. This is due to the outside of the flange is subjected to more strain in a thick sheet metal than in a thin sheet metal at one and the same inner diameter of the flange. This difference is more significant for Domex steels because they have a greater thickness range.

In order to obtain the best possible flanging results, the punching tools must be in good condition. Ultra high strength steels (UHSS steels) can require somewhat greater interior corner radius in order to avoid cracking. This can be achieved by increasing the clearance or the die radius.

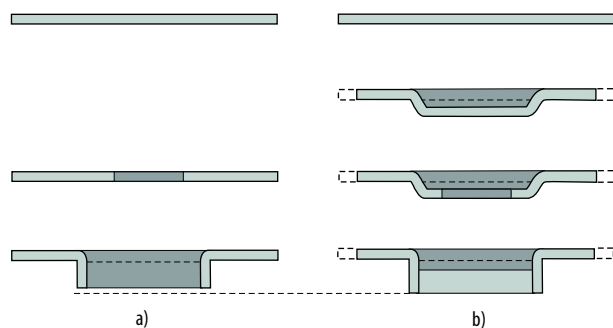
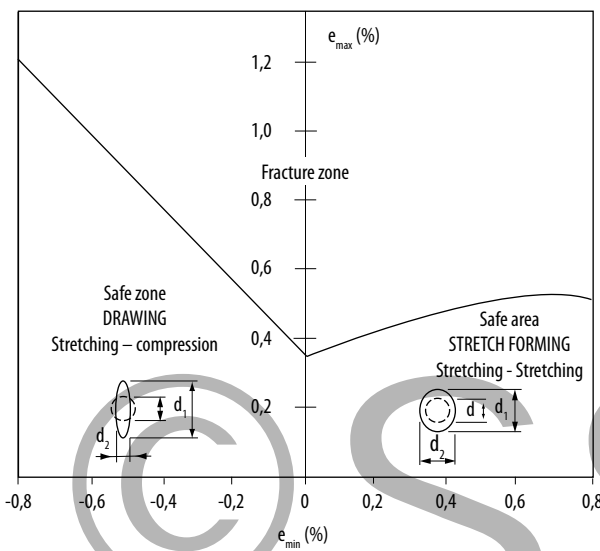


Figure 6.44: A comparison between flanging without pre-pressing, figure a) and flanging with pre-pressing, figure b). The diameter of the punched hole is the same in figures a) and b). The same applies for the inner diameter of the final flange, but pre-pressing gives a higher flange in figure b).



Forming limit curve (FLC)

FLC is used to establish how large deformation the material can withstand at a certain strain path or a certain deformation condition. *Figure 6.45* shows an outline of the FLC curve.

FLC is often determined with the help of rectangular test blanks that are formed with a semicircular punch until they fracture. A circular or a grid pattern has been etched on the test blanks and the most deformed area next to the fracture, or local contraction (necking), is measured. The strain in this area is expressed by the main strain values e_{\max} and e_{\min} . By using specimen of different formats it is possible to simulate different strain conditions, from drawing via plane strain to stretch forming, and a whole FLC can be established. *Figure 6.46* shows an example of pressed specimens. Different pattern sizes can be used, but in general the size is 2 or 5 mm.

The left part of the FLC in *figure 6.45* corresponds to forming where the degree of drawing increases to the left of the curve. Similarly, the right side corresponds to a forming where the degree of stretch forming increases to the right.

The FLC is dependent on the thickness, which is why it is not possible to compare different thicknesses. FLC is based straight deformation paths. If the material is to be stretched in one direction first and then in another, it is possible to achieve higher levels in the diagram.

Figure 6.45: An outline diagram of the forming limit curve (FLC). The curve marks the limit between the area where the sheet metal withstands the strain (below) and the area where the sheet metal fractures (above).

The most interesting area in the FLC curve is at $e_{\min} = 0$. This corresponds to plane strain, which is the case during bending. Many fractures observed during forming occur in the area around $e_{\min} = 0$.

The effect on forming when choosing a high strength steel

The formability of high strength steels is generally worse than that of mild steels. An increase in strength is often followed by a reduction in thickness for the purpose of reducing weight. Higher strength and reduced thickness can affect:

- Elastic springback
- Tendency for formation of wrinkles and creases
- Formability
- Stress on tools

Springback

Springback in connection with bending has been described in chapter 6.4.1. Springback phenomenon in connection with presswork operations is the same, but the problem becomes more complex because these often involve stretching and/or drawing and bending. The shape of the component is also more complex.

Measures for reducing springback during presswork operations

The basic thought for minimizing springback is the same as for bending. There are three different alternatives that can be used.

Overcrown the forming tool so that the springback component would have the correct geometry. Testing your way is time-consuming and many machine hours are required to rebuild the tool. A good alternative to reduce the testing time is to simulate springback and build the tool from scratch.

Make sure that the deformation in the springback areas is sufficient. This can be done by a blank holder and draw beads.

Design a stiff component where the springback areas are held back by neighboring areas, such as an indented radius.

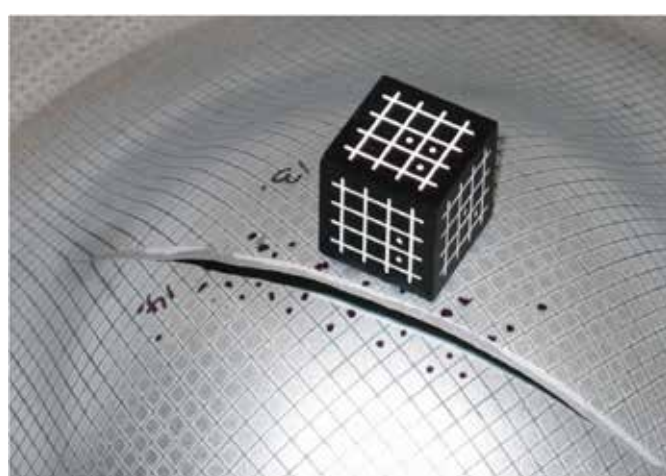
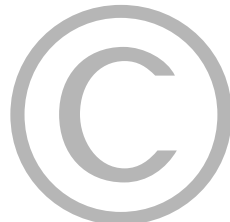


Figure 6.46: Example of a pressed sample for preparation of a FLC.



SSAB

Formation of wrinkles

During drawing, the compression stress results in the formation of wrinkles if the sheet metal is not well guided between the tool components. Flange wrinkling and wrinkling can be formed in part in large, flat areas, *figure 6.47*, component a, and in part in radii and edges over which the sheet is drawn, *figure 6.47*, component b. In both cases, the wrinkles are caused by compressive stress and excess material.

In general, reduced thickness and higher strength increase the risk of wrinkles. Stretching of the sheet metal in the final stage of the presswork operation, especially for flat sections, is made more difficult due to strain hardening.

There are many ways to counteract the formation of wrinkles. One of them is to increase the blank holder force. The increase, however, must not be too big. Otherwise a fracture will be observed. A greater draw depth of a component results in a smaller blank holder span between formation of wrinkles and fracture, the so-called blank holder window. *Figure 6.48* exemplifies this relation.

Another way is to use greater edge radii on large flat sections. This way the stretching of the material over the edge is facilitated. Greater corner radii also make the forming easier.

If the component has been formed, draw beads can be added in order to restrain and guide the excess material. This way formation of wrinkles is avoided. The blank holder force increases locally over the beads and the risk of fracture must therefore be taken into account. The problem with wrinkle formation is present primarily for cold rolled and metal coated high strength products. Hot rolled products often have a larger thickness, which is positive as far as prevention of wrinkles is concerned.

Formability

An increase in strength generally leads to a reduction of the r and n values. These parameters must be as high as possible to ensure best formability.



Figure 6.47: Example flange wrinkle formation, component a) and wrinkle formation, component b).

All hot rolled steel from SSAB has an r value ≈ 1 , which corresponds to a randomly oriented microstructure. The drawability of these steels is good as compared to other materials in the same strength and thickness range. Cold rolled micro-alloyed steels achieve their formability through a high r value. Some of the structure from the cold rolling process remains thus giving greater strength in thickness direction than in plane direction. Dual phase steels (DP) lack the structure of the cold rolling process and have an r value ≈ 1 , their formability is instead achieved through phase transformation and gives a high n-value.

Friction is an important factor for formability. The lubrication conditions are of greatest significance for the friction. The effect of the lubricant on the formability in general is dependent on the viscosity: higher viscosity results in better formability. An increase in strength requires an increase in the blank holder pressure if a component with an accurate shape is to be produced. This means also that a lubricant with high viscosity must be used. When selecting a lubricant, there are other factors to take into account. Application, anti-corrosion, aging of the oil, degreasing, the environment, etc. The choice of oil must therefore be considered from multiple perspectives.

The forming limit curve (FLC) is a good aid when determining formability, during FE simulations, for example. The FLC can be used both for cold and hot rolled steels. More information about the forming limit curve (FLC) can be found in the Forming Handbook.

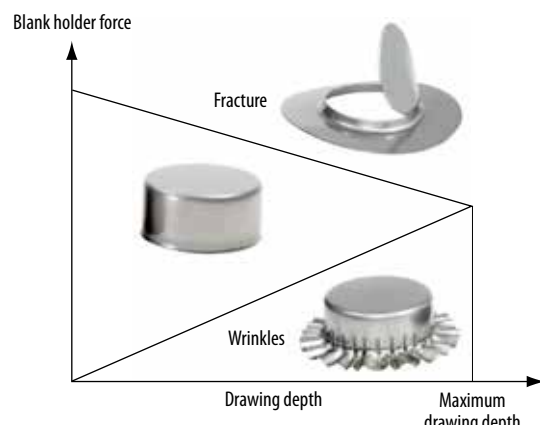


Figure 6.48: The blank holder force must lie within the marked area to avoid wrinkling and fracture at a certain drawing depth [6.12].



Figure 6.49: Components from the automotive industry where light weight, good formability and crash properties are sought after.

Stress on the tools

The need for maintenance and repair of the tools are usually dependent on two factors. Either the sheet metal smears the tool, which results in scratches in subsequent components, or the tool is worn out, as a result of which the form of the components is not accurate.

There are three damage mechanisms during forming that can be observed in the three active parts of the tool:

- Wear (abrasive or adhesive) which is associated with the work piece, the type of forming operation and the friction forces in the point of sliding contact.
- Plastic deformation, which occurs when the stress exceeds the flow stress (hardness) of the material of the tool.
- Pick-up (Galling) that occurs when workpiece material is built up on the tool. The galling mechanism is closely associated with adhesive wear.

The limiting damage mechanism during forming of high strength steels consists of wear in general and then in particular of abrasive wear, but adhesive wear and pick-up is observed when high friction forces are created during the forming of high strength steels.

A serious problem in forming tools is that galling causes scratches on the formed component. Galling is observed primarily at very high contact pressure. The tendency for galling increases for high strength and thick materials.

Galling can be counteracted via lubrication. The tendency for galling is reduced in tools with high surface finish and in tools where the surface hardness is increased. Higher surface hardness can be achieved through nitriding or chromium plating or via PVD- or CVD coating.

Certain results indicate that hot galvanized sheet metals are better able to withstand galling than plain sheet metals of the same strength [6.13]. Even for hot galvanized sheet metals the tendency for galling increases with the increase in strength.

The risk of galling increases with the increase of contact pressure and length of sliding contact in the tool.

Counteracting galling:

- Reduced friction (via lubrication, for example)
- Finer tool surface quality
- Increased tool surface hardness
- Increased sheet metal hardness



Figure 6.50: Back support Docol 1400M.

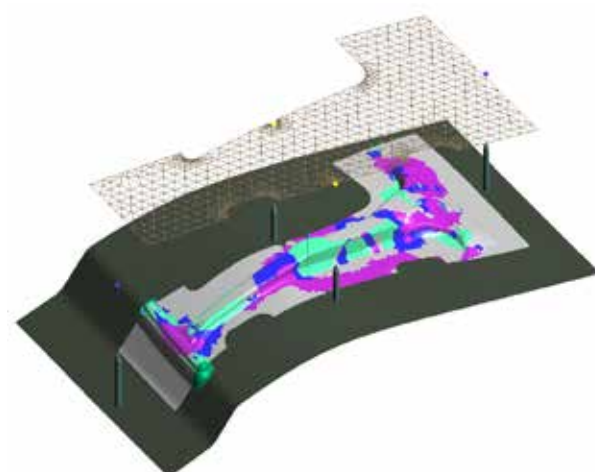


Figure 6.51: FEM simulation has become a vital tool in the field of sheet metal forming. Simulations make it easy to optimize the design, select the right material and significantly reduce the break-in period on forming tools. The illustration shows a B-pillar of Docol 800 DP.

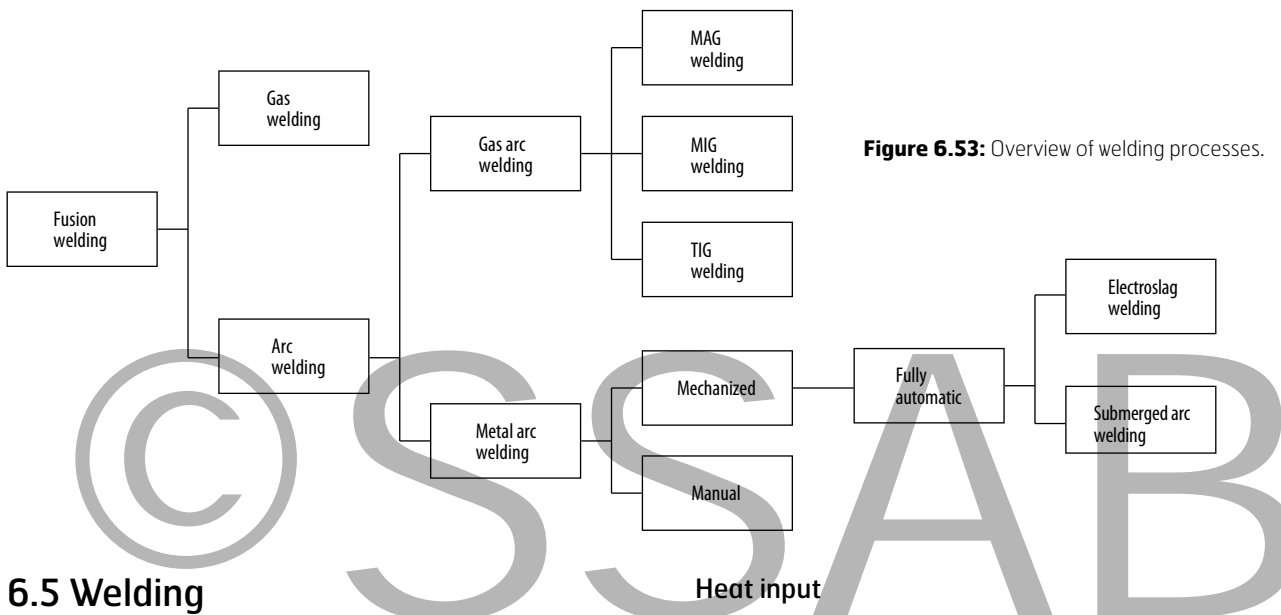


Figure 6.53: Overview of welding processes.

6.5 Welding

There are many different methods for joining steels, of which welding is the most common. Welding is divided into two main methods, fusion welding, cf. figure 6.53 and pressure welding. During fusion welding, the steel is heated locally to its melting temperature at which the work pieces are fused together. This is done without applying any pressure or using filler metals. For pressure welding the fusion takes place with or without heat, while pressure is used to carry out the welding.

6.5.1 Fusion welding

Of all fusion welding processes, the MAG (Metal Active Gas) welding method is the most common in the industry. This applies for both soft and high strength materials. Other possible fusion welding processes include MMA, TIG, plasma, laser and laser-hybrid welding.

Weldability

If a steel can be welded using a certain method without taking any special precautionary methods and without any normal changes in the process to give rise to apprehension regarding the reliability of the structure, the steel is regarded as weldable by this method. If, on the other hand, a normal welding process leads to such changes in the material that there is a serious risk for the structure not to comply with the above mentioned requirements or if material defects, such as cracking, are observed during or immediately after the welding, special precautionary measures must be taken (such as increased working temperature). In that case it is a matter of limited weldability steels.

In order for the steel to be regarded as weldable, the welded joint must be free from all kinds of cracks, and properties such as strength and toughness must be good. The strength and toughness in the joint must not be much poorer than those of the basic material so that the material can function well in the structure as a whole. This is usually referred to as good functional stability of the joint.

Heat input

The term heat input is used to describe how much heat is supplied to the material during fusion welding. The following formula is used to calculate the heat input:

$$E = \frac{U \cdot I \cdot 60}{V \cdot 1000} \text{ kJ / mm} \quad (\text{Eq. 6.5})$$

U – voltage

I – current

V – welding speed (mm/min)

The reason why it is important to know what heat input is used during welding is that high strength steels are somewhat more sensitive to high heat input as compared to soft steels. Too high a heat input can impair the mechanical properties of the welded joint. When welding high strength steels, low heat input is preferable both from a strength and from a toughness point of view.

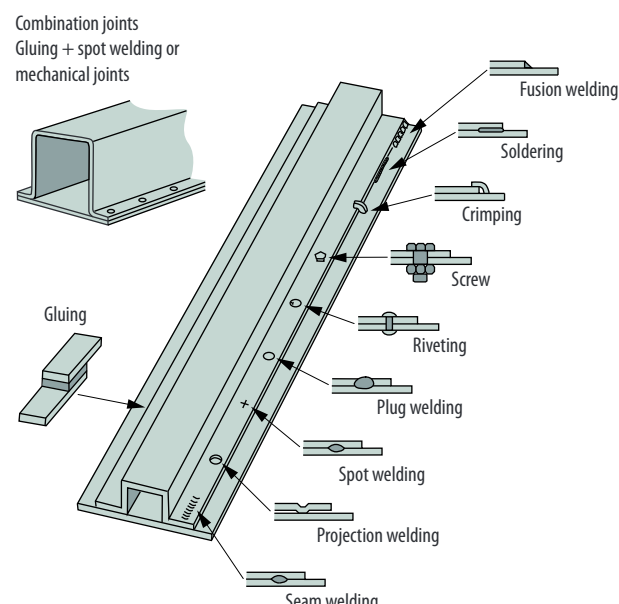


Figure 6.52: Different joining methods.



Heat affected zone

During welding, the steel is heated to a very high temperature which alters the microstructure of the steel in the welding area. The part of the material affected by the welding heat is called HAZ (heat affected zone). HAZ is divided into different subzones depending on how the material is affected by the heat from the arc. The size of HAZ varies depending on the cooling time ($\Delta t_{8/5}$). The cooling time is in turn dependent on many factors such as heat input, plate thickness joint type, welding process, etc. If the toughness and strength requirements are very high, the heat-affected zone shall be as limited as possible. *Figure 6.54* shows the nomenclature used for different zones and limits in accordance with the technical glossary of the Swedish Welding Commission [6.18]. Weld metal is the material that has been fused during the welding process.

Welding defects

Different defects/imperfections that can occur in connection with welding constitute notches with the consequence that local stress concentrations occur when load is applied. The shape and extension of the defect affect the notch effect. A crack in the welded joint is a much greater notch than a few pores, for example, which are relatively unimportant. Depending on the type of the defect that can occur in a welded joint, the acceptance limits differ and are usually regulated by different types of quality class designations. Compliance with requirements is usually verified by different types of tests, such as radiography (X-ray) for example.

Different types of cracks that can occur in the welded joint in connection with welding are usually due to the chemical composition of the steel and filler metals. These welding defects can be cold cracks, hot cracks, etc. and are therefore referred to as "material dependent welding defects". Defects such as incomplete penetration, slag inclusion, etc. are defects that can occur because of an inadequate welding procedure.

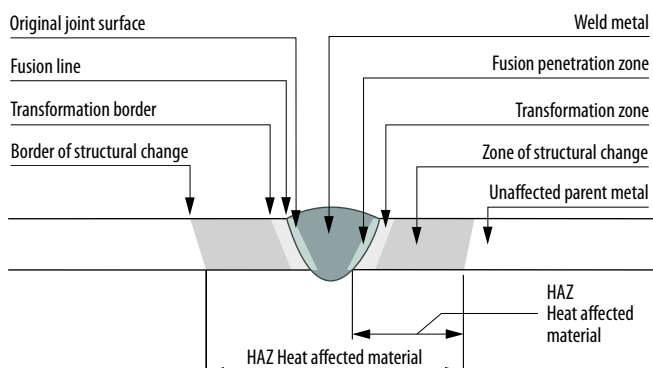
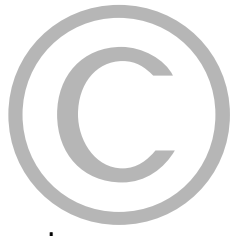


Figure 6.54: Heat-affected zone during welding.



SSAB

Cold cracks

These cracks normally occur in the heat affected zone (HAZ) and are normally oriented parallel to the fusion line, cf. *figure 6.55*. The cracks form at a temperature below 200°C, hence the name cold cracks. The cracks do not always reach the surface and even if they do, they are very difficult to discover with a naked eye.

In order for cold cracks to form, the combined effect of the following is necessary:

- brittle microstructure
- presence of hydrogen
- high stress

The risk for cold crack formation in connection with fusion welding is associated with the alloying content of the steel. In order to describe the quantity of alloying elements different types of formulas are used for determining the carbon equivalent of the steel. The most common is CE_{IIW} which has been developed by the International Institute of Welding.

$$CE_{IIW} = C + \frac{Mn}{6} + \frac{Cr + Mo + V}{5} + \frac{Cu + Ni}{15} \quad (\text{Eqn. 6.6})$$

The lower the carbon equivalent value, the lower the precautionary measures required to keep a joint free from cold cracks.

Hydrogen can be supplied to the weld in part as moisture via the filler metals or through impurities on the joint surface (rust, frost, etc. on the fusion face), in part via the atmosphere. Most of the hydrogen usually comes from the filler metal. In case of MAG welding, for example, with wire electrodes or gas shielded cored electrodes, the filler metal contributes with hydrogen levels of 2–4 ml/100g weld metal, which is regarded as very low.

Residual stresses always occurs in connection with welding due to shrinkage when the weld cools down. It is not unusual that these stress types are on a par with the yield point of the steel and/or the weld metal. Stress is also the factor that is most difficult to affect.

Hot cracks

Unlike cold cracks, hot cracks occur at very high temperatures, above 1200°C, and are usually located in the middle of the weld metal, along the weld, cf. *figure 6.55*. Hot cracks are usually very easy to notice without special aids because they are often open on the surface. However, there can also be hot cracks in the weld, which are not visible.

High carbon, sulfur, phosphorus and niobium content in the weld metal encourage hot crack formation. The quantity of these elements in the weld metal is determined by the composition and the degree of fusion of the parent material. To reduce the risk of formation of this type of cracks, make sure that the height of the weld run does not exceed the width of the run, cf. *figure 6.56*.

Defects influenced by the welding procedure

“Defects influenced by the welding procedure” refers to defects that have occurred because the welding operator/welder has used an incorrect welding procedure and not because the steel is the cause of the welding defect. There are many different welding defects of this kind. An overview of the most common ones can be found in *figure 6.57*.

Welding processes

There are many different fusion welding processes for welding thin plates, the most common of which are:

- gas metal arc welding (MAG, TIG)
- manual metal arc welding
- submerged arc welding
- laser welding

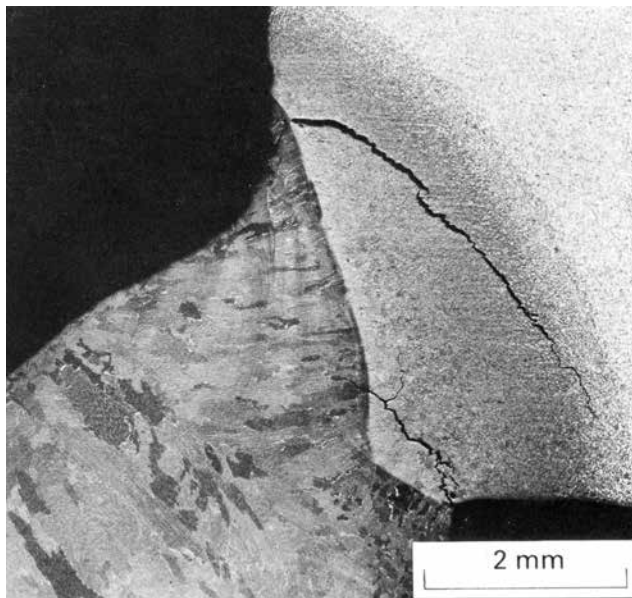


Figure 6.55: Cold and hot crack, respectively [6.17].

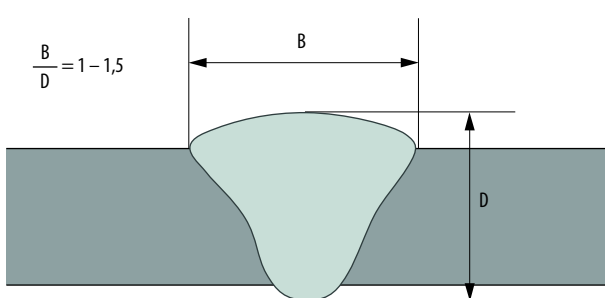


Figure 6.56: Recommended weld depth or width, respectively [6.17].

Welding defect/ imperfection	Cause	Measure
Lack of fusion	<ul style="list-style-type: none"> - Too low heat input - Joint angle too small - Too low/high welding speed - Incorrect torch angle - Electrode stick out too long - Oscillation too wide - Convex beads 	<ul style="list-style-type: none"> - Higher arc voltage - Increase the joint angle - Adjust the welding speed - Correct the torch angle - Adjust the electrode stick out - Add more beads - Fill the sides
Root defect	<ul style="list-style-type: none"> - Incorrect torch angle - Root face too large - Too low heat input - Too small root gap 	<ul style="list-style-type: none"> - Correct the torch angle - Reduce the root face - Increase the heat input - Increase the root gap, stitch closer - Use backing
End crater/Pipe	- Incorrect weld finish	<ul style="list-style-type: none"> - When finishing the welding the electric arc may not be broken immediately, it must go above the end crater so that it is filled, after which the electric arc can be broken.
Undercuts	<ul style="list-style-type: none"> - Incorrect torch angle - Voltage too high - Incorrect torch waving technique - Too high a welding speed. 	<ul style="list-style-type: none"> - Adjust the torch angle to the welded joint - Adjust the welding voltage in relation to the weld current. - During oscillation, the edges must be carefully filled - Adjust the welding speed in relation to the current
Pores	<ul style="list-style-type: none"> - Impurities on the parent material - Moist filler metals - Draught - Too low or too high gas flow - Torch angle too big - Clogged gas nozzle 	<ul style="list-style-type: none"> - Clean the material - Protect the welded steel against draughts. - Make sure that the right gas flow is obtained at the gas nozzle - Clean the gas nozzle from spatter
Reinforcement of Weld/ Root Reinforcement	<ul style="list-style-type: none"> - Incorrect planning of the beads - Welding speed too high/low - Too big a root gap - Root face too small 	<ul style="list-style-type: none"> - Plan the size of the beads so that the right joint volume will be obtained for the final layer - Adjust the welding speed to the weld current and arc voltage. - Reduce the root gap - Increase the root face surface
Spatter/Ignition marks	<ul style="list-style-type: none"> - Arc voltage too high - Impurities on the joint surface - Rusty material - Incorrect start location 	<ul style="list-style-type: none"> - Adjust the arc voltage to the current and welding speed - Clean the material from dirt and rust - Grind the material at the weld - Start in the welded joint, or alternatively, use start plates
Edge misalignment	<ul style="list-style-type: none"> - Slovenly tack welding of work pieces - Improperly fixed - Too big a distance between tack welds 	<ul style="list-style-type: none"> - Use fixture - Careful fitting - Smaller distance between tack welds

Figure 6.57: Different types of welding defects influenced by the welding operator [6.17].

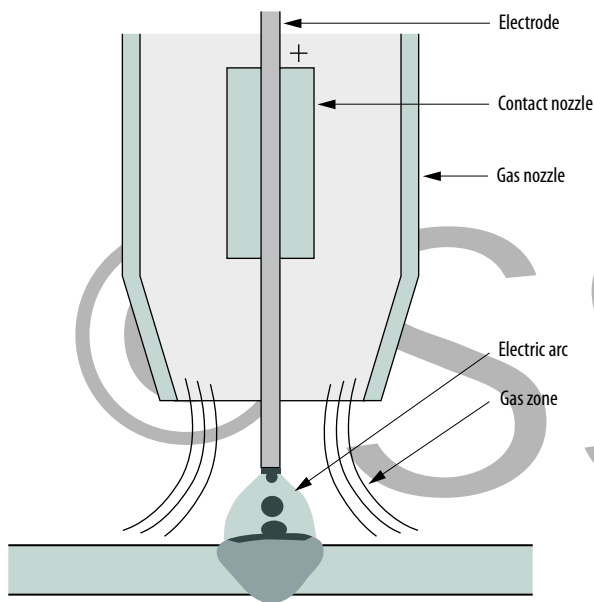


Figure 6.58: MAG welding [6.17].

SSAB

MAG welding

The most common welding process for thin plates is MAG welding. A DC source is used to create an arc between the continuously fed electrode and the work piece. The electric arc fuses the joint edges simultaneously with the fusion of the electrode material, cf. figure 6.58. The process, inclusive of fused material, is shielded by a shielding gas, usually consisting of argon/CO₂ mixtures.

The method can be used manually, but is also suited for automated welding where the productivity can be very high. Solid electrodes are often used as filler metal, but the use of cored wires is growing. The strong development of power sources recently, which has resulted in a very low heat input, has contributed to making it possible to MAG-weld plate thickness of approximately 0.5 mm.

In the case of lower heat input (less deformations in thin plates), MIGsoldering can be applied. The same equipment is used here as for MAG welding. It is only the electrode materials and the shielding gas that are different.

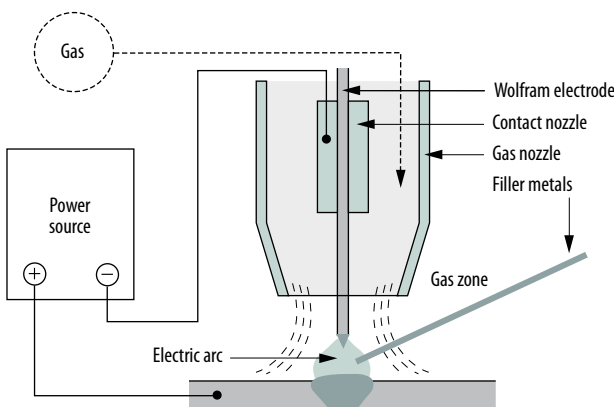


Figure 6.59: TIG welding [6.17].

TIG welding

A DC power source is used during TIG welding for creating an electric arc between a fixed, non-fusing electrode and the joint. In order for the electrodes not to melt at the high temperature developed by the electric arc, the used electrodes are made of wolfram alloys. Any filler metals must be added manually from the side during manual welding, cf. figure 6.59.

If the welding is properly performed, the method offers very high weld quality where the weld metal has a uniform and soft connection to the parent material. The relatively low productivity of the method limits its use to special materials and/or very small plate thicknesses.

A special area of application for the TIG welding process is "TIG dressing". The method is used to remelt the area between the weld metal and the parent material (weld toe) with the result that the connecting angle and the radius increase in the weld toe, while at the same time possible defects such as undercuts, are removed. The TIG treatment helps improve the fatigue strength of the welded joint.

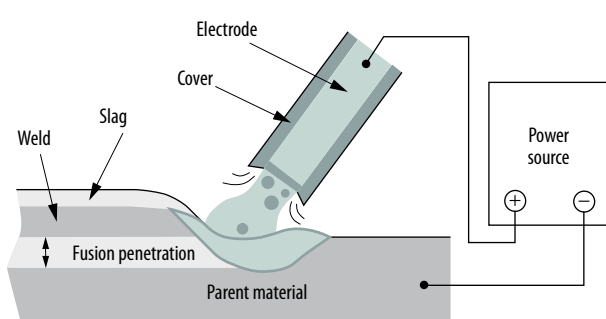


Figure 6.60: Metal arc welding [6.17].

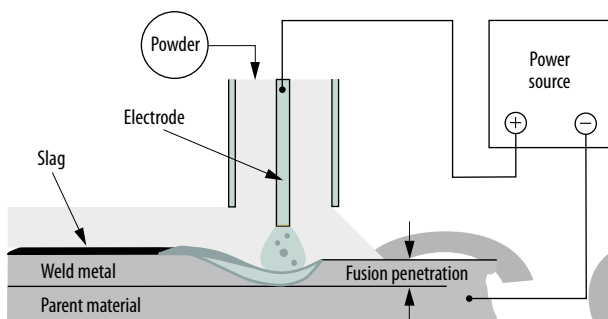


Figure 6.61: Submerged arc welding [6.17].

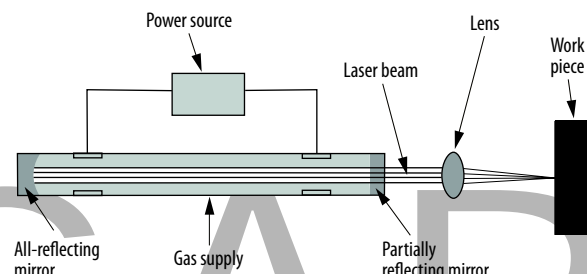


Figure 6.62: Laser welding (CO₂) [6.17].

Manual metal arc welding

During manual metal arc welding, an electric arc is created between a covered electrode and the work piece. At the same time as the joint melts in the entire electric arc, the electrode melts as well and drops of molten filler metal are transported into the joint via the electric arc, cf. figure 6.60. The electrode consists of a core wire and a cover where the chemical composition is generally basic, rutile or acid. The basic and rutile electrodes are most common.

Manual metal arc welding is primarily a manual method and is used advantageously where MAG welding is not appropriate, such as for outdoor welding, for example. Metal arc welding can be performed in plate thickness from approximately 2 mm or more. The method is low-productive as compared to MAG welding, primarily because of the frequent electrode replacement and slag operations.

Submerged arc welding

During submerged arc welding, a DC, an AC or a combination of both power sources is used to create one or several electric arcs (tandem welding) between the electrode/electrodes and the work piece. The method is somewhat reminiscent of MAG welding with the steady fed electrode but instead of shielding the process with a shielding gas as in the case of MAG welding, a powder is used whose composition is similar to the composition of the cover of the covered electrodes in the case of metal arc welding, cf. figure 6.61.

The method is usually fully mechanized and is advantageously used with thicker plates where the deposition rates (weld metal kg/h) can be very high. The method, however, can be used in thinner plates but not usually with thicknesses of less than 4 mm.

Laser welding

A CO₂ laser or an Nd:YAG laser is usually used in laser welding. The big difference between Nd:YAG and CO₂ laser is usually the wave length of the laser beam. Because of the short wave length of the Nd:YAG laser, the beam can be guided along long stretches via optic fiber, whereas welding with CO₂ laser uses mirrors to transport the laser beam to the weld, cf. figure 6.62. The beam is focused to a few tenths of a millimeter. The focal point is placed on or

just below the top of the work piece. Shielding gas is supplied for the purpose of:

- Protecting the weld from the detrimental effect of the atmosphere.
- Protecting the focus lens/mirror from material spatter and metal vapor.
- Preventing or minimizing the plasma from ionized metal vapor that is formed above the work piece. This plasma absorbs laser energy and prevents it from reaching the work piece.

A relatively deep and narrow weld is obtained by laser welding. The welding is based on the so called key hole effect, cf. figure 6.63. The key hole consists of a cavity filled with evaporated metal which is surrounded by fused metal.

Laser welding is most frequently used with thin plates where lap joints are usually used. Welding is done with or without filler metal.

Laser welding in thicker plates and butt welded joints places very high requirements on joint fitting to deliver a good weld. Recently this method has been developed in combination with others methods, the so called laser hybrid, which has resulted in reducing the high joint fitting requirements significantly. Because of the tendency to laser hybrid methods, this method has attracted interest even in the case of thicker plates.

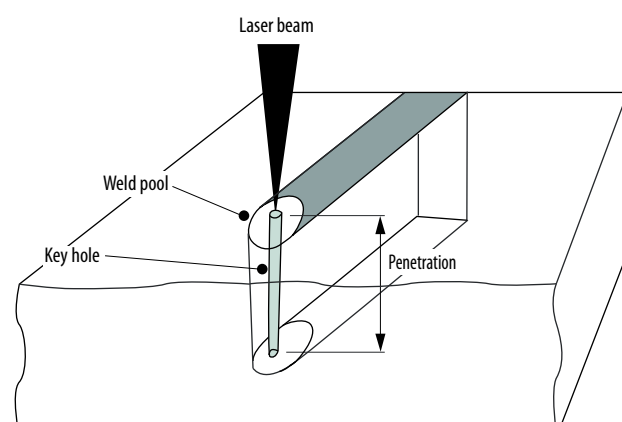
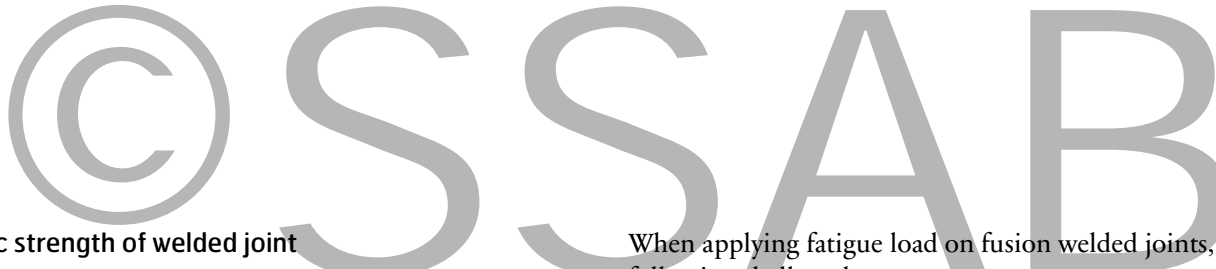


Figure 6.63: Laser welding principle.



Static strength of welded joint

A common requirement to a welded joint is that the static strength (tensile strength) shall not lie below the minimum requirement that applies for the parent material. In practice, this means that both weld metals and the heat-affected zone must have sufficient strength. The strength of the welded joint is affected by multiple factors such as choice of filler metal, steel composition, heat input, plate thickness, joint type, etc.

According to SSAB's recommendation, matching filler metals shall always be used if there is uncertainty as to what strength is required in the specific situation. In most cases, however, undermatching filler metals are used, for example:

- when the weld is in a low stress area
- for fillet welds
- for welding to a standard soft steel
- if the weld reinforcement can be maintained – in the case of the most fatigue-stressed joints
- if low hardness is desired in the weld metal

A basic prerequisite for using undermatching filler metal is that it is acceptable according to current product standards.

Fatigue strength of the welded joint

The fatigue strength of the welded joint is considerably lower than the fatigue strength of the unwelded plate. As a result, the fatigue strength of the welded joint is often crucial for the carrying capacity of the entire structure. A weld contributes to an increased notch effect, which increases the local stress, which in turn is the fundamental reason why welds have lower fatigue strength as compared to unwelded material.

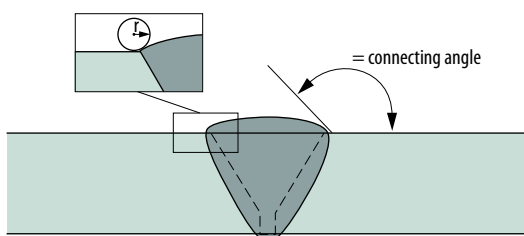


Figure 6.64: The connecting angle and radius in the transition between weld metal and weld metal [6.17].

When applying fatigue load on fusion welded joints, the following shall apply:

- the weld geometry (micro and macro geometry) determines the fatigue strength of the welded joint.
- the stress range is of decisive importance for the service life of the welded joint.

In order to use the high strength Domex steels in the best way possible in welded, fatigue-loaded structures, it is important to customize the structure and manufacturing methods to the high work stress.

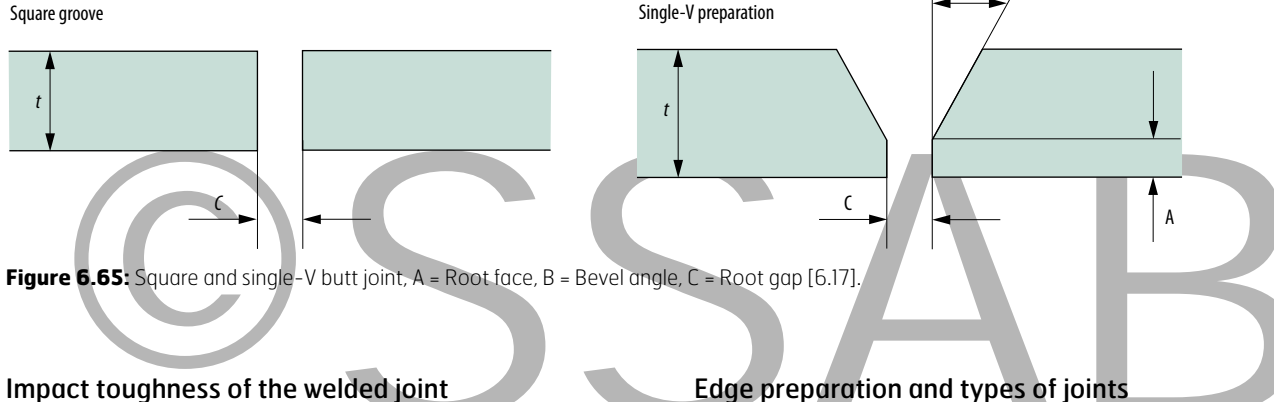
The following recommendations increase the fatigue strength/service life of the welded structure:

- If possible, try to create a good micro geometry by, for example, using butt welds instead of fillet welds.
- The welder should strive to create a favorable micro geometry. Make sure that you comply with the requirements of the selected quality class. Welding defects that the welder should avoid and therefore be very careful about, include undercuts, root defects, lack of fusion and "cold laps"; cf. figure 6.54. Try to create a smooth weld toe with a large angle and radius between the weld and the parent material, cf. figure 6.64.
- Other geometric deviations that should be avoided are edge and angular displacement.

If the structure includes individual welds with very high stresses, it can be cost-efficient to apply any of the available post weld treatment methods:

- TIG dressing – burr grinding
- peening – shoot peening

The principle of these methods is, through remelting or mechanical treatment, to create a favorable geometry near the weld toe while at the same time remove any welding defects (TIG treatment and grinding) in this area. The fatigue strength can be increased by 30–100% of the post weld treated welded joint.



Impact toughness of the welded joint

To avoid brittle fracture in the welded structure at impact and/or crashes at low temperature, the impact toughness must be good enough. The lowest impact toughness is normally found in the heat-affected zone of the welded joint.

The impact toughness depends upon the microstructure of the welded joint, which in turn depends on many different factors such as:

- choice of filler metal
- steel type
- heat input
- plate thickness
- welding process
- joint type
- etc.

Beside the choice of filler metal that complies with impact toughness requirements, heat input is the most important aspect to consider. As a basic rule, you should always strive to use a low heat supply with multiple-bead structure to limit the so called coarse-grained zone in HAZ where the worst impact strength is found.

6.5.2 Fusion welding in hot rolled steel

Hot rolled steel from SSAB is manufactured in thicknesses from about 2 to 16 mm. This section covers:

- Cold forming steel
- Weathering steels
- Boron steel
- Wear strip

The chapter provides basic information for welding of hot rolled steel, for more information see SSAB joining and welding handbook or contact SSAB for more information.

Edge preparation and types of joints

The methods usually applied for preparing high strength Strenx steels is thermal cutting or any form of machining such as milling. For thinner Strenx steels, it is possible to use a standard cut edge (square butt joint).

Edge preparation of the Strenx high strength steel is carried out in the same manner as edge preparation of common soft steels. An increase in work temperature during thermal cutting is not necessary. If thermal cutting is used, a thin oxide layer will form on the surface that has to be removed before welding.

Welded joints strength

The most common joint types for Strenx steels are square and single-V butt joints. Square butt joints are used for thin plates with a thickness of up to 3–4 mm. If the thickness is greater, single-V butt joints are used, cf. figure 6.65.

During welding of Strenx cold formed steels with yield strength above 550 MPa, soft zones are formed in the heat affected zone, cf. figure 6.66.

The width of the soft zones and the hardness are determined by cooling time (heat input, plate thickness, work temperature, etc.). If normal heat input is used, these soft zones are of no importance for the strength. If on the other hand, high heat input is used, the soft zones become more wide-spread while at the same time the hardness is reduced even more, which can cause the strength of the welded joint to fall to a level that is lower than that of the parent material.

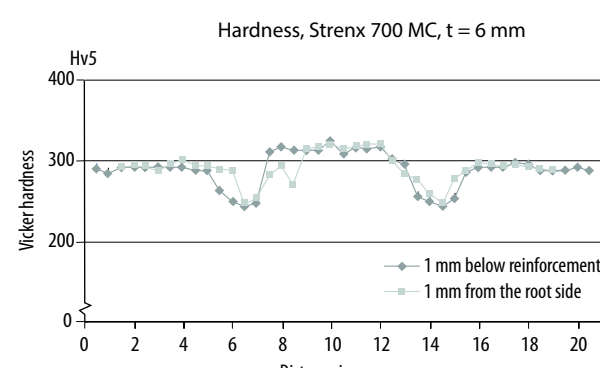


Figure 6.66: Typical hardness profile for Strenx 700 MC, t = 6 mm where recommended heat inputs are used [6.17].

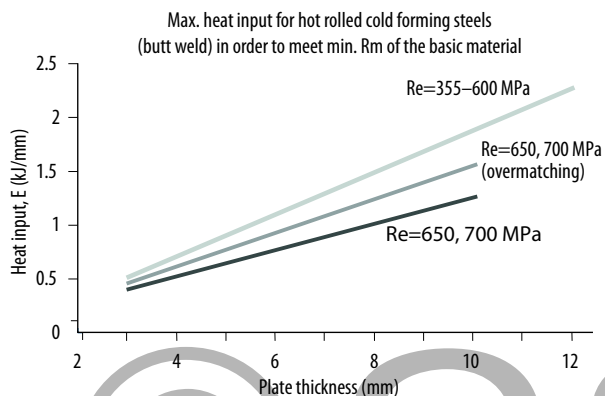


Figure 6.67: Recommended maximum heat input for hot rolled cold forming steels. (butt weld, matching filler metals, reinforcement removed by grinding [6.17].

In figure 6.67 you can see the maximum recommended heat input that is applicable for different hot rolled steels.

If the welding concerns fillet welded joints, the maximum recommended heat input can be increased by approx. 30–40%.

Multi pass welding can cause the temperature in the welded joint to increase to a level that is detrimental for the material and that results in a strength reduction. This is most critical at shorter welds of less than 500 mm because the temperature does not have enough time to decrease in the material before the next bead is welded. To limit a temperature increase that would be detrimental for the material, it is possible to apply a maximum interpass temperature, meaning that the temperature at the start point of the next bead may not exceed the specified value. The following recommendations apply for maximum interpass temperature:

$$Re = 355 - 550 \text{ MPa} \quad 150^\circ \text{ C}$$

$$Re = 600 - 700 \text{ MPa} \quad 100^\circ \text{ C}$$

Impact toughness of the welded joint

In figure 6.68 you can find the maximum recommended heat input to fulfill the minimum impact toughness requirement (50 J/cm^2) at -20° C for hotrolled cold forming steels.

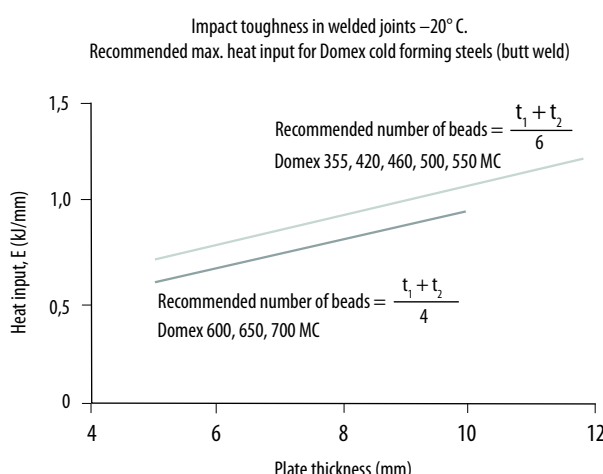


Figure 6.68: Maximum heat inputs as well as suitable choice of beads number for Domex cold formed steel to comply with the impact toughness requirement 50 J/cm^2 at -20° C (longitudinal test, butt weld) [6.17].

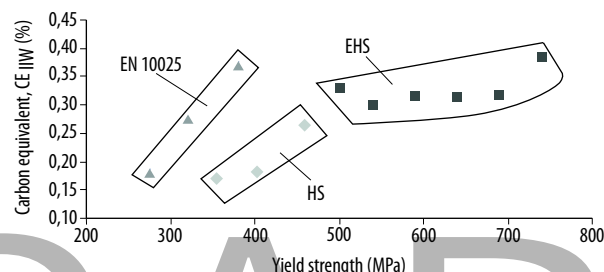


Figure 6.69: Comparison between the carbon equivalent and the yield strength of hot rolled cold forming steel and the standardized steels in EN 10025 [6.17].

In practice, these recommendations mean that 1–2 beads can be used for thicknesses up to 6 mm in cold forming steels with maximum yield strength of 550 MPa. For thicker plates (>6mm) it is recommended to increase the number of beads even further.

For steels of the highest strength, $Re = 600 \text{ MPa}$ and higher, 3–5 beads in the thickness range 6–10 mm are recommended.

Filler metals for cold forming steels

Examples of recommended filler metals for hot rolled cold forming steels can be found at ssabdirekt.com. The specified filler metals “match”, which means that the filler metals have the same strength as the steel or greater.

The risk of cold crack formation in connection with welding in the cold forming steels is very small, primarily depending on the lean steel composition of the steel. Despite the high strength, the carbon equivalent of the steel is not higher than that of conventional structural steels of much lower strength, cf. figure 6.69.

Thanks to the low carbon equivalent of hot rolled cold forming steels, there is a large selection of filler metals to choose from. The filler metals, however, should give a maximum hydrogen content of $10 \text{ ml}/100\text{g}$ weld metal for extra high strength steels (EHS), cf. table 6.5.

With these recommendations, rutile electrodes (MMA) can be used for welding high strength cold forming steels whereas basic electrodes are recommended for the extra high strength cold forming steels. During MAG welding, both rutile and basic cored wires can be used, regardless of steel strength.

It is important to remember that the filler metals have to be stored and handled in accordance with the filler metal manufacturer's instructions in order to minimize the risk of undesired welding defects during welding.

Steel type	H ₂ /100 g weld metal
Cold forming steel (HS) $\leq 420 \text{ MC}$	$\leq 30 \text{ ml}$
Cold forming steel (EHS) $> 420 \text{ MC}$	$\leq 10 \text{ ml}$

Table 6.5: Recommended maximum hydrogen content added for the different cold formed steels.

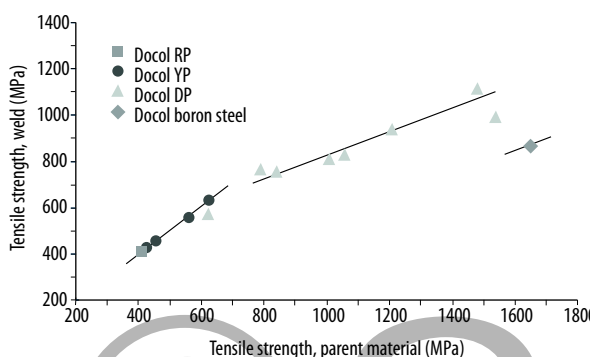


Figure 6.70: Strength of welded joints for different Docol steels (tensile tests across the welded joint, reinforcement removed by grinding, matching electrodes, MAG welding, 1 bead, heat input 0.11 – 0.17 kJ/mm) [6.17].

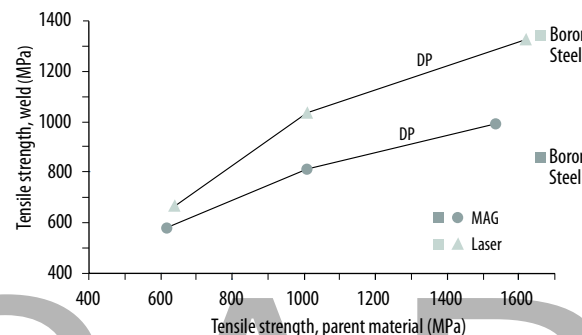


Figure 6.71: A strength comparison between MAG and laser welded joints for Docol DP and boron steel (thicknesses 1.6 – 2.0 mm, butt weld, tensile test across the welded joint, reinforcement removed by grinding, matching filler metals for MAG, no filler metal for laser welding) [6.17].

Filler metals for weather resistant steel

The type of electrodes developed especially for this type of steel is recommended for welding. These electrodes have high content of nickel and copper in order to give the weld metal a composition that offers good corrosion protection.

Conventional electrodes for welding of “standard” steels can also be used. As compared to the parent material, the weld can have somewhat reduced corrosion resistance.

Filler metals for hot rolled boron steel (014B, 024B)

Boron steel has higher alloy content as compared to cold forming steel. Despite that fact, fusion welding of boron steels is possible. To avoid cold crack formation, it is important to use welding processes that give low hydrogen contents $\leq 5\text{ml}/100\text{ g}$ in weld metal.

It is recommended to perform the welding before the quenching operation of the material. This way the difference between the hardness of the welded joint in the weld metal and in the parent material is small. If electrodes with low strength are used, the hardenability will be reduced thus the strength of the weld metal will be lower than that of the parent material. If the weld can be placed in an area with low wear resistance requirements, this will not pose a problem.

If the welding takes place after hardening and if high strength or high wear requirements apply for the weld, high strength filler metals must be used in order not to have too big a difference between the weld and the parent material. Filler metal examples can be found at ssabdirekt.com.

6.5.3 Fusion welding in Docol steel

Filler metals

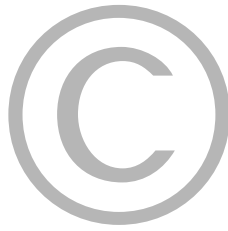
Examples of recommended filler metals for Docol steels can be found on ssabdirekt.com. The filler materials are matching or somewhat undermatching for Docol steels of the highest strength. Undermatching filler materials, however, can be normally used without reducing the strength of the welded joint significantly as compared to matching filler materials (MAG-welding).

For the weather resistant cold rolled steels (Cor-Ten and Docol W) filler metals customized for this type of steel are recommended. These filler metals are alloyed with e.g. copper and nickel to get a corrosion resistance that corresponds to the corrosion resistance of the steel.

Strength of welded joints

The strength of the welded joint is somewhat lower than that of the parent material in the case of Docol steels, whereas the strength is higher than that of Docol 600 DP. The reason why is that soft zones are formed in the heat affected zone and the failure is observed in one of these soft zones during tensile tests across the weld. The strength decrease is somewhat bigger for Docol steels with the absolute highest strength, cf. figure 6.70.

If greater weld strength is required, laser welding can be chosen. With laser welding, the heat supply is, of course, lower which results in reduced size of soft zones in the heat affected area, which result in increased strength of the welded joint, cf. figure 6.71.



6.5.4 Fusion welding of metal-coated thin plates

Metal-coated thin plates are somewhat more difficult to weld as compared to uncoated thin plates. Special measures must therefore be taken in order to achieve a satisfactory result.

Filler metals

When welding metal-coated thin plates, soft filler metals are usually recommended. It is only for the steels with a yield strength from 500 MPa and above where filler metals of higher strength can be warranted.

A list of recommended filler metals can be found at ssabdirekt.com.

There is a flux-cored wire for MAG welding, which has been especially developed for welding zinc-coated plates [6.17]. Single pass welding is recommended and it is important to ensure that the electrode is connected to the negative pole. This wire gives less spatter and pores, as well as a more uniform weld as compared to conventional solid wires. A disadvantage, however, is that this cored electrode leaves a thin layer of slag on top of the weld.

The effect of zinc on fusion welding

The main reason why metal-coated plates are more difficult to weld than standard uncoted plates is the zinc in the metal layer, which is quickly vaporized during the welding process. This affects the electric arc and in some cases makes it difficult to complete the welding. Spatter and pores are commonly observed during welding of zinc-coated plates.

The factors that have to be considered during fusion welding of metal-coated plates are [6.17]:

- it is difficult to achieve a stable electric arc
- an increased number of pores in the weld
- more spatter
- reduced fusion penetration
- increased amount of welding fumes



Recommendations

The best solution from a welding perspective is to locally grind the coating to remove it. In order to preserve a good corrosion resistance after the welding, some form of subsequent anti-corrosion treatment will be required, regardless of whether the coating has been removed or not. Such subsequent treatment can be, for example, applying a paint rich in zinc.

If it is not possible to remove the coating by grinding, one of the following measures or more are recommended [6.17]:

- Use as thin a coating layer as possible
- Reduce the welding speed
- During MAG welding use a shielding gas with high CO₂ content (especially for thick coatings)
- if possible, use a thin gap between the plates (lap welds)
- Spray the plate with “anti-spatter” oil before the welding
- During MAG welding, use a flux-filled cored wire designed for welding of zinc-coated plates
- Use MIG brazing with copper wire

Corrosion of welded joints

Since the zinc layer evaporates in front of the arc the corrosive properties of the welded joint deteriorate. If you want to improve the corrosive properties of the joint, the following are recommended [6.17]:

1. Cleaning the surface.
2. Preliminary treatment (brushing, scraping, grinding or sand shot peening).
3. Applying an epoxy paint that is rich in zinc.



6.5.5 Electrical resistance welding

Electrical resistance welding is a very common method for joining thin plates. Spot welding is the most common of methods, but projection welding and seam welding are also used.

Electrical resistance welding principle

During resistance welding, plates are joined without adding any filler metal. Electrical resistance welding is a pressure welding process, i.e. the fusion faces of the work piece are exposed to pressure during the welding process. The weld is heated up by using an electric current that is led through the work piece. The heat input is directly associated with the electric resistance of the weld spot.

Since the electric resistance of steel plates and the contact resistance between the plates are relatively small and the welding is done for a short time, very high current is required in order to allow sufficient heat to build up. Sufficient heat is the heat that causes the material to melt locally between the joint surfaces so that a so called weld nugget is formed. A prerequisite for a good and reproducible weld is to remove oxide scale, impurities and other coatings with high electric resistance before welding.

A great advantage of resistance-welded components is that the deformation of the plates is small as compared to fusion welding, for example.

Electrical resistance welding is a very common method for joining thin plates in thicknesses of up to 3 mm. Plates thicker than 3 mm can be resistance welded too, but the equipment must meet very high requirements such as being able to withstand high electrode forces. Fusion welding is therefore a much more common method for joining thicker plates.

Spot welding

Spot welding is the most common method for joining thin plates (plate thickness < 3 mm).

During spot welding, weld current is supplied through rod-shaped electrodes which simultaneously transfer the compressive force. The material is heated up quickly to the desired maximum temperature (cf. figure 6.72) after which the current supply is discontinued. However, the pressure on the weld is maintained for a short time after the current has been cut off in order to allow the weld to cool down and obtain sufficient strength before the electrode force is released.

The welding variables that have the greatest influence on the quality of the spot weld are:

- electrode tip diameter
- electrode force (F)
- squeeze time (T_A)
- weld time (T_s)
- weld current (I_s)
- holding time (T_H)

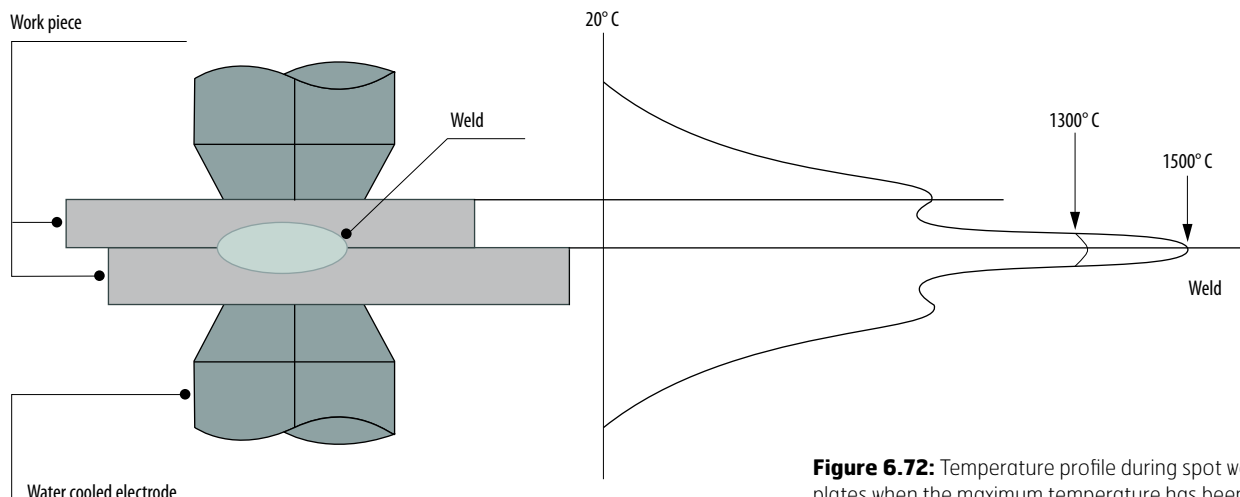


Figure 6.72: Temperature profile during spot welding of thin plates when the maximum temperature has been achieved.

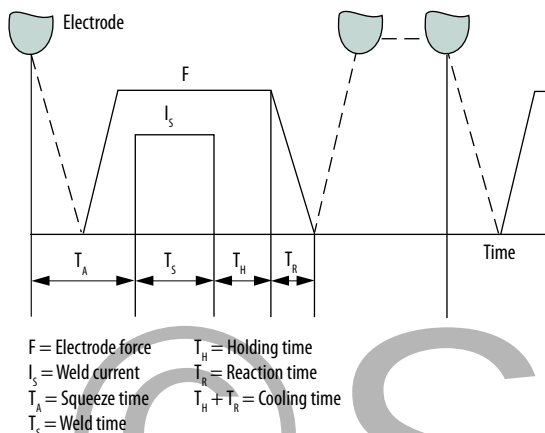


Figure 6.73: Welding process and parameters during spot welding.

The spot welding procedure can be seen in figure 6.73. During the spot welding cycle, the electrode force is accumulated during the squeezetime T_A . The weld current is supplied during the weld time T_s . The weld is cooled down during the holding time T_H after which the electrode force is released. The spot weld is cooled by the electrodes during the reaction time as well, until the electrodes let go completely. Reaction time + holding time are referred to as cooling time.

Both alternating current (AC) and direct current (DC) machines are used for spot welding. DC machines are most common in the automotive industry.

The rod-shaped electrodes must have good electrical and thermal conductivity and at the same time have high strength at elevated temperatures in order to prevent the electrodes from deforming during the welding process. Because of the high temperature strength requirement, copper electrodes are not allowed. Small quantities of other elements (such as chrome and zirconium) must be added in combination with copper in order to meet the strength requirements. The electrodes are cooled with water all the time because their good cooling is essential. To maintain the weld quality, it is also important to inspect the electrodes at regular intervals. If the contact surface has increased, it must be formed to the right diameter. To reduce the cost, different replaceable electrode ends, in part electrode caps and in part male electrode caps. Electrode caps are very common in the automotive industry, for example.

When setting welding parameters it is a good idea to use as basis the steel type, thickness and surface coating of the plates that going to be spot welded.

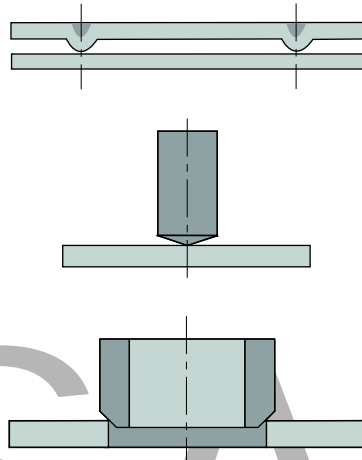


Figure 6.74: Different projection welding variants.

The following working methods are recommended:

1. Select the electrode tip diameter and the electrode force.
2. Set the squeeze time, the weld time and the holding time.
3. Finally, adjust the weld current by test welding.

The electrode force affects the contact resistance between the plates which is important for obtaining the right amount of heat input. The squeeze time shall be as short as possible, but still long enough for building up the full electrode force before supplying the weld current. The weld time shall be so long that a sufficient size of weld nugget is formed. The holding time shall in turn be sufficient for the weld to get strong enough before the joint or welding rod is moved. The current shall be at least so high that a satisfactory weld is obtained but at the same time not too high that spatter is formed during welding. The interval during which the current is allowed to vary is referred to as "available welding current range" and the size of the interval is a measure of the material's weldability.

Projection welding

During projection welding, the work piece components are shaped so that the weld surfaces would be raised and current and pressure can be concentrated there without any special electrode design to be necessary. In figure 6.74 you can see several different projection welding variants. The purpose of the electrodes is to transfer the current to the work piece on a relatively large surface, while at the same time fix the parts into the right position. The elec-

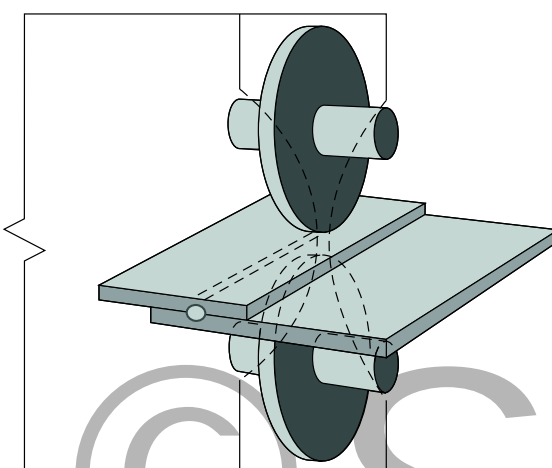


Figure 6.75: Seam welding.

trodes are less worn down than during spot welding and do not leave any imprints on the work piece surface.

A type of projection welding of thin plates is when a projection has been pressed into the plate steel and the plate are then welded together. One more projection welding variant is when a weld nut is welded to a plate. In that case, the weld nut can have a single projection (usually three or four projections) or with an annular projection (ring shaped projection).

Seam welding

Seam welding is used for welding thin plates in lap joints. During seam welding electrodes in the form of rollers are used to transfer the current and force to the plates, cf. figure 6.75. In general, one of the electrodes is operating, i.e. it feeds the plates while at the same time a continuous weld is achieved.

From a technical welding perspective, seam welding resembles spot welding. The electrode force, however, is kept constant during the entire welding operation, while at the same time welding speed is added as a new welding parameter. The welding can be carried out so that spots overlap (close welding) or they can be placed at a certain distance depending on the density and strength requirements for the weld.

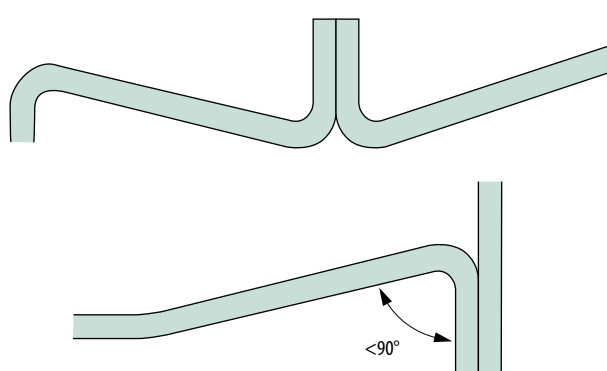


Figure 6.76: Example of inappropriate joint shapes during spot welding.

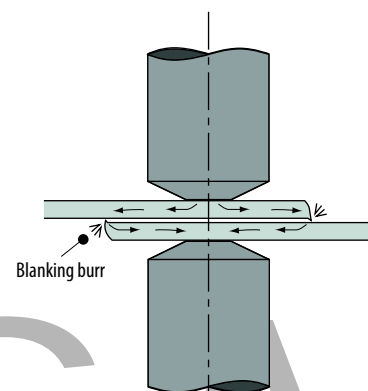


Figure 6.77: Sheared edges turned the wrong way cause leak current.

Structural instructions

Regarding structures that have to be resistance welded, remember that the electrodes must be easily accessible. Accessibility must be so good that the electrodes can be applied on the joints without coming into contact with neighboring plate surfaces. When the accessibility is good, standard electrodes, electrode arms and electrode holders can be used, which reduces the manufacturing cost. In figure 6.76 you can see a few examples of improper joint shapes in spot welding from accessibility perspective. Special electrodes are required for the welding of such components. The risk for inferior weld quality, however, is greater for this type of electrodes than for straight electrodes. It is also important to remember that blanking burr on the plate, if any, can be turned "right" so as to avoid current leakage through the burr (see figure 6.77). Problems associated with blanking burr mainly occur with thick plates. If a high electrode force is used, the risk of blanking burr problems is smaller. It is also important to select small enough a flange radius so as not to obstruct the fit-up of electrodes to the flange (cf. figure 6.78). Machine wear can be a cause for too big a flange radius.

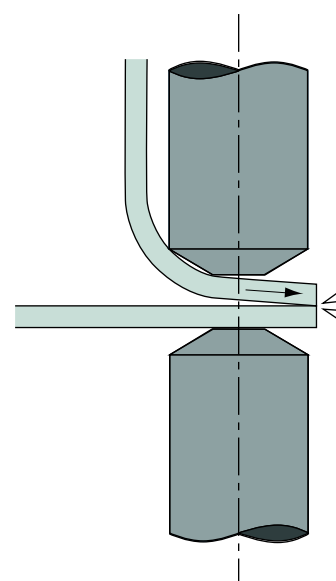
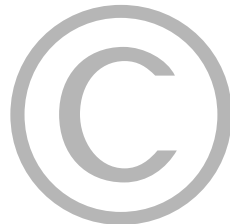


Figure 6.78: Spot welding where the flange radius is correct or too big, respectively.



SSAB

During spot welding of thin plates it is very important to know the minimum measures that apply for:

- flange width/overlap
- edge distance
- distance between welds

The flange width and the overlap must be big enough for the electrodes to fit and to be properly placed on the plate surfaces. The electrodes must not be placed too close to the plate edge and the distance between weld spots must be sufficient. The guideline values for flange width, overlap, edge distance and weld point distance can be found in *table 6.6*. *Figure 6.79* contains the definitions of the used designations. If the distance between the weld spots is smaller than the measures specified in *table 6.6*, there is a risk that the weld spot diameter would be too small as a result of leak current (shunt current) via previously welded spots. The strength of the spot welds will then be reduced. If it is not possible to increase the distance between spot welds, leak currents can be compensated by increasing the welding current. There are also welding machines with adaptive weld sensors which are able to compensate shunt currents via previously welded spots.

t mm	L mm	e mm		K mm
		Two plates	Three plates	
0,5	10	10	13	5
0,7	10	14	18	5
0,8	12	16	20	6
0,9	12	18	22	6
1	13	20	25	7
1,2	14	25	32	7
1,5	16	30	38	8
2	18	40	50	9
2,5	20	45	63	10
3	22	50	75	11
4	26	65	100	13
5	29	90	125	13

Table 6.6: Minimum flange width/overlap, spot distance and edge distance during spot welding. Designations – cf. figure 6.79.

The values in *table 6.6* apply for welding plates of the same thickness. When welding plates with different thicknesses, the flange width and the spot distance are selected according to the thickest plate.

To obtain good spot welding quality, the difference in the thickness of the plates shall not be too big. For a 2-plate joint, the thickness ratio between the plates may not be below 3:1 [3.17]. When welding a 3-plate joint with a big difference in the thickness of the plates (for example, two thick plates and one thin), try to place the thinnest plate in the middle.

The following minimum distance from the weld (the center of the weld) to the edge of the plate is recommended [3.17]:

- Flat profile: $1.25 \cdot L$ (where L is the width of the profile, cf. *figure 6.79*)
- Crowned profile: $5\sqrt{t}$ mm (t is the plate thickness)
or if expressed as a minimum overlap length:
- Flat profile: $2,5 \cdot L$
- Crowned profile: $10\sqrt{t}$ mm (t is the plate thickness)

Just as in the case of spot welding, there is leakage current if two parallel seam welds are too close to one another. It is therefore recommended for seam welds to be situated at least $16 \cdot$ plate thicknesses from one another (center-to-center distance).

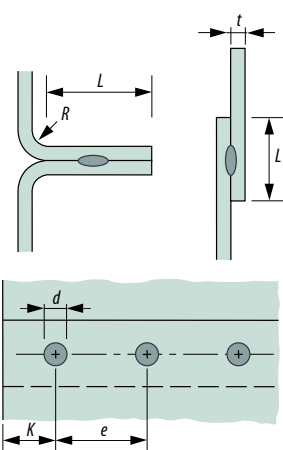
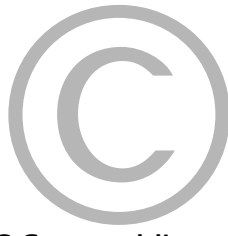


Figure 6.79: Spot welded joints. Clarification to designations used in table 6.1.



CSSAB

6.5.6 Spot welding

The following section describes testing, weld effects, geometry, failure type, service life and strength of spot welded joints.

Testing of spot welded joints

Tests must be conducted in order to confirm that the joints meet the current quality requirements.

The most common methods for testing spot welded joints are:

- visual inspection
- chisel test
- Peel test with a chisel
- Peel test with a roller
- metallographic examination– shear or tensile test

During an visual inspection (with a naked eye or through a magnifying glass) it is usually possible to determine whether the joint meets the appearance requirements. Examples of this type of requirement include that the surface of the welds may not be damaged by burn marks, it must be free from too deep indentations from the electrode and there must not be any spatter during the welding.

Chisel tests are used to check the strength of the welds. A chisel is hammered in alongside the spot weld. The plate must be able to withstand a relatively large deformation without the weld spot failing. This is a sign that it is a strong weld. This method does not offer an exact strength determination. If required, an exact determination of the strength can be obtained through other methods (please see below).

The peel test with a chisel is the best suited strength test for workshops. In this case, the joint is broken up with the help of a rounded chisel. A plug is pulled out and a hole is left in one of the plates. The size of the plug is measured. It shall be big enough and shall be able to comply with the prescribed minimum diameter. The plug diameter is directly associated with the strength of the weld. If the minimum plug diameter requirements are met, the minimum strength requirement will also be considered fulfilled.

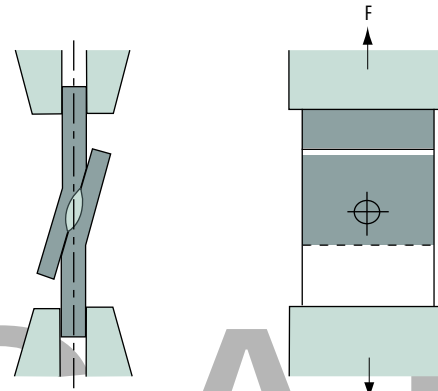


Figure 6.80: Shear tensile test of spot welded joints [6.17].

A variant of the chisel test is the peel test with a roller where the test is done manually or mechanical equipment is used for tearing apart. The assessment of the plug diameter, etc. is done in the same manner as for the chisel test.

A metallographic examination is also conducted sometimes. It involves a cut through the spot weld. After grinding, polishing and etching, the sample is examined under a microscope with regard to the weld nugget diameter and any possible defects such as pores, cracks, etc. In connection with this metallographic examination, a hardness measurement of the weld is also made in order to see how the hardness varies in the different weld zones.

Shear tension testing (cf. figure 6.80) or tensile tests (cf. figure 6.81) are used for determining the strength of a spot weld more accurately. Tensile tests are also called cross tensile tests depending on the appearance of the sample.

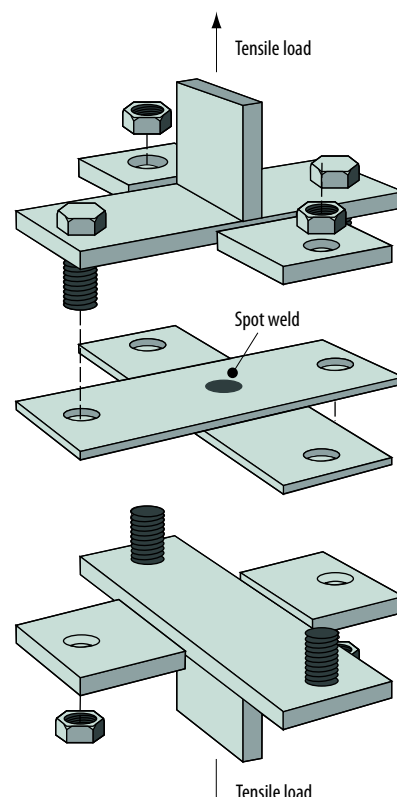


Figure 6.81: Tensile test of a spot welded joint in a cross tension test.

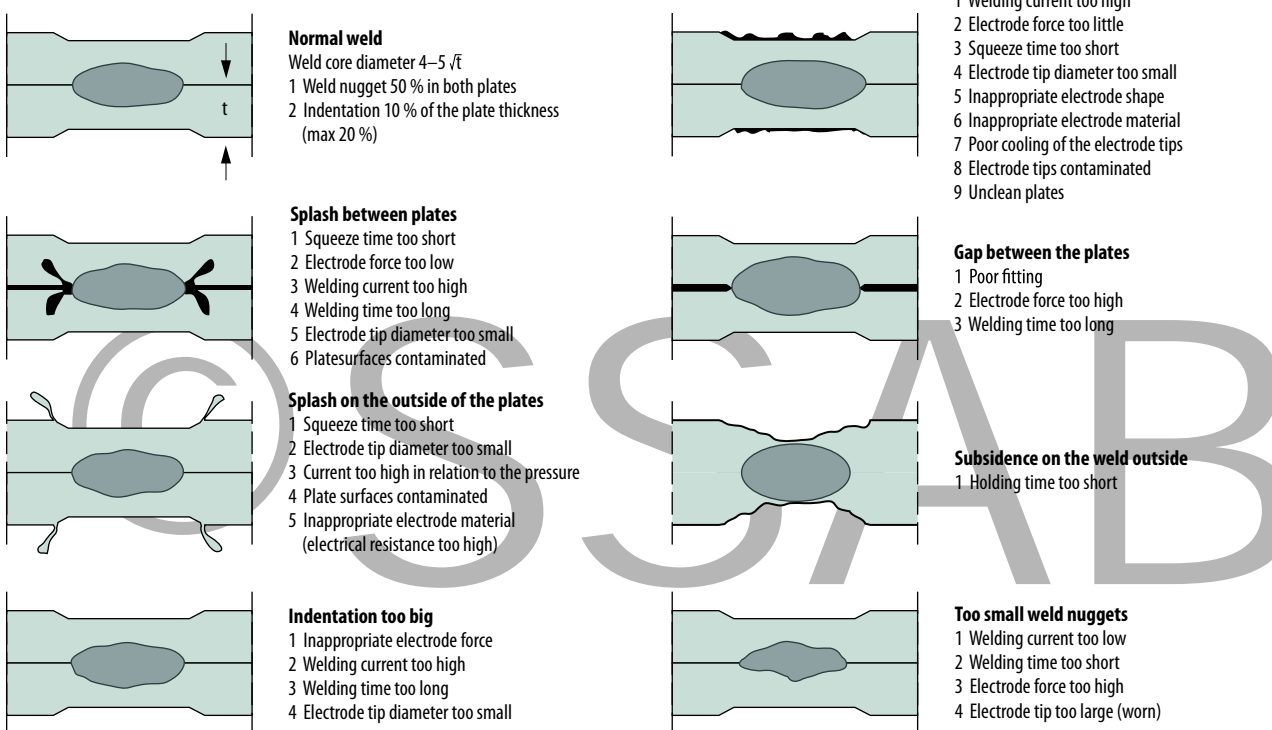


Figure 6.82: Example of causes of welding defects during spot welding.

Recommendations to avoid welding defects

Welding defects in resistance welded joints can be contingent upon many different things. For example, inappropriate material has been welded or the weld has been performed inappropriately. A general rule is that standard thin plates are very easy to weld since the chemical composition and plate surfaces are well-adapted for resistance welding. If a problem involving weld defects occurs, it is often due to using inappropriate welding parameters. For recommendations about proper welding variable settings for the different thin plate types, please refer to sections 6.5.7–6.5.9.

Figure 6.82 contains examples of some welding defect causes observed after spot welding of thin plates. As evident from the figure, there is often more than one possible cause for welding defects.

Weldability

In order to determine the weldability of a steel (how suitable it is for welding) for spot welding, one of the following methods is usually applied:

- Width of the weldability lobe – type of failure
- Useful life of electrodes

The type of failure relates to the appearance of the fracture in the various peel tests, tearing or cross tensile tests.

Only the first two methods above are used for cold rolled uncoated plates because the useful life of the electrodes in this case is normally so long that it is considered unnecessary to test it. On the other hand, the useful life of electrodes in the case of zinc-coated plates where the electrode wear is stronger is an important property.

Width of the weldability lobe

In order to be able to determine how easy it will be to spot weld a steel, a welding lobe is prepared (cf. figure 6.83). For different welding periods a welding lobe exhibits the allowed variation in welding current ("available welding current range") for obtaining a spot weld with an approved diameter without spatter. The diameter of the electrode tip and the electrode force are kept constant during the test. A wide welding lobe (a large "available welding current range") is a sign that the steel has good weldability.

It is evident from figure 6.83 that if the welding current is too high, spatter will form, which will impair the quality of the weld and is likely to damage the welding equipment. If the current is too low, the plug diameter of the weld will be too small (which results in low strength). The definition "Plug diameter too small", i.e. the smallest approved plug diameter, is not unambiguous and many values can occur. An electrode diameter of $5\sqrt{t}$ mm is often used for welding lobes, where t is the thickness in mm of the thinnest plate. A standard requirement associated with this is a minimum plug diameter of $3.5\sqrt{t}$ mm.

As far as electrode diameter and minimum plug diameter for welding lobes are concerned, it is very common amongst plate manufacturers to discuss with the customer the use of other values. For example, it is common to use the electrode diameter that the customer uses during production welding together with the minimum prescribed plug diameter in accordance with the respective company's quality standards.

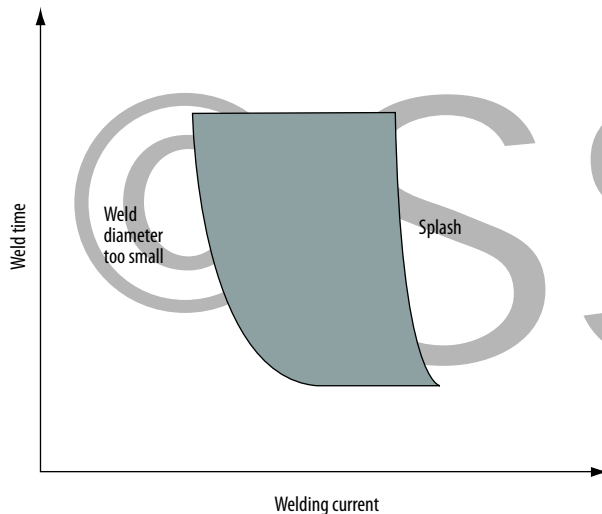


Figure 6.83: Weldability lobe for spot welding.

Type of failure

Three different failures can be observed during testing (such as breaking or tensile tests) of spot welds (cf. figure 6.84).

- A. Full plug failure
- B. Partial plug failure
- C. Interfacial failure

Full plug failure if the material fails around the weld. It is this type of failure that is sought and it is easy to measure the diameter of the plug as compared to the set requirements.

In some cases the failure can occur in the interface between both plates so there is a plug where a bit is missing. This type of failure is called partial plug failure and it can occur if the steel that has been welded has a high alloying content of, for example, carbon or any other alloying elements or if inappropriate welding variables are used.

If the failure is on the interface between both plates, the failure type is "interfacial failure". Steels with very high alloying content can get this type of failure. If a steel exhibits interfacial failure, the steel is regarded as a steel of poor weldability.

Useful life of the electrode

The useful life of the electrodes is very long with spot welding of standard cold rolled uncoated plate. Usually up to 10,000 spot welds can be made before the electrodes are flattened/deformed with an enlarged contact surface as a result. Because of the enlarged contact surface, the current density (energy/unit of surface) reduces so that the weld nugget will be smaller, resulting in a weld with lower strength. The electrodes must then be dressed so that they resume their design form.

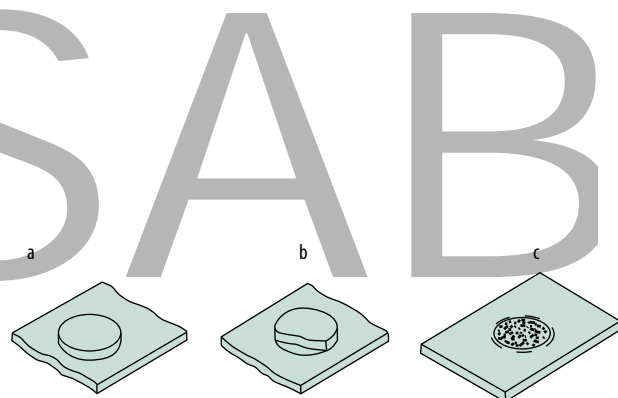


Figure 6.84: Different types of failures in spot welded joints a) full plug failure, b) partial plug failure, c) interfacial failure.

When the zinc-coated thin plate is spot welded, the electrode's useful life is significantly shortened than in the case of welding of uncoated thin plates. The reason why is that zinc from the plate surface is absorbed in the copper surface of the electrode during the welding and the result is a zinc and copper alloy that has properties other than the properties of the original electrode surface. In the case of zinc-coated plates, measuring of the useful life of the electrodes is often one of the tests conducted to describe the weldability of the current plate.

Static strength of spot welds

When a spot weld is exposed to shear stress, the forces act primarily on the plate plane, but also a small peelload is observed because of the rotation of the plate around the weld when the stress is applied. The factors that primarily affect the shear strength of the spot weld are:

- plate thickness
- spot weld diameter
- tensile strength of the plate

Spot welds in high strength steels have higher static shear tensile strength than standard soft steels because the strength of these steels is higher. In order to meet the strength requirements it is very important to achieve the required plug diameter.

The load type is of great importance for the strength of the spot weld. The tensile strength (the strength perpendicular to the plate plane) is lower than the shear strength. The tensile strength is determined as previously mentioned with the help of cross tensile strength



(cf. *figure 6.81*). It should also be mentioned that the strength of the plate is not so important for the tensile strength as it is for the shear strength.

Since the shear strength of spot welds is higher than the tensile strength the design of the structure shall be such that spot welds are exposed to shear stress and not to tensile or peel stress. For more detailed information about dimensioning of spot welded joints, please refer to section 4.6.1.

Plate thickness mm	Weldspot diameter mm	Electrode tip diameter mm	Electrode force kN	Welding time per	Current kA
0,6	4	5	1,40–1,70	5–8	6
0,8	4	5	1,60–2,30	6–10	7
0,9	5	6	1,70–2,45	8–11	8
1	5	6	2,10–2,90	9–12	9
1,2	5	6	2,50–3,40	10–13	9,5
1,5	6	7	3,30–4,30	12–16	10
2,0	6	7	3,90–5,40	16–20	11
2,5	7	8	5,40–7,00	22–26	12,5
3	7	8	6,30–8,50	24–30	14

Table 6.7: Example of spot welding parameters that give good weld quality for soft Docol steels.

6.5.7 Resistance welding in cold rolled steel

Soft Docol steel

Resistance welding of soft cold rolled steels is simple. These steels are characterised by very lean compositions as well as good surface-qualities, which allows for problem free welding. Neither the corrosion-protecting oil film nor residues from lubrication from pressing causes problems when welding. If dust or dirt has contaminated the surface during storage of the plate, it must be removed before welding takes place. Otherwise, welding can be difficult and the useful life of the electrode will be reduced.

Where problems have occurred during resistance welding of soft cold rolled steels, it is primarily due to inappropriate structural design or inappropriate choice of welding parameters.

Recommended welding variables for soft cold rolled steels

It is recommended to use standard CopperChromeZirconium electrodes for soft cold rolled steels.

As a rule of thumb, during spot welding of cold rolled soft plates, the following welding variable values are used (t is the thickness of the thin plate in mm):

- electrode tip diameter, approx. $5\sqrt{t}$ mm
- electrode force, approx. $2200 \cdot t$ N
- weld time, approx. $10 \cdot t$ per for AC machines
($200 \cdot t$ ms for MFDC machines).

The squeeze time is contingent upon the spot welding machine that is used but 30 per (600 ms) is often sufficient. For the holding time, a standard value is 10 per (200 ms) but shorter times such as 0.5 x the welding time have been reported to be good to use. In the last step, the welding current must be adjusted through test welding after the other welding parameters have been set.

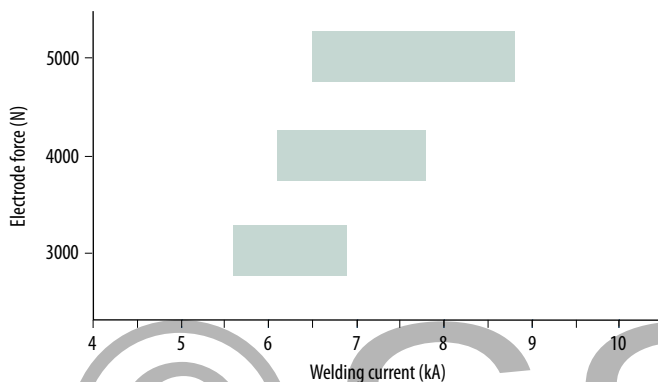


Figure 6.85: Influence of the electrode force on the available current range during spot welding of Docol 1000 DP (plate thickness 1.2 mm) to itself (Welding data: AC machine, standard flat CuCrZr electrodes, electrode tip diameter 6 mm, holding time – 10 cycles; welding time – 14 per. Maximum permissible current = maximum without splash. Minimum permissible current = plug diameter equal to 70% of the electrode tip diameter).

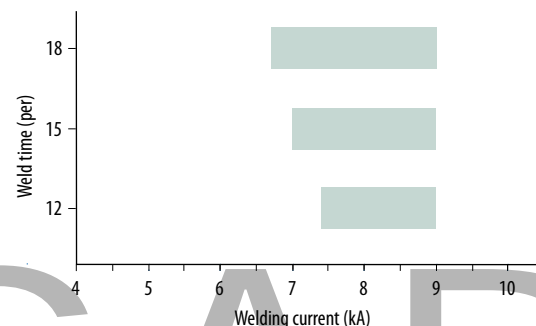


Figure 6.86: Influence of the welding time on the available current range during spot welding of Docol 800 DP (plate thickness 1.5 mm) to itself (Welding data: AC machine, standard flat CuCrZr electrodes, electrode tip diameter 6 mm, holding time – 10 cycles; electrode force – 5100 N. Max. permissible current = max. without splash. Min. permissible current = plug diameter equal to 70% of the electrode tip diameter).

Soft cold rolled steels exhibit wide weldability lobes and the fracture type is entirely full plug failure. The weldability of these steels is very good. *Table 6.7* shows examples of welding parameters that give good weld quality for welding of standard soft cold rolled steels (both plates have the same thickness).

High strength cold rolled steels

High strength steels (HS/EHS/UHS) can be resistance welded to other soft steels and to itself. Since these steels have higher electric resistance and poorer thermal conductivity as compared to mild steels, the welding parameters should be altered somewhat in order to ensure good welding results. The importance of changing the welding parameters increases with the increased strength and increasing content of alloying elements content of the steel.

Spot welding in high strength cold rolled steels

Electrode types and electrode tip diameters, no changes are normally necessary as compared to welding of mild steels.

The following are recommended with regard to welding parameters:

A. Welding to another mild steel.

- increase the electrode force by approx. 20–30%
- welding time, squeeze time and hold time the same as for mild steels

B. Welding to itself

- increase the electrode force by approx. 20–50 %
- increase the welding time by 20 %
- squeezing time and hold time the same as for mild steels

The lower electrode force values in the range above apply for HS steels and the higher – for UHS steels of the higher strength.

As far as welding current is concerned, suitable values are obtained through spot welding after the other welding parameters have been set. The recommendation here is to first increase the current until splash occurs, and then to reduce the current somewhat.

It is easiest to receive good welding quality with the welding parameters recommended here. If for some reason (such as limitation in machine equipment) it is not possible to increase the electrode force, welding can still go well. The risk for lower welding quality (such as smaller welding diameter than the desired) is greater and in this case it is easier to end up outside the weldability lobe. The importance of increasing the electrode force increases with increased strength of the plate.

Figure 6.85 shows an example of how the increase in electrode force results in a higher available current range for UHS steels (Docol 1000 DP 1.2 mm thickness). It is also evident that the increase in force requires higher welding current. Increased welding time results also in an increase of the available current range. This can be seen in the example in *figure 6.86* where Docol 800 DP of thickness 1.5 mm has been welded to itself.

When a high strength steel is used as a replacement of a mild steel, the plate thickness of the high strength steel is smaller. Since welding variables such as electrode force and welding time, are associated with the thickness of the plate, too big changes of the welding parameters as compared to soft steels are not necessary when welding high strength steels.

How big the available current range is may vary. It is contingent primarily on the type of welding equipment and how often electrodes are dressed. As a rough rule of thumb, the range should be at least 1 kA and should preferably be greater than 1.5 kA.

Welding parameters obtained during tests of flat plates might need to be modified somewhat when welding formed plates. The reason is that formed plate does not always have the same good fit as flat plates. Sometimes the electrode force is additionally increased to obtain good results.

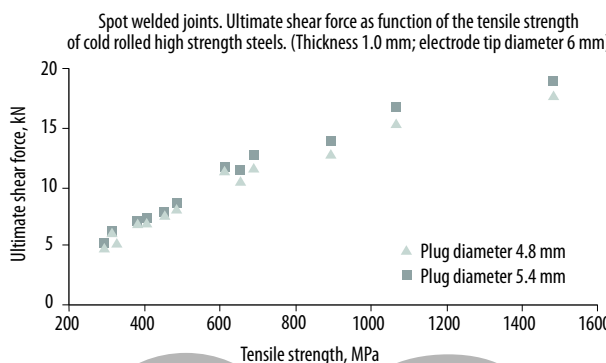


Figure 6.87: Ultimate shear force function of the tensile strength in spot welded joints of cold rolled high strength steels (1 spot weld, 2 plate joint, the same thickness and steel type in both plates, coupon size 150 x 40 mm, overlap 38 mm, 2 different plug diameters 80% and 90% of the electrode tip diam.). Thickness 1.0 mm; electrode tip diameter 6 mm

As mentioned earlier, fracture type (cf. figure 6.84) is sometimes used during peel tests as a measure of the weldability of the material in resistance welding. The type of fracture is determined principally by the steel composition and welding parameters. High contents of carbon and to a certain extent also of other elements (such as phosphorus, sulfur, manganese, etc.) increase the probability of partial plug failures.

During spot welding of high strength cold rolled steels, the following types of fracture normally apply:

Steel	Type of fracture type
Welding of soft steels	Full plug failure for all steels
Welding to itself	Full plug failure
– Docol RP/BH/YP	Full plug failure
– Docol DP to 800 DP	Full plug failure
– Docol 1000/1200/1400 DP	Full plug failure most often but sometimes partial plug failures
– Cold rolled boron steel	Sometimes full plug failures but most often partial plug failures

Table 6.8 contains examples of results measured during spot weld testing of different high strength cold rolled steels. The results show that the available welding current range is large if appropriate welding parameters are used. The failure type observed in all cases was full plug failure.

At ssabdirekt.com you can find examples of plug diameter-current curves for several cold rolled steels. A plug diameter-current curve makes it easy to read the available welding current range regardless of the minimum plug diameter that has been used as an available current range requirement.

Static strength of high strength cold rolled steels

Figure 6.87 and figure 6.88 show the measured ultimate tensile force values for joints with one spot weld in high strength cold rolled steels as a function of the tensile strength of the steel. The measurements have been made on 2-plated joints where both plates are of the same steel

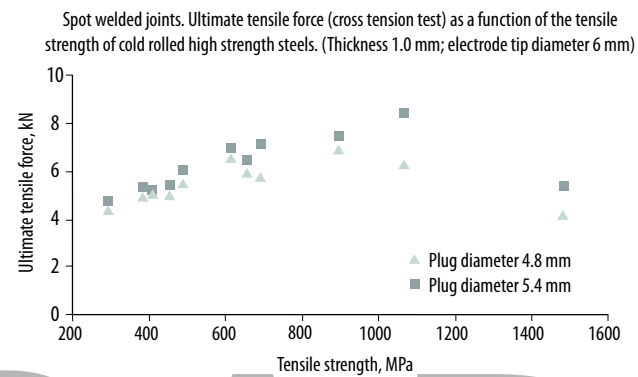


Figure 6.88: Ultimate tensile force (cross tension tests) as a function of the tensile strength of cold rolled high strength steels (1 spot weld, 2 plate joints, the same thickness and steel type in both plates, coupon size 150 x 40 mm, 2 different plug diameters 80% and 90% of the electrode tip diam.). Thickness 1.0 mm; electrode tip diameter 6 mm

type and thickness. Both shear specimens and cross tension specimen have been examined. The welds have been carried out in a stationary AC machine and for plate thickness of 1.0 mm an electrode diameter of 6 mm was used. The strength measurements have been made for different plug diameters (80 % and respectively 90 % of the electrode tip diameter).

Figure 6.87 and figure 6.88 shows that the plate thickness and the plug diameter increasing the strength, but also that:

1. The ultimate shear force increases with the increase in steel strength.
2. Regarding the ultimate tensile force (cross tensile tests), the impact of the steel strength is much smaller than in the case of ultimate shear force.
3. The ultimate force during cross tensile tests is lower than the ultimate shear force.
4. The difference between ultimate shear force and ultimate tensile force increases with the increase of steel strength.

Steel 1/steel 2 thickness mm	Welding data ¹⁾	Available current range ²⁾		Type of failure
		Range (kA)	min-max (kA)	
Docol 600 DP / Docol 600 DP (1,0/1,0)	5/3400/99/10/13	2,2	5,7–7,9	Plugs
Docol 600 DL / Docol 600 DL (1,5/1,5)	8/4500/30/10/15	2,5	8,5–11,0	Plugs
Docol 800 DP / Docol 800 DP (1,5/1,5)	8/4000/30/10/15	2,3	5,4–7,7	Plugs
Docol 1000 DP / Docol 1000 DP (1,2/1,2)	6/4000/99/10/14	2,2	5,5–7,7	Plugs
Docol 1200 M / Docol 1200 M (1,5/1,5)	6/4500/30/10/15	2,5	6,2–8,7	Plugs
Docol 1400 M / Docol 1400 M (1,0/1,0)	6/4000/99/10/12	2,1	5,8–7,9	Plugs

¹⁾ Electrode tip diameter (mm)/electrode force (N)/squeezing time/holding time/welding time (cycles).

²⁾ Minimum value: Plug diameter = 70 % x electrode tip diameter. Max value: The highest value without splash.

Table 6.8: Examples of measured available current ranges (cross tension test) during spot welding of different high strength cold rolled steels.



6.5.8 Resistance welding in hot rolled steel

Fusion welding is the most common welding process for hot rolled steels. It is possible, however, to resistance weld most hot rolled steels provided that the oxide scale has been removed first (by pickling, for example). The plates should preferably not be thick because very high electrode forces will then be required, which is not possible when using standard equipment. In practice, resistance welding of plates with thickness above 3 mm is very rare. A welding machine with sufficient capacity makes it possible to weld plates thicker than 3 mm.

Soft hot rolled steels

Thin plates of pickled soft hot rolled steels are very much like the soft cold rolled steels as far as electrical resistance welding is concerned. The reason for this is that both steel families have very similar steel compositions (low carbon content in combination with otherwise low alloying content). Just as with cold rolled steels, wide weldability lobes are achieved during spot welding of soft hot rolled steels and the failure type during the test is full plug failure.

The following recommendations apply for resistance welding of soft hot rolled steels:

1. Use pickled steel from which all millscale had been removed.
2. Make sure that the current welding equipment has sufficient electrode force.
3. Use the same welding parameters as those recommended for soft cold rolled steels.

High strength hot rolled steels

Pickled HS/EHS hot rolled cold forming steels with thin thicknesses (max. 3 mm) can be resistance welded as well. Both HS and EHS cold formed steels have very lean steel compositions, which is advantageous during resistance welding. To set appropriate welding parameters, it is recommended to use the same settings as for cold rolled HS/EHS/UHS steels which sometimes means that the electrode force should be somewhat higher as compared to soft steels.

6.5.9 Resistance welding in zinc-coated thin plates

Zinc-coated thin plates can be welded by using most welding processes. Resistance welding is, however, the most common method and is often preferred to MAG welding because resistance welding damage the zinc layer less and causes less deformation of the plates. With resistance welding it is also easier to receive a good welding results (MAG welding often result in spatter and pores, cf. section 6.5.1).

In order to achieve good welding results, we recommend changing the welding parameters a little bit as compared to welding of standard uncoated plates. An acceptable weldability lobe width is normally obtained with changed welding parameters. The type of failure and strength do not differ significantly from the equivalent uncoated steels. In order not to have welding fume problems, we recommend the use of an effective welding fume extraction system.

Useful life of electrodes

The greatest difference between spot welding of zinc-coated plates and uncoated plates is the useful life of electrodes, which is shorter for zinc-coated plates. One of the reasons why this is so is that zinc from the plate surface is accumulated on the surface of the copper electrode during welding. As a result, the electrode surface is altered.

The following recommendations apply for extending the useful life of electrodes as much as possible when spot welding zinc-coated plates:

1. The coat should not be thicker than the necessary.
2. Make sure that the cooling of the electrodes is effective.
3. The welding current and the welding time shall not exceed the necessary.

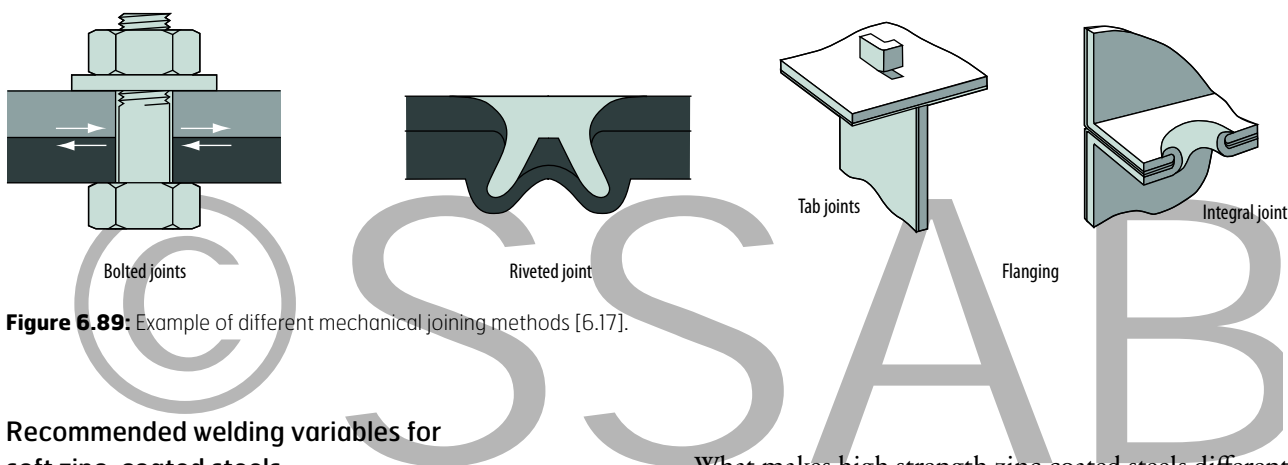


Figure 6.89: Example of different mechanical joining methods [6.17].

Recommended welding variables for soft zinc-coated steels

During spot welding of zinc-coated steels, the same size and type of electrodes are recommended as for welding uncoated plates. The following changes to the welding parameters are recommended for soft zinc-coated steels as compared to soft uncoated steels:

- increased electrode force (approx. 20–50 %)
- increased welding time (approx. 20–50 %)
- increased welding current (up to 50 %)

Recommended welding variables for high strength zinc-coated steels

Even with spot welding of high strength zinc-coated steels, the same size and type of electrodes are recommended as for uncoated steels. The following changes to the welding parameters are recommended for high strength zinc-coated steels as compared to soft uncoated steels:

- increased electrode force (approx. 20–70 %)
- increased welding time (approx. 20–50 %)
- increased welding current (up to 50 %)

What makes high strength zinc-coated steels different from soft zinc-coated steels is primarily that the electrode force and the welding time for the high strength steels need to be increased somewhat.

Table 6.9 shows examples of results measured during spot weld tests of zinc-coated 600 DP and zinc-coated 800 DP. The results show that great allowed current ranges are obtained with the increase in electrode forces and welding times that have been used here. The failure type in all cases is full plug failure.

6.6 Mechanical joining

6.6.1 Mechanical joining methods

There are many different types of mechanical joining methods, the most common of which are:

- bolted joints
- riveted joints
- integral joints

See figure 6.89.

Common for these methods is that the joining operation is cold, which gives many advantages as compared to welding, such as:

- no heat-affected zone
- the surface layer (zinc, color) is not considerably damaged
- different types of materials can be joined together, such as steel to aluminum

Screwed joints

Joining by screwed joints is one of the most common joining methods. Screwed joints can be divided into "screwed joints for thicker plates" (bolted joints) as well as "screws in thin plate joints" (different types of plate screws, drilling, tapping, etc.) see figure 6.90.

The principle that applies for screwed joints is that tightening takes place so that clamping force is formed in

Steel 1/steel 2 thickness, mm	Welding data ¹⁾	Allowed current range ²⁾		Type of failure
		Range (kA)	min-max (kA)	
600DP ³⁾ 600 DP (1,5/1,5)	6,0/4500/ 30/20/19	2,0	6,9 - 8,9	Plug
800DP ⁴⁾ 800 DP (1,5/1,5)	8,0/4000/ 30/10/17	3,0	9,8 - 12,8	Plug

¹⁾ Electrode tip diameter (mm)/electrode force (N)/squeezing time/holding time/welding time (cycles).

²⁾ Minimum value: Plug diameter = 70 % x electrode tip diameter. Max value: The highest value without splash

³⁾ Coating thickness Z100, 7 µm (both steels)

⁴⁾ Coating thickness Z140, 10 µm (double-sided, coated)

Table 6.9: Examples of measured allowed current ranges during spot welding of zinc-coated 600 DP and zinc-coated 800 DP (single phase stationary AC machine, CuCrZr electrodes).

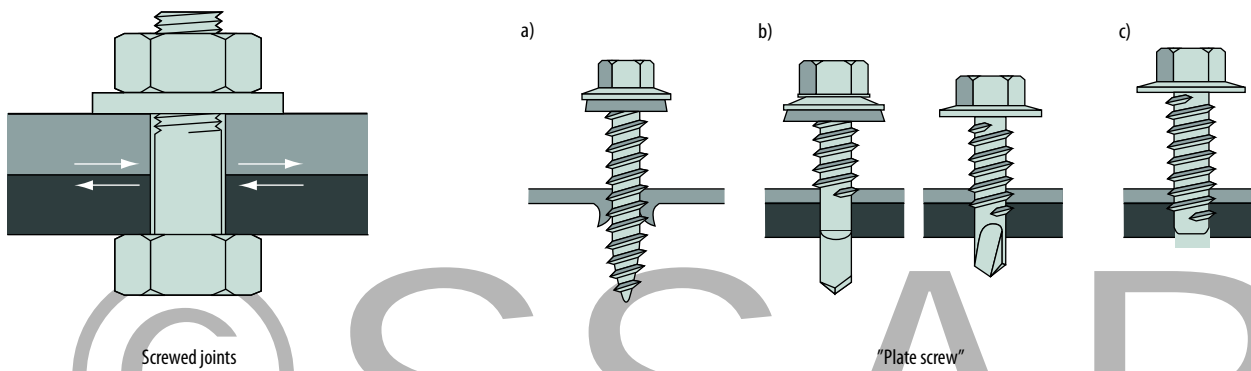


Figure 6.90: Examples of different types of screws for thin plates [6.17].

the joint to prevent transversal movements between the plates. The simpler “thin plate joints” keep components together without any major requirement on clamping force.

Some of the greatest advantages with screwed joints include:

- it is possible to join different materials
- the joints can be dismantled
- high strength (both static and fatigue strength)

Clinching

No additional joining elements are used in clinching. The principle is to form the plates together between a punch and a die so as to obtain a mechanical lock between them, see *figure 6.91*.

Figure 6.91 illustrates the locking mechanism clearly. The top plate has been pressed under the bottom plate.

There are many different types of clinched joints, but the most common one of them is the non shear clinched joint that does not cut through the plate, as well as the part shear clinched joint, which partially cuts through the plate, cf. *figure 6.92*.

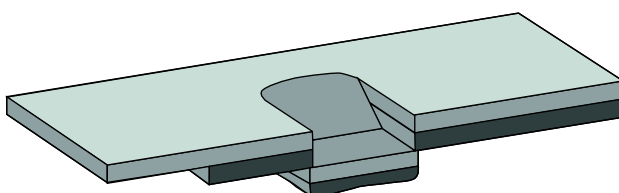


Figure 6.92: Part shear clinched joint [6.17].

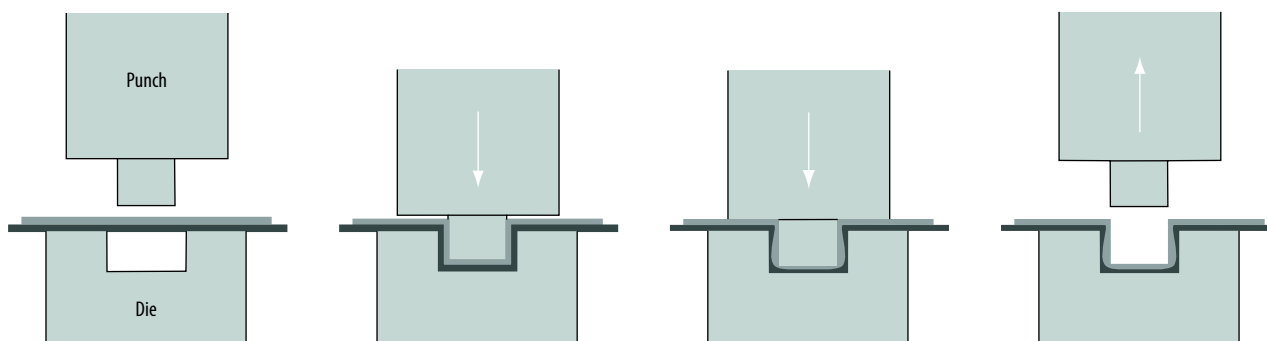


Figure 6.91: Clinching principle [6.17].



Strength of butt riveted joints

The strength of a clinched joints is lower than that of a spot weld. To compensate for the lower strength, you can:

- increase the number of clinched joints
- increase the size of the clinched joints

The strength of clinched joints increases with the increase in plate strength, cf. figure 6.93.

It is very important to remember that stress on clinched joints has to be applied in the shearing direction because the peel strength is much lower. The peel strength is usually approx. 25–30 % of the shear strength.

The fatigue strength of clinched joints is somewhat lower than that of spot welds if the number of load cycles is low (<106). On the other hand is the fatigue strength higher for clinched joints subjected to shear loading if the number of load cycles is high.

Self piercing riveting

Self piercing riveting is using a rivet to join the plates together. The rivet is pressed through the top plate with the help of a punch. The die then forces the bottom part of the rivet to expand and form as well as to lock the plates to one another, see figure 6.94.

Punch riveting of thin plates is carried out in different types of lap joints and is common where resistance welding produces unsatisfactory results, such as in the case of metal coated (thick zinc layer), painted or film coated thin plates. Another advantage is that it is possible to join different materials, such as a plate to aluminum.

Self piercing riveting of thin plates can be carried out in thicknesses from 0.5 to 3 mm. The total thickness may not exceed 6 mm [6.17].

Punch riveting has more advantages as compared to spot welding, such as:

- joining thin plates with another material, such as aluminum
- better fatigue properties
- no or little need for post treatment – very small or no damages on the coated material
- no heat impact
- good working environment
- process monitoring possible
- low need for energy

Disadvantages include:

- requires filler metals (rivets)
- most rivet types create a projection on one side (the die side)
- lower static strength
- punch forces are required

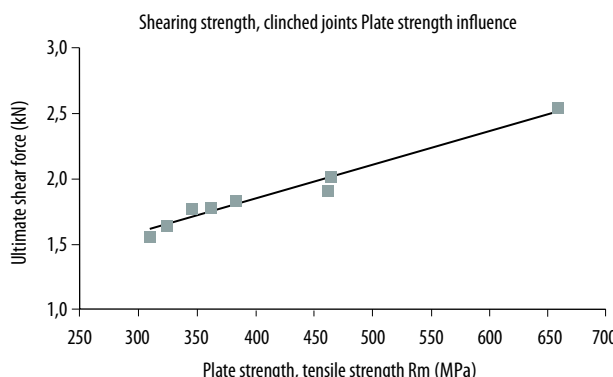


Figure 6.93: Plate strength influence on the shear strength of clinched joints. (Non shear Tog-L-Loc clinched joint with bottom diameter of 7 mm, 2-plate lap joints t approx. 0.7 mm, specimen size 120 x 40 mm with an overlap of 40 mm, steel grades are, DCO1, Docol 600 DP, zinc-coated F36 11 mm, zinc-coated B500 7 mm, zinc-coated 350 YP 20 mm). [6.17].

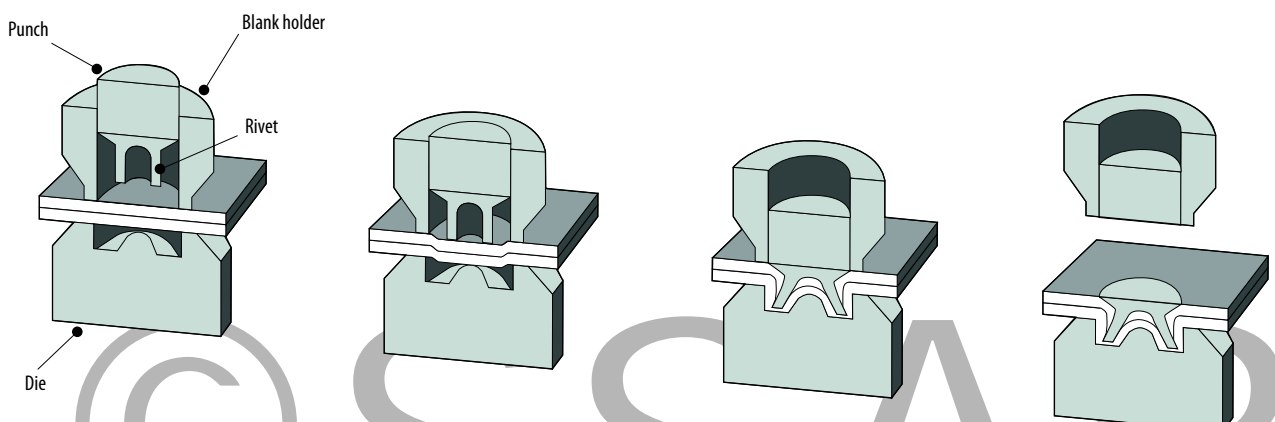


Figure 6.94: The principle of self piercing riveting with a semi tubular rivet [6.17].

Strength of self pierced riveted joints

Just as in the case of clinching, the static strength is determined primarily by:

- the strength of the plates
- the plate thickness

The rivet size and type also affect the strength of the joint. For highest strength, select a rivet with as large a diameter as possible.

When the strength of the plates is increased, there is a great linear increase of the shear strength of the self pierced riveted joints, cf. figure 6.95.

Just as in the case of riveted joints, the strength during peel load is considerably lower. It is therefore important to always try to ensure that the joints are exposed to shear load.

The fatigue strength is better in self pierced riveted joints than in clinched joints.

Punch riveted joints in high strength steels exhibit better fatigue strength than joints of low strength steel. In the case of spot welding, this effect is not observed. High strength spot welded steels exhibit the same fatigue strength as soft steels [6.17].

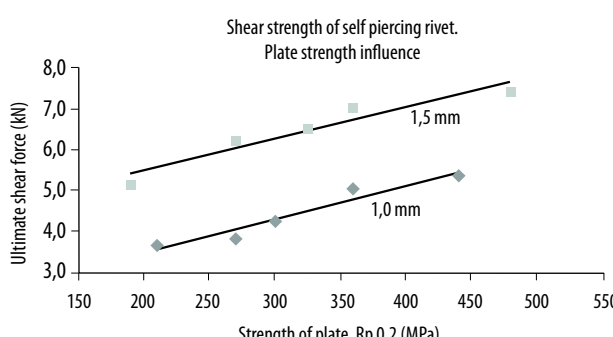


Figure 6.95: Plate strength influence on the shear strength of self pierced riveted joints (Semi tubular rivet, rivet size 5.3 x 5.0 mm respectively 5.3 x 6.5 mm, 2-plate lap joints t=1.0 respectively 1.5 mm, specimen size 194 x 45 mm, overlap 16 mm, the steel types that have been tested correspond to steels DC01, Docol 260 RP, Docol 340 YP, Docol 500 DP and Docol 420 YP) [6.17].

6.7 Bonding

Bonding of thin plates has been used in the industry for several decennia and is still used today, so structural bonding is one of the fastest-growing joining techniques within the automotive industry [6.17].

Adhesive joints have many advantages as compared to other joining methods, such as:

- with the bonding method different types of materials can be joined together, such as steels, plastics, aluminum, copper, etc.
- adhesive functions as an isolator that prevents the formation of galvanic elements
- it is possible to join parts with great differences in dimension without any deformations in the construction
- the joints are waterproof.
- better fatigue strength (better stress distribution)
- good damping properties, less noise and less vibrations
- no heat affected zone such as in the case of welding, for example

The plate surface

During bonding, it is of utmost importance that the plate surface be known and reproducible in order for as good bonding results as possible to be achieved. Remember that both cold rolled and metal-coated plates are delivered with many different surface conditions.

The adhesive that shall be used must wet the surface that is to be bonded. If the adhesive has higher surface tension than the plate surface, no wetting will be achieved, and therefore no adhesion.

To improve adhesion, some cutting-off by means of brushing by a "Scotch-Brite", for example, may be necessary. The plate surface can also be adapted for bonding through a light washing operation where a standard soap solution is used and rinsed. Using with a detergent should generally be avoided because of both the internal and external environment.

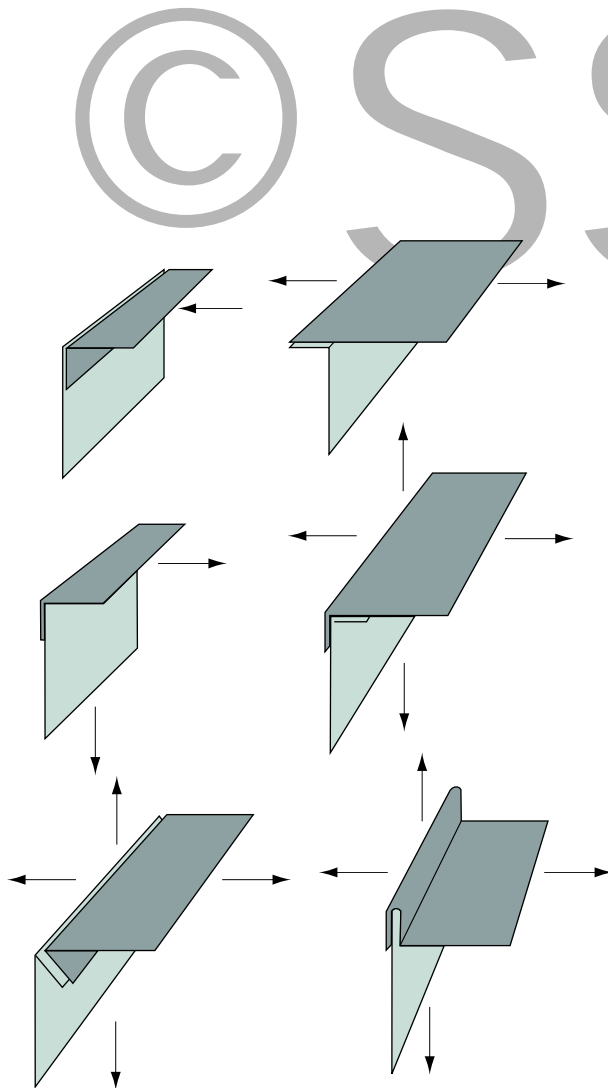


Figure 6.96: Example of appropriate joint designs in thin plate bonding [6.17].

Joint design

The most common joint type in bonding is the single lap joint. This type of joint is also very easy to prepare from a pure production perspective.

Adhesive joints should preferably be designed so as to be exposed to shear stress, cf. figure 6.96. This is so because the peel and the cleavage strength are distinctly lower than the shear strength. In thin plate structures, however, it is difficult to completely avoid peel and cleavage loads [6.17].

Long-term durability

The long-term durability of an adhesive joint depends a lot on what the adhesive joint is exposed to during operation, such as:

- moisture
- heat
- stress
- light (UV)
- etc.

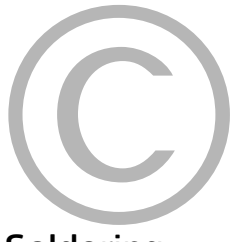
In the case of joints exposed to moisture, the long-term resistance is contingent upon how stable and resistant the oxides formed by the metal are. How well the adhesive is in contact with the surface profile is also very important [6.20], in other words, the choice of adhesive in relation to the surface that is to be bonded is very important.

The long-term resistance can be improved many times by first painting the plate surface with a primer. If adhesive joints with better long-term resistance are required, paint or film-coated thin plates can be an alternative [6.20].

Adhesive types and adhesive application

Adhesive types can be divided by how the transition from fluid to solid form takes place. This transition can take place either through physical or chemical solidification. The physically solidifying adhesive is usually referred to as hot melt adhesive, whereas the chemically solidifying adhesive is called curing adhesive. The industrial application of adhesives is often automatic and not seldom using robots.

Read more about bonding in SSAB's Joining Handbook.



6.8 Soldering

Soldering is a joining method that can be an alternative to welding when, for example, thin plates have to be joined with other metallic materials (brass, copper, etc.). During soldering, the soldering spot is heated to the working temperature of the solder (the filler metal) which is always lower than the melting temperature of the material that will be soldered. Metallic bonding between the solder and the parent material then takes place through a bonding zone, cf. *figure 6.97*.

The solder (filler metal) shall always be selected based on the materials that will be joined together. To make it possible to join parent materials through soldering, the surface must be clean and oxides must be removed. To remove the oxides and prevent oxide formation during the soldering process, use flux. The fluxing agent must be suitable for the solder and the material that will be soldered.

The following are required to create a soldered joint with good properties:

- a well-cleaned oxide-free surface
- that the solder is intended for the materials that have to be soldered
- that the fluxing agent is suitable for both the solder and the parent material
- right work piece temperature

The gap between the work pieces is very important for achieving a good capillary effect and should be within the range 0.05–0.5 mm. Too big or respectively too little gap impairs the strength of the soldered joint.

Soldering methods

There are a few different soldering methods, but the most common for thin plate soldering is brazing. Brazing takes place at temperatures higher than 450° C and produces joints that are much stronger than in the case of soldering (tin soldering).

Thin plate soldering

In case of thin plate soldering, it is important to make sure that the current material can withstand the temperature that will be used in the soldering process. High strength thin plates can be sensitive to high temperatures during long periods, which in turn can result in a reduction of strength in the heated area. If the soldered joint can be placed in an area with low stress, the soldering can be used without jeopardizing the functional stability of the structure.

For more detailed information, please see the Joining Handbook [6.17].



Figure 6.97: The different zones of the soldered joint [6.17].

6.9 Straightening

In general, the same methods can be used for straightening high strength as for mild steels. Consideration to the higher material strength must, of course, be taken. For roll flattening, amongst other things, this means a harder guideline setting.

6.9.1 Roll flattening

Roll flattening is done in the same way for both mild- and high strength plates. The same calculation methods can be applied for setting guideline values or for dimensioning of roll diameter, C-C measures and motors. However, it is clearly more difficult to straighten high strength steels because of the higher yield point and higher residual stresses.

The result, i.e. the flatness of the straightened plate and the distribution of residual stresses, must be checked during the run. The guideline values might need to be adjusted because residual stresses for example can be changed at the end of the coil.

6.10 Surface treatment

The surface treatment of high strength steels follows the same rules as the surface treatment of mild steels. The temperature of the plate, however, may not exceed 200° C for martensitic steels, 300° C for DP steels and 650° C for HSLA steels.

6.10.1 Cleaning and surface treatment

The purpose of cleaning is to remove impurities that can lead to bad adhesion or cause different types of surface defects and corrosion. Satisfactory cleaning is a prerequisite for good surface treatment results.

The surface that has to be cleaned can be contaminated with any different types of dirts:

Water-soluble substances:

Salts, hand sweat, residual flux agent, pickling paste, etc.

Non-water soluble substances:

Anti-corrosive agents, greases, waxes, lubricants

Electrochemically active substances:

Soot, oxide scale, oxides

Hot rolled strips always have surface oxides which have to be removed prior to surface treatment. This is normally done through blasting or pickling.

There is often an oil on hot rolled pickled and cold rolled strips. It protects against corrosion during storage and transportation. It is easy to remove after standard storage, but after long-term inappropriate storage where exposed

to moisture, heat, direct sunlight, etc. the aging of the oil makes it difficult to remove. The cleaning agent must be appropriate for removing particles from the manufacturing process such as carbon and iron particles, grinding dust, etc.

An oil similar to the oil used in cold rolled steels or a chemical passivation treatment is used to achieve good anti-corrosion protection during transportation and storage of metal-coated strips.

Mechanical cleaning

Good mechanical cleaning refers to blasting, brushing, grinding and tumbling. Blasting can be done at different degrees of precision. In SS-EN ISO 8501-1:2007 you can find the standardized values. The greater the corrosion protection requirement, the more precise the blasting of the surfaces has to be. The precision is given in classes Sa 1, 2, 2½ and 3. A higher number means better blasting. Blasting can be done manually or in automatic installations.

There are different types of blasting agents. Single use blasting agents are e.g. cheap by-products from metal manufacturing, natural minerals or polymer materials. Reusable blasting agents can be cast iron or corundum (aluminum oxide). When choosing a blasting agent, it is important to remember that the agent sticks to the surface during blasting. Therefore, the material you choose should cause as little damage as possible. Noble or un-noble materials can cause bimetallic cells with blistering formation in the paint layer. In blasting equipments where the agent is reused it is important to make sure that the surface is free from large grease quantities before the blasting. Otherwise there is a risk for grease to adhere on the blasting agent and spread to other surfaces.

The material shall be dry during blasting and the temperature of the product must be at least 3° C above the dew point. After the blasting, the remaining blasting agent has to be removed from the surface immediately and the subsequent painting done as soon as possible.

Degreasing

The most common degreasing agents in the manufacturing industry are water-based alkaline cleaners. They contain alkalis (such as sodium or potassium hydroxide, sodium carbonate, sodium silicate) for removal of dirt and pH increase, dispersants such as tensides and emulsifiers, softeners and corrosion inhibitors.

Depending on the degree of contamination and on the nature of impurities, different strong agents can be selected. The capacity to remove oil and grease increases with pH. The choice of alkali depends on the material to be treated whereas the choice of tenside depends on the impurities and on the process. Products are available in both liquid and powder form. The agents are diluted with water to the

right concentration and applied on the surface, either by spraying or by dipping. Rinsing in one or several steps takes place afterwards, followed by forced drying.

Organic solvents are used when the material is easily corroded or when the surface is only contaminated by substances that are easy to dissolve in the selected solvent, such as oil and grease. Because the cleaning agent is usually left to evaporate from the surface, the impurities dissolved in the solvent will accumulate on the surface. It is therefore important to use a cleaning agent with low content of impurities. This can be achieved by cleaning the solvent often or by multiple-step cleaning.

Organic solvents are classified as harmful to the health according to the criteria of the National Board of Occupational Safety and their use is regulated in Sweden. Chlorinated solvents that have been used for industrial degreasing, trichloroethylene (tri) and methylene chloride, are forbidden but may be used if the Swedish Chemicals Agency grants exemption. Their use, however, has decreased significantly in the past years because of the transition to water-based systems.

Pickling

Pickling is a standard pretreatment before metal coating or painting. Corrosion products and oxides on the steel are removed by dipping the material into a strong acid, usually hydrochloric acid or sulfuric acid. After the pickling process, the material is carefully rinsed in order to remove all acid residues.

The predominant pickling acid used in Europe is hydrochloric acid. It usually gives good pickling results even at low temperatures (=room temperature). Usually, acid contents of 5–20 weight % are used. The maximum temperature in open baths is 40° C because the hydrochloric acid emits hazardous and corrosive fumes. In case of pickling in closed facilities baths, the temperature can be increased to 90° C.

When using sulfuric acid, the acid concentration has to be 15–20 weight % and the bath shall have a temperature of 60–80° C in order to give satisfactory pickling results.

Often, the pickling bath contains an inhibitor. It shall prevent the acid attack on the bare steel surface and affect the dissolving of the oxide layer as little as possible.

6.10.2 Non-metallic, non-organic coatings

Chromating

Chromating is a chemical conversion coating that is used on aluminum and zinc. The metal surface reacts with a chromium containing solution, and a thin coating is formed.

Chromating is used to:

- Give the material a temporary corrosion protection during transportation and storage
- Give the surface a decorative appearance
- Improve the adhesion of a paint or varnish

Chromating is carried out by dipping or spraying in an acidic chromate solution. The thickness of the layer varies depending on the chromate type and on the product that is to be chromated. Thin transparent layers, approx. 0.1 µm, function as corrosion protection during storage and transportation. Yellow coatings, approx. 1 µm, are used primarily as a pretreatment to painting, but also as temporary corrosion protection on galvanized components. Green chromating forms a thick layer, approx. 3 µm, that is used when the aim is a decorative surface.

All chromating solutions contain hexavalent chromium that can cause allergic skin reactions and are classified as poisonous, mutagenic and cancerogenic. Via the EU directives (ROHS, Restriction of Hazardous Substances and WEEE, Waste Electronic and Electrical Equipment) the electronic industry has imposed a ban on 1 July 2006 banning the use of hexavalent chromium for inhibition and anticorrosion protection. The automotive industry followed and the ELV (End of Life Vehicle) directive came into force on 1 July 2007. It bans the use of products containing hexavalent chromium as inhibitor and corrosion protection in up-to-2,500 kg vehicles.

SSAB's hot dip galvanized strip is protected against corrosion during storage and transportation by a thin coating, approx. 0.1 µm, free from hexavalent chromium. For more information about metal-coated thin strips, please see our environmental declarations.

Against the background of chromating-related environmental problems that exist today, extensive work is being done to find alternative chemicals, cf. the section on TOC (Thin Organic Coatings).

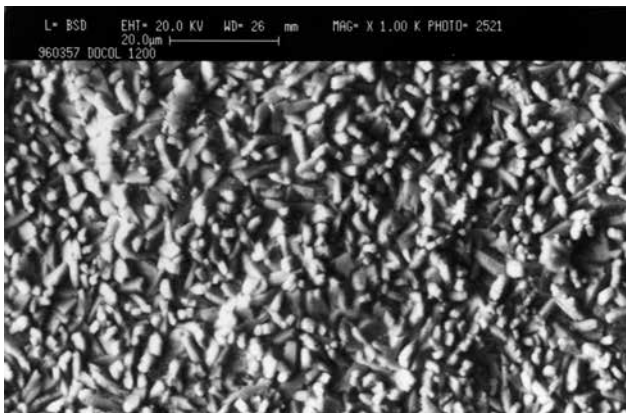


Figure 6.98: Docol 1200 DP phosphatized in a zinc-manganese phosphatization process.

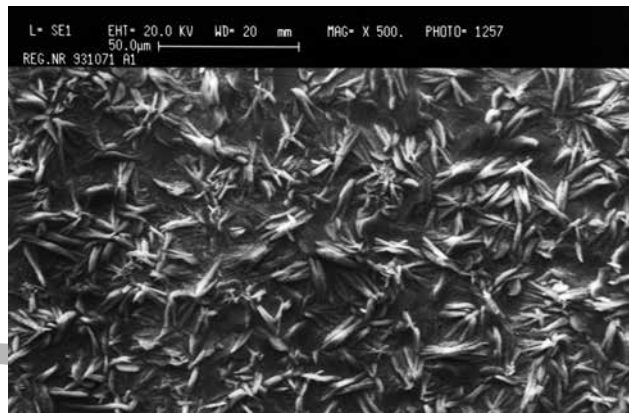


Figure 6.99: Zinc-manganese phosphatized steel.

Phosphatization

Phosphatization is a chemical reaction between a metallic surface and an aqueous solution, containing primarily phosphoric acid and one or several metal salts. A metal phosphate layer forms on the surface. Phosphatized materials are primarily steel, zinc, galvanized steel and aluminum.

Phosphatization is used as:

- pretreatment for painting
- lubricant carrier
- temporary corrosion protection
- break-in support in engines

The most common phosphatization processes as a pretreatment for painting are iron, zinc and 3-cation phosphatization. The latter is the most advanced process and is used when the adhesion and corrosion protection requirements are very tough, such as in the automotive industry. 3-cation phosphatization is also somewhat illogically referred to as zing-manganese phosphatization because it also contains nickel. There are also environmentally friendly nickel free alternatives to 3-cation phosphatization. During the phosphatization process the solution reacts with the metal surface and phosphates of the abovementioned metals are formed.

When the requirements are somewhat lower, zinc phosphatization is used. For even easier and cheaper applications iron phosphatization can be a suitable pretreatment.

Zinc-phosphate coatings are used as a lubricant carrier during different cold drawing operations, such as tube and wire drawing and cold-heading. The layer is quite porous and can carry significant amounts of lubricant thus contributing to reducing the friction and the wear on the machine.

Phosphate coatings for temporary corrosion protection of machine components, etc. often consist of zinc phosphate, manganese phosphate or zinc-calcium phosphate of relatively thick layers, approx. 10 g/m².

Protection against wear on gear and pistons often consists of manganese phosphate. The layer has a certain lubricating effect but also binds with oil, which can be important when breaking-in different motor parts.

The phosphatization of steel as pretreatment for painting is usually no problem, neither on mild steels nor on

high strength materials. The most important thing is to have a clean surface before phosphatization to ensure fast nucleation and phosphate layer growth. This promotes the formation of a fine crystalline coating for best paint adhesion results. *Figure 6.98* shows a phosphate layer on a high strength steel material phosphated by a zinc-manganese phosphatization process. Phosphatization of hot-dip galvanized materials in the same process is also of high quality, see *figure 6.99*.

When phosphatization is used as pretreatment prior to painting, the last step of the pretreatment process is often a passivation treatment. Traditionally, chromate solutions have been used, but they have now been replaced by solutions based on zirconium or titanium salts.

Enameling

Enamel consists of several inorganic substances, primarily oxides. Up to approx 50–60 different substances can be included in an enamel depending on the desired properties. By fusing all these substances at high temperature and allowing them to cool down, the hard enamel, 60–70 % of which consist of glass, is formed.

The enamel can be applied on the substrate in many different ways and is burnt at 800–840° C. Application takes place via dipping or spraying. Modern application methods include electro dipping enameling and electrostatic application. The latter method is a direct method of applying dry powder onto the component. In order to achieve good enameling results, the steel must have special properties suitable for enameling. The chemical composition of the steel and the reactivity of the surface are two parameters that are important for the enameling.

The enamel can be given many different properties. It can be wear resistant and be used as a corrosion protection. The enamel is useful when a high chemical resistance is desirable. It is insensitive to bacteria which is useful in hospital environments. The enamel is also resistant to heat and UV-radiation.

In conventional two-layer enameling the first layer is a primer that will provide good adhesion to the base material and a satisfactory basis for the top enamel. When the top enamel is applied the desired properties and appearance of the component is achieved. To obtain a good qual-

GreenCoat – Nordic quality steel for harsh weather and greener living

GreenCoat® is SSAB's brand for innovative, eco-conscious color coated steel solutions for the building industry. GreenCoat is the greenest product portfolio of high quality color coated steel for exterior building applications and also one of the most comprehensive for the entire building industry.

All products come with premium Nordic quality steel in the substrate, which is recognized worldwide as one of the best steels available on the market. On top, most GreenCoat products feature a Bio-based Technology (BT) coating where a substantial portion of the traditional fossil oil is replaced by Swedish rapeseed oil, which is unique on the market. The unique, patented BT coatings do not only offer environmental advantages, but also increased performance.

GreenCoat products are highly resistant to corrosion, UV radiation as well as scratches. They provide builders with a lightweight material that is easy to work with even down to -15°C.

Binders	Drying or curing method	Comments
Alkyd	Oven- or air drying, 1-component	A large group with different properties. Not recommended for galvanized surfaces.
Acrylates	Oven- or air drying, 1-component and 2-component	High outdoor resistance. Limited resistance to solvents. Suitable for galvanized surfaces.
Epoxy	Oven- or air drying, 1-component and 2-component	Good adhesion. Low chalking resistance during outdoor use. The use of epoxy is regulated in the Occupational Health and Safety directives AFS 2005:18.
Oxiranester	2-component	Good adhesion but sensitive to surface cleanliness.
Polyester	Oven-drying, 1-component	Good mechanical properties and chemical resistance. Accurate curing is important.
Polyurethane	Oven- or air drying, 1-component and 2-component	Good outdoor hardness and chemical resistance. The use of polyurethane is subject to the Occupational Health and Safety directives AFS 2005:18.

Table 6.10: Binders that keep the paint together and give it its adhesion.

ity enamel the carbon content of the steel must be < 0.1 % and the steel surface pretreated, i.e. cleaned and pickled, before the application of the primer.

For direct enameling only one layer is applied, which places higher requirements on the substrate than two-layer enameling. Direct enameling requires the steel material to have a very low carbon content < 0.005 %. Prior to enameling the detail is pickled and a thin nickel coating ($1\text{g}/\text{m}^2$) is applied for best adhesion. Common applications are e.g. grate tops and other exposed components.

A third type of enameling is also used. This is in principle a direct enameling, but the enamel applied is a primer unlike a normal direct enameling where the enamel is a top coating. In general, the pretreatment of this type of enameling consists solely of degreasing. Typical applications are baking sheets and oven fittings.

6.10.3 Organic coatings

Passivations and TOC (Thin Organic Coatings)

TOC are coatings with a thickness of 1–2 µm that have been developed to replace previously used chromate-containing surface treatments. The coatings have been developed to become more multifunctional than their predecessor and can have the following functions:

- Temporary corrosion and handling protection during transportation, storage and processing.
- Dry and stick-free surface.
- Ensure an improved lubrication during various forming operations.
- Serve as a good surface for painting.

TOC coatings can be applied both on steel and metal coated surfaces and we distinguish between temporary and permanent coatings. Temporary coatings can be removed by conventional cleaning methods such as alkaline clean-

ing, whereas permanent coatings cannot be removed. Temporary coatings shall be used if subsequent process steps, such as painting, require a completely clean surface. There are two types of temporary corrosion protection. Dry corrosion protection, thickness 0.2 – 0.05 µm, whose only function is corrosion protection and dry lubricants, thickness 1–2 µm, where corrosion protection is combined with a lubricating additive which improves the processing properties.

Permanent coatings are currently used on metal coated steels. The simplest type is passivations, thickness 0.01–0.1 µm. They have replaced the traditional chromate-containing passivations due to the toxicity of hexavalent chromium. The next category comprises somewhat thicker coatings, 1–2 µm, often acrylate polymers with a lubricant additive. In addition to good corrosion protection, they have good lubricating properties and protect against handling damage, such as fingerprints. They can also be used as a basis for painting but this should be thoroughly evaluated for each paint system. The third category comprises weldable primers (pretreatment primers) which are primarily used in the automotive industry to increase the corrosion protection in cavities and hem flanges. These coatings are 3–7 µm thick and contain conductive components that make them weldable.

Paint

Painting is an organic surface treatment that gives a surface an esthetic appearance and/or protection.

A paint consists of the following components:
The binder keeps the paint together and provides adhesion, mechanical properties and protection against corrosion. Different types of paints are often named after the type of binder, such as alkyds, polyesters or polyurethanes, cf. table 6.10.

- Pigments and additives are particles with different composition that give the layer its color, coverage and corrosion protection.
- Solvents shall give the paint its right viscosity upon application.

In case of a surface treatment that involves the application of multiple paint layers, the first one, the primer, shall give adhesion to the substrate and improve the corrosion protection. The intermediate coat is used to give adhesion to the primer and moderates the thickness of the entire paint layer. The top coat shall give good resistance to the environment and an esthetically attractive surface (color and gloss).

Paints can also be divided by the agent that is used to apply the paint:

- waterborne
- solventborne
- powder
- wet paints with 100 % dry content

Environmental and financial issues is the driving force towards the use of paints with a reduced organic solvents. This can be achieved by using waterborne paints, increase the dry content of solvent borne paints or by completely switching to solvent-free paints. The latter can either be powder coatings or wet paints with 100% dry content where the binding agent is in liquid form.

Paint application

In order for a coating system to achieve the right properties, all substeps in the process must be thoroughly conducted. Depending on the requirements of the product, some of the following treatments can be included:

- cleaning
- chemical pretreatment
- metallic coating
- primer
- intermediate coat
- top coat

Paint can be applied by different spraying or dipping procedures selected based on the product requirements, economy and paint type. Dip coating requires the product to be clean in order not to contaminate the bath.

The transfer efficiency is high and even surfaces that are difficult to reach are painted. This particularly applies if electrodeposition (ED) is used. This method gives a low variation of coating thickness and good penetration of paint in partially closed areas.

Spray application can be carried out as low-pressure spraying, high-pressure spraying or electrostatic spraying. Low-pressure spraying provides a good surface finish, but bad paint utilization, approx. 50–60%, and low penetration

depth. High pressure application and electrostatic painting give better paint utilization, approx. 60–85%, but the surface finish is worse.

In some cases it is possible to paint before treatment and forming. The painting is integrated in the steel production process in a coil coating line. After cleaning and pretreatment, the paint roll coated. On SSAB's coil coated products the paint is applied in two layers, first the primer and then the top coat.

Corrosion protection by painting

The principal method for protection of steel constructions against corrosion is by painting. Four factors other than the environment and the structural design, are of decisive importance for the quality of corrosion protection painting, namely:

- the pretreatment
- the application
- the paint material
- the paint layer thickness

The best help in choosing the right surface treatment can be found in SS-EN 1090-2. It refers to corrosivity categories pursuant to standard SS-EN ISO 12944-2 and recommends appropriate corrosion protection systems according to standard SS-EN ISO 12944-5.

Coil coating

At SSAB's coating lines, a hot-dip galvanized steel strip is painted in a continuous line. First, the strip is chemically and mechanically cleaned and pretreated. The purpose of the pretreatment is to improve the adhesion between the steel surface and the coating. The coating takes place in two steps, first a primer and then a top coat. The paint is applied by rollers which gives good possibilities for reproducing the thickness and appearance of the paint layer. The curing of the paint takes place in ovens, one for the primer and one for the top coat. Different paint systems can be selected depending on the requirements to the product, cf. figure 6.100.

Polyester

Polyester is currently the most common paint system for coil coating in Europe. The polyester is a thin coating, usually 27 µm. It has uniform properties in terms of hardness, bendability, scratch-, and chemical-resistance.

Polyester is used, for example, in industrial buildings and in corrosivity categories up to C3. Common applications include roof and facade plates and roofing tiles. The polyester is also common in the construction industry where it can be tailored for different gloss and flexibility.

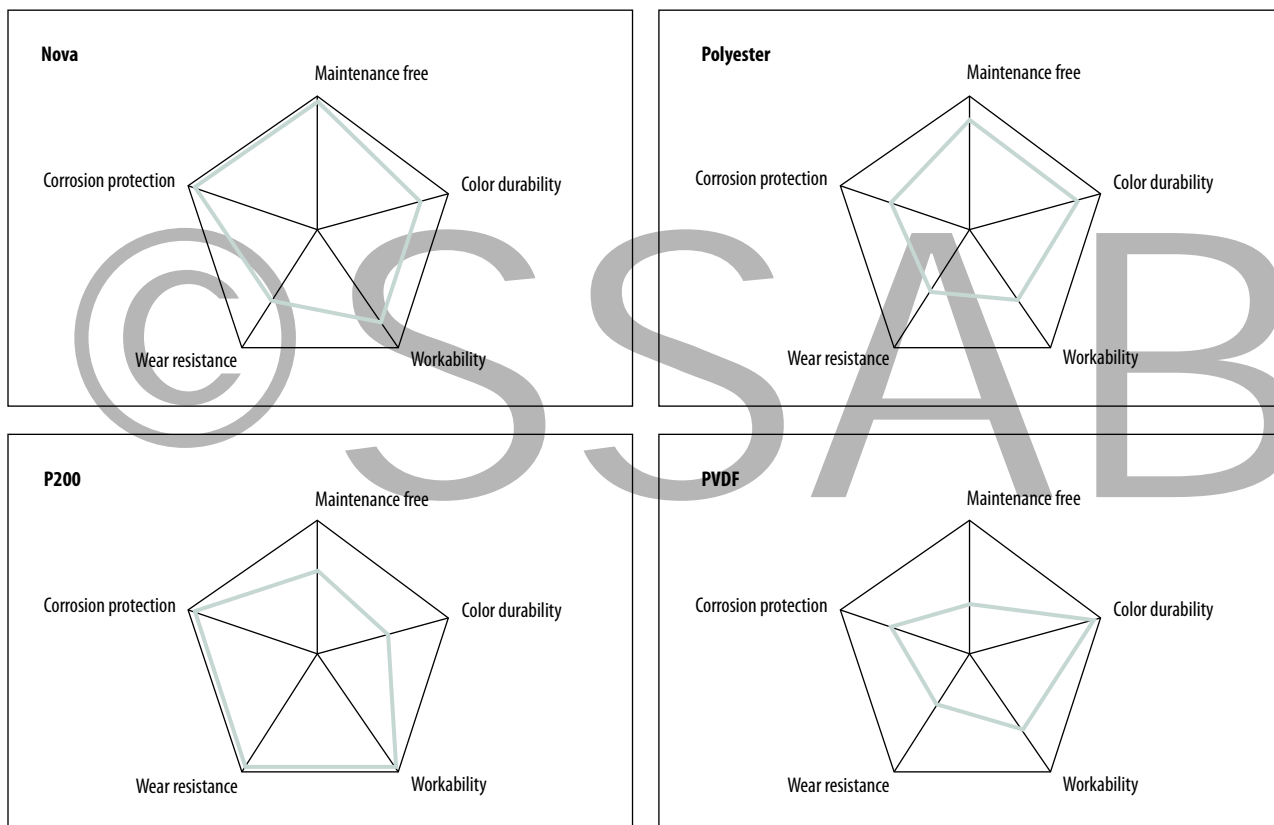


Figure 6.100: Paint system – the most important properties for outdoor use.

SSAB has also a high build polyester coating, 50 µm, with improved corrosion protection, flexibility and mechanical durability. It has a structured, wear-resistant surface thanks to the polymer particles in the top coat. It is used for roofing, rainwater systems and facades in of corrosivity category up to C4.

Plastisol

Plastisol coatings have a thickness of approx. 200 µm. It has an embossed surface and is scratch-resistant, has good formability and corrosion protection. It can be used in corrosivity category up to C4.

Prelaq 200 is used for facades and fittings in corrosive environments. Due to low UV-stability it shall not be used in Central and Southern Europe.

PVDF – Polyvinylidene Fluoride

PVDF has the best color and gloss durability and its formability is very good too. The coating has a thickness of 27 µm and is used in environments with corrosivity category of up to C3.

PVDF is primarily used in façade wall cassettes for buildings with high color and gloss requirements. Protection foil can be used to protect the surface during handling and assembly and then removed once the works are finished.

6.10.4 Metallic coatings

Continuous metal coating

In case of continuous application of strips and wires, after cleaning and oxide reduction, the steel strip is entering a molten bath. To obtain the right layer thickness, the excess is blown away by air-knives at the molten bath exit. Normal layer thicknesses for this type of processes are 5–25 µm per side. After exiting the molten bath, the strip is cooled down to room temperature before being skin passed (customer option) and applied with transport protection (oil or passivation) and coiled. SSAB's continuously hot-dip galvanized products are manufactured this way.

An alternative way to apply the metal coating is to electrolytically precipitate a layer on the surface. The strip goes through several cells where the process takes place. Coatings of up to 10 µm per side can be produced with this method, either pure zinc coatings, or zinc-nickel or zinc-iron coatings.

General galvanizing

General galvanizing is the most common hot-dip galvanizing procedure. During general galvanizing, a zinc coating is applied, 70–200 µm thick, depending on the steel grade and process variables. General galvanizing gives the detail very good corrosion protection and is a preferred method

Composition weight %	Cold rolled steel	Hot rolled steel
Si + P < 0,03	OK for normal requirements. Thickness according to standard, gloss layer. The following apply for high surface requirements: Si < 0.03 and Si + 2.5P < 0.04	OK for normal requirements. Thickness according to standard, shiny appearance. The following apply for high surface requirements: Si < 0.02 and Si + 2.5P < 0.09
0,03 < Si + P ≤ 0,14	Not suitable!	Not suitable!
0,15 < Si < 0,21	Coating thicker than standard. Check for internal oxidation that changes the surface reactivity.	Coating thicker than standard.
0,22 < Si < 0,28	Coating much thicker than standard. Gray appearance.	Coating much thicker than standard. Gray appearance.
0,29 < Si < 0,35	High coating thickness with a certain brittleness. Gray appearance.	High coating thickness with a certain brittleness. Gray appearance.

Table 6.11: Structural steels suitable for general galvanizing.

for corrosive environments of corrosivity category 2 to 5 according to SS-EN ISO 12944-2.

General galvanizing can take place through a wet or a dry process. In both methods the steel surfaces must be degreased, then usually pickled in hydrochloric acid or ferrous chloride and rinsed in water before immersion in molten zinc at a temperature of 450–460° C. In the wet process, a flux agent (ammonium chloride) is placed on the zinc surface. The humid steel components are dipped through the flux layer into the zinc bath and then taken up through a flux-free bath surface. In the dry process, after being pickled and rinsed, the steel components are dipped into a water solution of zinc/ammonium chloride and then dried. A thin layer of flux salt remains on the steel surface and the subsequent dipping in the zinc bath does not require any additional flux agent. After the galvanizing, the steel is cooled down in air or water. In most common structural steels silicon and phosphorus have the greatest influence on the structure and thickness of the zinc layer. *Table 6.11* shows structural steels suitable for general galvanizing:

See also SS-EN ISO 1461: Hot-dip galvanized coatings on fabricated iron- and steel articles - Specifications and Test Methods.

Steels with silicon content above 0.35 weight % can be hot dip galvanized too, but the layer thickness significantly increases with the dipping time. Thick zinc layers are generally more brittle and have to be handled with care. Impacts during transportation can cause the layer to lose adhesion.

Steels not suitable for general galvanizing have Si+P between 0.03 and 0.15 weight %. The zinc strongly reacts with these steels, Sandelin effect, *figure 6.101*, and results in thick, brittle and dark gray layer, often with bad adhesion.

The advices above applies for both hot rolled and cold rolled steels. However, there is an important difference between steels with Si+P content just above the unsuitable range (0.03 % < Si+P < 0.15 %). Since the cold rolled material is annealed after the cold rolling process, some of the silicon enriched and oxidized on the outermost surface. This silicon is inactive during the general galvanizing, which means the content of active silicon decreases, ending up in the unsuitable range with an undesirable zinc layer growth. The problem can be avoided if the material

is pickled prior to galvanizing at which the affected zones is removed. There is a certain variation, however, both in the annealing and in the pickling process, so in order to completely eliminate the risk, we recommend using other steels, e.g. steels with Si+P<0.030 % or Si+P=0.25 to 0.35 %.

In the case of high temperature galvanizing, 540–560° C, the composition of the steel has a minor influence on the properties of the layer. The structure of the layer is governed by the cooling process after the dipping.

The fatigue strength after general galvanizing of high strength steels with a yield point above 650 MPa is reduced by up to 35%. Only a marginal decrease is achieved with steels with lower yield strength.

To select the right steel grade, always inform the steel supplier if you intend to use general galvanizing. Recommendations can also be obtained from the trade organization Nordic Galvanizers. Rephos steels are not recommended for general galvanizing.

Zinc plating

Zinc plating is the most common electrolytic coating method. It gives the component an appealing and a relatively good corrosion protection. A common scope of application is for fasteners. The zinc plating layer is usually 5–25 µm thick but it may vary on the object depending on design and fixture. To improve to the corrosion protection, the product is sometimes painted after zinc plating.

Zinc plating of high strength steels implies a risk for hydrogen embrittlement if the tensile strength is greater than 1000 MPa (equivalent to HRC 35 or HV 345). Hydrogen embrittlement reduces the strength of the component and fracture can be observed directly or years after the surface treatment. Hydrogen embrittlement is due to the absorption and diffusion of atomic hydrogen to stress concentration areas. It makes no difference whether the tensile stress is caused by external or residual stress. When hydrogen accumulates in high stress areas, crack development is facilitated resulting in a brittle, intercrystalline fracture. The risk for hydrogen embrittlement can be reduced through baking. Temperatures and times can be found in standard SS-ISO 9588 and are depending upon the tensile strength of the steel.

SSAB's steel grades with strength of up to Docol 1000 DP can be zinc-plated without problem. During zinc-plating of

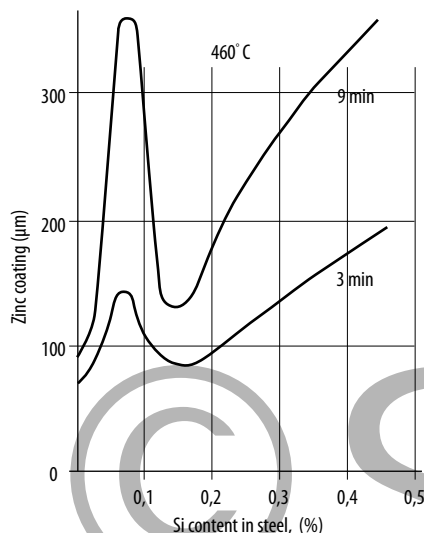


Figure 6.101: In the Sandelin curve you can see the effect of the Si content on the thickness of the zinc layer general galvanizing for 3 or 9 min dipping time.

our martensitic steels, Docol 1200 M and Docol 1400 M, the outcome is dependent upon the process. Thorough tests and assessments in the intended production facility are required for each individual product. Alternatively, surface treatments that do not generate hydrogen, such as Geomet or Delta MKS, can be chosen for certain applications.

Nickel- and chrome-plating

The most common application of nickel plating is for decorative purposes. Simultaneously the corrosion protection properties of the nickel layer can be utilized. In the case of bright nickel plating, it is common to apply a thin surface chrome layer, approx. 0,3 µm, in order to keep the gloss for a longer period of time.

Nickel can be applied in very thick layers, up to 250 µm and can be made very hard, up to 500 HV. Thick layers are often required if the layer shall be a satisfactory corrosion protection of the steel. Nickel is more noble than steel meaning that the layer has to cover the basic metal completely and must be free from pores in order to provide good corrosion protection.

Chrome plating is used in thin layers onto nickel coatings, see above or as hard chromium plating as corrosion and wear protection.

When hard chromium plating is used the layer thickness can vary considerably from 5 to 500 µm depending on the requirements on the component. Hardness values above 1100 HV can be achieved.

PVD and CVD coatings

Surface treatment methods where the materials are evaporated first and then condensed on a surface are referred to as gas phase methods. The gas phase methods are often divided into two technical areas: PVD (Physical Vapor Deposition) and CVD (Chemical Vapor Deposition). Everything from pure metal layers, via different alloys to different variants of nitrides, carbides and oxides and/or mixtures of these, as well as both homogenous and alloyed structures can be fabricated with the help of these methods. The fundamental difference between PVD and CVD is how the material is supplied to the surface.

In the PVD process, the coating material, such as Ti or Cr, is vaporized from solid phase to gas phase. Some

methods require an electric voltage between the article and the reaction chamber for transporting the vaporized material to the surface where it will be condensed. The process takes place at a pressure ranging from 10–6 to 10–4 Pa. To form wear-resistant nitrides, carbides or oxides, a small quantity of reactive gas is supplied (such as nitrogen, methane or oxygen). The layer thickness is usually between 2 and 7 µm depending on the application.

In the CVD process the components are placed in a coating reactor. The reactor is then heated to a temperature between 960 and 1,020°C depending on the process and on the steel grade of the component. After that a gas mixture is fed into the reactor. The gas composition determines the composition of the layer formed on the surface. The gas mixture can be changed during the course of the process so the layer composition varies with the layer thickness. The layer thickness normally ranges from 5 to 7 µm.

Coatings are often used on tools or components exposed to wear or any other type of mechanical abrasion.

The PVD technique has also been used in continuous coating lines for steel strips. The materials applied on the steel surface have been primarily zinc, aluminum and magnesium.

SSAB steel grade	Uddeholm tool steel	Tool hardness (HRC)
460 LAD 500 LAD 500 DP	Calmax Unimax Caldie Sleipner Sverker 21 Vanadis 4 Extra Vancron 40	56–62
600 DP 600 CP 780 CP 800 DP 800 DFX	Calmax Unimax Caldie Sleipner Vanadis 4 Extra Vanadis 6 Vancron 40	58–64
800 DP 800 DFX 1000 DPX ROLL 800 ROLL 1000	Caldie Sleipner Vanadis 4 Extra Vancron 40	≥ 60

Table 6.12: Recommended tool steel for punching in zinc-coated strip steel.

6.11 Tool steel for high strength steels

The hardness of high strength steels requires very hard tool steel to avoid tool deformation and minimize wear.

6.11.1 Tool steel for punching operations

Tool steel wear will increase when shearing high strength steels. It is therefore important to select good tool steel for best economy. The following information is general. If you have a specific inquiry, do not hesitate to contact special tool steel experts (Uddeholm Tooling).

6.11.2 Tool steel for punching

The press force increases with higher strength of sheet metal. Greater blank holder force is often necessary too in order to avoid wrinkle formation. This results in high local contact pressure that places high requirements on the tool material and its surface.

6.11.3 Coating of tools

Besides the conventional surface transformation methods, there are two other common surface treatment methods for increasing the surface hardness of a tool: PVD or resp. CVD. With these methods, tool surfaces can be coated with very hard nitride or carbide layers that improve the friction properties and wear resistance of the surfaces. A combination of nitriding of the surface and a PVD layer, the so called Duplex treatment has proven to work well while forming high strength steels. With all types of surface treatments it is important to have a substrate material that can carry the hard surface layer without plastic deformation or fatigue and a high surface quality of the tool that is to be coated.

SSAB steel grade	Uddeholm tool steel	Tool hardness (HRC)
Docol 500 LA Docol 500 DP Docol 500 DL	Calmax Unimax Caldie Sleipner Sverker 21 Vanadis 4 Extra Vancron 40	≥ 56
Docol 600 DP Docol 600 DL	Caldie Sleipner Vanadis 4 Extra Vanadis 6 Vancron 10 Vanadis 40	≥ 58
Docol 800 DP Docol 800 DL Docol 1000 DP Docol ROLL 800 Docol ROLL 1000 Docol 100 DP+ZE Docol 1000EP	Caldie Sleipner Sverker 21 Vanadis 4 Extra Vanadis 6 Vancron 40	≥ 60
Docol 1200 M Docol 1400 M Docol 1500 M Docol WEAR 450 Docol 1200 MZE Docol 1400 MZE	Caldie Sleipner Vanadis 4 Extra	60–62

Table 6.13: Recommended tool steel for punching in cold rolled steel.

PVD (Physical Vapor Deposition)

PVD coating is carried out in a vacuum chamber. The layer thickness is usually 3–4 µm.

The coating temperature ranges from approx. 400 to 550° C thanks to which many high alloyed tool steels can be coated in hardened and tempered conditions without reduction in the basic hardness. Low temperature coatings (200° C) are also available where the tool steel is tempered at a lower temperature. One limitation of the method, however, is that the inside of the holes can only be coated to a depth corresponding to the diameter of the hole.

CVD (Chemical Vapor Deposition)

The coating usually takes place through a chemical reaction and a uniform layer is formed over the entire exposed tool surface (even in the holes). The layer thickness is usually approx. 3–10 µm. The adhesion is very good.

Since the process temperature is high 800–1,100° C, the tools must be hardened and tempered to the right hardness in connection with CVD treatment. The thermal treatment requirement makes it more difficult to handle narrow tool tolerances than it is the case with PVD treatment. Multiple layers and layer combinations can be achieved, cf. table 6.15.

Figure 6.102 provides an overview of the hardness levels that can be achieved through coating. The comparison has been made with the help of hardened steel and cemented carbide.

Strength R_m (MPa)	Steel Type Uddeholm/AISI/W.-Nr.	Coating		Tool Hardness (HRC)
		Type	Useful Life	
350–570	Calmax/-/1.2358	Nitriding/PVD	Medium	≥ 58
	Rigor/A2/1.2363	PVD/CVD	Medium	
	Sverker 21/D2/1.2379	PVD/CVD	Medium	
	Caldie	PVD/CVD	Medium-Long	
	Sleipner	PVD/CVD	Medium-Long	
	Vanadis 4 Extra	PVD/CVD	Long	
	Vancron 40	No coating		
570–800	Calmax/-/1.2358	Duplex (Nitriding+PVD)	All	≥ 60
	Sverker 21/D2/1.2379	PVD/CVD	All	
	Caldie	PVD/CVD	All	
	Sleipner	PVD/CVD	All	
	Vanadis 4 Extra	PVD/CVD	All	
	Vanadis 6	PVD/CVD	All	
	Vancron 40	No coating		
800–1400	Caldie	PVD/CVD	All	≥ 60
	Sleipner	PVD/CVD	All	
	Vanadis 4 Extra	PVD/CVD	All	
	Vanadis 6	PVD/CVD	All	
	Vanadis 10	PVD/CVD	All	
	Vancron 40	No coating		

Table 6.14: A table of some standard coatings.

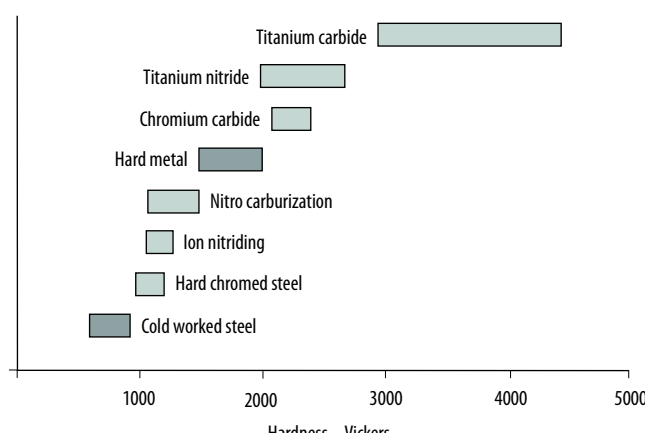


Figure 6.102: Layer hardness as compared to the hardness of thermal treated steels and cemented carbide [6.14].

		CVD	PPD
Titanium carbide	TiC	X	
Titanium nitride	TiN	X	X
Titanium carbonitride	Ti _x C _y N _z	X	X
Chromium nitride	CrN		X
Titanium aluminum nitride	Ti _x Al _y N _z		X

Table 6.15: A table of some standard coatings.

6.12 References

- [6.1] Lysaght, J.
Sheet Steel fabrication handbook
Ltd, Port Kembla, Australien 1983.
- [6.2] LUFORM – *Stansning och hålklippning*
Broschyr, SSAB Svenskt stål AB, Luleå 1982.
- [6.3] Schneider, B., Hohemarkstrasse, KG.
Normalien fur Stanzwerkzeuge
Broschyr, p.89–91, D-6370 OBERURSEL, Germany.
- [6.4] Palmers, G., Weidemann C.,
Finklippning av höghållfast och rostfria martensitiska stål
IVF –resultat 73613, Sveriges Mekanförbund, Stockholm 1973.
- [6.5] Wickström, S.
Finklippning av plåtdetaljer
IVF resultat 73612, Sveriges Mekanförbund, Stockholm 1973.
- [6.6] Speedsteel – *Feinschneiden durch ASP noch wirtschaftlicher*.
Broschyr, Kloster Spedsteel AB, Söderfors 1984.
- [6.7] *Stål för klipp- och pressverktyg*.
Broschyr, SSAB Svenskt Stål AB, Oxelösund 1985.
- [6.8] Schmanser, H. R.
Erfahrungen mit beschichteten Schneidstempeln.
Werkstatt und Betrieb Vol 120, s. 642–646, 1987,
- [6.9] *Bearbetning av OX –plåt*.
Broschyr, SSAB Svenskt Stål AB, Oxelösund 1985.
- [6.10] *Karlebo handbok*
Utgåva nr 13, Maskinaktiebolaget Karlebo 1986.
- [6.11] *Termisk skärning*.
Svetskommisionen, AG 42, Kompendium, temadag AGA,
Lidingö 1987.
- [6.12] Salmi, T.
Laser i tunnplåtsbearbetning
Särtryck från Verkstäderna, nr 15, sid 37–39, 1983.
- [6.13] *Bockning av tunnplåt*
IVF –resultat 78623, Sveriges Mekanförbund, Stockholm
1978.
- [6.14] Lundh, H.
Analys av återfädring vid bockning med bottenslag
Teknisk rapport nr 860057, SSAB Svenskt Stål AB, Borlänge.
- [6.15] *Fogningshandboken – Sammanfogning av höghållfast stål*.
SSAB Tunnplåt AB, Borlänge 2004.
- [6.16] *Svetsteknisk ordlista*.
Svetskommisionen, 1968.
- [6.17] *Motståndssvetsning (Handbok)*
Svetskommisionen, 1987 (ISBN 91 7082 436 3)
- [6.18] [6.19] SS-EN ISO 8501-1:2001
Behandling av ståltytor före beläggning med målningsfärg och liknande produkter. Del 1: Rostgrader och förbehandlingsgrader för obelagd stål och för stål, från vars hela yta tidigare beläggning avlägsnas.
SIS Förlag AB 2001.
- [6.20] *Handbok i metallrengöring*.
IM, IVL och YKI. Stockholm 1995.
- [6.21] *Handbok i industriell rengöring*.
IVF. Mölndal 1994.
- [6.22] *Lärobok i elektrolytisk och kemisk ytbehandling*.
Band I–III. Sveriges Galvanotekniska Förening. Linköping
1990.
- [6.23] *Industriell lackering – Handbok för val av miljöanpassade processer*.
IVF, KI och SP. 1995.
- [6.24] BSK 99.
Boverkets handbok om stålkonstruktioner.
Boverket, 1999
- [6.25] *Handbok i rotskyddsmålning*.
Bulletin nr 107. Korrosionsinstitutet. Stockholm 1999.
- [6.26] *Anvisningar för provning av rotskyddsmålning genom fältexponering*.
Korrosionsinstitutet rapport 1993:8. Stockholm 1993.
- [6.27] Hirn, A.
Varmförzinkning av svåra stål.
Institutet för metallforskning. Stockholm 1994.
- [6.28] *Väteförsprödning – mekanismer, orsaker och åtgärder*.
IVF-skrift 97823. Mölndal 1997.
- [6.29] EN ISO 9013:2002
Termisk skärning – klassificering av termiskt skurna ytor – kvalitetsnivåer för formavvikelse och toleranser.
SIS Förlag AB 2002.
- [6.30] Ivarson, A.
On the Physics and Chemical Thermodynamics of Laser Cutting.
Ph.D. thesis, Luleå University of Technology, Sweden 1993.

Price: 95 €

ISBN: 978-91-637-1032-2



SSAB is a leading global provider of high-strength steel. SSAB offers products developed in close cooperation with customers to create a stronger, lighter and more sustainable world.

SSAB has employees in over 45 countries and production facilities in Sweden and the United States. SSAB is listed on the NASDAQ OMX Nordic Exchange in Stockholm.

1008-EN-Design Handbook-VI-2012. Höglund Design AB. Österbergs Tryckeri.

SSAB EMEA

SE-781 84 Borlänge
Sweden

Tel +46 243 700 00
Fax +46 243 720 00
E-mail: info@ssab.com

www.ssab.com

SSAB

This handbook contains general suggestions and information without any expressed or implied warranty of any kind. SSAB hereby expressly disclaims all liability of any kind, including any damages, in connection with the use of the information and for their suitability for individual applications. It is the responsibility of the user of this brochure to adapt the recommendations contained therein to the requirements of individual applications.